

ABSTRACT

Title of Document: ASSESSMENT OF NITROGEN STATUS AND VEGETATION COMPOSITION IN TIDAL FRESHWATER MARSHES USING PARTIAL LEAST SQUARES REGRESSION MODELS OF HYPERSPECTRAL CANOPY REFLECTANCE

Emily Poynter Jenkins, Master of Science, 2006

Directed By: Assistant Professor David R. Tilley
Biological Resources Engineering

Hyperspectral canopy reflectance was used to predict sub-surface water nutrients, vegetation composition, and canopy nutrients, which could lead to more useful means for assessing the status of wetlands. Thirty field quadrats at two tidal freshwater marsh sites on the Nanticoke River (Maryland) were treated with five nitrogen levels. During the 2004-05 growing seasons, hyperspectral canopy reflectance was measured using a spectroradiometer with 1nm resolution across the visible and near – infrared spectrum (350-1075 nm), water samples were collected using lysimeters, species cover was quantified, and biomass was collected and analyzed for canopy nutrients. ANOVA was used to determine whether nitrogen affected reflectance, species composition, canopy N and P, and partial least squares regression was used to develop reflectance models predictive of these ecosystem properties. Results indicated that hyperspectral radiometry could be used as a remote sensing tool for quantifying sub-surface water nitrogen, vegetation composition, and canopy nutrients in tidal freshwater marshes.

ASSESSMENT OF NITROGEN STATUS AND VEGETATION COMPOSITION
IN TIDAL FRESHWATER MARSHES USING PARTIAL LEAST SQUARES
REGRESSION MODELS OF HYPERSPECTRAL CANOPY REFLECTANCE

By

Emily Poynter Jenkins

Thesis submitted to the Faculty of the Graduate School of the
University of Maryland, College Park, in partial fulfillment
of the requirements for the degree of
Master of Science
2006

Advisory Committee:
Dr. David R. Tilley, Chair
Dr. Andrew H. Baldwin
Dr. Patrick C. Kangas

Dedication

To Conrad and Alec, who, from the beginning, cheerfully accompanied me every step of the way,

To Dick Leinenkugel, who was there when I was both overwhelmed and overjoyed,
and to Mike, who always listened.

Acknowledgements

I would like to thank the following associations for major funding for this project: the Department of Interior's U.S. Geological Survey through the University of Maryland's Water Resources Research Center (Agreement #1HQGR0084), D. Tilley P.I., the Department of Commerce's National Oceanic and Atmospheric Administration through Maryland Sea Grant College (Agreement #NA16RG2207), D. Tilley P.I., and The Nature Conservancy through the Biodiversity Conservation Research Fund (Agreement #05230504-MDDC), E.P. Jenkins and D. Tilley Co-P.I.

I sincerely thank Dr. David Tilley, Assistant Professor, University of Maryland at College Park, for his leadership in the development of this research, continual guidance throughout the project, and encouragement to present my work at academic conferences. I also thank Dr. Andrew Baldwin, Associate Professor and Acting Chair, Biological Resources Engineering Department, University of Maryland at College Park, for his assistance in launching the project and instruction on plant identification, and Dr. Patrick Kangas, Associate Professor, University of Maryland at College Park, for his suggestions and support. Also, many thanks go to my colleagues, Jeff Mentzer, Jose-Luis Izursa, Laura Schumann, and Alex MacLeod, as well as Jim Carleton, Kimberly Monahan, Dave Blersch, and Tommy Griffeth for assistance in field work.

Table of Contents

Dedication	ii
Acknowledgements	iii
Table of Contents	iv
List of Tables	vi
List of Figures	x
Chapter 1: Introduction	1
1.1 Problem definition	1
1.2 Literature Review	2
1.3 Objectives	9
1.4 Plan of Study	10
Chapter 2: Materials and Methods	11
2.1 Site Description	11
2.2 Experimental Design	11
2.3 Data Collection	16
2.4 Data Analysis	21
2.4.1 <i>Reflectance Transformations for ANOVA and PLS Modeling</i>	23
2.4.2 <i>Dependent Data Transformations for ANOVA and PLS Modeling</i>	35
Chapter 3: Results	42
3.1 Marsh Water Quality	42
3.1.1 <i>Seasonal dynamics of sub-surface nutrients</i>	42
3.1.2 <i>Fertilization and Site Effects on NH₃</i>	48
3.1.3 <i>Fertilization and Site Effects on NO₃</i>	55
3.1.4 <i>Fertilization and Site Effects on Total Nitrogen</i>	59
3.1.5 <i>Fertilization and Site Effects on Total Phosphorus</i>	65
3.2 Marsh Vegetation Composition	67
3.2.1 <i>Pattern of dominant species over the growing season at each site</i>	67
3.2.2 <i>Fertilization effects on vegetation cover</i>	72
3.2.3 <i>Nitrogen fertilization effects on canopy nutrients</i>	138
3.3 Marsh Canopy Reflectance Response	144
3.3.1 <i>Seasonal dynamics of canopy reflectance</i>	144
3.3.2 <i>Detection of nitrogen effect on reflectance indices</i>	146
3.3.3 <i>Detection of nitrogen and marsh-type effects on canopy reflectance</i>	159
3.3.4 <i>Detection of nitrogen effects on transformed canopy reflectance</i>	166
3.4 Partial Least Squares (PLS) Modeling	170
3.4.1 <i>Prediction of nitrogen and phosphorus in marsh sub-surface water</i>	170
3.4.2 <i>Prediction of canopy nutrients</i>	240
3.4.3 <i>Prediction of vegetation composition and surface cover</i>	244
Chapter 4: Discussion	259
4.1 Nitrogen fertilization effect on sub-surface marsh N and P levels	259
4.2 Nitrogen fertilization effect on vegetation composition & canopy nutrients ..	261
4.3 Effects of fertilizer and vegetation on canopy reflectance	262
4.4 Models predictive of nutrient level, vegetation cover, and canopy nutrients ..	264

4.5 Spectral bands significant to nutrient availability	267
4.6 Conclusions	268
4.7 Implications	269
APPENDIX A List of Abbreviations.....	271
APPENDIX B Spectral Bands Used in ANOVA and PLS-regressions.....	272
APPENDIX C PLS Regressions for Vegetation Composition.....	288
APPENDIX D Raw vegetation data across the 2004-05 seasons.....	362
Literature Cited	408

List of Tables

Table 2.1	Definition of nitrogen treatments	15
Table 2.2	Cover Class System	20
Table 2.3	Summary of spectral transformation	41
Table 2.4	Summary of water quality transformations	41
Table 2.5	Summary of vegetation transformations	41
Table 3.1.1	Repeated measures ANOVA model for ammonia	48
Table 3.1.2	Treatment and time ANOVA model for ammonia	49
Table 3.1.3	Treatment and site ANOVA model for ammonia	49
Table 3.1.4	Repeated measures ANOVA model for Log (NH ₃)	50
Table 3.1.5	Treatment and time ANOVA model for Log (NH ₃)	51
Table 3.1.6	Treatment and site ANOVA model for Log (NH ₃)	51
Table 3.1.7	Repeated measures ANOVA model for nitrate	55
Table 3.1.8	Treatment and time ANOVA model for nitrate	55
Table 3.1.9	Treatment and site ANOVA model for nitrate	56
Table 3.1.10	Repeated measures ANOVA model for total nitrogen	59
Table 3.1.11	Treatment and time ANOVA model for total nitrogen	60
Table 3.1.12	Treatment and site ANOVA model for total nitrogen	60
Table 3.1.13	Repeated measures ANOVA model for Log (TN)	61
Table 3.1.14	Treatment and time ANOVA model for Log (TN)	61
Table 3.1.15	Treatment and site ANOVA model for Log (TN)	62
Table 3.1.16	Repeated measures ANOVA model for total phosphorus	65
Table 3.1.17	Treatment and site ANOVA model for total phosphorus	65

Table 3.2.1	Treatment and time ANOVA model for <i>P. australis</i>	74
Table 3.2.2	Treatment and time ANOVA model for <i>A. calamus</i>	78
Table 3.2.3	Repeated measures ANOVA model for <i>P. arifolium</i> cover	82
Table 3.2.4	Treatment and time ANOVA model for <i>P. arifolium</i>	82
Table 3.2.5	Treatment and site ANOVA model for <i>P. arifolium</i>	82
Table 3.2.6	Repeated measures ANOVA model for <i>P. virginica</i> cover	89
Table 3.2.7	Treatment and time ANOVA model for <i>P. virginica</i>	89
Table 3.2.8	Treatment and site ANOVA model for <i>P. virginica</i>	89
Table 3.2.9	Repeated measures ANOVA model for <i>Typha</i> cover	95
Table 3.2.10	Treatment and time ANOVA model for <i>Typha</i> species	95
Table 3.2.11	Treatment and site ANOVA model for <i>Typha</i> species	96
Table 3.2.12	Repeated measures ANOVA model for <i>I. capensis</i> cover	101
Table 3.2.13	Treatment and time ANOVA model for <i>I. capensis</i>	101
Table 3.2.14	Treatment and site ANOVA model for <i>I. capensis</i>	101
Table 3.2.15	Repeated measures ANOVA model for LAI	108
Table 3.2.16	Treatment and time ANOVA model for LAI	108
Table 3.2.17	Treatment and site ANOVA model for LAI	108
Table 3.2.18	Repeated measures ANOVA model for species richness	115
Table 3.2.19	Treatment and time ANOVA model for species richness	115
Table 3.2.20	Treatment and site ANOVA model for species richness	115
Table 3.2.21	Repeated measures ANOVA model for dead material	122
Table 3.2.22	Treatment and time ANOVA model for dead material	122
Table 3.2.23	Treatment and site ANOVA model for dead material	122

Table 3.2.24	Repeated measures ANOVA model for diversity index	129
Table 3.2.25	Treatment and time ANOVA model for diversity index	129
Table 3.2.26	Treatment and site ANOVA model for diversity index	129
Table 3.2.27	Canopy nitrogen of the top six species according to nitrogen treatment	140
Table 3.2.28	Canopy phosphorus of the top six species according to nitrogen treatment	141
Table 3.4.1	PLS regressions for ammonia on <i>Phragmites</i> -dominant and <i>Phragmites</i> -absent sites	171
Table 3.4.2	PLS-regression transformations tested on spectrum and ammonia concentration at both sites	173
Table 3.4.3	PLS-regression for ammonia at the <i>Phragmites</i> -absent site	175
Table 3.4.4	PLS-regression transformations tested on spectrum and ammonia concentrations at the <i>Phragmites</i> -absent site	177
Table 3.4.5	PLS-regression for ammonia at the <i>Phragmites</i> -dominant site	181
Table 3.4.6	PLS-regression transformations tested on ammonia concentrations at the <i>Phragmites</i> -dominant site	183
Table 3.4.7	PLS-regression for nitrate at combined <i>Phragmites</i> -dominant and <i>Phragmites</i> -absent sites	192
Table 3.4.8	PLS-regression transformations tested on nitrate concentrations at the two marsh sites	194
Table 3.4.9	PLS-regression for nitrate at the <i>Phragmites</i> -dominant site	198
Table 3.4.10	PLS-regression transformations tested on nitrate concentrations at the <i>Phragmites</i> -dominant site	200
Table 3.4.11	PLS-regression for nitrate concentration at the <i>Phragmites</i> -absent site	201
Table 3.4.12	PLS-regression transformations tested on nitrate concentrations at the <i>Phragmites</i> -absent site	203

Table 3.4.13	PLS-regressions for total nitrogen at the <i>Phragmites</i> -dominant site	213
Table 3.4.14	PLS-regression transformations tested on total nitrogen concentrations collected from the <i>Phragmites</i> -dominant site	215
Table 3.4.15	PLS-regression for total nitrogen at the <i>Phragmites</i> -absent site	216
Table 3.4.16	PLS-regressions transformations performed on the total nitrogen concentrations collected from the <i>Phragmites</i> -absent site	218
Table 3.4.17	PLS-regression for total phosphorus at the <i>Phragmites</i> -dominant site	226
Table 3.4.18	PLS-regression transformations tested on total phosphorus concentrations collected at the <i>Phragmites</i> -dominant site	228
Table 3.4.19	PLS-regression for total phosphorus at the <i>Phragmites</i> -absent site	231
Table 3.4.20	PLS-regressions transformations tested on total phosphorus concentrations collected at the <i>Phragmites</i> -absent site	233
Table 3.4.21	PLS-regressions for leaf N, leaf P, and biomass	240
Table 3.4.22	PLS-regressions for canopy N of the plot and relative to total biomass	241
Table 3.4.23	The best PLS-regressions for each species cover at individual marsh sites	244
Table 3.4.24	The best PLS models of each species cover applied to the opposite marsh site	245
Table 3.4.25	The best PLS-regression(s) for each vegetation characteristic at individual marsh sites	256
Table 3.4.26	The best PLS models of each vegetation characteristic applied to the opposite marsh site	257

List of Figures

Figure 2.1	Location of Maryland, USA	12
Figure 2.2	Location of marsh sites on Delmarva Peninsula	13
Figure 2.3	Map of the Nanticoke River identifying the two marsh sites, and layout of plots according to fertilization treatment	14
Figure 2.4	Diagram of the lay-out for each 1 m ² plot.	15
Figure 2.5	Canopy reflectance measured at the <i>Phragmites</i> -absent site	17
Figure 2.6	Sub-surface water collected at the <i>Phragmites</i> -dominant site	18
Figure 2.7	Typical untransformed spectral reflectance curve	24
Figure 2.8	Truncated spectral reflectance curve	25
Figure 2.9	Normalized (R/R ₄₁₀) spectral curve	26
Figure 2.10	Inverse (1/R) spectral curve	27
Figure 2.11	Log of a reflectance curve	28
Figure 2.12	Norris 1 st derivative reflectance curve	29
Figure 2.13	S. Golay 1 st derivative reflectance curve	30
Figure 2.14	Norris 1 st derivative reflectance curve with five adjacent bands averaged together	30
Figure 2.15	Norris 1 st derivative reflectance curve with ten adjacent bands averaged together	31
Figure 2.16	S. Golay 2 nd derivative reflectance curve	32
Figure 2.17	Multiplicative scatter correction (MSC) curve	33
Figure 2.18	Absorbance curve	34
Figure 2.19	Kubelka-Munk absorbance curve	35
Figure 2.20	Frequency distribution of NH ₃ concentrations	36

Figure 2.21	Distribution of Log (NH ₃)	37
Figure 2.22	Distribution of the square root (NH ₃)	38
Figure 2.23	Distribution of the arcsine of the square root (NH ₃)	39
Figure 2.24	Distribution of the fourth root (NH ₃)	40
Figure 3.1.1	Ammonia over time according to N treatments	43
Figure 3.1.2	Predicted ammonia levels according to N treatments	44
Figure 3.1.3	Nitrate over time according to N treatments	45
Figure 3.1.4	Total phosphorus over time according to N treatments	46
Figure 3.1.5	Total nitrogen over time according to N treatments	46
Figure 3.1.6	Ammonia, nitrate, and total phosphorus concentrations in 2005 according to N treatments	47
Figure 3.1.7	Log ammonia at the <i>Phragmites</i> -dominant site for each sample date according to nitrogen treatment	53
Figure 3.1.8	Log ammonia at the <i>Phragmites</i> -absent site for each sample date according to nitrogen treatment	54
Figure 3.1.9	Nitrate at the <i>Phragmites</i> -dominant site for each sample date according to nitrogen treatment	57
Figure 3.1.10	Nitrate at the <i>Phragmites</i> -absent site for each sample date according to nitrogen treatment	58
Figure 3.1.11	Log nitrogen at the <i>Phragmites</i> -dominant site for each sample date according to nitrogen treatment	63
Figure 3.1.12	Log nitrogen at the <i>Phragmites</i> -absent site for each sample date according to nitrogen treatment	64
Figure 3.2.1	Mean percent cover of all species at the <i>Phragmites</i> -dominant site in June, July, August and September, 2004	69
Figure 3.2.2	Mean percent cover of all species at the <i>Phragmites</i> -absent site in June, July, August and September, 2004	72

Figure 3.2.3	<i>P. australis</i> over time at the <i>Phragmites</i> -dominant and <i>Phragmites</i> -absent sites	74
Figure 3.2.4	<i>P. australis</i> at the <i>Phragmites</i> -dominant site for each sample date according to nitrogen treatment	76
Figure 3.2.5	<i>A. calamus</i> over time at the <i>Phragmites</i> -dominant and <i>Phragmites</i> -absent sites	77
Figure 3.2.6	<i>A. calamus</i> cover at the <i>Phragmites</i> -dominant site for each sample date according to nitrogen treatment	80
Figure 3.2.7	<i>P. arifolium</i> over time at the <i>Phragmites</i> -dominant and <i>Phragmites</i> -absent sites	81
Figure 3.2.8	<i>P. arifolium</i> cover at the <i>Phragmites</i> -dominant site for each sample date according to nitrogen treatment	85
Figure 3.2.9	<i>P. arifolium</i> cover at the <i>Phragmites</i> -absent site for each sample date according to nitrogen treatment	87
Figure 3.2.10	<i>P. virginica</i> over time at the <i>Phragmites</i> -dominant and <i>Phragmites</i> -absent sites	88
Figure 3.2.11	<i>P. virginica</i> cover at the <i>Phragmites</i> -dominant site for each sample date according to nitrogen treatment	91
Figure 3.2.12	<i>P. virginica</i> cover at the <i>Phragmites</i> -absent site for each sample date according to nitrogen treatment	92
Figure 3.2.13	<i>P. virginica</i> cover according to nitrogen treatment for each sample date in 2005 at both sites	93
Figure 3.2.14	<i>Typha</i> species over time at the <i>Phragmites</i> -dominant and <i>Phragmites</i> -absent sites	95
Figure 3.2.15	<i>Typha</i> species cover at the <i>Phragmites</i> -absent site for each sample date according to nitrogen treatment	99
Figure 3.2.16	<i>I. capensis</i> over time at the <i>Phragmites</i> -dominant and <i>Phragmites</i> -absent sites	100
Figure 3.2.17	<i>I. capensis</i> cover at the <i>Phragmites</i> -dominant site for each sample date according to nitrogen treatment	104

Figure 3.2.18	<i>I. capensis</i> cover at the <i>Phragmites</i> -absent site for each sample date according to nitrogen treatment	106
Figure 3.2.19	LAI over time at the <i>Phragmites</i> -dominant and <i>Phragmites</i> -absent sites	107
Figure 3.2.20	LAI at the <i>Phragmites</i> -dominant site for each sample date according to nitrogen treatment	111
Figure 3.2.21	LAI at the <i>Phragmites</i> -absent site for each sample date according to nitrogen treatment	113
Figure 3.2.22	Species richness over time at the <i>Phragmites</i> -dominant and <i>Phragmites</i> -absent sites	114
Figure 3.2.23	Species richness at the <i>Phragmites</i> -dominant site for each sample date according to nitrogen treatment	118
Figure 3.2.24	Species richness at the <i>Phragmites</i> -absent site for each sample date according to nitrogen treatment	120
Figure 3.2.25	Dead material over time at the <i>Phragmites</i> -dominant and <i>Phragmites</i> -absent sites	121
Figure 3.2.26	Dead material at the <i>Phragmites</i> -dominant site for each sample date according to nitrogen treatment	125
Figure 3.2.27	Dead material at the <i>Phragmites</i> -absent site for each sample date according to nitrogen treatment	127
Figure 3.2.28	Shannon-Wiener diversity over time at the <i>Phragmites</i> -dominant and <i>Phragmites</i> -absent sites	128
Figure 3.2.29	Diversity index at the <i>Phragmites</i> -dominant site for each sample date according to nitrogen treatment	132
Figure 3.2.30	Diversity index at the <i>Phragmites</i> -absent site for each sample date according to nitrogen treatment	134
Figure 3.2.31	Biomass at the <i>Phragmites</i> -absent site according to nitrogen treatment on 8/02/05	135
Figure 3.2.32	Biomass at the <i>Phragmites</i> -dominant site according to nitrogen treatment on 8/02/05	135
Figure 3.2.33	Biomass and LAI linear regression	136

Figure 3.2.34	Biomass and Shannon diversity index linear regression	137
Figure 3.2.35	Biomass and species richness linear regression	137
Figure 3.2.36	Canopy nitrogen at the <i>Phragmites</i> -absent site according to nitrogen treatment on 8/02/05	138
Figure 3.2.37	Canopy nitrogen at the <i>Phragmites</i> -dominant site according to nitrogen treatment on 8/02/05	139
Figure 3.2.38	Canopy phosphorus at the <i>Phragmites</i> -absent site according to nitrogen treatment on 8/02/05	139
Figure 3.2.39	Canopy phosphorus at the <i>Phragmites</i> -dominant site according to nitrogen treatment on 8/02/05	140
Figure 3.2.40	Biomass and canopy nitrogen linear regression	141
Figure 3.2.41	Biomass and canopy phosphorus linear regression	142
Figure 3.2.42	Canopy nitrogen and phosphorus linear regression	142
Figure 3.2.43	Canopy nitrogen and sub-surface ammonia linear regression	143
Figure 3.2.44	Canopy phosphorus and sub-surface phosphorus linear regression	143
Figure 3.3.1	Hyperspectral reflectance of the two marsh sites in late May, mid-July, and late-September for unfertilized plots	144
Figure 3.3.2	Reflectance of unfertilized plots for combined marsh sites for blue, green, red near-infrared wavebands	145
Figure 3.3.3	Reflectance of highly fertilized plots for combined marsh sites for blue, green, red, and near-infrared wavebands	146
Figure 3.3.4	R_{493}/R_{678} at the <i>Phragmites</i> -dominant site for each date according to nitrogen treatment	148
Figure 3.3.5	R_{493}/R_{678} at the <i>Phragmites</i> -absent site for each date according to nitrogen treatment	149
Figure 3.3.6	R_{415}/R_{710} at the <i>Phragmites</i> -dominant site for each date according to nitrogen treatment	150

Figure 3.3.7	R_{415}/R_{710} at the <i>Phragmites</i> -absent site for each date according to nitrogen treatment	151
Figure 3.3.8	R_{564}/R_{768} at the <i>Phragmites</i> -dominant site for each date according to nitrogen treatment	152
Figure 3.3.9	R_{564}/R_{768} at the <i>Phragmites</i> -absent site for each date according to nitrogen treatment	153
Figure 3.3.10	PRI at the <i>Phragmites</i> -dominant site for each date according to nitrogen treatment	155
Figure 3.3.11	PRI at the <i>Phragmites</i> -absent site for each date according to nitrogen treatment	156
Figure 3.3.12	NDVI at the <i>Phragmites</i> -dominant site for each date according to nitrogen treatment	157
Figure 3.3.13	NDVI at the <i>Phragmites</i> -absent site for each date according to nitrogen treatment	158
Figure 3.3.14	Mean reflectance of each marsh site prior to nitrogen fertilization (5/25/04)	159
Figure 3.3.15	Significance of interaction effect on spectral bands between nitrogen treatment and site for all dates	161
Figure 3.3.16	Significance of N main effect on spectral bands for all dates	162
Figure 3.3.17	Significance of site main effect on spectral bands for all dates	163
Figure 3.3.18	Significance of nitrogen treatment main effect on spectral bands for individual sites	165
Figure 3.3.19	Significance of nitrogen treatment main effect on the 2 nd derivative of canopy reflectance for individual sites	168
Figure 3.3.20	Significant spectral bands for the 2 nd derivative of reflectance	169
Figure 3.4.1	Predicted vs measured ammonia PLS-regression for the two marsh sites using untransformed reflectance (9/21/04)	174
Figure 3.4.2	Predicted vs measured ammonia PLS-regression for the <i>Phragmites</i> -absent site (9/21/04)	178

Figure 3.4.3	Predicted vs measured log (NH ₃) PLS-regression using the 1 st derivative reflectance for the <i>Phragmites</i> -absent site	179
Figure 3.4.4	Predicted vs measured ammonia PLS-regression at the <i>Phragmites</i> -dominant site (8/02/05)	184
Figure 3.4.5	(a) Significant spectral bands for ammonia according to PLS-regressions at the two marsh sites, (b) Spectral bands significant for ten or more ammonia regressions at the two marsh sites	185
Figure 3.4.6	(a) Significant spectral bands for ammonia according to PLS-regressions at the <i>Phragmites</i> -absent site (b) Spectral bands significant for ten or more ammonia regressions at the <i>Phragmites</i> -absent site	187
Figure 3.4.7	(a) Significant spectral bands for ammonia according to PLS-regressions at the <i>Phragmites</i> -dominant site (b) Spectral bands significant for ten or more ammonia regressions at the <i>Phragmites</i> -dominant site	189
Figure 3.4.8	Predicted vs measured nitrate PLS-regression for combined sites using untransformed 8/02/05 data	191
Figure 3.4.9	Predicted vs measured nitrate PLS-regression at the <i>Phragmites</i> -dominant site	195
Figure 3.4.10	Predicted vs measured nitrate PLS-regression at the <i>Phragmites</i> -dominant site using the 1 st derivative of the 9/21/04 spectra	197
Figure 3.4.11	Predicted vs measured log of nitrate PLS-regression at the <i>Phragmites</i> -absent site which used the 1 st derivative of the 9/21/04 reflectance	204
Figure 3.4.12	Predicted vs measured nitrate PLS-regression of the <i>Phragmites</i> -absent site which used the inverse reflectance from 8/24/04	205
Figure 3.4.13	(a) Significant spectral bands for nitrate according to PLS-regressions at the two marsh sites (b) Spectral bands significant for ten or more nitrate regressions at the two marsh sites	207

Figure 3.4.14	(a) Significant spectral bands for nitrate according to PLS-regressions at the <i>Phragmites</i> -dominant site (b) Spectral bands significant for ten or more regressions for nitrate at the <i>Phragmites</i> -dominant site	209
Figure 3.4.15	(a) Significant spectral bands for nitrate according to PLS-regressions at the <i>Phragmites</i> -absent site (b) Spectral bands significant for ten or more regressions for nitrate at the <i>Phragmites</i> -absent site	211
Figure 3.4.16	Predicted vs measured log of total nitrogen PLS-regression at the <i>Phragmites</i> -dominant site which used the 1 st derivative of the 6/29/04 reflectance	216
Figure 3.4.17	Predicted vs measured total nitrogen PLS-regression at the <i>Phragmites</i> -absent site which used the 2 nd derivative of the 8/24/04 reflectance	220
Figure 3.4.18	(a) Significant spectral bands for total nitrogen according to PLS-regressions at the <i>Phragmites</i> -dominant site (b) Spectral band significant for ten or more regression for total nitrogen at the <i>Phragmites</i> -dominant site	222
Figure 3.4.19	(a) Significant spectral bands for total nitrogen according to PLS-regressions at the <i>Phragmites</i> -absent site (b) Spectral bands significant for ten or more regressions for total nitrogen at the <i>Phragmites</i> -absent site	224
Figure 3.4.20	Predicted vs measured log of total phosphorus PLS-regression at the <i>Phragmites</i> -dominant site which used the 1 st derivative of the 9/21/04 reflectance	229
Figure 3.4.21	Predicted vs measured total phosphorus PLS-regression at the <i>Phragmites</i> -dominant site which used the 1 st derivative of the 9/21/04 reflectance	230
Figure 3.4.22	Predicted vs measured total phosphorus PLS-regression at the <i>Phragmites</i> -absent site which used untransformed spectra from 7/19/04	234
Figure 3.4.23	(a) Significant spectral bands for total phosphorus according to PLS-regressions at the <i>Phragmites</i> -dominant site (b) Spectral bands significant for ten or more regressions for total phosphorus at the <i>Phragmites</i> -dominant site	236

Figure 3.4.24	(a) Significant spectral bands for total phosphorus according to PLS-regressions at the <i>Phragmites</i> -absent site (b) Spectral bands significant for ten or more regressions for total phosphorus at the <i>Phragmites</i> -absent site	238
Figure 3.4.25	PLS regression coefficients for canopy N of the plot and relative to total biomass	241
Figure 3.4.26	PLS regression coefficients for canopy N, canopy P, biomass, and several transformations	242
Figure 3.4.27	Mean species cover for the five most common species present at the <i>Phragmites</i> -dominant site	246
Figure 3.4.28	Mean species cover for the four most common species present at the <i>Phragmites</i> -absent site	247
Figure 3.4.27	Significant spectral bands used for the best PLS models at the <i>Phragmites</i> -dominant site	244
Figure 3.4.28	Significant spectral bands used for the best PLS models at the <i>Phragmites</i> -absent site	245
Figure 3.4.29	PLS regression coefficients for <i>P. australis</i> cover	248
Figure 3.4.30	PLS regression coefficients for <i>A. calamus</i> cover	249
Figure 3.4.31	PLS regression coefficients for <i>P. arifolium</i> cover	250
Figure 3.4.32	PLS regression coefficients for <i>P. virginica</i> cover	251
Figure 3.4.33	PLS regression coefficients for <i>Typha</i> species cover	252
Figure 3.4.34	PLS regression coefficients for <i>I. capensis</i> cover	253
Figure 3.4.35	PLS regression coefficients for dead material	254
Figure 3.4.36	PLS regression coefficients for exposed soil	255

Chapter 1: Introduction

1.1 Problem definition

Tidal freshwater wetlands are unique ecosystems, important to the world for a variety of reasons. They are used for recreational purposes, commercial fisheries, and are rich in biodiversity. For example, more bird species inhabit tidal freshwater marshes than any other type of marsh (Mitsch and Gosselink 2000). Functional values of wetlands include stabilizing the water supply throughout floods and droughts, protecting the shorelines, recharging the groundwater, and cleansing polluted waters (Mitsch and Gosselink 2000). Wetlands behave as a filter between land and water bodies (Zhang et al., 1997), removing sediments, nutrients, and organic pollutants from the water source, thereby improving the quality of the water before it reaches the water body (Krieger 2003; Poe et al., 2003).

Unfortunately, coastal marshes are one of the ecosystems often subject to continual exploitation, modification, and destruction (Zhang et al., 1997; Rosso et al., 2005). Tidal freshwater marshes, due to their inland coastal position, are at a high risk to be affected by human interactions, such as soil erosion from construction sites and croplands, discharge from waste treatment plants, and agricultural runoff (Kahn and Kemp 1985; Mitsch and Gosselink 2000). Nutrient non-point source pollution from agricultural runoff is an especially large, well-known problem. Agricultural crops use only 40-60% of their applied nitrogen fertilizer (Poe et al., 2003), allowing large

amounts of nitrogen to enter bodies of water, especially wetlands since they are usually located on the border between land and either lakes or rivers.

Over the last few years, the awareness of the importance of wetlands has increased and laws and regulations have been established to protect and restore wetlands (Mitsch and Gosselink 2000). Under the Clean Water Act, states must monitor wetlands regularly to ensure the water quality standards are met (USEPA 2002). Currently, the methods used to monitor nutrients in a wetland are labor-intensive and time-consuming (Rosso et al., 2005). An alternative method, therefore, such as remote sensing, is needed that can quickly and accurately quantify nitrogen and other nutrients in large areas of wetlands to detect ecosystem stressors, predict habitat changes, and monitor invasive species (Tiner 2004; Maheu-Giroux et al., 2005; Rosso et al., 2005; Salem et al., 2005).

1.2 Literature Review

Marsh response to nitrogen

Nitrogen from agricultural runoff, wastewater treatment facilities, and other sources is known to cause eutrophication in open-water aquatic systems, stimulating algal blooms and causing a loss of submerged aquatic vegetation, a decrease in fish populations, and a decline in biodiversity (Mitsch and Gosselink 1993; Rabalais 2002). Fortunately, wetlands are capable of filtering nitrogen from water sources and releasing it as nitrogen gas through denitrification before nitrogen reaches open aquatic systems (Buscot and Varma 2005; Philippot and Germon 2005).

As nitrogen enters the wetland as urea, $(\text{NH}_2)_2\text{CO}$, it is rapidly transformed to ammonia and carbon dioxide with the catalyst enzyme, urease (Payne 1981; Thoren et al., 2004). While carbon dioxide is released to the atmosphere, ammonia is converted by autotrophic microorganisms, such as *Nitrosomonas* and *Nitrobacter*, to nitrate through nitrification. Nitrate, a soluble compound, can be taken up by plants, but can also be easily leached out of the soil and pollute nearby water bodies, unless wetlands perform denitrification, a four-step anaerobic process controlled by microorganisms, which changes nitrate into dinitrogen gas (Philippot and Germon 2005).

Remote sensing in marshes

At the Earth's surface, solar energy is reflected, absorbed, or transmitted from all materials (Larcher 2003). The ratio of reflected energy to the total energy as a function of wavelength is called hyperspectral reflectance and can be measured with a spectroradiometer, which reports the spectral reflectance in hundreds of narrow (1 to 10 nm) and contiguous wavelength bands (Shippert 2004).

Hyperspectral reflectance, as well as other remote sensing techniques, can be used to extract biophysical information about a vegetation canopy from the interaction between solar irradiance and the canopy (Hurcom et al., 1996). In plants, chlorophyll and other leaf pigments are responsible for leaf energy absorption and reflection; low concentrations of chlorophyll result in less energy absorption and

more reflectance. Since chlorophyll concentrations are affected by nutrients, like nitrogen and phosphorus, hyperspectral reflectance can be used to indirectly quantify the availability of nutrients.

Some of the earliest work to quantify nitrogen concentrations in marshes through remote sensing was established by Tilley et al. (2003), where relationships between water column ammonia and reflectance indices were discovered. In 2005, Becker et al. discovered a correlation between eight hyperspectral bands and vegetation characteristics within freshwater marshes and Phillips et al. (2005) found spectral differences between vegetation communities in freshwater marshes using GIS remote sensing. Analysis for both vegetation studies was performed on vegetation data collected in August and early September, during peak biomass (Becker et al., 2005; Phillips et al., 2005). Vegetation changes in a coastal saltwater marsh were successfully mapped using digital airborne remote sensing (Thomson et al., 2004), as were *P. australis* communities in linear wetland corridors using color aerial photography imaging (Maheu-Giroux et al., 2005). The US Fish and Wildlife Service have also used remote sensing techniques to monitor wetland trends (Tiner 2004).

Besides nutrient and vegetation trends, remote sensing has also been proven to detect environmental stressors in wetlands. Oil spills in freshwater wetlands were identified using hyperspectral imagery (Salem et al., 2005), and significant differences between treatments of heavy metals and oil were found in wetland plants using hyperspectral reflectance (Rosso et al., 2005). The alterations in the plant's biochemistry and

cellular composition from environmental stressors produce measurable changes in reflectance (Rosso et al., 2005). For example, plants exposed to heavy metals exhibited a darker canopy and therefore a lower reflectance, than healthy plants (Schuerger et al., 2003; Wilson et al., 2004).

Other applications involving hyperspectral reflectance measurements include classifying the trophic status of lakes (Koponen et al., 2002), determining coral reef community structures (Hochberg et al., 2003), evaluating nitrogen concentrations in the wetland crop, rice (Xue et al., 2004), assessing wetland plant stress due to flooding (Anderson and Perry 1996), and correlating leaf nitrogen concentration to canopy hyperspectral reflectance in a forest (Smith et al., 2003; Townsend et al., 2003). Hyperspectral reflectance has also correctly identified moss species in Antarctica (Lovelock and Robinson 2002) and salt-water vegetation species in coastal wetlands (Silvestri et al., 2003).

Several studies relating hyperspectral reflectance to the identification of species at the canopy level have been performed on agricultural crops to investigate and improve the area of precision agriculture. Studies have shown high accuracy (up to 80%) in distinguishing soybean crops from weeds, such as the cocklebur (*Xanthium strumarium*) (Henry et al., 2004), sicklepod (*Cassia obtusifolia*) (Chang et al., 2004), and morningglory (*Ipomoea lacunosa*) (Koger et al., 2004).

Partial Least Squares Regression

In order to correlate biological responses to reflectance data, partial least squares (PLS) regression has been used to develop predictive models of biological responses using full-spectrum data. PLS regression is an eigenvector analysis that reduces the full-spectrum data (independent matrix, X) to a smaller set of independent latent factors (i.e., PLS-components) with the dependent variable (biological responses) used directly during the spectral decomposition process. PLS uses the factors to predict responses in a population (Esbensen 2002; Smith et al., 2002).

Two data sets, called the training set and test set, are used to compute the model parameters in a PLS regression. The training set establishes the multivariate model for (X,Y) then predicts the Y matrix from the X as previously described. The test set is a new set of data that is used to test the model under realistic conditions in a process called test set validation. Since two data sets cannot always be obtained for validation purposes, another validation method, called cross-validation, can also be used (Petisco et al., 2005). In cross validation each biological response and spectra are iteratively excluded and a prediction of the sample value is made based on an equation developed with the remaining samples. The process is repeated until every sample has been left out once. The prediction residuals are combined to compute the validation equation statistics and RMSEP (Smith et al., 2003).

Martens uncertainty test eliminates useless predictors in a multivariate calibration.

The test is based on the standard deviation of regression coefficients computed from values in the cross validation process. If the regression coefficient contains the value zero at the 95% confidence interval, it is eliminated from the model (Forina et al., 2004).

PLS and hyperspectral reflectance

PLS has become a useful method of analyzing spectral information. Petisco et al. (2005) and Smith et al. (2002) used PLS to develop predictive models of leaf nitrogen concentrations from near-infrared spectroscopy (NIRS) and hyperspectral remote sensing. A PLS regression model has predicted the LAI, chlorophyll and leaf nitrogen concentrations from reflectance data (Filella et al., 1995; Casa and Jones 2003; Zhang et al., 2003, Fridgen and Varco 2004). PLS has also been used to successfully predict and interpret heavy metal stress in wetland plants (Wilson et al., 2004), nitrogen concentrations in wheat (Hansen and Schjoerring 2003), and species composition and structure in grasslands (Schmidtlein and Sassin 2004).

Reflectance indices

Researchers have often used individual reflectance bands, ratios, or indices to relate hyperspectral data to biological and ecological properties. One of the most common reflectance bands used for analysis is the red edge (RE), defined as the wavelength of maximum slope at the red-NIR transition. The RE increases with higher chlorophyll content and is therefore generally responsive to changes in nitrogen and other nutrient

levels (Smith et al., 2003). To reduce data noise, a sensitive waveband is normalized by a non-sensitive waveband to form a ratio, such as a blue to red reflectance ratio (R_{415}/R_{710}). Other popular ratios for data analysis include the blue to red ratio (R_{493}/R_{678}), and the green to red ratio (R_{564}/R_{768}). Reflectance indices, or combinations of reflectance bands, used to relate spectral data to biological and ecological properties include the normalized difference vegetation index ($NDVI = (R_{nir} - R_{red}) / (R_{nir} + R_{red})$) and photochemical reflectance index ($PRI = (R_{531} - R_{570}) / (R_{531} + R_{570})$).

Spectral indices like the NDVI can accurately predict LAI of crops with a coefficient of determination as high as 0.95 (Hansen and Schjoerring 2003; Haboudane et al., 2004). Other agricultural crop studies have correlated LAI to a specific wavelength, such as green, R_{560} , or a simple ratio of spectral bands like R_{810}/R_{560} (Xue et al., 2004).

Simple reflectance ratios have also been used to link reflectance measurements to nutrient concentrations. Tilley et al. (2003) showed that a reflectance ratio (R_{493}/R_{678}) explained 54% of ammonia concentrations in wetland water columns. A blue to red ratio (R_{415}/R_{710}) used by Read et al. (2002) strongly indicated leaf nitrogen in cotton (*Gossypium hirsutum*), and ratios of the near-infrared (NIR) to the visible (VIS) linked canopy nitrogen to fertilization rate in corn (*Zea mays*) (Diker and Bausch 2003). Other reflectance indicators of nitrogen include a higher reflectance curve in the NIR for fertilized plants (Tilley et al., 2004; Xue et al., 2004), and a correlation

between nitrogen and NDVI (Li et al., 2001, Bronson et al., 2005). The PRI and red-edge were both able to detect nitrogen ammonia levels in plants in research conducted by Strachan et al. (2002) and Tilley et al. (2003). Others, including Carter and Miller (1994), Tarpley et al. (2000), and Fridgen and Varco (2004) have used the RE as an indicator of chlorophyll in the plant, which is indirectly related to canopy nitrogen concentrations.

LandSat ETM+

The Landsat program is a series of optical and infrared remote sensing satellites used for land observation. The Landsat ETM+ (Enhanced Thematic Mapper Plus) provides high-resolution image information on the Earth's surface through an eight-band multispectral radiometer. The four wavebands referred to in this project are the blue (450-520 nm), green (520-600 nm), red (630-690 nm), and near-infrared (760-900 nm) (USGS 2004).

1.3 Objectives

The objectives of this study were to:

1. Determine the effects of applying nitrogen as urea on sub-surface marsh nitrogen and phosphorus levels.
2. Determine whether nitrogen fertilization affected the vegetation composition and concentration of the canopy nitrogen and phosphorus of a tidal freshwater marsh.
3. Determine whether nitrogen fertilization or vegetation composition affected canopy reflectance of a tidal freshwater marsh.

4. Develop spectroradiometric models predictive of sub-surface water nutrient concentrations, vegetation composition, and canopy nitrogen and phosphorus in tidal freshwater marshes using partial least squares (PLS) regression.
5. Identify which spectral bands offer the most information about nutrient availability in tidal freshwater marshes.

1.4 Plan of Study

1. To determine the effects of applying nitrogen on sub-surface nitrogen and phosphorus levels, a field experiment involving two sites of a tidal freshwater marsh and five nitrogen treatment types was conducted. Sub-surface water quality samples were analyzed throughout the 2004-5 marsh growing seasons.
2. To determine if nitrogen affected the vegetation composition and leaf nitrogen and phosphorus in a tidal freshwater marsh, percent cover of vegetation species was measured over the course of the field experiment and vegetation was harvested and analyzed for nitrogen on the last sample date in 2005.
3. To determine whether nitrogen fertilization or vegetation composition affected the canopy reflectance of a tidal freshwater marsh, canopy reflectance was measured with a spectroradiometer over the two growing seasons.
4. Partial least squares regression was used to establish models predictive of sub-surface water nutrient concentrations, vegetation composition, and canopy nitrogen and phosphorus.
5. Significant spectral bands were identified for sub-surface water nutrients in ANOVA's and PLS regression models, then compiled and compared.

Chapter 2: Materials and Methods

2.1 Site Description

Experimental plots were established in a tidal freshwater marsh along the Nanticoke River (lat 38°31'20" N, long 75°45'23" W) on the Eastern Shore of Maryland near Sharptown (Figures 2.1 and 2.2). The climate on the peninsula is humid with an average precipitation of 112 cm (Denver et al., 2001). Land use on the peninsula is mostly agricultural, specifically corn, soybeans, and chicken farms. Wetlands are common in the riparian and coastal zones, inland forests, and depressions (Denver et al., 2001). Land use within the Nanticoke watershed is 43% forested areas, 38% agricultural, 16% wetlands, and 3% urban (MD DNR 1994).

2.2 Experimental Design

The experimental design used in the study was that of a completely randomized design. Two sites were established at the experimental marsh. The two sites shared many characteristics with each other, including an overlap of several vegetative species. One site was primarily dominated by the species *Phragmites australis* (Cav.) Trin ex Steud (henceforth referred to as the *Phragmites*-dominant site), while the other site contained no *P. australis* (the *Phragmites*-absent site). The *Phragmites*-dominant site had a roughly rectangular area of 1500 m² (150 m along the river, 10 m inland), while the *Phragmites*-absent site had a rectangular area of about 4000 m² (100 m along the river, 40 m inland) (Figure 2.3).

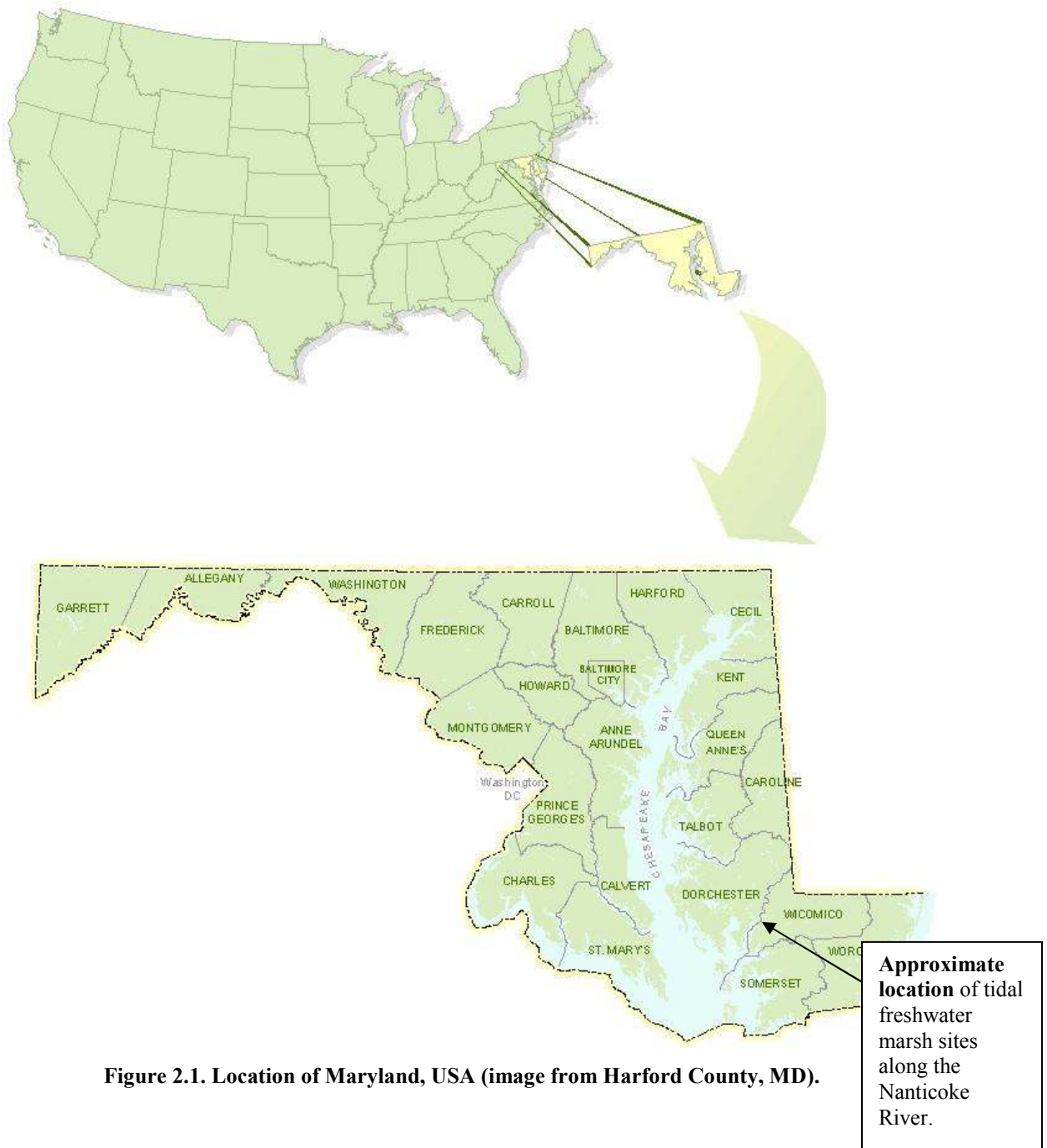
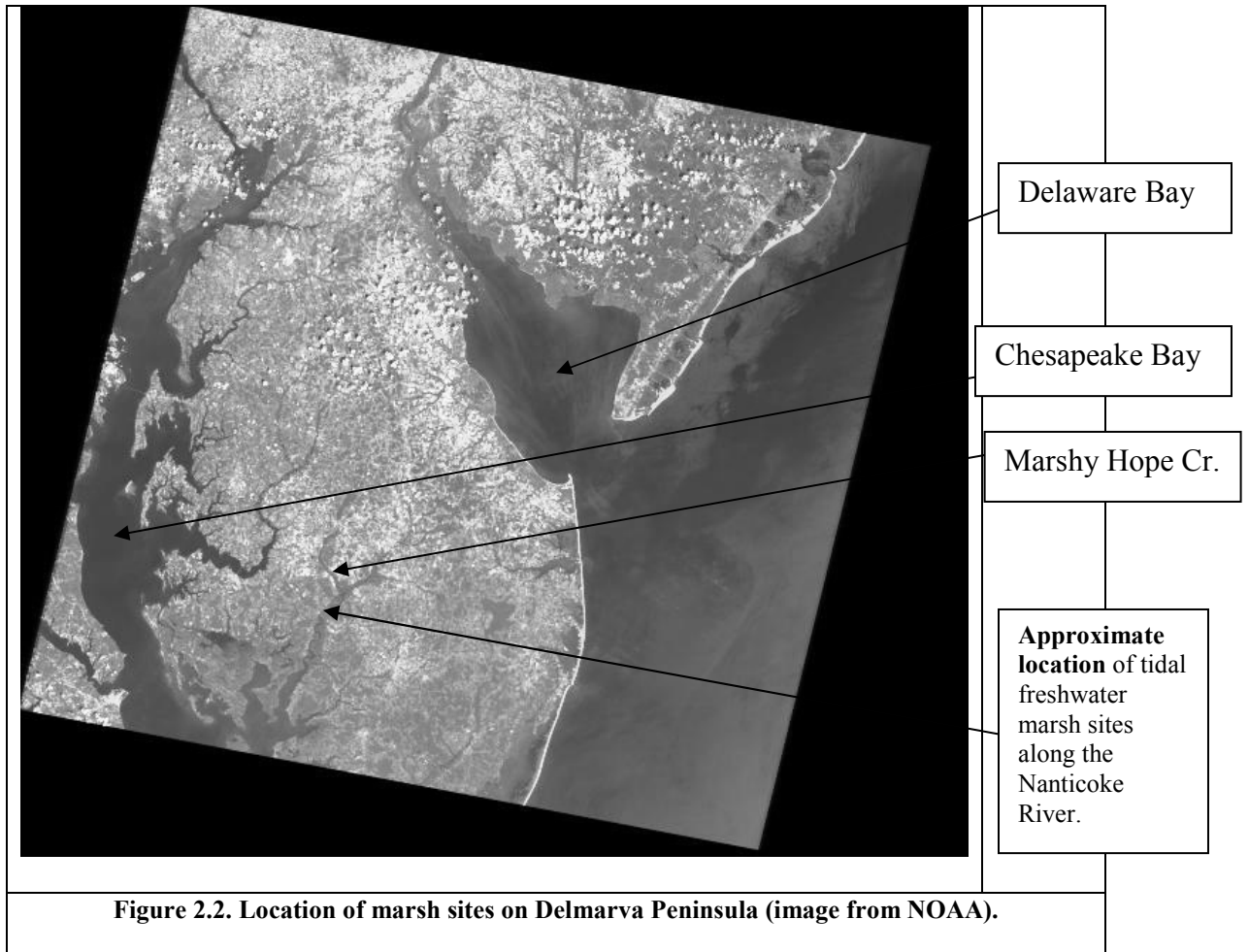


Figure 2.1. Location of Maryland, USA (image from Harford County, MD).



Plots were randomly located within each site based on a developed coordinate system where the x-axis lay parallel to the Nanticoke River and the y-axis cut inland. X-, then y-coordinates were randomly generated to determine the corner of each plot, providing plots were no closer than 10 m, if possible.

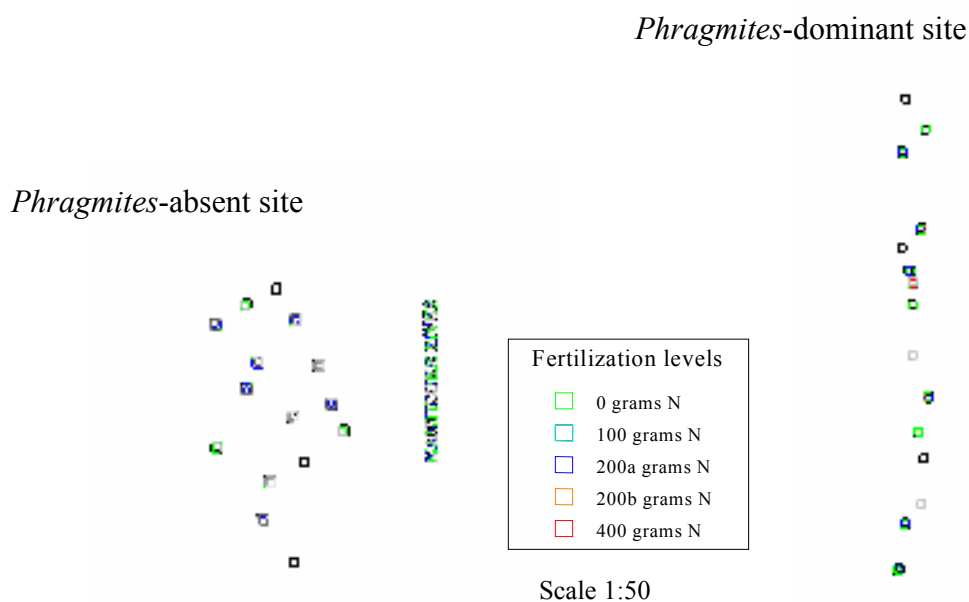


Figure 2.3. Map of the Nanticoke River identifying the location of the two marsh sites and layout of plots according to fertilization treatment.

On June 3, 2004, each plot was randomly chosen to receive one of five treatments of nitrogen as urea (0, 100, 200a, 200b, or 400 g-urea). Four 30 cm deep boreholes (2.5 cm diameter) were drilled into each plot, each equidistant from the plot center to its edge (Figure 2.4). Each borehole received urea either inserted in a micro-porous

dialysis tube (SpectroPor, Spectrum Labs, Rancho Dominguez, CA) or poured directly into the borehole (Feller et al., 1999). The dialysis tubes provided a slow time-release of nitrogen over the growing season, simulating a constant source of nitrogen pollution, while the boreholes created an immediate increase of nitrogen concentration in the soil, simulating a once occurring nitrogen hotspot. Boreholes not receiving urea were filled with inert perlite. The five treatments, summarized in Table 2.1, were a combination of the four urea amounts and the two application methods. Every treatment was replicated three times at each marsh site. Urea was reapplied in an identical manner during the second growing season on June 6, 2005.

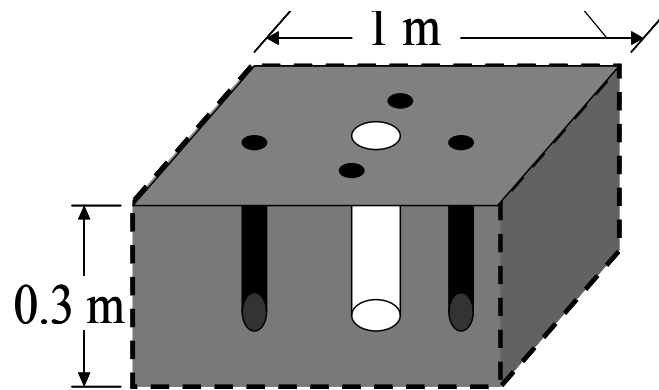


Figure 2.4. Diagram of the lay-out for each 1 m² plot. A lysimeter was installed 30 cm deep in the center of each plot. Four boreholes were drilled, one on each side of the plot halfway between the center and the edge of the plot.

Table 2.1. Definition of nitrogen treatments.

Treatment Code	Number of Urea-filled Dialysis Tubes (D)	Number of Urea-filled Bore Holes	Nitrogen as urea (g-urea)
Ambient	0	0	0
N100	1	0	100
N200/1D	1	1	200
N200/2D	2	0	200
N400	2	2	400

Ceramic-tipped lysimeters (Soil Moisture Inc, CA) were installed in the center of each plot at a depth of 30 cm and covered by a layer of Bentonite to prevent water and air leaks. Two colored polyethylene tubes connected to the lysimeters ran to the edge of the plot for water sample collection. The black tube was used to connect a hand operated pump/vacuum to pressurize and evacuate the lysimeters. The green tube was used to fill sample containers with sub-surface water. The lysimeters were purged of all water before the vacuum was set, and then both tubes were folded closed to hold the vacuum until the sample water was extracted.

2.3 Data Collection

Canopy reflectance, sub-surface water nutrients, percent cover class, and leaf area index (LAI) at all plots were measured biweekly in June 2004 following initial fertilization in late May, then once monthly from July through September 2004. The same measurements were taken for the following year (2005) in early June and early August. Biomass and canopy nutrients were measured at the conclusion of the experiment, in August 2005.

An ASD Handheld SpectroRadiometer (Analytical Spectral Device, Boulder, CO) was used to measure canopy reflectance from 325-1075 nm (750 spectral bands) of each marsh plot. Spectroradiometric measurements were taken in full sunlight between 10 am and 3 pm. The radiometer was attached to a uni-pod fixed at a 20° angle to a long plastic rod that was anchored into the ground approximately 1.5 m away from the middle of the north side of each plot (Figure 2.5). The radiometer's

25° field-of-view bare-optic sensor pointed straight down towards the plot, 3.5 m above the ground surface, such that the entire 1 m² plot was viewed. Percent reflectance was calculated by dividing the canopy reflectance readings by the reflectance of a calibrated Spectralon white panel (Labsphere, Inc., North Sutton, NH), which was held on a long pole directly under the radiometer before plot readings were taken. The spectroradiometer collected ten 76 or 168 millisecond readings of each plot canopy which were later averaged to estimate mean plot reflectance.



Figure 2.5. Canopy reflectance measured at the *Phragmites*-absent site (8/24/04). The radiometer is mounted on the long pole centered over the plot, and is reading the reflectance of the calibrated white panel. The sample plot is marked by the long, thin pole with flagging at one corner and a smaller pole, not visible here, at the opposite corner.

Sub-surface water samples of 250 mL were taken from the 400 mL lysimeter by first purging the lysimeter with the hand pump (Figure 2.6). A vacuum was then set and

left for 6 to 24 hours to allow the lysimeter to draw in sub-surface water. A water sample was pumped from the lysimeter at each plot to a labeled sample bottle and preserved on ice at a pH of 2 until analysis testing was conducted. A full water sample was not always attained at each site; occasionally the lysimeter did not have a sufficient amount of time to pull enough water to fill a sample container.



Figure 2.6. Sub-surface water collected at the *Phragmites*-dominant site (6/16/04). Water was collected 6 to 24 hours after the vacuum was set on the lysimeter.

Water samples were analyzed using the Hach DR/2010 Spectrophotometer (Hach Company, Loveland, CO) for ammonia, nitrate, total phosphorus, and total nitrogen. Method #8038 for ammonia mixed Mineral Stabilizer, Polyvinyl Alcohol dispersing Agent, and Nessler Reagent to each water sample and measured ammonia at 425 nm, using deionized water as the blank. Method #8039 used NitraVer 5 Nitrate Reagent Powder to analyze nitrate at 500 nm against the original sample as a blank. Total

phosphorus was analyzed according to Method #8190, which used Potassium Persulfate and heat before the sample was measured at 890 nm. Total nitrogen analysis required Method #8075, which first involved digestion of the sample with the Digesdahl heater (Hach Company, Loveland, CO), and evaluation of nitrogen concentration at 460 nm. For quality control, several ammonia and nitrate concentration solutions were prepared, split in half, and analyzed using Hach DR/2010 Spectrophotometer methods, while the other half was analyzed at Washington Suburban Sanitary Commission (WSSC). WSSC used automated flow injection analysis methods to analyze ammonia using method EPA 350.1 (Lachat 10-107-06-1-A) (Lachat Instruments, Milwaukee, WI) and nitrate with EPA 353.2 (Lachat 10-107-04-1-A) (Lachat Instruments, Milwaukee, WI). Both the Hach DR/2010 and WSSC analyses yielded similar ammonia and nitrate concentrations.

The surface cover of vegetation, dead material (i.e., brown, senescent), surface water, exposed soil, and bentonite/perlite (installed with the lysimeters and N-fertilizations) was quantified for each plot according to a cover class system used by the North Carolina Vegetation Survey (Peet et al., 1998). The cover of each plant species found within the one-meter quadrat was recorded and assigned a classification number (Table 2.2) based on its percent cover of the quadrat. The cover class system had higher resolution at the lower end of the scale than at the higher end.

Species richness was determined by summing the number of species observed at each plot, and the diversity index was calculated according to the Shannon-Wiener diversity index (H):

$$H = -\sum (n_i/N) \ln(n_i/N)$$

where n_i is the cover of each species i , and N the total cover of all species.

Table 2.2. Cover Class System (Peet et al., 1998)

Class	Cover Range
1	a trace amount
2	0-1%
3	1-2%
4	2-5%
5	5-10%
6	10-25%
7	25-50%
8	50-75%
9	75-95%
10	95-100%

The leaf area index (LAI) of each plot was measured and recorded with an LAI-2000 Plant Canopy Analyzer (Li-Cor, Lincoln, NE). The optical sensor of the LAI-2000 was held above the canopy for one reading, then within the plot at approximately 10 cm above ground level for two consecutive readings to estimate LAI as the area of foliage per unit area of ground.

Total biomass of each plot was collected on 8/02/05 after other measurements were collected. All standing vegetation in the plot was cut at ground level and bagged for transport. At the lab, biomass at each plot was sorted according to species, dried at 70 °C, and weighed. The dried tissue was ground and sent to the University of Delaware Soil Testing Program for canopy nitrogen and phosphorus analysis. Total

nitrogen and total carbon in the tissue was measured by the combustion technique using an Elementar Vario-Max CN analyzer (Elementar Americas, Inc., Mt. Laurel, NJ). Samples were digested for elemental composition using a CEM MARS-5 microwave digestion system (CEM Corporation, Matthews, NC). Digests were analyzed for P, K, Ca, Mg, Mn, Cu, Zn, Fe, B, S and Al by emission spectroscopy using a Thermo IRIS Intrepid II – XSP Duo View inductively coupled plasma-optical emission spectrometer (Thermo Electron Corp., Madison, WI).

2.4 Data Analysis

Analysis of variance (ANOVA) was conducted to study treatment effects on sub-surface water nutrient concentrations, vegetation composition data, biomass, canopy nitrogen and phosphorus concentrations, and spectral band reflectance and reflectance indices. Reflectance indices examined included three simple reflectance ratios (R_{493}/R_{678} , R_{415}/R_{710} , and R_{564}/R_{768}), the Photochemical Reflectance Index (PRI), and a standard Normalized Difference Vegetation Index (NDVI).

I conducted repeated measures ANOVAs to determine the effect of time, site, treatment, and their interactions on each parameter. Time effects were further investigated with treatment effect at individual sites using repeated measures ANOVA. I also used a univariate general linear model ANOVA at each sample date, with fixed factors as treatment and site, to determine whether nitrogen, site, or their interaction produced significant responses in sub-surface water nutrient concentrations, vegetation cover composition data, biomass, canopy nutrient

concentrations, and reflectance at each narrow spectral band. Comparison of means was examined using the least significant difference (LSD) test in SPSS for Windows (SPSS Inc., Chicago, IL) for each sample date and marsh site. Significant differences were defined at the 0.05 probability level.

Linear regressions were used to determine relationships between reflectance and time, sub-surface water nutrients and canopy nutrients, as well as biomass and LAI, diversity, species richness, and canopy nutrients.

Partial least squares regression was used to develop models of hyperspectral reflectance predictive of sub-surface water nitrogen (in forms of ammonia, nitrate, and total nitrogen) and total phosphorus, as well as cover of vegetation, dead material, exposed soil, LAI, species richness, diversity index, canopy nitrogen and phosphorus, and biomass. All PLS regressions were performed using Unscrambler 9.0 (Camo Process AS, Oslo, Norway).

For validation of the PLS model, both the full-cross method (i.e. leave-one-out) and the test set method were performed. The optimal number of PLS-components (i.e. independent latent factors) included in the final model corresponded to the model with the minimum root mean square error of prediction (RMSEP), which is the square root of the residual mean square that estimates the common within-group standard deviation. The Martens Uncertainty Test within Unscrambler was applied to each

PLS regression to determine significant spectral bands. Bands found to be insignificant were removed and a new model was built with remaining bands.

2.4.1 Reflectance Transformations for ANOVA and PLS Modeling

Several data preprocessing transformations were performed on spectroradiometric data during ANOVA and PLS-regression modeling. Pre-processing transformations used on reflectance data included:

- a truncated reflectance curve,
- normalized reflectance,
- inverse reflectance,
- log of the reflectance,
- Norris method first derivative of the reflectance,
- Golay method first derivative of the reflectance
- Golay method second derivative of the reflectance,
- multiplicative scatter correction (MSC),
- absorbance transformation, and
- Kubelka-Munk transformation.

All transformations were performed on all data so comparisons could be made between transformations.

An example of a typical untransformed reflectance curve for the tidal freshwater marsh is shown in Figure 2.7. Examples of each transformation are based on their typical reflectance curve.

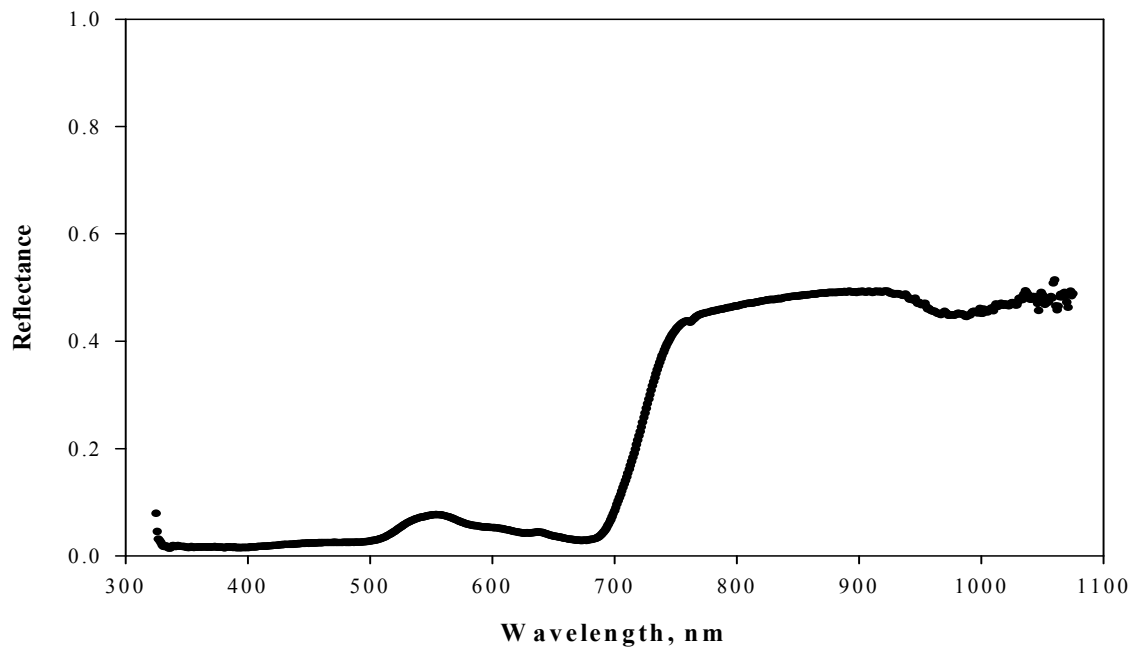


Figure 2.7. A typical untransformed spectral reflectance curve for the tidal freshwater marsh canopy during the middle of the 2004 growing season.

Truncated reflectance curve

The truncated reflectance curve, included only untransformed spectral bands between 400 and 950 nm (Figure 2.8). By using the truncated curve, much of the noise reported by the radiometer at each end of its range was eliminated.

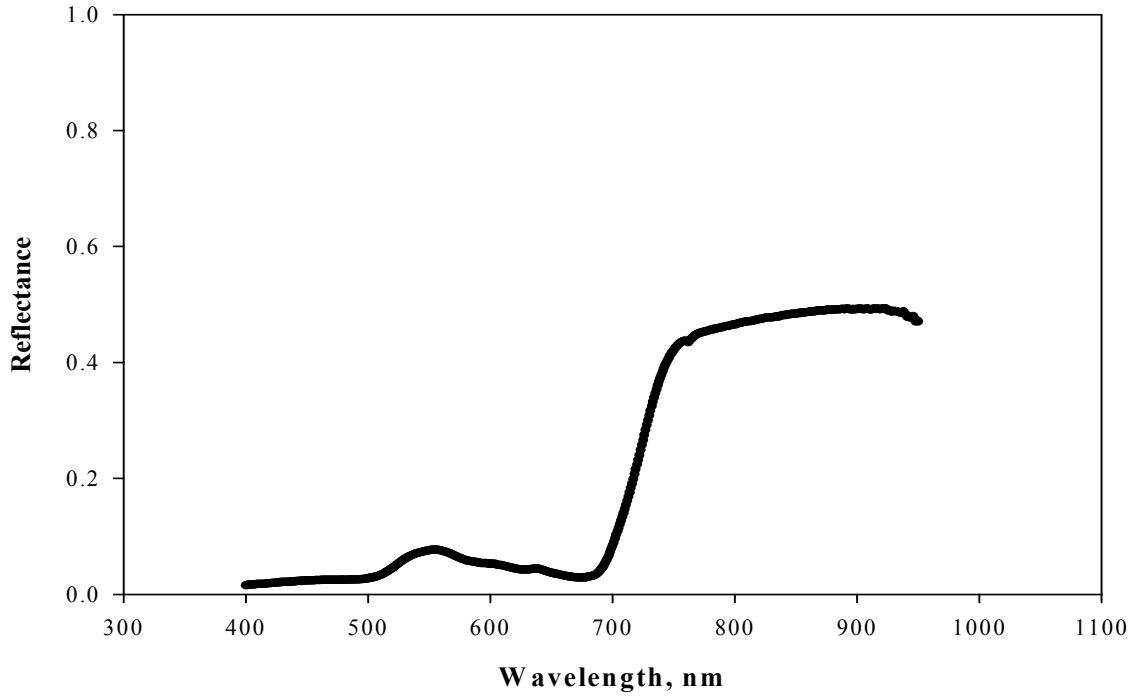


Figure 2.8. A truncated (400-950nm) spectral reflectance curve for the tidal freshwater marsh canopy during the growing season.

Normalized reflectance curve

Normalization of reflectance curves was performed to compensate for small reflectance variations in individual plots (Figure 2.9). To normalize the data, the reflectance at each spectral band was divided by the reflectance at spectral band R_{410} (see equation 1).

$$R_{\text{norm}} = R_{\lambda} / R_{410} \quad \text{Equation 1}$$

R_{410} was chosen as the normalization wavelength because the amount of reflectance at R_{410} had the lowest variance of all spectral bands. The normalized reflectance curve rescaled the original curve, thereby removing variation.

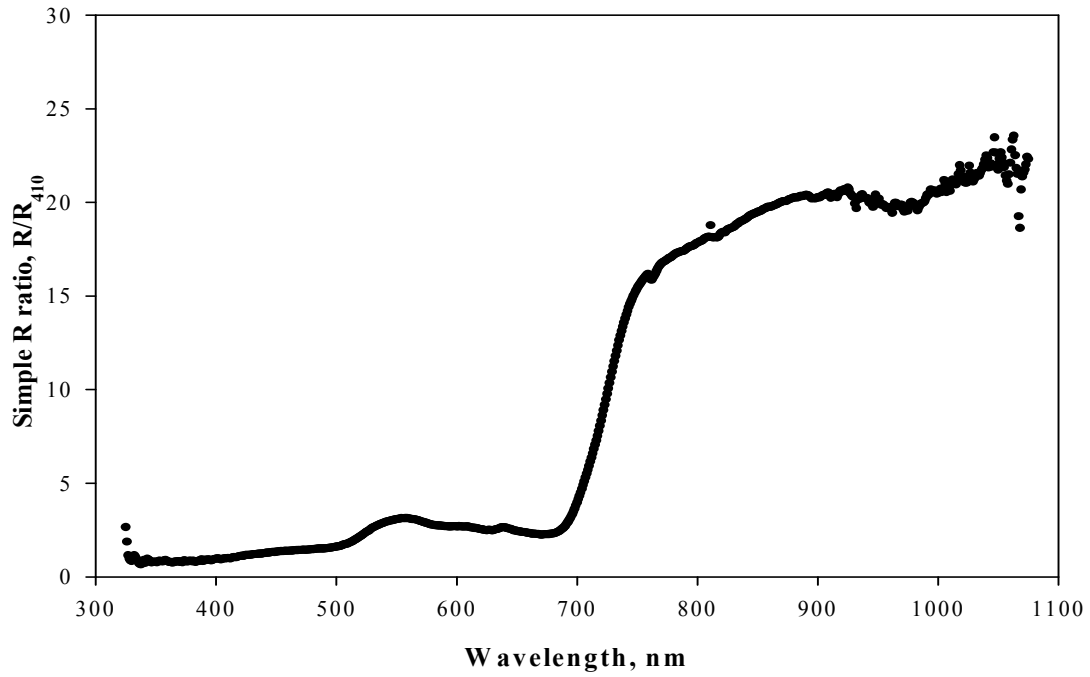


Figure 2.9. Normalized (R/R_{410}) (and not truncated) spectral curve for a tidal freshwater marsh canopy.

Inverse reflectance curve

The inverse of the typical reflectance curve is shown in Figure 2.10 and is characterized by taking one over the reflectance at each spectral band (Equation 2).

$$R_{\text{inv}} = 1/R \quad \text{Equation 2}$$

The inverse transformation is often used in traditional statistics to improve data normality; for spectroradiometric data, it inverts the reflectance curve.

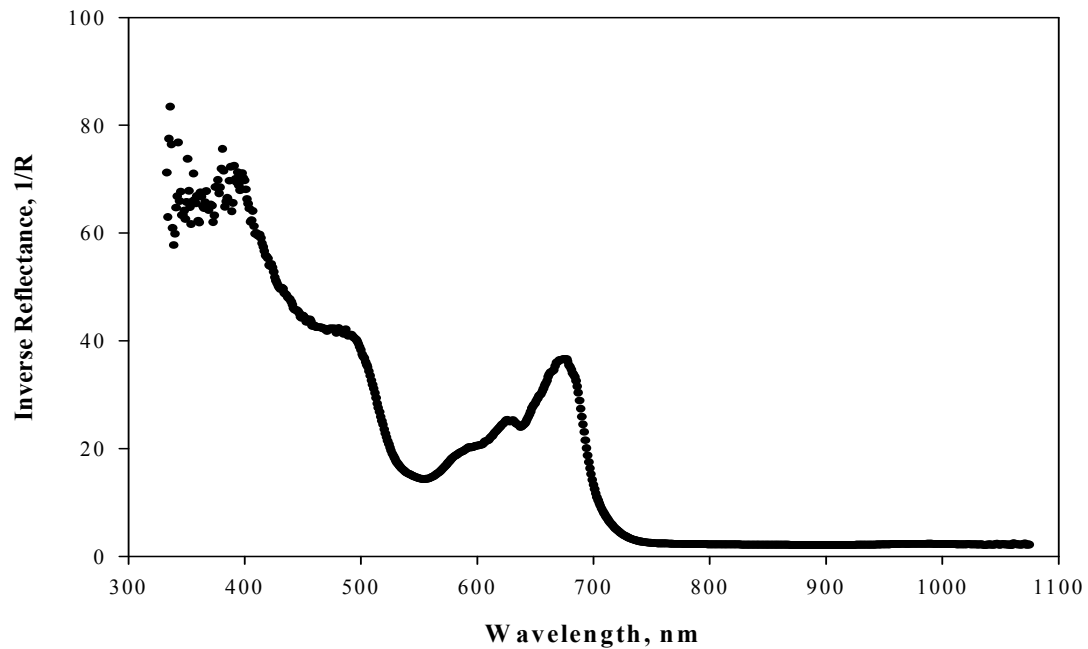


Figure 2.10. An inverse (1/R) spectral curve for a tidal freshwater marsh canopy.

Log reflectance curve

Figure 2.11 shows the log of the reflectance performed for each spectral band's reflectance (Equation 3).

$$\log R = \log_{10} R \quad \text{Equation 3}$$

The log of the reflectance ($\log R$) converted the multiplicative relationship of the reflectance and dependent variable to an additive one in an attempt to improve the linearity of the regression relationship. Multiplicative relationships assume that factors change the dependent variable by multiplication or division, while additive models assume factors change the dependent variable by addition or subtraction and hence give a more linear relationship than multiplicative models. Several researchers have used the log transformation to find relationships between leaf nitrogen and reflectance information (Grossman et al., 1996; Retisco et al., 2005).

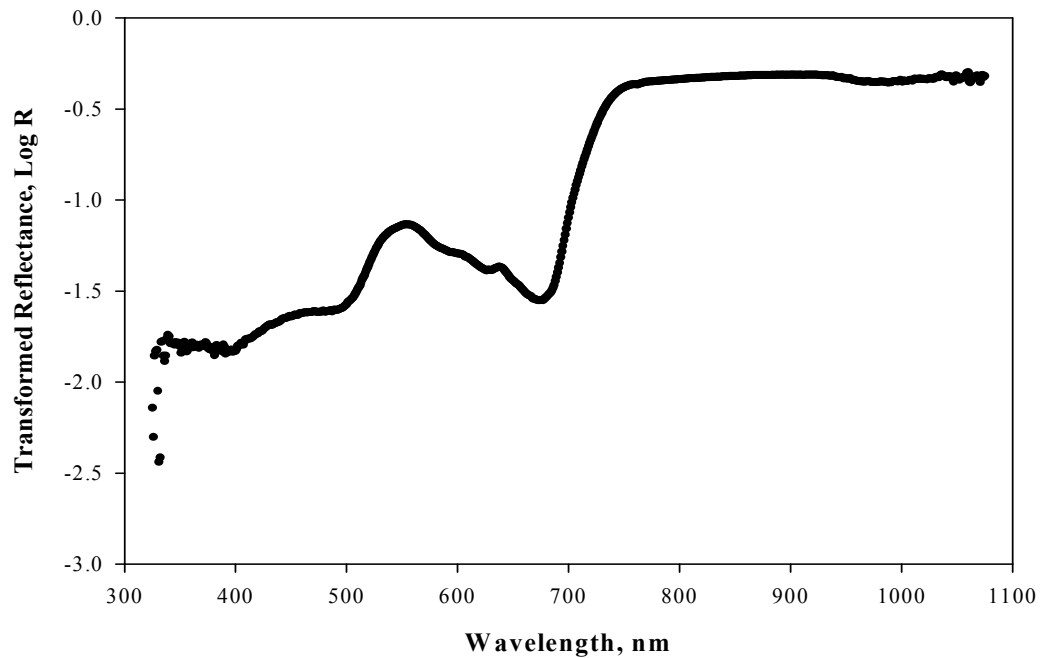


Figure 2.11. The log of a reflectance curve for a tidal freshwater marsh canopy.

First derivative of a reflectance curve

The first derivative of the reflectance curve is a measure of the slope for the spectral curve at every band and results in a spectrum in which peaks and valleys correspond with inflection points in the reflectance spectra (Equation 4). The first derivative typically is used to correct baseline shifts, resolve overlapping spectral peaks, and minimize low-frequency variation (Smith et al., 2002).

$$1^{\text{st}} \text{ derivative } R = d(R_{\lambda})/d\lambda \quad \text{Equation 4}$$

Two different methods can be used in the program Unscrambler to differentiate spectral data: the Norris method and the Savitzky- Golay (Golay) method. The Norris method only calculates 1st derivatives, while the Golay method can calculate 1st and higher order derivatives. Both methods include a smoothing factor in their

separate algorithms which determines how many adjacent bands will be used in the derivation.

The 1st derivative (Norris) of a plot reflectance curve (Figure 2.12), the Golay 1st derivative of a reflectance curve (Figure 2.13), the 1st derivative (Norris) with a smoothing factor of 5 bands (Figure 2.14), and the 1st derivative (Norris) with a smoothing factor of 10 bands (Figure 2.15), all show the same major spectral features (eg. peak at 700 nm), but differ slightly where derivatives were small (eg. between 600 – 700 nm).

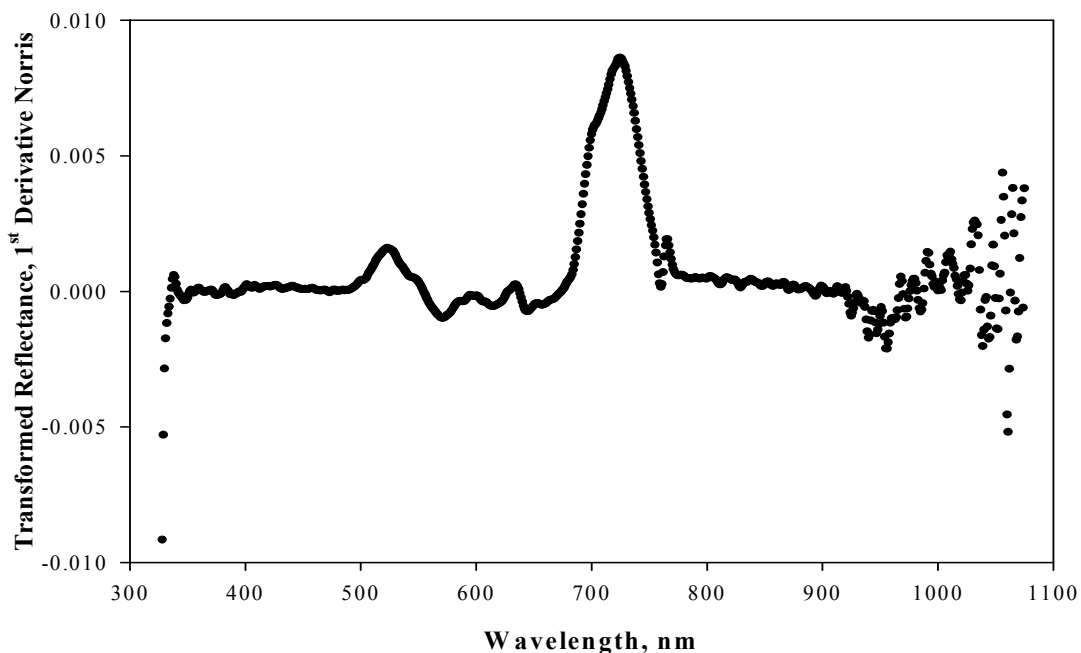


Figure 2.12. The Norris 1st derivative reflectance curve for a tidal freshwater marsh canopy

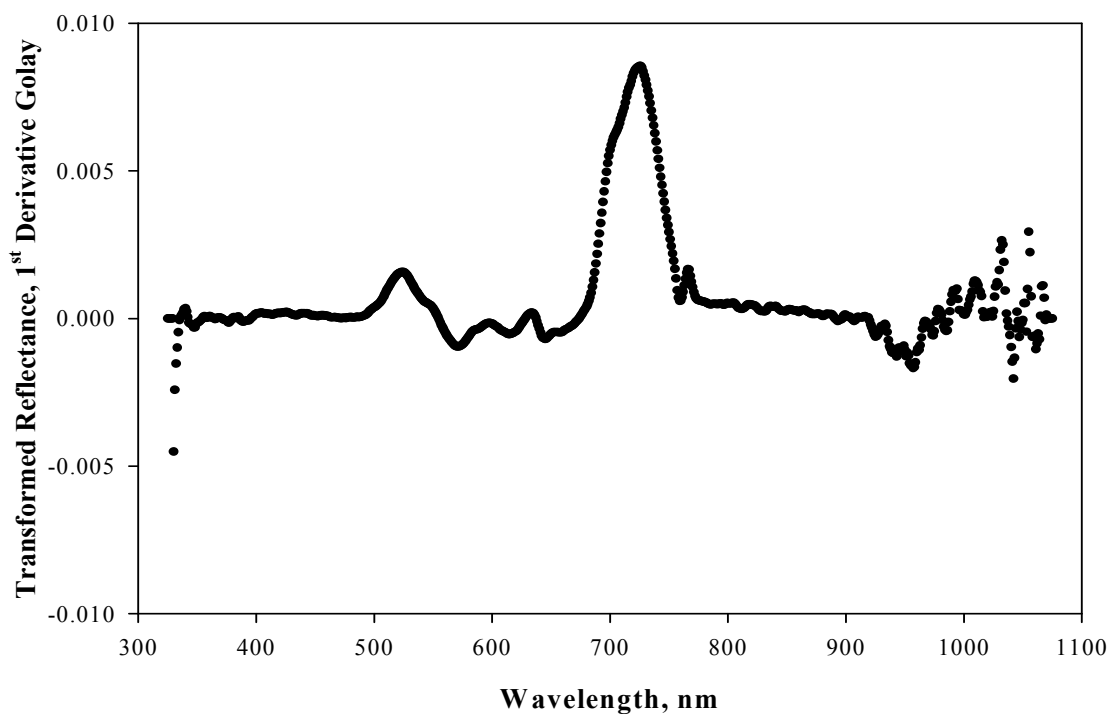


Figure 2.13. The S. Golay 1st derivative reflectance curve for a tidal freshwater marsh canopy

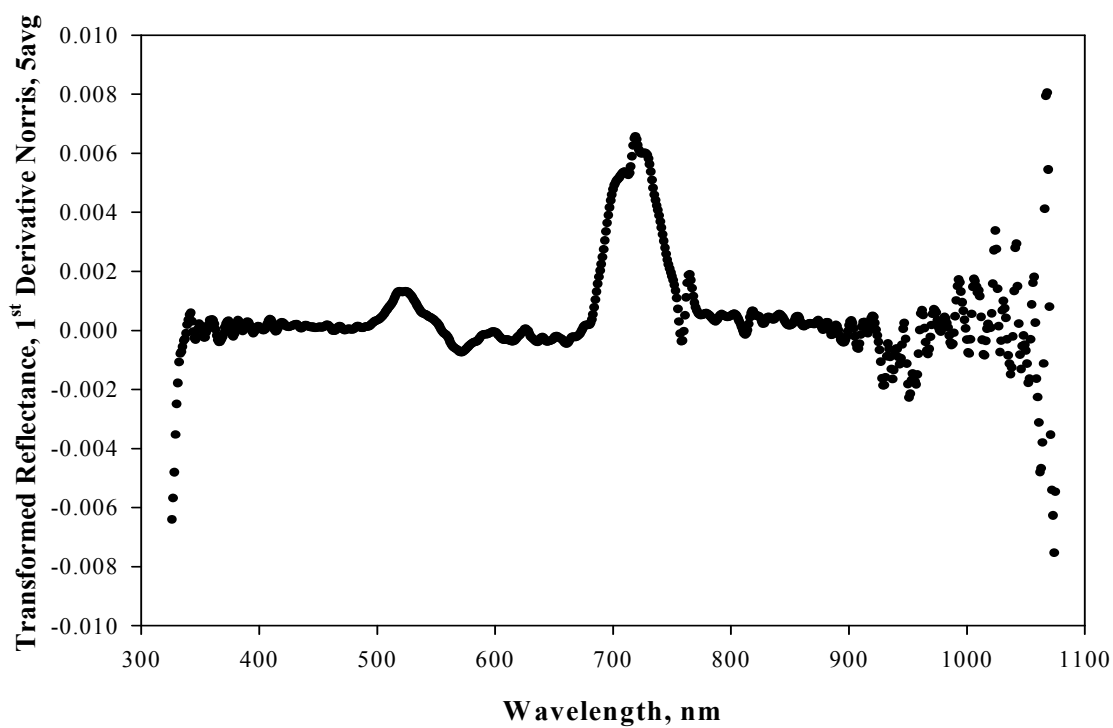


Figure 2.14. The Norris 1st derivative reflectance curve for a tidal freshwater marsh canopy, with five adjacent bands averaged together.

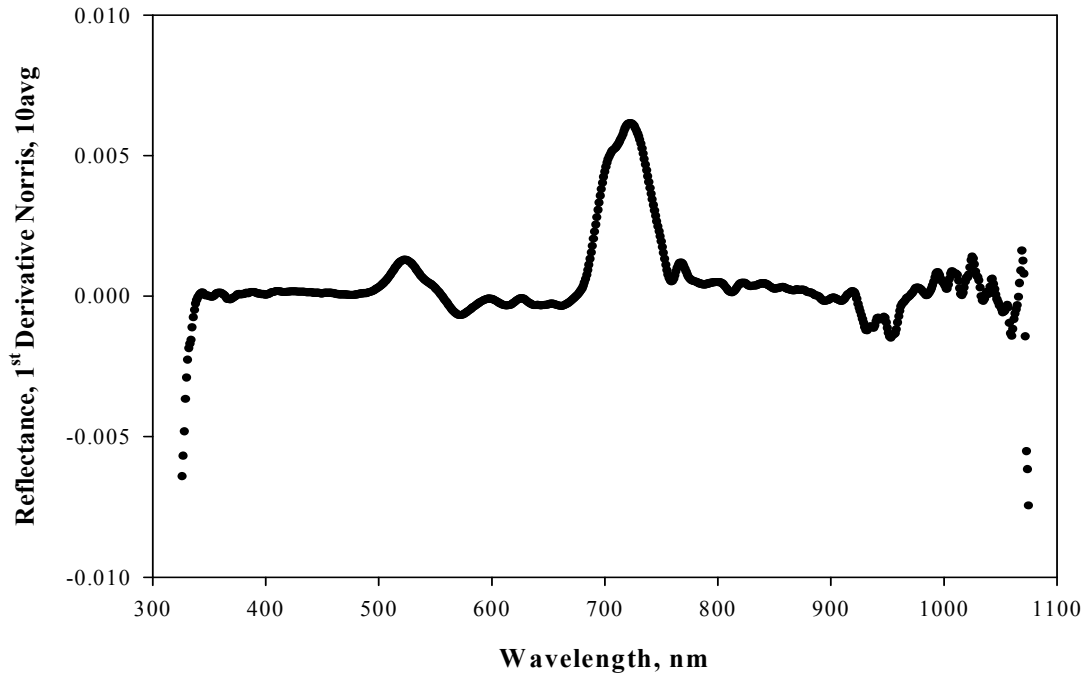


Figure 2.15. The Norris 1st derivative reflectance curve for a tidal freshwater marsh canopy, with ten adjacent bands averaged together.

Second derivative of a reflectance curve

Second derivatives correct scatter effects in reflectance curves to better correlate hyperspectral data to vegetation components (Becker et al, 2005) and nitrogen concentrations (Smith et al., 2002; Petisco et al., 2004). The equation for the second derivative of reflectance is shown in Equation 5.

$$2^{\text{nd}} \text{ derivative } R = d^2R/d\lambda^2 \quad \text{Equation 5}$$

For Golay 2nd derivatives we always averaged 10 adjacent spectral bands. Figure 2.16 displays the 2nd derivative of the reflectance curve of a typical tidal freshwater marsh canopy.

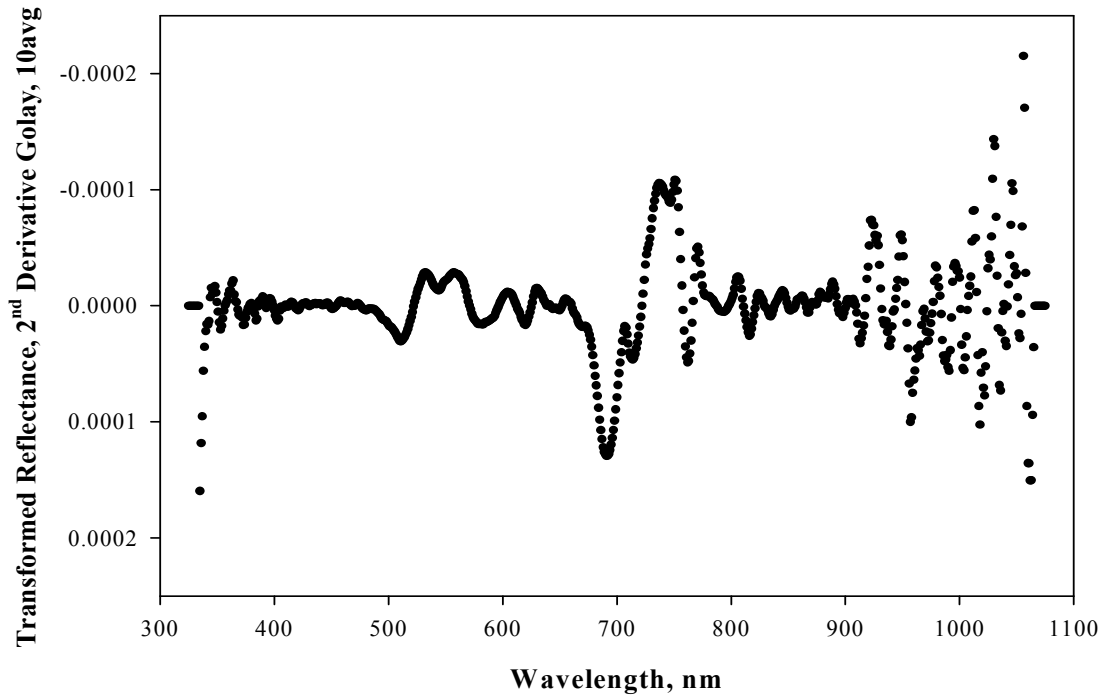


Figure 2.16. The S. Golay 2nd derivative (averaging 10 wavebands) for a typical tidal freshwater marsh canopy.

Multiplicative scatter correction (MSC) of a reflectance curve

Multiplicative scatter correction (MSC) removes both multiplicative and additive light scattering effects from the spectral data. Scatter effects in reflectance data may be caused by background effects and air temperature and pressure variations, all of which are composed of multiplicative and additive effects. MSC removes all effects with a corrective regression model (Equation 6).

$$R_{MSC} = [R_{\lambda} - A(i)] / B(i) \quad \text{Equation 6}$$

(A = intercept of the regression line, B = slope of the regression line, i = sample)

Figure 2.17 illustrates the MSC transformation of a typical reflectance curve of a tidal freshwater marsh canopy.

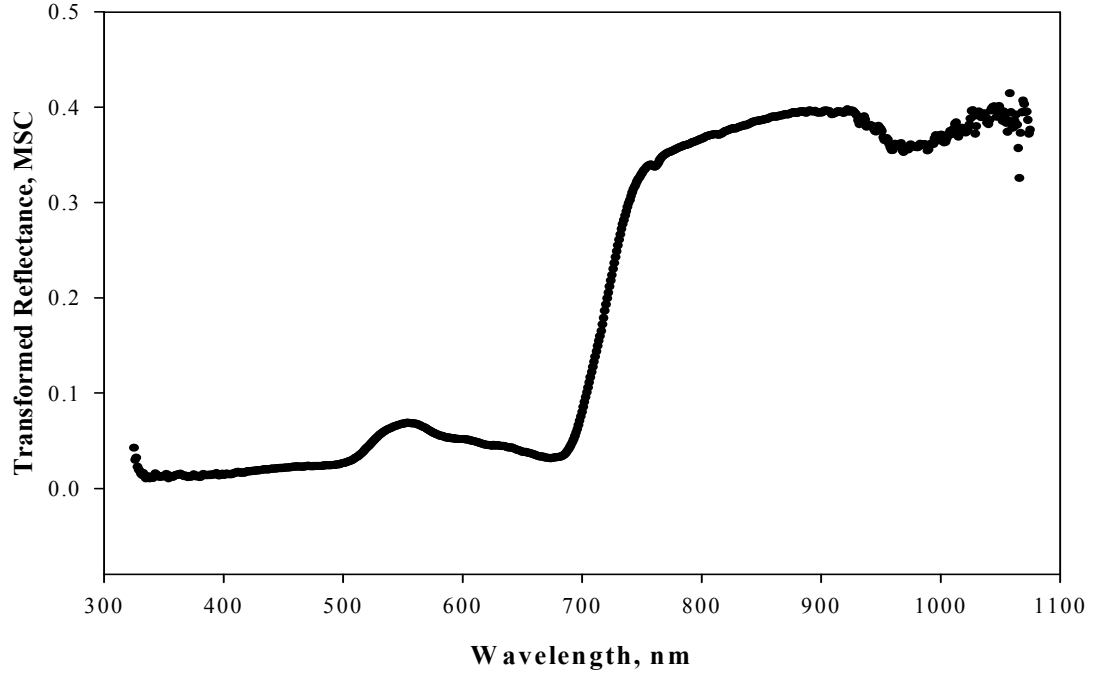


Figure 2.17. A multiplicative scatter correction (MSC) curve for a typical tidal freshwater marsh canopy.

Absorbance curve

Reflectance curves transformed into absorbance curves using Equation 7 have been correlated to vegetation components in PLS-regressions (Grossman et al., 1996; Smith et al., 2002; Petisco et al, 2005).

$$R_{abs} = \log_{10}(1/R_{\lambda}) \quad \text{Equation 7}$$

The absorbance transformation combines the inverse and log transformations, which yields an inverse reflectance curve minimizing the differences between high and low reflectance bands (Figure 2.18).

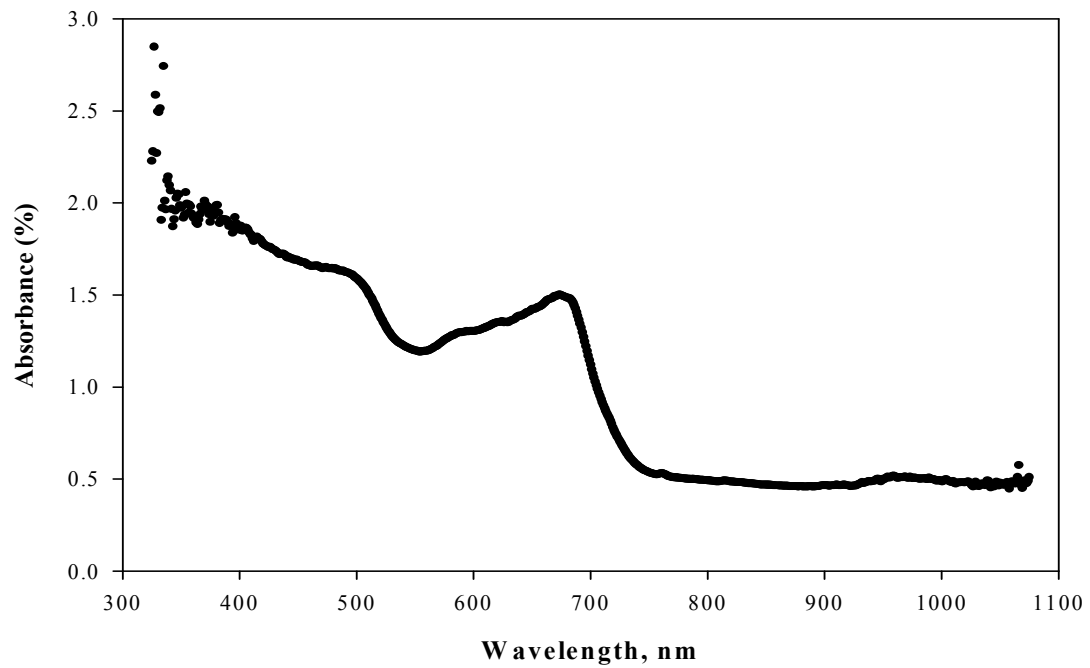


Figure 2.18. An absorbance curve for a tidal freshwater marsh canopy

Kubelka-Munk transformation of a reflectance curve

Reflectance curves were also transformed into Kubelka-Munk units (Equation 8).

The Kubelka-Munk transformation is a type of inverse reflectance function that helps to reduce scattering effects in reflectance data (Figure 2.19).

$$R_{KM} = (1 - R_{\lambda})^2 / (2R_{\lambda}) \quad \text{Equation 8}$$

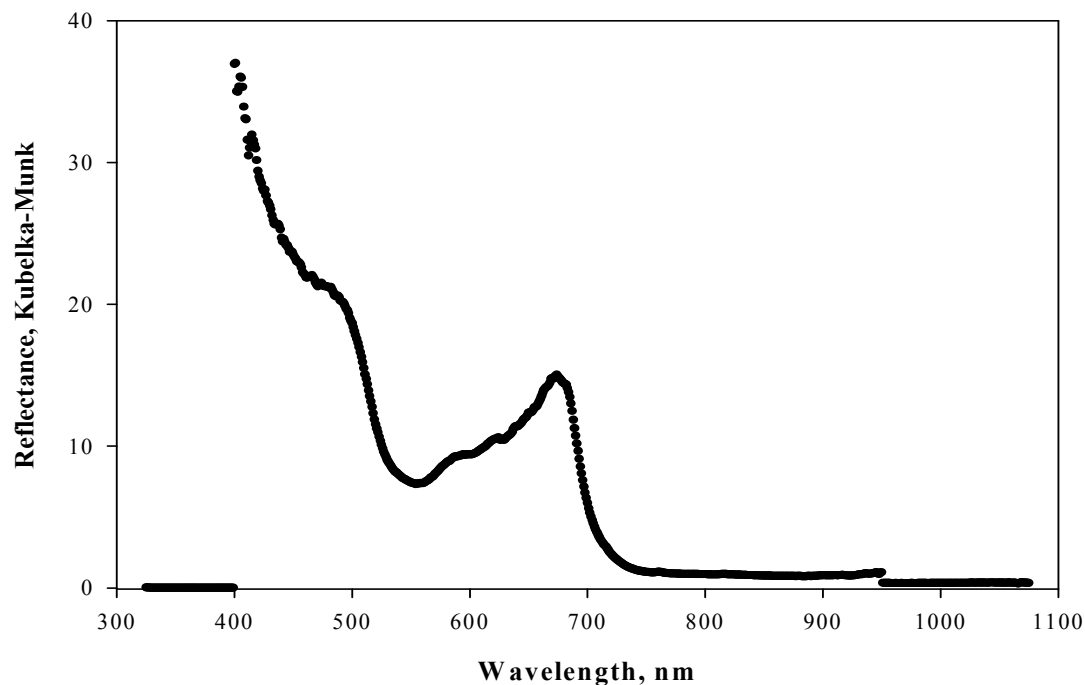


Figure 2.19. A Kubelka-Munk absorbance curve for a tidal freshwater marsh canopy.

2.4.2 Dependent Data Transformations for ANOVA and PLS Modeling

Water quality and vegetation component transformations used for all ANOVA and PLS-modeling included the log of concentration, the square root of concentration, arcsine of the square root of concentration, and the fourth root concentration. The untransformed water quality data had skewed frequency distributions with a few high concentrations and a majority of low concentrations. For example, NH_3 untransformed concentrations are shown in Figures 2.20, demonstrating the skewed distribution. Examples of the effect of each transformation on water quality data are shown in Figures 2.21 – 2.24.

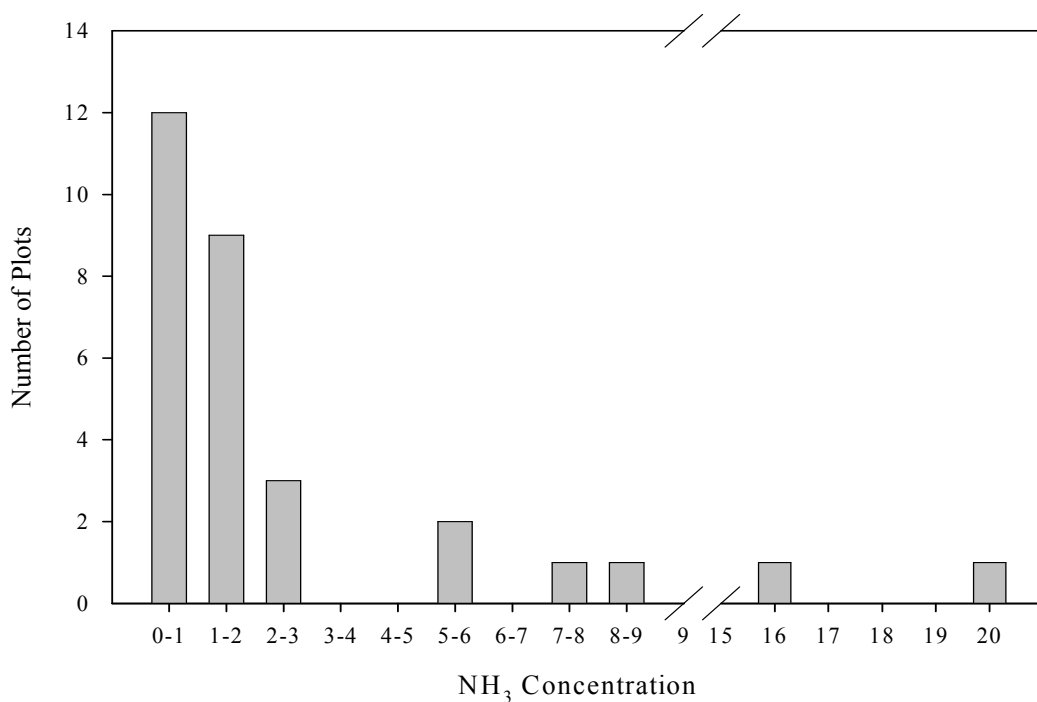


Figure 2.20. The frequency distribution of NH₃ concentrations for plots at the two marsh sites on 8/24/04.

Log of concentration

The log of the concentration (Figure 2.21) produced a more normal distribution than the untransformed data (Figure 2.20). For the log transformation shown in Figure 2.22, the \log_{10} was taken of each concentration (Equation 9).

$$\log \text{ Conc} = \log_{10}(\text{Conc})$$

Equation 9

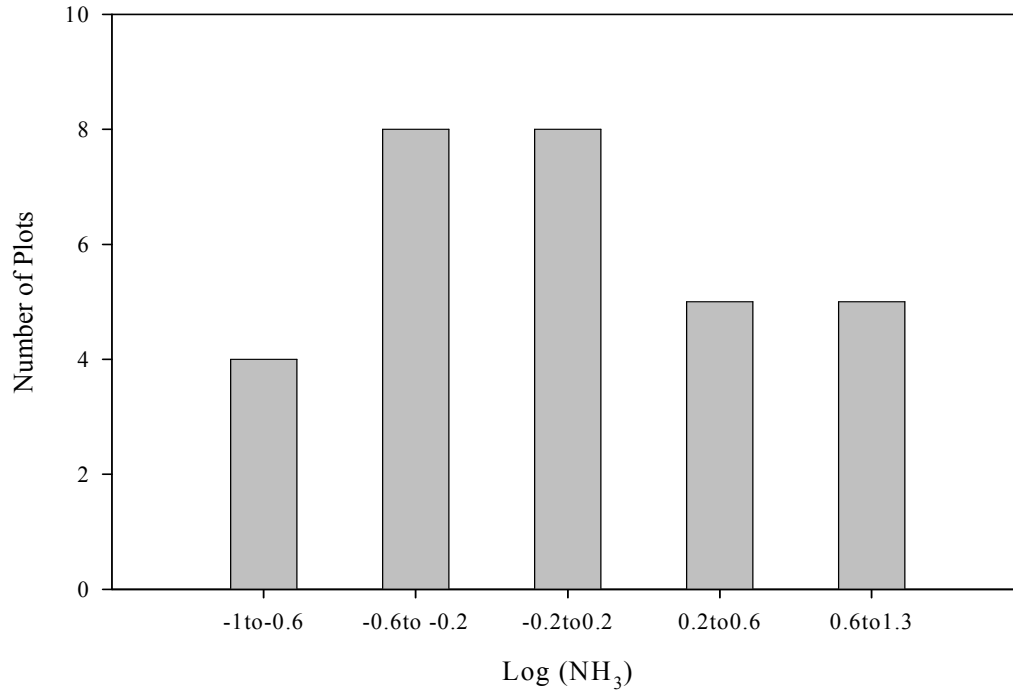


Figure 2.21. The distribution of the Log (NH₃) transformation for plots at the two marsh sites on sample date 8/24/04.

Square root of concentration

The square root of the dependent variable is commonly used in statistics to create a normal distribution from skewed data (Equation 10). Figure 2.22 shows the transformed distribution for the square root of the concentration.

$$\text{Conc}_{\text{sqrt}} = (\text{Conc})^{1/2}$$

Equation 10

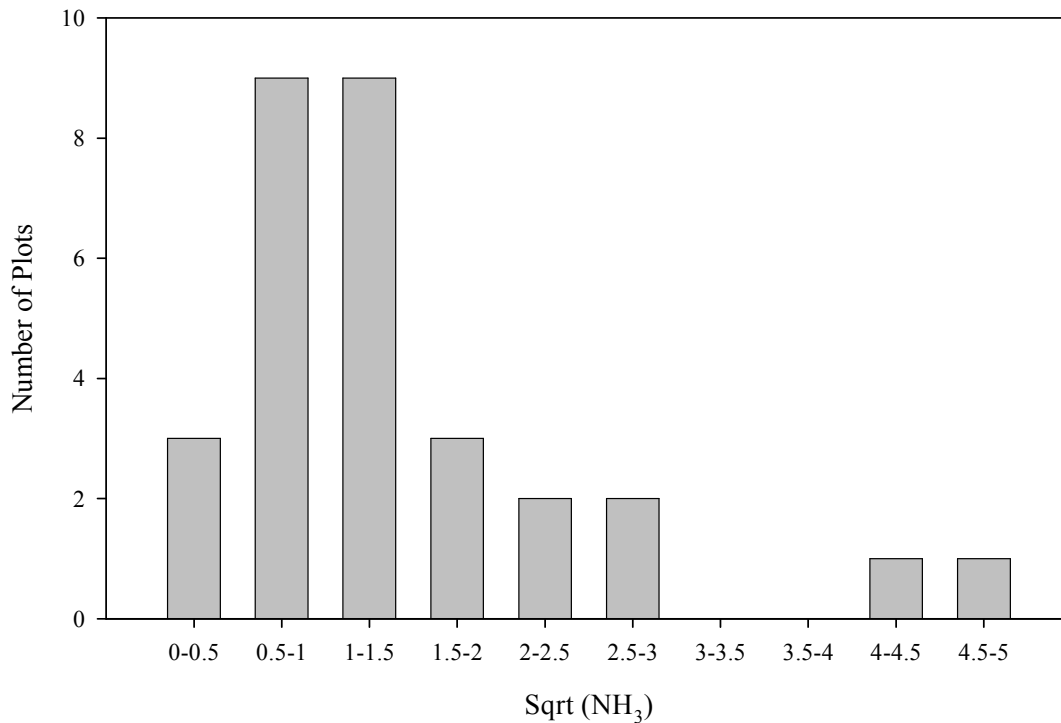


Figure 2.22. The distribution of the square root transformation of NH₃ for plots at the two marsh sites on sample date 8/24/04.

Arcsine of the square root of concentration

The arcsine of the square root of concentration transformation (Equation 11) has been used to normalize the dependent variable data in statistics. The transformed distribution had a much smaller range, but still had a skewed distribution (Figure 2.23).

$$\text{Conc}_{\text{arcsin}} = \text{Arcsine}(\text{sqrt}(\text{Conc}))$$

Equation 11

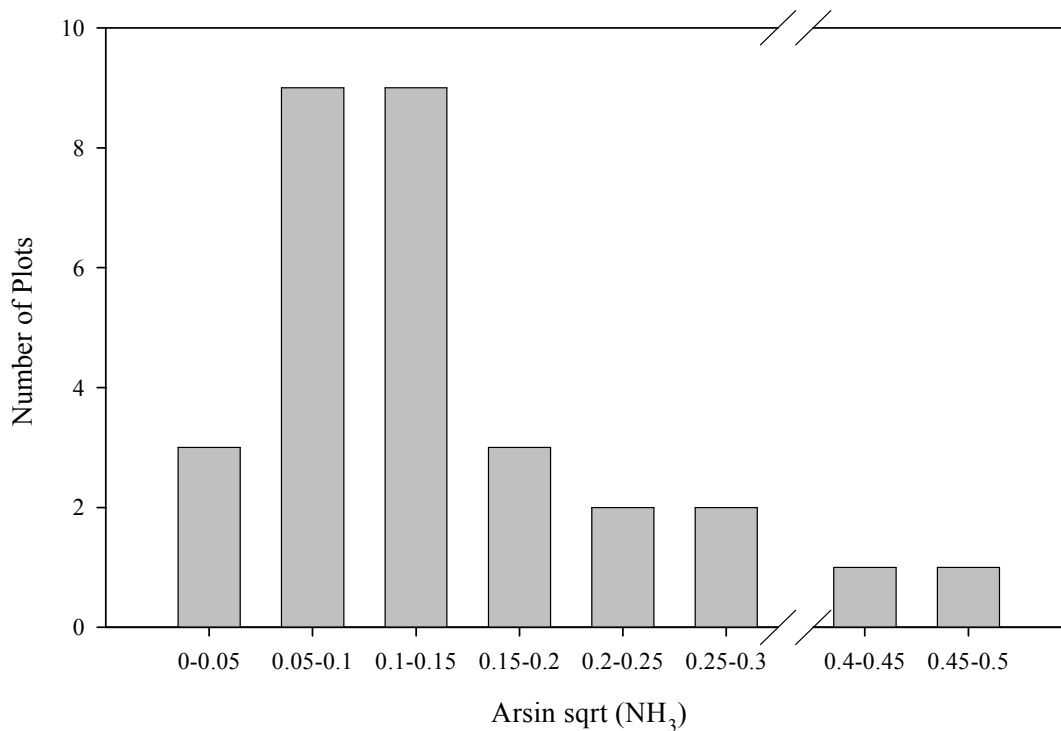


Figure 2.23. The distribution of the arcsine of the square root transformation of NH₃ for plots at the two marsh sites on sample date 8/24/04.

Fourth root of concentration

The fourth root of the concentration is similar to both the square root and arcsine of the square root transformations, in that it improves normality and decreases the range of the distribution. Equation 12 shows the process taken to transform the dependent data and Figure 2.24 illustrates the transformation distribution.

$$\text{Conc}_{4 \text{ root}} = (\text{Conc})^{1/4} \quad \text{Equation 12}$$

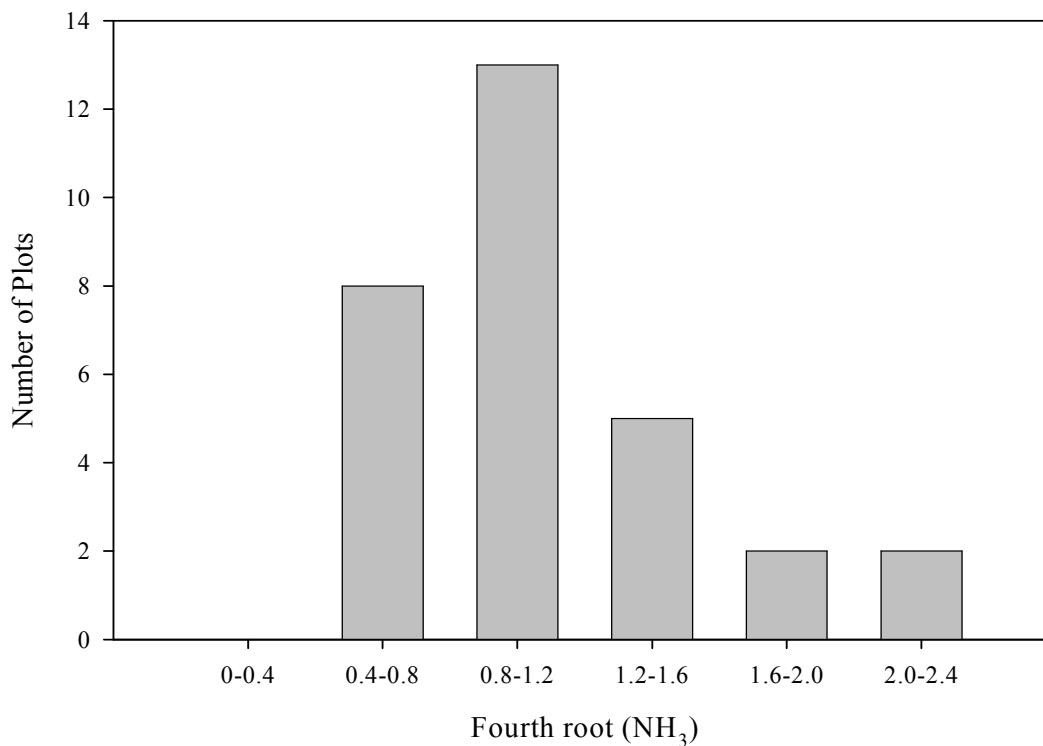


Figure 2.24. An example of the distribution of the fourth root transformation of NH_3 for plots at the two marsh sites on sample date 8/24/04

Vegetation component transformations

Vegetation component transformations included the log of vegetation cover, the square root of cover, arcsine of the square root of cover, and the fourth root of cover.

The untransformed vegetation component data were not as skewed as the water quality data, although the transformations did improve normality.

Summary of transformations

Table 2.3 summarizes all reflectance transformations used. Tables 2.4 and 2.5 summarize the water quality transformations and vegetation component transformations performed on the data, respectively.

Table 2.3. Summary of spectral transformations.

Spectral Transformations	
Untransformed	All wavebands used, no transformations
Truncated spectra	Wavebands 400-950nm used
Normalized spectra	Each waveband divided by waveband 410 (Reflectance/R410)
Transform 1/R	One over each waveband
Log R	Log of each waveband
Norris 1st Derivative	1 st derivative of the reflectance curve by the Norris algorithm
Norris 1st Derivative, avg 5	1 st deriv. of the reflectance curve, Norris algorithm, smoothing factor = 5
Norris 1st Derivative, avg 10	1 st deriv. of the reflectance curve, Norris algorithm, smoothing factor = 10
Golay 1st Derivative	1 st deriv. of the reflectance curve by the S. Golay algorithm
Golay 1st Derivative, avg 5	1 st deriv. of the reflectance curve, S. Golay algorithm, smoothing factor = 5
Golay 1st Derivative, avg 10	1 st deriv. of the reflectance curve, S. Golay algorithm, smoothing factor = 10
Golay 2nd Derivative, avg 10	2 nd deriv. of the reflectance curve, S. Golay algorithm, smoothing factor = 10
MSC Transformation	Multiplicative scatter correction reduces multiplicative and additive effects
Absorbance Transformation	Converting reflectance units to absorbance units
Kubelka-Munk Transformation	Converting reflectance units to Kubelka-Munk absorbance units

Table 2.4. Summary of water quality transformations.

Water Quality Data Transformations	
Untransformed	Water quality data as measured
Log (Conc)	Log of each water quality concentration
Square root (Conc)	Square root of each water quality concentration
Arcsine sqrt (Conc)	Arcsine of the square root of each concentration
4th root (Conc)	Fourth root of each concentration

Table 2.5. Summary of vegetation transformations.

Vegetation Data Transformations	
Untransformed	Vegetation data as measured
Log (Veg)	Log of vegetation data
Square root (Veg)	Square root of vegetation data
Arcsine sqrt (Veg)	Arcsine of the square root of vegetation data
4th root Veg	Fourth root of vegetation data

Chapter 3: Results

The results chapter reports on the seasonal dynamics of marsh water quality, vegetation composition, and canopy reflectance. The effects of nitrogen fertilization on water quality and species, analyzed with ANOVA, are also reported. Partial least squares (PLS) models for water quality, leaf nitrogen, and vegetation composition predictions are included, as well as a comparison of significant spectral bands detected in the PLS models and selected during ANOVA.

3.1 Marsh Water Quality

The addition of nitrogen as urea increased the ammonia, nitrate, and total nitrogen concentrations in the sub-surface water, particularly at the *Phragmites*-dominant site for the majority of the 2004 season (June – August). Total phosphorus concentrations did not change with nitrogen application. The effects of nitrogen as urea on sub-surface nutrients over the 2004 growing season are illustrated in section 3.1.1, and analyzed in sections 3.1.2 – 3.1.5.

3.1.1 Seasonal dynamics of sub-surface nutrients

Ammonia, nitrate, total phosphorus, and total nitrogen sub-surface water concentrations fluctuated throughout the growing season, with each treatment yielding a different seasonal pattern of concentration. Figure 3.1.1 shows the mean ammonia concentrations of sub-surface water for each nitrogen treatment during the 2004 growing season. In general the highest urea application generated the highest ammonia concentration. However N100 had the second highest ammonia concentration until 7/19/04. Most treatments increased in ammonia concentration

early in the season, peaked in mid- to late-June, then decreased slowly through 9/21/04, as expected. Ambient conditions, predictably, remained fairly constant at background ammonia levels of around 1 mg-N/L. Surprisingly, N200/1D was also constant throughout the season at levels only slightly above ambient conditions at around 2 mg-N/L.

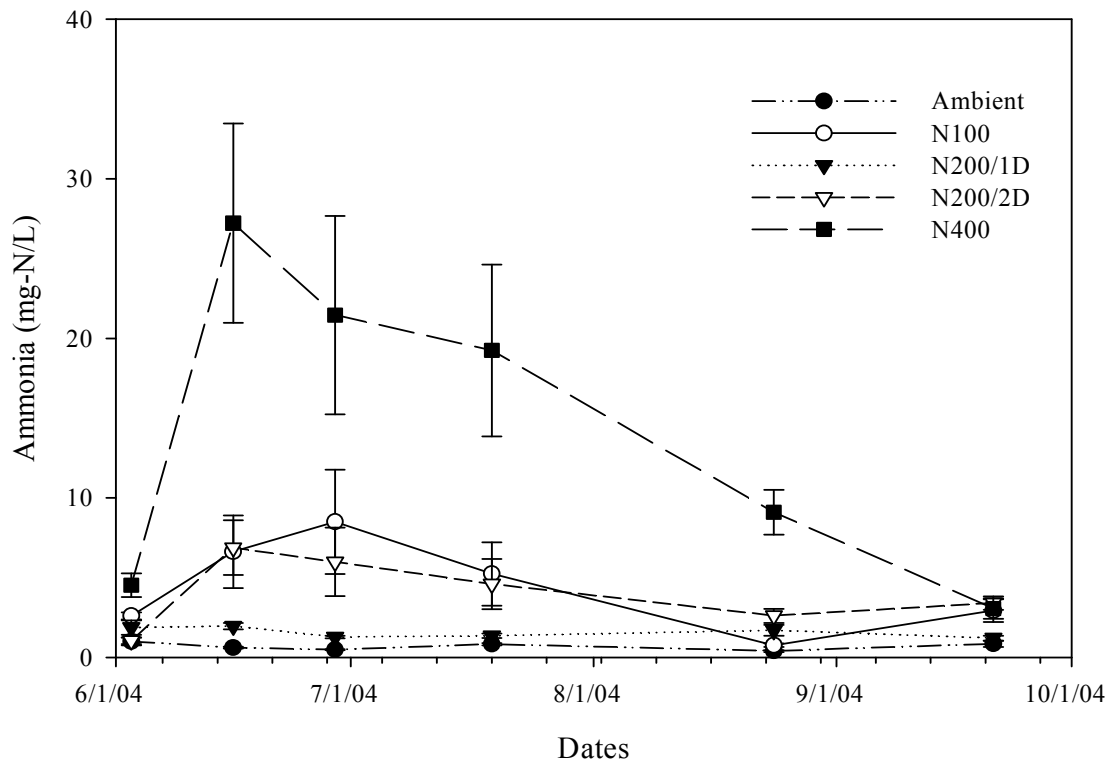


Figure 3.1.1. Mean and standard errors of ammonia concentrations by urea treatment at the two marsh sites during the 2004 growing season.

The simulated model for nitrogen release over time developed by Tilley et al. (2004) (Figure 3.1.2) graphically fits the observed concentrations in my study (Figure 3.1.1). N400 increased quickly in both the observed and predicted model, while N200/2D also peaked early before slowly declining through the remaining season.

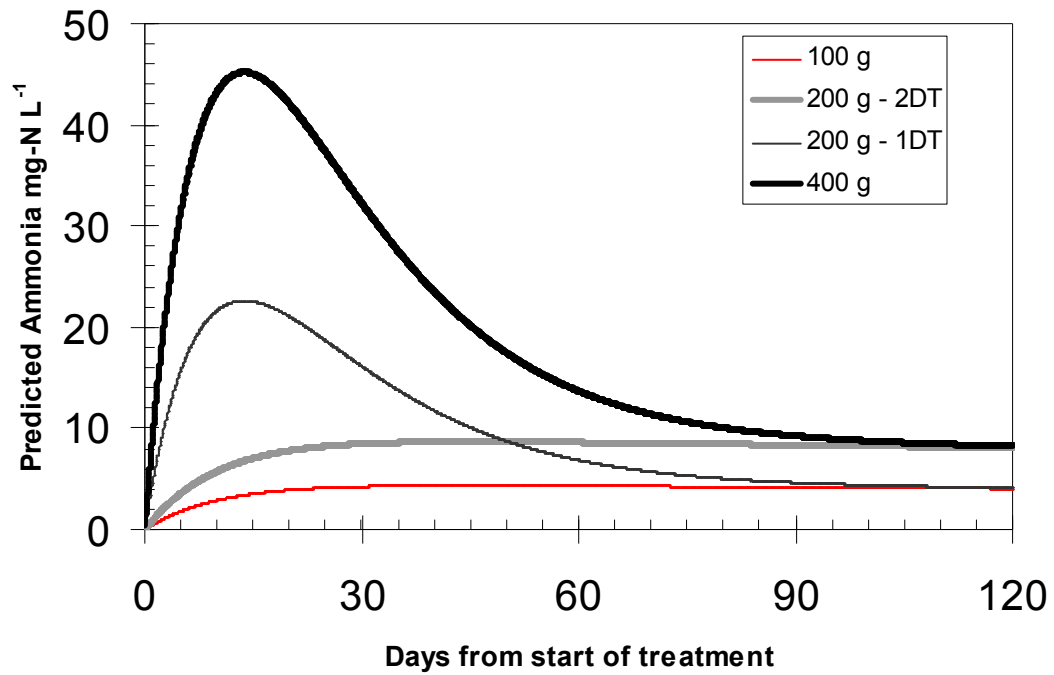


Figure 3.1.2 Predicted sub-surface water ammonia levels in marsh experimental plots based on a simulation model developed and calibrated on experiments with dialysis tubes in the laboratory (Tilley et al., 2004).

The addition of nitrogen increased nitrate concentrations in sub-surface water during the 2004 growing season (Figure 3.1.3). N400 had a higher nitrate concentration than other treatments until it decreased sharply after its peak on 7/19/04. Ambient conditions were fairly uniform across the 2004 season, remaining between 1.0 and 2.0 mg-N/L nitrate. N100 steadily increased after the 6/29/04 sample date.

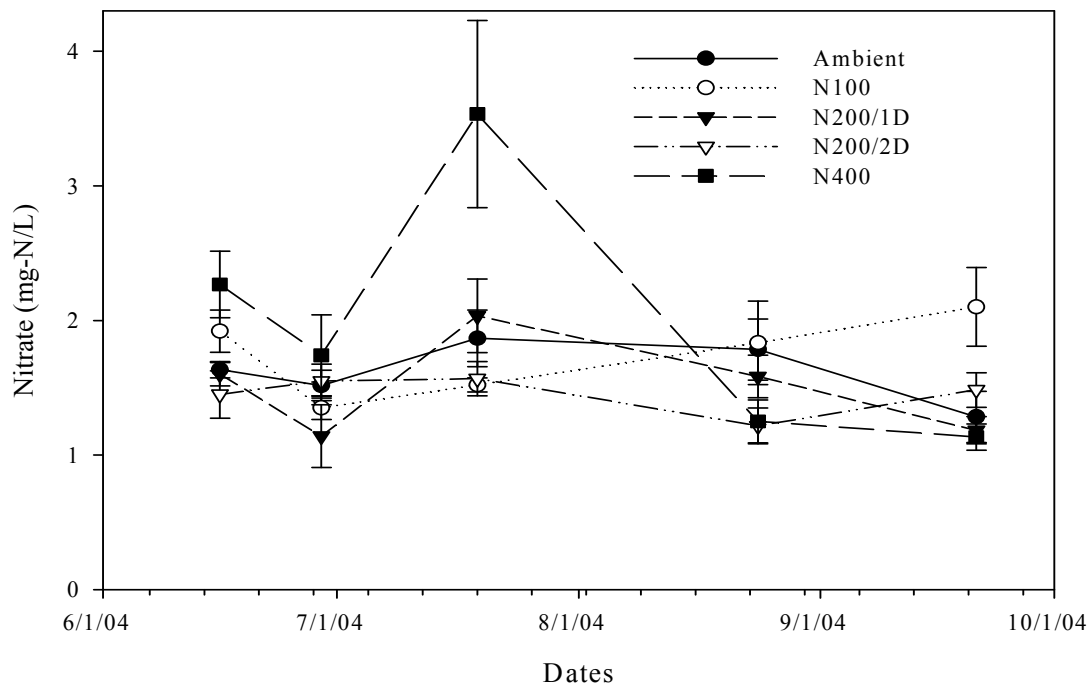


Figure 3.1.3. Mean and standard errors of nitrate concentration by urea treatment at the two marsh sites during the 2004 growing season.

Figure 3.1.4 displays mean total phosphorus concentrations of sub-surface water in both marsh sites for each nitrogen treatment during the 2004 growing season.

Although N200/2D began with the highest total phosphorus concentration on 6/16/04, all treatments fell into the range of 0.0 – 0.4 mg-P/L by the end of June, and remained in that range through the end of September.

As for total nitrogen concentrations over time, the highest nitrogen treatment produced the highest total nitrogen for the 2004 season, even on 7/19/04 when N400 dropped to about 15 mg - N/L from its average 30 mg - N/L (Figure 3.1.5). Ambient nitrogen conditions hovered slightly above 10 mg - N/L all summer, while N200/1D and N200/2D increased in total nitrogen concentration after 7/19/04.

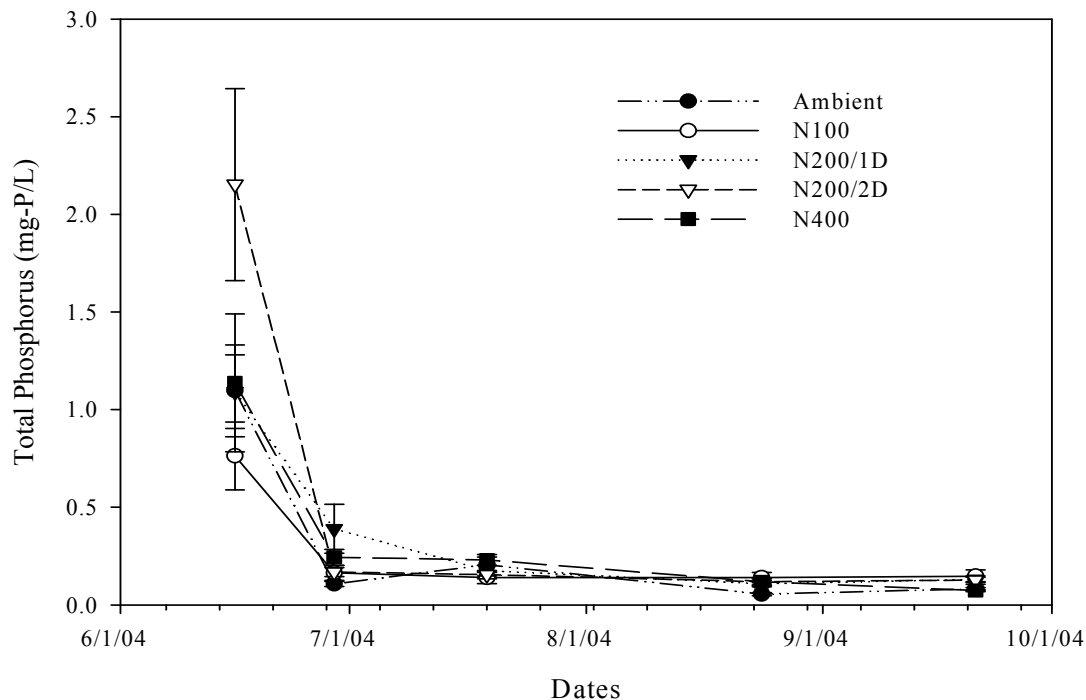


Figure 3.1.4. Mean and standard errors of total phosphorus concentration by urea treatment at the two marsh sites during the 2004 growing season.

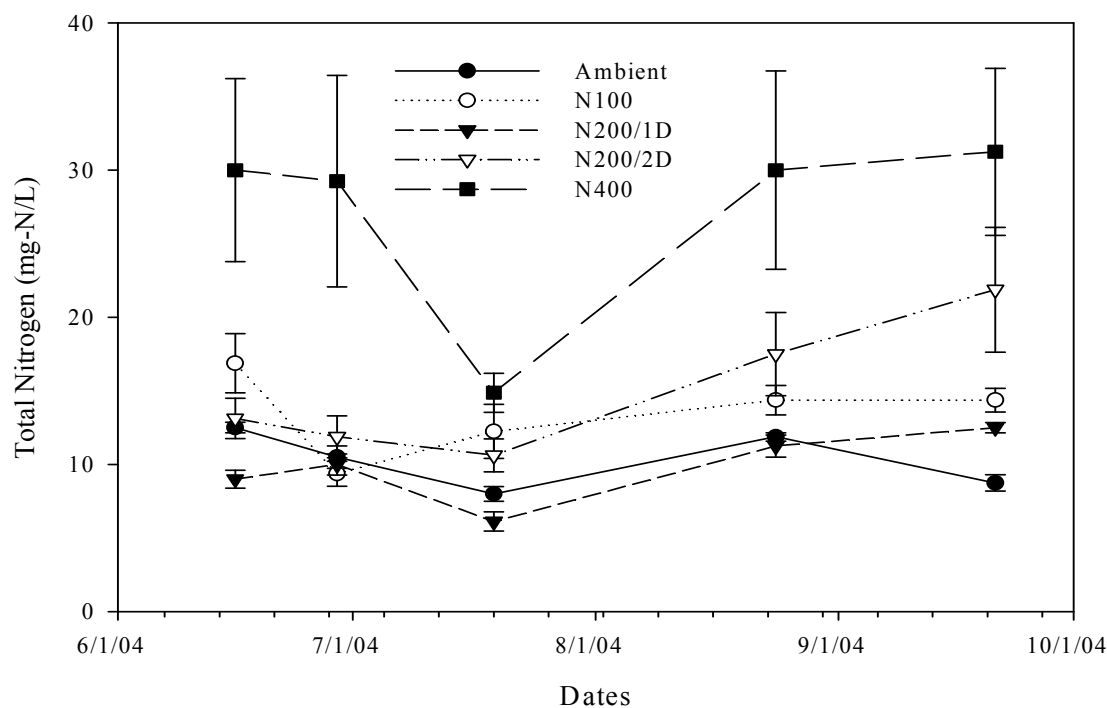


Figure 3.1.5. Mean and standard errors of total nitrogen concentrations by urea treatment at the two marsh sites during the 2004 growing season.

Mean ammonia, nitrate, and total phosphorus sub-surface water concentrations during the 2005 growing season are plotted in Figure 3.1.6. In the summer of 2005, ambient ammonia concentrations decreased, as did N200/2D, while all other treatments increased in ammonia. Nitrate concentration decreased for all treatments during the 2005 summer.

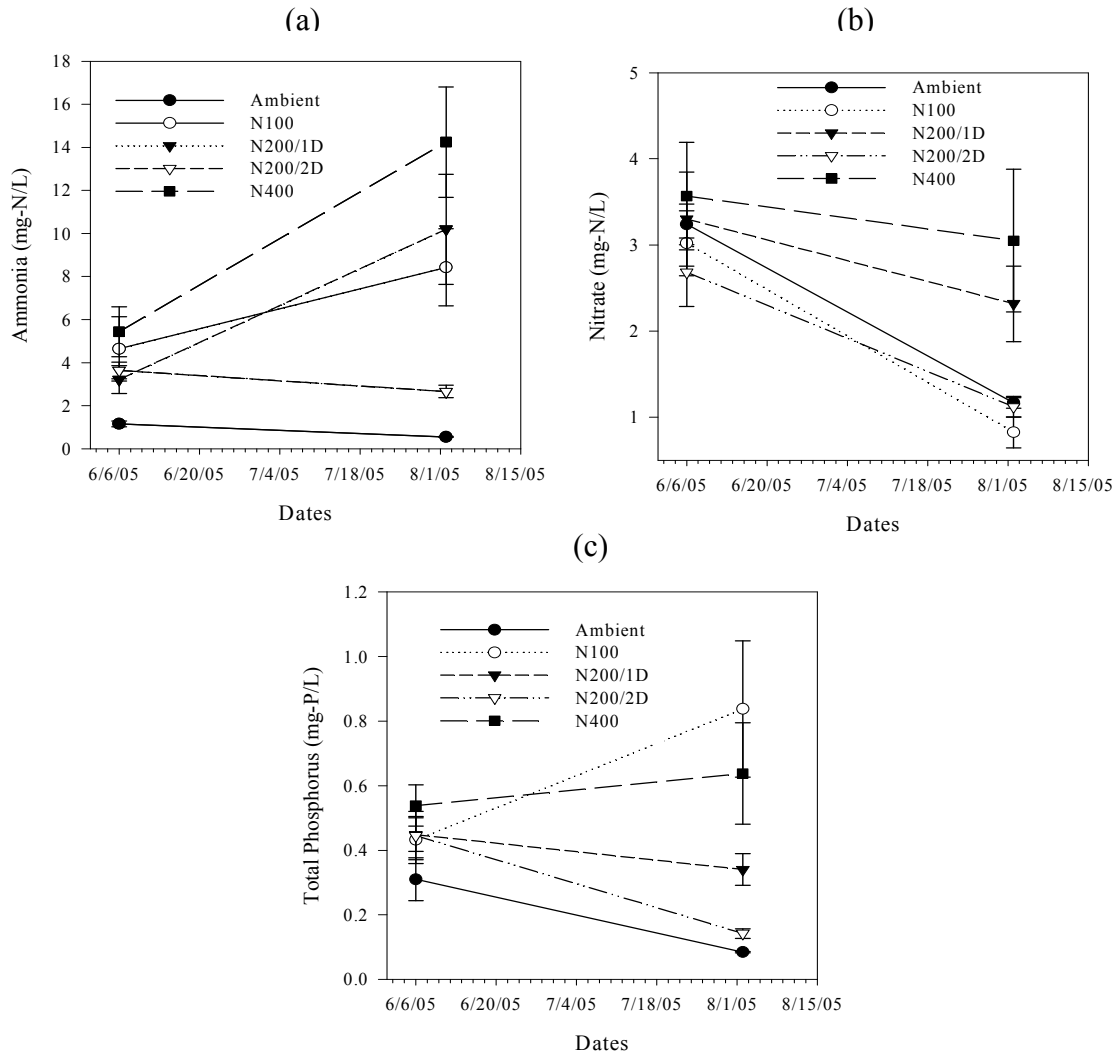


Figure 3.1.6. Mean and standard errors of (a) ammonia, (b) nitrate, and (c) total phosphorus concentrations by urea treatment at the two marsh sites during the 2005 growing season.

3.1.2 Fertilization and Site Effects on NH_3

A repeated measures analysis of variance (ANOVA) was conducted on all water quality nutrients to determine the significance of time and its interaction with nitrogen treatment and site effects, before main effects of nitrogen were considered.

Ammonia sub-surface water concentrations increased with the addition of nitrogen fertilization for the majority of the growing season (June – August) at both sites (Figures 3.1.7 and 3.1.8). Upon analysis, a strong time effect interfered with site and treatment effects (Tables 3.1.1 and 3.1.2), suggesting that nitrogen treatment effect be analyzed on each sample date (Table 3.1.3). Site effects interacted with nitrogen effects for several 2004 dates, but on 6/16/04 and 8/24/04, nitrogen treatment affected ammonia concentrations.

Table 3.1.1. Repeated measures ANOVA model for 2004 NH_3 concentrations. * <0.01, ** < 0.05, * < 0.10**

Source	Type III SS	df	MS	F	Sig
Site	1139.10	1	1139.10	4.14	0.058
Trt	5414.90	4	1353.72	4.92	0.008
Site * Trt	4518.07	4	1129.52	4.10	0.017
Error	4681.88	17	275.40		
Time	1682.02	5	336.40	5.40	0.000
Time * Site	512.07	5	102.41	1.64	0.157
Time * Trt	3062.82	20	153.14	2.46	0.002
Time * Site * Trt	3118.66	20	155.93	2.50	0.002***
Error (time)	5296.02	85	62.31		

Table 3.1.2 ANOVA model: Trt + Time + (Trt*Time) at each marsh site for NH₃. * <0.01, ** < 0.05, * < 0.10. PD site = *Phragmites*-dominant site; PA site = *Phragmites*-absent site**

Site	Source	Type III				
		SS	df	MS	F	Sig
PD site	Trt	8093.40	4	2023.35	4.89	0.027
	Time	1848.90	5	369.78	4.28	0.003
	Time * Trt	4832.07	20	241.60	2.80	0.003***
	Error	3308.61	8	413.58		
PA site	Trt	583.57	4	145.89	0.96	0.476
	Time	1848.90	5	369.78	4.28	0.003
	Time * Trt	4832.07	20	241.60	2.80	0.003***
	Error	1373.27	9	152.59		

Table 3.1.3. ANOVA model: Site + Trt + (Site*Trt) at all sample dates for NH₃. * <0.01, ** < 0.05, * < 0.10**

Date	Source	Type III				
		SS	df	MS	F	Sig
6/3/2004	Trt	25.43	4	6.36	5.10	0.005
	Site	52.80	1	52.80	42.40	0.000
	Trt*Site	24.02	4	6.01	4.82	0.007***
	Error	24.91	20	1.25		
6/16/2004	Trt	2725.52	4	681.38	2.36	0.090*
	Site	212.01	1	212.01	0.73	0.402
	Trt*Site	1145.47	4	286.37	0.99	0.436
	Error	5482.44	19	288.55		
6/29/2004	Trt	2159.96	4	539.99	2.77	0.059
	Site	483.54	1	483.54	2.48	0.132
	Trt*Site	2842.42	4	710.61	3.65	0.024**
	Error	3502.85	18	194.60		
7/19/2004	Trt	1354.41	4	338.60	2.08	0.122
	Site	363.73	1	363.73	2.23	0.151
	Trt*Site	1689.34	4	422.34	2.59	0.068*
	Error	3257.54	20	162.88		
8/24/2004	Trt	304.59	4	76.15	6.29	0.002***
	Site	45.63	1	45.63	3.77	0.066*
	Trt*Site	57.49	4	14.37	1.19	0.347
	Error	242.18	20	12.11		
9/21/2004	Trt	33.12	4	8.28	1.22	0.332
	Site	0.20	1	0.20	0.03	0.865
	Trt*Site	37.04	4	9.26	1.37	0.280
	Error	135.26	20	6.76		

Since time and site both influenced nitrogen effects on ammonia concentrations, nitrogen treatment effects on individual sample dates and marsh sites were then analyzed. When nitrogen effects were investigated with untransformed data, however, sample variances were unequal, so the log transformation of ammonia concentrations was used for analysis.

Time interacted with site and treatment for the log of ammonia data as well (Table 3.1.4). At the *Phragmites*-dominant site, there was a nitrogen*time interaction effect, but at the *Phragmites*-absent site, there was a time effect instead of an interaction effect (Table 3.1.5). When nitrogen and site effects were analyzed on each sample date, site effect was significant for only two dates (6/03/04 and 8/24/04) because several others had site*treatment interactions (Table 3.1.6). Nitrogen treatment had an effect on log ammonia concentrations on 6/16/04 and 8/24/04, which matched sample dates with treatment effects for untransformed data (Table 3.1.3).

Table 3.1.4. Repeated measures ANOVA model for 2004 Log (NH₃) concentrations. * <0.01, ** < 0.05, * < 0.10**

Source	Type III SS	df	MS	F	Sig
Site	4.90	1	4.90	24.06	0.002
Trt	10.86	4	2.71	13.32	0.002
Site * Trt	2.50	3	0.83	4.10	0.057
Error	1.43	7	0.20		
Time	0.94	5	0.19	3.01	0.023
Time * Site	0.56	5	0.11	1.78	0.142
Time * Trt	1.82	20	0.09	1.45	0.162
Time * Site * Trt	3.11	15	0.21	3.33	0.002***
Error (time)	2.18	35	0.06		

Table 3.1.5 ANOVA model: Trt + Time + (Trt*Time) at each marsh site for Log (NH₃). * <0.01, ** < 0.05, * < 0.10. PD site = *Phragmites*-dominant site; PA site = *Phragmites*-absent site**

		Type III				
Site	Source	SS	df	MS	F	Sig
PD site	Trt	14.64	4	3.66	17.58	0.002
	Time	0.29	5	0.06	0.83	0.540
	Time * Trt	4.09	20	0.20	2.91	0.004***
	Error	1.25	6	0.21		
PA site	Trt	6.97	4	1.74	2.60	0.108
	Time	1.97	5	0.39	3.14	0.016**
	Time * Trt	3.02	20	0.15	1.20	0.297
	Error	6.04	9	0.67		

Table 3.1.6. ANOVA model: Site + Trt + (Site*Trt) at all sample dates for Log (NH₃)

*** <0.01, ** < 0.05, * < 0.10

		Type III				
Date	Source	SS	df	MS	F	Sig
6/3/2004	Trt	0.65	4	0.16	1.28	0.342
	Site	2.48	1	2.48	19.54	0.001***
	Trt*Site	0.09	3	0.03	0.23	0.875
	Error	1.27	10	0.13		
6/16/2004	Trt	5.67	4	1.42	6.79	0.001***
	Site	0.57	1	0.57	2.73	0.115
	Trt*Site	1.49	4	0.37	1.79	0.173
	Error	3.97	19	0.21		
6/29/2004	Trt	3.92	4	0.98	4.56	0.010
	Site	0.41	1	0.41	1.89	0.186
	Trt*Site	3.01	4	0.75	3.50	0.028**
	Error	3.87	18	0.21		
7/19/2004	Trt	2.64	4	0.66	3.41	0.028
	Site	0.93	1	0.93	4.80	0.040
	Trt*Site	2.37	4	0.59	3.07	0.040**
	Error	3.87	20	0.19		
8/24/2004	Trt	5.97	4	1.49	9.86	0.000***
	Site	0.80	1	0.80	5.31	0.032**
	Trt*Site	0.07	4	0.02	0.12	0.973
	Error	3.03	20	0.15		
9/21/2004	Trt	1.82	4	0.46	1.99	0.136
	Site	0.14	1	0.14	0.60	0.448
	Trt*Site	1.27	4	0.32	1.39	0.275
	Error	4.59	20	0.23		

Since the effect of nitrogen treatment on ammonia concentration was sensitive to time and site, nitrogen effects were analyzed on individual dates at each site (Figures 3.1.7 and 3.1.8). At the *Phragmites*-dominant site during the majority of the growing season (June – August), the higher application of urea resulted in higher ammonia concentrations. By the end of the growing season in September, the effect had diminished, but was still distinguishable, especially for the N200/2D treatment. During the second year, reapplication of urea resulted in elevated ammonia levels, although the consistency of the effect was less clear. Sample date 8/02/05 was missing ammonia concentrations for several plots, explaining the lack of a mean for N100 and the high standard errors for N200/1D and N400 (Figure 3.1.7h).

At the *Phragmites*-absent site, the urea fertilization was less conclusive. While there were hints that higher nitrogen application produced higher ammonia, statistically the effect was not detected except for one or two dates (Figure 3.1.8). The dialysis tube may have been punctured or opened at an N100 plot, which would have caused urea to diffuse more quickly than the designed rate, creating a higher log ammonia mean and standard error for N100. On sample dates 6/03/04 and 8/02/05, several ammonia concentrations were missing, accounting for the absent N100 mean (Figure 3.1.8a and 3.1.8h).

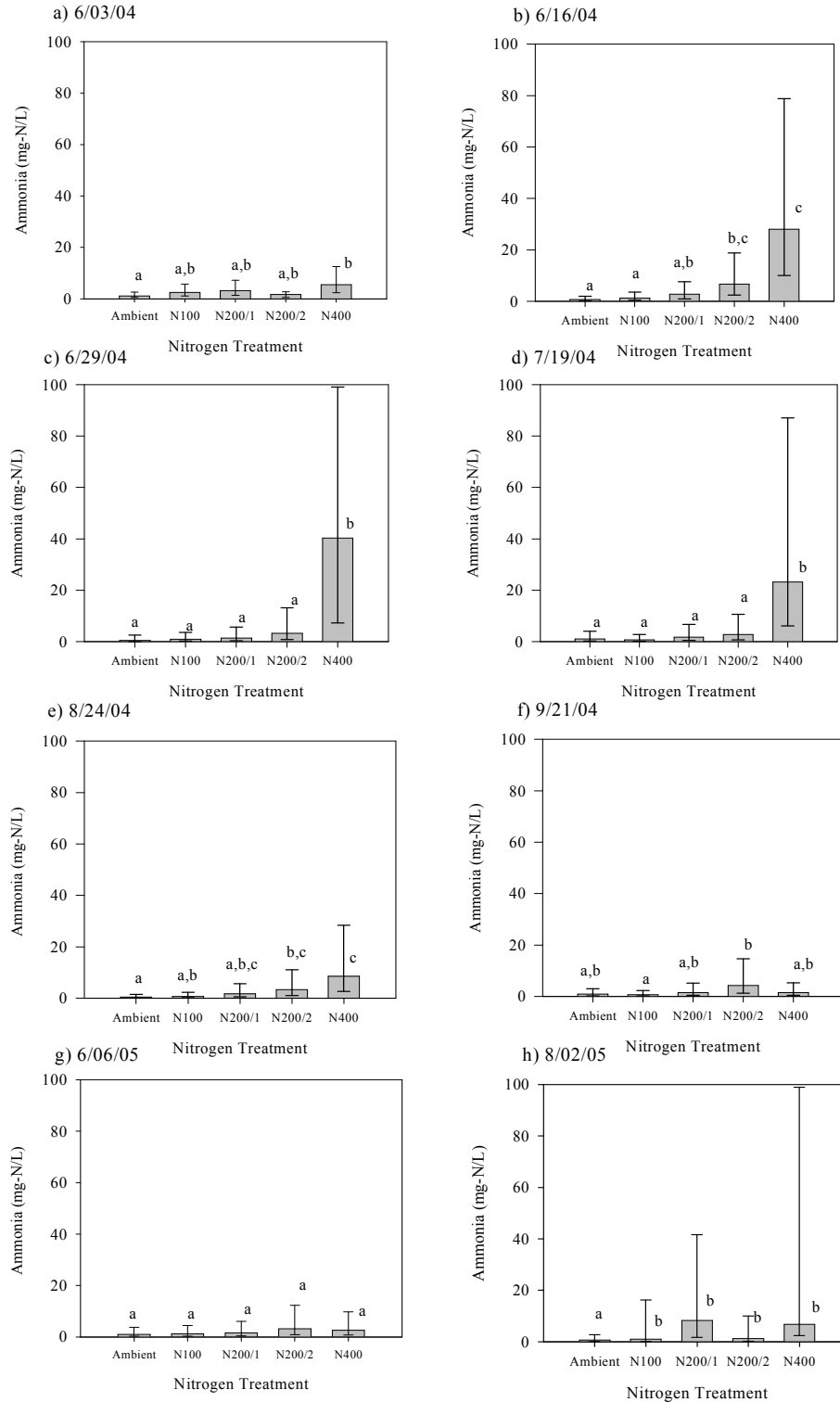


Figure 3.1.7. Geometric mean of ammonia concentrations (\pm 95% CL) of the *Phragmites*-dominant site according to nitrogen treatment over the 2004-5 growing seasons. Treatments with different letters indicate a significant difference between treatments ($p < 0.05$). Log of ammonia was the dependent variable in the one-way ANOVA model, with an LSD contrast.

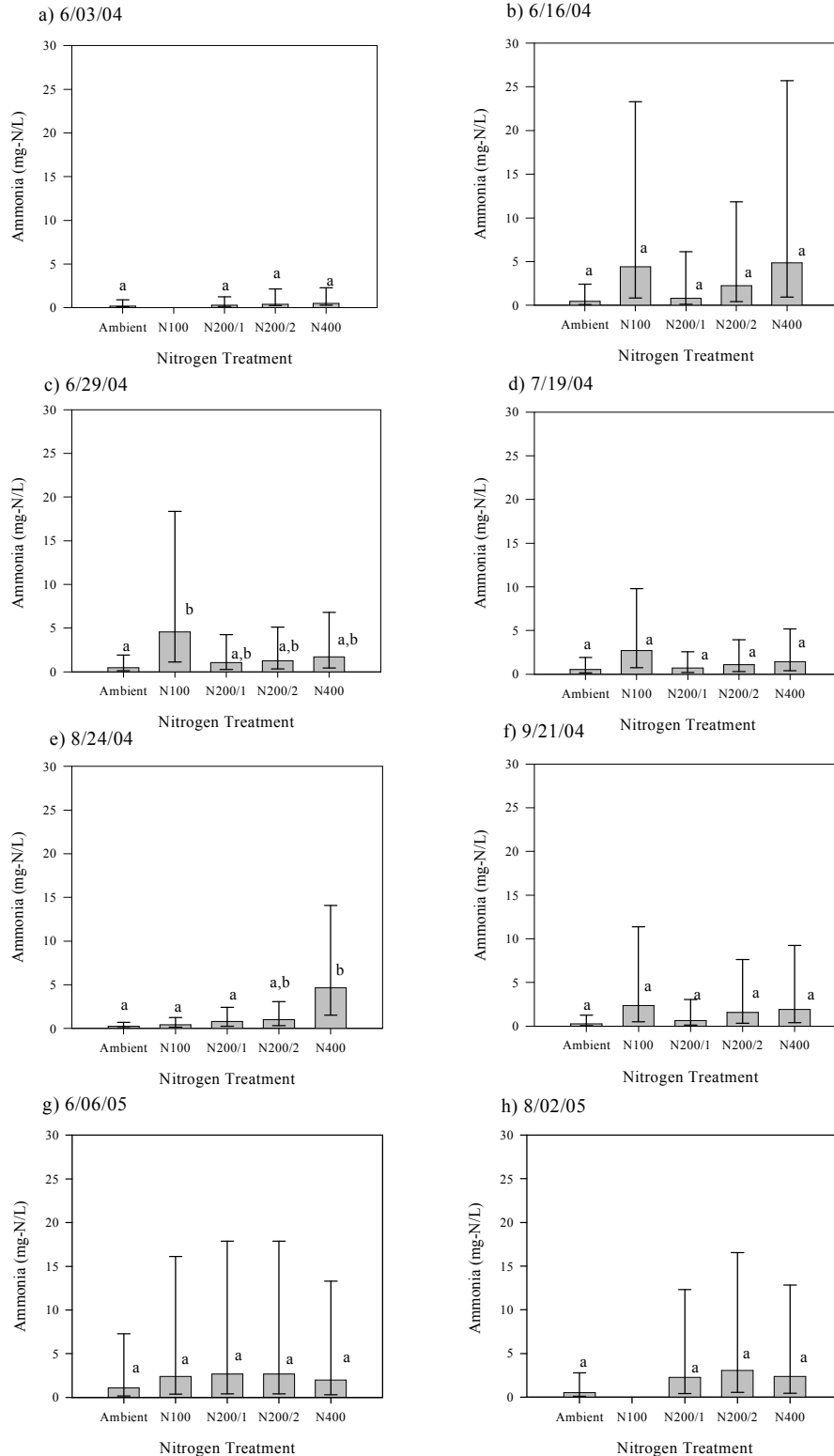


Figure 3.1.8. Geometric mean of ammonia concentrations (\pm 95% CL) of the *Phragmites*-absent site according to nitrogen treatment over the 2004-5 growing seasons. Treatments with different letters indicate a significant difference between treatments ($p < 0.05$). Log ammonia concentration was the dependent variable in the one-way ANOVA model with an LSD contrast. Sample date 8/02/05 had several missing NH_3 concentrations.

3.1.3 Fertilization and Site Effects on NO₃

Urea application increased nitrate concentrations at the *Phragmites*-dominant site on particular sample dates (Figure 3.1.9), while treatment differences were harder to distinguish at the *Phragmites*-absent site (Figure 3.1.10). Analysis proved that both time and site affected sub-surface nitrate concentrations (Table 3.1.7), so site, then time effects were isolated for the analysis. When individual sites were studied, only the *Phragmites*-absent site displayed a seasonal effect (Table 3.1.8). When individual dates were studied, only the end of the growing season (July – September) displayed a site effect (Table 3.1.9).

Table 3.1.7. Repeated measures ANOVA model for 2004 NO₃ concentrations. * <0.01, ** < 0.05, * < 0.10**

Source	Type III SS	df	MS	F	Sig
Site	11.58	1	11.58	3.84	0.069*
Trt	1.40	4	0.35	0.12	0.975
Site * Trt	2.03	4	0.51	0.17	0.951
Error	45.25	15	3.02		
Time	57.21	5	11.44	20.05	0.000***
Time * Site	5.33	5	1.07	1.87	0.110
Time * Trt	11.32	20	0.57	0.99	0.482
Time * Site * Trt	15.96	20	0.80	1.40	0.150
Error (time)	42.80	75	0.57		

Table 3.1.8. ANOVA model: Trt + Time + (Trt*Time) for each marsh site for NO₃. * <0.01, ** < 0.05, * < 0.10. PD site = *Phragmites*-dominant site; PA site = *Phragmites*-absent site**

Site	Source	Type III SS	df	MS	F	Sig
PD site	Trt	2.80	4	0.70	0.11	0.977
	Time	7.45	4	1.86	2.09	0.109
	Time * Trt	20.13	16	1.26	1.41	0.207
	Error	24.97	28	0.89		
PA site	Trt	1.27	4	0.32	0.31	0.861
	Time	3.24	4	0.81	2.95	0.035**
	Time * Trt	4.12	16	0.26	0.94	0.539
	Error	8.78	32	0.27		

Table 3.1.9. ANOVA model: Site + Trt + (Site*Trt) at all sample dates for NO₃. * <0.01, ** < 0.05, * < 0.10**

Date	Source	Type III SS	df	MS	F	Sig
6/16/2004	Trt	2.55	4	0.64	0.84	0.520
	Site	1.57	1	1.57	2.06	0.168
	Trt*Site	1.63	4	0.41	0.53	0.713
	Error	13.72	18	0.76		
6/29/2004	Trt	1.01	4	0.25	0.26	0.898
	Site	1.73	1	1.73	1.81	0.198
	Trt*Site	2.48	4	0.62	0.65	0.637
	Error	15.35	16	0.96		
7/19/2004	Trt	18.49	4	4.62	1.59	0.215
	Site	16.13	1	16.13	5.56	0.029**
	Trt*Site	17.87	4	4.47	1.54	0.229
	Error	58.05	20	2.90		
8/24/2004	Trt	2.01	4	0.50	0.46	0.765
	Site	8.97	1	8.97	8.17	0.010**
	Trt*Site	1.65	4	0.41	0.38	0.824
	Error	21.96	20	1.10		
9/21/2004	Trt	3.73	4	0.93	1.33	0.295
	Site	5.38	1	5.38	7.64	0.012**
	Trt*Site	4.19	4	1.05	1.49	0.243
	Error	14.07	20	0.70		

Nitrogen effects on nitrate concentrations were then analyzed at individual sites on each sample date in 2004-5 (Figures 3.1.0 and 3.1.10). At the *Phragmites*-dominant site, only two dates displayed a nitrogen effect. Nitrate concentration for N400 was low at the end of the 2004 season and high at the beginning of the 2005 season (Figure 3.1.9). On sample date 8/02/05, several nitrate concentrations were missing and a nitrogen contrast could not be conducted. At the *Phragmites*-absent site, no differences in nitrate concentrations among nitrogen treatments were detected in the 2004-5 growing seasons (Figure 3.1.10).

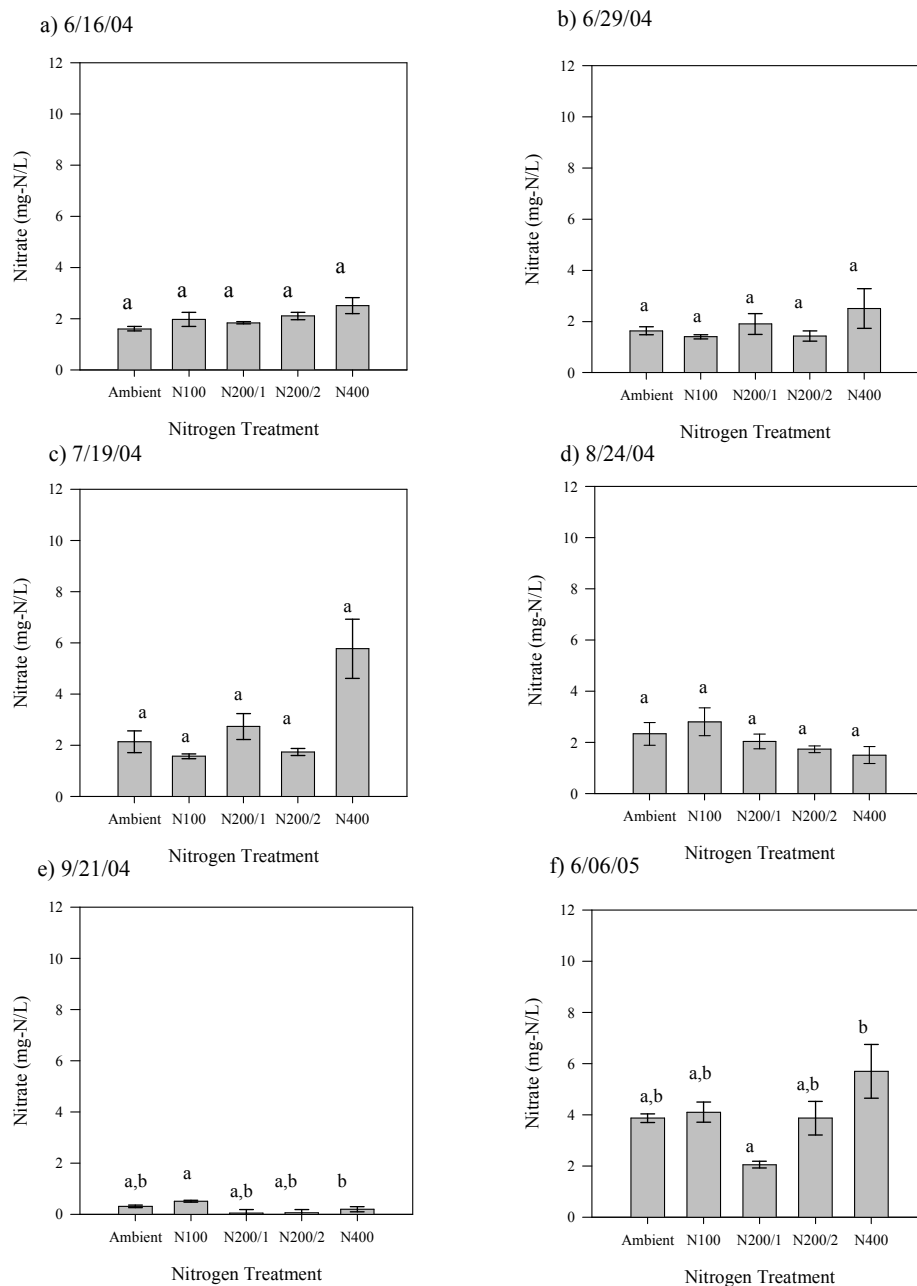


Figure 3.1.9. Mean nitrate concentrations and standard errors of the *Phragmites*-dominant site according to nitrogen treatment over the 2004-5 growing seasons. Treatments with different letters indicate a significant difference between treatments ($p=0.05$). Nitrate concentration was the dependent variable in the one-way ANOVA model against treatment with an LSD contrast.

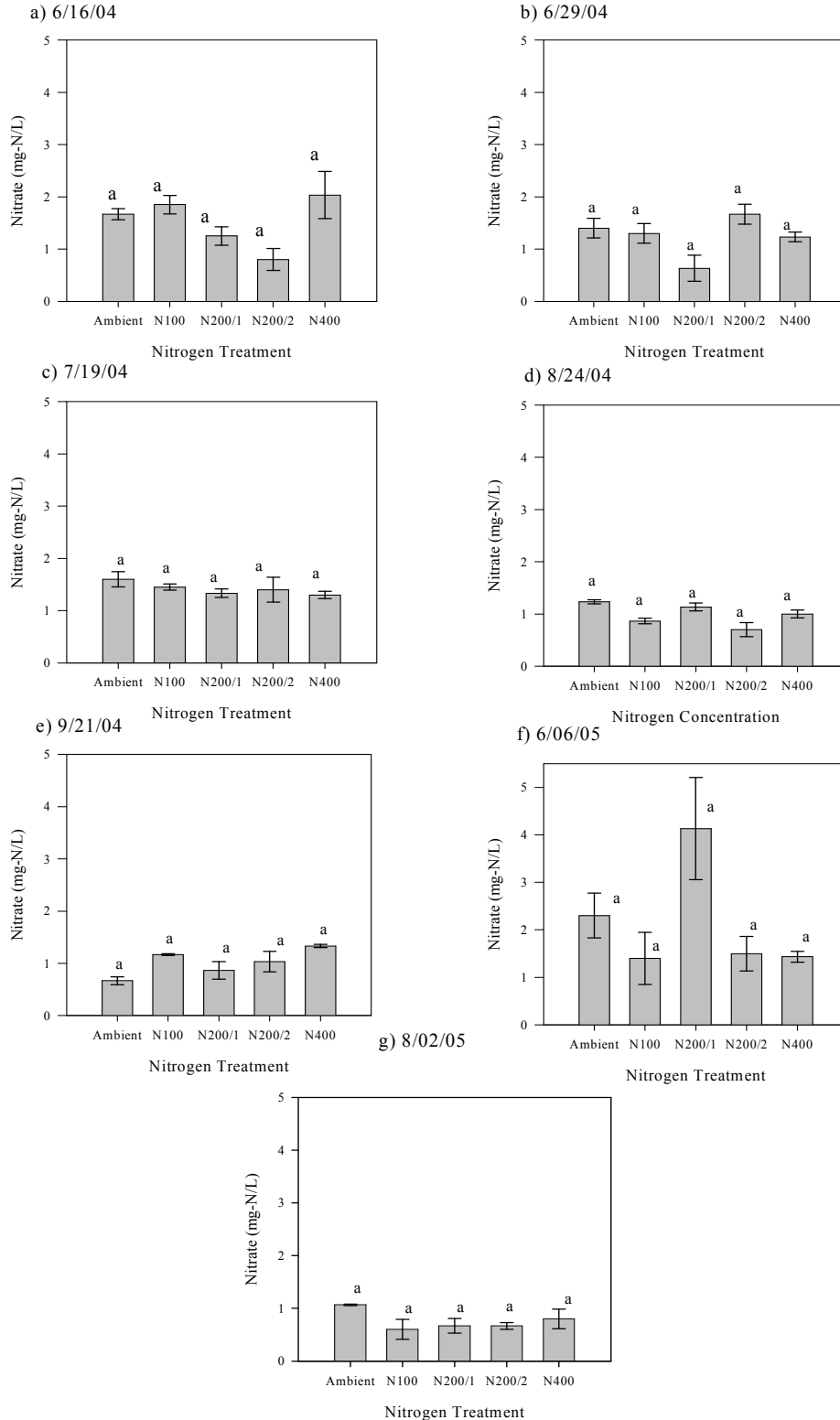


Figure 3.1.10. Mean nitrate concentrations and standard errors of the *Phragmites*-absent site according to nitrogen treatment over the 2004-5 growing seasons. Treatments with different letters indicate a significant difference between treatments ($p=0.05$). Nitrate concentration was the dependent variable in the one-way ANOVA model with an LSD contrast.

3.1.4 Fertilization and Site Effects on Total Nitrogen

The addition of urea increased total nitrogen at the *Phragmites*-dominant site on particular dates (Figure 3.1.11), but did not conclusively change total nitrogen at the *Phragmites*-absent site (Figure 3.1.12). Not only did each site's total nitrogen levels respond differently to additional urea, but there was also a clear seasonal effect at each site (Table 3.1.11). Time had an interaction effect with both site and treatment (Table 3.1.10). Analysis of time, nitrogen, and their interaction at each marsh site found that time was significant at both sites (Table 3.1.11). Analysis of nitrogen, site, and their interaction analyzed on each 2004 sample date found that no site*treatment interaction effect was significant on 6/29/04 and 7/19/04 (Table 3.1.12).

Table 3.1.10. Repeated measures ANOVA model for 2004 total nitrogen concentrations. * <0.01, ** < 0.05, * < 0.10**

Source	Type III SS	df	MS	F	Sig
Site	1890.10	1	1890.10	3.08	0.097
Trt	7391.14	4	1847.78	3.01	0.048
Site * Trt	7012.22	4	1753.05	2.86	0.056
Error	10437.41	17	613.97		
Time	6948.40	5	1389.68	18.73	0.000
Time * Site	1431.03	5	286.21	3.86	0.003
Time * Trt	2707.80	20	135.39	1.83	0.030
Time * Site * Trt	2486.99	20	124.35	1.68	0.054*
Error (time)	6305.78	85	74.19		

Table 3.1.11 ANOVA model: Trt + Time + (Trt*Time) at each marsh site for total nitrogen.
 *** <0.01, ** < 0.05, * < 0.10. PD site = *Phragmites*-dominant site; PA site = *Phragmites*-absent site

Site	Source	Type III		MS	F	Sig
		SS	df			
PD site	Trt	12239.13	4	3059.78	2.46	0.130
	Time	6330.03	5	1266.01	9.22	0.000***
	Time * Trt	4220.04	20	211.00	1.54	0.122
	Error	9968.66	8	1246.08		
PA site	Trt	341.02	4	85.25	1.64	0.247
	Time	1854.83	5	370.97	20.47	0.000***
	Time * Trt	428.74	20	21.44	1.18	0.312
	Error	468.75	9	52.08		

Table 3.1.12. ANOVA model: Site + Trt + (Site*Trt) at all sample dates for total nitrogen.
 *** <0.01, ** < 0.05, * < 0.10

Date	Source	Type III		MS	F	Sig
		SS	df			
6/16/2004	Trt	1523.83	4	380.96	1.61	0.214
	Site	206.36	1	206.36	0.87	0.363
	Trt*Site	1811.72	4	452.93	1.91	0.150
	Error	4507.03	19	237.21		
6/29/2004	Trt	2276.60	4	569.15	3.07	0.043
	Site	843.86	1	843.86	4.55	0.047
	Trt*Site	2533.80	4	633.45	3.42	0.030**
	Error	3335.16	18	185.29		
7/19/2004	Trt	285.19	4	71.30	2.37	0.087
	Site	56.72	1	56.72	1.89	0.185
	Trt*Site	408.94	4	102.23	3.40	0.028**
	Error	601.50	20	30.08		
8/24/2004	Trt	1412.81	4	353.20	1.12	0.376
	Site	826.87	1	826.87	2.62	0.121
	Trt*Site	1137.19	4	284.30	0.90	0.483
	Error	6318.75	20	315.94		
9/21/2004	Trt	1915.31	4	478.83	1.55	0.227
	Site	480.00	1	480.00	1.55	0.227
	Trt*Site	1005.94	4	251.48	0.81	0.532
	Error	6187.50	20	309.38		

Mean total nitrogen contrasts did not exhibit homogeneity of sample variances, so a log (base 10) transform was performed on the data to improve variance equality. A time*site interaction, as well as a site*treatment interaction on log of total nitrogen concentrations (Table 3.1.13) demonstrated the need to analyze nitrogen effects at individual sites for each sample date. When nitrogen and time were analyzed at each marsh site, both were significant at the *Phragmites*-dominant site (Table 3.1.14). When nitrogen and site were analyzed on each date, a site effect was observed on 8/24/04 and a nitrogen effect was found on 9/21/04 (Table 3.1.15).

Table 3.1.13. Repeated measures ANOVA model for 2004 Log (TKN) concentrations. * <0.01, ** < 0.05, * < 0.10**

Source	Type III SS	df	MS	F	Sig
Site	0.22	1	0.22	1.26	0.277
Trt	2.29	4	0.57	3.28	0.036
Site * Trt	1.76	4	0.44	2.53	0.079*
Error	2.96	17	0.17		
Time	0.66	4	0.16	5.43	0.001
Time * Site	0.74	4	0.18	6.10	0.000***
Time * Trt	0.31	16	0.02	0.65	0.830
Time * Site * Trt	0.51	16	0.03	1.06	0.413
Error (time)	2.05	68	0.03		

Table 3.1.14 ANOVA model: Trt + Time + (Trt*Time) at each marsh site for Log (TKN). * <0.01, ** < 0.05, * < 0.10. PD site = *Phragmites*-dominant site; PA site = *Phragmites*-absent site**

Site	Source	Type III SS	df	MS	F	Sig
PD site	Trt	3.27	4	0.82	2.82	0.099*
	Time	1.15	4	0.29	9.92	0.000***
	Time * Trt	0.38	16	0.02	0.82	0.656
	Error	0.93	32	0.03		
PA site	Trt	0.31	4	0.08	1.07	0.426
	Time	0.20	4	0.05	1.63	0.187
	Time * Trt	0.44	16	0.03	0.88	0.594
	Error	1.13	36	0.03		

Table 3.1.15. ANOVA model: Site + Trt + (Site*Trt) at all sample dates for Log (TKN). * <0.01, ** < 0.05, * < 0.10**

Date	Source	Type III SS	df	MS	F	Sig
6/16/2004	Trt	0.48	4	0.12	2.21	0.107
	Site	0.01	1	0.01	0.10	0.757
	Trt*Site	0.45	4	0.11	2.09	0.122
	Error	1.03	19	0.05		
6/29/2004	Trt	0.47	4	0.12	1.60	0.217
	Site	0.16	1	0.16	2.15	0.159
	Trt*Site	0.63	4	0.16	2.12	0.120
	Error	1.33	18	0.07		
7/19/2004	Trt	0.25	4	0.06	1.81	0.168
	Site	0.32	1	0.32	9.32	0.007
	Trt*Site	0.46	4	0.12	3.34	0.031**
	Error	0.66	19	0.03		
8/24/2004	Trt	0.28	4	0.07	1.10	0.382
	Site	0.32	1	0.32	5.06	0.036**
	Trt*Site	0.16	4	0.04	0.65	0.631
	Error	1.26	20	0.06		
9/21/2004	Trt	0.66	4	0.16	2.32	0.092*
	Site	0.08	1	0.08	1.11	0.304
	Trt*Site	0.19	4	0.05	0.66	0.627
	Error	1.41	20	0.07		

Since the effect of nitrogen treatment on log of total nitrogen concentrations was sensitive to time and site, nitrogen treatment effects were evaluated on individual dates at each site. Mean log total nitrogen concentrations for the *Phragmites*-dominant site showed several nitrogen effects. Specifically N400 produced higher log nitrogen concentrations than other treatments for the majority of the 2004 growing season (Figure 3.1.11). At the *Phragmites*-absent site, N100 had a higher log total nitrogen concentration than other treatments on 6/16/04 and 7/19/04, possibly due to a break in the dialysis tube at one of the N100 plots (Figure 3.1.12a and c).

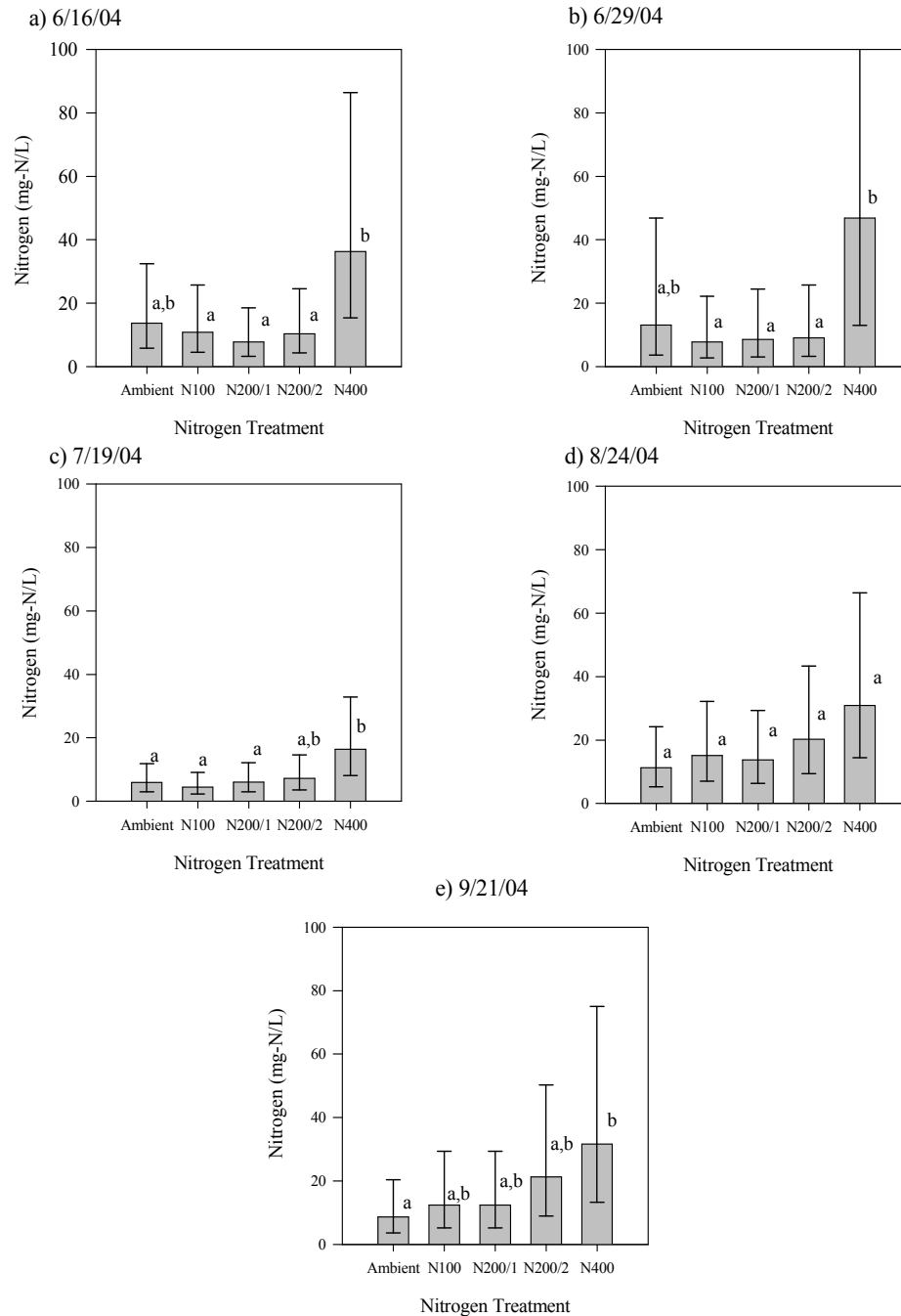


Figure 3.1.11. Geometric mean of total nitrogen concentrations (\pm 95% CL) of the *Phragmites*-dominant site according to nitrogen treatment over the 2004-5 growing seasons. Treatments with different letters indicate a significant difference between treatments ($p=0.05$). Log total nitrogen concentration was the dependent variable in the one-way ANOVA model against treatment with an LSD contrast.

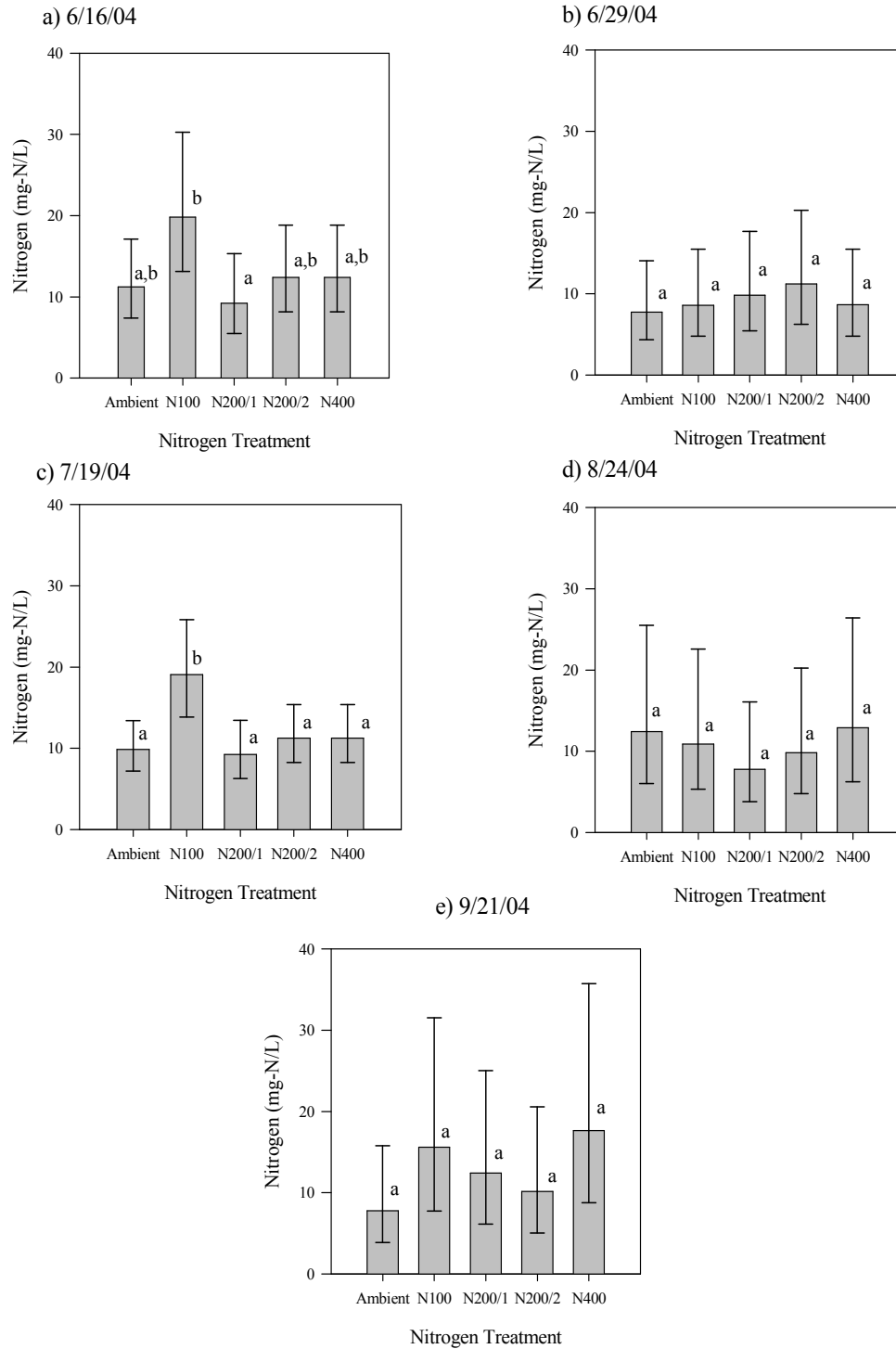


Figure 3.1.12. Geometric mean of total nitrogen concentrations (\pm 95% CL) of the *Phragmites*-absent site according to nitrogen treatment over the 2004-5 growing seasons. Treatments with different letters indicate a significant difference between treatments ($p=0.05$). Log total nitrogen concentration was the dependent variable in the one-way ANOVA model with an LSD contrast.

3.1.5 Fertilization and Site Effects on Total Phosphorus

Addition of nitrogen did not change total phosphorus levels throughout the experimental study period. Time, however, had an effect on phosphorus (Table 3.1.16), so nitrogen and site effects were analyzed on each sample date in 2004-5 (Table 3.1.17). No nitrogen or site effects on total phosphorus were determined on any 2004-5 sample date (Table 3.1.17).

Table 3.1.16. Repeated measures ANOVA model for 2004 TP concentrations. * <0.01, ** < 0.05, * < 0.10**

Source	Type III SS	df	MS	F	Sig
Site	0.10	1	0.10	0.14	0.716
Trt	1.90	4	0.47	0.66	0.628
Site * Trt	2.33	4	0.58	0.81	0.535
Error	11.47	16	0.72		
Time	22.72	5	4.54	7.79	0.000***
Time * Site	0.82	5	0.16	0.28	0.922
Time * Trt	8.67	20	0.43	0.74	0.769
Time * Site * Trt	4.26	20	0.21	0.37	0.993
Error (time)	46.65	80	0.58		

Table 3.1.17. ANOVA model: Site + Trt + (Site*Trt) at all sample dates for TP. * <0.01, ** < 0.05, * < 0.10**

Date	Source	Type III SS	df	MS	F	Sig
6/3/2004	Trt	0.08	4	0.02	0.65	0.634
	Site	0.05	1	0.05	1.86	0.188
	Trt*Site	0.16	4	0.04	1.32	0.296
	Error	0.59	20	0.03		
6/16/2004	Trt	6.67	4	1.67	0.49	0.746
	Site	0.31	1	0.31	0.09	0.766
	Trt*Site	4.11	4	1.03	0.30	0.875
	Error	65.21	19	3.43		
6/29/2004	Trt	0.27	4	0.07	0.57	0.688
	Site	0.00	1	0.00	0.01	0.920
	Trt*Site	0.51	4	0.13	1.08	0.398
	Error	2.02	17	0.12		

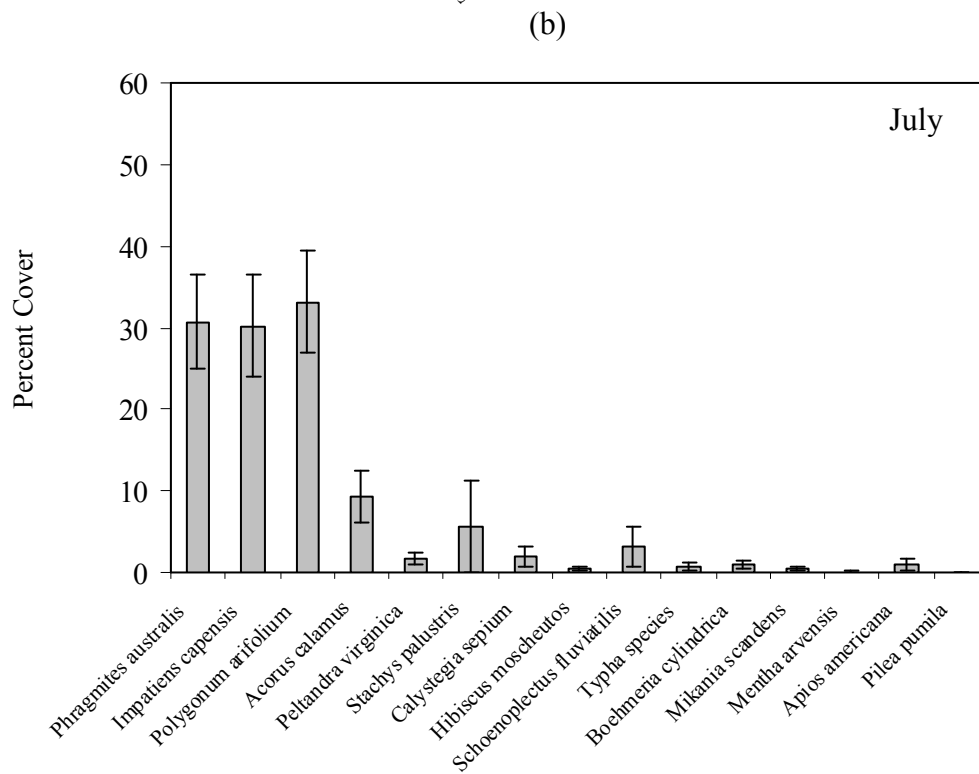
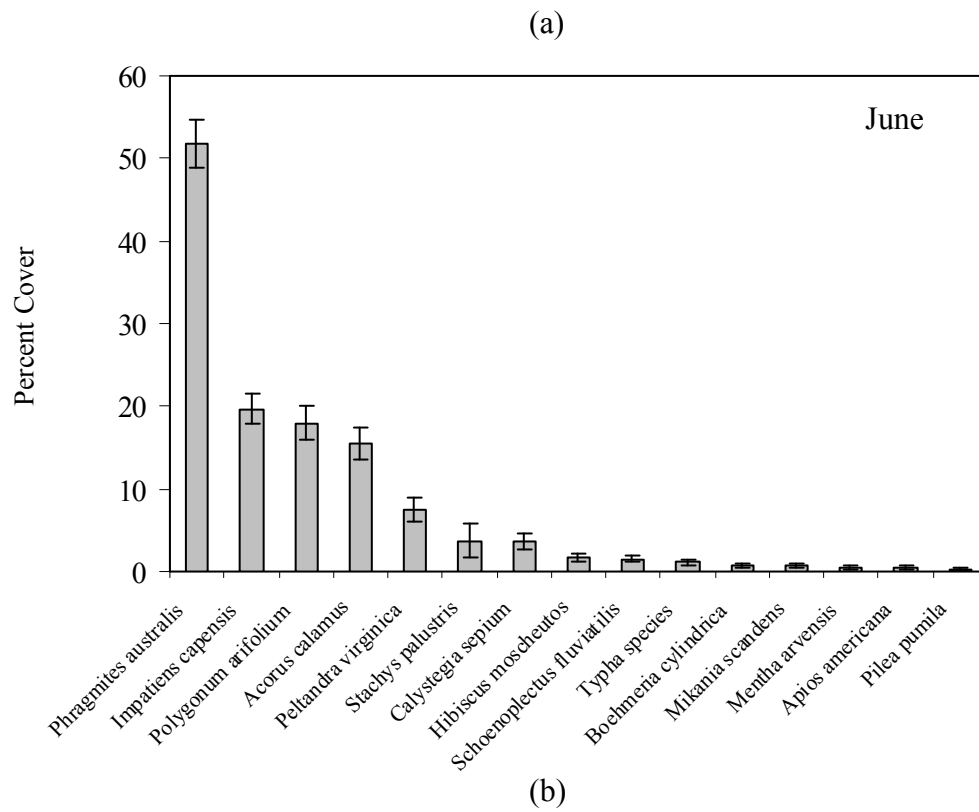
Date	Source	Type III SS	df	MS	F	Sig
7/19/2004	Trt	0.03	4	0.01	0.34	0.851
	Site	0.00	1	0.00	0.00	0.972
	Trt*Site	0.19	4	0.05	2.01	0.131
	Error	0.48	20	0.02		
8/24/2004	Trt	0.02	4	0.01	0.62	0.656
	Site	0.03	1	0.03	2.74	0.113
	Trt*Site	0.02	4	0.00	0.39	0.812
	Error	0.20	20	0.01		
9/21/2004	Trt	0.02	4	0.01	0.74	0.578
	Site	0.02	1	0.02	2.46	0.133
	Trt*Site	0.06	4	0.02	1.89	0.151
	Error	0.17	20	0.01		

3.2 Marsh Vegetation Composition

Nitrogen fertilization affected species differently. For some species, such as *P. australis*, *P. virginica*, *Typha* species, and dead material, cover was low for high additions of nitrogen as urea. Other species, like *A. calamus*, *P. arifolium*, and *I. capensis* had a low cover for a slight addition of nitrogen that increased with high nitrogen fertilization. Both leaf area index and species richness were high for a large addition of nitrogen.

3.2.1 Pattern of dominant species over the growing season at each site

The vegetation at the tidal freshwater marsh was very diverse, with at least forty species identified during the growing season. Along with a high diversity, the vegetation composition changed seasonally as cover of early dominant species was reduced and minor species became the more widespread. Figure 3.2.1 illustrates the diversity of the *Phragmites*-dominant site and the changes in dominant species as the summer progressed. In June, *Phragmites australis* was clearly the dominant species at the *Phragmites*-dominant site (Figure 3.2.1a), but in July both *Impatiens capensis* and *Polygonum arifolium* had equal percent covers to *P. australis* (Figure 3.2.1b) and by August *P. arifolium* was more prominent than both *P. australis* and *I. capensis* at the site (Figure 3.2.1c). As *P. arifolium* began to senesce in September, *I. capensis* became the dominant species (Figure 3.2.1d). By September, a few species that had minor representation early in the season became more prevalent (~ 10% cover) (Figure 3.2.1d).



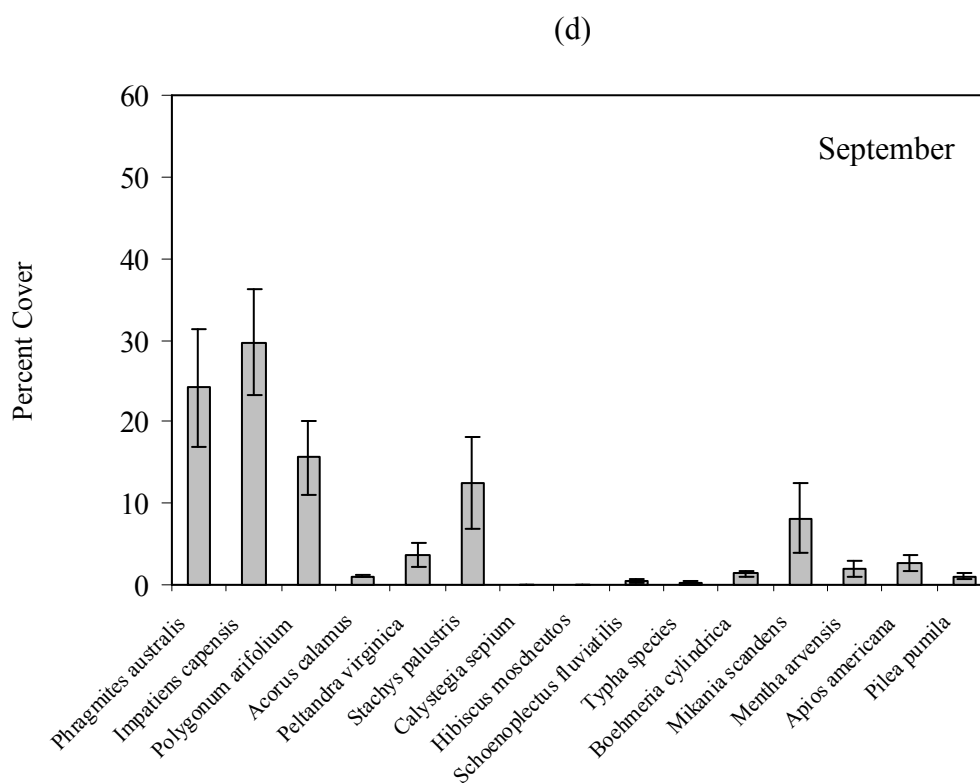
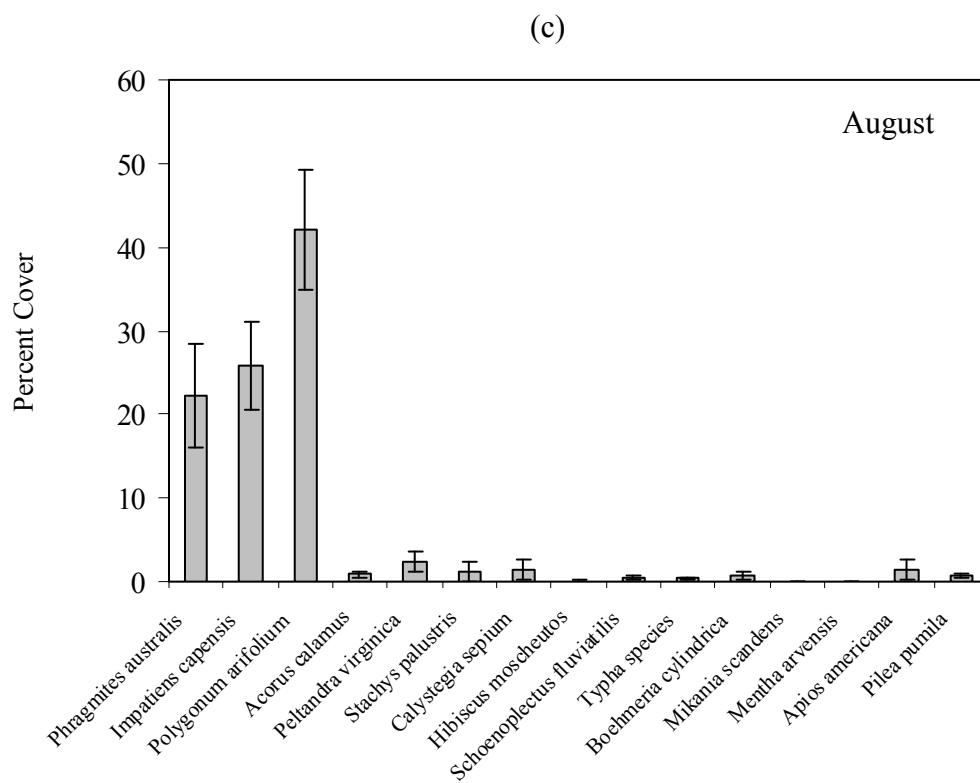
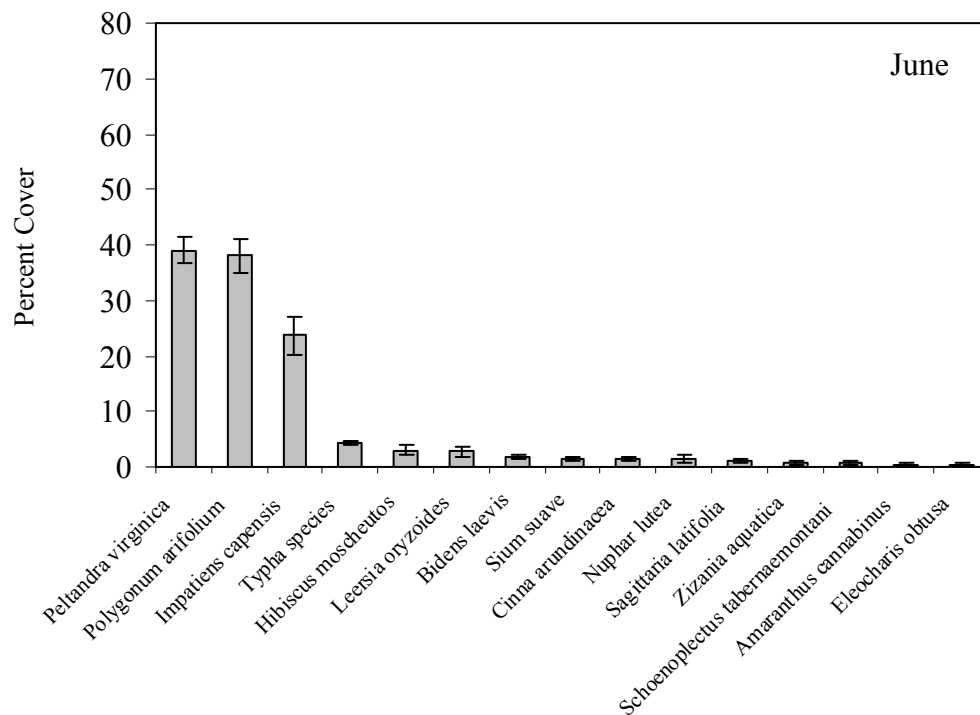


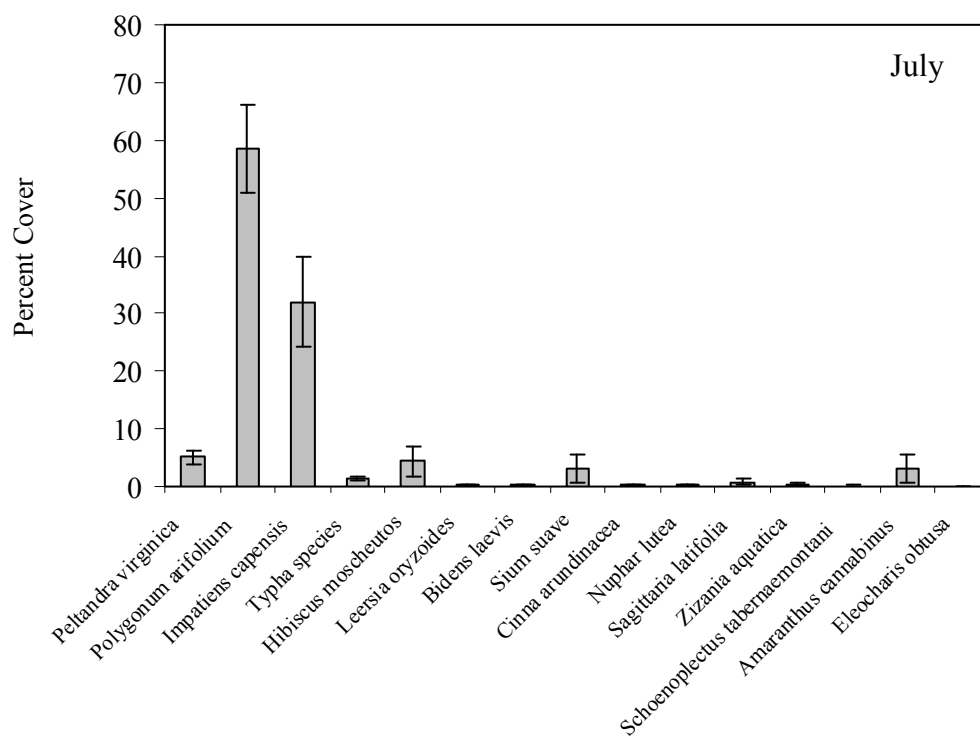
Figure 3.2.1. Mean percent cover of all species in each plot at the *Phragmites*-dominant site (plots = 15) in (a) June, (b) July, (c) August, and (d) September of 2004.

Not only did the marsh have high species richness, but each marsh site had a very different vegetation composition. The *Phragmites*-absent site had no *P. australis*, but instead was dominated by *P. virginica* and *P. arifolium* in June (Figure 3.2.2a). In July, *P. virginica* had been out-competed by *P. arifolium* and *I. capensis* (Figure 3.2.2b), and by August, almost every species had been out-competed by *P. arifolium* (Figure 3.2.2c). All species were senescing in September, although *P. arifolium* was still the dominant species at the *Phragmites*-absent site (Figure 3.2.2d).

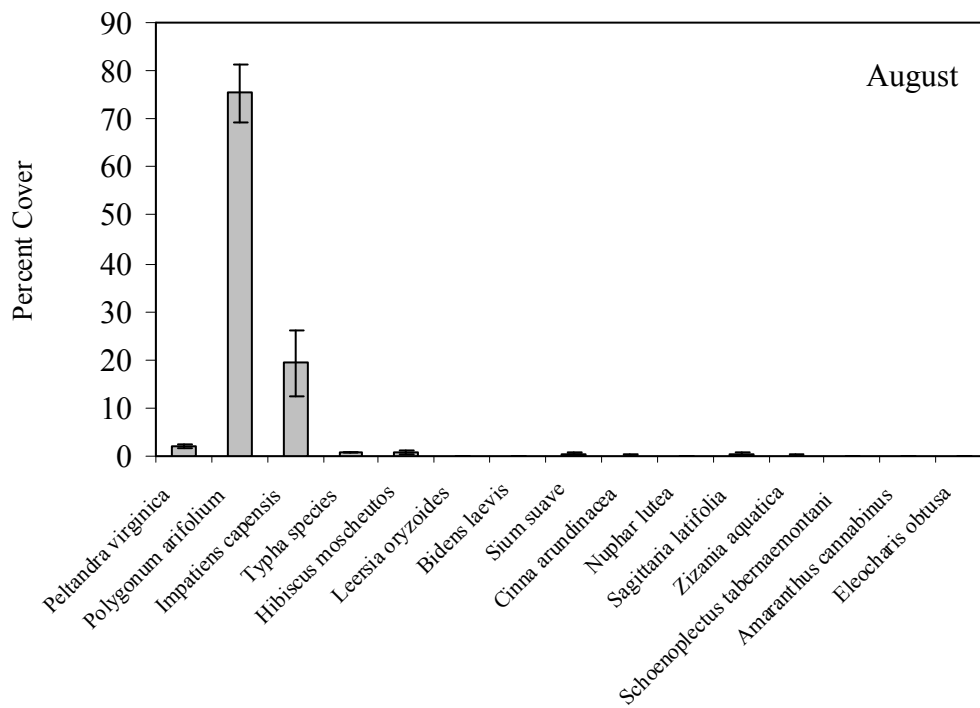
(a)



(b)



(c)



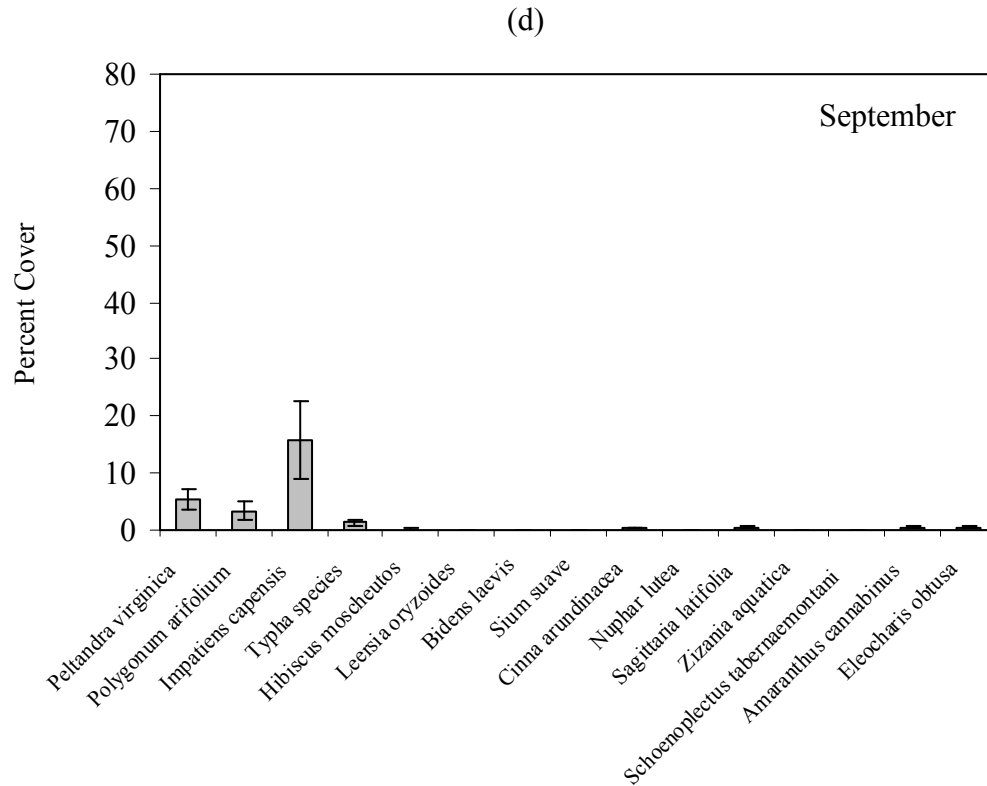


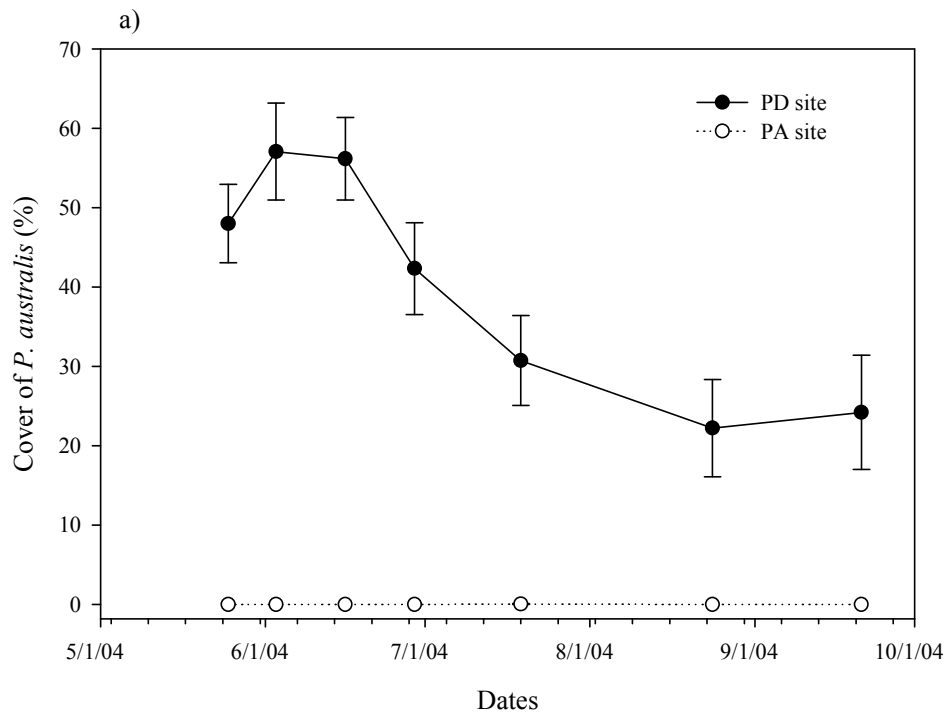
Figure 3.2.2. Mean percent cover of all species in each plot at the *Phragmites*-absent site (plots = 15) in (a) June, (b) July, (c) August, and (d) September of 2004.

3.2.2 Fertilization effects on vegetation cover

To determine if nitrogen fertilization affected vegetation composition, six prominent species, *Phragmites australis*, *Polygonum arifolium*, *Impatiens capensis*, *Typha* species, *Acorus calamus*, and *Peltandra virginica*, were chosen for analysis of nitrogen treatment effects. These species were in the top four dominant species at each site (see Figures 3.2.1a and 3.2.2a). In addition to analyzing nitrogen effects on species, we analyzed whether nitrogen affected leaf area index, species richness, percent cover of dead material, and species diversity.

Effects on P. australis

Evaluation of nitrogen effects on *P. australis* began by determining the effect of site and time on the species. Since the marsh sites were categorized as either dominated by *Phragmites* or devoid of *Phragmites*, there was a clear difference in *P. australis* cover between sites (Figure 3.2.3). The treatment and time effects were evaluated for the *Phragmites*-dominant site, and although no treatment effect was observed, time affected *P. australis* cover (Table 3.2.1), suggesting that nitrogen effects be analyzed on individual sample dates.



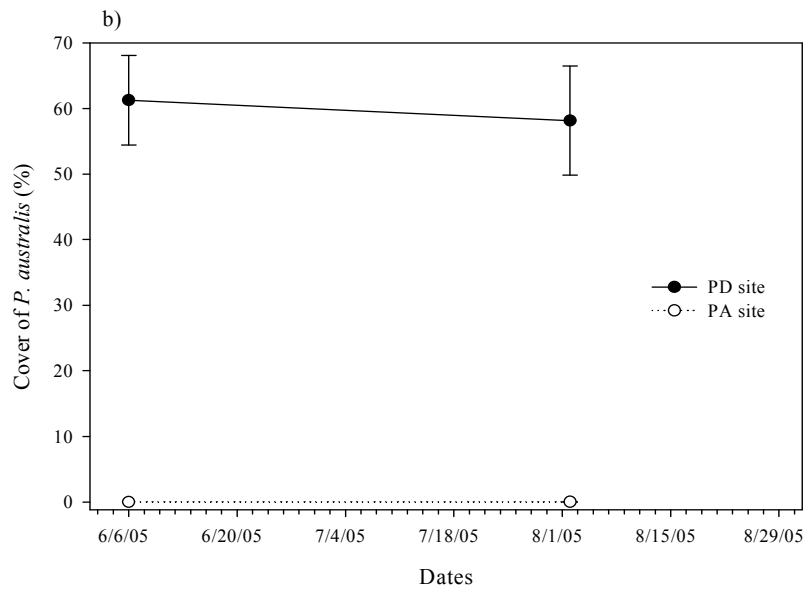
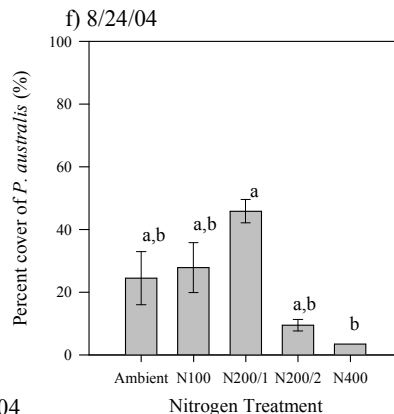
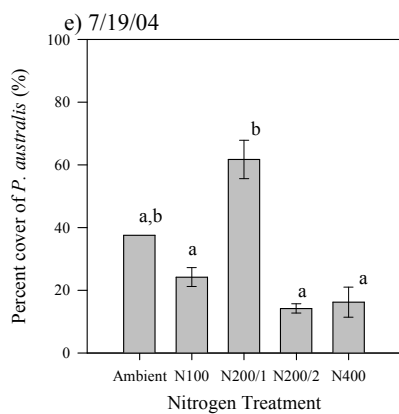
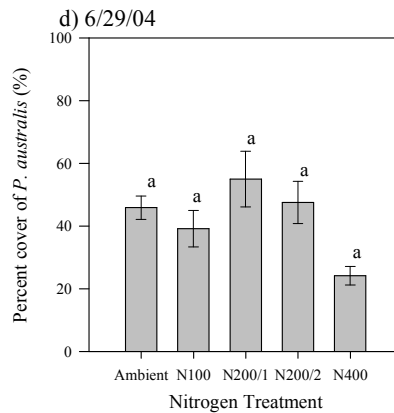
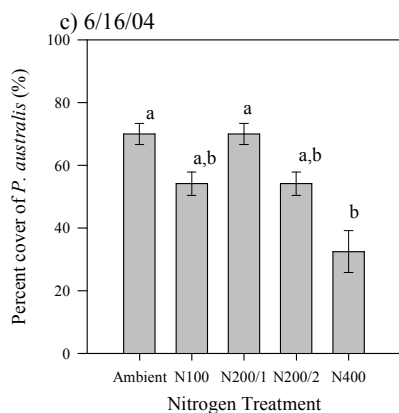
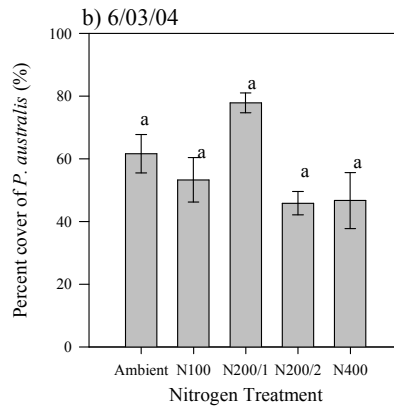
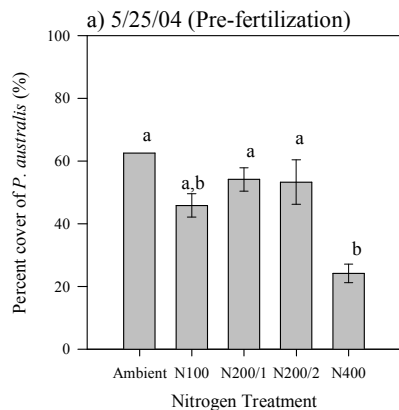


Figure 3.2.3. Mean percent cover and standard errors of *P. australis* for the *Phragmites*-dominant and *Phragmites*-absent sites across the (a) 2004 and (b) 2005 growing seasons.

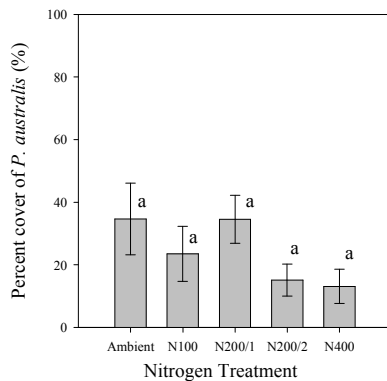
Table 3.2.1 ANOVA model: Trt + Time + (Trt*Time) of *P. australis* percent cover for the *Phragmites*-dominant site. *** <0.01, ** < 0.05, * < 0.10

Site	Source	Type III			F	Sig
		SS	df	MS		
PD site	Trt	14340.13	4	3585.03	1.69	0.228
	Time	19097.48	6	3182.91	16.18	0.000***
	Time * Trt	3956.40	24	164.85	0.84	0.677
	Error	11805.40	60	196.76		

Figure 3.2.4 shows nitrogen effect on *P. australis* percent cover for each sample date in 2004 and 2005 at the *Phragmites*-dominant site. In general throughout the growing season, *P. australis* percent cover was high for medium nitrogen fertilization (N200/1D) (Figure 3.2.4).



g) 9/21/04



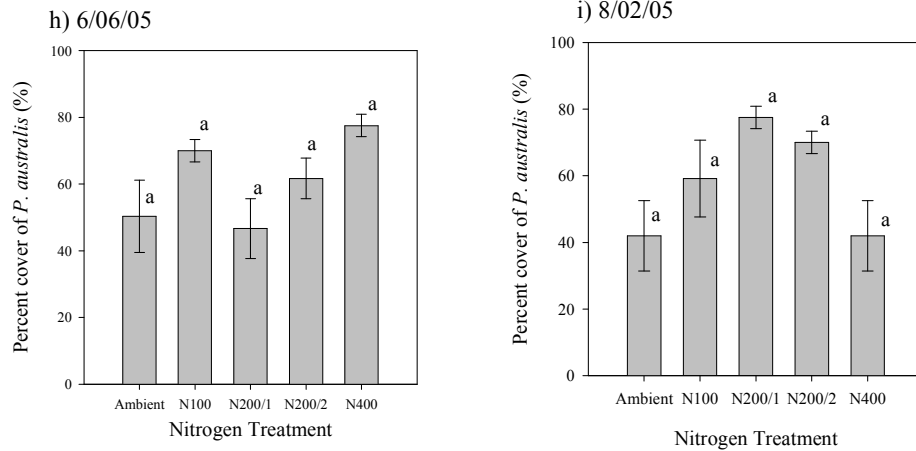


Figure 3.2.4. Mean *P. australis* percent cover and standard errors of the *Phragmites*-dominant site according to nitrogen treatment over the 2004-5 growing seasons. Treatments with different letters indicate a significant difference between treatments ($p < 0.05$). Percent *P. australis* was the dependent variable in the one-way ANOVA model, with an LSD contrast.

Effects on A. calamus

Seasonal and site effects influenced *A. calamus* cover. A clear site effect existed, as *A. calamus* was only found in trace amounts at the *Phragmites*-absent site, but up to 25% cover at the *Phragmites*-dominant site (Figure 3.2.5). Treatment and time analysis at the *Phragmites*-dominant site demonstrated that time did not interact with the treatment effect, but significantly affected *A. calamus* percent cover (Table 3.2.2). The direct seasonal effects on *A. calamus* cover illustrated *A. calamus* peaked on 6/16/04, then decreased in cover through 9/21/04 (Figure 3.2.5).

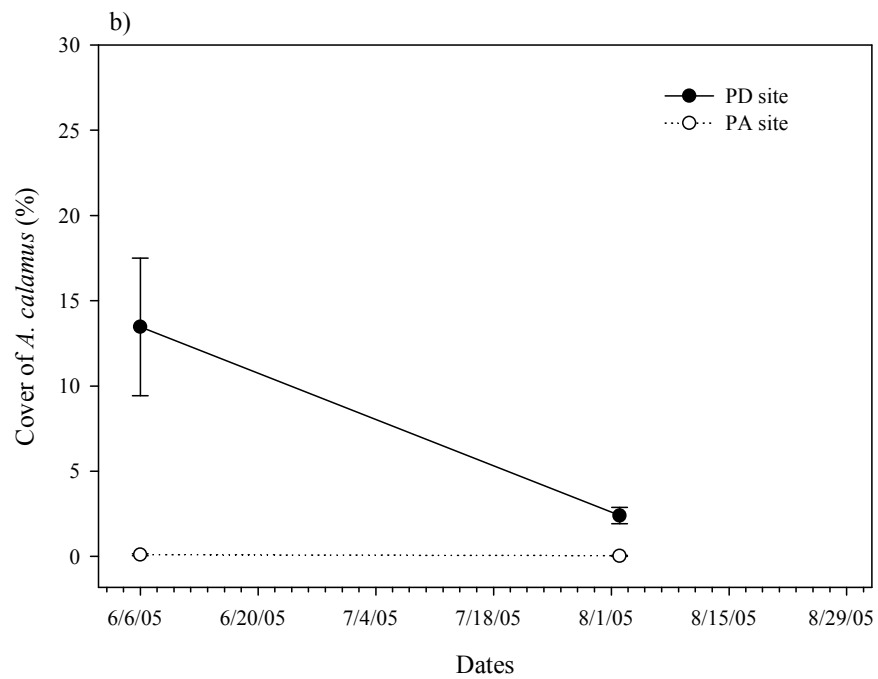
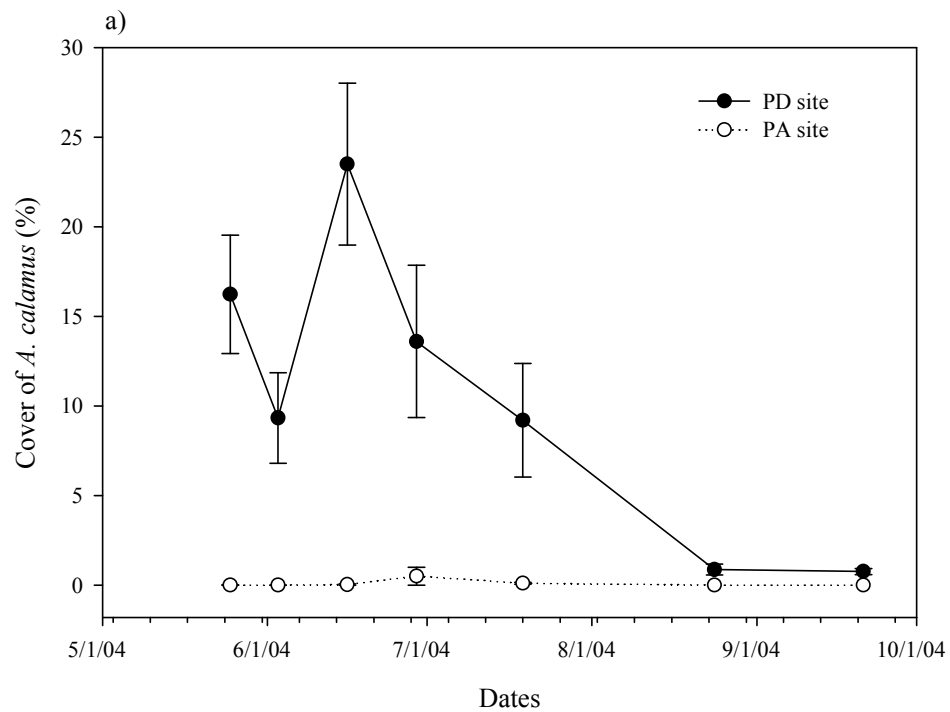
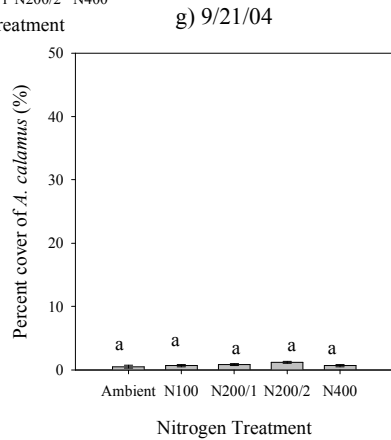
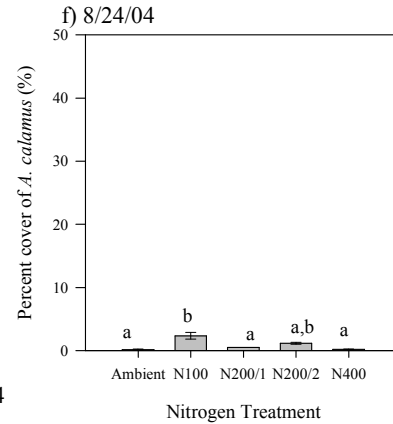
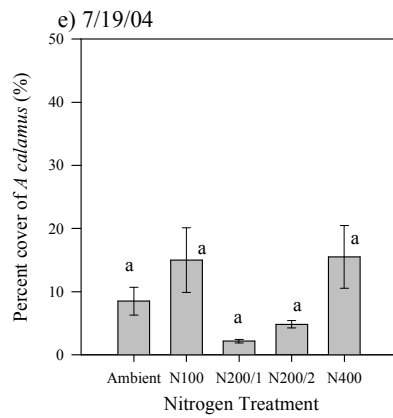
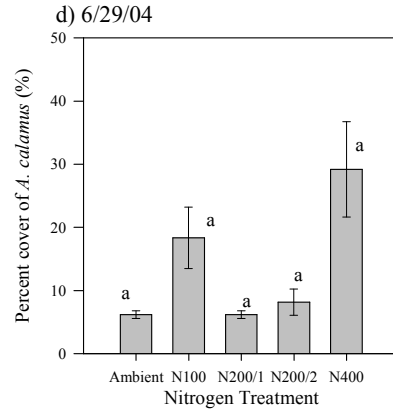
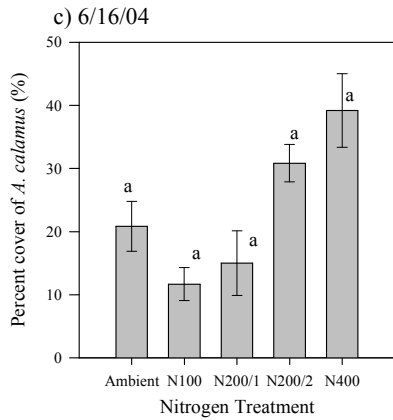
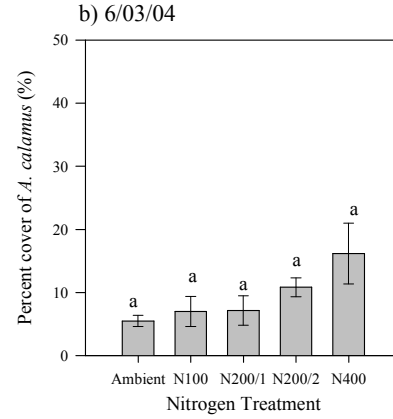
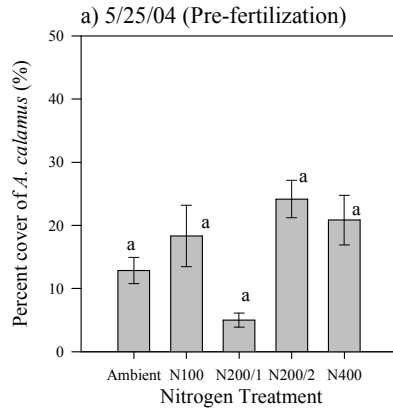


Figure 3.2.5. Mean percent cover and standard errors of *A. calamus* for the *Phragmites*-dominant and *Phragmites*-absent sites across the (a) 2004 and (b) 2005 growing seasons.

Table 3.2.2. ANOVA model: Trt + Time + (Trt*Time) at the *Phragmites*-dominant site for *A. calamus* percent cover. * <0.01, ** < 0.05, * < 0.10**

Site	Source	Type III SS	df	MS	F	Sig
PD site	Trt	1751.09	4	437.77	0.89	0.506
	Time	6030.10	6	1005.02	12.56	0.000***
	Time * Trt	2356.94	24	98.21	1.23	0.257
	Error	4802.35	60	80.04		

Nitrogen was not found to affect the cover of *A. calamus* during the majority of the growing season (Figure 3.2.6). However, when *A. calamus* cover was low (<10%) in the late season, there was a slight elevation in its cover for the lowest nitrogen treatment. In general, *A. calamus* percent cover was low for medium nitrogen fertilization and high for large urea applications.



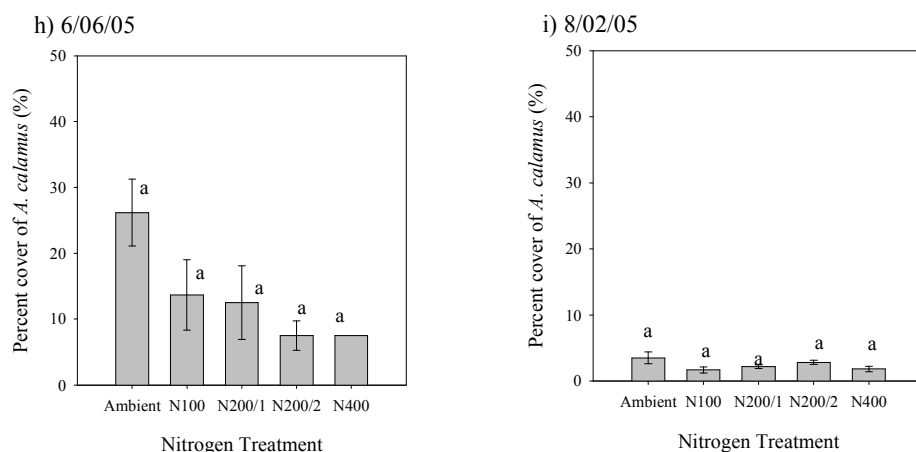


Figure 3.2.6. Mean *A. calamus* percent cover and standard errors of the *Phragmites*-dominant site according to nitrogen treatment over the 2004-5 growing seasons. Treatments with different letters indicate a significant difference between treatments ($p < 0.05$). Percent *A. calamus* was the dependent variable in the one-way ANOVA model, with an LSD contrast.

Effects on P. arifolium

Before nitrogen effects were analyzed on *P. arifolium*, site and time effects were evaluated. The *Phragmites*-absent site had a higher percent cover of *P. arifolium* than the *Phragmites*-dominant site for the majority of the season (Figure 3.2.7).

Upon analysis, the site*time interaction was significant (Table 3.2.3) and time had a strong effect at each site (Table 3.2.4), which indicated that each date and each site needed to be analyzed separately to detect nitrogen effects (Table 3.2.5). When site and nitrogen effects were analyzed on each sample date, *P. arifolium* cover was significantly different between the two marsh sites at every date except for the pre-fertilization date, 5/25/04.

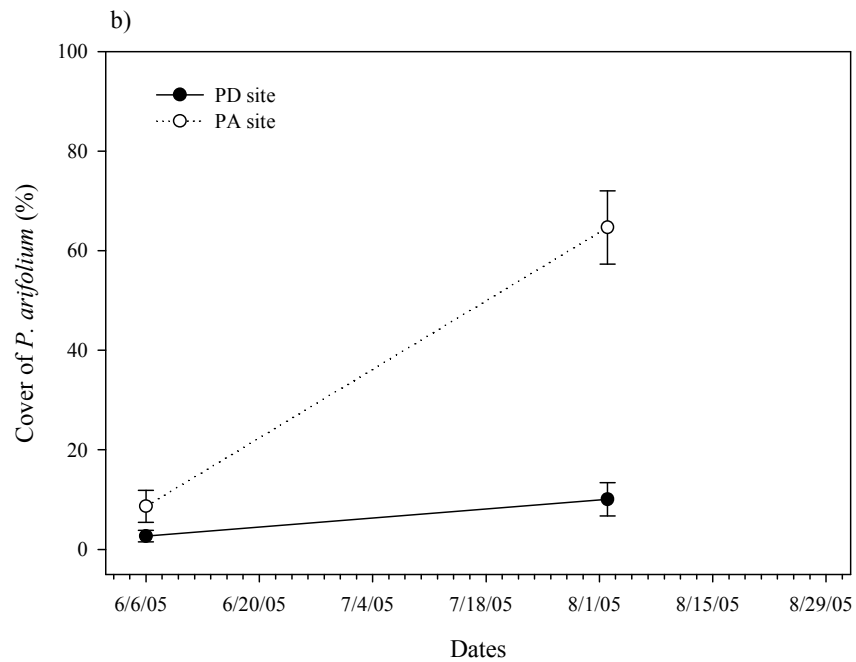
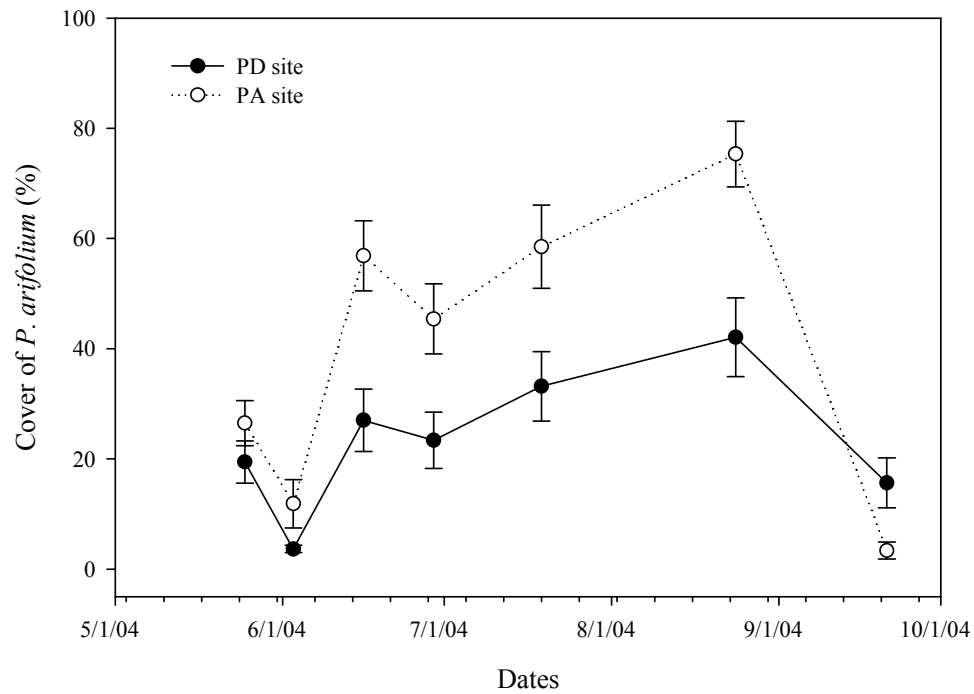


Figure 3.2.7. Mean percent cover and standard errors of *P. arifolium* for the *Phragmites*-dominant and *Phragmites*-absent sites across the (a) 2004 and (b) 2005 growing seasons.

Table 3.2.3 Repeated measures ANOVA model for 2004 *P. arifolium* populations. * <0.01, ** < 0.05, * < 0.10**

Source	Type III SS	df	MS	F	Sig
Site	12900.00	1	12900.00	7.80	0.012
Trt	3002.09	4	750.52	0.45	0.768
Site * Trt	5766.44	4	1441.61	0.87	0.499
Error	31404.83	19	1652.89		
Time	63362.18	6	10560.36	39.34	0.000
Time * Site	10248.99	6	1708.16	6.36	0.000***
Time * Trt	4037.68	24	168.24	0.63	0.907
Time * Site * Trt	5654.33	24	235.60	0.88	0.631
Error (time)	30598.87	114	268.41		

Table 3.2.4. ANOVA model: Trt + Time + (Trt*Time) at each marsh site for *P. arifolium* percent cover. * <0.01, ** < 0.05, * < 0.10**

Site	Source	Type III SS	df	MS	F	Sig
PD site	Trt	3227.29	4	806.82	0.54	0.708
	Time	12746.78	6	2124.46	7.14	0.000***
	Time * Trt	4127.70	24	171.99	0.58	0.929
	Error	16078.00	54	297.74		
PA site	Trt	6318.66	4	1579.67	0.87	0.512
	Time	63270.26	6	10545.04	43.57	0.000***
	Time * Trt	5463.87	24	227.66	0.94	0.551
	Error	14520.87	60	242.01		

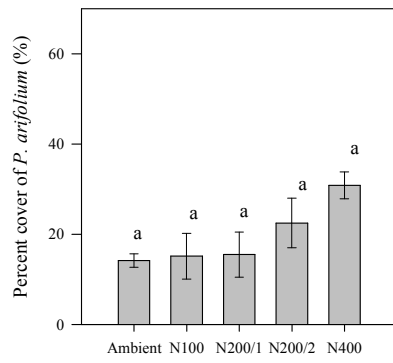
Table 3.2.5 ANOVA model: Site + Trt + (Site*Trt) at all sample dates for *P. arifolium*. * <0.01, ** < 0.05, * < 0.10**

Date	Source	Type III SS	df	MS	F	Sig
5/25/2004	Site	336.79	1	336.79	1.17	0.294
	Trt	537.08	4	134.27	0.47	0.760
	Site * Trt	366.11	4	91.53	0.32	0.863
	Error	5483.33	19	288.60		
6/3/2004	Site	508.41	1	508.41	3.83	0.064*
	Trt	653.33	4	163.33	1.23	0.330
	Site * Trt	860.13	4	215.03	1.62	0.208
	Error	2655.50	20	132.78		
6/16/2004	Site	6675.21	1	6675.21	13.41	0.002***
	Trt	2724.17	4	681.04	1.37	0.280
	Site * Trt	2513.33	4	628.33	1.26	0.318
	Error	9958.33	20	497.92		

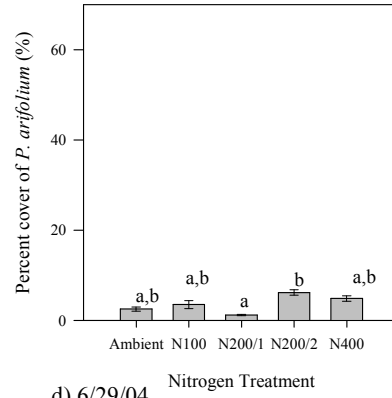
Date	Source	Type III SS	df	MS	F	Sig
6/29/2004	Site	3641.01	1	3641.01	6.88	0.016**
	Trt	352.80	4	88.20	0.17	0.953
	Site * Trt	3134.87	4	783.72	1.48	0.245
	Error	10585.17	20	529.26		
7/19/2004	Site	4813.33	1	4813.33	5.68	0.027**
	Trt	1937.42	4	484.35	0.57	0.686
	Site * Trt	1304.08	4	326.02	0.38	0.817
	Error	16938.83	20	846.94		
8/24/2004	Site	8300.03	1	8300.03	11.03	0.003***
	Trt	1196.13	4	299.03	0.40	0.808
	Site * Trt	1925.97	4	481.49	0.64	0.640
	Error	15050.67	20	752.53		
9/21/2004	Site	1127.92	1	1127.92	5.83	0.025**
	Trt	346.08	4	86.52	0.45	0.773
	Site * Trt	530.69	4	132.67	0.69	0.610
	Error	3869.87	20	193.49		
6/6/2005	Site	270.00	1	270.00	3.25	0.086*
	Trt	260.00	4	65.00	0.78	0.549
	Site * Trt	545.67	4	136.42	1.64	0.202
	Error	1659.00	20	82.95		
8/2/2005	Site	22358.70	1	22358.70	40.43	0.000***
	Trt	1579.72	4	394.93	0.71	0.592
	Site * Trt	1099.88	4	274.97	0.50	0.738
	Error	11061.67	20	553.08		

Nitrogen was not found to affect the cover of *P. arifolium* during the majority of the growing season at the *Phragmites*-dominant site (Figure 3.2.8). Generally across the season, *P. arifolium* cover was low for medium nitrogen fertilization, especially on 6/03/04. *P. arifolium* cover was at its lowest of the season on 6/03/04 and standard errors were small (Figure 3.2.7a). At all other sample dates in 2004, the percent cover of *P. arifolium* was fairly high and standard errors were large, which lessened the statistical sensitivity.

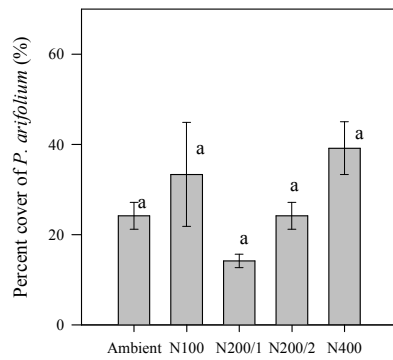
a) 5/25/04 (Pre-fertilization)



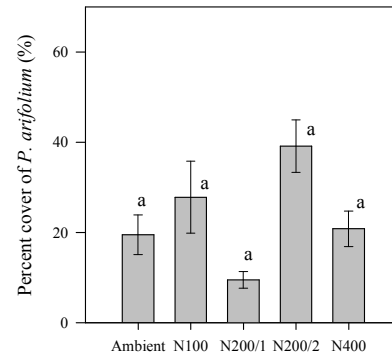
b) 6/03/04



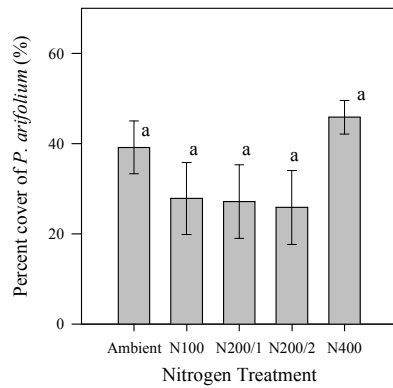
c) 6/16/04 Nitrogen Treatment



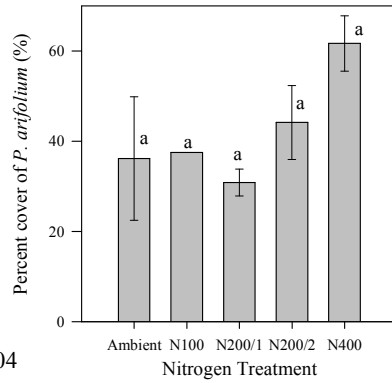
d) 6/29/04 Nitrogen Treatment



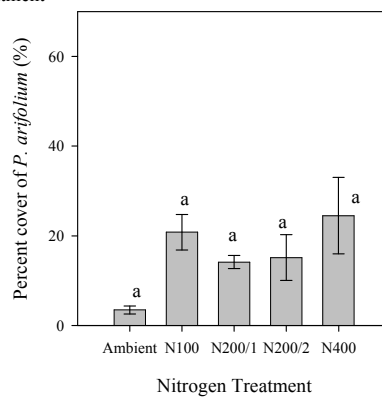
e) 7/19/04 Nitrogen Treatment



f) 8/24/04 Nitrogen Treatment



g) 9/21/04



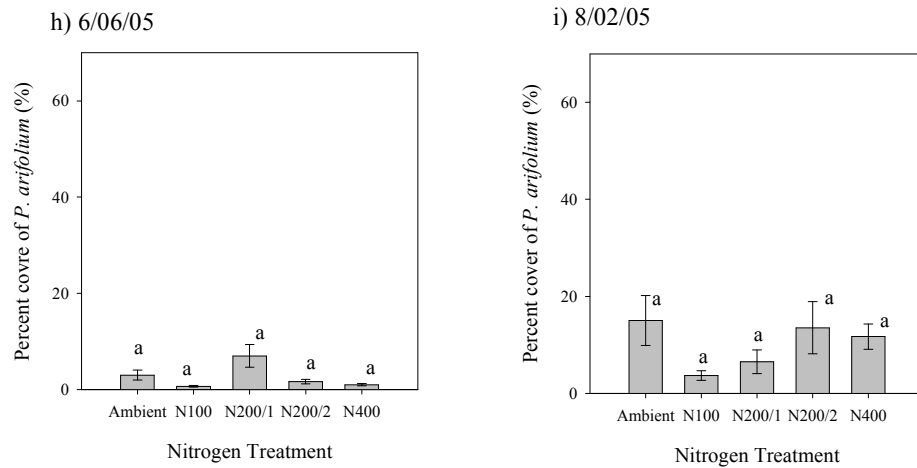
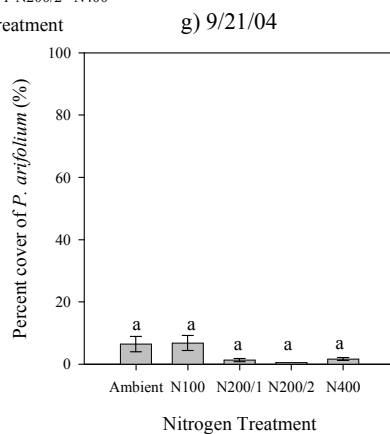
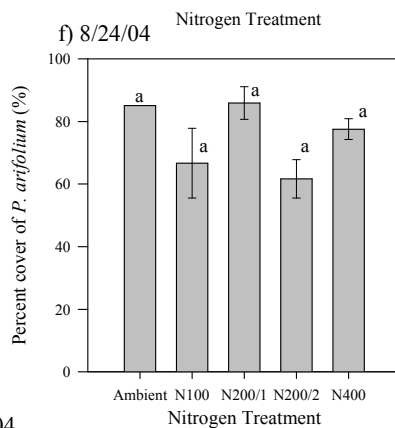
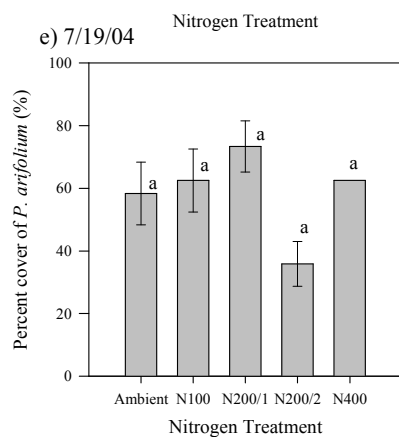
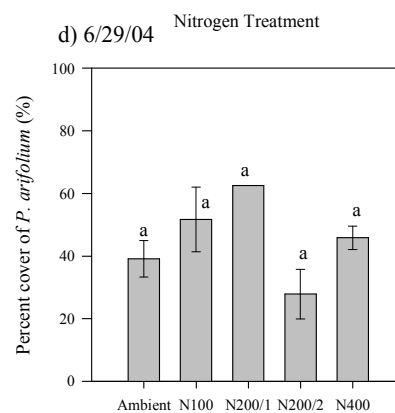
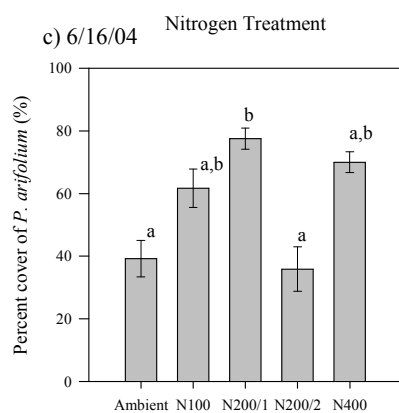
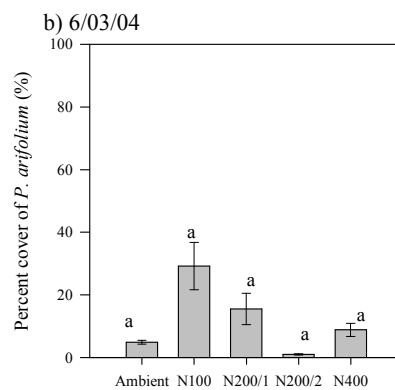
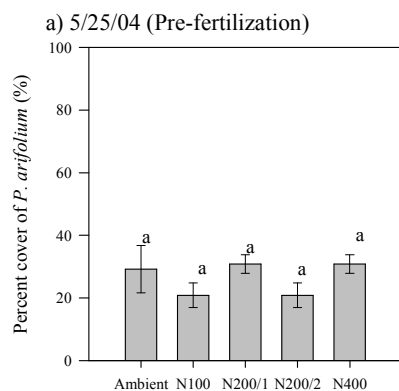


Figure 3.2.8. Mean *P. arifolium* percent cover and standard errors of the *Phragmites*-dominant site according to nitrogen treatment over the 2004-5 growing seasons. Treatments with different letters indicate a significant difference between treatments ($p < 0.05$). Percent *P. arifolium* was the dependent variable in the one-way ANOVA model, with an LSD contrast.

Analysis of the nitrogen effect on *P. arifolium* on each date at the *Phragmites*-absent site was similar to the *Phragmites*-dominant site analysis in that only one date showed a nitrogen effect on *P. arifolium* cover (Figure 3.2.9). Only on 6/16/04 did N200/1D have a greater percent cover of *P. arifolium* (Figure 3.2.9c).



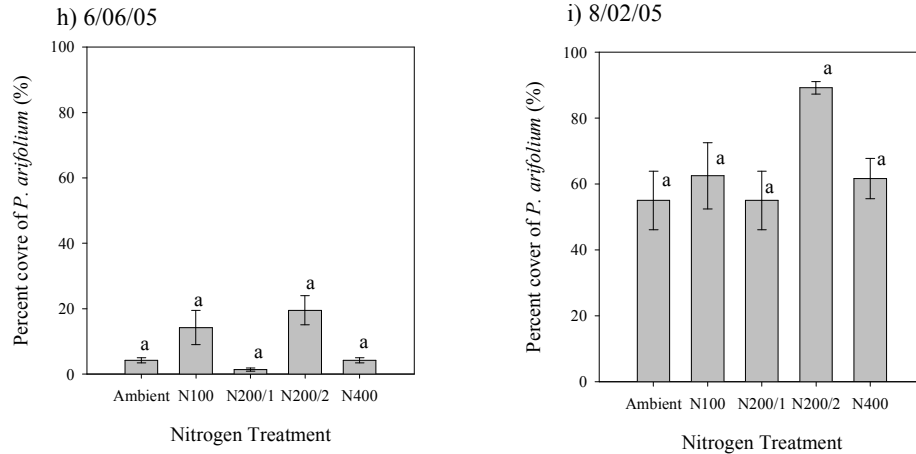


Figure 3.2.9. Mean *P. arifolium* percent cover and standard errors of the *Phragmites*-absent site according to nitrogen treatment over the 2004-5 growing seasons. Treatments with different letters indicate a significant difference between treatments ($p < 0.05$). Percent *P. arifolium* was the dependent variable in the one-way ANOVA model, with an LSD contrast.

Effects on P. virginica

Nitrogen fertilization effects on *P. virginica* were analyzed by first determining the effect of site and time on *P. virginica* percent cover. Figure 3.2.10 shows that percent cover of *P. virginica* decreased at both sites over the growing season until it was approximately the same at each in August (Figure 3.2.10). Upon analysis, site was found to have an interaction effect on percent cover of *P. virginica* with both the nitrogen and time effects (Table 3.2.6). When individual sites were studied for time and nitrogen effects on *P. virginica*, the time effect on percent cover of *P. virginica* was highly significant for both sites and the nitrogen effect was significant at the *Phragmites*-absent site (Table 3.2.7). Since time had a great effect on percent cover, site and nitrogen effects were studied at each sample date, which determined that site was significant on all sample dates before August (Table 3.2.8).

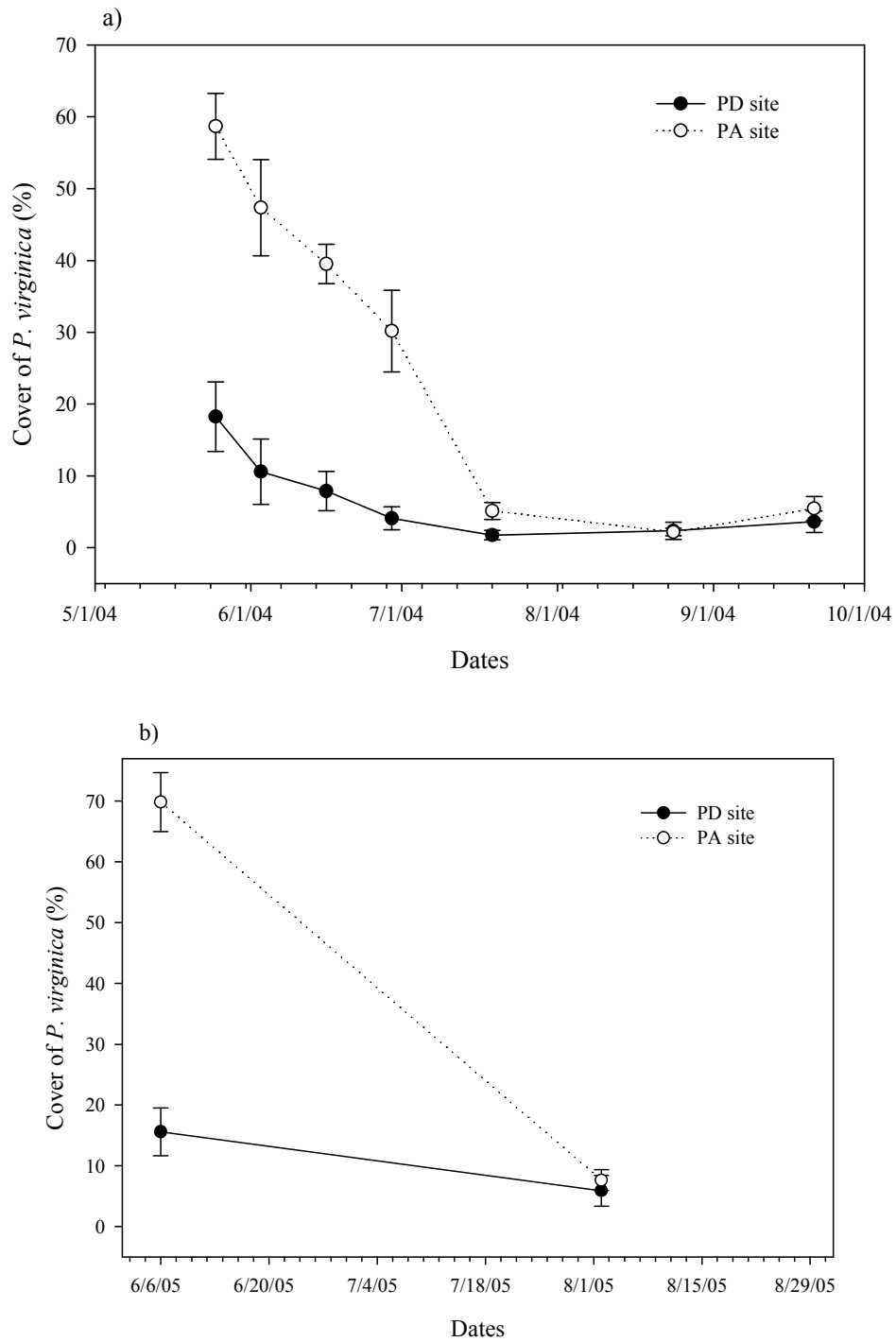


Figure 3.2.10. Mean percent cover and standard errors of *P. virginica* for the *Phragmites*-dominant and *Phragmites*-absent sites across the (a) 2004 and (b) 2005 growing seasons.

Table 3.2.6 Repeated measures ANOVA model for 2004 *P. virginica* populations. * <0.01, ** < 0.05, * < 0.10**

Source	Type III SS	df	MS	F	Sig
Site	20986.00	1	20986.00	63.79	0.000
Trt	2024.79	4	506.20	1.54	0.229
Site * Trt	3257.26	4	814.31	2.48	0.077*
Error	6580.04	20	329.00		
Time	36156.45	6	6026.07	45.27	0.000
Time * Site	14134.06	6	2355.68	17.70	0.000***
Time * Trt	3816.17	24	159.01	1.19	0.261
Time * Site * Trt	3780.91	24	157.54	1.18	0.271
Error (time)	15974.92	120	133.12		

Table 3.2.7. ANOVA model: Trt + Time + (Trt*Time) at each marsh site for *P. virginica* percent cover. * <0.01, ** < 0.05, * < 0.10**

Site	Source	Type III SS	df	MS	F	Sig
PD site	Trt	1342.06	4	335.51	0.89	0.507
	Time	3137.11	6	522.85	5.84	0.000***
	Time * Trt	1757.47	24	73.23	0.82	0.701
	Error	5373.49	60	89.56		
PA site	Trt	3939.99	4	985.00	3.53	0.048**
	Time	47153.40	6	7858.90	44.48	0.000***
	Time * Trt	5839.62	24	243.32	1.38	0.159
	Error	10601.43	60	176.69		

Table 3.2.8 ANOVA model: Site + Trt + (Site*Trt) at all sample dates for *P. virginica*. * <0.01, ** < 0.05, * < 0.10**

Date	Source	Type III SS	df	MS	F	Sig
5/25/2004	Site	12261.41	1	12261.41	41.68	0.000***
	Trt	1307.47	4	326.87	1.11	0.379
	Site * Trt	2158.13	4	539.53	1.83	0.162
	Error	5883.17	20	294.16		
6/3/2004	Site	10138.41	1	10138.41	23.45	0.000***
	Trt	2532.30	4	633.07	1.46	0.250
	Site * Trt	2589.47	4	647.37	1.50	0.241
	Error	8647.00	20	432.35		
6/16/2004	Site	7505.01	1	7505.01	61.24	0.000***
	Trt	181.95	4	45.49	0.37	0.826
	Site * Trt	537.28	4	134.32	1.10	0.386
	Error	2451.00	20	122.55		

Date	Source	Type III SS	df	MS	F	Sig
6/29/2004	Site	5105.16	1	5105.16	23.34	0.000***
	Trt	1637.74	4	409.44	1.87	0.155
	Site * Trt	1317.87	4	329.47	1.51	0.238
	Error	4374.44	20	218.72		
7/19/2004	Site	84.67	1	84.67	6.92	0.016
	Trt	21.08	4	5.27	0.43	0.785
	Site * Trt	116.73	4	29.18	2.38	0.086*
	Error	244.89	20	12.24		
8/24/2004	Site	0.20	1	0.20	0.01	0.905
	Trt	43.00	4	10.75	0.79	0.545
	Site * Trt	48.62	4	12.15	0.89	0.486
	Error	271.84	20	13.59		
9/21/2004	Site	25.21	1	25.21	0.74	0.400
	Trt	117.43	4	29.36	0.86	0.505
	Site * Trt	270.07	4	67.52	1.98	0.137
	Error	682.64	20	34.13		
6/6/2005	Site	22059.41	1	22059.41	81.21	0.000***
	Trt	461.05	4	115.26	0.42	0.789
	Site * Trt	2297.22	4	574.30	2.11	0.117
	Error	5432.67	20	271.63		
8/2/2005	Site	22.45	1	22.45	0.31	0.586
	Trt	134.67	4	33.67	0.46	0.765
	Site * Trt	375.41	4	93.85	1.28	0.311
	Error	1465.67	20	73.28		

Nitrogen effects on *P. virginica* percent cover for individual dates and sites were evaluated. Figure 3.2.11 shows no nitrogen effect on *P. virginica* percent cover for 2004 sample dates at the *Phragmites*-dominant site. At the *Phragmites*-absent site, N400 was significantly lower on 6/03/04 (Figure 3.2.12). By 7/19/04, *P. virginica* had been out-competed at the *Phragmites*-absent site by other species, primarily *P. arifolium* (Figure 3.2.7a). No nitrogen effects on percent *P. virginica* cover were detected in the 2005 season for either site (Figure 3.2.13).

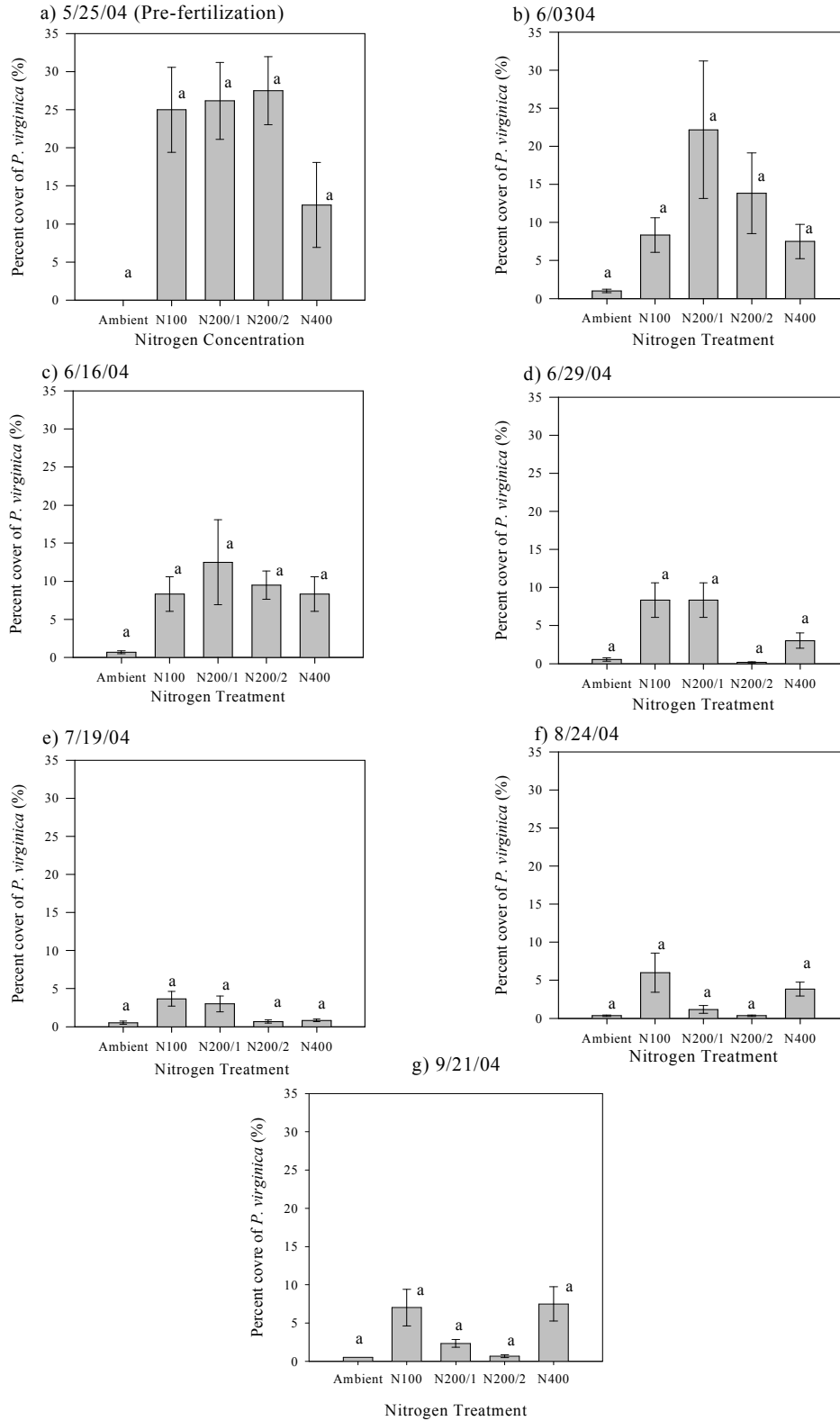


Figure 3.2.11. Mean *P. virginica* percent cover and standard errors of the *Phragmites*-dominant site according to nitrogen treatment over the 2004 growing season. Treatments with different letters indicate a significant difference between treatments ($p < 0.05$). Percent *P. virginica* was the dependent variable in the one-way ANOVA model, with an LSD contrast.

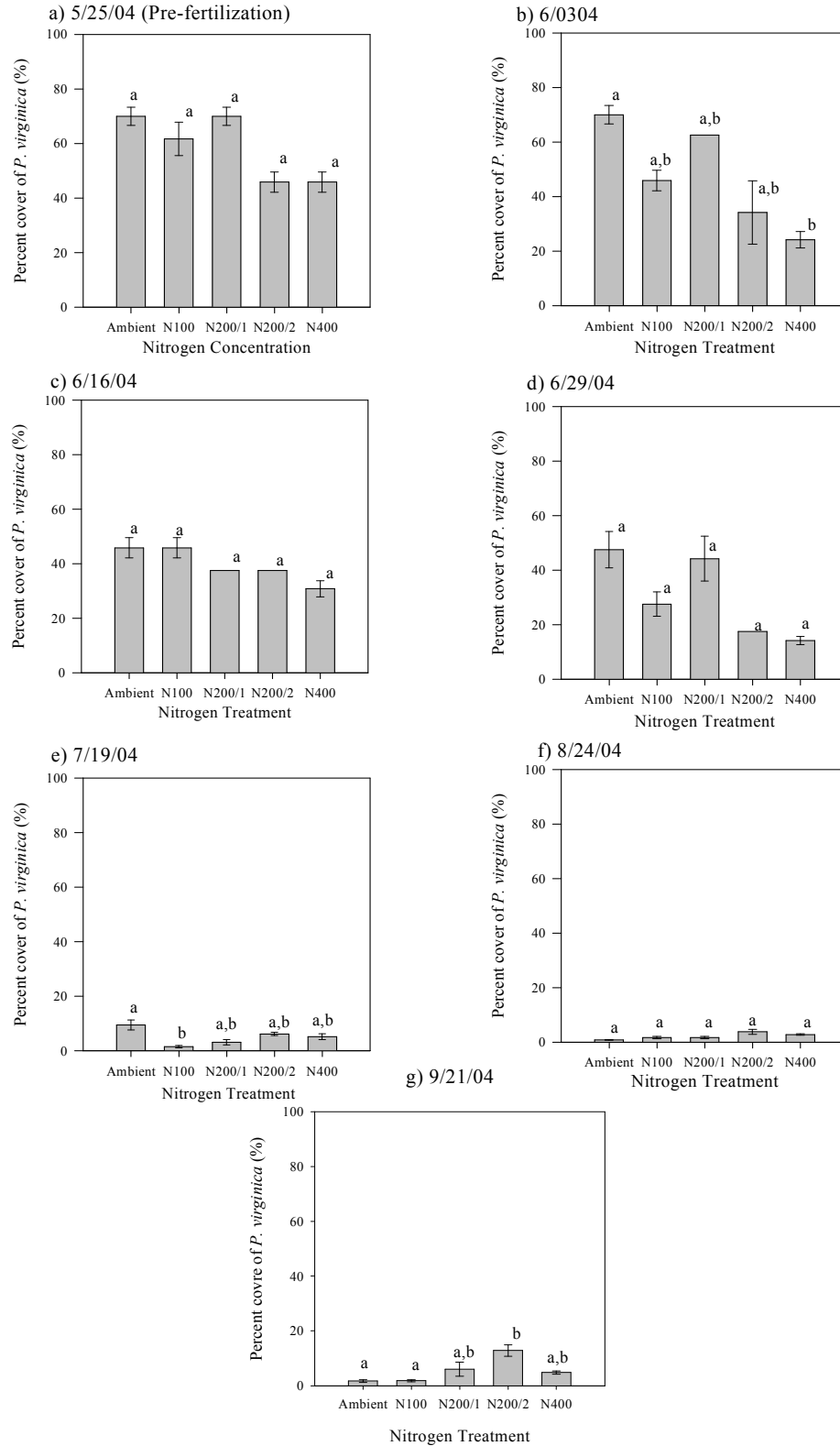


Figure 3.2.12. Mean *P. virginica* percent cover and standard errors of the *Phragmites*-absent site according to nitrogen treatment over the 2004 growing season. Treatments with different letters indicate a significant difference between treatments ($p < 0.05$). Percent *P. virginica* was the dependent variable in the one-way ANOVA model, with an LSD contrast.

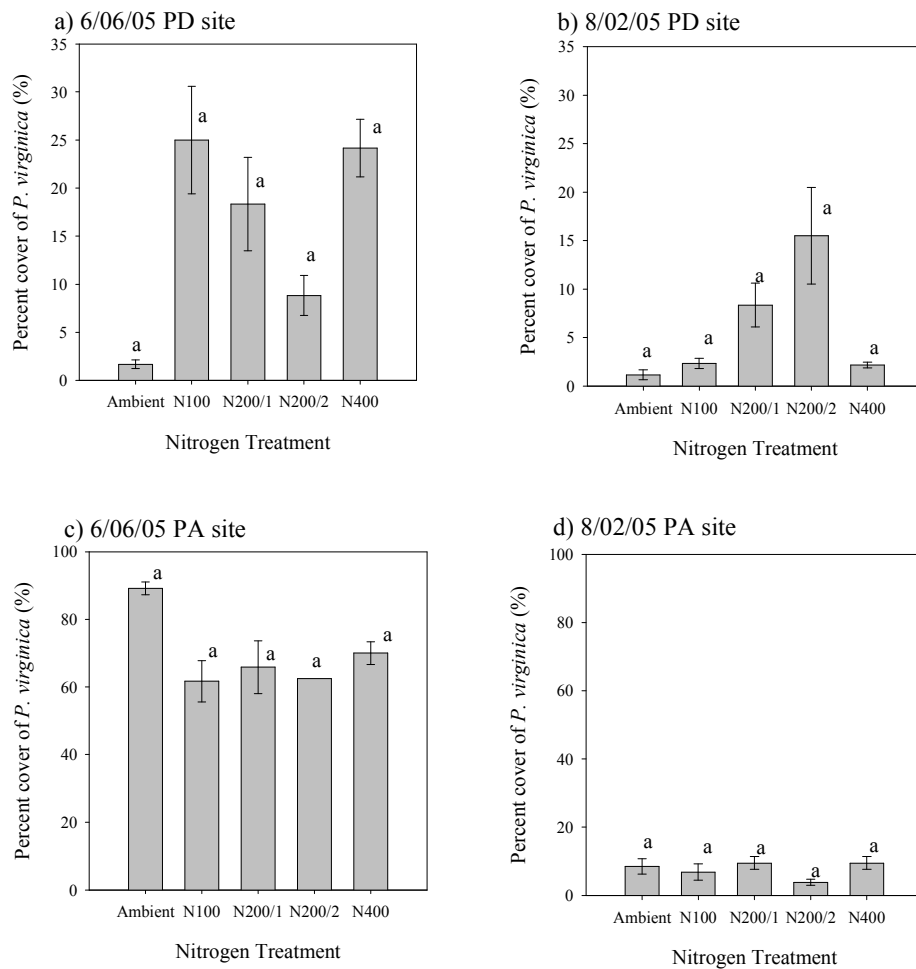
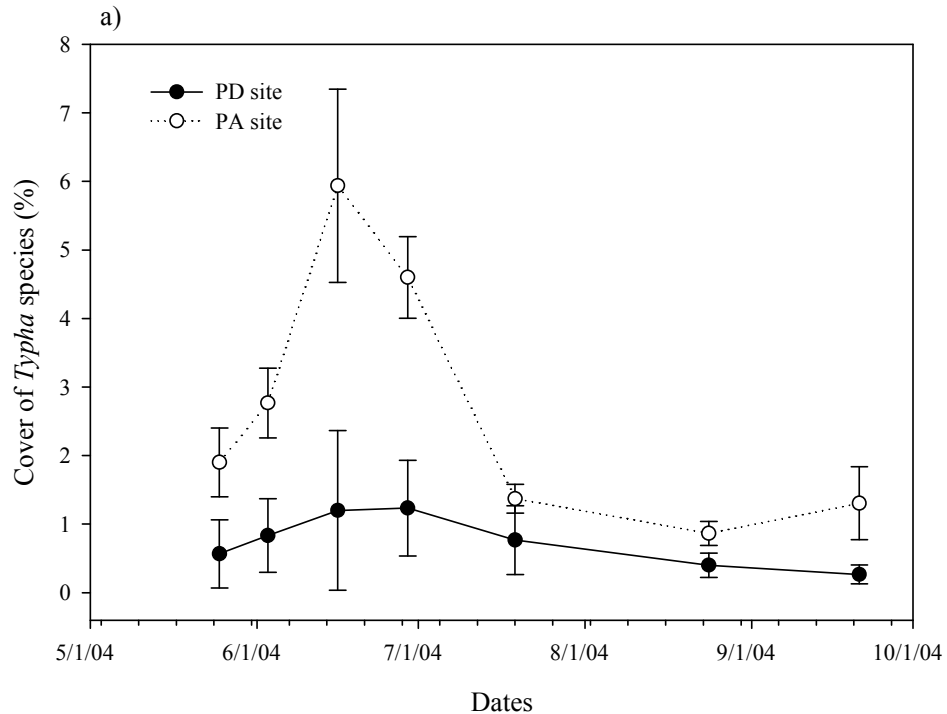


Figure 3.2.13. Mean *P. virginica* percent cover and standard errors according to nitrogen treatment over the 2005 growing seasons at both the *Phragmites*-dominant and *Phragmites*-absent site. (a) 6/06/05 *Phragmites*-dominant site, (b) 8/02/05 *Phragmites*-dominant site, (c) 6/06/05 *Phragmites*-absent site, (d) 8/02/05 *Phragmites*-absent site. Treatments with different letters indicate a significant difference between treatments ($p < 0.05$). Percent *P. virginica* was the dependent variable in the one-way ANOVA model, with an LSD contrast.

Effects on Typha species

The effect of nitrogen fertilization on *Typha* species percent cover was analyzed after site and time effects were determined. The two marsh sites appeared to differ from each other, especially in June when the *Phragmites*-absent site had a greater *Typha* species percent cover than the *Phragmites*-dominant site (Figure 3.2.14). In the analysis, site had an interaction effect with time (Table 3.2.9), so nitrogen effects at

individual sites (Table 3.2.10) and on individual dates (Table 3.2.11) were then analyzed. As expected, no time effect on *Typha* species was detected at the *Phragmites*-dominant site, unlike the *Phragmites*-absent site where a large time effect was distinguished (Table 3.2.10). When site and nitrogen effects were studied on each sample date, it was discovered that *Typha* species had a higher percent cover at the *Phragmites*-absent site than at the *Phragmites*-dominant site in June (Table 3.2.11). Also, in late June (6/29/04), a nitrogen effect on *Typha* species percent cover was detected (Table 3.2.11).



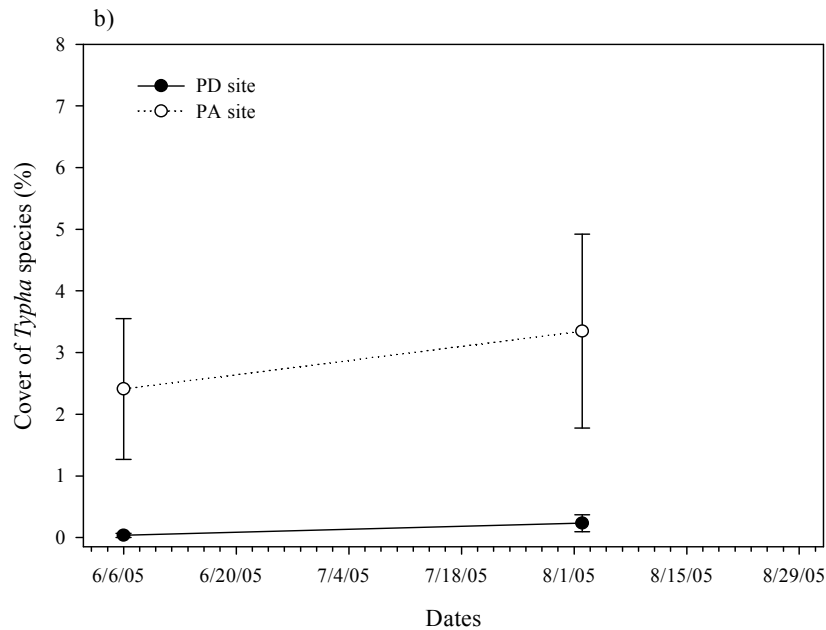


Figure 3.2.14. Mean percent cover and standard errors of *Typha* species for the *Phragmites*-dominant and *Phragmites*-absent sites across the (a) 2004 and (b) 2005 growing seasons.

Table 3.2.9 Repeated measures ANOVA model for 2004 *Typha* species populations. *** <0.01, ** < 0.05, * < 0.10

Source	Type III SS	df	MS	F	Sig
Site	178.20	1	178.20	10.77	0.004
Trt	92.09	4	23.02	1.39	0.275
Site * Trt	72.81	4	18.20	1.10	0.385
Error	314.46	19	16.55		
Time	202.82	6	33.80	7.29	0.000
Time * Site	96.51	6	16.08	3.47	0.003***
Time * Trt	110.52	24	4.61	0.99	0.481
Time * Site * Trt	106.20	24	4.42	0.95	0.531
Error (time)	528.65	114	4.64		

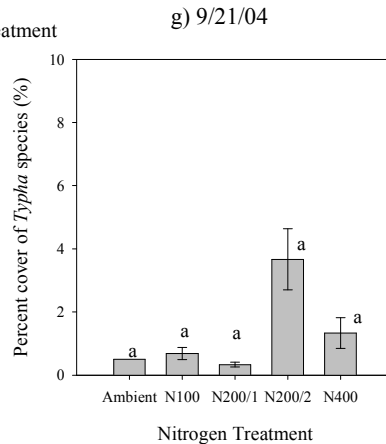
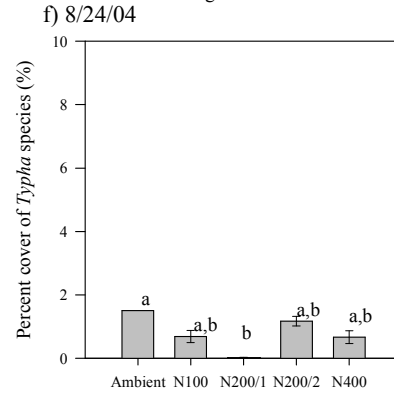
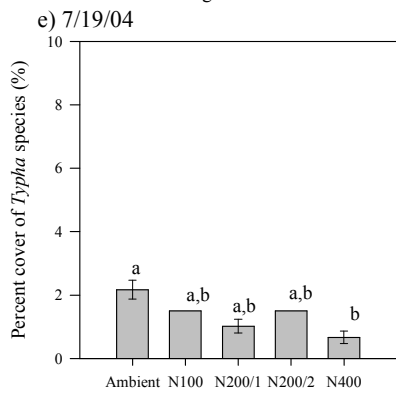
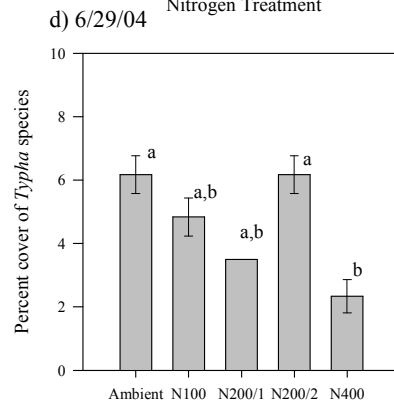
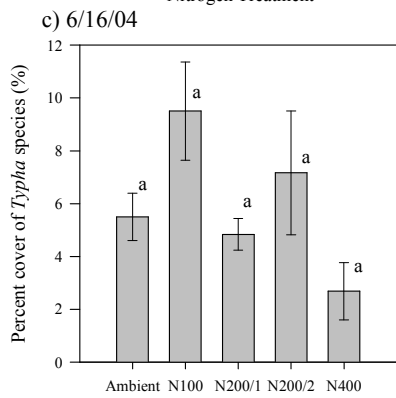
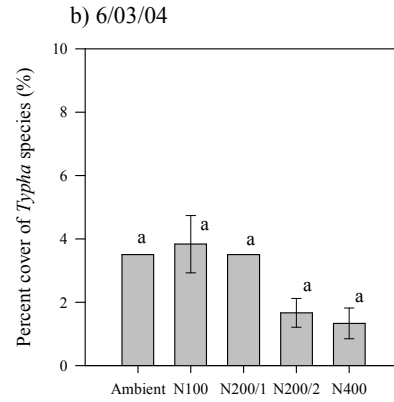
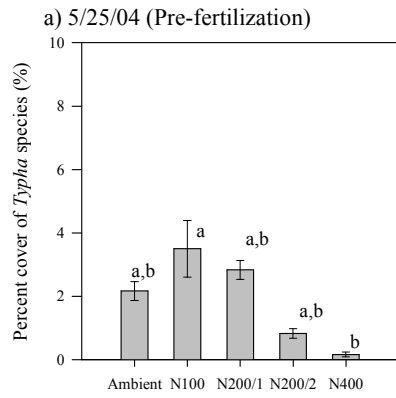
Table 3.2.10. ANOVA model: Trt + Time + (Trt*Time) at each marsh site for *Typha* species percent cover. *** <0.01, ** < 0.05, * < 0.10

Site	Source	Type III SS	df	MS	F	Sig
PD site	Trt	100.40	4	25.10	1.47	0.282
	Time	12.50	6	2.08	0.64	0.695
	Time * Trt	97.00	24	4.04	1.25	0.240
	Error	194.14	60	3.24		
PA site	Trt	65.77	4	16.44	1.03	0.443
	Time	274.36	6	45.73	7.38	0.000***
	Time * Trt	117.77	24	4.91	0.79	0.730
	Error	334.51	54	6.19		

Table 3.2.11 ANOVA model: Site + Trt + (Site*Trt) at all sample dates for *Typha* species. * <0.01, ** < 0.05, * < 0.10**

Date	Source	Type III SS	df	MS	F	Sig
5/25/2004	Site	13.33	1	13.33	4.07	0.057
	Trt	10.37	4	2.59	0.79	0.544
	Site * Trt	29.17	4	7.29	2.23	0.103
	Error	65.50	20	3.28		
6/3/2004	Site	28.03	1	28.03	8.29	0.009
	Trt	9.30	4	2.33	0.69	0.609
	Site * Trt	37.80	4	9.45	2.79	0.054*
	Error	67.67	20	3.38		
6/16/2004	Site	168.27	1	168.27	6.20	0.022**
	Trt	100.89	4	25.22	0.93	0.467
	Site * Trt	58.28	4	14.57	0.54	0.710
	Error	542.57	20	27.13		
6/29/2004	Site	85.01	1	85.01	19.81	0.000***
	Trt	60.67	4	15.17	3.53	0.025**
	Site * Trt	29.53	4	7.38	1.72	0.185
	Error	85.83	20	4.29		
7/19/2004	Site	2.73	1	2.73	1.20	0.287
	Trt	3.56	4	0.89	0.39	0.813
	Site * Trt	12.40	4	3.10	1.36	0.283
	Error	45.57	20	2.28		
8/24/2004	Site	1.19	1	1.19	2.53	0.128
	Trt	2.92	4	0.73	1.55	0.227
	Site * Trt	0.96	4	0.24	0.51	0.728
	Error	8.94	19	0.47		
9/21/2004	Site	8.06	1	8.06	4.04	0.058
	Trt	11.01	4	2.75	1.38	0.277
	Site * Trt	12.27	4	3.07	1.54	0.230
	Error	39.94	20	2.00		
6/6/2005	Site	42.25	1	42.25	4.58	0.045**
	Trt	44.16	4	11.04	1.20	0.343
	Site * Trt	45.07	4	11.27	1.22	0.333
	Error	184.39	20	9.22		
8/2/2005	Site	72.70	1	72.70	5.80	0.026
	Trt	132.55	4	33.14	2.64	0.064
	Site * Trt	138.74	4	34.68	2.77	0.056*
	Error	250.66	20	12.53		

To analyze the nitrogen effect on *Typha* species percent cover without site and time effects, nitrogen treatments were evaluated at the *Phragmites*-absent site for each sample date (Figure 3.2.15). Overall, *Typha* species percent cover was visually lower for N400, and in late June (6/29/04), *Typha* species percent cover for N400 was significantly lower than other treatments (Figure 3.2.15d). Interestingly, one of the nitrogen additions (N200/2D) increased mean cover of *Typha* species by September (Figure 3.2.15g), which was present during the early part of the next season and remained until the last measurement in August (Figure 3.2.15i)



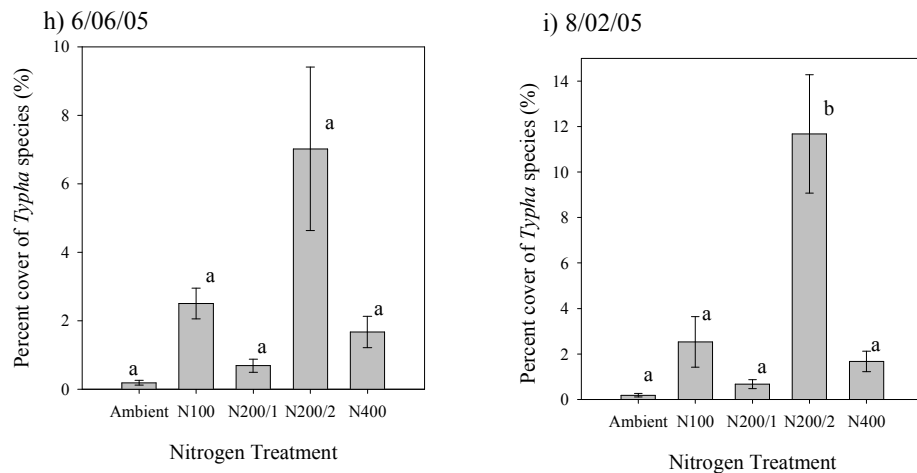


Figure 3.2.15. Mean *Typha* species percent cover and standard errors of the *Phragmites*-absent site according to nitrogen treatment over the 2004-5 growing seasons. Treatments with different letters indicate a significant difference between treatments ($p < 0.05$). Percent *Typha* species was the dependent variable in the one-way ANOVA model, with an LSD contrast.

Effects on I. capensis

To determine if nitrogen fertilization affected *I. capensis* percent cover, site and time effects were first evaluated. Although the marsh sites appeared to have similar percent covers of *I. capensis* over the growing season (Figure 3.2.16), the site effect did interact with time for *I. capensis* percent cover (Table 3.2.12). Time effect on *I. capensis* percent cover was also noticed at both marsh sites when analyzed individually (Table 3.2.13). A nitrogen effect was also detected at the *Phragmites*-dominant site (Table 3.2.13). When time effects were eliminated by analyzing site and nitrogen effects on each sample date, marsh sites were not found to be different from each other in *I. capensis* percent cover (Table 3.2.14). Interestingly, a strong treatment effect was discovered for *I. capensis* on 8/02/05 (Table 3.2.14).

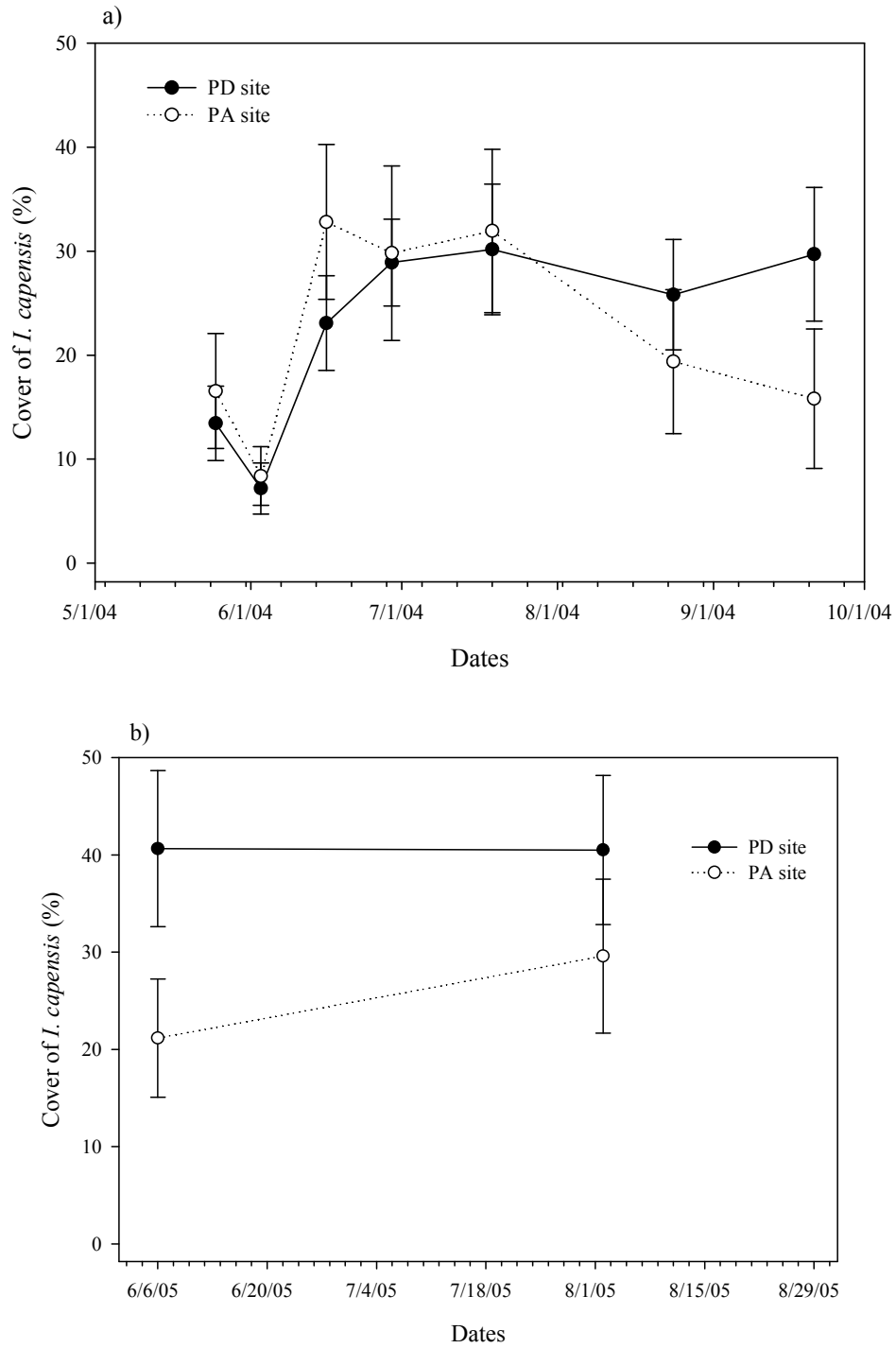


Figure 3.2.16. Mean percent cover and standard errors of *I. capensis* for the *Phragmites*-dominant and *Phragmites*-absent sites across the (a) 2004 and (b) 2005 growing seasons.

Table 3.2.12 Repeated measures ANOVA model for 2004 *I. capensis* populations. * <0.01, ** < 0.05, * < 0.10**

Source	Type III SS	df	MS	F	Sig
Site	14.07	1	14.07	0.01	0.943
Trt	11672.14	4	2918.03	1.10	0.384
Site * Trt	3876.63	4	969.16	0.37	0.831
Error	53101.11	20	2655.06		
Time	12688.49	6	2114.75	11.40	0.000
Time * Site	2566.69	6	427.78	2.31	0.038**
Time * Trt	6287.41	24	261.98	1.41	0.115
Time * Site * Trt	4678.89	24	194.95	1.05	0.410
Error (time)	22257.13	120	185.48		

Table 3.2.13. ANOVA model: Trt + Time + (Trt*Time) at each marsh site for *I. capensis* percent cover. * <0.01, ** < 0.05, * < 0.10**

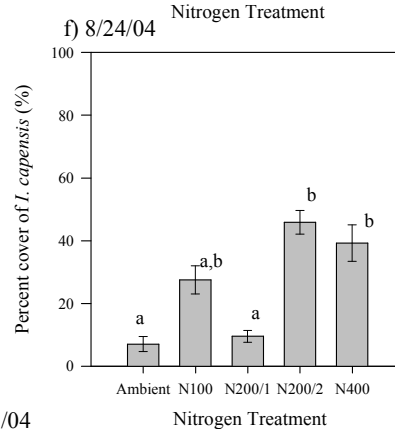
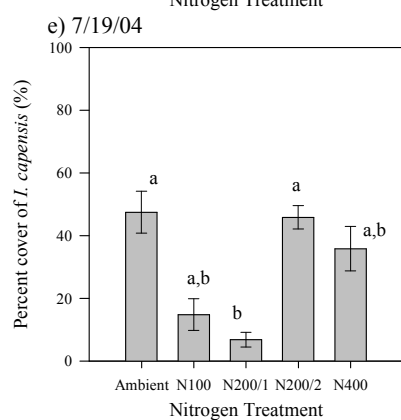
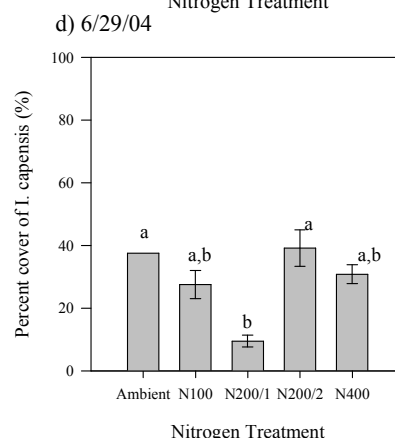
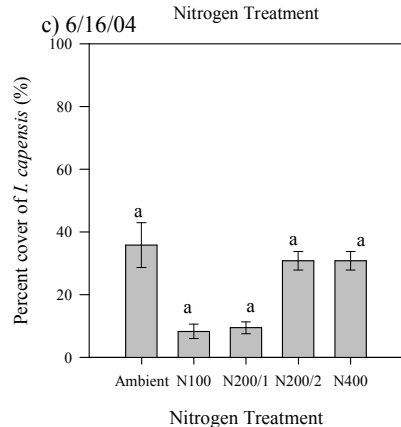
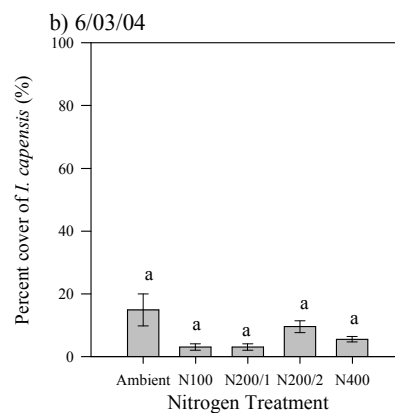
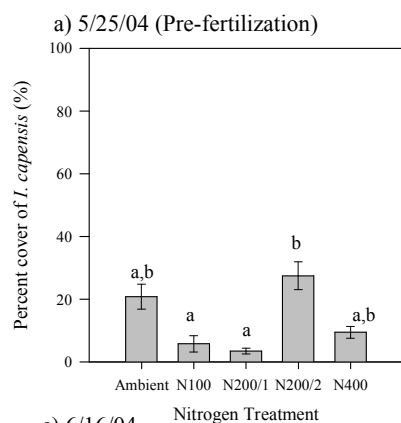
Site	Source	Type III SS	df	MS	F	Sig
PD site	Trt	11801.94	4	2950.48	6.60	0.007***
	Time	7198.87	6	1199.81	5.98	0.000***
	Time * Trt	6535.41	24	272.31	1.36	0.170
	Error	12047.67	60	200.79		
PA site	Trt	3746.83	4	936.71	0.19	0.937
	Time	8056.31	6	1342.72	7.89	0.000***
	Time * Trt	4430.89	24	184.62	1.08	0.387
	Error	10209.46	60	170.16		

Table 3.2.14 ANOVA model: Site + Trt + (Site*Trt) at all sample dates for *I. capensis*. * <0.01, ** < 0.05, * < 0.10**

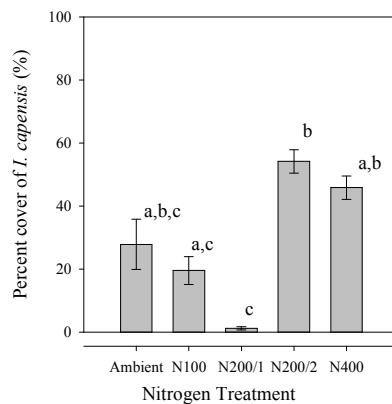
Date	Source	Type III SS	df	MS	F	Sig
5/25/2004	Site	72.23	1	72.23	0.19	0.666
	Trt	797.54	4	199.39	0.53	0.714
	Site * Trt	793.14	4	198.28	0.53	0.716
	Error	7504.84	20	375.24		
6/3/2004	Site	10.74	1	10.74	0.09	0.769
	Trt	203.64	4	50.91	0.42	0.793
	Site * Trt	297.51	4	74.38	0.61	0.659
	Error	2431.70	20	121.59		
6/16/2004	Site	710.53	1	710.53	1.21	0.284
	Trt	2537.78	4	634.45	1.08	0.391
	Site * Trt	1758.72	4	439.68	0.75	0.569
	Error	11715.33	20	585.77		

Date	Source	Type III SS	df	MS	F	Sig
6/29/2004	Site	6.07	1	6.07	0.01	0.932
	Trt	1362.45	4	340.61	0.42	0.795
	Site * Trt	696.72	4	174.18	0.21	0.928
	Error	16380.83	20	819.04		
7/19/2004	Site	23.41	1	23.41	0.03	0.860
	Trt	4773.05	4	1193.26	1.62	0.209
	Site * Trt	1743.38	4	435.85	0.59	0.673
	Error	14761.83	20	738.09		
8/24/2004	Site	310.09	1	310.09	0.57	0.459
	Trt	3908.95	4	977.24	1.80	0.169
	Site * Trt	1237.58	4	309.40	0.57	0.688
	Error	10860.17	20	543.01		
9/21/2004	Site	1447.69	1	1447.69	2.47	0.131
	Trt	4376.13	4	1094.03	1.87	0.155
	Site * Trt	2028.47	4	507.12	0.87	0.501
	Error	11703.54	20	585.18		
6/6/2005	Site	2843.11	1	2843.11	3.98	0.060*
	Trt	4055.44	4	1013.86	1.42	0.264
	Site * Trt	2916.48	4	729.12	1.02	0.421
	Error	14298.09	20	714.90		
8/2/2005	Site	891.07	1	891.07	1.35	0.260
	Trt	11240.18	4	2810.05	4.24	0.012**
	Site * Trt	990.28	4	247.57	0.37	0.825
	Error	13247.64	20	662.38		

Nitrogen effects on *I. capensis* percent cover were analyzed at each marsh site and sample date so that site and time effects would not influence nitrogen effects. At the *Phragmites*-dominant site, percent cover for N200/1D was lower than other treatments in late-June through September (Figure 3.2.17). *I. capensis* percent cover was visually higher for high fertilization treatments, as well as ambient conditions, while middle treatments yielded a low percent cover. Also, in the 2005 growing season, N400 yielded a higher percent *I. capensis* cover than other treatments (Figure 3.2.17i).



g) 9/21/04



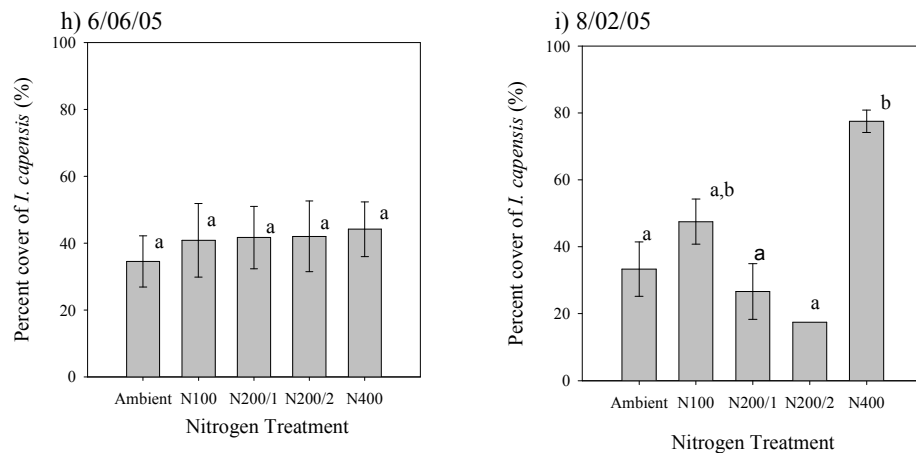
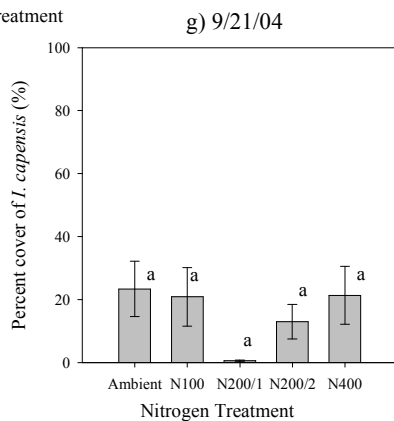
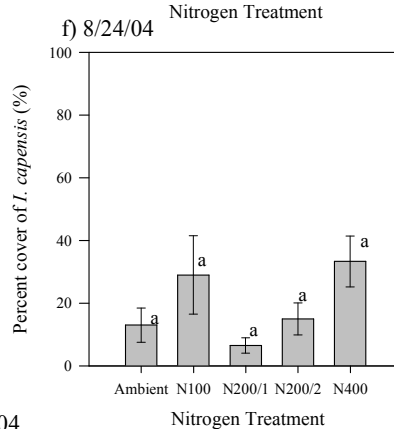
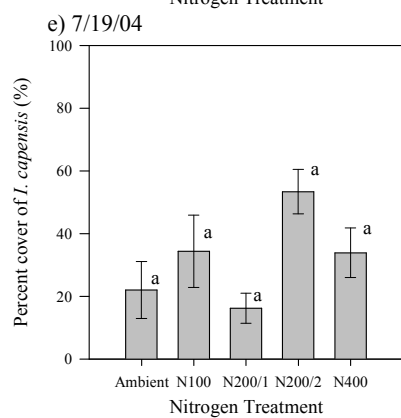
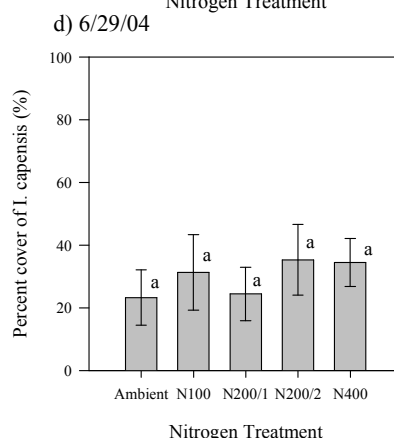
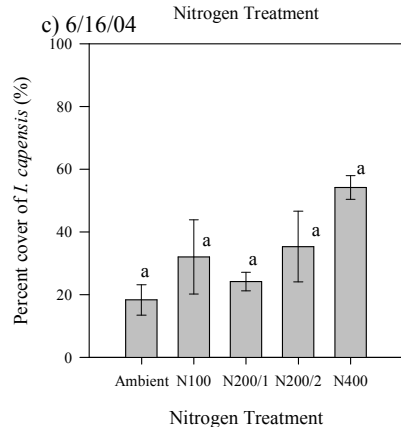
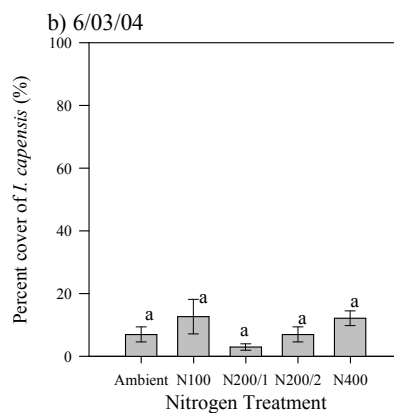
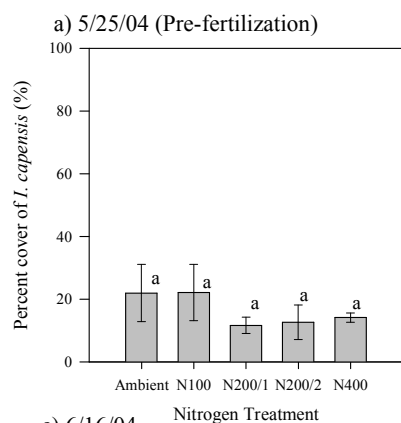


Figure 3.2.17. Mean *I. capensis* percent cover and standard errors of the *Phragmites*-dominant site according to nitrogen treatment over the 2004-5 growing seasons. Treatments with different letters indicate a significant difference between treatments ($p < 0.05$). Percent *I. capensis* was the dependent variable in the one-way ANOVA model, with an LSD contrast.

No nitrogen effects were discovered at the *Phragmites*-absent site for percent *I. capensis* in the 2004 growing season (Figure 3.2.18). However, in the 2005 growing season, sample date 6/06/05 showed that N400 had a significantly greater percent cover of *I. capensis* than all other treatments (Figure 3.2.18h).



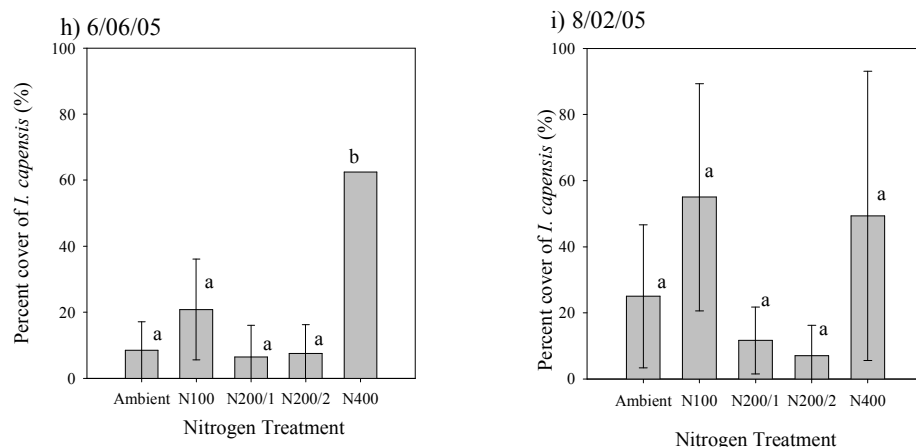


Figure 3.2.18. Mean *I. capensis* percent cover and standard errors of the *Phragmites*-absent site according to nitrogen treatment over the 2004-5 growing seasons. Treatments with different letters indicate a significant difference between treatments ($p < 0.05$). Percent *I. capensis* was the dependent variable in the one-way ANOVA model, with an LSD contrast.

Effects on Leaf Area Index

Leaf area index was analyzed to determine if it was affected by nitrogen fertilization.

Since LAI appeared to be higher at the *Phragmites*-dominant site than at the

Phragmites-absent site, and both sites followed the same trend over time (Figure

3.2.19), site and time effects were evaluated before nitrogen effects were considered.

Results indicated that there were strong site and time effects on LAI (Table 3.2.15),

so nitrogen effects at individual sites and dates were evaluated. Time influenced LAI

at the *Phragmites*-dominant site, but interacted with nitrogen effects at the

Phragmites-absent site (Table 3.2.16). When individual dates were analyzed, site

effects were detected on dates that had the lowest LAIs (Table 3.2.17 and Figure

3.2.19a). A nitrogen effect was revealed on 6/16/04 (Table 3.2.17), which was also

the date that both sites had a high LAI (Figure 3.2.19a).

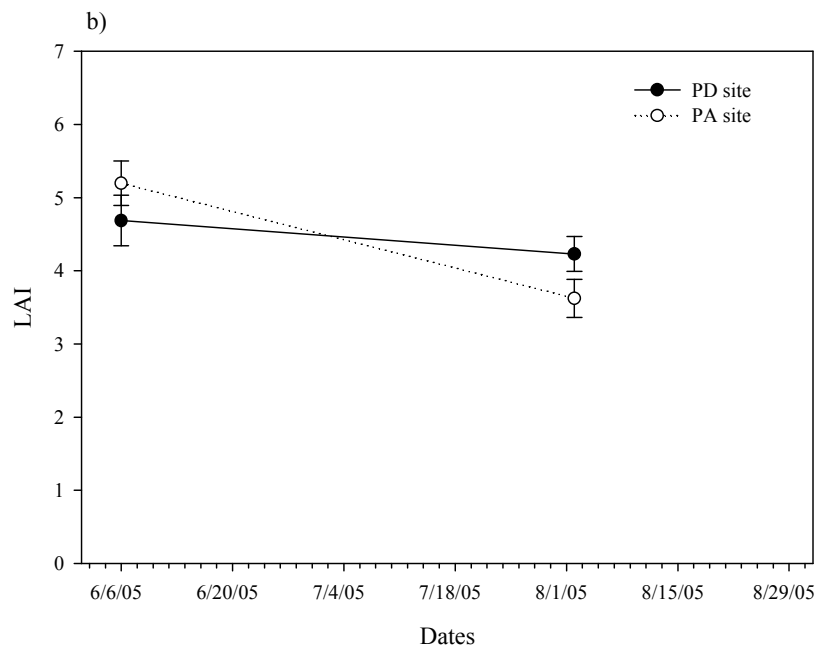
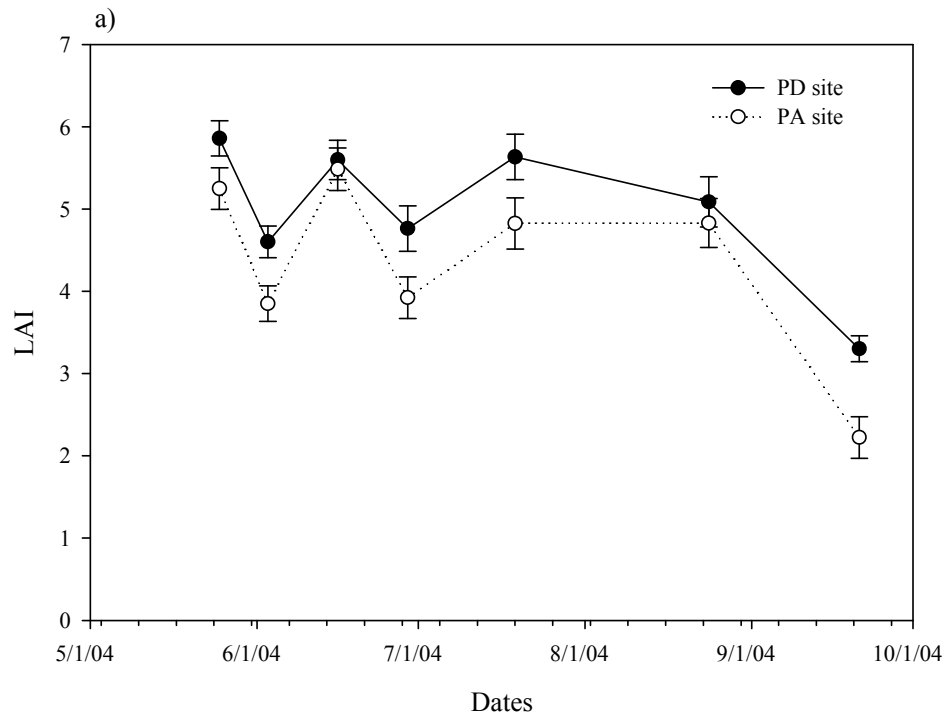


Figure 3.2.19. Mean LAI and standard errors for the *Phragmites*-dominant and *Phragmites*-absent sites across the (a) 2004 and (b) 2005 growing seasons.

Table 3.2.15 Repeated measures ANOVA model for 2004 LAI. * <0.01, ** < 0.05, * < 0.10**

Source	Type III SS	df	MS	F	Sig
Site	17.20	1	17.20	7.35	0.014**
Trt	11.72	4	2.93	1.25	0.325
Site * Trt	11.25	4	2.81	1.20	0.344
Error	42.14	18	2.34		
Time	160.71	6	26.79	38.08	0.000***
Time * Site	5.21	6	0.87	1.23	0.295
Time * Trt	17.45	24	0.73	1.03	0.431
Time * Site * Trt	18.09	24	0.75	1.07	0.388
Error (time)	75.96	108	0.70		

Table 3.2.16. ANOVA model: Trt + Time + (Trt*Time) at each marsh site for LAI. * <0.01, ** < 0.05, * < 0.10**

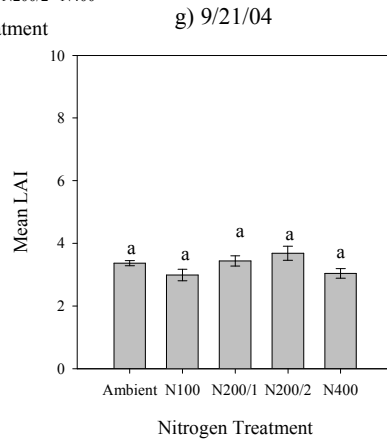
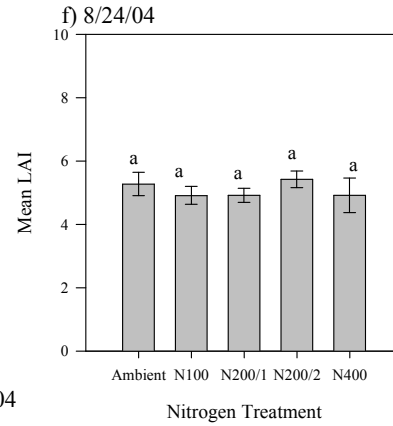
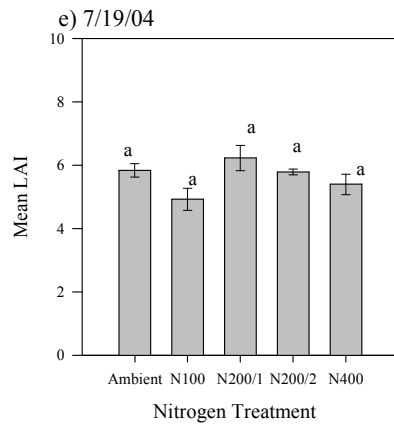
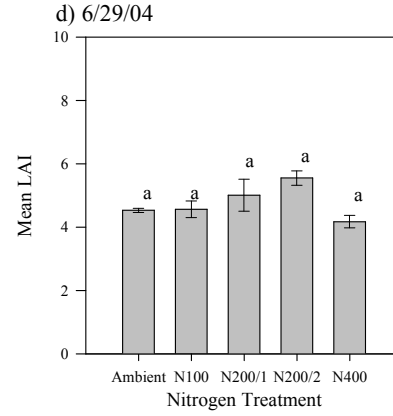
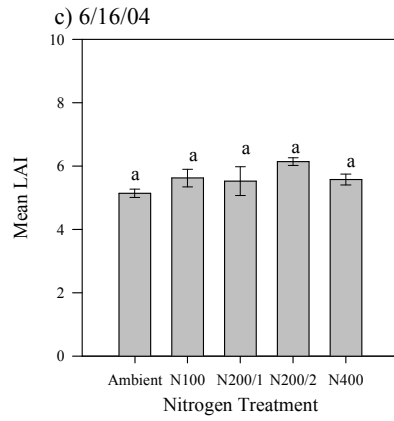
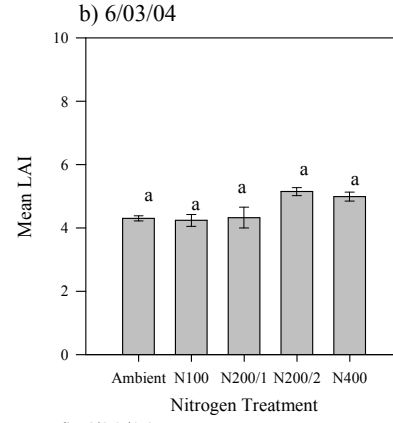
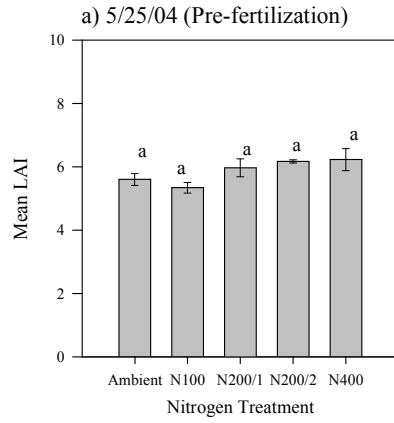
Site	Source	Type III SS	df	MS	F	Sig
PD site	Trt	6.72	4	1.68	0.61	0.664
	Time	69.05	6	11.51	15.18	0.000***
	Time * Trt	6.83	24	0.28	0.38	0.995
	Error	45.48	60	0.76		
PA site	Trt	16.95	4	4.24	2.32	0.145
	Time	94.55	6	15.76	24.82	0.000
	Time * Trt	27.21	24	1.13	1.79	0.044**
	Error	30.48	48	0.64		

Table 3.2.17 ANOVA model: Site + Trt + (Site*Trt) at all sample dates for LAI. * <0.01, ** < 0.05, * < 0.10**

Date	Source	Type III SS	df	MS	F	Sig
5/25/2004	Site	2.80	1	2.80	2.90	0.104
	Trt	2.23	4	0.56	0.58	0.683
	Site * Trt	1.78	4	0.44	0.46	0.764
	Error	19.31	20	0.97		
6/3/2004	Site	3.43	1	3.43	6.13	0.023**
	Trt	4.18	4	1.05	1.87	0.158
	Site * Trt	2.35	4	0.59	1.05	0.409
	Error	10.65	19	0.56		
6/16/2004	Site	0.10	1	0.10	0.13	0.726
	Trt	7.17	4	1.79	2.35	0.089*
	Site * Trt	3.55	4	0.89	1.16	0.356
	Error	15.24	20	0.76		

Date	Source	Type III SS	df	MS	F	Sig
6/29/2004	Site	5.29	1	5.29	5.32	0.032**
	Trt	3.09	4	0.77	0.78	0.553
	Site * Trt	6.33	4	1.58	1.59	0.215
	Error	19.88	20	0.99		
7/19/2004	Site	4.90	1	4.90	5.73	0.027
	Trt	7.81	4	1.95	2.28	0.096
	Site * Trt	11.45	4	2.86	3.34	0.030**
	Error	17.12	20	0.86		
8/24/2004	Site	0.53	1	0.53	0.37	0.548
	Trt	2.95	4	0.74	0.52	0.720
	Site * Trt	7.10	4	1.77	1.26	0.322
	Error	26.85	19	1.41		
9/21/2004	Site	8.73	1	8.73	11.23	0.003***
	Trt	2.84	4	0.71	0.91	0.475
	Site * Trt	0.28	4	0.07	0.09	0.984
	Error	15.54	20	0.78		
6/6/2005	Site	1.95	1	1.95	1.47	0.239
	Trt	11.56	4	2.89	2.18	0.108
	Site * Trt	6.30	4	1.57	1.19	0.347
	Error	26.52	20	1.33		
8/2/2005	Site	2.75	1	2.75	2.65	0.119
	Trt	3.06	4	0.77	0.74	0.577
	Site * Trt	2.38	4	0.59	0.57	0.685
	Error	20.76	20	1.04		

Nitrogen effects on LAI were analyzed at individual sites and dates so site and time effects would not interfere with treatment effects. Leaf area index was not affected by nitrogen on any date at the *Phragmites*-dominant site (Figure 3.2.20). All treatments had very uniform LAIs across treatments for both the 2004 and 2005 growing seasons.



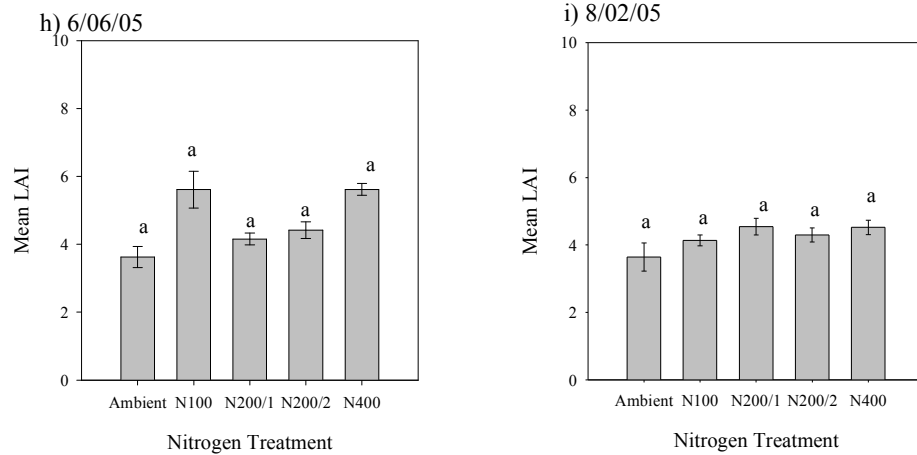
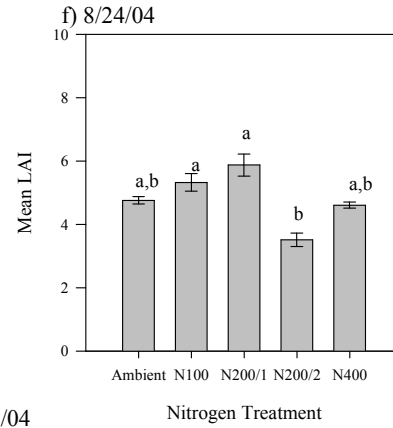
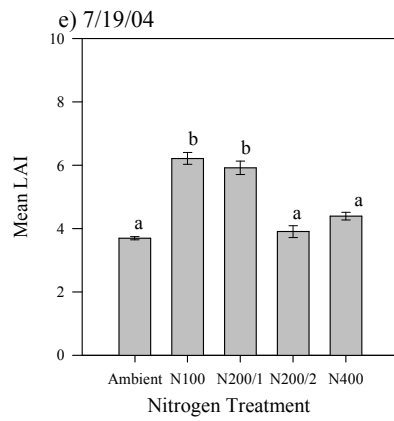
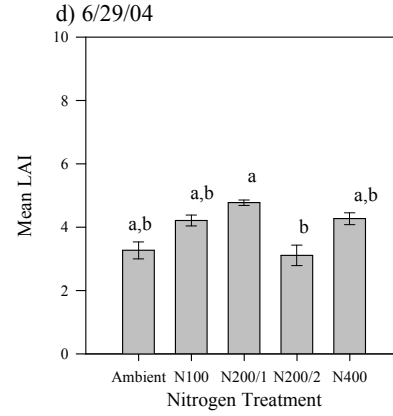
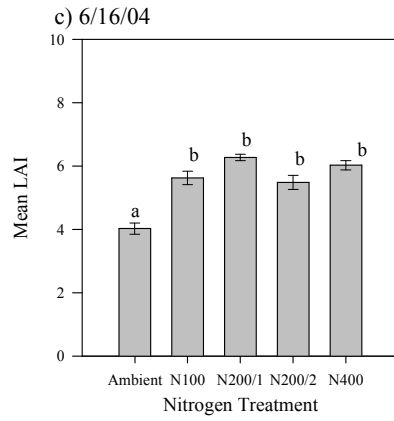
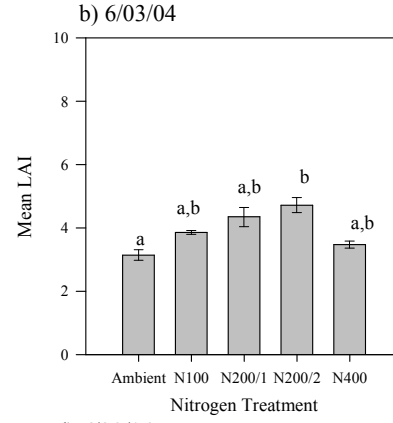
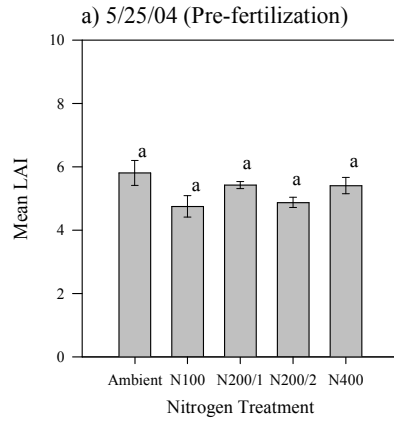
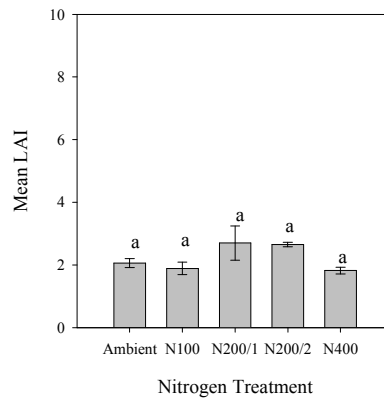


Figure 3.2.20. Mean LAI and standard errors at the *Phragmites*-dominant site according to nitrogen treatment over the 2004-5 growing seasons. Treatments with different letters indicate a significant difference between treatments ($p < 0.05$). LAI was the dependent variable in the one-way ANOVA model, with an LSD contrast.

At the *Phragmites*-absent site, additional nitrogen appeared to increase LAI during the early growing season (Figure 3.2.21), but the effect disappeared by September. Sample dates in 2005 showed no significant treatment effects (Figures 3.2.21h and 3.2.21i).



g) 9/21/04



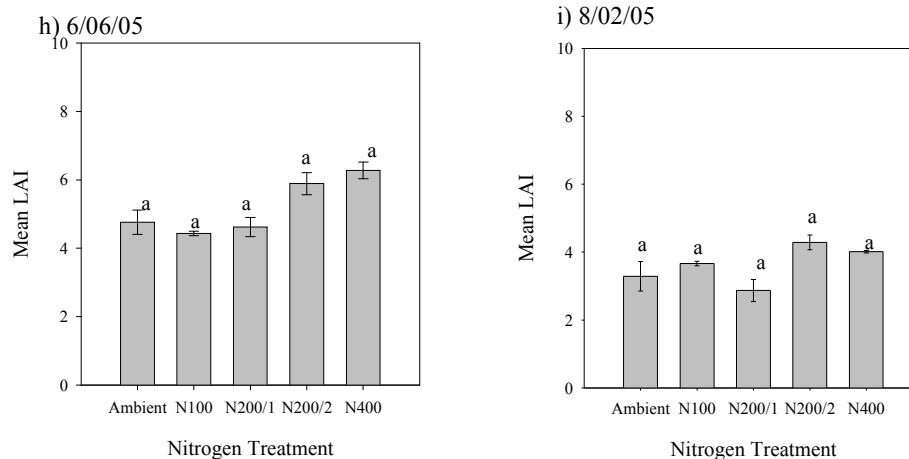


Figure 3.2.21. Mean LAI and standard errors at the *Phragmites*-absent site according to nitrogen treatment over the 2004-5 growing seasons. Treatments with different letters indicate a significant difference between treatments ($p < 0.05$). LAI was the dependent variable in the one-way ANOVA model, with an LSD contrast.

Effects on Species Richness

Nitrogen effects on species richness were analyzed after both site and time effects were evaluated. Figure 3.2.22 shows the progression of species richness at each site over the season. Both sites had 6 – 8 species present for the majority of the summer until late August when species began to senesce. Upon analysis, it was established that site and time interacted to affect species richness (Table 3.2.18). Time and treatment were evaluated at each site, revealing a strong time effect on species richness (Table 3.2.19). When time effects were eliminated by analyzing site and nitrogen effects at every date, a nitrogen effect was distinguished on 6/29/04 when sites had similar species richness and site effects were expectedly noted on dates that had the most difference between species richness (Table 3.2.20 and Figure 3.2.22a).

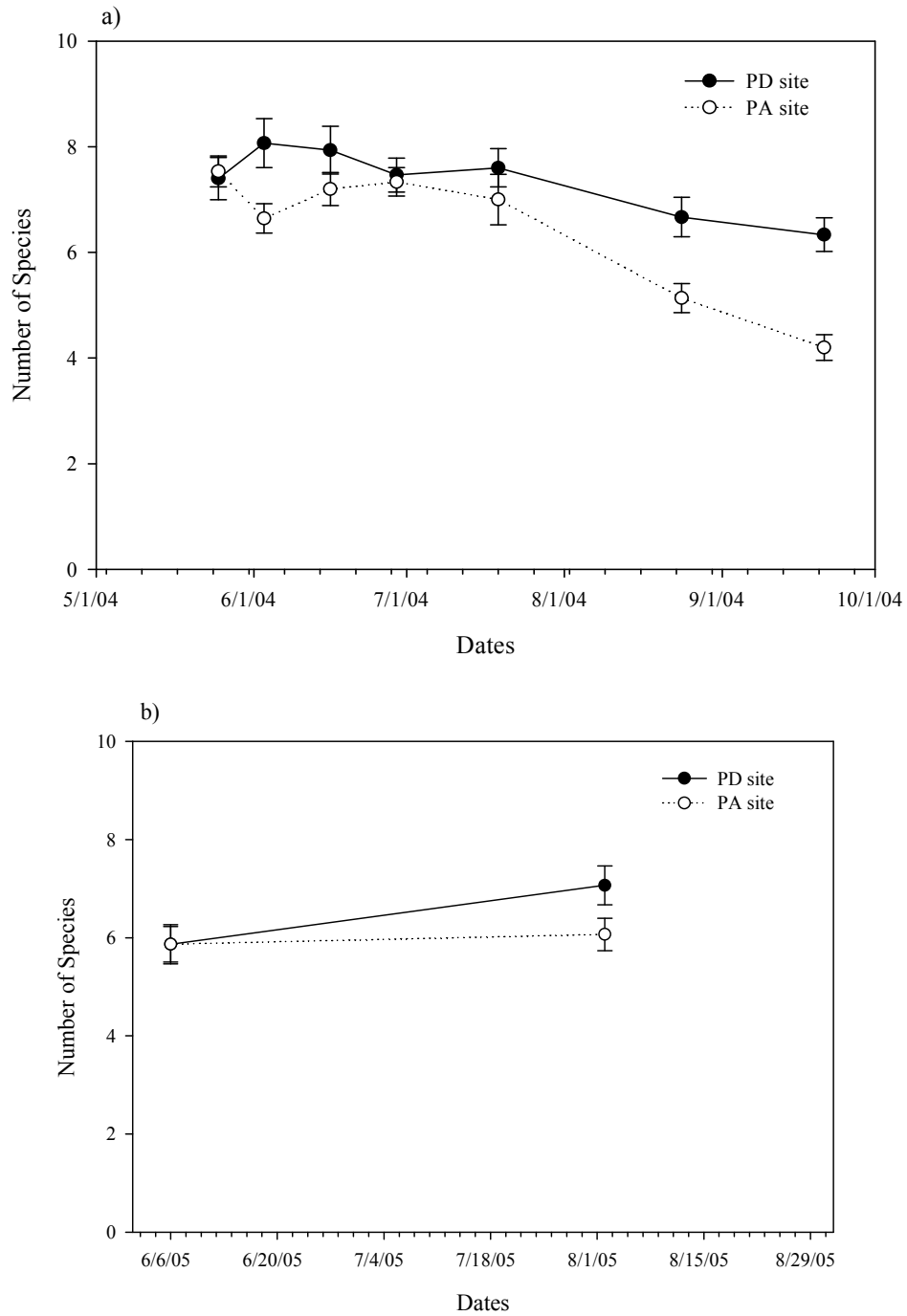


Figure 3.2.22. Mean number of species and standard errors for the *Phragmites*-dominant and *Phragmites*-absent sites across the (a) 2004 and (b) 2005 growing seasons.

Table 3.2.18 Repeated measures ANOVA model for 2004 species richness. * <0.01, ** < 0.05, * < 0.10**

Source	Type III SS	df	MS	F	Sig
Site	54.38	1	54.38	11.51	0.003
Trt	50.99	4	12.75	2.70	0.062
Site * Trt	26.52	4	6.63	1.40	0.271
Error	89.79	19	4.73		
Time	139.32	6	23.22	21.51	0.000
Time * Site	24.88	6	4.15	3.84	0.002***
Time * Trt	16.51	24	0.69	0.64	0.899
Time * Site * Trt	19.15	24	0.80	0.74	0.801
Error (time)	123.05	114	1.08		

Table 3.2.19 ANOVA model: Trt + Time + (Trt*Time) at each marsh site for species richness. * <0.01, ** < 0.05, * < 0.10**

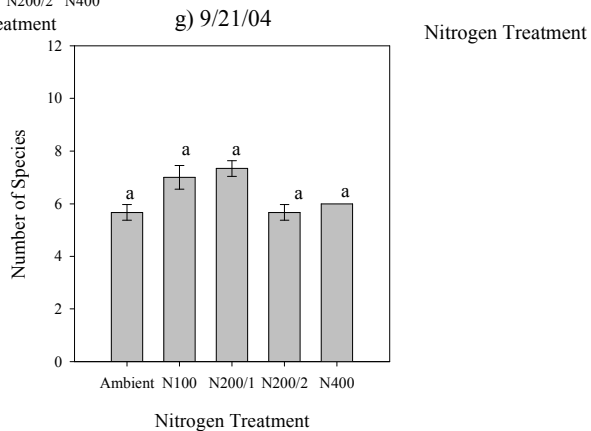
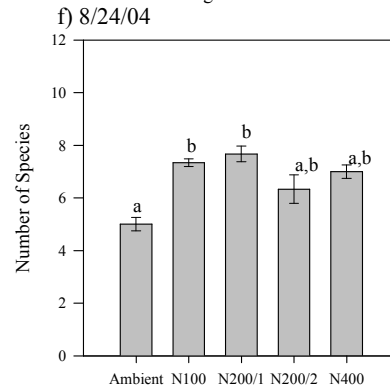
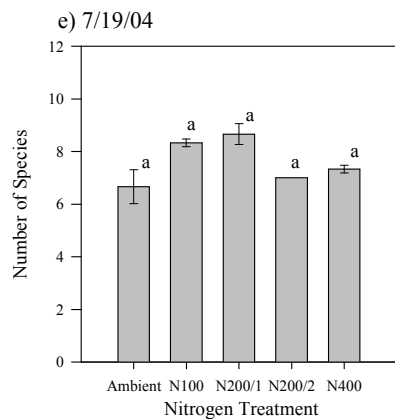
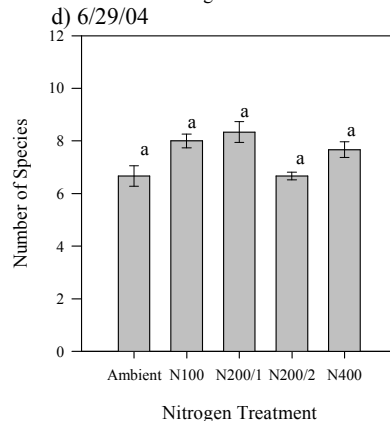
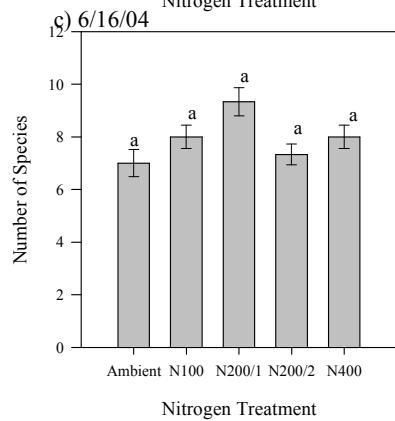
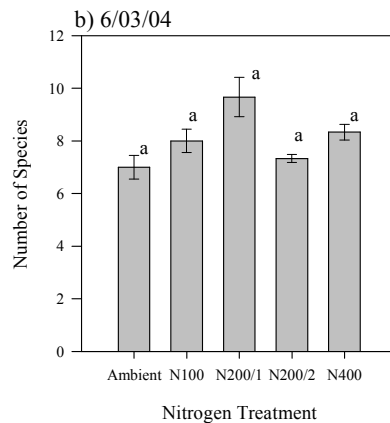
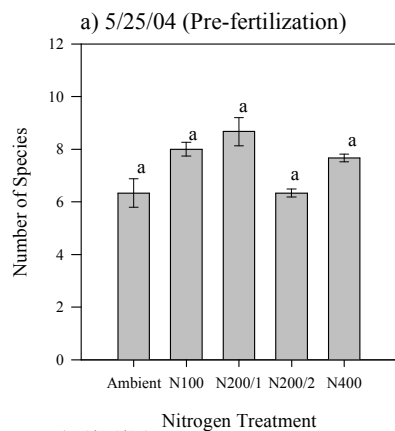
Site	Source	Type III SS	df	MS	F	Sig
PD site	Trt	65.01	4	16.25	2.14	0.150
	Time	36.50	6	6.08	4.96	0.000***
	Time * Trt	7.12	24	0.30	0.24	1.000
	Error	73.52	60	1.23		
PA site	Trt	14.44	4	3.61	2.33	0.135
	Time	123.57	6	20.59	22.46	0.000***
	Time * Trt	27.41	24	1.14	1.25	0.248
	Error	49.52	54	0.92		

Table 3.2.20 ANOVA model: Site + Trt + (Site*Trt) at all sample dates for species richness. * <0.01, ** < 0.05, * < 0.10**

Date	Source	Type III SS	df	MS	F	Sig
5/25/2004	Site	0.13	1	0.13	0.07	0.788
	Trt	9.13	4	2.28	1.27	0.315
	Site * Trt	6.20	4	1.55	0.86	0.504
	Error	36.00	20	1.80		
6/3/2004	Site	14.67	1	14.67	6.17	0.022**
	Trt	9.97	4	2.49	1.05	0.409
	Site * Trt	4.69	4	1.17	0.49	0.741
	Error	45.17	19	2.38		
6/16/2004	Site	4.03	1	4.03	1.95	0.178
	Trt	15.87	4	3.97	1.92	0.146
	Site * Trt	6.13	4	1.53	0.74	0.575
	Error	41.33	20	2.07		

Date	Source	Type III SS	df	MS	F	Sig
6/29/2004	Site	0.13	1	0.13	0.12	0.735
	Trt	10.87	4	2.72	2.40	0.084*
	Site * Trt	3.53	4	0.88	0.78	0.552
	Error	22.67	20	1.13		
7/19/2004	Site	2.70	1	2.70	1.45	0.243
	Trt	15.80	4	3.95	2.12	0.117
	Site * Trt	22.47	4	5.62	3.01	0.043**
	Error	37.33	20	1.87		
8/24/2004	Site	17.63	1	17.63	13.23	0.002
	Trt	4.20	4	1.05	0.79	0.547
	Site * Trt	14.20	4	3.55	2.66	0.063*
	Error	26.67	20	1.33		
9/21/2004	Site	34.13	1	34.13	27.68	0.000***
	Trt	1.53	4	0.38	0.31	0.867
	Site * Trt	7.53	4	1.88	1.53	0.232
	Error	24.67	20	1.23		
6/6/2005	Site	0.00	1	0.00	0.00	1.000
	Trt	11.47	4	2.87	1.32	0.296
	Site * Trt	6.67	4	1.67	0.77	0.558
	Error	43.33	20	2.17		
8/2/2005	Site	7.50	1	7.50	3.52	0.075*
	Trt	1.53	4	0.38	0.18	0.946
	Site * Trt	11.67	4	2.92	1.37	0.281
	Error	42.67	20	2.13		

Since site and time effects on species richness were both present, nitrogen effects were further analyzed on individual sites at each sample date. At the *Phragmites*-dominant site, the number of species present across the growing season was not affected by nitrogen fertilization for the majority of the 2004-5 seasons (Figure 3.2.23). Only on the 8/24/04 did nitrogen addition appear to increase species richness over the control (Figure 3.2.23f).



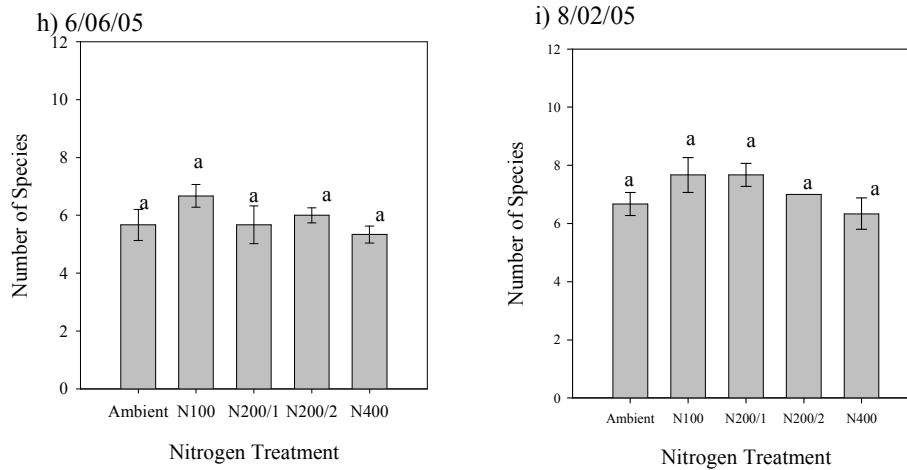
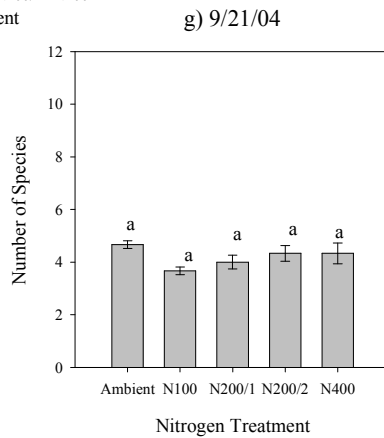
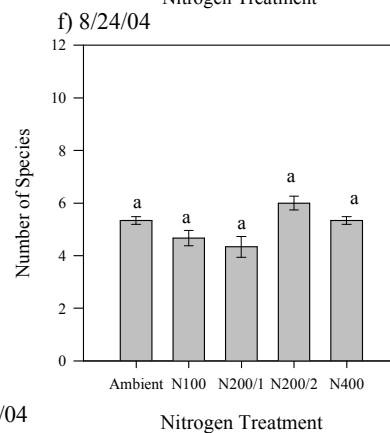
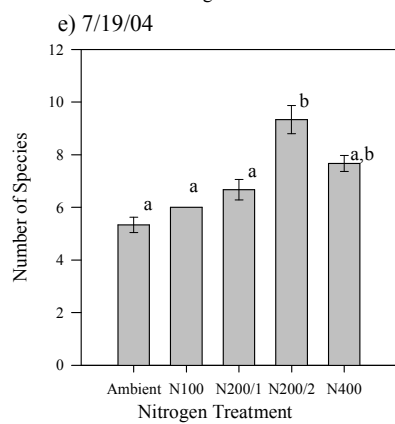
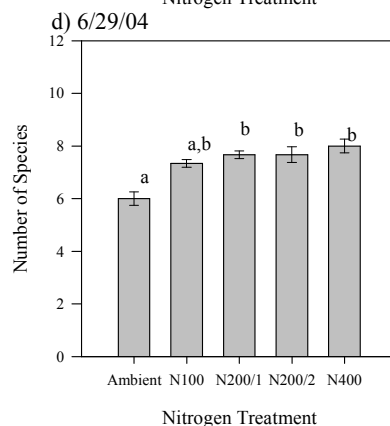
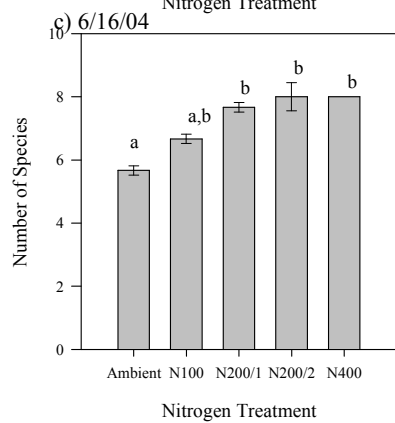
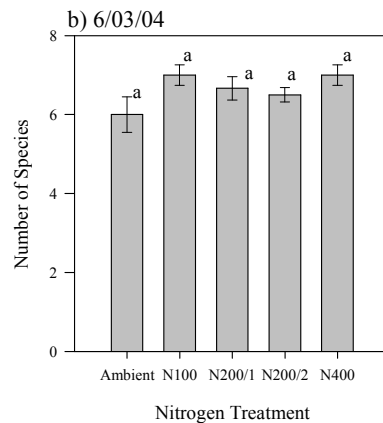
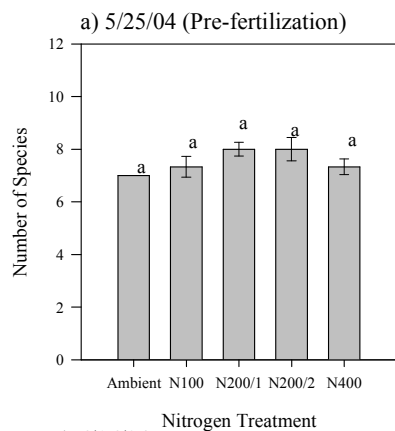


Figure 3.2.23. Mean species richness and standard errors at the *Phragmites*-dominant site according to nitrogen treatment over the 2004-5 growing seasons. Treatments with different letters indicate a significant difference between treatments ($p < 0.05$). Species richness was the dependent variable in the one-way ANOVA model, with an LSD contrast.

At the *Phragmites*-absent site the addition of nitrogen increased species richness early in the growing season (mid-June – July) but the effect disappeared by August (Figure 3.2.24). From mid-June through mid-July, the middle nitrogen fertilizer treatments (N200/1D and N200/2D) yielded significantly more species than ambient conditions (Figure 3.2.24c-e). N200/2D also produced higher species richness on 6/06/05 (Figure 3.2.24h).



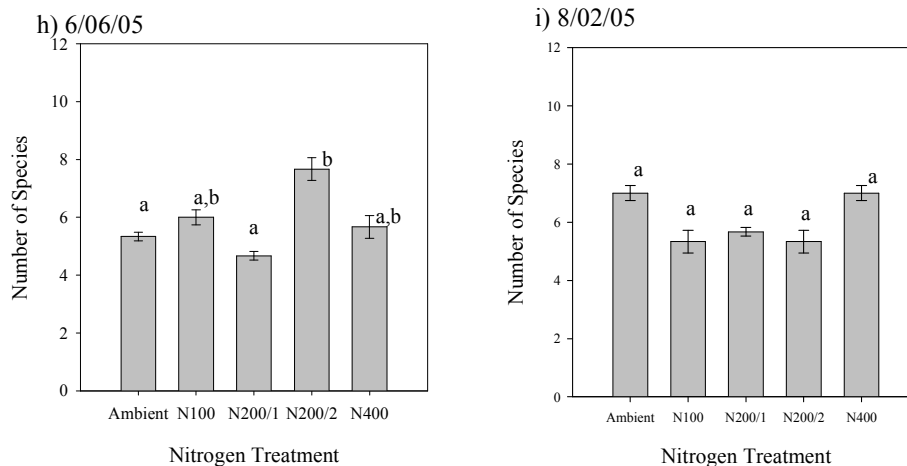


Figure 3.2.24. Mean species richness and standard errors at the *Phragmites*-absent site according to nitrogen treatment over the 2004-5 growing seasons. Treatments with different letters indicate a significant difference between treatments ($p < 0.05$). Species richness was the dependent variable in the one-way ANOVA model, with an LSD contrast.

Effects on dead material

Nitrogen fertilization effect on percent cover of dead material in the marsh was analyzed by first investigating site and time effects. The site effect on percent dead material cover over time, illustrated in Figure 3.2.25, was found to interact with the time effect (Table 3.2.21), so nitrogen effects were analyzed with time at individual sites and with site on each date. Time effects on percent dead material cover were highly significant at both sites and nitrogen effects were discovered at the *Phragmites*-dominant site (Table 3.2.22). Site effects on dead material percent cover were found for the majority of the growing season, while nitrogen effects were not detected on any date (Table 3.2.23).

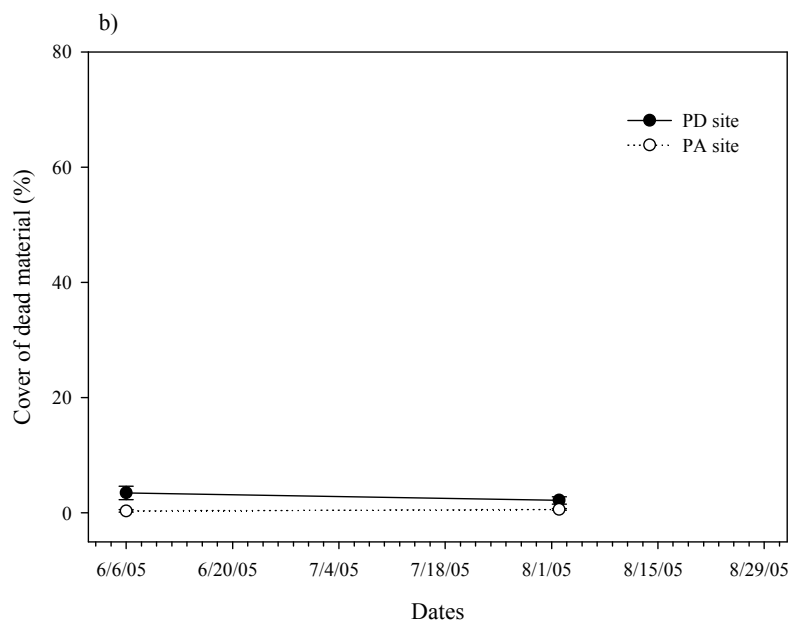
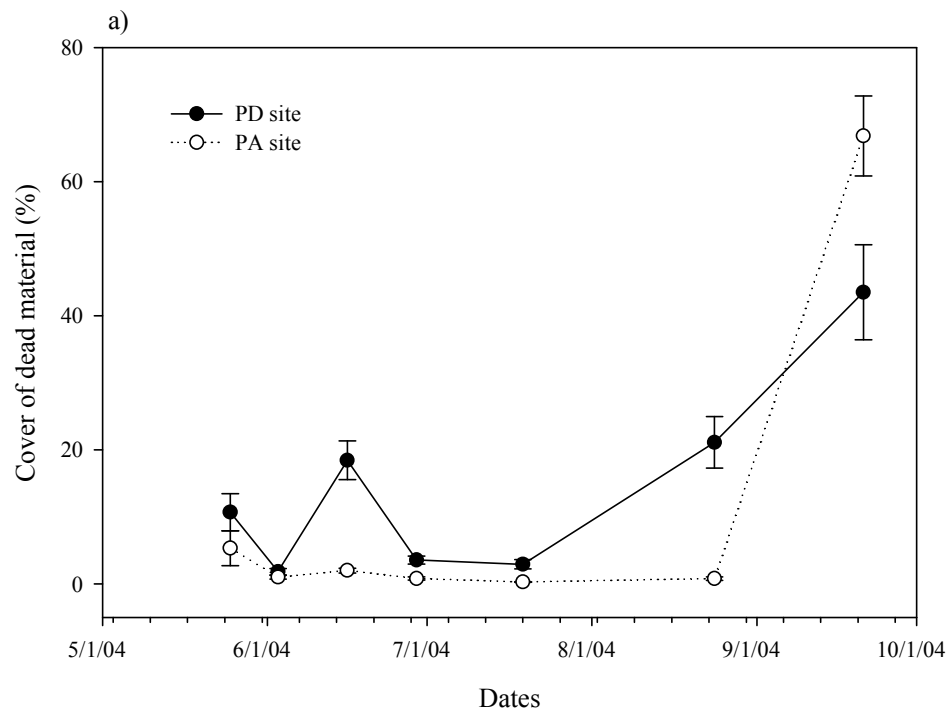


Figure 3.2.25. Mean percent cover of dead material and standard errors for the *Phragmites*-dominant and *Phragmites*-absent sites across the (a) 2004 and (b) 2005 growing seasons.

Table 3.2.21 Repeated measures ANOVA model for 2004 percent dead material. * <0.01, ** < 0.05, * < 0.10**

Source	Type III SS	df	MS	F	Sig
Site	671.61	1	671.61	4.68	0.043
Trt	1615.37	4	403.84	2.81	0.053
Site * Trt	960.34	4	240.09	1.67	0.196
Error	2870.76	20	143.54		
Time	65863.92	6	10977.32	86.68	0.000
Time * Site	8864.38	6	1477.40	11.67	0.000***
Time * Trt	3612.48	24	150.52	1.19	0.266
Time * Site * Trt	1974.80	24	82.28	0.65	0.889
Error (time)	15197.85	120	126.65		

Table 3.2.22 ANOVA model: Trt + Time + (Trt*Time) at each marsh site for dead material. * <0.01, ** < 0.05, * < 0.10**

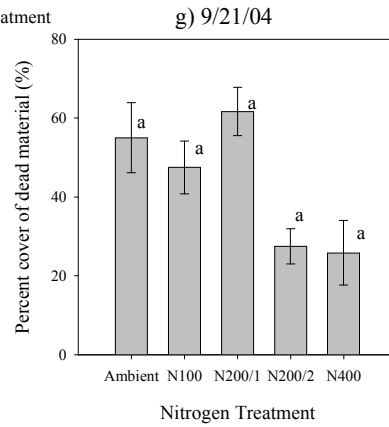
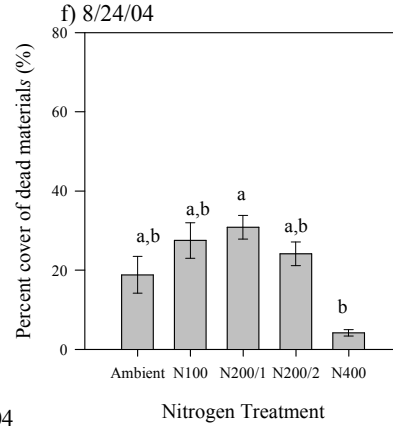
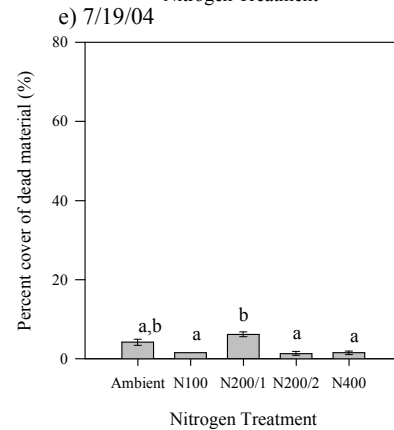
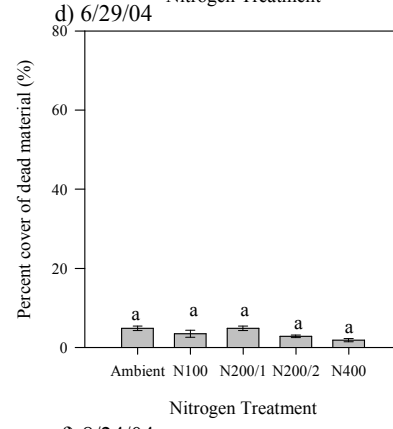
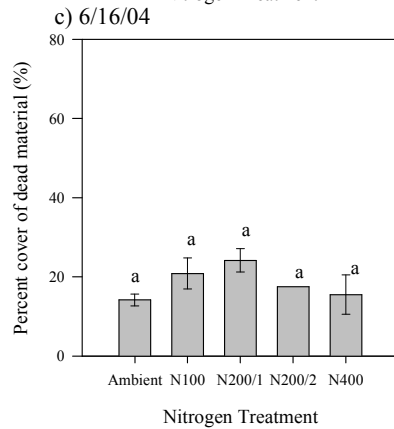
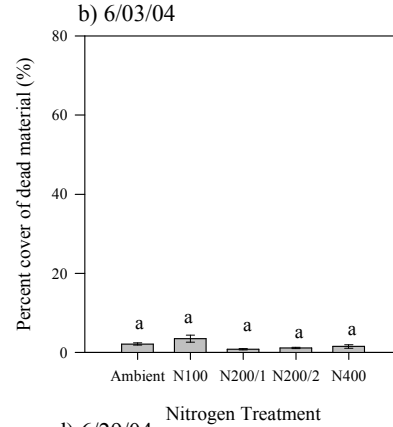
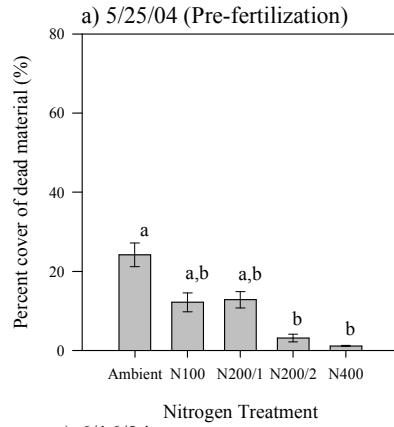
Site	Source	Type III SS	df	MS	F	Sig
PD site	Trt	2294.57	4	573.64	2.69	0.093*
	Time	19921.76	6	3320.29	21.20	0.000***
	Time * Trt	3450.90	24	143.79	0.92	0.578
	Error	9395.58	60	156.59		
PA site	Trt	281.14	4	70.28	0.96	0.472
	Time	54806.53	6	9134.42	94.46	0.000***
	Time * Trt	2136.38	24	89.02	0.92	0.576
	Error	5802.27	60	96.70		

Table 3.2.23 ANOVA model: Site + Trt + (Site*Trt) at all sample dates for percent dead material. * <0.01, ** < 0.05, * < 0.10**

Date	Source	Type III SS	df	MS	F	Sig
5/25/2004	Site	215.74	1	215.74	2.50	0.129
	Trt	353.37	4	88.34	1.03	0.418
	Site * Trt	943.79	4	235.95	2.74	0.058*
	Error	1723.54	20	86.18		
6/3/2004	Site	5.13	1	5.13	2.15	0.158
	Trt	5.03	4	1.26	0.53	0.717
	Site * Trt	12.37	4	3.09	1.30	0.305
	Error	47.74	20	2.39		
6/16/2004	Site	2025.41	1	2025.41	25.93	0.000***
	Trt	111.80	4	27.95	0.36	0.836
	Site * Trt	94.47	4	23.62	0.30	0.873
	Error	1562.17	20	78.11		

Date	Source	Type III SS	df	MS	F	Sig
6/29/2004	Site	57.96	1	57.96	18.58	0.000***
	Trt	11.07	4	2.77	0.89	0.490
	Site * Trt	12.44	4	3.11	1.00	0.432
	Error	62.41	20	3.12		
7/19/2004	Site	52.67	1	52.67	24.45	0.000
	Trt	29.16	4	7.29	3.38	0.029
	Site * Trt	26.69	4	6.67	3.10	0.039**
	Error	43.08	20	2.15		
8/24/2004	Site	3095.75	1	3095.75	34.15	0.000***
	Trt	609.92	4	152.48	1.68	0.194
	Site * Trt	703.72	4	175.93	1.94	0.143
	Error	1813.02	20	90.65		
9/21/2004	Site	4083.33	1	4083.33	6.37	0.020**
	Trt	4107.50	4	1026.88	1.60	0.213
	Site * Trt	1141.67	4	285.42	0.45	0.774
	Error	12816.67	20	640.83		
6/6/2005	Site	73.48	1	73.48	10.06	0.005
	Trt	75.23	4	18.81	2.58	0.069
	Site * Trt	76.87	4	19.22	2.63	0.065*
	Error	146.06	20	7.30		
8/2/2005	Site	19.04	1	19.04	5.21	0.034**
	Trt	10.53	4	2.63	0.72	0.588
	Site * Trt	6.48	4	1.62	0.44	0.776
	Error	73.11	20	3.66		

Since nitrogen effects on percent dead material cover were sensitive to time and site, the effect of nitrogen was analyzed on individual dates at each site. At the *Phragmites*-dominant site, percent dead material for N400 was lower than other treatments in July and August (Figure 3.2.26e and f).



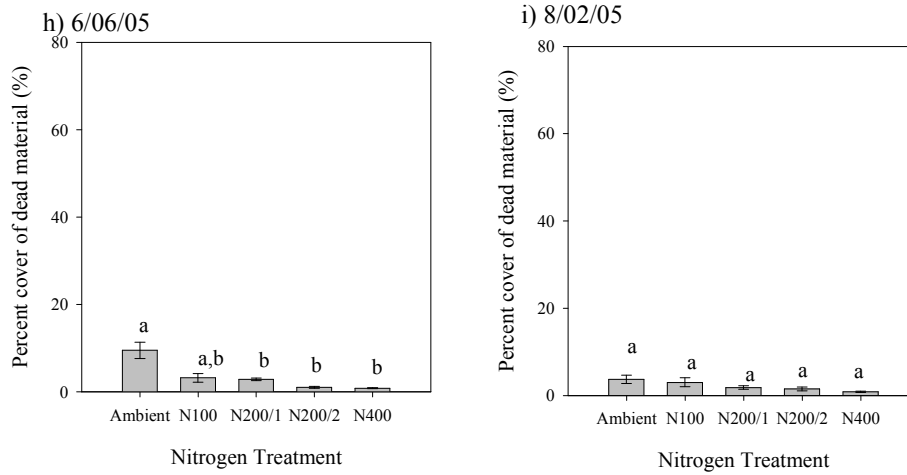
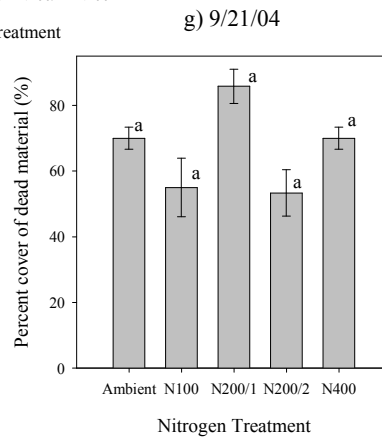
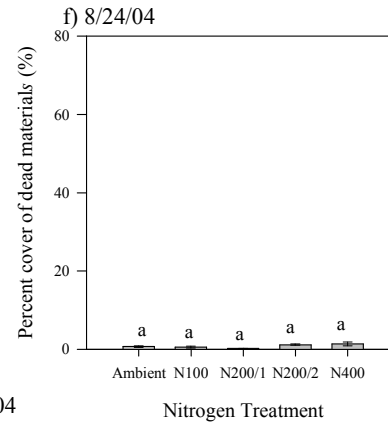
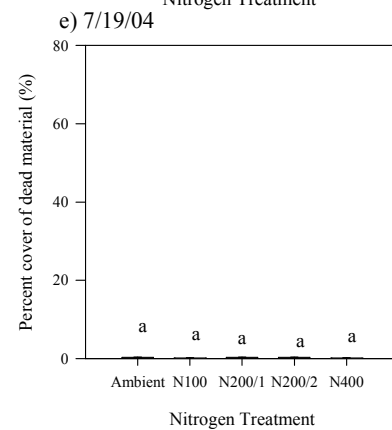
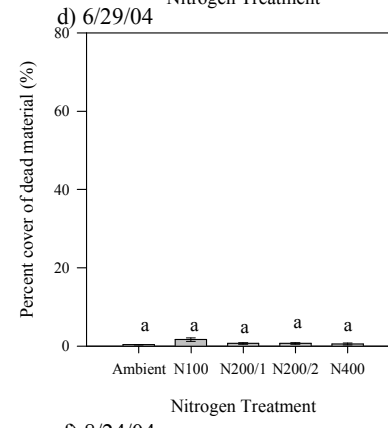
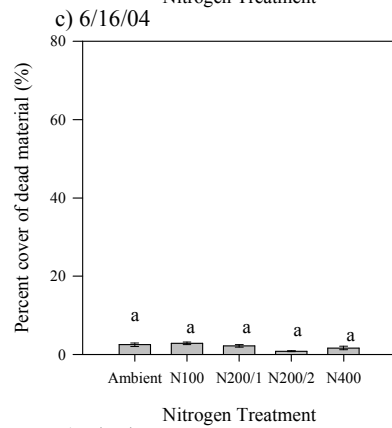
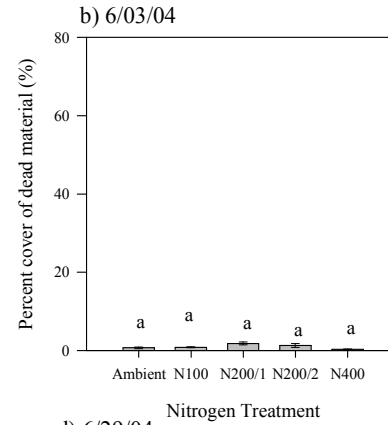
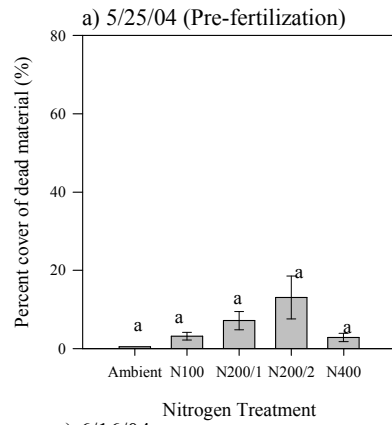


Figure 3.2.26. Mean percent dead material and standard errors at the *Phragmites*-dominant site according to nitrogen treatment over the 2004-5 growing seasons. Treatments with different letters indicate a significant difference between treatments ($p < 0.05$). Percent dead material was the dependent variable in the one-way ANOVA model, with an LSD contrast.

At the *Phragmites*-absent site, no nitrogen effects existed for percent dead material cover on any date in 2004 or 2005 (Figure 3.2.27). Percent cover of dead material followed the same pattern across time for all treatments, where very little dead matter existed during the growing season until September when percent mean reached approximately 60%.



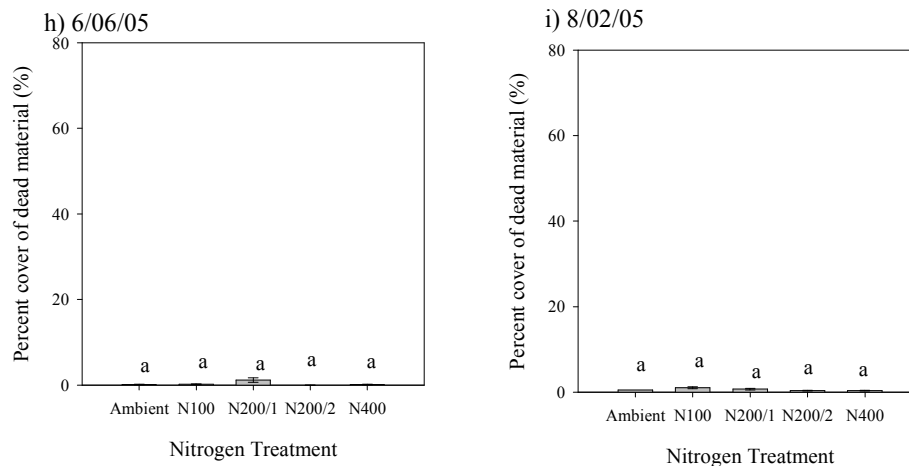


Figure 3.2.27. Mean percent dead material and standard errors at the *Phragmites*-absent site according to nitrogen treatment over the 2004-5 growing seasons. Treatments with different letters indicate a significant difference between treatments ($p < 0.05$). Percent dead material was the dependent variable in the one-way ANOVA model, with an LSD contrast.

Effects on Shannon-Wiener Diversity Index

The Shannon-Wiener diversity index was evaluated for nitrogen effects, as well as site and time effects for the 2004-5 growing seasons. The *Phragmites*-dominant site visually had a higher Shannon-Wiener species diversity index than the *Phragmites*-absent site and retained a high diversity index for the majority of the 2004 season, while the *Phragmites*-absent site's diversity index fell to below a value of 1.0 in mid-July (Figure 3.2.28). The visual differences between sites and sample dates were statistically proven with an interaction effect between site and time (Table 3.2.24). Analysis of time and treatment at each site found a strong time effect at both sites (Table 3.2.25). Analysis of site and treatment at each date found a site effect at the majority of sample dates, particularly those near the end of the growing season (Table 3.2.26). Also, a minor nitrogen effect on diversity index was found early in the 2004 season, on 6/03/04 and 6/16/04 (Table 3.2.26).

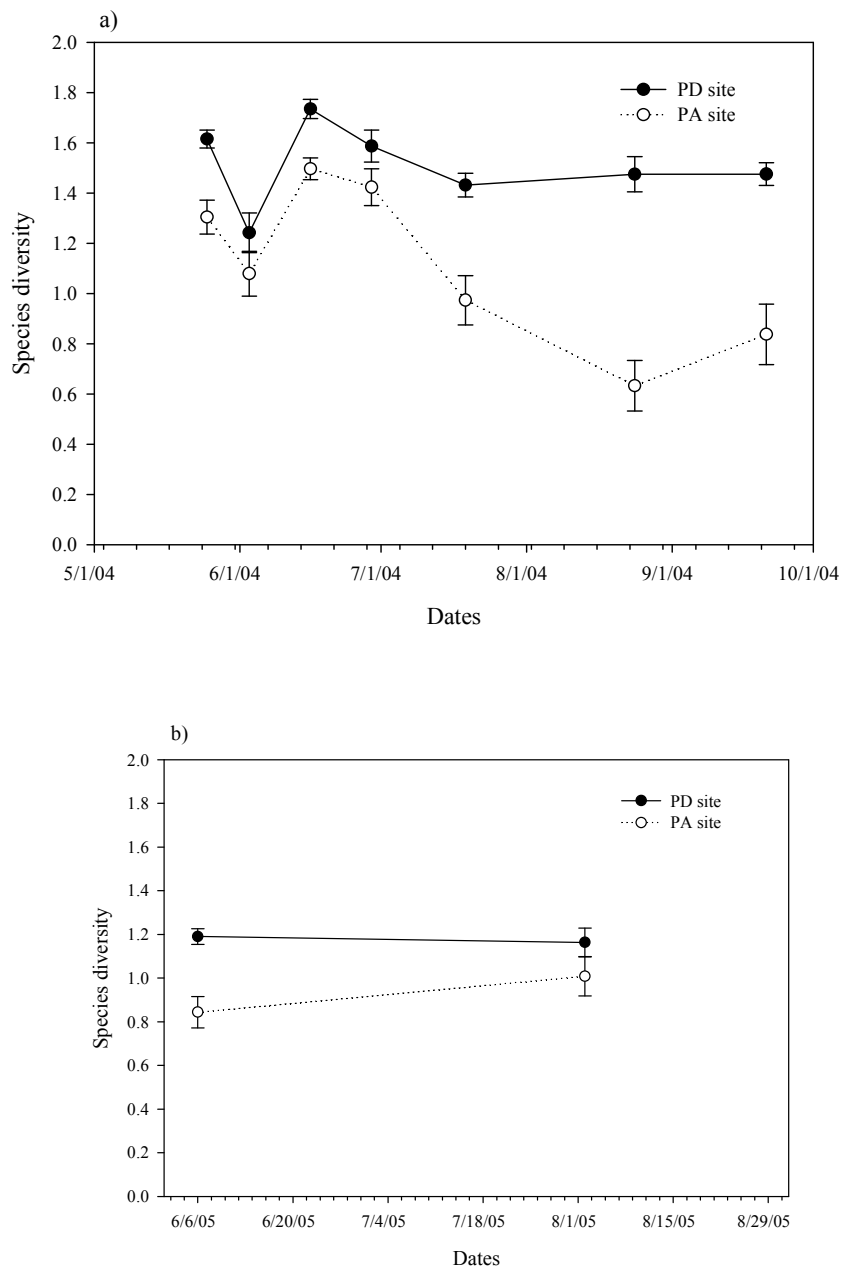


Figure 3.2.28. Mean Shannon-Wiener diversity and standard errors for the *Phragmites*-dominant and *Phragmites*-absent sites across the (a) 2004 and (b) 2005 growing seasons.

Table 3.2.24 Repeated measures ANOVA model for 2004 Shannon-Wiener diversity index. * <0.01, ** < 0.05, * < 0.10**

Source	Type III SS	df	MS	F	Sig
Site	8.72	1	8.72	59.65	0.000
Trt	0.83	4	0.21	1.42	0.266
Site * Trt	0.91	4	0.23	1.55	0.228
Error	2.78	19	0.15		
Time	7.58	6	1.26	20.34	0.000
Time * Site	2.69	6	0.45	7.23	0.000***
Time * Trt	1.13	24	0.05	0.76	0.780
Time * Site * Trt	1.72	24	0.07	1.15	0.300
Error (time)	7.08	114	0.06		

Table 3.2.25 ANOVA model: Trt + Time + (Trt*Time) at each marsh site for Shannon-Wiener diversity index. * <0.01, ** < 0.05, * < 0.10**

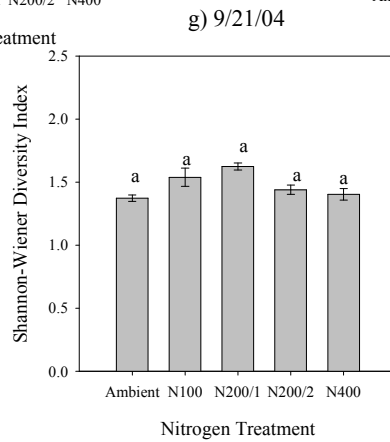
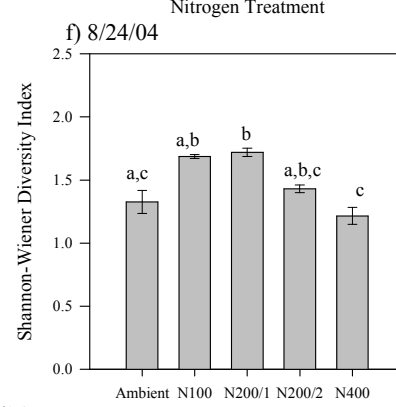
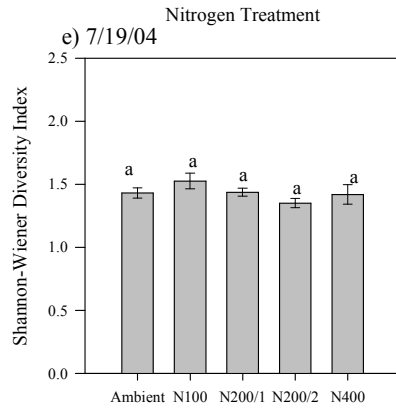
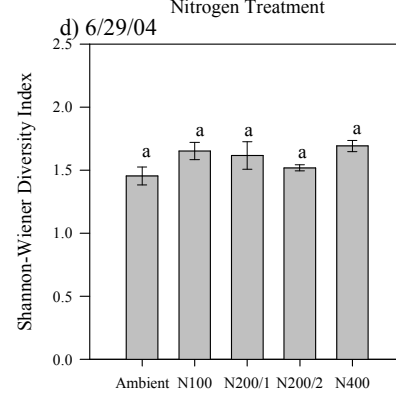
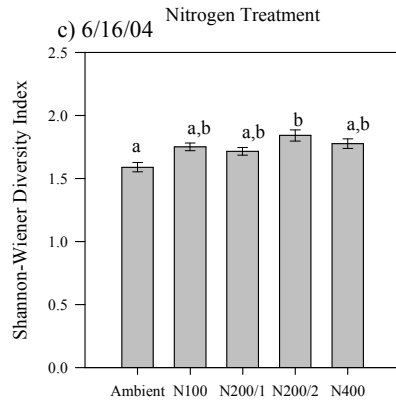
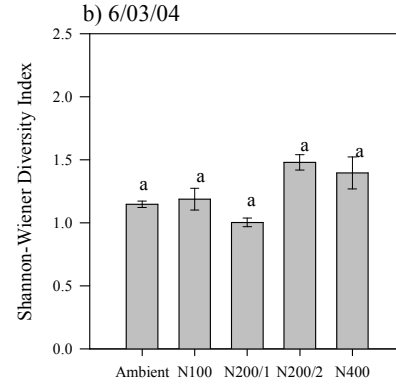
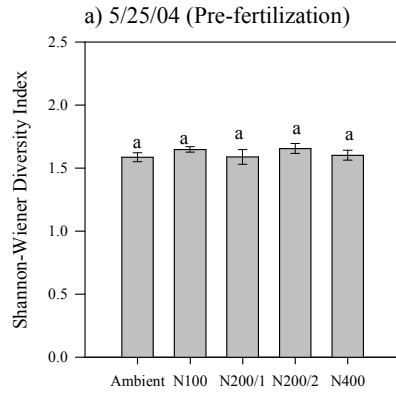
Site	Source	Type III SS	df	MS	F	Sig
PD site	Trt	0.28	4	0.07	0.88	0.509
	Time	2.22	6	0.37	9.27	0.000***
	Time * Trt	1.16	24	0.05	1.21	0.269
	Error	2.39	60	0.04		
PA site	Trt	1.40	4	0.35	1.60	0.256
	Time	7.79	6	1.30	14.95	0.000***
	Time * Trt	1.69	24	0.07	0.81	0.705
	Error	4.69	54	0.09		

Table 3.2.26 ANOVA model: Site + Trt + (Site*Trt) at all sample dates for the Shannon-Wiener diversity index. * <0.01, ** < 0.05, * < 0.10**

Date	Source	Type III SS	df	MS	F	Sig
5/25/2004	Site	0.73	1	0.73	21.61	0.000***
	Trt	0.30	4	0.07	2.21	0.105
	Site * Trt	0.25	4	0.06	1.83	0.162
	Error	0.67	20	0.03		
6/3/2004	Site	0.19	1	0.19	2.16	0.158
	Trt	0.83	4	0.21	2.30	0.096*
	Site * Trt	0.29	4	0.07	0.79	0.543
	Error	1.71	19	0.09		
6/16/2004	Site	0.43	1	0.43	20.20	0.000***
	Trt	0.22	4	0.06	2.63	0.065*
	Site * Trt	0.05	4	0.01	0.64	0.640
	Error	0.42	20	0.02		

Date	Source	Type III SS	df	MS	F	Sig
6/29/2004	Site	0.20	1	0.20	2.83	0.108
	Trt	0.22	4	0.05	0.77	0.556
	Site * Trt	0.33	4	0.08	1.17	0.352
	Error	1.42	20	0.07		
7/19/2004	Site	1.58	1	1.58	18.44	0.000***
	Trt	0.21	4	0.05	0.60	0.666
	Site * Trt	0.56	4	0.14	1.64	0.203
	Error	1.71	20	0.09		
8/24/2004	Site	5.32	1	5.32	49.48	0.000***
	Trt	0.18	4	0.05	0.43	0.786
	Site * Trt	0.82	4	0.20	1.90	0.149
	Error	2.15	20	0.11		
9/21/2004	Site	3.05	1	3.05	24.27	0.000***
	Trt	0.25	4	0.06	0.49	0.741
	Site * Trt	0.69	4	0.17	1.38	0.277
	Error	2.51	20	0.13		
6/6/2005	Site	0.91	1	0.91	27.38	0.000
	Trt	0.18	4	0.05	1.37	0.278
	Site * Trt	0.51	4	0.13	3.87	0.017**
	Error	0.66	20	0.03		
8/2/2005	Site	0.18	1	0.18	1.92	0.181
	Trt	0.37	4	0.09	0.99	0.437
	Site * Trt	0.38	4	0.09	1.00	0.431
	Error	1.88	20	0.09		

Analysis of nitrogen effects on the Shannon-Wiener diversity index for individual dates at the *Phragmites*-dominant site found no nitrogen effects, except in late-August (8/24/04) when a high addition of nitrogen had a low diversity index and mid-fertilization had a very high diversity index (Figure 3.2.29f).



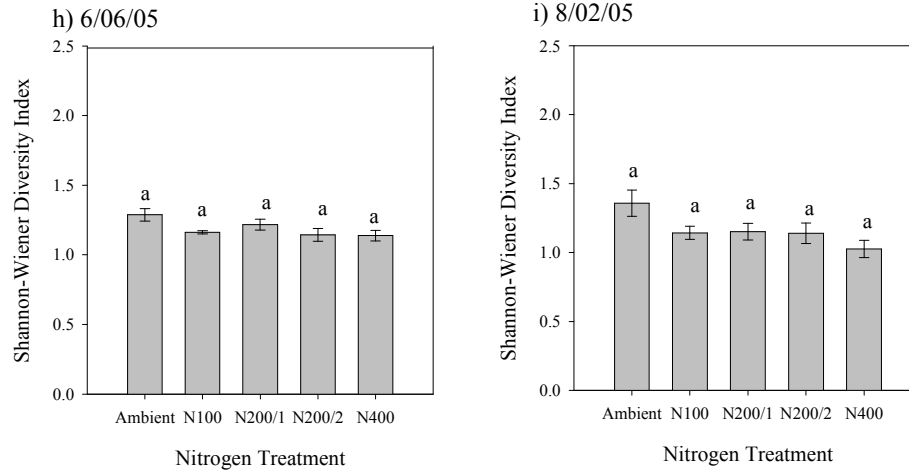
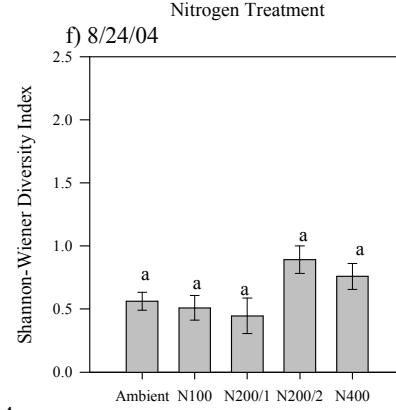
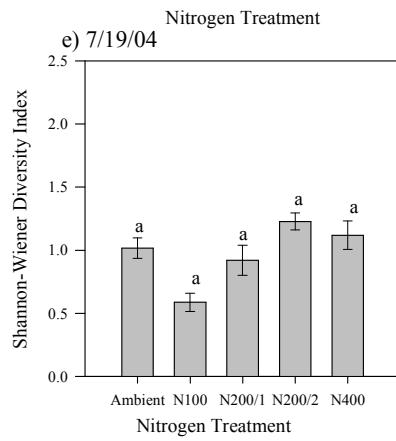
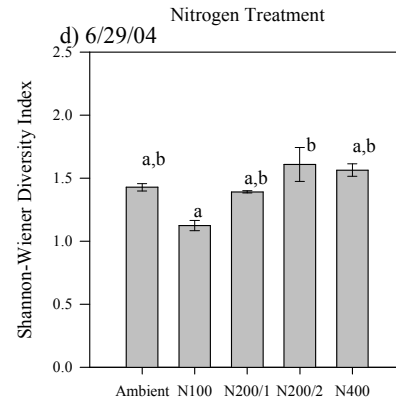
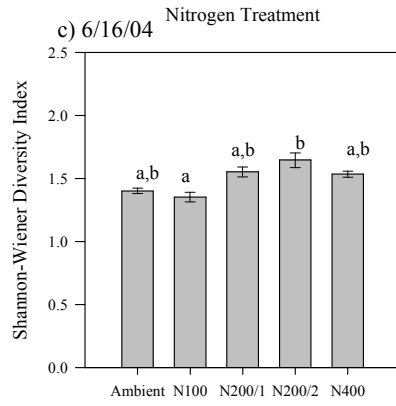
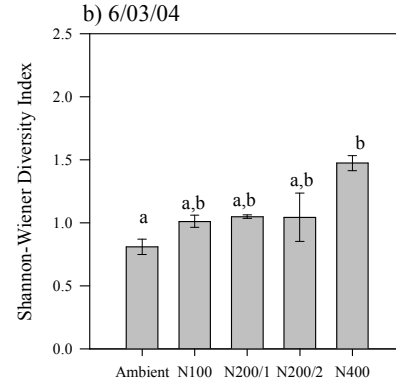
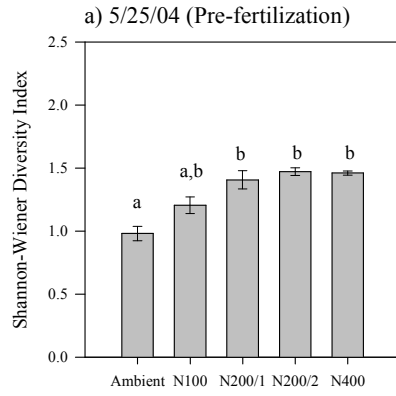
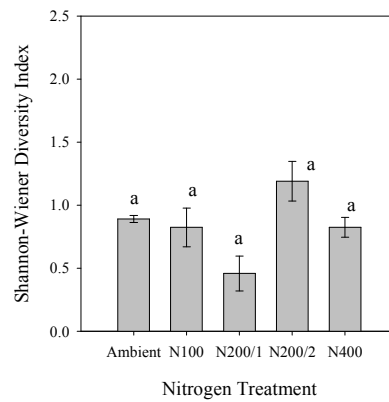


Figure 3.2.29. Mean diversity index and standard errors at the *Phragmites*-dominant site according to nitrogen treatment over the 2004-5 growing seasons. Treatments with different letters indicate a significant difference between treatments ($p < 0.05$). Diversity index was the dependent variable in the one-way ANOVA model, with an LSD contrast.

Detection of a nitrogen effect on Shannon-Wiener diversity index at the *Phragmites*-absent site was confounded by the fact that the pre-fertilization date was correlated to nitrogen treatment (Figure 3.2.30).



g) 9/21/04



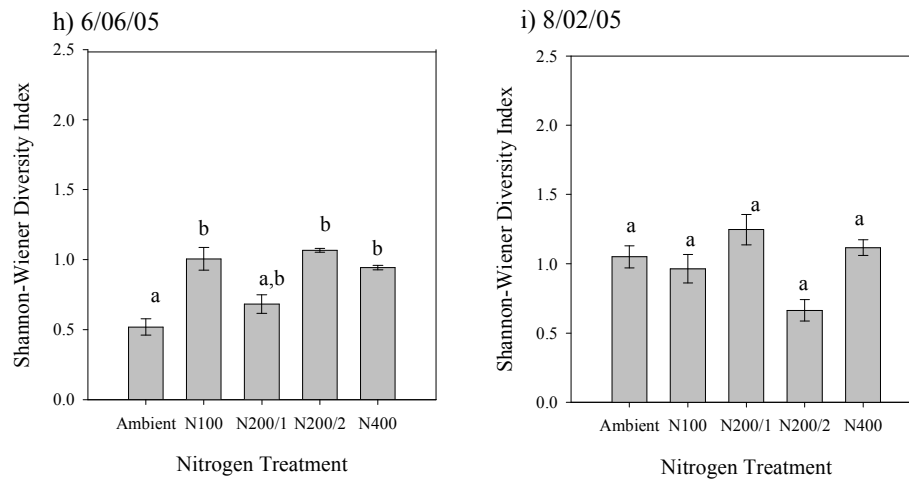


Figure 3.2.30. Mean diversity index and standard errors at the *Phragmites*-absent site according to nitrogen treatment over the 2004-5 growing seasons. Treatments with different letters indicate a significant difference between treatments ($p < 0.05$). Diversity index was the dependent variable in the one-way ANOVA model, with an LSD contrast.

Effects on Biomass

Plots given more urea had higher biomass at the *Phragmites*-absent site (Figure 3.2.31), but there was no difference among plots at the *Phragmites*-dominant site (Figure 3.2.32). *P. arifolium* and *I. capensis* dominated the *Phragmites*-absent site in August (Figure 3.2.2c), and both had a high cover at high levels of nitrogen fertilization, possibly contributing to the high biomass at high fertilization levels. Conversely, the *Phragmites*-dominant site was dominated by *P. arifolium*, *I. capensis*, and *P. australis* in August (Figure 3.2.1c). While *P. arifolium* and *I. capensis* cover had high cover at high levels of fertilization, *P. australis* had a low cover at high levels of fertilization. The differences in nitrogen effects on the dominant species at the *Phragmites*-dominant site may have influenced the biomass at that site. It's also notable that mean biomass at the *Phragmites*-dominant control plots was nearly five times the amount at the *Phragmites*-absent site. Also, the addition of N200/2D as urea doubled the biomass at the *Phragmites*-absent site.

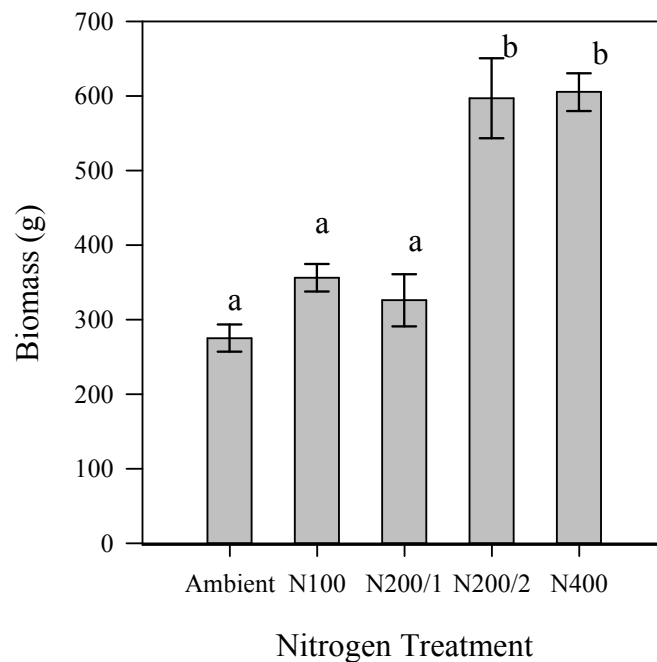


Figure 3.2.31. Mean biomass and standard errors at the *Phragmites*-absent site according to nitrogen treatment on 8/02/05. Treatments with different letters indicate a significant difference between treatments ($p<0.05$).

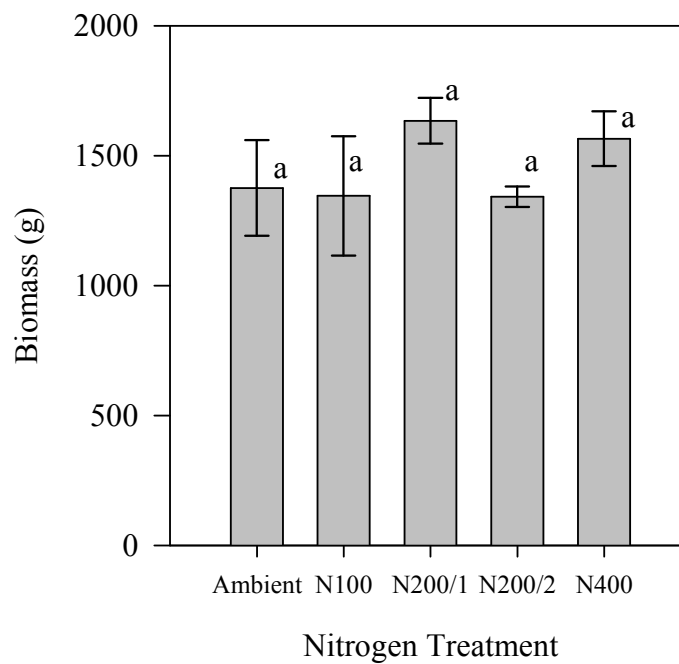


Figure 3.2.32. Mean biomass and standard errors at the *Phragmites*-dominant site according to nitrogen treatment on 8/02/05. Treatments with different letters indicate a significant difference between treatments ($p<0.05$).

LAI was positively related to plot biomass (Fig. 3.2.33). However, neither species richness, nor Shannon diversity were related to biomass (Figure 3.2.34 and 3.2.35).

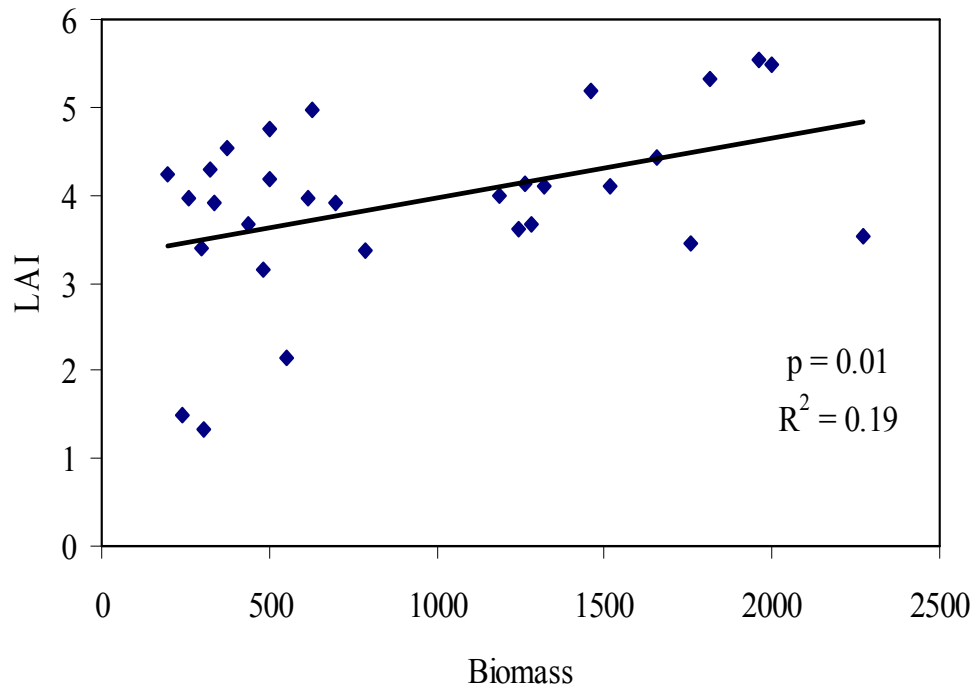


Figure 3.2.33. Biomass and LAI linear regression for all plots (n = 30) on 8/02/05.

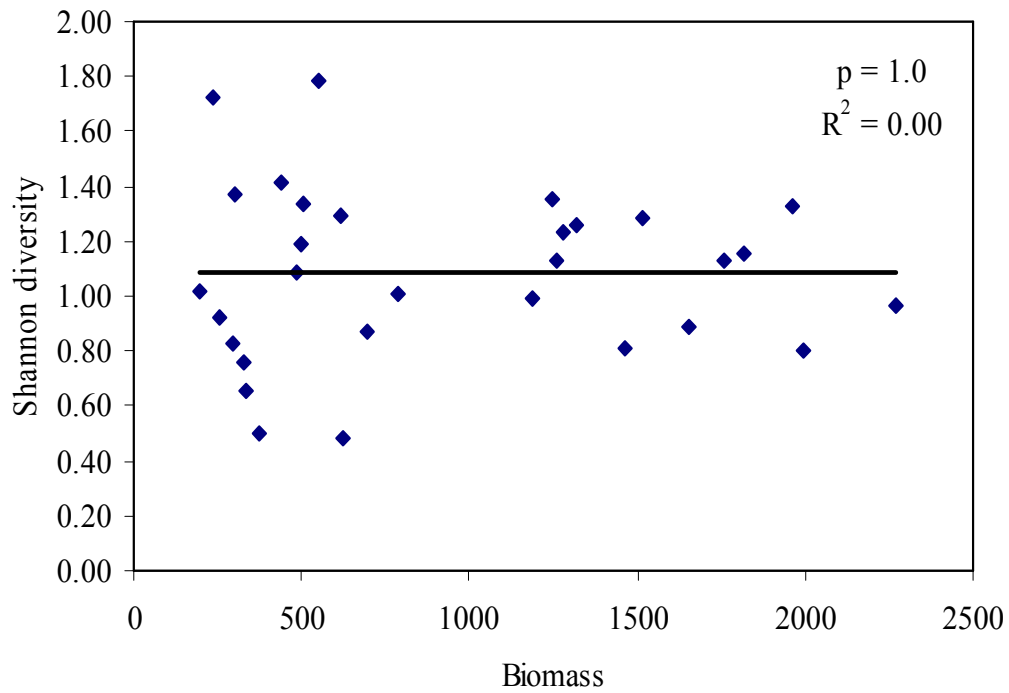


Figure 3.2.34. Biomass and Shannon diversity index linear regression for all plots (n = 30) on 8/02/05.

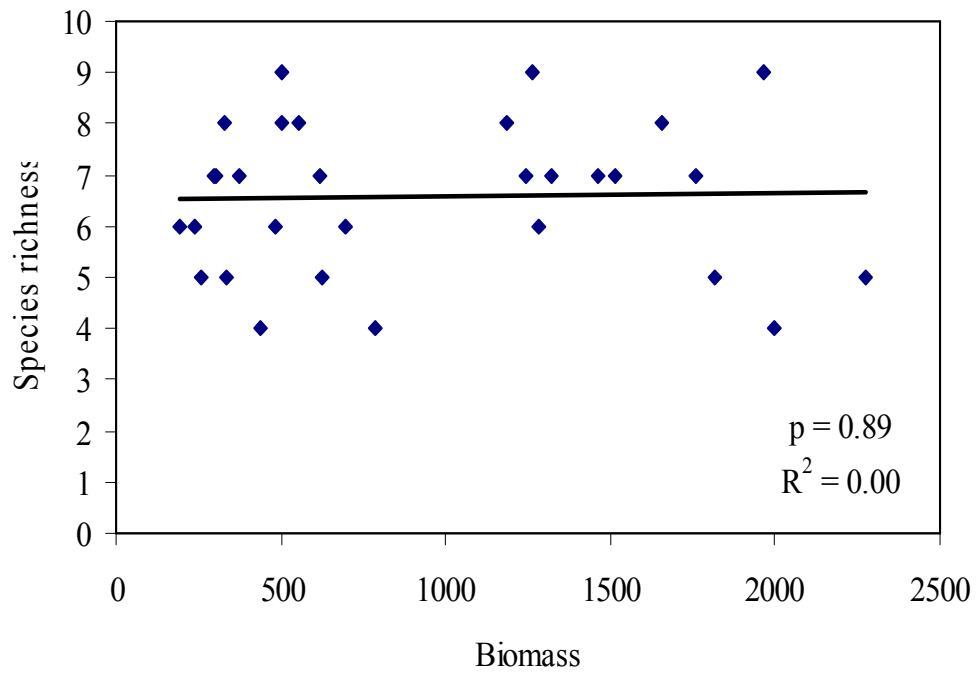


Figure 3.2.35. Biomass and species richness linear regression for all plots (n = 30) on 8/02/05.

3.2.3 Nitrogen fertilization effects on canopy nutrients

The addition of nitrogen increased canopy nitrogen at the *Phragmites*-absent site (Figure 3.2.36), but did not conclusively increase vegetation nitrogen concentration at the *Phragmites*-dominant site (Figure 3.2.37). Nitrogen fertilization also increased canopy phosphorus at the *Phragmites*-absent site (Figure 3.2.38), but did not alter phosphorus at the *Phragmites*-dominant site (Figure 3.2.39).

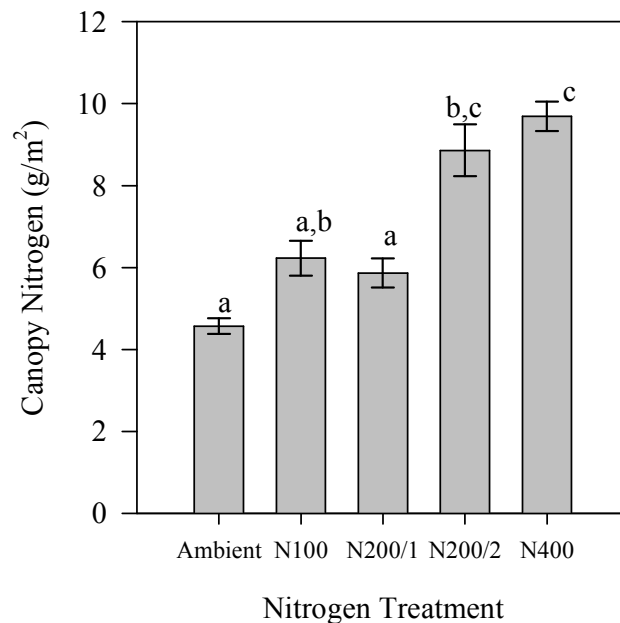


Figure 3.2.36. Mean canopy nitrogen and standard errors at the *Phragmites*-absent site according to nitrogen treatment on 8/02/05. Treatments with different letters indicate a significant difference between treatments ($p < 0.05$).

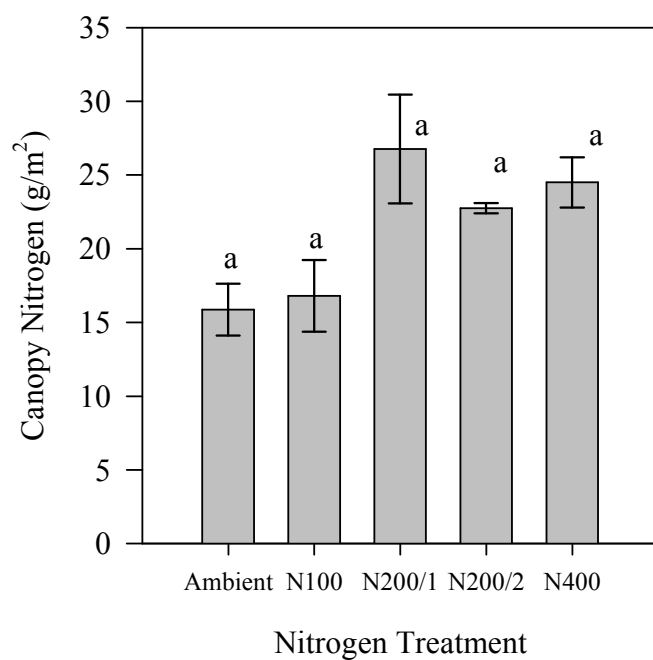


Figure 3.2.37. Mean canopy nitrogen and standard errors at the *Phragmites*-dominant site according to nitrogen treatment on 8/02/05. Treatments with different letters indicate a significant difference between treatments ($p < 0.05$).

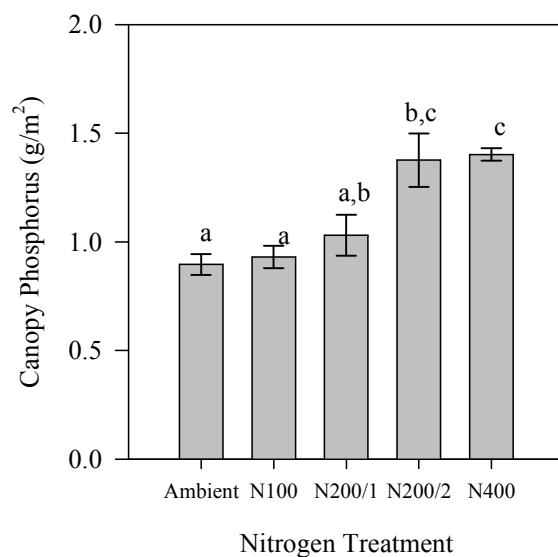


Figure 3.2.38. Mean canopy phosphorus and standard errors at the *Phragmites*-absent site according to nitrogen treatment on 8/02/05. Treatments with different letters indicate a significant difference between treatments ($p < 0.10$).

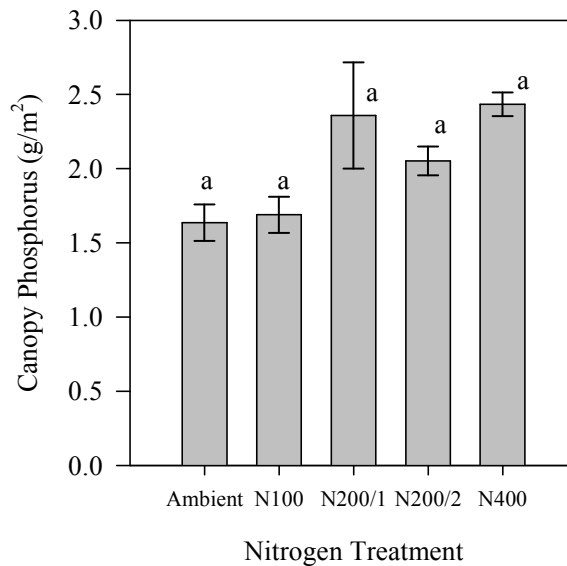


Figure 3.2.39. Mean canopy phosphorus and standard errors at the *Phragmites*-dominant site according to nitrogen treatment on 8/02/05. Treatments with different letters indicate a significant difference between treatments ($p < 0.10$).

The mean canopy nitrogen and phosphorus for each of the top six species is shown according to nitrogen treatment (Tables 3.2.27 and 3.2.28). *A. calamus* and *Typha* species both had high canopy nitrogen and phosphorus with a large addition of urea, whereas *I. capensis* and *P. arifolium* had high canopy nitrogen and phosphorus with low fertilization and high fertilization (Tables 3.2.27 and 3.2.28). *P. virginica* had high canopy nitrogen and phosphorus with medium fertilization (Tables 3.2.27 and 3.2.28).

Table 3.2.27. Mean canopy nitrogen (g/m²) for the top six species according to nitrogen treatment on 8/02/05.

Species	N0				
	(control)	N100	N200/1D	N200/2D	N400
<i>A. calamus</i>	1.22	1.68	1.68	1.49	2.04
<i>I. capensis</i>	0.96	1.15	0.64	0.77	2.62
<i>P. virginica</i>	1.45	1.75	2.49	1.53	1.41
<i>P. australis</i>	11.94	12.59	21.40	17.87	18.16
<i>P. arifolium</i>	1.71	2.27	1.67	3.48	2.45
<i>Typha</i> sp.	0.30	0.52	0.29	1.28	0.99

Table 3.2.28. Mean canopy phosphorus (g/m^2) for the top six species according to nitrogen treatment on 8/02/05.

Species	N0 (control)	N100	N200/1D	N200/2D	N400
<i>A. calamus</i>	0.18	0.27	0.26	0.25	0.36
<i>I. capensis</i>	0.13	0.15	0.07	0.08	0.30
<i>P. virginica</i>	0.31	0.30	0.45	0.27	0.23
<i>P. australis</i>	1.03	1.04	1.62	1.34	1.52
<i>P. arifolium</i>	0.32	0.34	0.30	0.56	0.34
<i>Typha</i> sp.	0.04	0.06	0.04	0.15	0.17

Patterns in species canopy nutrients for each treatment mimic nitrogen effects on species percent cover, which suggests a correlation between biomass and canopy nutrients. Canopy nitrogen was positively related to biomass (Figure 3.2.40), as was canopy phosphorus (Figure 3.2.41).

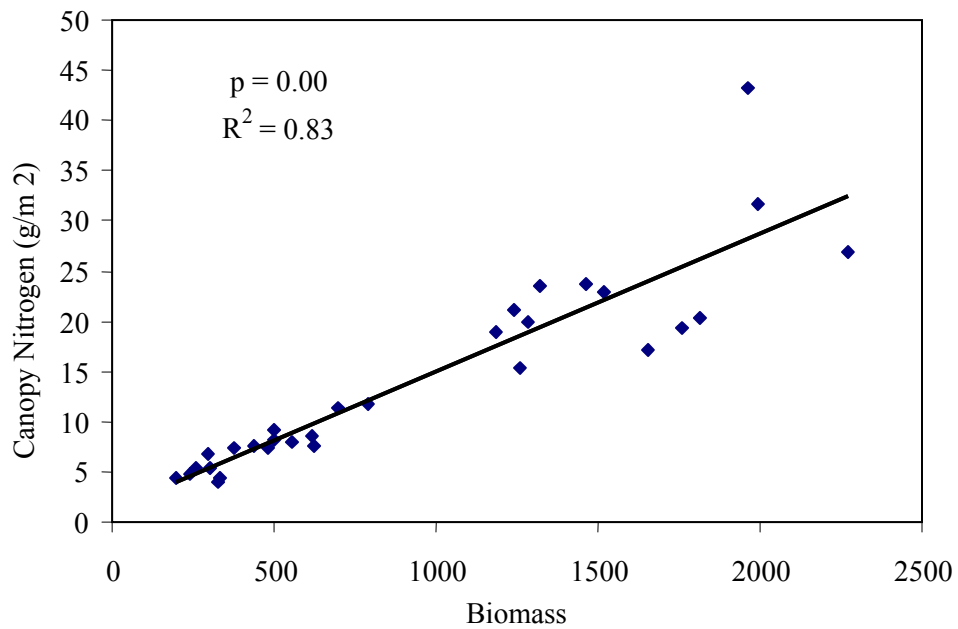


Figure 3.2.40. Biomass and canopy nitrogen linear regression for all plots (n = 30) on 8/02/05.

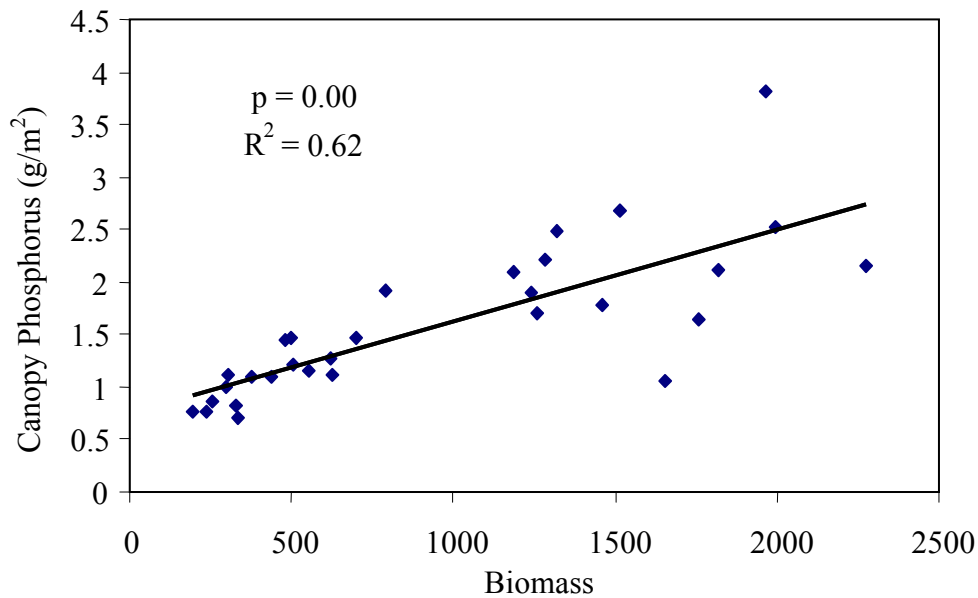


Figure 3.2.41. Biomass and canopy phosphorus linear regression for all plots (n = 30) on 8/02/05. Canopy nitrogen was also positively related to canopy phosphorus (Figure 3.2.42),

but not to sub-surface water ammonia (Figure 3.2.43). Likewise, canopy phosphorus was not related to sub-surface total phosphorus (Figure 3.2.44).

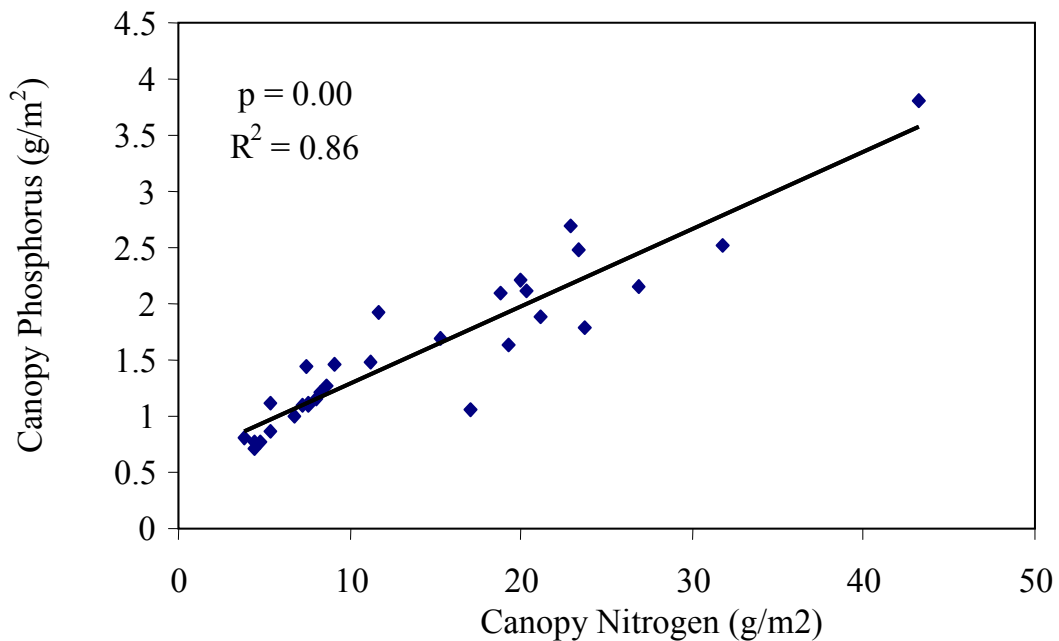


Figure 3.2.42. Canopy nitrogen and phosphorus linear regression for all plots (n = 30) on 8/02/05.

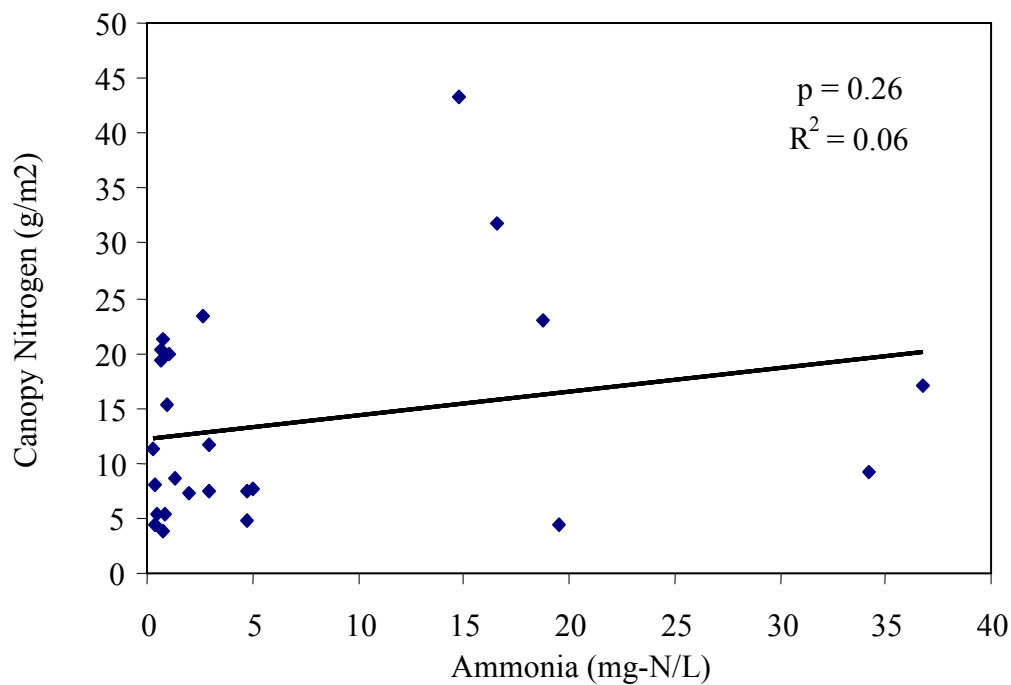


Figure 3.2.43. Sub-surface water ammonia and canopy nitrogen linear regression for all plots (n = 30) on 8/02/05.

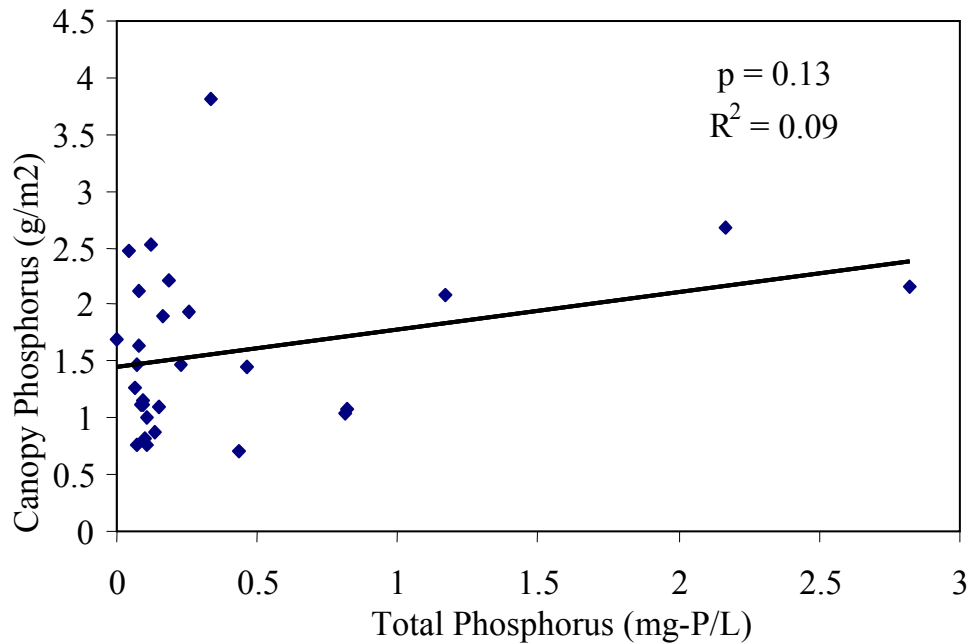


Figure 3.2.44. Sub-surface water total phosphorus and canopy phosphorus linear regression for all plots (n = 30) on 8/02/05.

3.3 Marsh Canopy Reflectance Response

Marsh canopy reflectance was analyzed to determine its response to nitrogen fertilization and vegetation composition. Basic trends of the reflectance over the growing season are outlined in the following section, as are ANOVA's to evaluate the effect of time, site and nitrogen on canopy reflectance.

3.3.1 Seasonal dynamics of canopy reflectance

Since nutrient concentrations and vegetation communities changed over time, canopy reflectance was analyzed to determine its seasonal dynamics. Figure 3.3.1 shows the mean canopy hyperspectral reflectance of six unfertilized plots within the two marsh sites in late May, mid-July, and late-September. As the summer progressed, the marsh canopy reflected less VNIR, except in the visible red waveband, which stayed relatively constant for all three dates.

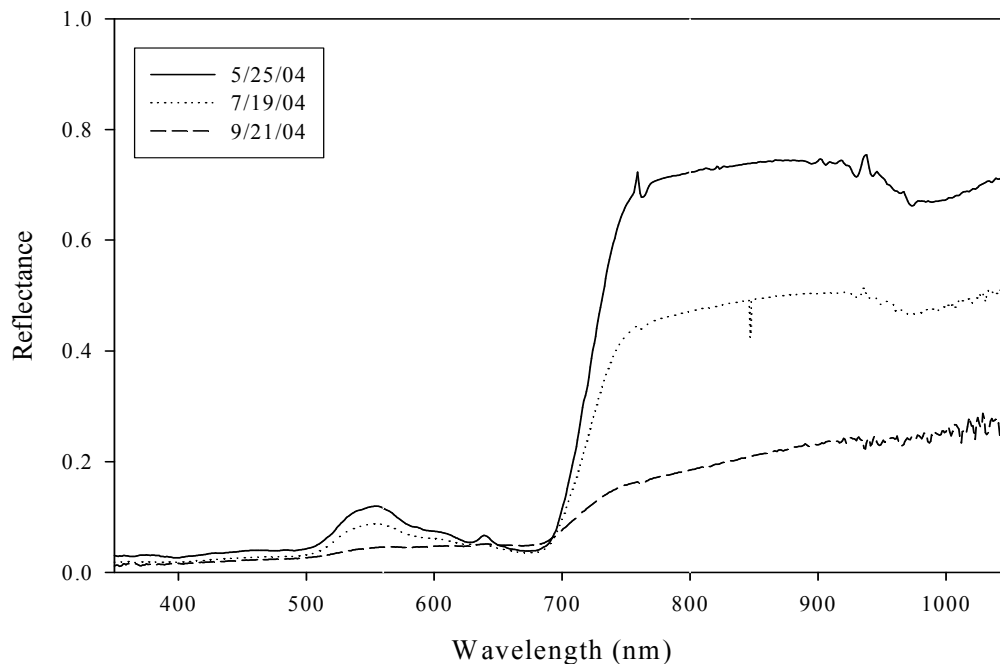


Figure 3.3.1. Mean hyperspectral reflectance of combined marsh sites in late May, mid-July, and late-September for unfertilized plots.

A linear regression was performed to quantify the seasonal effects on major multispectral waveband reflectance. Figures 3.3.2 and 3.3.3 illustrate the seasonal changes in the reflectance of the four Landsat TM wavebands (blue 450-520nm; green 520-600nm; red 630-690nm; near-infrared 760-900nm) for the unfertilized plots and the most heavily fertilized plots, respectively. The red waveband did not change in reflectance as the summer progressed for either the unfertilized or the heavily fertilized plots. The blue, green, and near-infrared wavebands declined throughout the summer for both the unfertilized and highly fertilized plots.

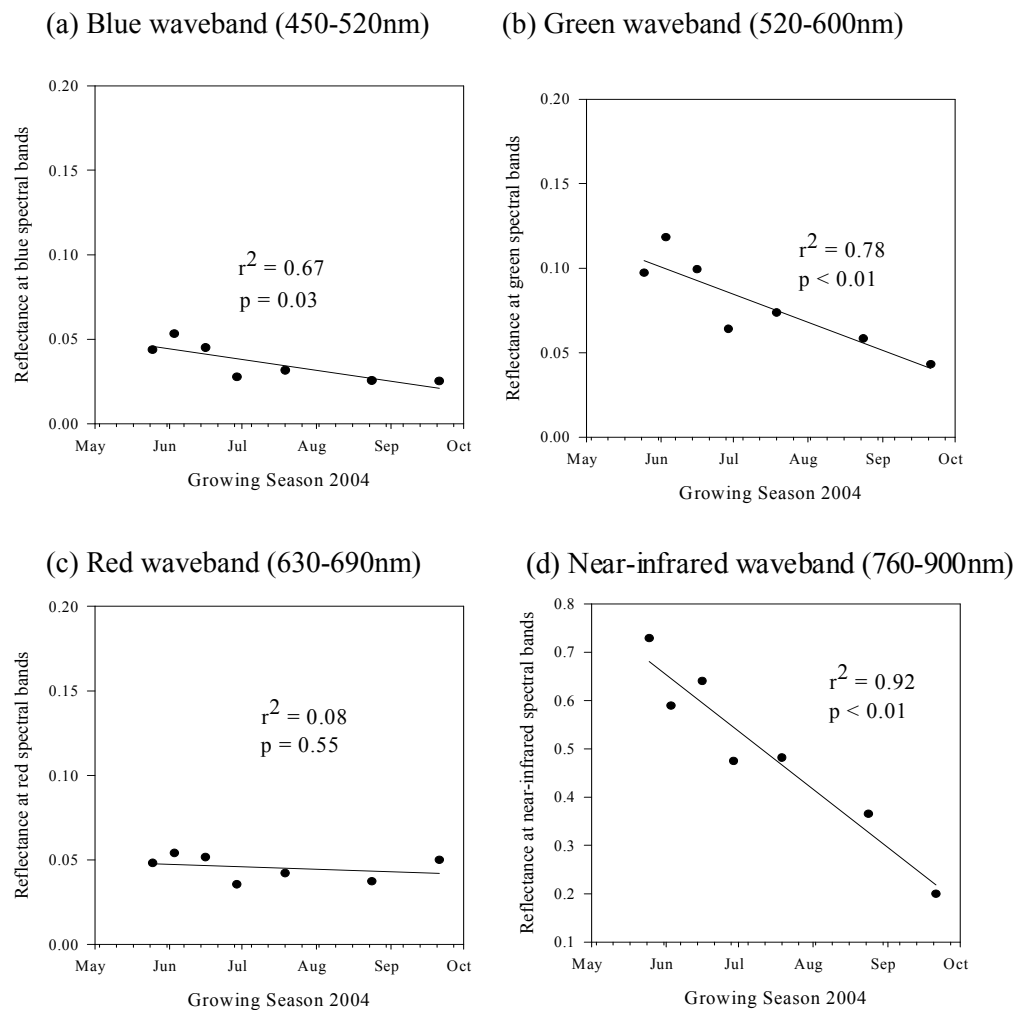
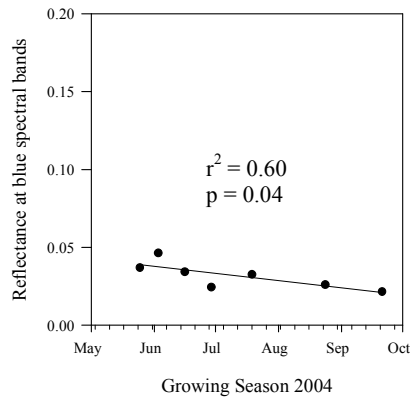
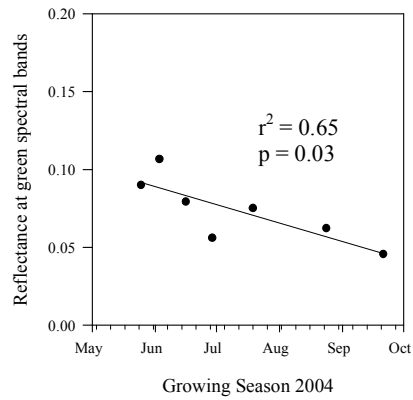


Figure 3.3.2. Mean reflectance of unfertilized plots (n = 6) for combined marsh sites throughout the 2004 growing season for (a) blue waveband (450-520nm) (b) green waveband (520-600nm), (c) red waveband (630-690nm), and (d) near-infrared waveband (760-900nm).

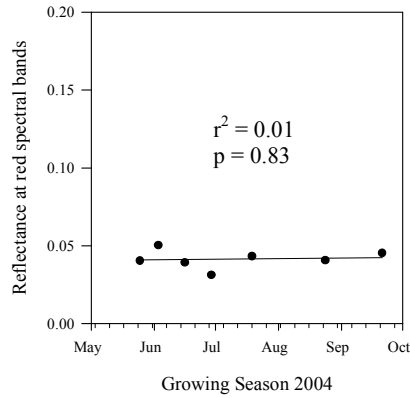
(a) Blue waveband (450-520nm)



(b) Green waveband (520-600nm)



(c) Red waveband (630-690nm)



(d) Near-infrared (760-900nm)

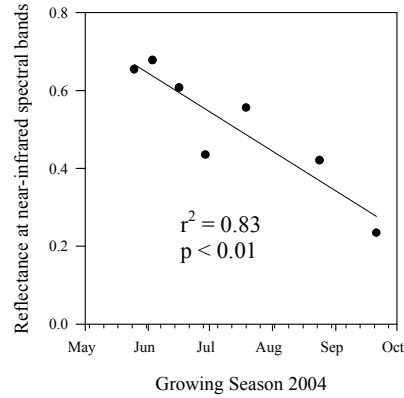


Figure 3.3.3. Mean reflectance of highly fertilized plots (n = 6) for combined marsh sites throughout the 2004 growing season for (a) blue waveband (450-520nm) (b) green waveband (520-600nm), (c) red waveband (630-690nm), and (d) near-infrared waveband (760-900nm).

3.3.2 Detection of nitrogen effect on reflectance indices

Three simple ratios, R_{493}/R_{678} , R_{415}/R_{710} and R_{564}/R_{768} , and two reflectance indices, PRI and NDVI, were analyzed for their response to nitrogen. A one-way ANOVA model with an LSD contrast was performed for the ratios and indices at each site on every sample date.

$$R_{493}/R_{678}$$

The simple ratio R_{493}/R_{678} did not distinguish between the different nitrogen treatments for the *Phragmites*-dominant site (Figure 3.3.4), however the ratio was

higher at the end of the growing season (9/21/04) for the higher nitrogen treatment at the *Phragmites*-absent site (Figure 3.3.5).

$$R_{415}/R_{710}$$

Figures 3.3.6 and 3.3.7 show differences among treatments for the simple ratio R_{415}/R_{710} for the *Phragmites*-dominant and *Phragmites*-absent site, respectively.

Similar to the R_{493}/R_{678} ratio, the R_{415}/R_{710} ratio was not generally different during peak growing season, but rather was different at the end in September, but only for the *Phragmites*-dominant site (Figure 3.3.6).

$$R_{564}/R_{768}$$

The simple ratio R_{564}/R_{768} could only differentiate between nitrogen treatments at the end of the growing season for the *Phragmites*-dominant site (Figure 3.3.8), which was similar to the R_{415}/R_{710} ratio.

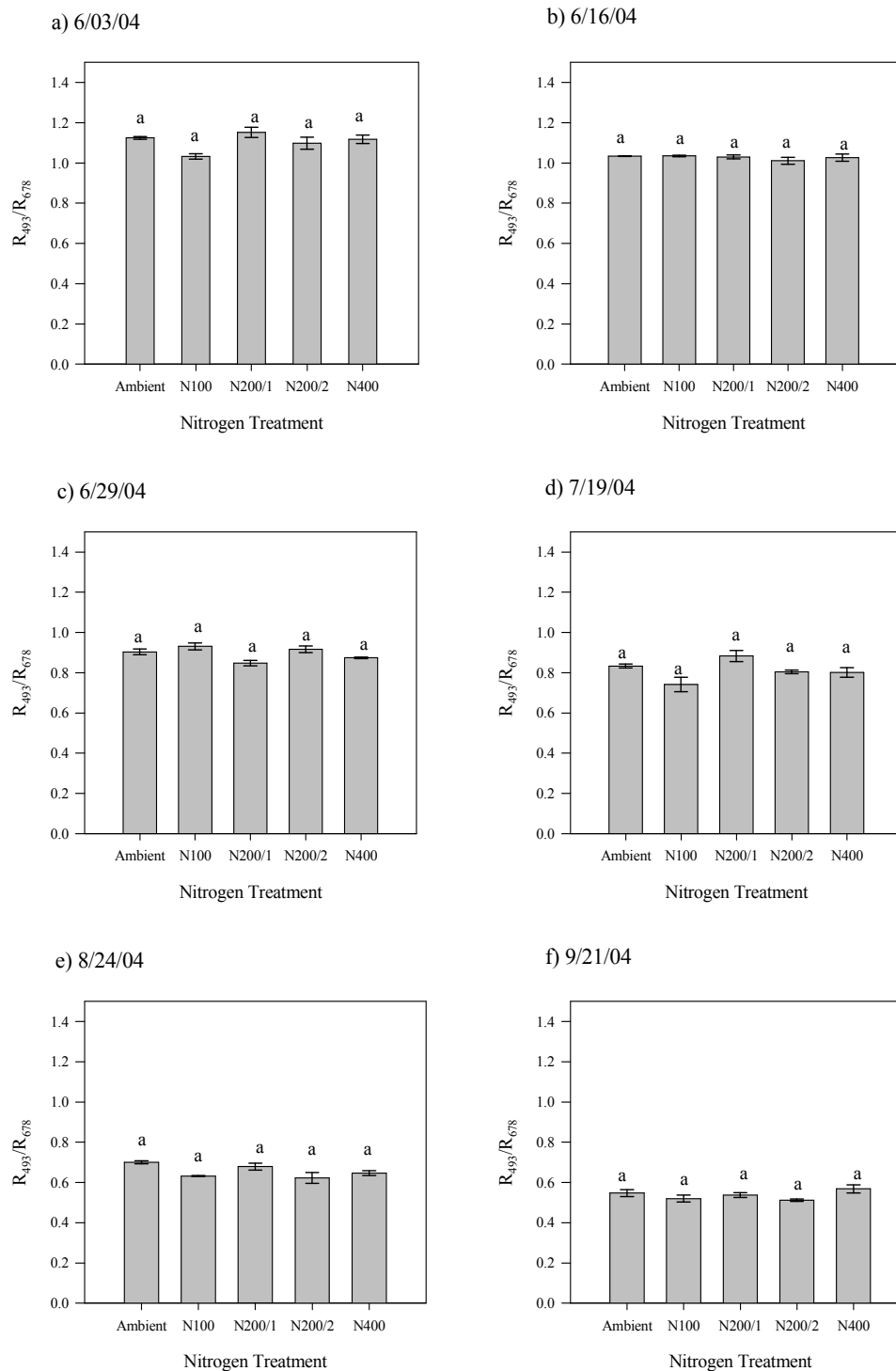


Figure 3.3.4. Mean R_{493}/R_{678} values and standard errors of the *Phragmites*-dominant site according to nitrogen treatment over the 2004 growing season. Treatments with different letters indicate a significant difference between treatments ($p < 0.05$). Ratio R_{493}/R_{678} was the dependent variable in the one-way ANOVA model, with an LSD contrast.

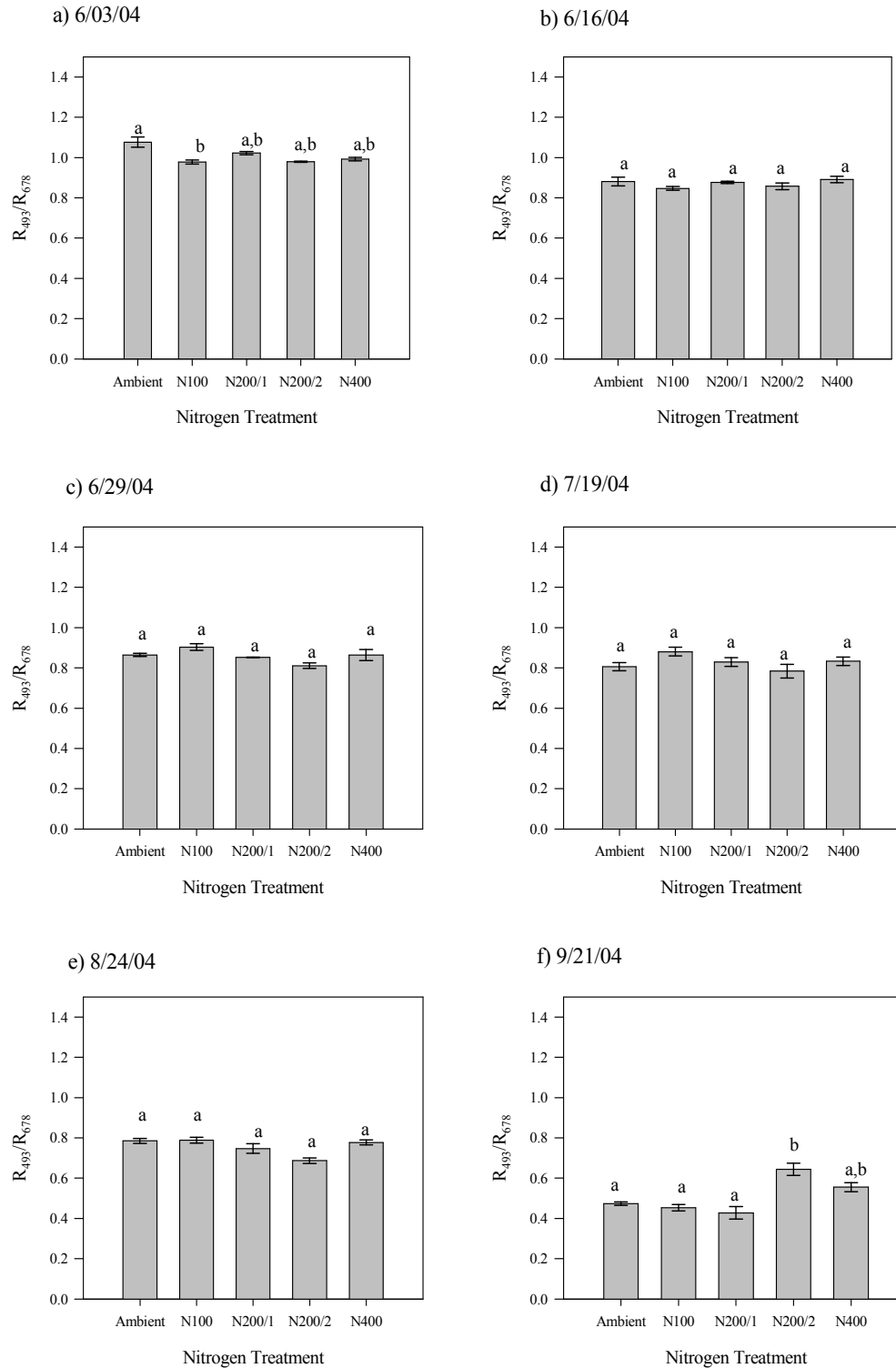


Figure 3.3.5. Mean R_{493}/R_{678} values and standard errors of the *Phragmites*-absent site according to nitrogen treatment over the 2004 growing season. Treatments with different letters indicate a significant difference between treatments ($p < 0.05$). Ratio R_{493}/R_{678} was the dependent variable in the one-way ANOVA model, with an LSD contrast.

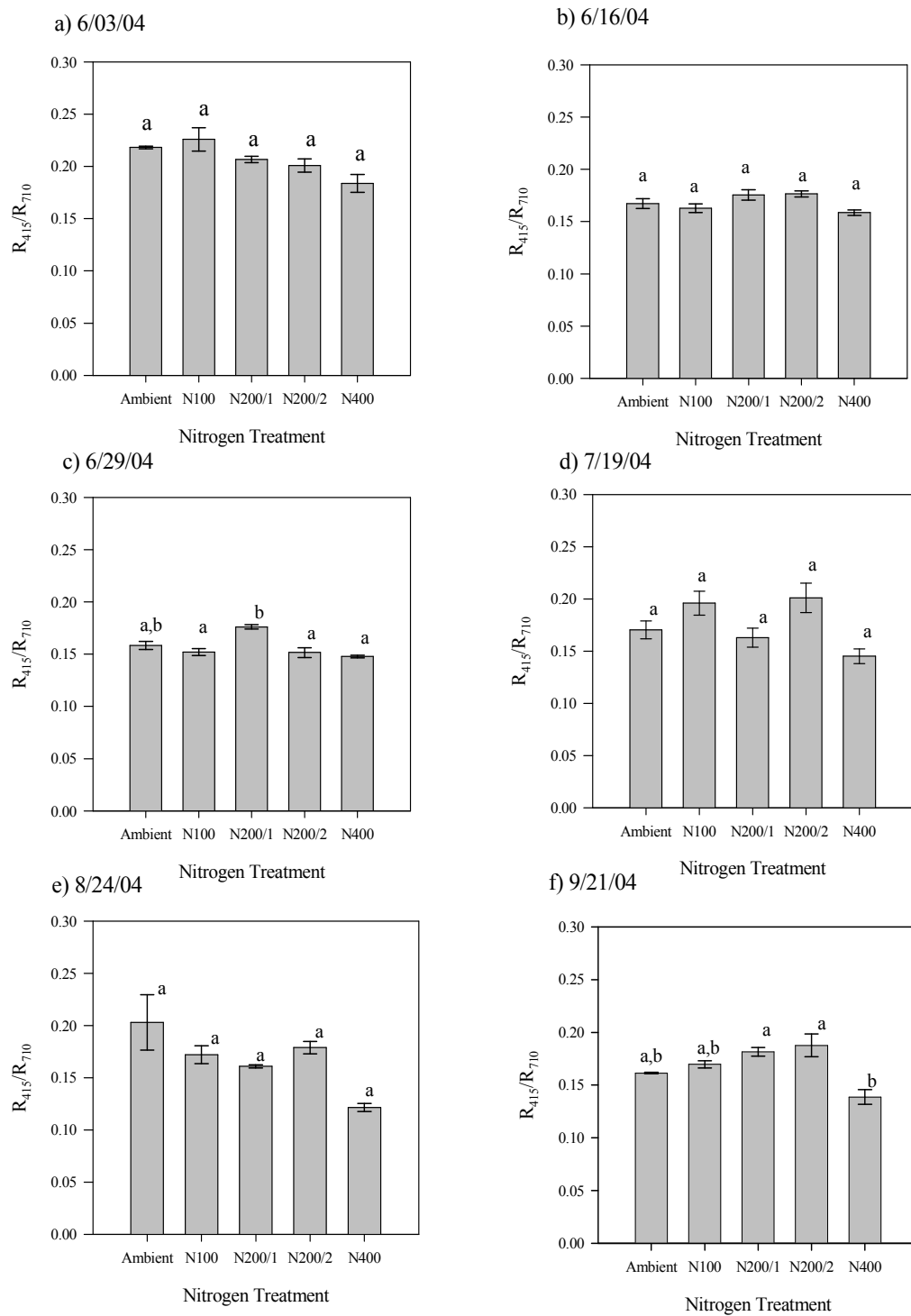


Figure 3.3.6. Mean R_{415}/R_{710} values and standard errors of the *Phragmites*-dominant site according to nitrogen treatment over the 2004 growing season. Treatments with different letters indicate a significant difference between treatments ($p < 0.05$). Ratio R_{415}/R_{710} was the dependent variable in the one-way ANOVA model, with an LSD contrast.

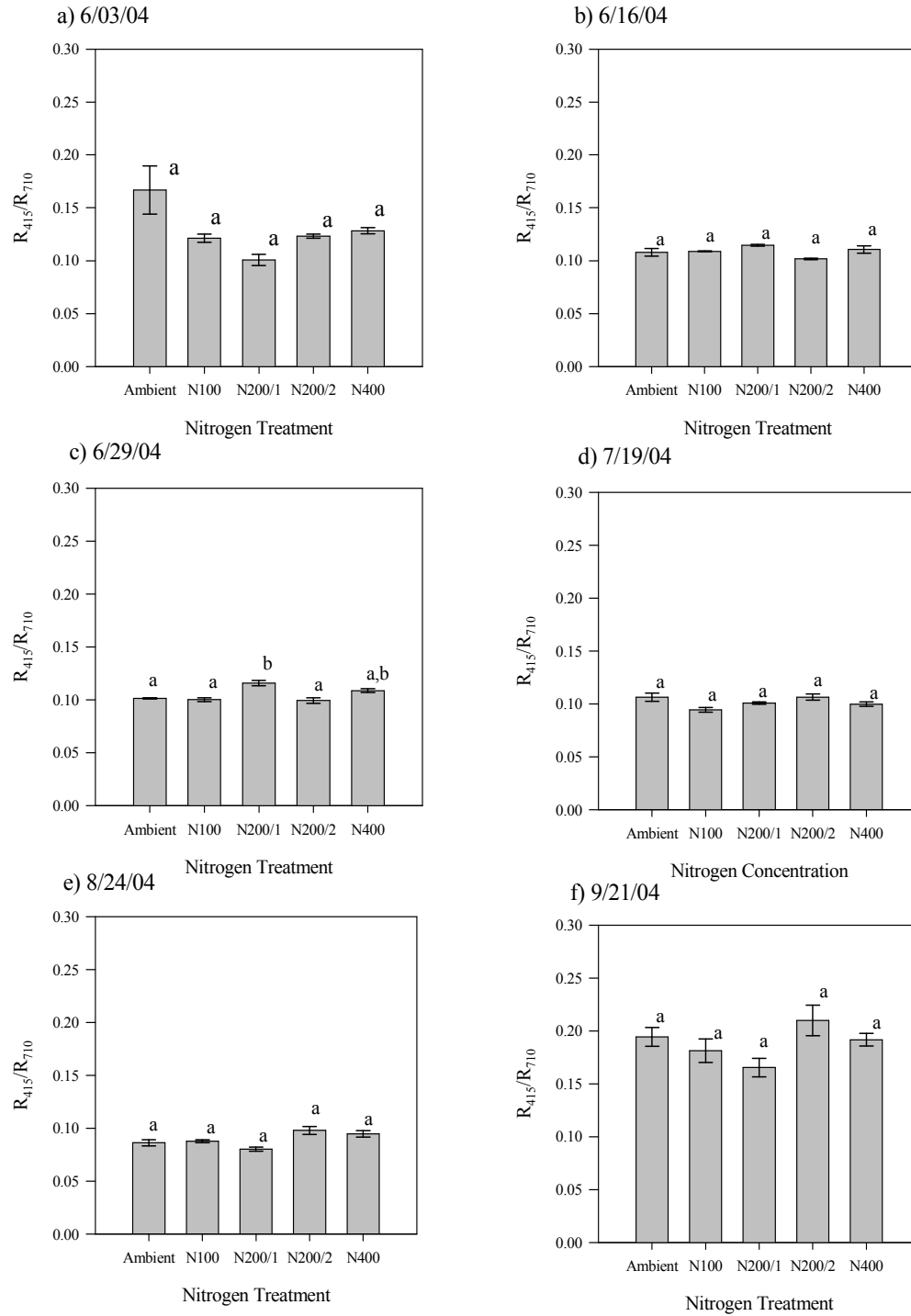


Figure 3.3.7. Mean R_{415}/R_{710} values and standard errors of the *Phragmites*-absent site according to nitrogen treatment over the 2004 growing season. Treatments with different letters indicate a significant difference between treatments ($p < 0.05$). Ratio R_{415}/R_{710} was the dependent variable in the one-way ANOVA model, with an LSD contrast.

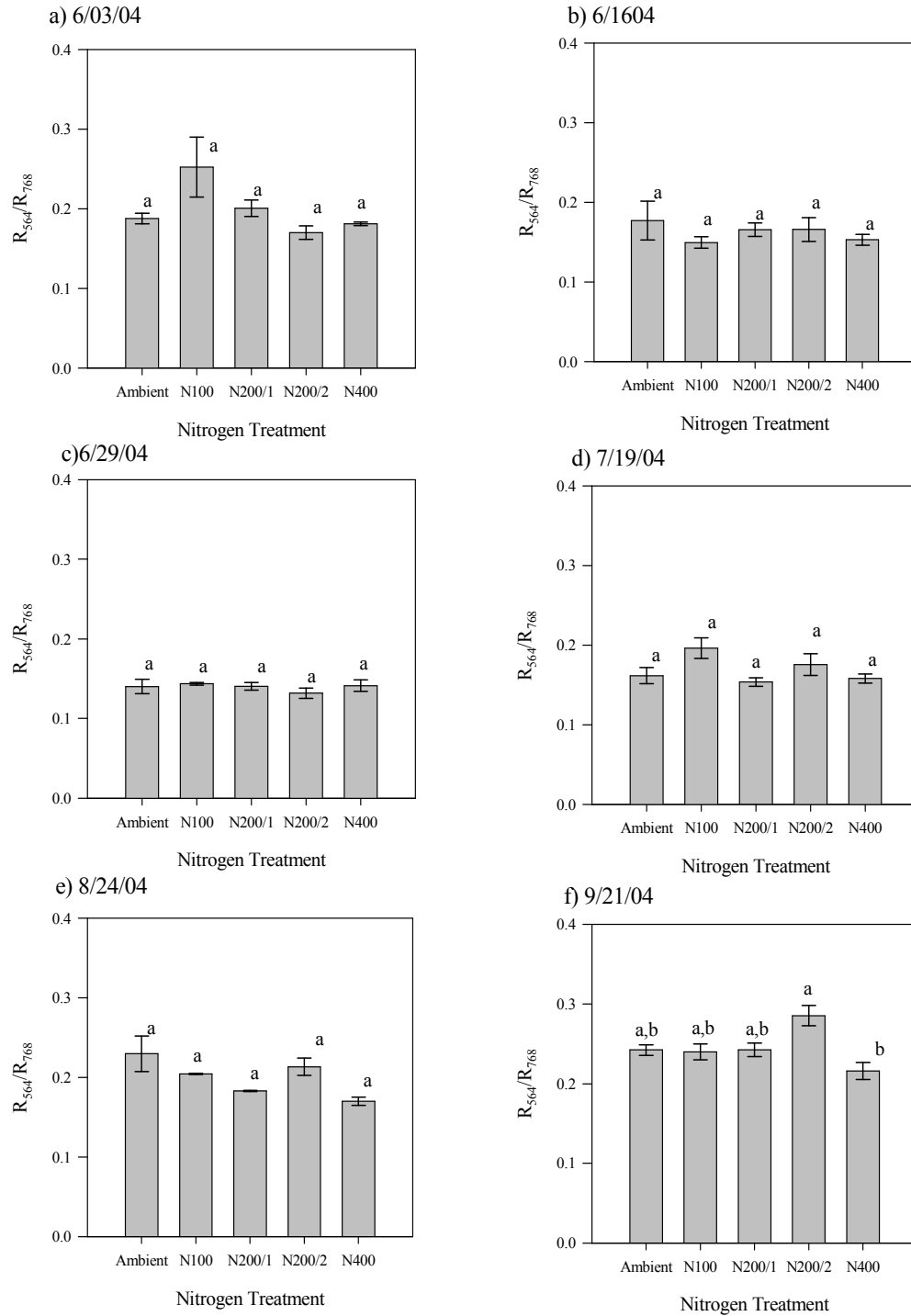


Figure 3.3.8. Mean R_{564}/R_{768} values and standard errors of the *Phragmites*-dominant site according to nitrogen treatment over the 2004 growing season. Treatments with different letters indicate a significant difference between treatments ($p < 0.05$). Ratio R_{564}/R_{768} was the dependent variable in the one-way ANOVA model, with an LSD contrast.

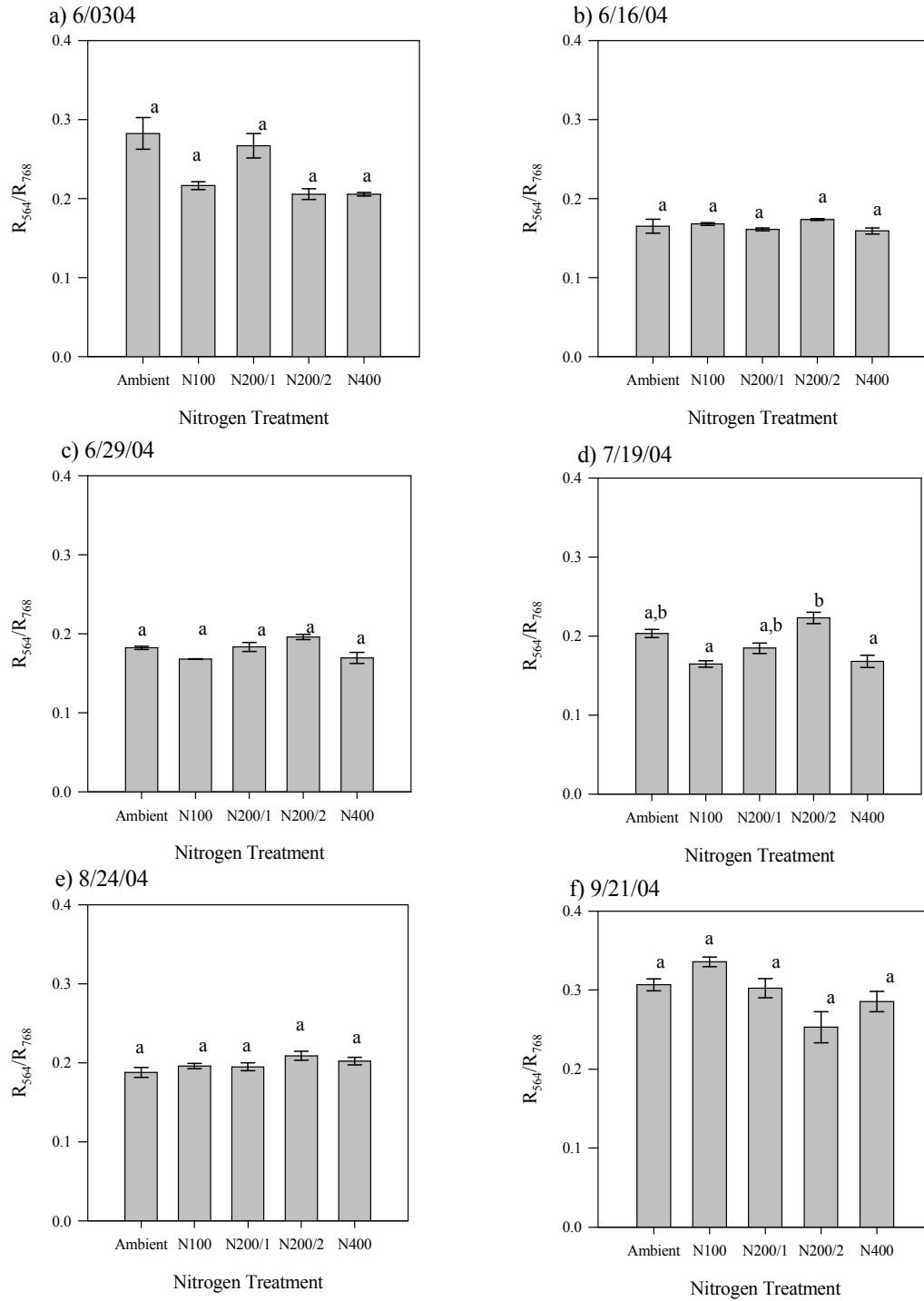


Figure 3.3.9. Mean R_{564}/R_{768} values and standard errors of the *Phragmites*-absent site according to nitrogen treatment over the 2004 growing season. Treatments with different letters indicate a significant difference between treatments ($p < 0.05$). Ratio R_{564}/R_{768} was the dependent variable in the one-way ANOVA model, with an LSD contrast.

PRI

At the *Phragmites*-dominant site no nitrogen effects were detected according to the PRI index $(R_{531}-R_{570})/(R_{531}+R_{570})$ (Figure 3.3.10). At the *Phragmites*-absent site, however, the PRI index was greater for N100 on 6/29/04 and greater for N200/2D on 9/21/04 (Figure 3.3.11), suggesting that PRI could be useful for detecting nitrogen effects during the end of the growing season.

NDVI

Figures 3.3.12 and 3.3.13 show differences in NDVI $(R_{nir}-R_{red})/(R_{nir}+R_{red})$ according to nitrogen treatment for both sites. NDVI was saturated at both sites for each treatment, including ambient conditions, which emphasizes the lush, dense vegetation conditions of the marsh. Only a few nitrogen effects on NDVI were found, including at the end of the growing season, the NDVI for the N200/2D treatment decreased at the *Phragmites*-dominant site (Figure 3.3.12) and increased at the *Phragmites*-absent site (Figure 3.3.13).

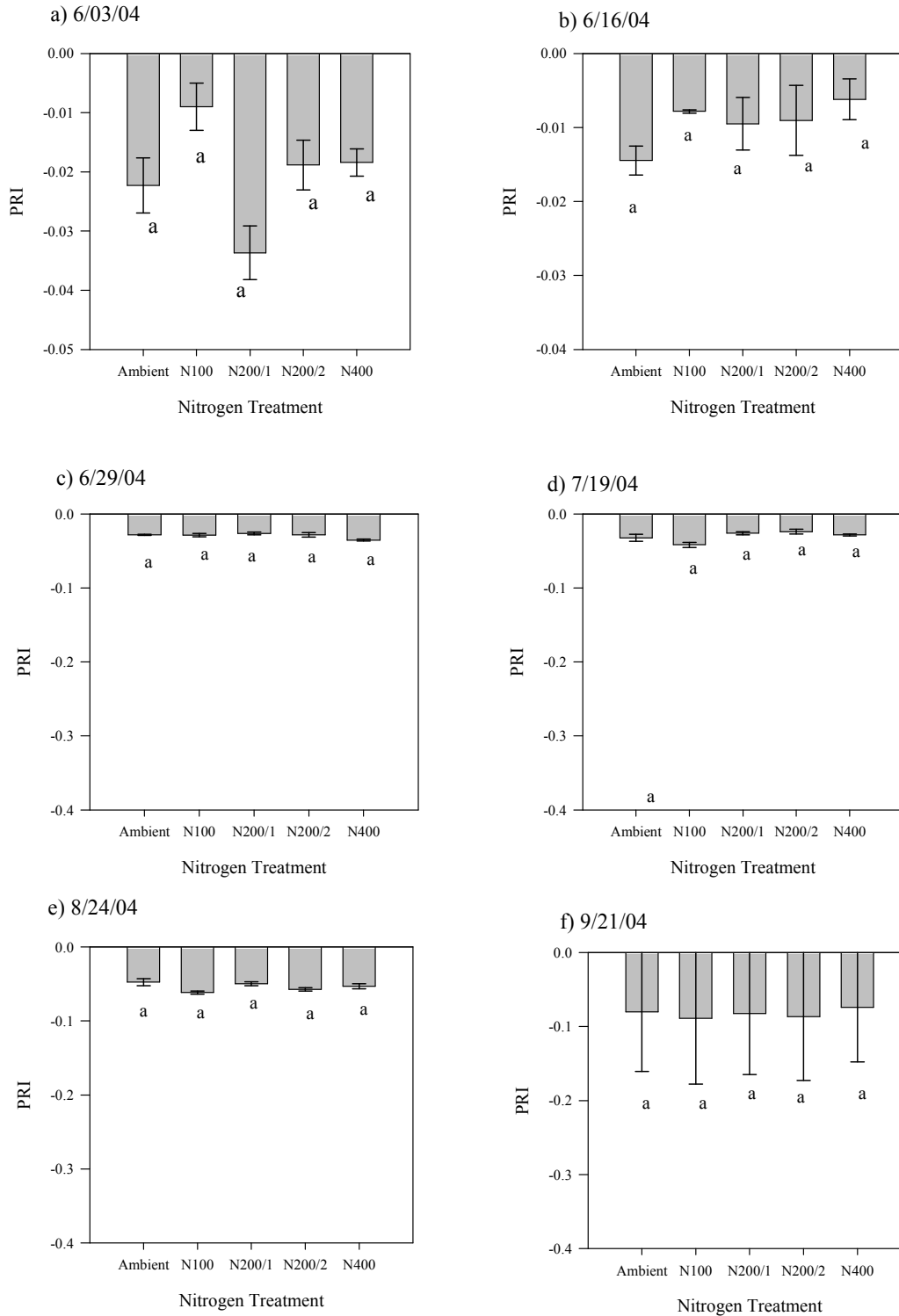


Figure 3.3.10. Mean PRI values and standard errors of the *Phragmites*-dominant site according to nitrogen treatment over the 2004 growing season. Treatments with different letters indicate a significant difference between treatments ($p < 0.05$). PRI index was the dependent variable in the one-way ANOVA model, with an LSD contrast.

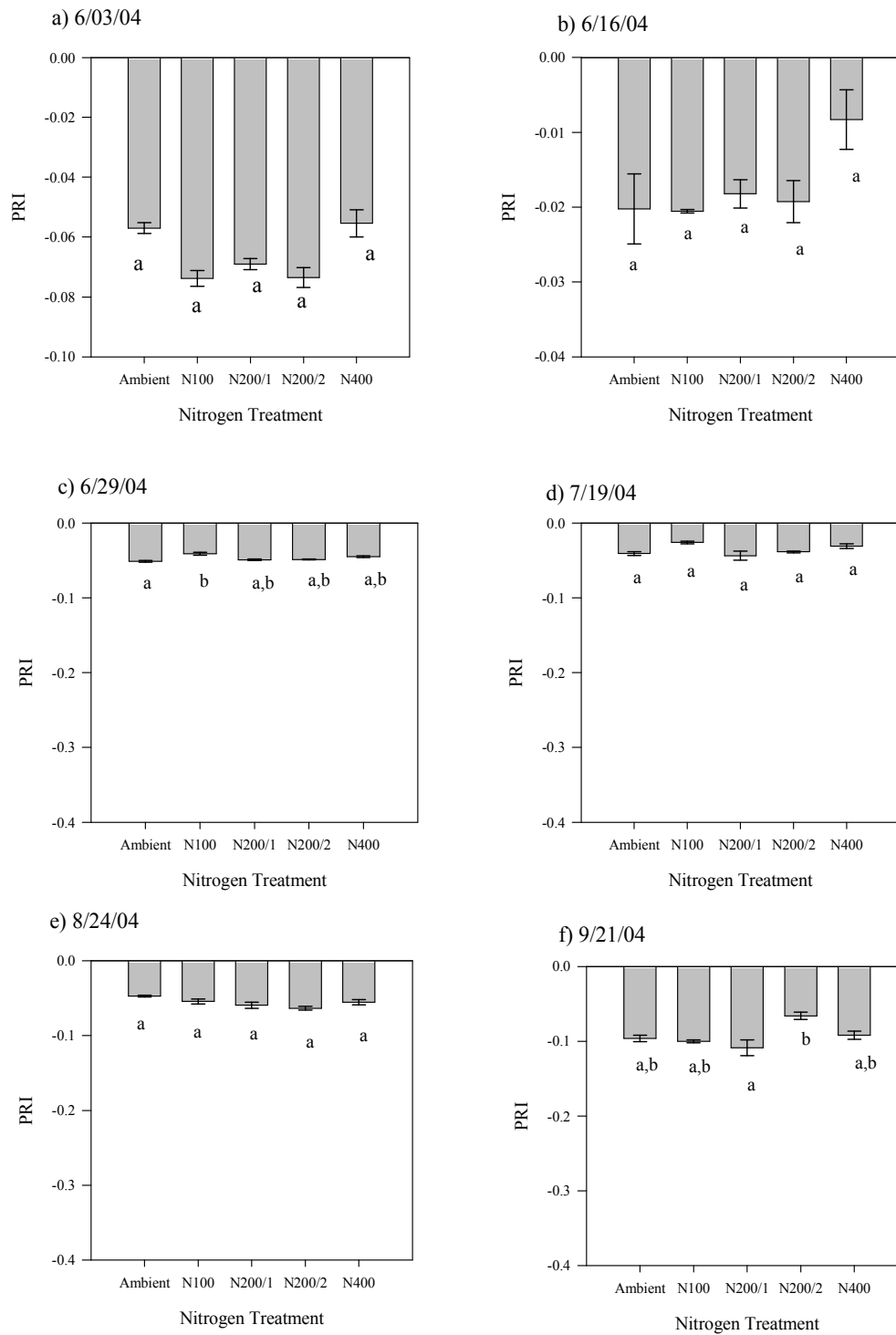


Figure 3.3.11. Mean PRI values and standard errors of the *Phragmites*-absent site according to nitrogen treatment over the 2004 growing season. Treatments with different letters indicate a significant difference between treatments ($p < 0.05$). PRI index was the dependent variable in the one-way ANOVA model, with an LSD contrast.

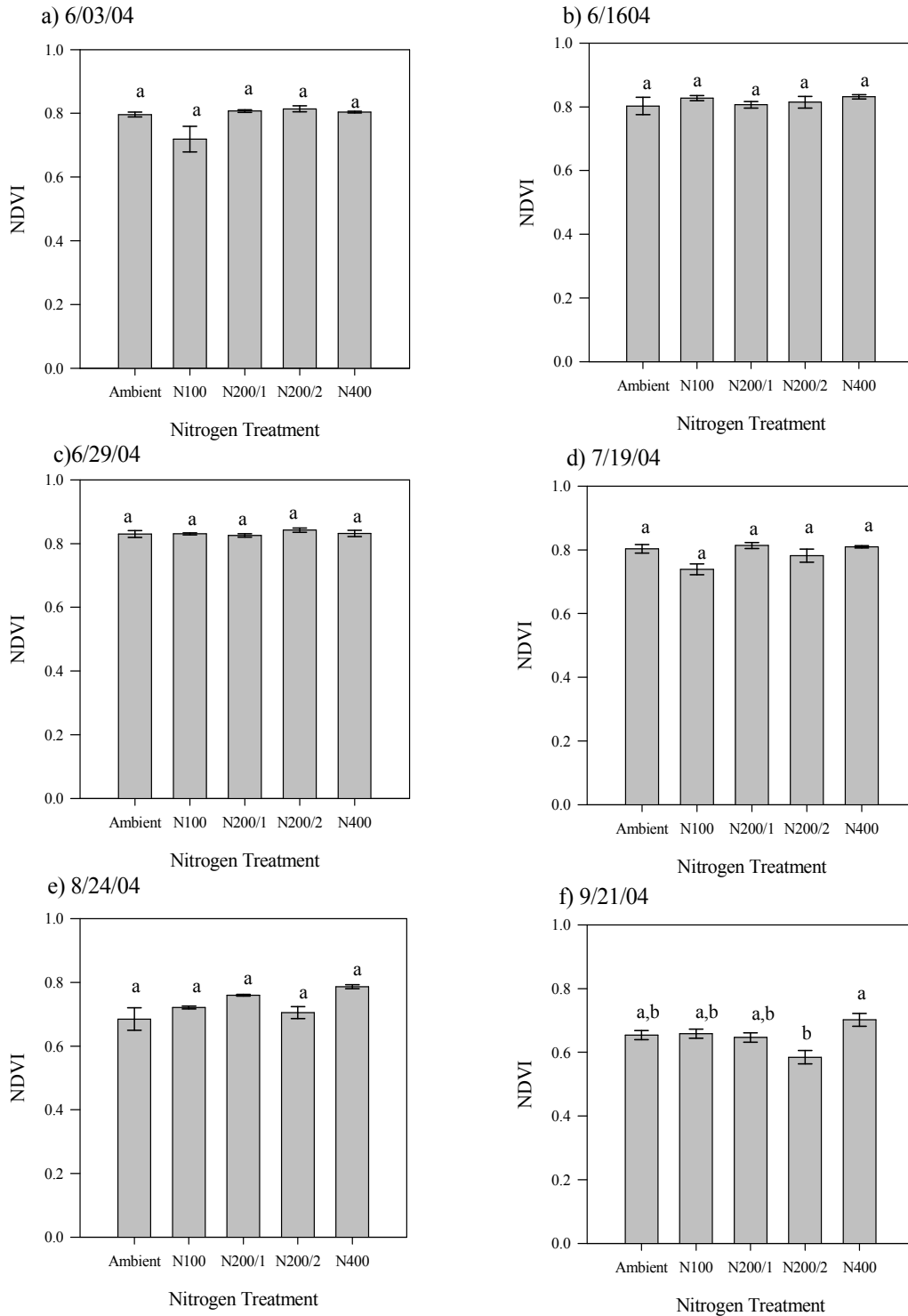


Figure 3.3.12. Mean NDVI values and standard errors of the *Phragmites*-dominant site according to nitrogen treatment over the 2004 growing season. Treatments with different letters indicate a significant difference between treatments ($p < 0.05$). NDVI index was the dependent variable in the one-way ANOVA model, with an LSD contrast.

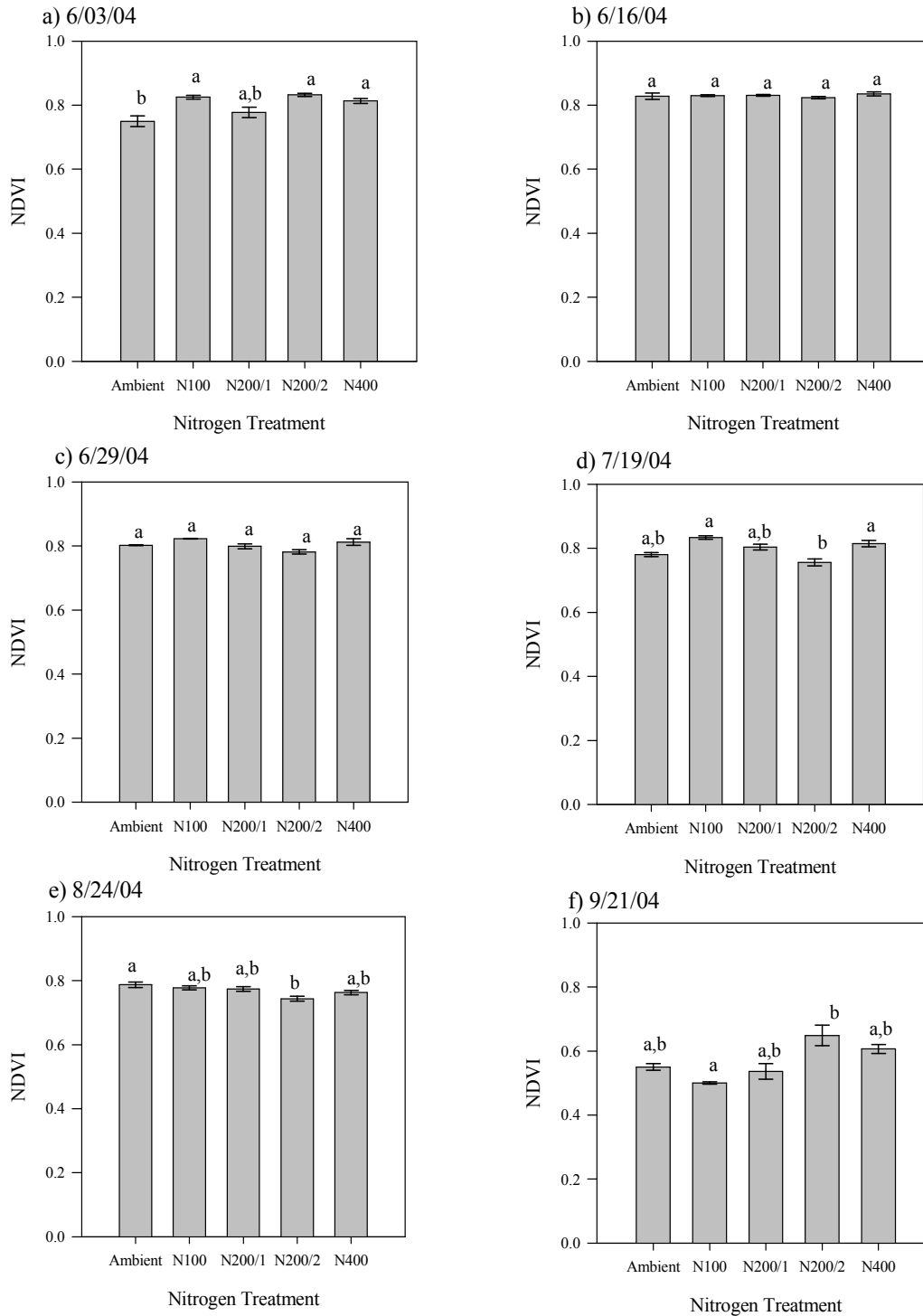


Figure 3.3.13. Mean NDVI values and standard errors of the *Phragmites*-absent site according to nitrogen treatment over the 2004 growing season. Treatments with different letters indicate a significant difference between treatments ($p < 0.05$). NDVI index was the dependent variable in the one-way ANOVA model, with an LSD contrast.

3.3.3 Detection of nitrogen and marsh-type effects on canopy reflectance

To determine if canopy reflectance of a highly diverse marsh was capable of distinguishing between nitrogen treatments, both nitrogen effects and vegetation composition effects at each site and sample date were analyzed. First, reflectance of each site was investigated. Figure 3.3.14 compares the mean reflectance curves for the *Phragmites*-dominant with the *Phragmites*-absent marsh site before fertilization. The figure shows the natural differences in reflectance between the two sites, which suggested the need to analyze treatment effects on canopy reflectance for each site separately.

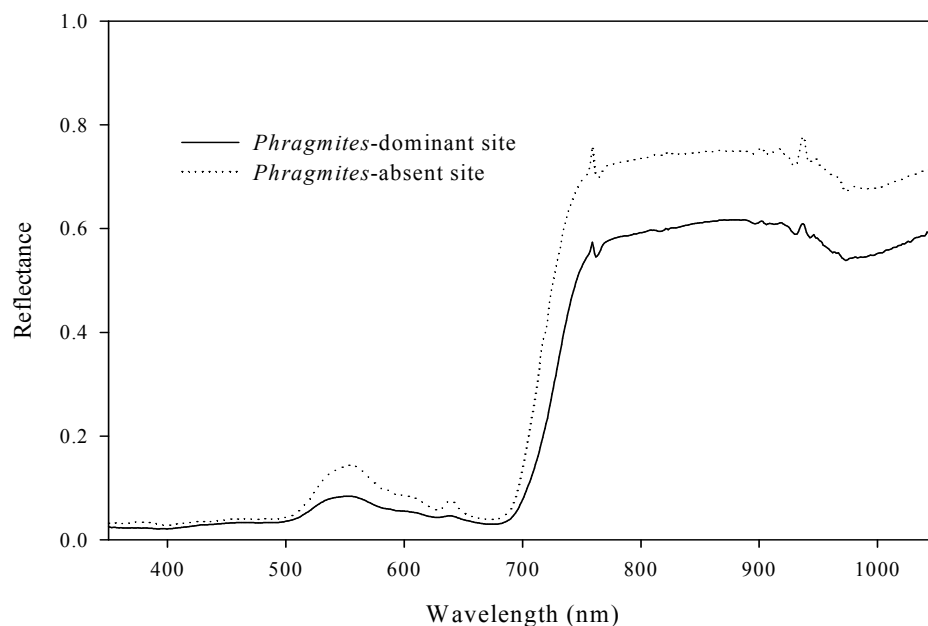


Figure 3.3.14. Mean reflectance of each marsh site prior to nitrogen fertilization (5/25/04).

Site, treatment and their interaction were analyzed in ANOVA to determine which spectral bands were most affected by site and treatment effects. Interactions between site and treatment were found in the red at the end of the growing season (9/21/04)

and in the green and red-edge at the beginning of the 2005 season (6/06/05) (Figure 3.3.15).

No nitrogen effect was detected for any spectral band on sample dates between May and August, 2004 (Figure 3.3.16). However there was a nitrogen effect in the NIR on both 9/21/04 and 6/06/05. Due to the site and treatment interaction in the visible range on both dates, only the NIR nitrogen effects were considered.

Site effects on wavebands were very significant for several sample dates across the growing season (Figure 3.3.17). Before fertilization every waveband had a different reflectance at the *Phragmites*-dominant than at the *Phragmites*-absent site (Figure 3.3.17a), which implied the differences between observed vegetative species at the two sites produced different reflectance curves. Throughout the rest of the growing season, site effects were most noticeable in the green, red-edge, and NIR in late-June through late-August (Figures 3.3.17d, e, f, and i), when most species were at their peak. Late in the growing season (9/21/04), both sites were beginning to senesce, so canopy reflectance between the two sites was not different (Figure 3.3.17g).

The addition of nitrogen did not affect any spectral band for any site or date, except at the *Phragmites*-absent site at the end of the growing season (9/21/04) and beginning of the 2005 season (6/06/05) (Figures 3.3.18l and n), indicating that nitrogen is not easily detectable during the peak of growing season.

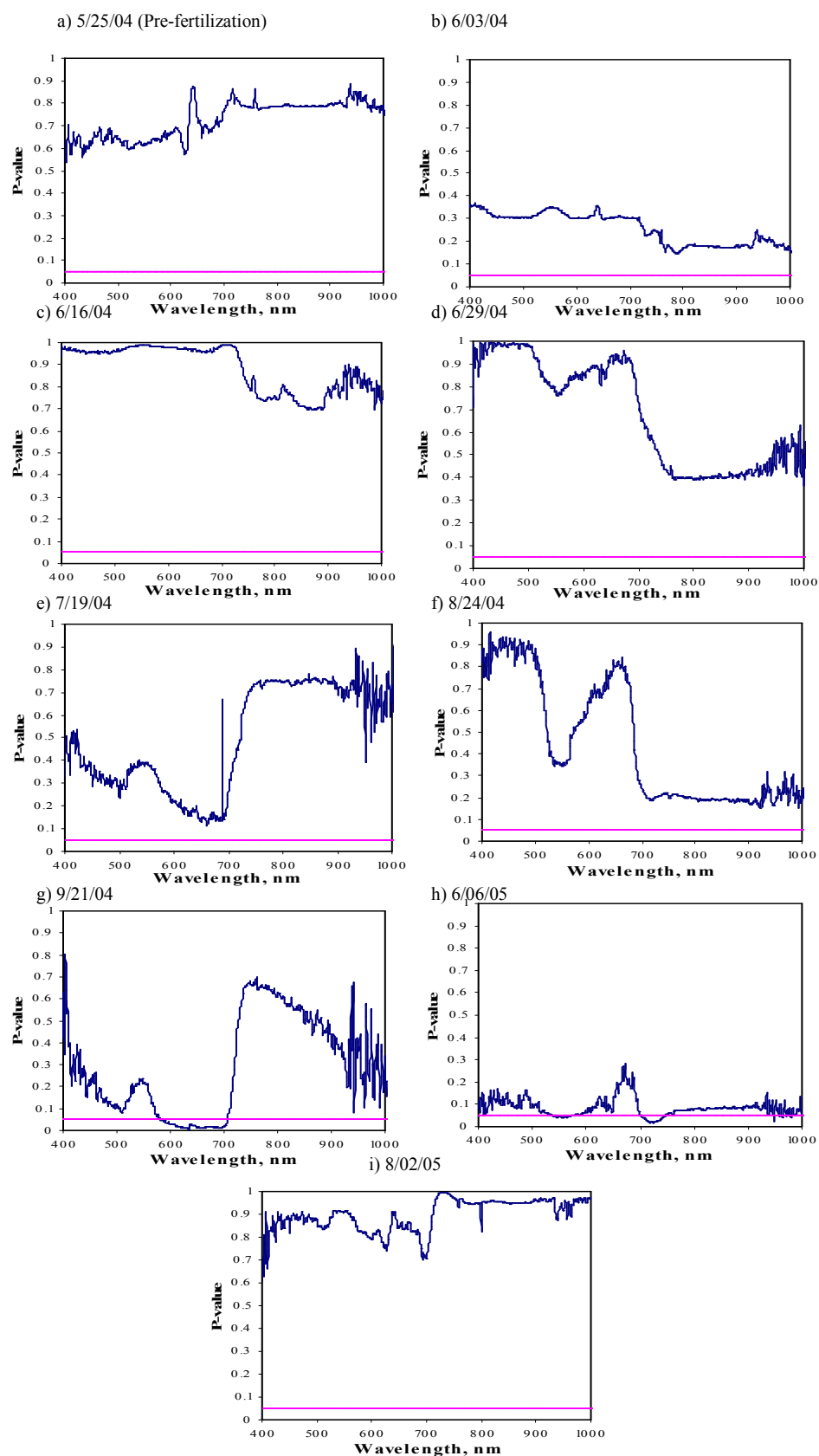


Figure 3.3.15. Significance of interaction effect between nitrogen treatment and site for all dates. ANOVA model: N trt + site + (N trt x site) (SPSS).

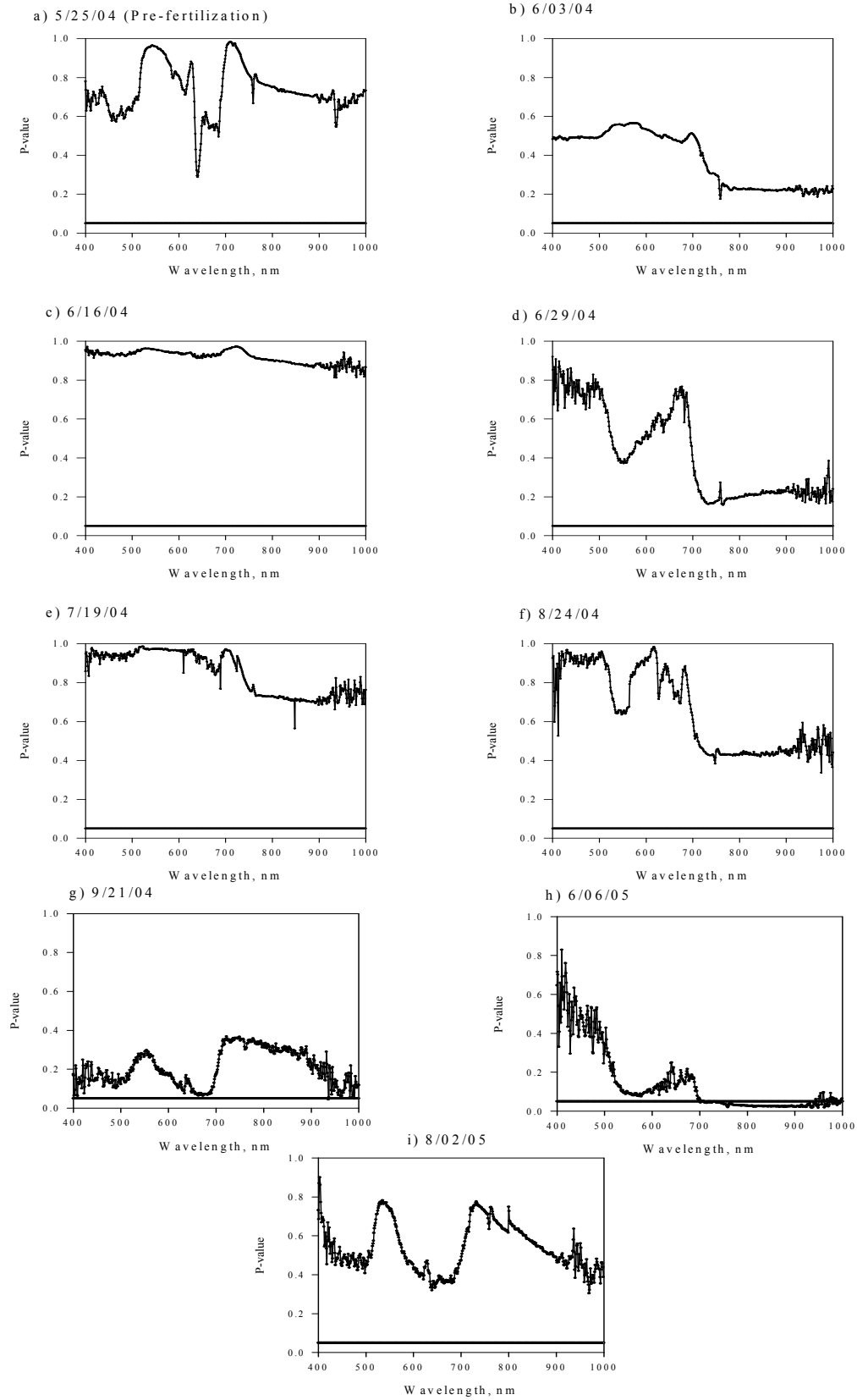


Figure 3.3.16. Significance of N main effect for all dates as analyzed in ANOVA (SPSS). ANOVA model: Ntrt + site + (Ntrt x site).

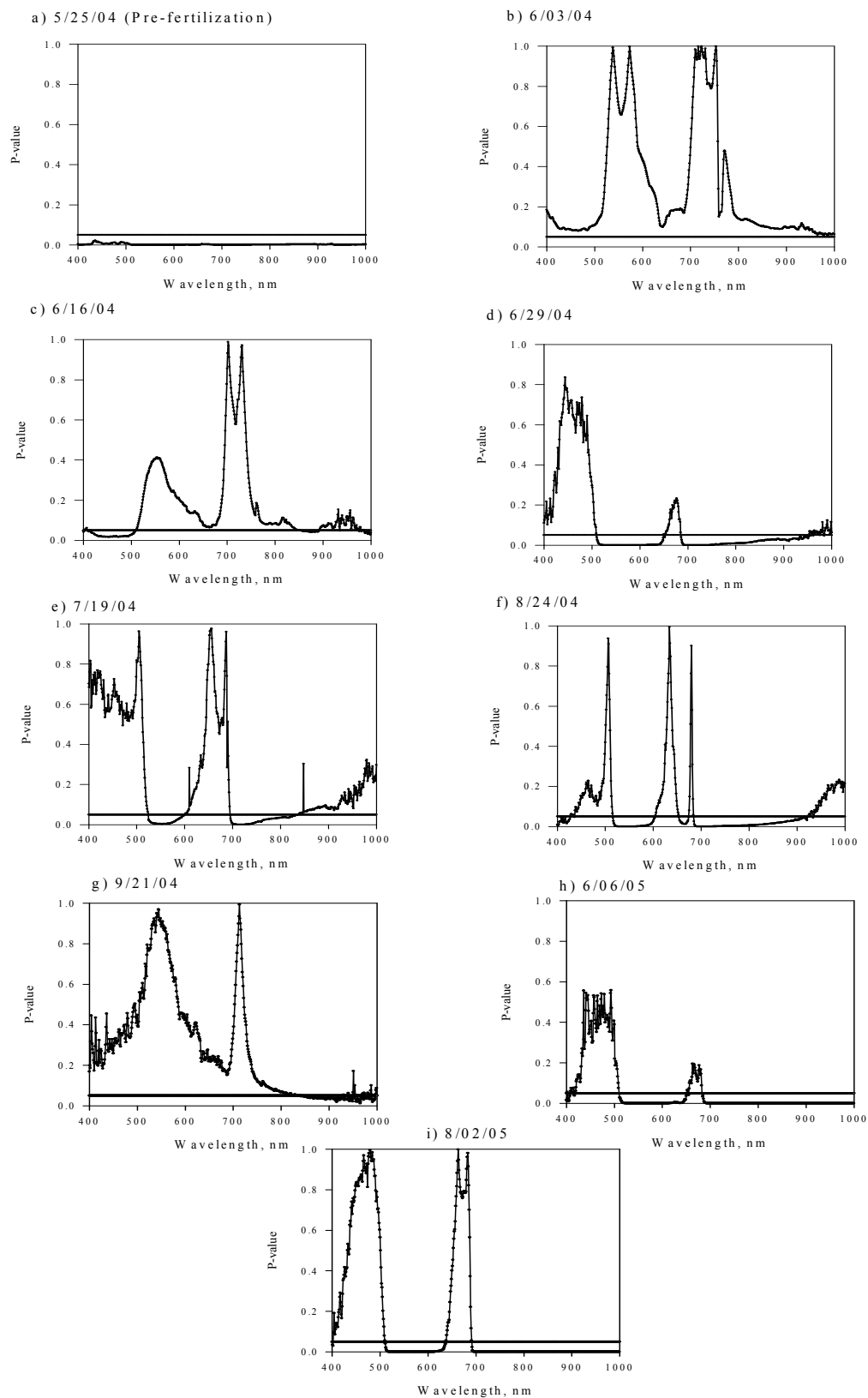
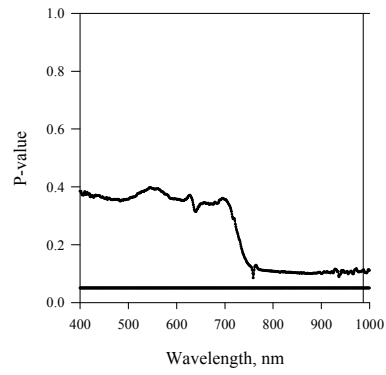
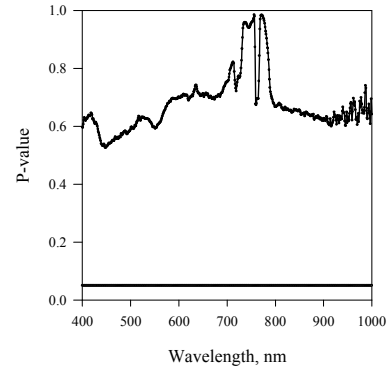


Figure 3.3.17. Significance of site main effect for all dates as analyzed in ANOVA (SPSS). ANOVA model: Ntrt + site +(Ntrt x site).

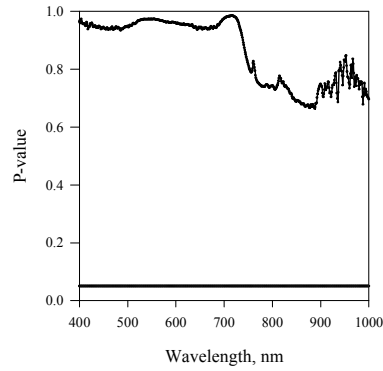
a) 6/03/04 *Phragmites*-dominant site



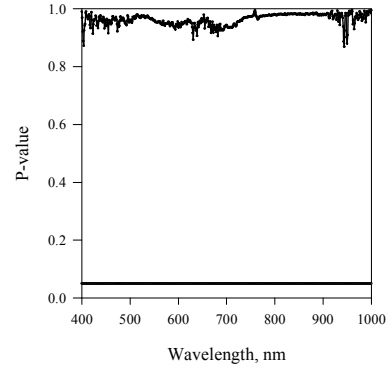
b) 6/03/04 *Phragmites*-absent site



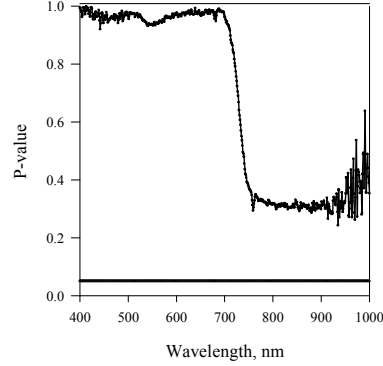
c) 6/16/04 *Phragmites*-dominant site



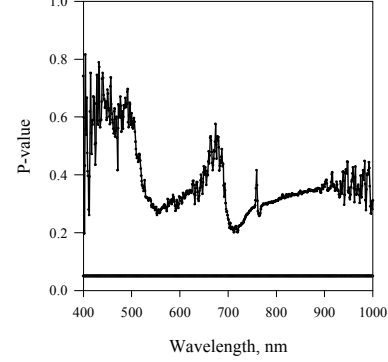
d) 6/16/04 *Phragmites*-absent site



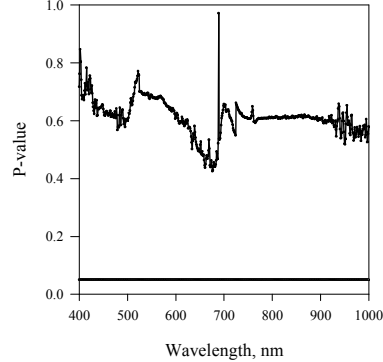
e) 6/29/04 *Phragmites*-dominant site



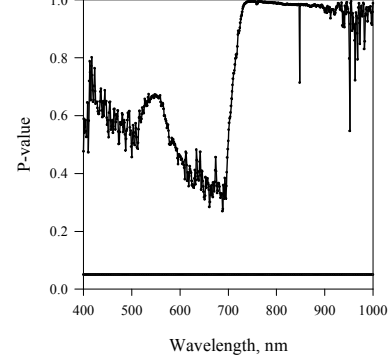
f) 6/29/04 *Phragmites*-absent site



g) 7/19/04 *Phragmites*-dominant site



h) 7/19/04 *Phragmites*-absent site



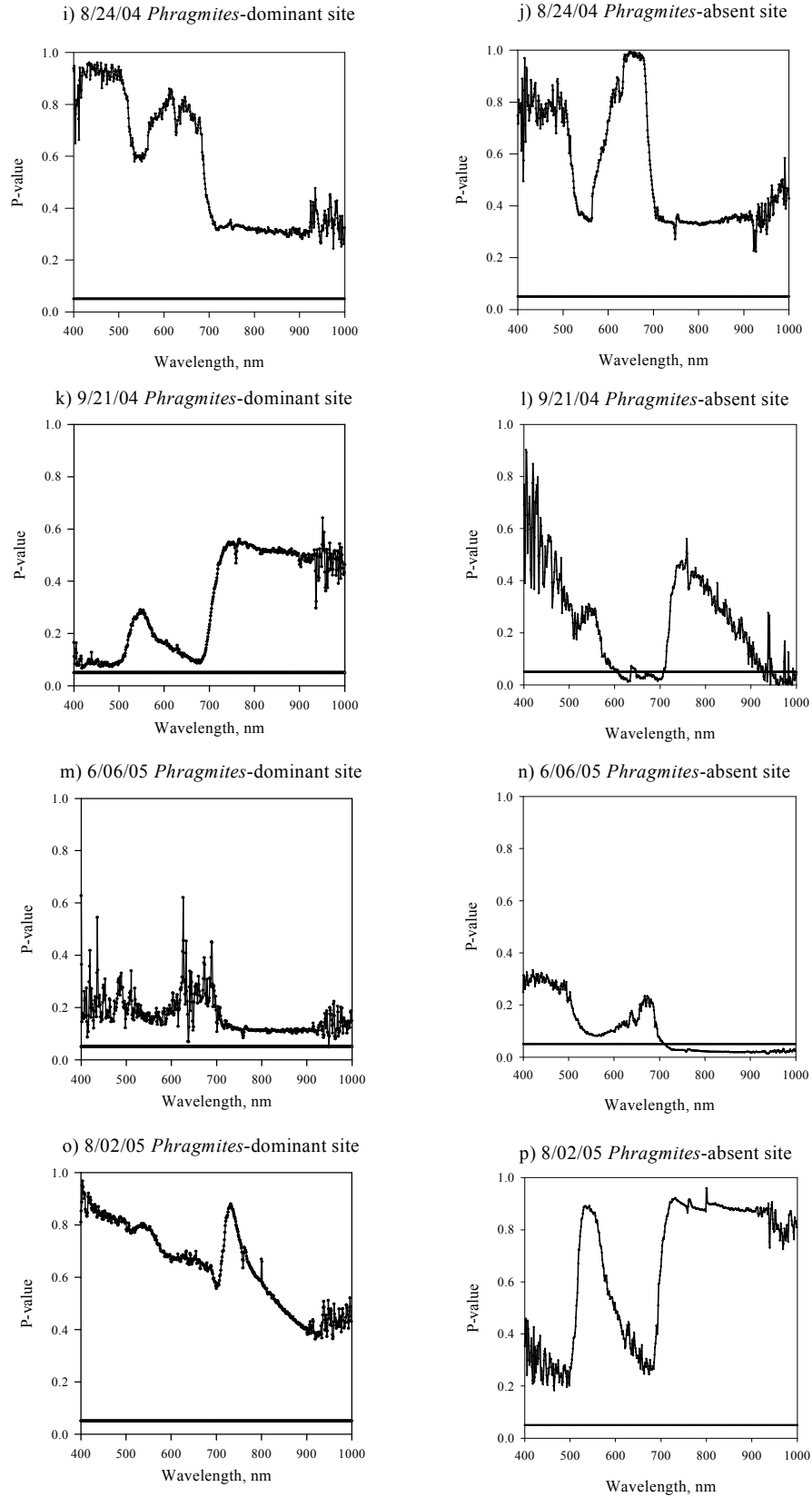


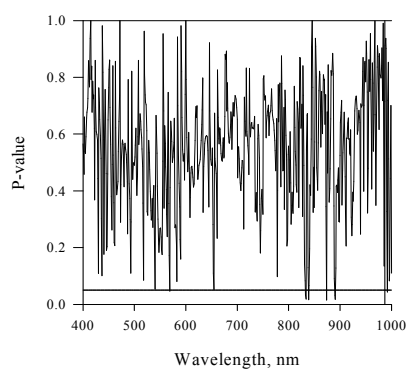
Figure 3.3.18. Significance of nitrogen treatment main effect for individual sites as analyzed in ANOVA. ANOVA model: reflectance = dependent variable, N trt = fixed factor.

3.3.4 Detection of nitrogen effects on transformed canopy reflectance

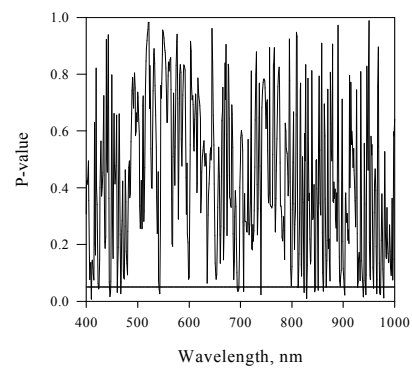
The first and second derivatives of the canopy reflectance were analyzed to determine if nitrogen fertilization affected marsh reflectance. Results from the first derivative analysis were not reported because the second derivative of the reflectance could discriminate more between nitrogen levels and was affected by more spectral bands.

Nitrogen had a significant effect on the second derivative of many spectral bands (Figure 3.3.19), which suggested that the second derivative of reflectance could be a stronger indicator of nitrogen levels than untransformed reflectance. There were more spectral bands affected by nitrogen during the middle growing season (June-August) than at the end (September) (Figure 3.3.20). Figure 3.3.20 summarizes which spectral bands were affected by nitrogen when using the second derivative of reflectance. The site summaries in the chart indicate spectral bands affected by nitrogen in three or more sample dates. In general, nitrogen most consistently affected the second derivative within the 500-750 nm spectrums for both sites, however there were a few spectral bands in the 400-500 and NIR portions of the spectrum for both marsh sites that responded to nitrogen. All significant spectral bands for each site are listed in the Appendix.

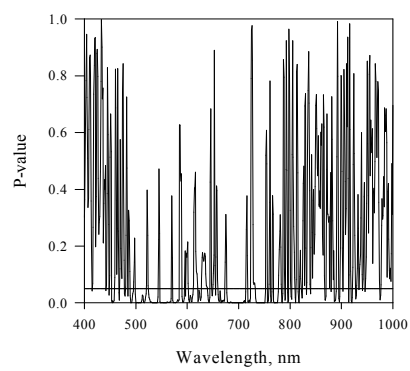
a) 6/03/04 *Phragmites*-dominant site



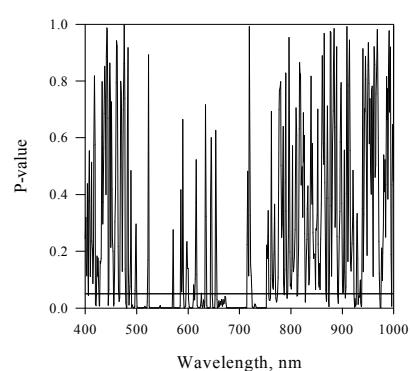
b) 6/03/04 *Phragmites* -absent site



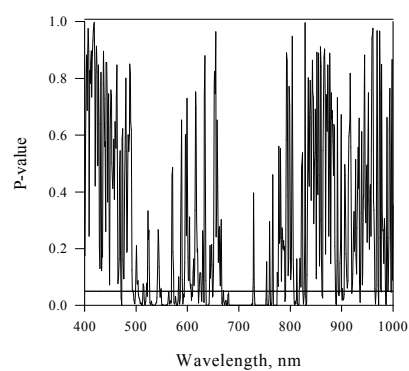
c) 6/16/04 *Phragmites*-dominant site



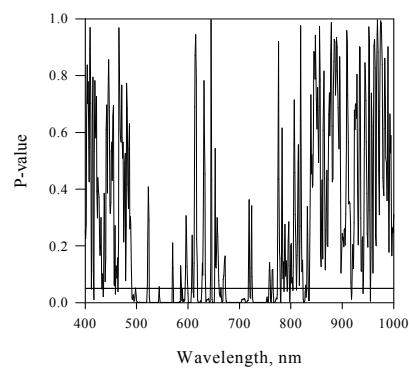
d) 6/16/04 *Phragmites*-absent site



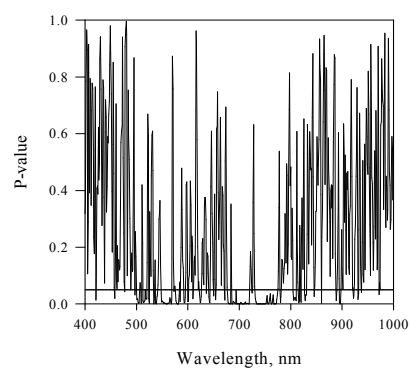
e) 6/29/04 *Phragmites*-dominant site



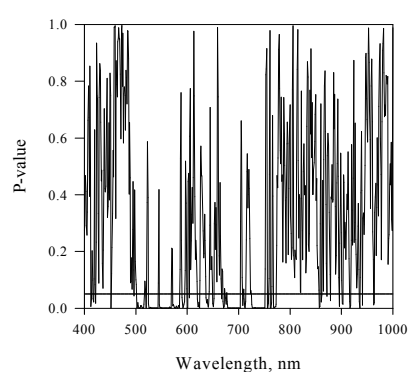
f) 6/29/04 *Phragmites*-absent site



g) 7/19/04 *Phragmites*-dominant site



h) 7/19/04 *Phragmites*-absent site



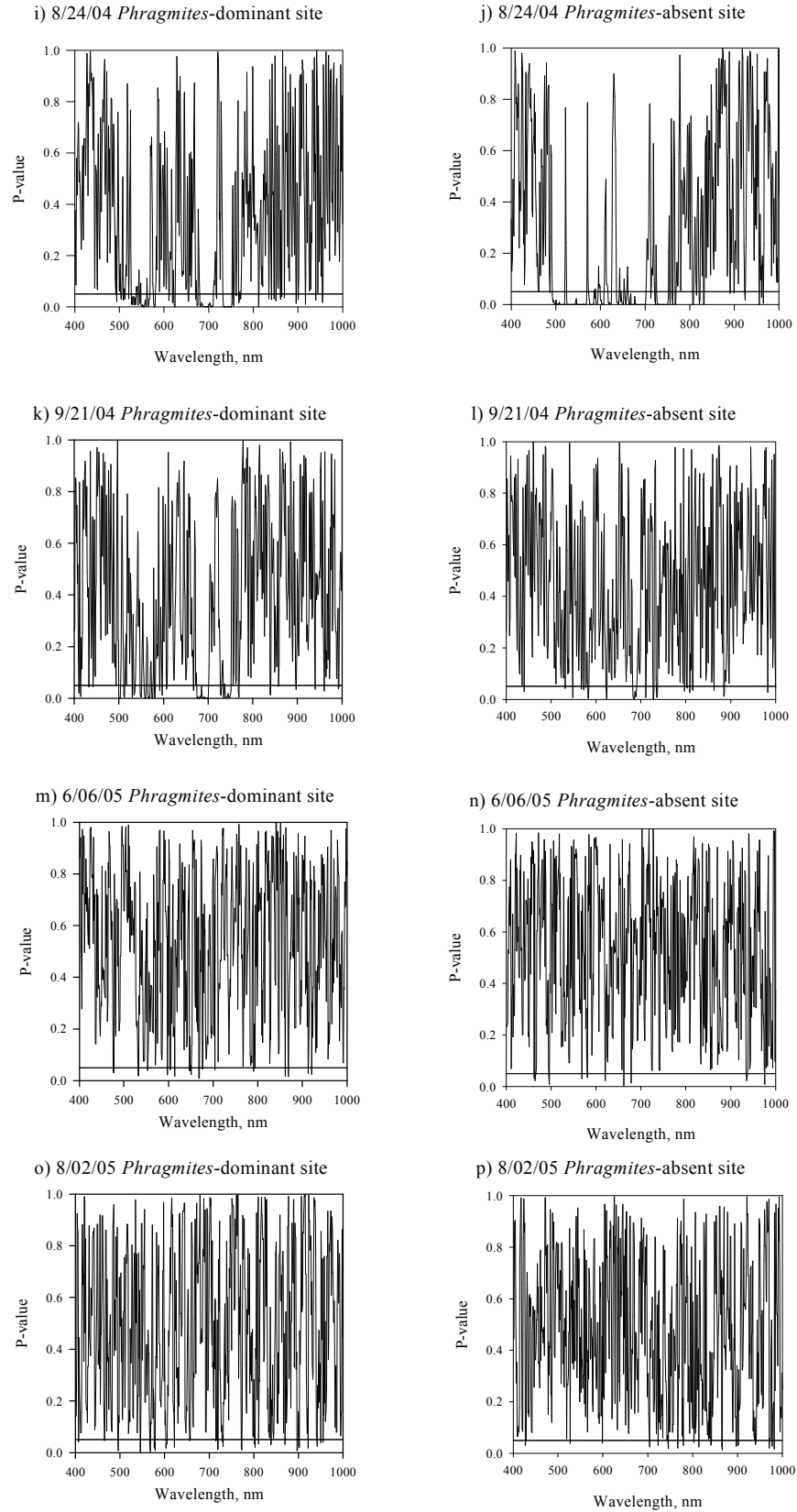


Figure 3.3.19. Significance of nitrogen treatment main effect for individual sites on the second derivative (Golay) of canopy reflectance as analyzed in an ANOVA model.

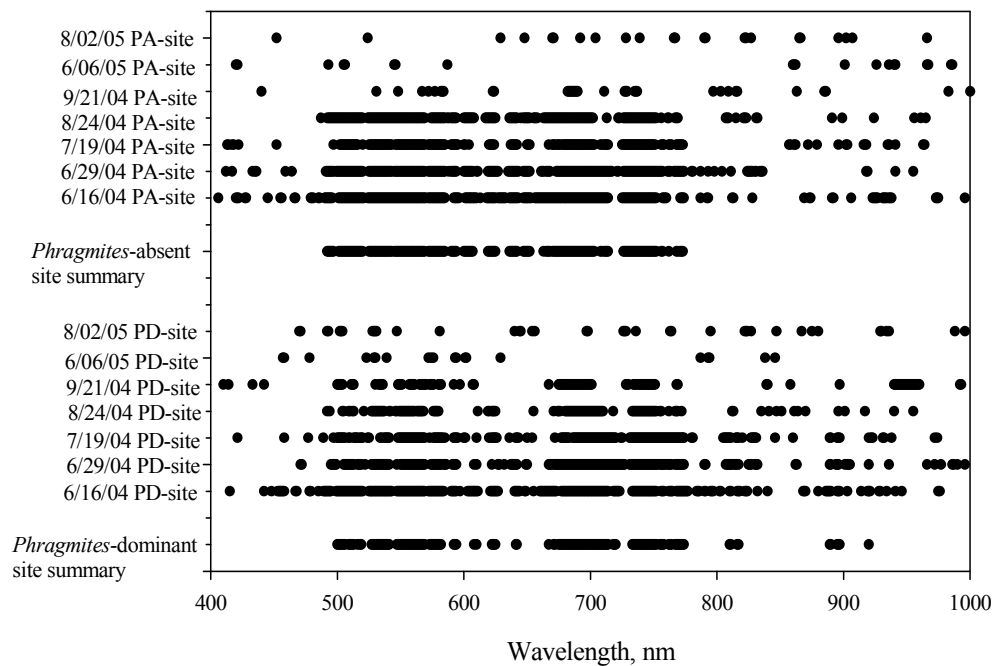


Figure 3.3.20. Spectral bands identified as significantly affected by N for the second derivative of reflectance (Golay). Site summaries indicate spectral bands affected by nitrogen for three or more dates.

3.4 Partial Least Squares (PLS) Modeling

Partial least squares (PLS) regressions were used to develop spectroradiometric models predictive of sub-surface water nutrient concentrations and vegetation composition in tidal freshwater marshes.

3.4.1 Prediction of nitrogen and phosphorus in marsh sub-surface water

Since remote assessment of nutrient concentrations in tidal freshwater marshes would be beneficial, we explored the ability of PLS-regressions to predict sub-surface ammonia, nitrate, total nitrogen and total phosphorus concentrations.

PLS models of Ammonia

PLS could not accurately predict ammonia concentrations at the two marsh sites, regardless of transformations employed (Tables 3.4.1 and 3.4.2). The best PLS model used eight spectral bands of untransformed spectra from 9/21/04 that were combined into four PLS-components with an RMSEP of 1.97 and $R^2 = 0.50$ (Figure 3.4.1).

Table 3.4.1. PLS-regressions for ammonia on *Phragmites*-dominant (PD) and *Phragmites*-absent (PA) sites. r = regression coefficient, RMSEP = root mean square error of prediction, PCs = PLS-components

Spectra Transformations	NH ₃ Transformations	Date	r	RMSEP	n	Name of plots removed	PCs	# bands used	Comments
Untransformed (350-1075nm)	none	9.21.04	0.71	1.97	28	PA 8-9	4	8	PA8-9 inaccurate reflectance curve
Norris 1 st Derivative	Log NH ₃	9.21.04	0.70	0.37	30	none	2	62	none
Untransformed (350-1075nm)	none	8.02.05	0.69	4.42	23	PD 3,6,8-10; PA 8,12	2	26	PD3,6,9-10, PA12 missing NH ₃ conc; PD8, PA8 high NH ₃ conc.
Log R	Sqrt NH ₃	9.21.04	0.66	0.57	29	PD 6	3	16	PD6 high reflectance
Golay 1 st Derivative	none	9.21.04	0.66	1.99	30	none	2	18	none
Golay 1 st Derivative	none	8.24.04	0.63	3.68	30	none	2	10	none
Norris 1 st Derivative	none	8.24.04	0.61	3.70	30	none	1	52	none
Avg 5 wavelengths	none	8.24.04	0.59	2.80	29	PD 1	1	no	PD1 high NH ₃ concentration
Golay 2 nd Derivative, avg 10	Log NH ₃	9.21.04	0.57	0.42	30	none	1	19	none
Truncated spectra (400-950nm)	none	6.06.05	0.56	2.16	28	PD1; PA7	6	27	PD1, PA7 high NH ₃ conc.
Untransformed (350-1075nm)	none	6.06.05	0.51	2.51	27	PD1; PA 3,7	10	29	PD1, PA7 high NH ₃ conc; PA3 low NH ₃ conc.
Truncated spectra (400-950nm)	Log NH ₃	8.24.04	0.48	0.47	27	PD 1,6; PA13	6	86	PD6 high reflectance; PD1, PA13 high NH ₃ conc.
MSC Transformation	none	8.24.04	0.47	3.13	28	PD 1,4	1	92	PD1 high NH ₃ conc.; PD4 spiked reflectance
Transform 1/R	none	8.24.04	0.45	1.60	26	PD 1,4,6; PA13	1	632	PD6 high refl.; PD4 low refl.; PD1,PA13 high NH3 conc.
Transform 1/R	none	9.21.04	0.43	2.45	30	none	2	128	none
Absorbance Transformation	none	8.24.04	0.42	1.63	26	PD 1,4,6; PA13PA	9	542	PD6 high reflect; PD4 low reflect; PD1, PA13 high NH ₃ conc.
Kubelka-Munk Transformation	none	8.24.04	0.42	2.12	28	PD 1,6	6	46	PD6 high reflectance; PD1 high concentration
Golay 2 nd Derivative, avg 10	none	9.21.04	0.42	1.67	28	PA 7,11	1	28	PA7,11 high NH ₃ concentration
Log R	Sqrt NH ₃	8.24.04	0.40	0.57	26	PD 1,4,6; PA13	1	554	PD6 high reflect; PD4 low reflect; PD1, PA13 high NH ₃ conc.
Log R	none	9.21.04	0.39	2.08	29	PA 7	3	105	PA7 high NH ₃ concentration
Truncated spectra (400-950nm)	none	8.24.04	0.35	4.49	30	none	3	29	none

Spectra Transformations	NH ₃ Transformations	Date	r	RMSEP	n	Name of plots removed	PCs	# bands used	Comments
Norris 1 st Derivative	Log NH ₃	8.24.04	0.35	0.56	30	none	2	65	none
Untransformed (350-1075nm)	none	6.16.04	0.34	5.69	25	PD 1,15; PA 2,5,11	2	262	PD15, PA2,11 high NH ₃ conc; PD1 low NH ₃ conc; PA5 missing NH ₃ conc.
Untransformed (350-1075nm)	none	8.24.04	0.34	1.71	26	PD 1,2,6; PA13	1	504	PD6 high reflect; PD2 low refl.; PD1, PA13 high NH ₃ conc
Golay 1 st Derivative, avg 5	none	8.24.04	0.33	4.47	30	none	3	10	none
Golay 2 nd Derivative, avg 10	Log NH ₃	8.24.04	0.33	0.56	30	none	2	25	none
Avg 10 wavelengths	none	8.24.04	0.33	1.69	27	PD 1,6; PA13	4	no	PD6 high reflectance; PD1, PA13 high NH ₃ concentration
Untransformed (350-1075nm)	none	6.29.04	0.32	6.38	26	PD 1,4,12; PA2	6	1	PD1, PA2 high NH ₃ conc; PD4,12 missing NH ₃ conc
Golay 1 st Derivative, avg 10	none	8.24.04	0.32	4.49	30	none	1	no	none
Norris 1 st Derivative, avg 10	none	8.24.04	0.31	4.72	30	none	5	no	none
Normalized spectra (R/R410)	none	8.24.04	0.24	4.62	30	none	2	no	none
Norris 1 st Derivative, avg 5	none	8.24.04	0.24	4.73	30	none	3	13	none
Truncated spectra (400-950nm)	Arcsine sqrt (NH ₃)	8.24.04	0.23	0.11	30	none	4	18	none
Truncated spectra (400-950nm)	Sqrt NH ₃	8.24.04	0.23	1.06	30	none	4	17	none
Transform 1/R	Arcsine sqrt (NH ₃)	8.24.04	0.23	0.07	27	PD 1,4,6	1	364	PD6 high reflectance; PD4 low reflectance; PD1 high NH ₃ conc.
Norris 1 st Derivative	Log NH ₃	8.02.05	0.21	0.64	23	PD 3,6,9-10; PA 3,8,12	1	21	PD3,6,9-10, PA12 missing NH ₃ conc; PA8 high NH ₃ conc; PA3 spiked reflect.
Golay 2 nd Derivative, avg 10	Log NH ₃	7.19.04	0.19	0.49	29	PD 1	1	18	PD1 high NH ₃ concentration
Truncated spectra (400-950nm)	4th rt NH ₃	8.24.04	0.17	0.41	30	none	4	14	none
Untransformed (350-1075nm)	none	7.19.04	0.16	7.91	29	PD1	2	55	PD1 high NH ₃ concentration
Truncated spectra, manual test set	none	8.24.04	0.16	2.86	10	PD6	1	no	PD6 high reflectance
Truncated spectra, random test set	none	8.24.04	0.09	1.65	10	PD 1,6	1	no	PD6 high reflectance; PD1 high NH ₃ concentration
Golay 2 nd Derivative, avg 10	none	8.24.04	0.02	2.26	28	PD 1,6	1	22	PD6 high reflectance; PD1 high NH ₃ concentration

Table 3.4.2. PLS-regression transformations tested on spectrum and ammonia concentration at both sites.

[illegible][illegible]

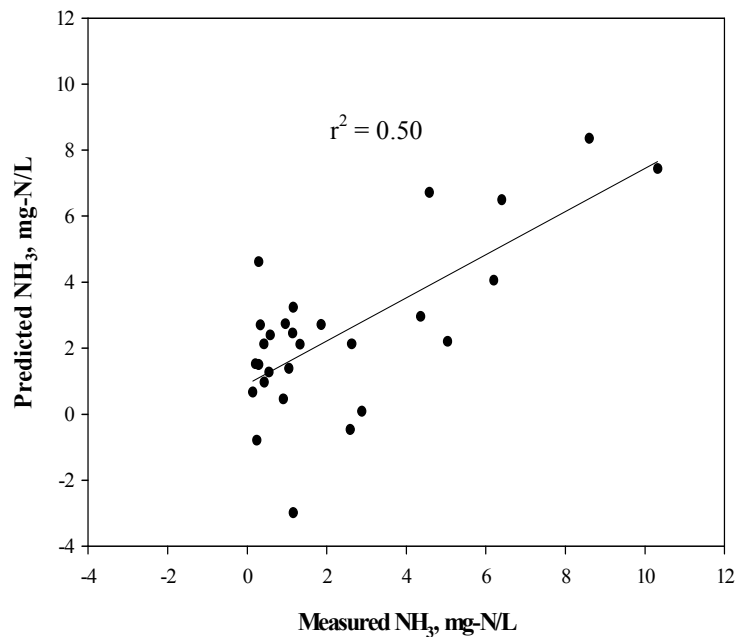


Figure 3.4.1. Predicted vs measured NH₃ PLS-regression for the two marsh sites using untransformed reflectance from 9/21/04 (350-1075nm). Eight spectral bands from 28 samples were used to create four PLS-components with RMSEP = 1.97, $r = 0.71$.

PLS could quantify ammonia concentrations at the *Phragmites*-absent and *Phragmites*-dominant site individually. At the *Phragmites*-absent site, PLS-regressions were most successful at correctly predicting ammonia concentrations with transformed (1st and 2nd derivative) spectra (Table 3.4.3), although the untransformed data (9/21/04) using 44 spectral bands that were combined into five PLS-components yielded an R^2 of 0.76 and RMSEP of 1.71 (Figure 3.4.2).

Table 3.4.3. PLS-regression for ammonia at the *Phragmites*-absent (PA) site. r = regression coefficient, RMSEP = root mean square error of prediction, PCs = PLS-components

Spectra Transformations	NH ₃ Transformations	Date	r	RMSEP	n	Name of plots removed	PCs	# bands used	Comments
Norris 1 st Derivative	Log NH ₃	8.02.05	0.91	0.24	14	Plot 12	2	49	Plot 12 missing NH ₃ data
Untransformed (350-1075nm)	none	9.21.04	0.87	1.71	15	none	5	44	none
Golay 2 nd Derivative, avg 10	Log NH ₃	9.21.04	0.84	0.31	15	none	2	17	none
Golay 2 nd Derivative, avg 10	Log NH ₃	8.24.04	0.82	0.31	15	none	3	38	none
Golay 2 nd Derivative, avg 10	none	9.21.04	0.82	1.79	15	none	3	12	none
Norris 1 st Derivative	Log NH ₃	9.21.04	0.65	0.44	15	none	2	24	none
Truncated spectra, random test	none	8.24.04	0.58	2.76	5	none	2	no	Remaining 10 plots used for calibration
Log R	none	9.21.04	0.58	2.56	15	none	1	12	none
Truncated spectra (400-950nm)	Log NH ₃	8.24.04	0.56	0.43	12	Plots 2,13,14	1	476	Plots 2,14 high reflect; Plot 13 high NH ₃
Truncated spectra (400-950nm)	4th rt NH ₃	8.24.04	0.54	0.24	12	Plots 2,13,14	1	482	Plots 2,14 high reflect; Plot 13 high NH ₃
Golay 2 nd Derivative, avg 10	none	8.24.04	0.54	1.22	14	Plot 13	2	78	Plot 13 high NH ₃ concentration
Truncated spectra (400-950nm)	none	6.06.05	0.52	5.22	15	none	5	12	none
Transform 1/R	none	9.21.04	0.52	2.84	15	none	1	3	none
Truncated spectra (400-950nm)	Arcsine sqrt (NH ₃)	8.24.04	0.49	0.05	12	Plots 2,13,14	1	472	Plots 2,14 high reflect; Plot 13 high NH ₃
Truncated spectra (400-950nm)	Sqrt NH ₃	8.24.04	0.49	0.51	12	Plots 2,13,14	1	469	Plots 2,14 high reflect; Plot 13 high NH ₃
Transform 1/R	Arcsine sqrt (NH ₃)	8.24.04	0.48	0.05	14	Plot 13	4	21	Plot 13 high NH ₃ concentration
Log R	Sqrt NH ₃	9.21.04	0.46	0.83	15	none	2	5	none
Norris 1 st Derivative, avg 10	none	8.24.04	0.40	1.31	14	Plot 13	1	24	Plot 13 high NH ₃ concentration
Norris 1 st Derivative	none	8.24.04	0.39	1.33	14	Plot 13	2	22	Plot 13 high NH ₃ concentration

Spectra Transformations	NH ₃ Transform- ations	Date	r	RMSEP	n	Name of plots removed	PCs	# bands used	Comments
Log R	Sqrt NH₃	8.24.04	0.37	0.53	13	Plots 2,13	1	381	Plot 2 high reflect; Plot 13 high NH ₃
Golay 1st Derivative	none	8.24.04	0.37	1.33	14	Plot 13	1	20	Plot 13 high NH ₃ concentration
Golay 1st Derivative, avg 5	none	8.24.04	0.37	1.33	14	Plot 13	1	19	Plot 13 high NH ₃ concentration
Golay 1st Derivative	none	9.21.04	0.37	0.37	14	Plot 7	3	6	Plot 7 high NH ₃ concentration
Truncated spectra (400-950nm)	none	8.24.04	0.33	0.75	12	Plots 2,11,13	1	31	Plot 2 high reflect; Plots 11,13 high NH ₃
Norris 1st Derivative	Log NH₃	8.24.04	0.32	0.54	15	none	2	7	none
Norris 1st Derivative, avg 5	none	8.24.04	0.31	1.34	14	Plot 13	1	25	Plot 13 high NH ₃ concentration
Transform 1/R	none	8.24.04	0.27	1.43	13	Plots 2,13	1	97	Plot 2 high reflect; Plot 13 high NH ₃
Golay 1st Derivative, avg 10	none	8.24.04	0.24	2.17	15	none	1	13	none
Untransformed d (350-1075nm)	none	6.29.04	0.20	1.30	14	Plot 2	2	8	Plot 2 high NH ₃ concentration
Truncated spectra, manual test	none	8.24.04	0.20	3.00	5	none	2	no	Remaining 10 plots used for calibration
Golay 2nd Derivative, avg 10	Log NH₃	7.19.04	0.19	0.24	14	Plot 2	1	8	Plot 2 high NH ₃ concentration
Kubelka-Munk Transformation	none	8.24.04	0.16	1.44	14	Plot 13	1	no	Plot 13 high NH ₃ concentration
Untransformed d (350-1075nm)	none	6.06.05	0.14	5.64	14	Plot 3	1	49	Plot 3 high reflectance curve
Absorbance Transformation	none	8.24.04	0.13	1.45	14	Plot 13	1	no	Plot 13 high NH ₃ concentration
MSC Transformation	none	8.24.04	0.12	1.41	14	Plot 13	1	9	Plot 13 high NH ₃ concentration
Untransformed d (350-1075nm)	none	8.24.04	0.08	1.52	14	Plot 13	1	no	Plot 13 high NH ₃ concentration
Normalized spectra (R/R410)	none	8.24.04	0.05	2.34	15	none	1	no	none
Untransformed d (350-1075nm)	none	8.02.05	0.03	10.46	14	Plot 12	1	no	Plot 12 missing NH ₃ data
Untransformed d (350-1075nm)	none	7.19.04	0.13	7.56	15	none	1	no	none
Untransformed d (350-1075nm)	none	6.16.04	0.35	15.27	14	Plot 5	1	no	Plot 5 missing NH ₃ data

Table 3.4.4. PLS-regression transformations tested on spectrum and ammonia concentrations at the *Phragmites*-absent site.

[illegible][illegible]

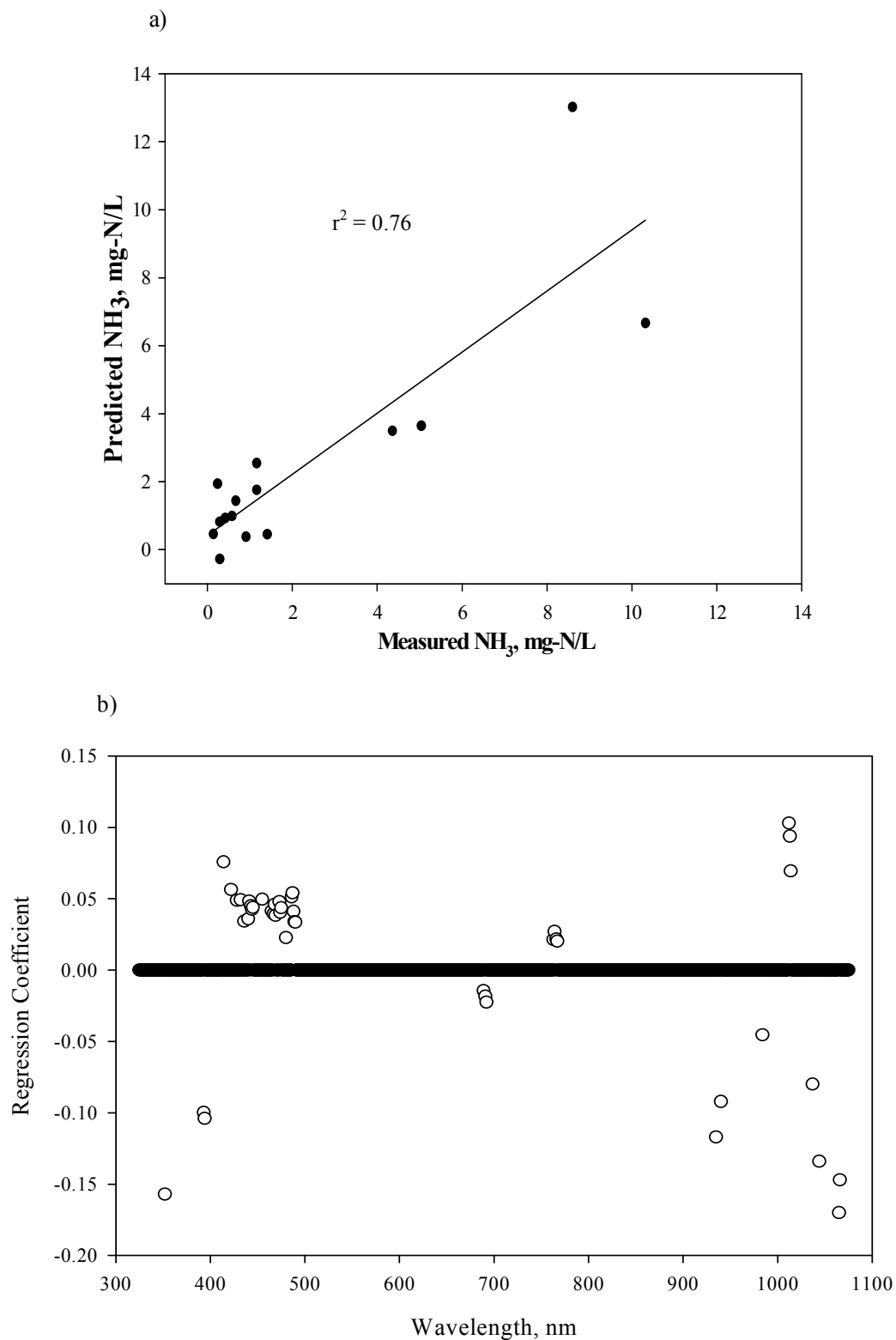


Figure 3.4.2. (a) Predicted vs measured ammonia PLS-regression which used 44 spectral bands to form five PLS-components with $r = 0.87$ and RMSEP of 1.71 for the *Phragmites*-absent site, 9/21/04 data. (b) Loading plot of regression coefficients for the PLS-regression.

The best PLS model at the *Phragmites*-absent site used the 1st derivative of the spectra and the log of ammonia concentration for a more normal distribution (Figure 3.4.3). Two PLS-components were created from the 49 spectral bands used in the model with $R^2 = 0.83$ and an RMSEP of 0.24.

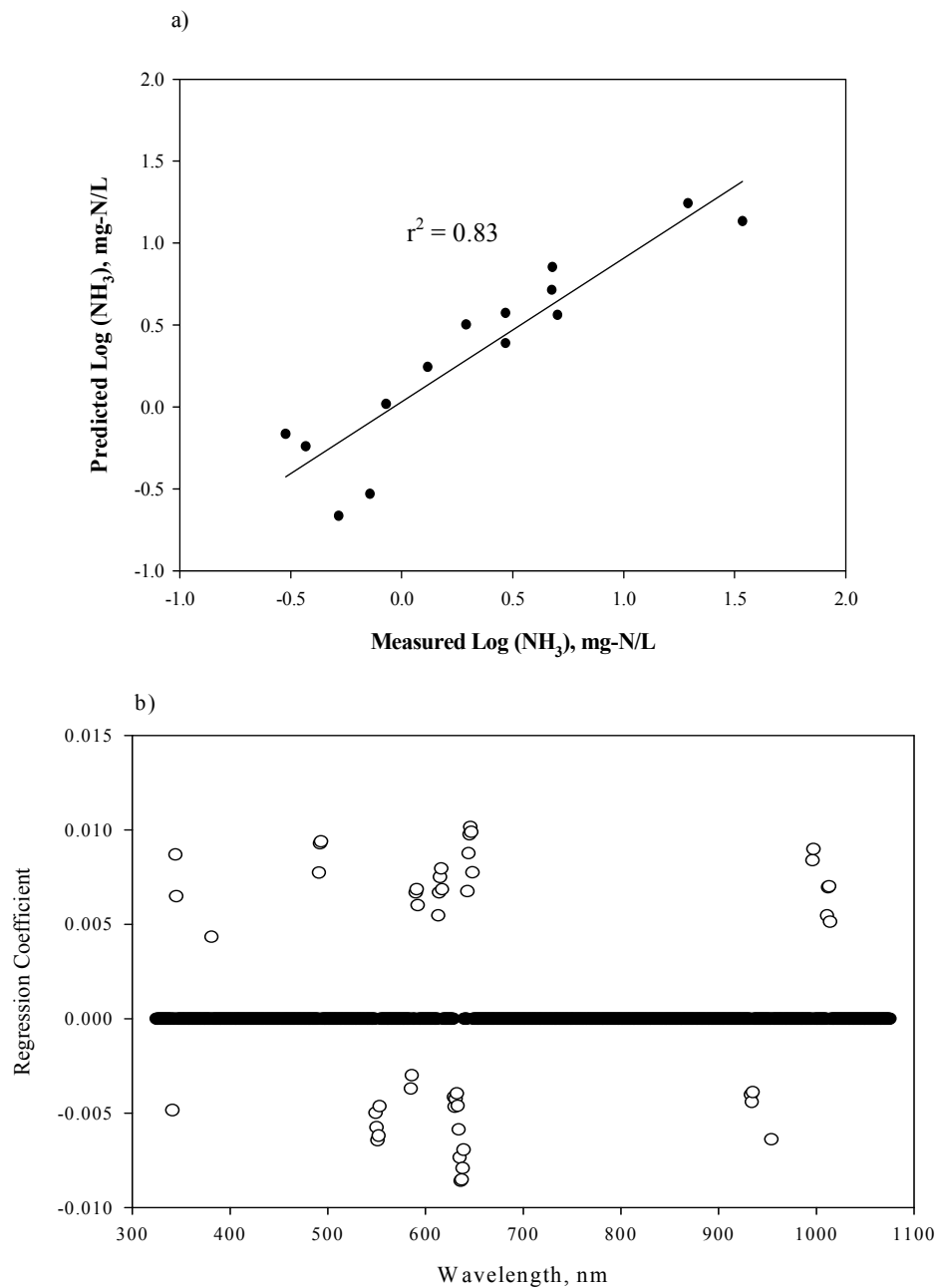


Figure 3.4.3. (a) *Phragmites*-absent site predicted vs measured log of ammonia PLS-regression using 49 spectral bands of the 1st derivative of the 8/02/05 reflectance to form two PLS-components with $r = 0.91$ and RMSEP of 0.24. (b) Loading plot of regression coefficients for the PLS-regression.

PLS was able to quantify ammonia concentrations at the *Phragmites*-dominant site with untransformed spectra during August and September of both years (Table 3.4.5). The most predictive model at the *Phragmites*-dominant site used untransformed spectra (8/02/05) and ten spectral bands in the visible red to form six PLS-components with RMSEP of 1.65 and $R^2 = 0.96$ (Figure 3.4.4).

Summaries of spectral bands used in each PLS-regression are given for combined marsh sites, and individual sites (Tables 3.4.5a, 3.4.6a, and 3.4.7a). Models for the two marsh sites used only a few spectral bands in the green and near-infrared in ten or more regressions (Figure 3.4.5b). At the *Phragmites*-absent site spectral bands used in ten or more PLS-regressions were generally located in the blue and green wavebands (Figure 3.4.6b). The *Phragmites*-dominant site displayed the most spectral bands used in ten or more PLS-regressions, particularly in the green, red-edge, and near-infrared (Figure 3.4.7b). A list of the illustrated bands, significant to ten or more regressions, can be found in the Appendix.

Table 3.4.5. PLS-regression for ammonia at the *Phragmites*-dominant (PD) site. r = regression coefficient, RMSEP = root mean square error of prediction, PCs = PLS-components

Spectra Transformations	NH ₃ Transformations	Date	r	RMSEP	n	Name of plots removed	PCs	# bands used	Comments
Untransformed (350-1075nm)	none	8.02.05	0.98	1.65	10	Plots 3,6,8-10	6	10	Plots 3,6,9-10 missing NH ₃ ; Plot 8 high NH ₃
Golay 2 nd Derivative, avg 10	none	9.21.04	0.88	0.80	14	Plot 10	2	103	Plot 10 high NH ₃ concentration
Truncated spectra (400-950nm)	Sqrt NH ₃	8.24.04	0.77	0.61	14	Plot 1	5	30	Plot 1 high NH ₃ concentration
Untransformed (350-1075nm)	none	9.21.04	0.73	1.18	14	Plot 6	3	278	Plot 6 high NH ₃ concentration
Truncated spectra (400-950nm)	Arcsine sqrt (NH ₃)	8.24.04	0.72	0.07	14	Plot 1	4	35	Plot 1 high NH ₃ concentration
Truncated spectra (400-950nm)	4th root NH ₃	8.24.04	0.70	0.26	14	Plot 1	4	36	Plot 1 high NH ₃ concentration
Norris 1 st Derivative	Log NH ₃	8.02.05	0.63	0.55	11	Plots 3,6,9-10	1	97	Plots 3,6,9-10 missing NH ₃ concentration
Golay 2 nd Derivative, avg 10	Log NH ₃	8.24.04	0.62	0.45	15	none	1	42	none
Golay 2 nd Derivative, avg 10	none	8.24.04	0.59	4.98	15	none	1	98	none
Golay 2 nd Derivative, avg 10	Log NH ₃	9.21.04	0.57	0.38	15	none	2	5	none
Norris 1 st Derivative	none	8.24.04	0.56	5.06	15	none	1	82	none
Norris 1 st Derivative	Log NH ₃	8.24.04	0.54	0.48	15	none	1	35	none
Golay 1 st Derivative, avg 10	none	8.24.04	0.53	5.09	15	none	1	92	none
Truncated spectra, manual test	none	8.24.04	0.52	3.23	5	Plot 6	1	no	Remaining 9 plots used for calib.
Untransformed (350-1075nm)	none	6.29.04	0.51	8.14	12	Plots 1,4,12	2	36	Plot 1 high NH ₃ conc; Plots 4,12 missing NH ₃
Golay 1 st Derivative	none	8.24.04	0.51	5.16	15	none	1	89	none
Golay 1 st Derivative, avg 5	none	8.24.04	0.51	5.16	15	none	1	90	none
Golay 2 nd Derivative, avg 10	Log NH ₃	7.19.04	0.49	0.58	15	none	2	148	none
Log R	none	9.21.04	0.49	1.79	15	none	2	228	none
Norris 1 st Derivative, avg 5	none	8.24.04	0.48	5.26	15	none	1	96	none
Norris 1 st Derivative, avg 10	none	8.24.04	0.48	5.27	15	none	1	105	none

Spectra Transformations	NH ₃ Transformations	Date	r	RMSEP	n	Name of plots removed	PCs	# bands used	Comments
Log R	Square root NH ₃	9.21.04	0.47	0.58	15	none	1	154	none
Avg 5 wavelengths	none	8.24.04	0.45	5.78	14	Plot 4	2	80	Plot 4 low reflectance
Untransformed (350-1075nm)	none	6.16.04	0.43	6.88	13	1,15	2	353	Plot 1 highest NH ₃ conc; Plot 15 lowest NH ₃
Truncated spectra (400-950nm)	Log NH ₃ Discrim.	8.24.04	0.43	0.57	15	none	9	no	none
Untransformed (350-1075nm)	Analysis	8.24.04	0.41	0.86	13	Plots 4,6	1	79	Plot 4 low reflect.; 6 high NH ₃ conc.
Kubelka-Munk Transformation	none	8.24.04	0.41	1.86	13	Plots 1,6	1	5	Plots 1,6 high NH ₃ conc.
Transform 1/R	none	9.21.04	0.41	1.83	15	none	1	277	none
Golay 1 st Derivative	none	9.21.04	0.41	2.10	15	none	1	39	none
Transform 1/R	none	8.24.04	0.40	1.94	12	Plots 1,4,6	1	517	Plots 1,6 high NH ₃ conc; Plot 4 low reflect.
Transform 1/R	Arcsine sqrt (NH ₃)	8.24.04	0.39	0.06	12	Plots 1,4,6	1	337	Plots 1,6 high NH ₃ conc; Plot 4 low reflect.
Avg 10 wavelengths	none	8.24.04	0.39	5.82	15	none	2	164	none
Log R	Sqrt NH ₃	8.24.04	0.38	0.63	12	Plots 1,4,6	2	264	Plots 1,6 high NH ₃ conc; Plot 4 low reflect.
Norris 1 st Derivative	Log NH ₃	9.21.04	0.38	0.47	15	none	1	39	none
Truncated spectra (400-950nm)	none	8.24.04	0.37	5.70	15	none	2	11	none
Normalized spectra (R/R410)	none	8.24.04	0.37	5.98	14	Plot 4	2	278	Plot 4 low reflectance
Untransformed (350-1075nm)	none	8.24.04	0.34	5.78	15	none	2	201	none
Untransformed (350-1075nm)	none	7.19.04	0.32	20.83	13	Plots 5,10	1	53	Plot 5 high reflectance; Plot 10 low reflectance
MSC Transformation	none	8.24.04	0.20	6.76	15	none	2	23	none
Absorbance Transformation	none	8.24.04	0.19	6.46	14	Plot 4	2	162	Plot 4 low reflectance
Untransformed (350-1075nm)	Excluding NH ₃ >8	8.24.04	0.17	2.12	13	Plots 1,6	1	no	Plots 1,6 NH ₃ concentration > 8mg/L
Truncated spectra, random test	none	8.24.04	0.10	6.01	4	Plot 6	1	no	Remaining 10 plots used for calib.
PLS2 Untransformed (350-1075)	NH ₃ , NO ₃	8.24.04	0.09	6.11	15	none	1	no	none
Untransformed (350-1075nm)	none	6.06.05	0.32	2.05	14	Plot 1	1	no	Plot 1 high NH ₃ concentration
Truncated spectra (400-950nm)	none	6.06.05	0.37	4.98	15	none	1	no	none

Table 3.4.6. PLS-regression transformations tested on ammonia concentrations at the *Phragmites*-dominant site.

[illegible][illegible]

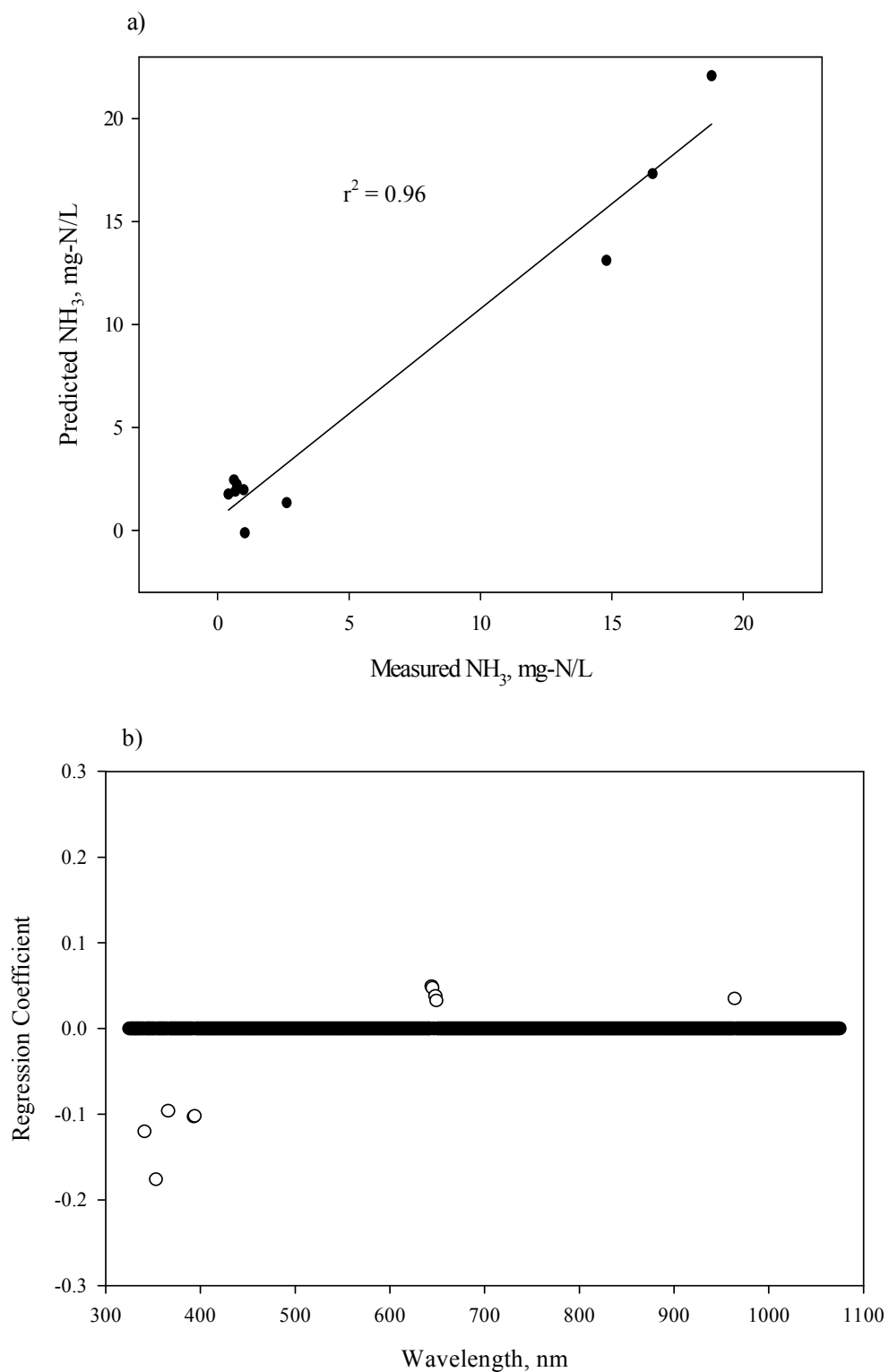


Figure 3.4.4. (a) Predicted vs measured ammonia PLS-regression at the *Phragmites*-dominant site which used ten spectral bands from 8/02/05 data to form six PLS-components with $r = 0.98$ and RMSEP = 1.65. (b) Loading plot of regression coefficients vs wavelength for the PLS-regression.

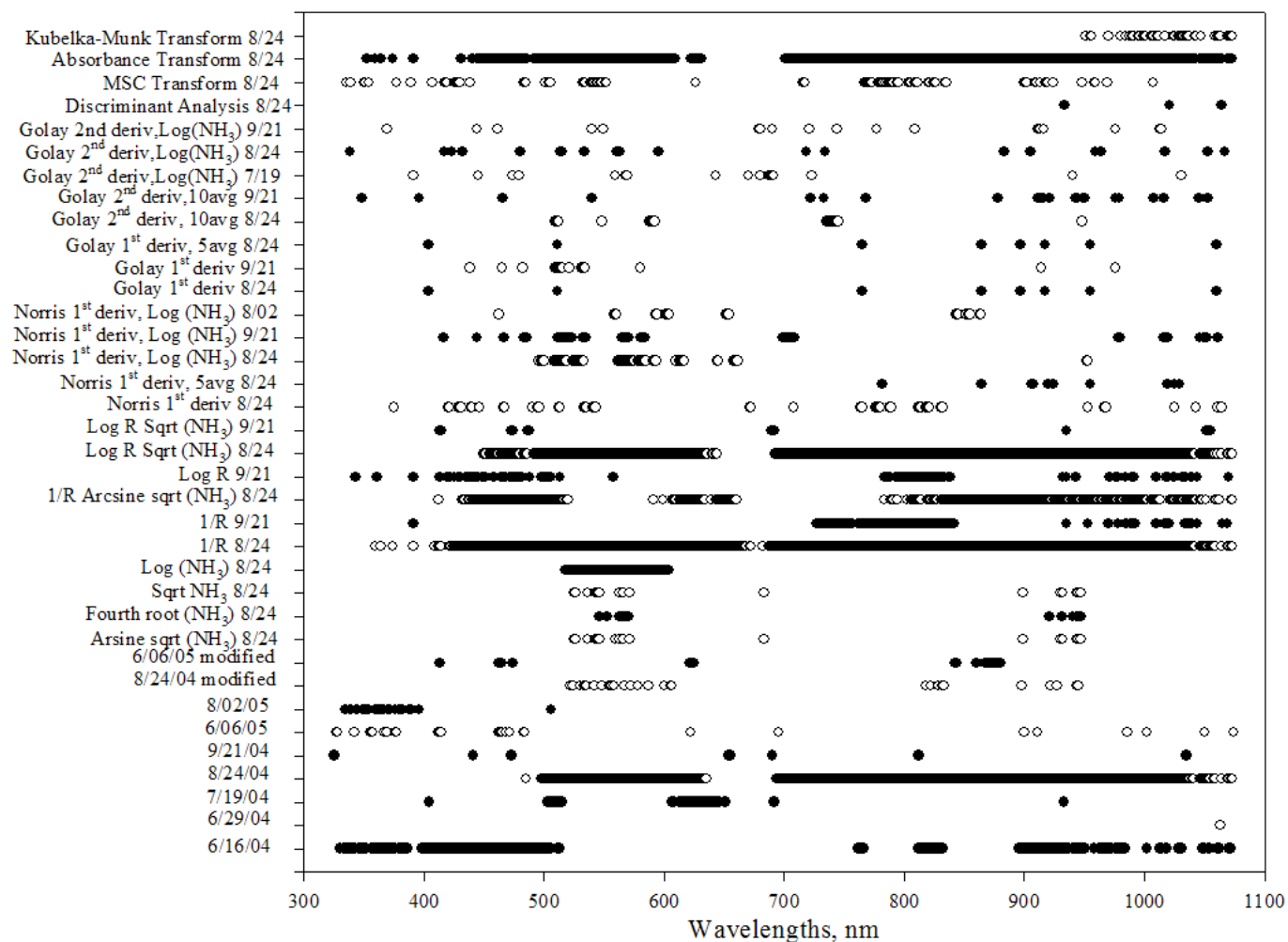


Figure 3.4.5a. Significant spectral bands for NH_3 according to PLS-regressions at the two marsh sites.

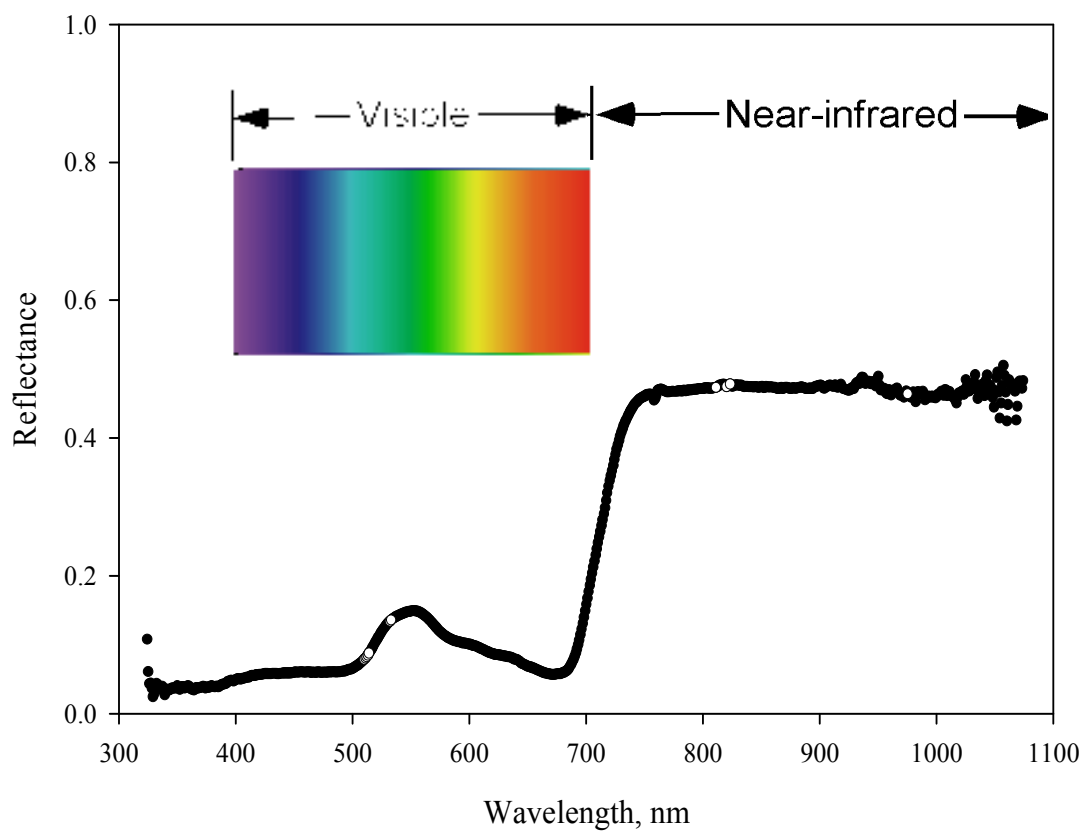


Figure 3.4.5b. Spectral bands significant for ten or more NH₃ regressions at the two marsh sites are indicated by an open circle.

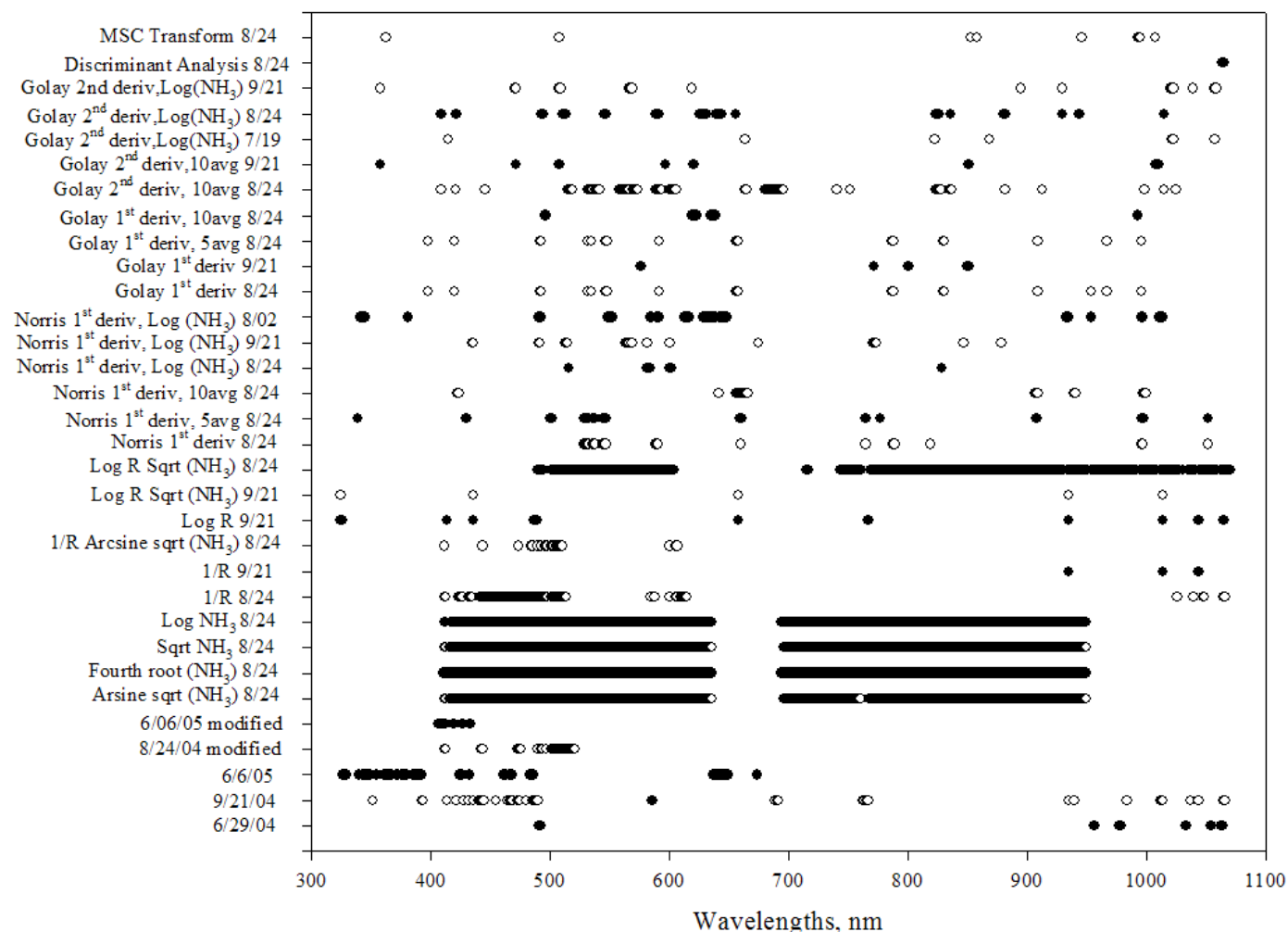


Figure 3.4.6a. Significant spectral bands for NH_3 according to PLS-regressions at the *Phragmites*-absent site.

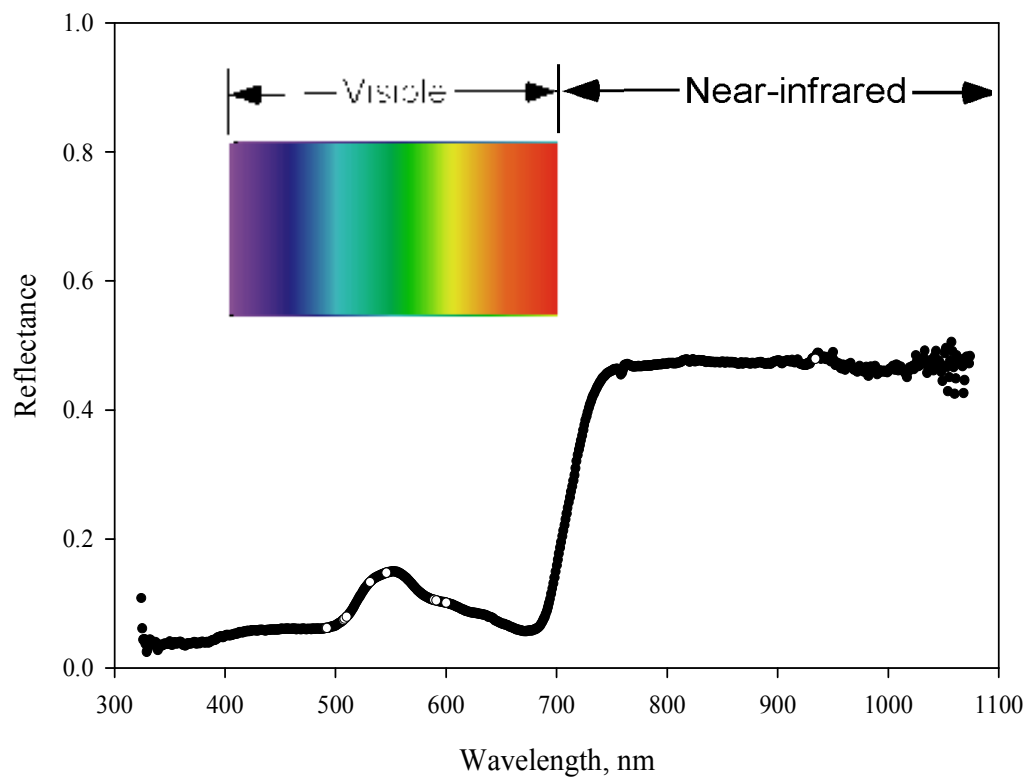


Figure 3.4.6b. Spectral bands significant for ten or more NH_3 regressions at the *Phragmites*-absent site are indicated by an open circle.

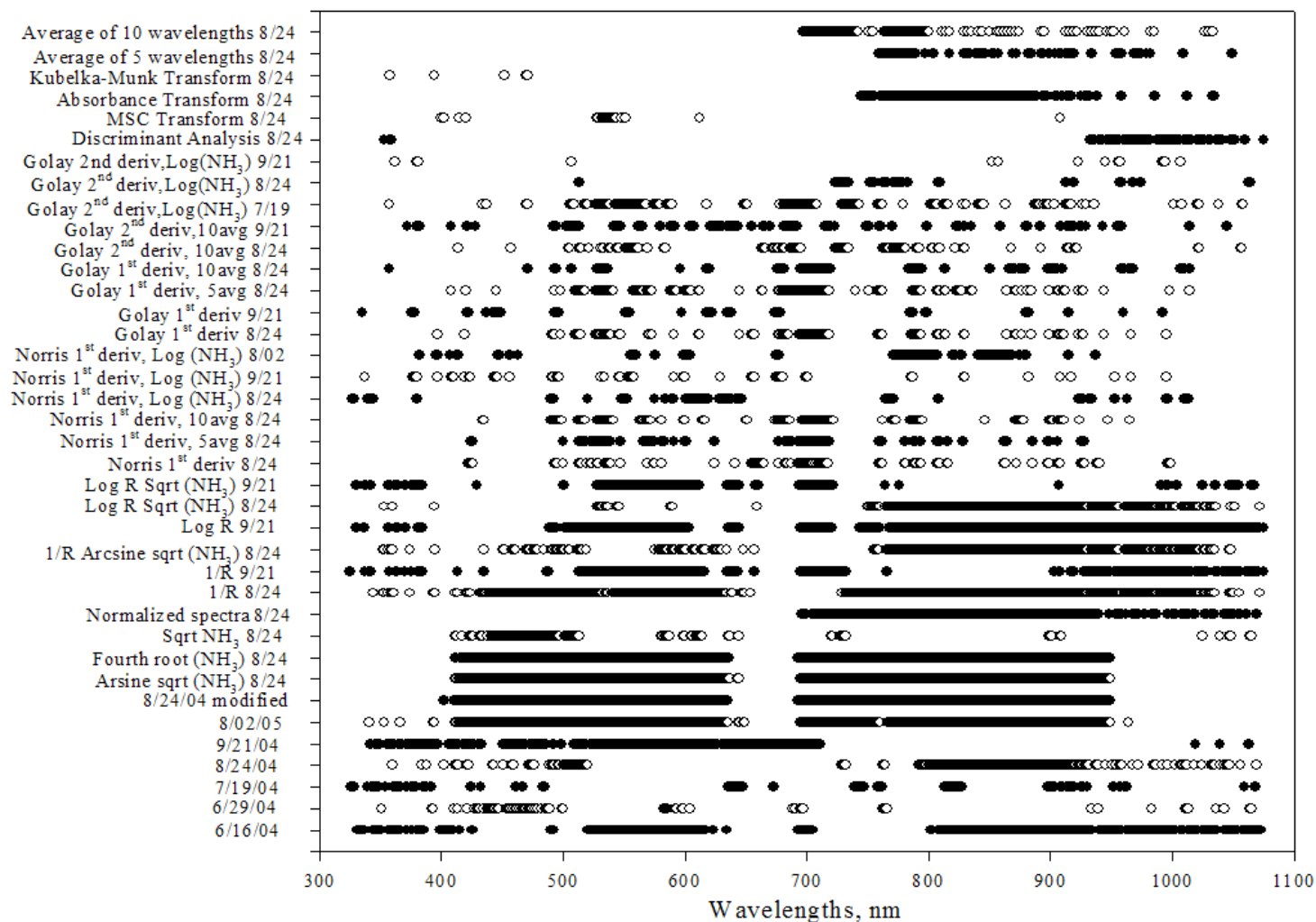


Figure 3.4.7a. Significant spectral bands for NH_3 according to PLS-regressions at the *Phragmites*-dominant site.

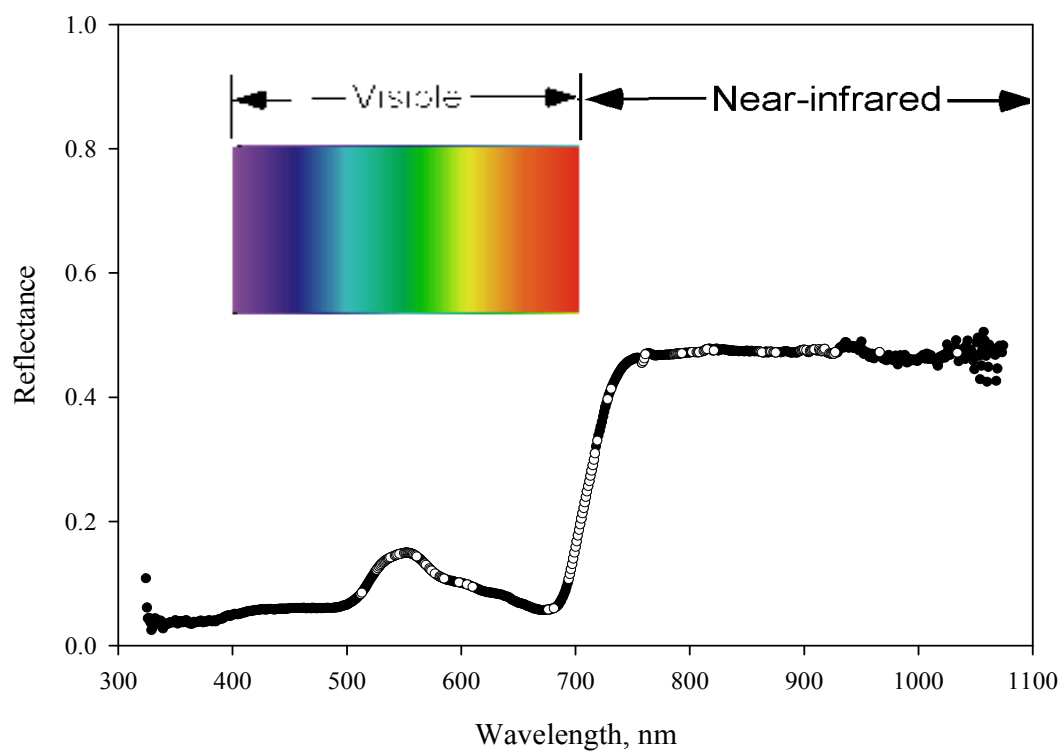


Figure 3.4.7b. Spectral bands significant for ten or more NH_3 regressions at the *Phragmites*-dominant site are indicated by an open circle.

PLS Models of Nitrate

PLS was able to quantify nitrate concentrations in sub-surface marsh water for the two sites during the end of the season (August and September). The best model predictive of nitrate used four untransformed spectral bands that were combined into two PLS-components with RMSEP of 1.5 and $R^2 = 0.67$ (Figure 3.4.8). Other models that quantified nitrate at the two marsh sites used the 1st or 2nd derivative of the spectra to reduce reflectance noise and the log of nitrate to normalize the sample distribution (Table 3.4.7).

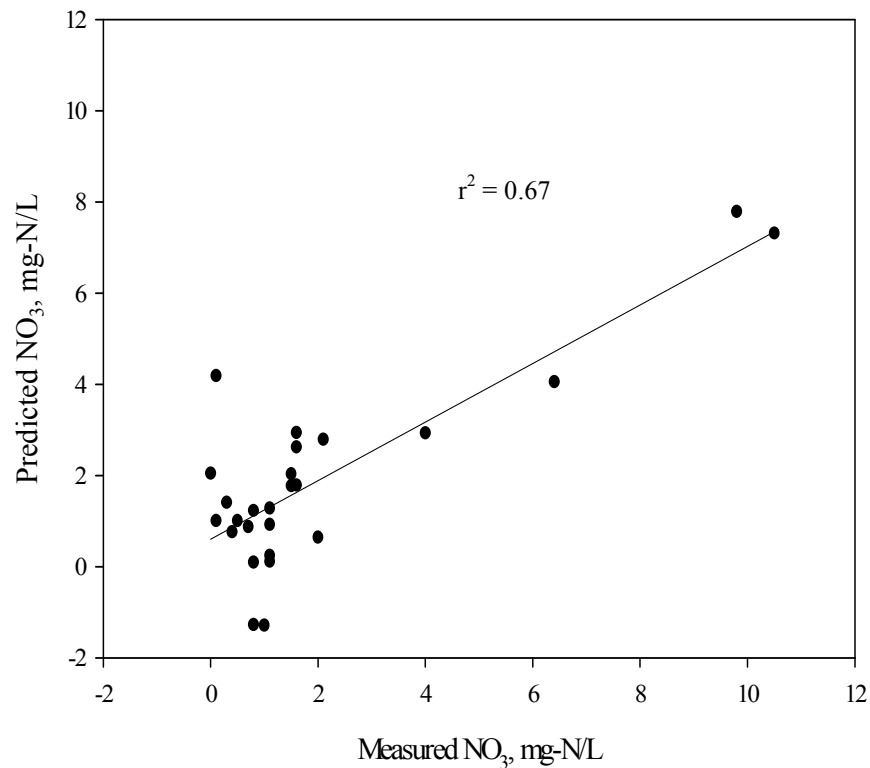


Figure 3.4.8. Predicted vs measured nitrate PLS-regression for combined sites using four spectral bands of untransformed data from 8/02/05 to form two PLS-components with $r = 0.82$, RMSEP = 1.50.

Table 3.4.7. PLS-regression for nitrate at combined *Phragmites*-dominant (PD) and *Phragmites*-absent (PA) sites. r = regression coefficient, RMSEP = root mean square error of prediction, PCs = PLS-components

Spectra Transformations	NO ₃ Transformations	Date	r	RMSEP	n	Name of plots removed	PCs	# bands used	Comments
Untransformed (350-1075nm)	none	8.02.05	0.82	1.50	26	PD 3,6,10; PA12	2	4	PD 3,6,10; PA12 missing NO3 data
Norris 1 st Derivative	Log NO ₃	8.02.05	0.80	0.30	26	PD 3,6,10; PA12	2	41	PD 3,6,10; PA12 missing NO3 data
Golay 2 nd Derivative, avg 10	Log NO ₃	9.21.04	0.73	0.21	30	none	1	26	none
Golay 2 nd Derivative, avg 10	none	9.21.04	0.71	0.69	30	none	2	28	none
Truncated spectra, manual test	none	8.24.04	0.60	0.79	10	none	2	none	Remainder used in calibration
Norris 1 st Derivative	none	8.24.04	0.60	0.87	30	none	2	30	none
Norris 1 st Derivative, avg 5	none	8.24.04	0.60	0.86	30	none	1	7	none
Norris 1 st Derivative, avg 10	none	8.24.04	0.57	0.88	30	none	1	18	none
Golay 1 st Derivative	none	8.24.04	0.57	0.88	30	none	2	39	none
Golay 1 st Derivative, avg 5	none	8.24.04	0.57	0.88	30	none	2	39	none
Untransformed (350-1075nm)	none	6.16.04	0.56	0.74	28	PA2,5	8	9	PA2,5 missing NO3 data
Transform 1/R	none	8.24.04	0.54	0.91	30	none	1	219	none
Kubelka-Munk Transformation	none	8.24.04	0.54	0.90	30	none	1	216	none
Golay 1 st Derivative, avg 10	none	8.24.04	0.52	0.93	30	none	2	51	none
Truncated spectra (400-950nm)	none	8.24.04	0.51	0.95	29	PD6	3	26	PD6 high reflectance
Golay 2 nd Derivative, avg 10	Log NO ₃	7.19.04	0.49	0.24	29	PA2	1	83	PA2 low NO3 conc.
Truncated spectra (400-950nm)	Log NO ₃	8.24.04	0.49	0.32	29	PD6	8	71	PD6 high reflectance
Truncated spectra (400-950nm)	Sqrt NO ₃	8.24.04	0.45	0.37	29	PD6	2	7	PD6 high reflectance

Spectra Transformations	NO ₃ Transformations	Date	r	RMSEP	n	Name of plots removed	PCs	# bands used	Comments
Untransformed (350-1075nm)	none	8.24.04	0.44	1.00	29	PD6	4	38	PD6 high reflectance
Log R	Sqrt NO ₃	8.24.04	0.44	0.37	30	none	5	139	none
Absorbance Transformation	none	8.24.04	0.44	0.97	30	none	1	271	none
Log R	Sqrt NO ₃	9.21.04	0.44	0.34	29	PA8	2	31	PA8 noisy reflectance
	Arcsine sqrt (NO ₃)								
Truncated spectra (400-950nm)	(NO ₃)	8.24.04	0.42	0.04	29	PD6	3	4	PD6 high reflectance
Truncated spectra, random test	none	8.24.04	0.42	1.35	10	none	1	none	Remainder used in calibration
	Arcsine sqrt (NO ₃)								
Transform 1/R	(NO ₃)	8.24.04	0.42	0.04	30	none	1	308	none
Truncated spectra (400-950nm)	4th root NO ₃	8.24.04	0.39	0.18	29	PD6	2	7	PD6 high reflectance
Golay 2 nd Derivative, avg 10	none	8.24.04	0.39	1.00	30	none	1	41	none
Golay 2 nd Derivative, avg 10	Log NO ₃	8.24.04	0.37	0.28	29	PD1	1	45	PD1 low NO3 conc.
Golay 1 st Derivative	none	9.21.04	0.36	0.63	29	PD3	2	30	PD3 high NO3 concentration
Normalized spectra (R/R410)	none	8.24.04	0.33	1.02	30	none	1	512	none
Norris 1 st Derivative	Log NO ₃	8.24.04	0.33	0.34	30	none	3	12	none
MSC Transformation	none	8.24.04	0.32	1.07	30	none	7	none	none
Norris 1 st Derivative	Log NO ₃	9.21.04	0.24	0.31	30	none	2	none	none
						PD14; PA			
Untransformed (350-1075nm)	none	6.06.05	0.21	2.31	27	12,15	2	60	PD4; PA 12,15 missing NO3 data
						PD4; PA			
Truncated spectra (400-950nm)	none	6.06.05	0.12	2.35	27	12,15	1	none	PD4; PA 12,15 missing NO3 data
						PD 3,12,14;			
Untransformed (350-1075nm)	none	6.29.04	-0.17	0.96	26	PA2	1	none	PD 3,12,14; PA2 missing NO3 data
Untransformed (350-1075nm)	none	9.21.04	-0.27	1.04	30	none	1	none	none
Transform 1/R	none	9.21.04	-0.27	1.03	30	none	1	56	none
Log R	none	9.21.04	-0.27	1.04	30	none	1	none	none
Untransformed (350-1075nm)	none	7.19.04	-0.32	2.07	30	none	1	none	none

Table 3.4.8. PLS-regression transformations tested on nitrate concentrations at the two marsh sites.

[illegible][illegible]

PLS was very successful in predicting nitrate at the *Phragmites*-dominant site, particularly during August and September of both years. The best PLS model at the *Phragmites*-dominant site used the same untransformed data (8/02/05) that was used in the best model for the two marsh sites. At the *Phragmites*-dominant site, the PLS model used 40 spectral bands to form seven PLS-components with RMSEP of 1.08 and $R^2 = 0.90$ (Figure 3.4.9).

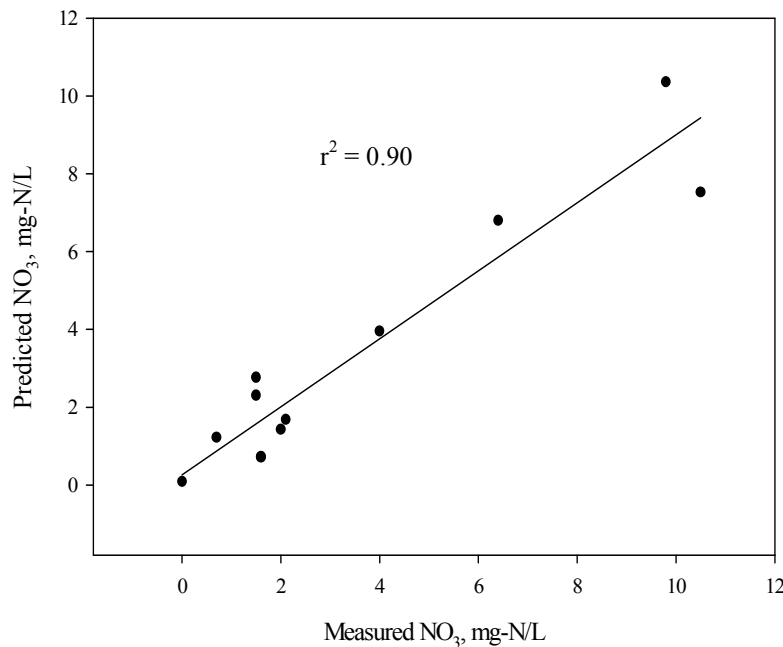


Figure 3.4.9. Predicted vs measured nitrate PLS-regression at the *Phragmites*-dominant site. Seven PLS-components were formed from 40 spectral bands of untransformed reflectance data from 8/02/05 with $r=0.95$ and RMSEP=1.08.

The 1st and 2nd derivatives were also used in models predictive of nitrate sub-surface concentrations at the *Phragmites*-dominant site. On 9/21/04, a PLS model using 75 spectral bands of the 1st derivative transformed reflectance yielded an RMSEP of 0.40 and $R^2 = 0.88$ (Figure 3.4.10).

Among the transformations yielding the best regressions at the *Phragmites*-dominant site were the 1st and 2nd derivatives of the reflectance curve, and the log of nitrate concentration (Table 3.4.9). Since several reflectance and nitrate transformations were used in the PLS-regressions, a complete summary of transformations performed on the *Phragmites*-dominant site data is given in Table 3.4.10.

At the *Phragmites*-absent site, nitrate was predicted correctly using PLS during August and September. During the end of the 2004 growing season, nitrate concentrations were, on average, between 1-2 mg-N/L at the *Phragmites*-absent site. PLS-regression was able to quantify this range using transformed (1st and 2nd derivative, inverse reflectance, normalized) spectra (Table 3.4.11). The best PLS model for the *Phragmites*-absent site used the log of nitrate and 75 spectral bands of 1st derivative transformed reflectance that established three PLS-components with RMSEP of 0.11 and R^2 of 0.81 (Figure 3.4.11). When the inverse reflectance of sample date 8/24/04 was used, PLS correctly predicted nitrate concentrations using 234 spectral bands of inverse reflectance, primarily in the near-infrared, to form six PLS-components with an RMSEP of 0.15 and R^2 of 0.79 (Figure 3.4.12).

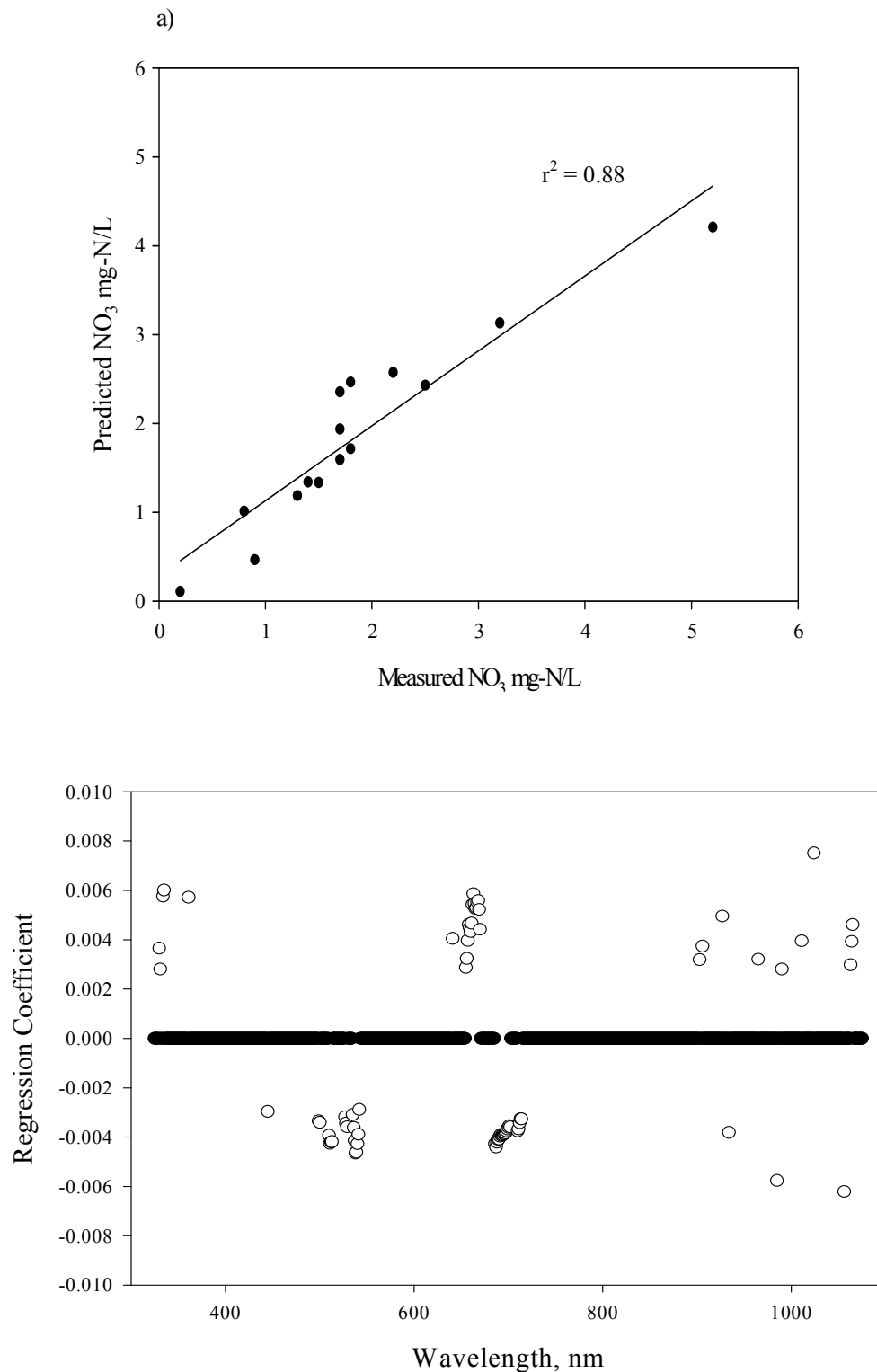


Figure 3.4.10. (a) Predicted vs measured nitrate PLS-regression at the *Phragmites*-dominant site using 75 spectral bands of the 1st derivative of the spectrum (9/21/04) to form seven PLS-components with $r = 0.94$ and RMSEP of 0.40. (b) Loading plot showing significant spectral bands used in the regression as open circles.

Table 3.4.9. PLS-regression for nitrate at the *Phragmites*-dominant (PD) site. r = regression coefficient, RMSEP = root mean square error of prediction, PCs = PLS-components

Spectra Transformations	NO ₃ Transformations	Date	r	RMSEP	n	Name of plots removed	PCs	# bands used	Comments
Untransformed (350-1075nm)	none	8.02.05	0.95	1.08	12	Plots 3,6,10	7	40	Plots 3,6,10 missing NO ₃ data
Golay 1 st Derivative	none	9.21.04	0.94	0.40	15	none	7	75	none
Golay 2 nd Derivative, avg 10	none	9.21.04	0.93	0.42	15	none	2	35	none
Norris 1 st Derivative	Log NO ₃	9.21.04	0.88	0.09	14	Plot 1	5	49	Plot 1 low NO ₃ conc
Norris 1 st Derivative	Log NO ₃	8.02.05	0.76	0.24	11	Plots 3,6,9,10	1	43	Plots 3,6,10 missing NO ₃ ; Plot 9 low NO ₃
Transform 1/R	none	9.21.04	0.69	0.83	15	none	10	19	none
Golay 2 nd Derivative, avg 10	Log NO ₃	9.21.04	0.67	0.23	15	none	1	10	none
Norris 1 st Derivative, avg 10	none	8.24.04	0.60	1.07	14	Plot 6	1	153	Plot 6 high reflectance
Golay 1 st Derivative, avg 10	none	8.24.04	0.58	1.10	14	Plot 6	1	130	Plot 6 high reflectance
Golay 1 st Derivative	none	8.24.04	0.57	1.10	14	Plot 6	1	138	Plot 6 high reflectance
Golay 1 st Derivative, avg 5	none	8.24.04	0.57	1.10	14	Plot 6	1	86	Plot 6 high reflectance
Truncated spectra, random test	none	8.24.04	0.56	2.21	5	none	1	none	none
Norris 1 st Derivative	none	8.24.04	0.53	1.12	14	Plot 6	1	99	Plot 6 high reflectance
Norris 1 st Derivative	Log NO ₃	8.24.04	0.53	0.18	13	Plots 1,6	1	88	Plot 1 low NO ₃ conc; Plot 6 high reflect.
Golay 2 nd Derivative, avg 10	Log NO ₃	7.19.04	0.50	0.31	15	none	1	15	none
Golay 2 nd Derivative, avg 10	none	8.24.04	0.49	1.12	15	none	1	31	none
Norris 1 st Derivative, avg 5	none	8.24.04	0.48	1.16	14	Plot 6	1	120	Plot 6 high reflectance
Golay 2 nd Derivative, avg 10	Log NO ₃	8.24.04	0.47	0.15	13	Plots 1,3	1	4	Plot 1 low NO ₃ conc; Plot 3 high NO ₃
Untransformed (350-1075nm)	none	8.24.04	0.46	1.26	14	Plot 6	3	171	Plot 6 high reflectance

Spectra Transformations	NO ₃ Transformations	Date	r	RMSEP	n	Name of plots removed	PCs	# bands used	Comments
Truncated spectra (400-950nm)	none	6.06.05	0.45	1.45	12	Plots 6,12,14	4	60	Plots 6,12 high NO ₃ ; Plot 14 missing NO ₃
MSC Transformation	none	8.24.04	0.35	1.19	15	none	1	64	none
Absorbance Transformation	none	8.24.04	0.35	1.24	14	Plot 6	1	141	Plot 6 high reflectance
Kubelka-Munk Transformation	none	8.24.04	0.33	1.25	14	Plot 6	1	149	Plot 6 high reflectance
Transform 1/R	none	8.24.04	0.32	1.25	14	Plot 6	1	108	Plot 6 high reflectance
Truncated spectra (400-950nm)	none	8.24.04	0.28	1.32	14	Plot 6	1	123	Plot 6 high reflectance
Transform 1/R	Arcsine sqrt (NO ₃)	8.24.04	0.28	0.05	14	Plot 6	1	85	Plot 6 high reflectance
Log R	Sqrt NO ₃	8.24.04	0.27	0.46	14	Plot 6	1	136	Plot 6 high reflectance
Truncated spectra (400-950nm)	4th root NO ₃	8.24.04	0.26	0.23	13	Plots 6,15	1	104	Plots 6,15 high reflect
Truncated spectra (400-950nm)	Arcsine sqrt (NO ₃)	8.24.04	0.24	0.05	14	Plot 6	1	105	Plot 6 high reflectance
Truncated spectra (400-950nm)	Sqrt NO ₃	8.24.04	0.24	0.48	14	Plot 6	1	104	Plot 6 high reflectance
Truncated spectra, manual test	none	8.24.04	0.21	2.60	5	none	1	none	none
Truncated spectra (400-950nm)	Log NO ₃	8.24.04	0.19	0.42	13	Plots 6,15	1	79	Plots 6,15 high reflect
Untransformed (350-1075nm)	none	9.21.04	0.17	1.22	14	Plot 2	1	21	Plot 2 high reflectance
Untransformed (350-1075nm)	none	6.16.04	0.16	0.71	15	none	1	236	none
Log R	none	9.21.04	0.11	1.22	14	Plot 2	1	4	Plot 2 high reflectance
Untransformed (350-1075nm)	none	6.06.05	0.04	1.86	13	Plots 6,14	1	224	Plot 6 high NO ₃ ; Plot 14 missing NO ₃
Log R	Sqrt NO ₃	9.21.04	0.03	0.43	15	none	1	none	none
Untransformed (350-1075nm)	none	7.19.04	0.27	2.64	15	none	1	none	none
Normalized spectra (R/R410)	none	8.24.04	0.53	1.70	15	none	1	none	none
Untransformed (350-1075nm)	none	6.29.04	0.75	1.26	12	Plots 3,12,14	1	none	Plots 3,12,14 missing NO ₃ data

Table 3.4.10. PLS-regression transformations tested on nitrate concentrations at the *Phragmites*-dominant site.

[illegible][illegible]

Table 3.4.11. PLS-regression for nitrate concentration at the *Phragmites*-absent (PA) site. r = regression coefficient, RMSEP = root mean square error of prediction, PCs = PLS-components

Spectra Transformations	NO ₃ Transformations	Date	r	RMSEP	n	Name of plots removed	PCs	# bands used	Comments
Norris 1 st Derivative	Log NO ₃	9.21.04	0.90	0.11	14	Plot 10	3	75	Plot 10 high NO ₃ conc
Transform 1/R	none	8.24.04	0.89	0.15	15	none	6	234	none
Absorbance Transformation	none	8.24.04	0.88	0.16	15	none	6	247	none
Normalized spectra (R/R410)	none	8.24.04	0.86	0.17	14	Plot 1	10	11	Plot 1 high reflectance
Golay 1 st Derivative	none	8.24.04	0.83	0.18	15	none	5	182	none
Golay 1 st Derivative, avg 5	none	8.24.04	0.83	0.18	15	none	5	182	none
Golay 2 nd Derivative	Log NO ₃	8.24.04	0.83	0.06	14	Plot 6	4	23	Plot 6 low NO ₃ conc.
Golay 1 st Derivative	none	9.21.04	0.83	0.23	14	Plot 10	2	25	Plot 10 high NO ₃ conc
Norris 1 st Derivative	none	8.24.04	0.79	0.20	15	none	3	181	none
Golay 2 nd Derivative, avg 10	none	8.24.04	0.77	0.21	15	none	1	3	none
Golay 2 nd Derivative	Log NO ₃	9.21.04	0.77	0.18	14	Plot 10	3	17	Plot 10 high NO ₃ conc
Norris 1 st Derivative	Log NO ₃	8.02.05	0.76	0.24	14	Plot 12	4	160	Plot 12 missing NO ₃ data
Norris 1 st Derivative, avg 10	none	8.24.04	0.76	0.21	15	none	9	206	none
Transform 1/R	none	9.21.04	0.76	0.27	13	Plots 10,13	2	17	Plot 10 high NO ₃ ; Plot 13 low reflect.
Untransformed (350-1075nm)	none	6.29.04	0.75	0.38	12	Plots 2,3,10	2	14	Plot 2 missing NO ₃ ; Plots 3,10 high NO ₃
Norris 1 st Derivative	Log NO ₃	8.24.04	0.75	0.07	14	Plot 6	3	134	Plot 6 low NO ₃ conc.
Golay 1 st Derivative, avg 10	none	8.24.04	0.74	0.24	15	none	6	252	none
Golay 2 nd Derivative	none	9.21.04	0.74	0.27	14	Plot 10	1	16	Plot 10 high NO ₃ conc
Kubelka-Munk Transformation	none	8.24.04	0.73	0.22	15	none	2	3	none
Norris 1 st Derivative, avg 5	none	8.24.04	0.72	0.23	15	none	3	174	none

Spectra Transformations	NO ₃ Transformations	Date	r	RMSEP	n	Name of plots removed	PCs	# bands used	Comments
Log R	Sqrt NO₃	8.24.04	0.71	0.17	14	Plot 1	8	191	Plot 1 high reflectance
Truncated spectra (400-950nm)	none	6.06.05	0.69	1.61	12	Plots 3,12,15	4	13	Plot 3 high reflect; Plots 12, 15 missing NO ₃
Untransformed (350-1075nm)	none	8.02.05	0.66	0.28	13	Plots 11,12	1	23	Plot 11 high NO ₃ conc; Plot 12 missing NO ₃
Transform 1/R	Arcsine sqrt (NO₃)	8.24.04	0.60	0.02	15	none	2	14	none
Truncated spectra (400-950nm)	none	9.21.04	0.60	0.33	14	Plot 10	3	5	Plot 10 high NO ₃ conc
Golay 2nd Derivative	Log NO₃	7.19.04	0.57	0.16	14	Plot 2	2	11	Plot 2 low NO ₃ conc
MSC Transformation	none	8.24.04	0.56	0.28	15	none	2	37	none
Untransformed (350-1075nm)	none	9.21.04	0.56	0.35	14	Plot 10	3	167	Plot 10 high NO ₃ conc
Untransformed (350-1075nm)	none	6.16.04	0.53	0.78	13	Plots 2, 5	2	12	Plots 2,5 missing NO ₃ data
Truncated spectra, random test	none	8.24.04	0.53	0.31	10	none	1	none	Remainder used in calibration
Untransformed (350-1075nm)	none	7.19.04	0.51	0.39	14	Plot 2	1	462	Plot 2 low NO ₃ conc
Untransformed (350-1075nm)	none	8.24.04	0.51	0.31	14	Plot 1	3	229	Plot 1 high reflectance
Log R	Sqrt NO₃	9.21.04	0.51	0.22	14	Plot 10	3	52	Plot 10 high NO ₃ conc
Truncated spectra, manual test	none	8.24.04	0.50	0.42	10	none	1	none	Remainder used in calibration
Truncated spectra (400-950nm)	Arcsine sqrt (NO₃)	8.24.04	0.43	0.02	14	Plot 1	6	none	Plot 1 high reflectance
Truncated spectra (400-950nm)	4th root NO₃	8.24.04	0.37	0.12	14	Plot 1	6	none	Plot 1 high reflectance
Truncated spectra (400-950nm)	Sqrt NO₃	8.24.04	0.31	0.21	15	none	2	none	none
Truncated spectra (400-950nm)	Log NO₃	8.24.04	0.20	0.29	15	none	2	none	none
Untransformed (350-1075nm)	none	6.06.05	0.06	-	12	Plots 3,12,15	1	none	Plot 3 high reflect; Plots 12, 15 missing NO ₃
Log R	none	9.21.04	0.31	0.59	14	Plots 10	1	none	Plot 10 high NO ₃ conc

Table 3.4.12. PLS-regression transformations tested on nitrate concentrations at the *Phragmites*-absent site.

[illegible]

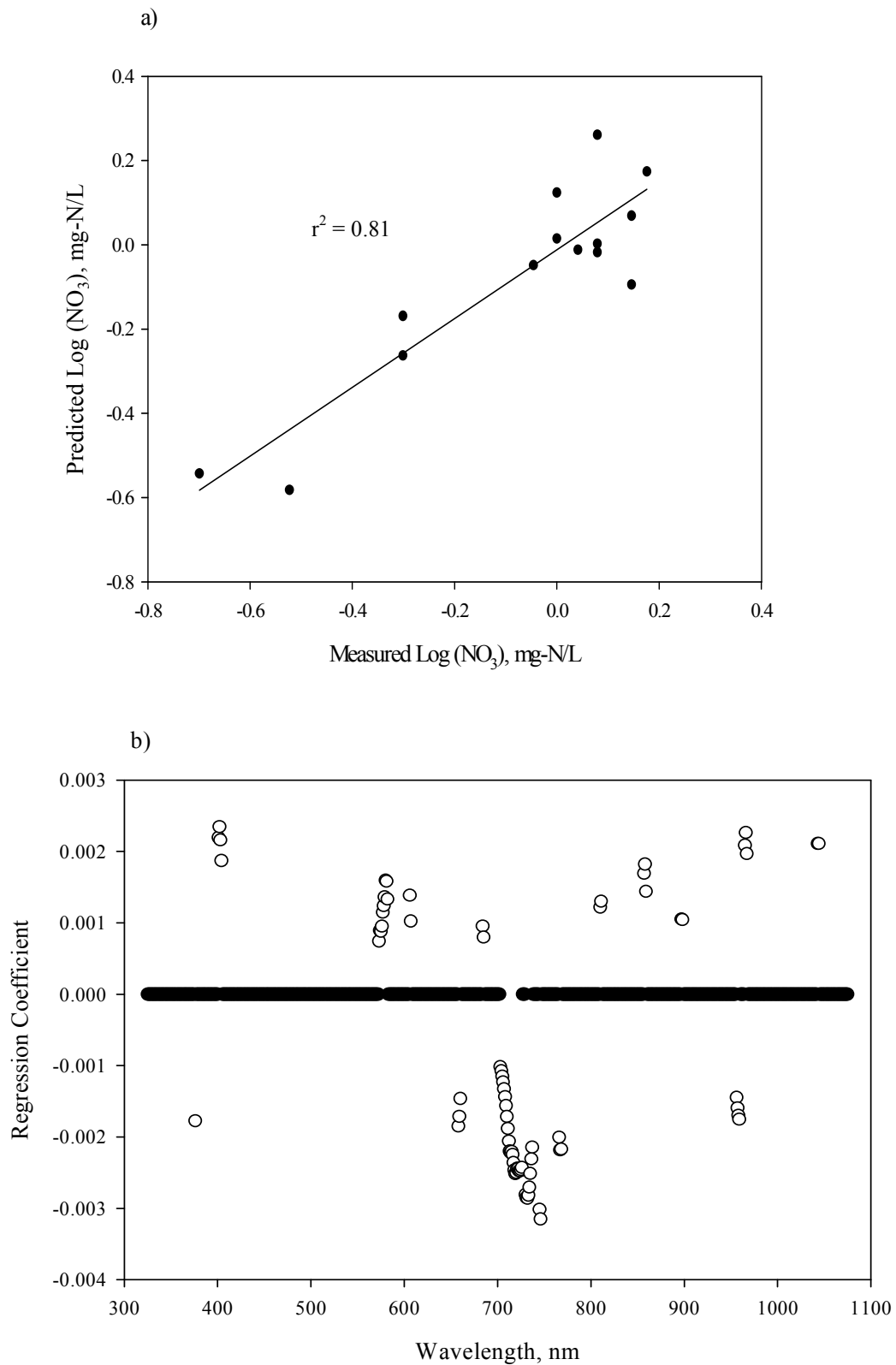


Figure 3.4.11. (a) Predicted vs measured log of nitrate PLS-regression at the *Phragmites*-absent site which used 75 spectral bands of the 1st derivative of the 9/21/04 reflectance to form three PLS-components with $r = 0.90$ and RMSEP of 0.11. (b) Loading plot showing significant spectral bands used in the regression as open circles.

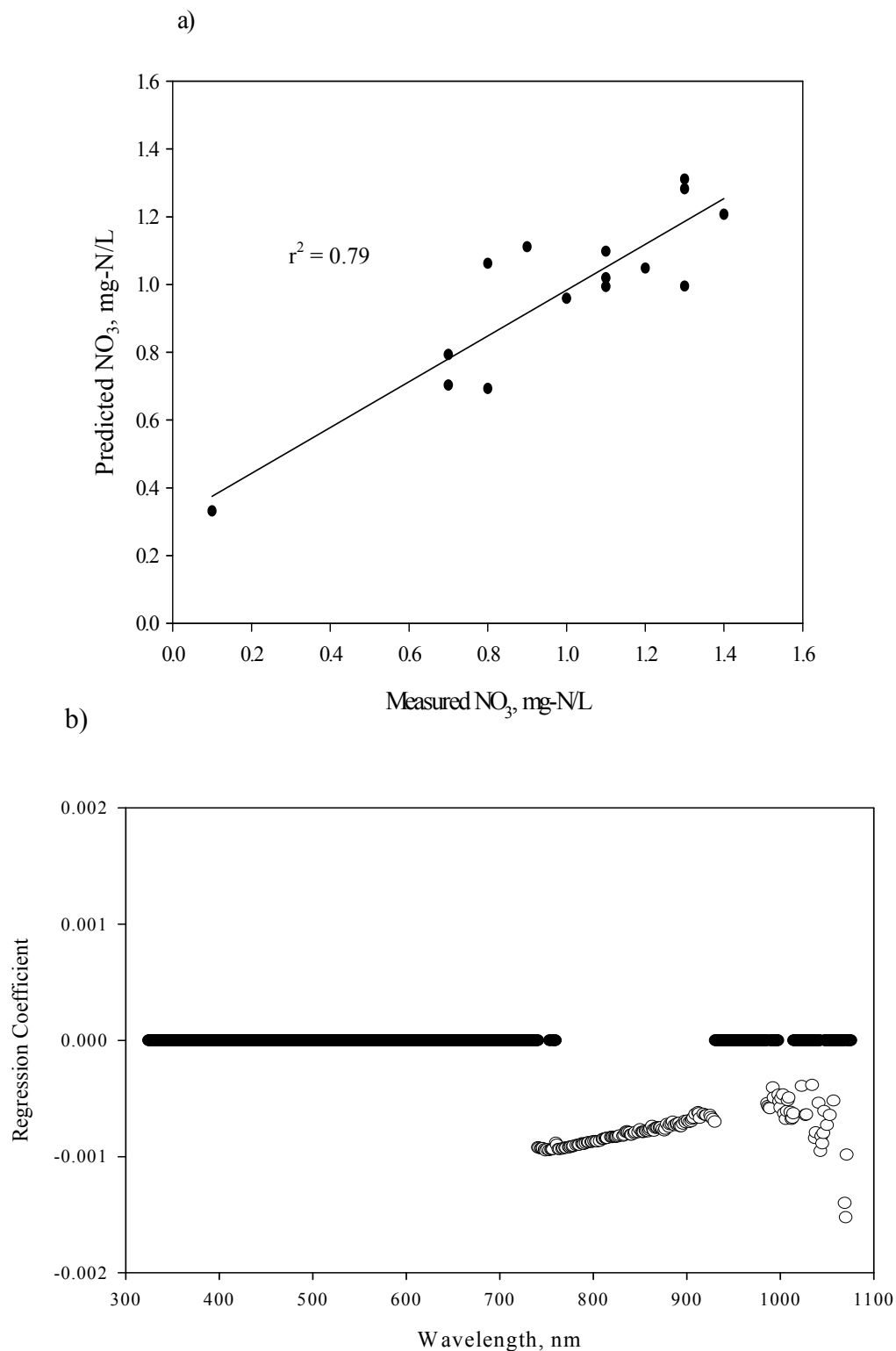


Figure 3.4.12. (a) Predicted vs measured nitrate PLS-regression of the *Phragmites*-absent site which used 234 spectral bands of the inverse reflectance from 8/24/04 to form six PLS-components with $r = 0.89$ and RMSEP of 0.15. (b) Loading plot showing significant spectral bands used in the regression as open circles.

Spectral bands used in the PLS models for the two marsh sites, the *Phragmites*-dominant site, and the *Phragmites*-absent site were examined for reflectance trends. A summary of spectral bands used in PLS models at the two marsh sites shows that several regressions used bands in the visible green, red-edge, and near-infrared (Figure 3.4.13a). Ten or more regressions used only spectral bands in the green (530-590 nm) (Figure 3.4.13b).

At the *Phragmites*-dominant site, many regressions had significant spectral bands in throughout the visible and near-infrared, but only bands in the blue and green range (500-600 nm) were significant for ten or more regressions (Figure 3.4.14).

For the *Phragmites*-absent site, regressions used several spectral bands between 500-600 nm, as well as the red-edge (700-720nm), but the spectral bands used in ten or more regressions included only the red-edge spectral bands and a few spectral bands in the blue and green wavebands (Figure 3.4.15). A list of the illustrated bands, significant to ten or more regressions for both sites, can be found in the Appendix.

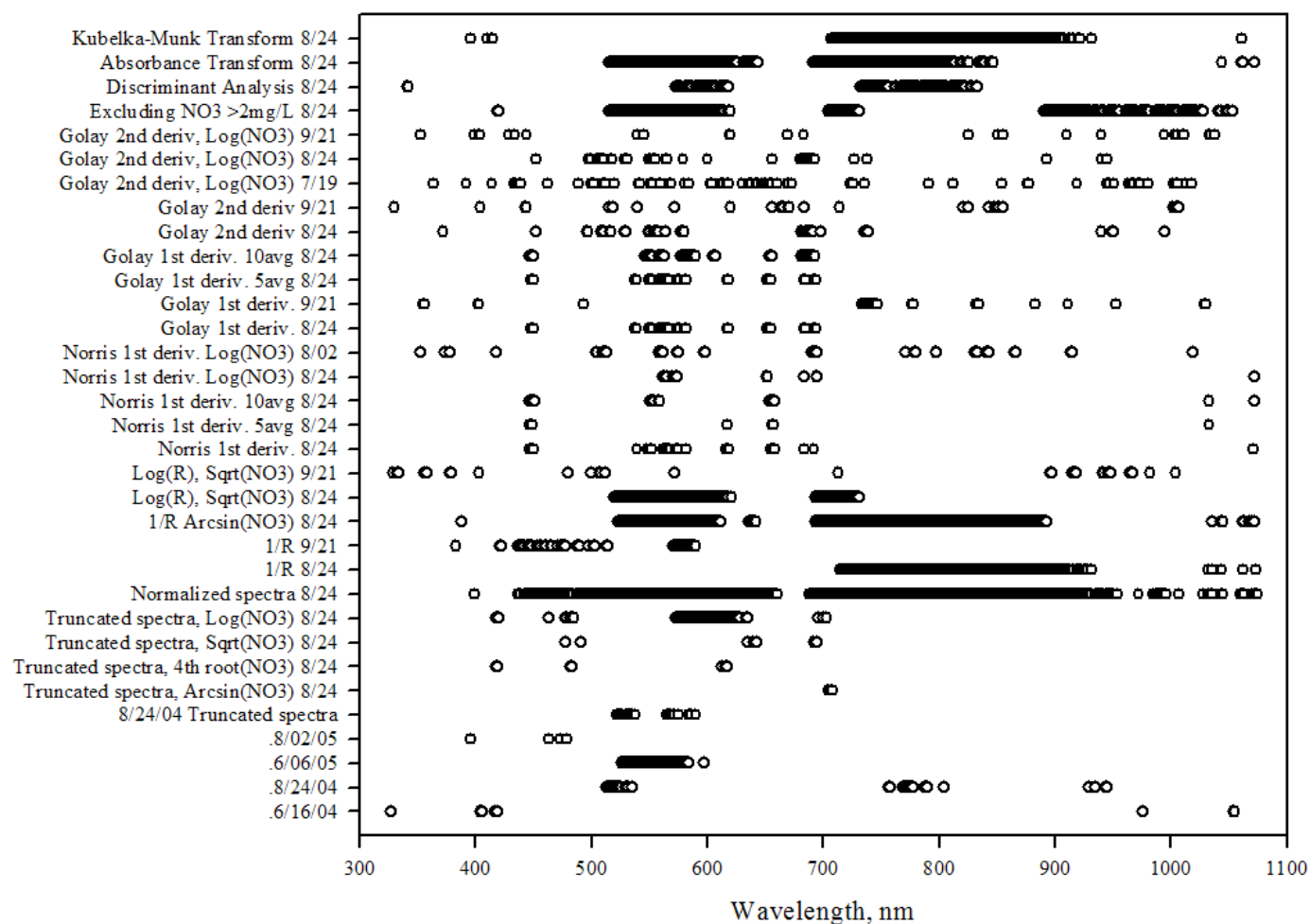


Figure 3.4.13a. Significant spectral bands for NO_3 according to PLS-regressions at the two marsh sites.

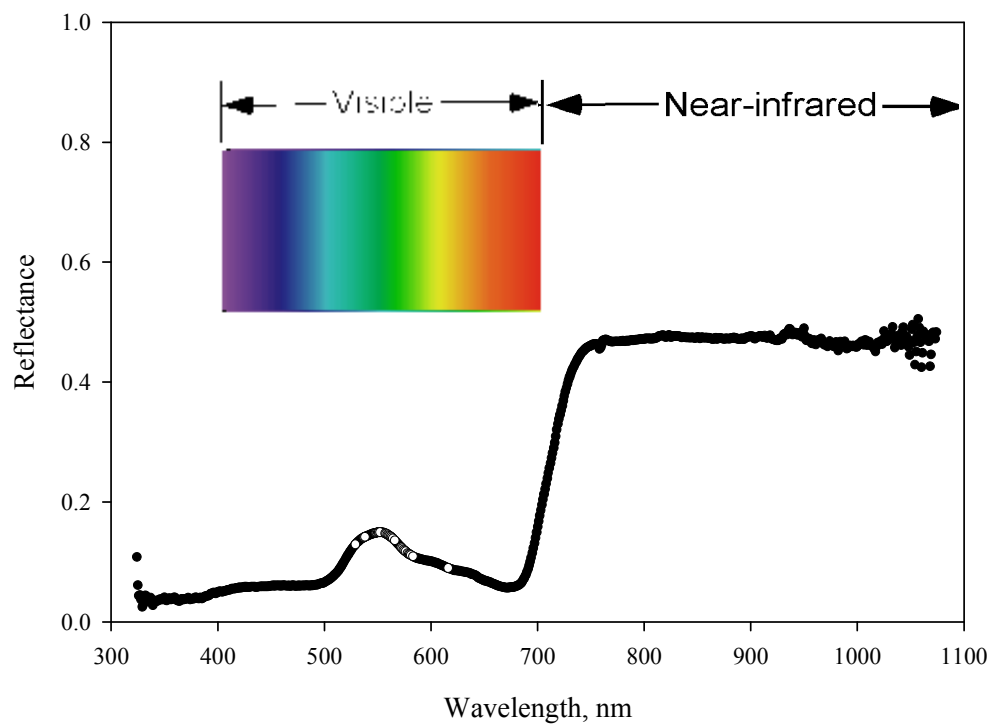


Figure 3.4.13b. Spectral bands significant for ten or more nitrate regressions at the two marsh sites are indicated by an open circle.

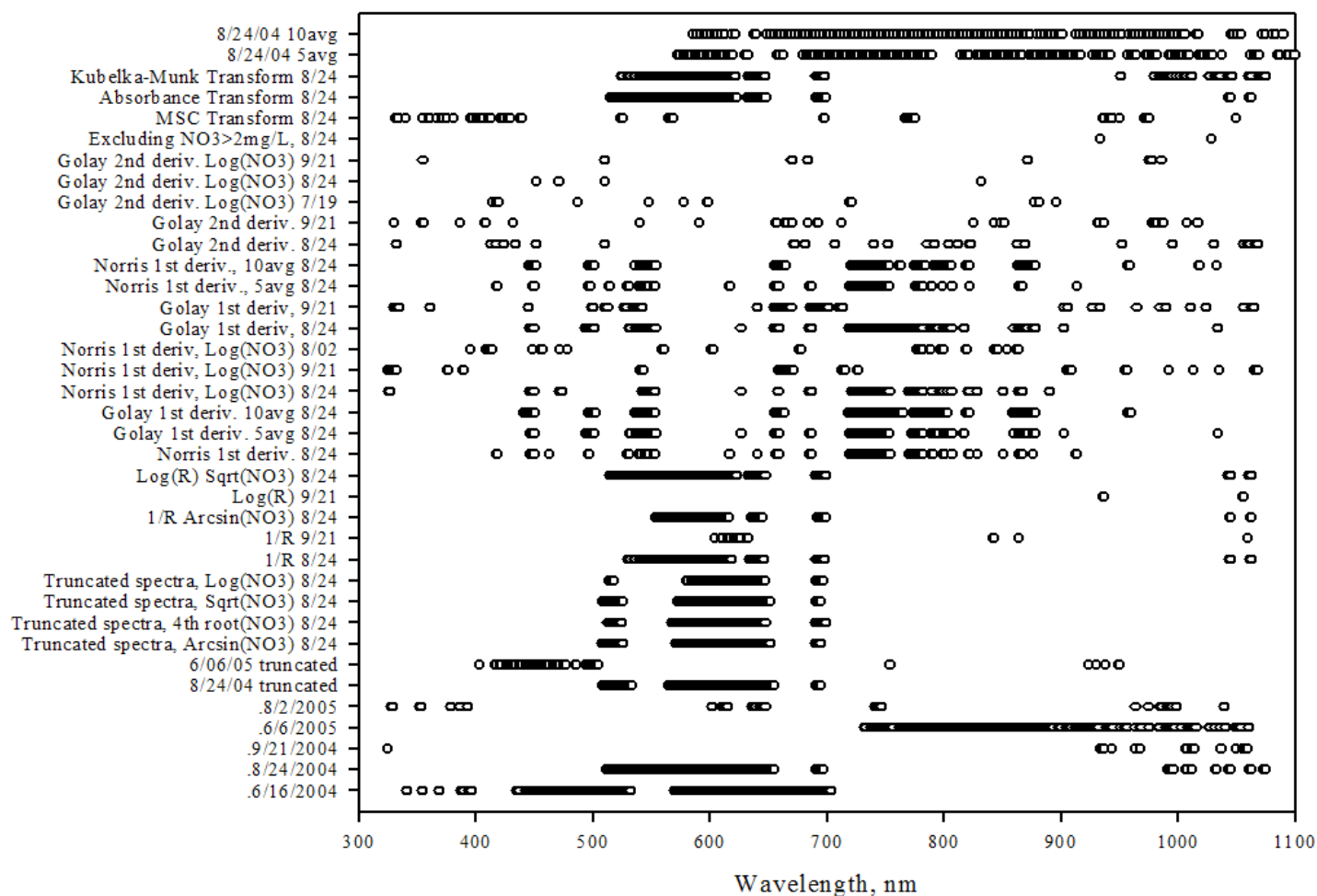


Figure 3.4.14a. Significant spectral bands for NO_3 according to PLS-regressions at the *Phragmites*-dominant site.

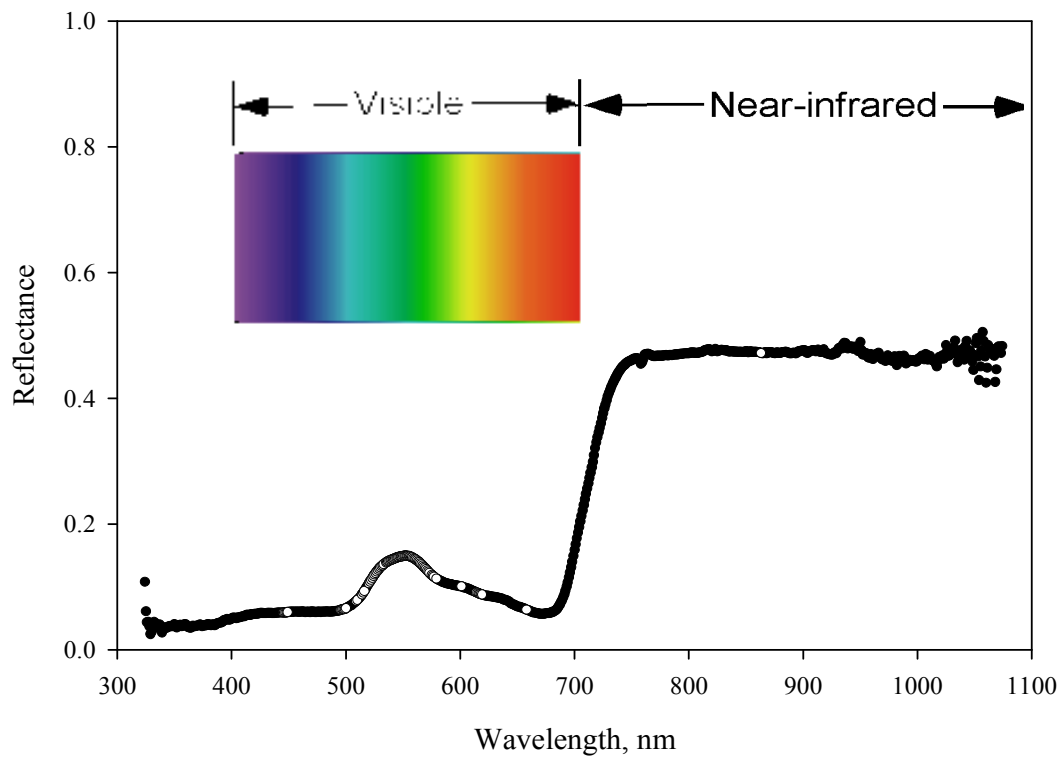


Figure 3.4.14b. Spectral bands significant for ten or more regressions for nitrate at the *Phragmites*-dominant site are indicated by an open circle.

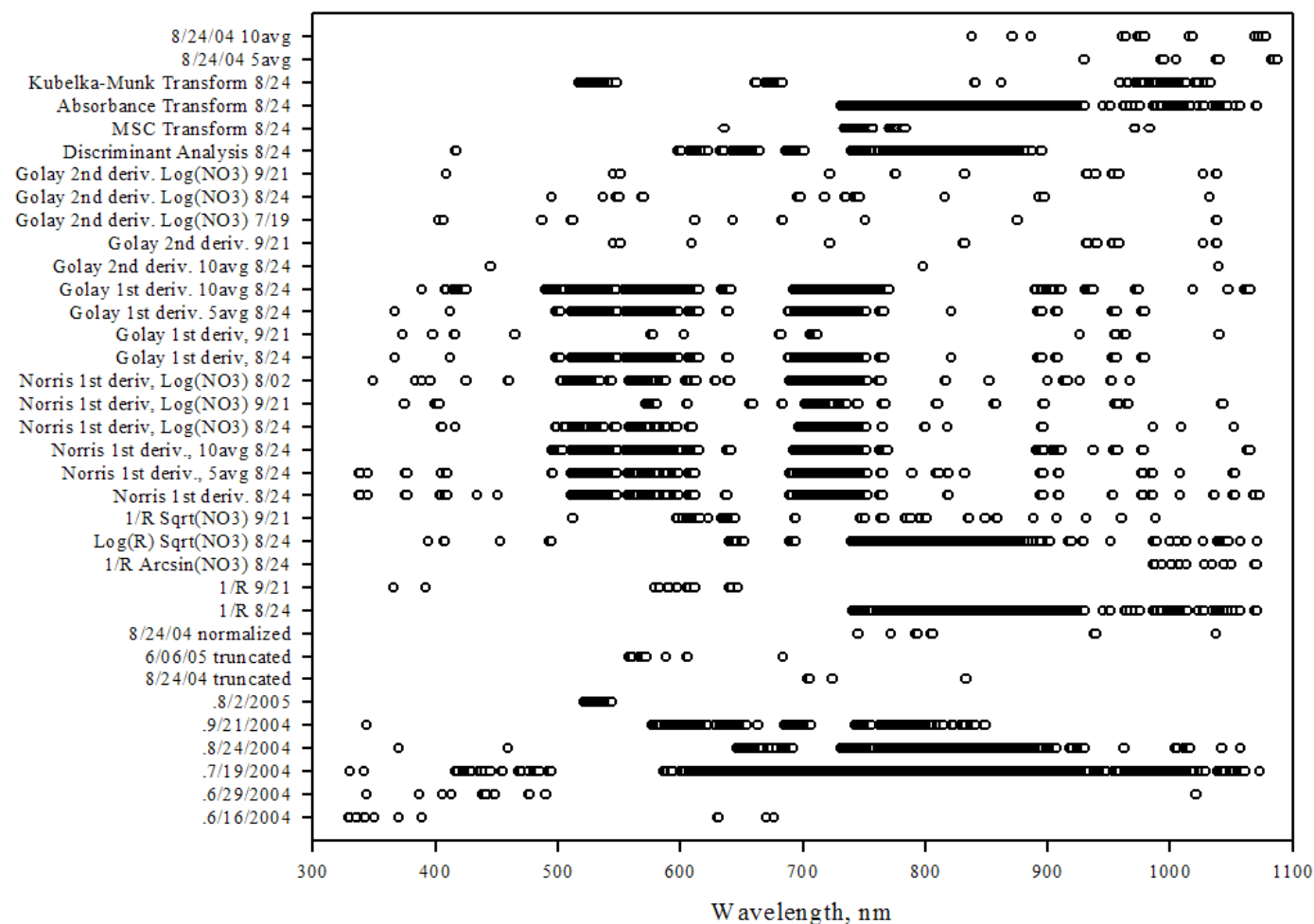


Figure 3.4.15a. Significant spectral bands for NO_3 according to PLS-regressions at the *Phragmites*-absent site.

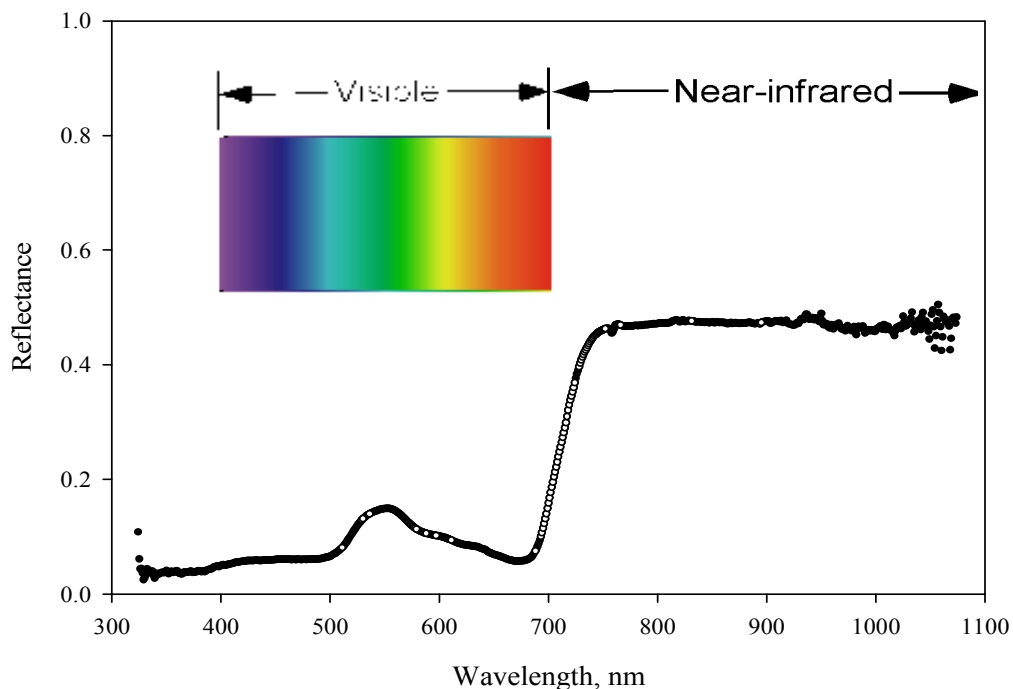


Figure 3.4.15b. Spectral bands significant for ten or more regressions for nitrate at the *Phragmites*-absent site are indicated by an open circle.

PLS Models of Total Nitrogen

Spectroradiometric PLS models were able to predict total nitrogen concentrations in sub-surface marsh water at both the *Phragmites*-dominant and *Phragmites*-absent sites. Models at both sites used transformations of the canopy reflectance (1st and 2nd derivatives) and nitrogen concentration (Log) to quantify nitrogen concentrations during July and August (Tables 3.4.13 and 3.4.15). At the *Phragmites*-dominant site, the highest correlated model used the log of nitrogen concentration on 6/29/04 and 33 spectral bands of 1st derivative transformed reflectance to form three PLS-components with RMSEP of 0.09 and $R^2 = 0.88$ (Figure 3.4.16). Log nitrogen concentrations were uniformly distributed and had discrete values due to the Hach Digestion procedure used to analyze total Kjeldahl nitrogen.

Table 3.4.13. PLS-regression for total nitrogen at the *Phragmites*-dominant (PD) site. r = regression coefficient, RMSEP = root mean square error of prediction, PCs = PLS-components

Spectra Transformations	TKN Transformations	Date	r	RMSEP	n	Name of plots removed	PCs	Number of sig. spectral bands	Comments
Norris 1 st Derivative	Log TKN	6.29.04	0.94	0.09	12	Plots 1,4,12	3	33	Plots 4,12 missing TKN; Plot 1 high TKN
Norris 1 st Derivative	none	7.19.04	0.93	2.82	14	Plot 5	5	28	Plot 5 high reflectance
Norris 1 st Derivative	Log TKN	7.19.04	0.93	0.10	14	Plot 5	6	34	Plot 5 high reflectance
Golay 2 nd Derivative, avg 10	Log TKN	6.29.04	0.91	0.11	12	Plots 1,4,12	1	31	Plots 4,12 missing TKN; Plot 1 high TKN
Golay 2 nd Derivative, avg 10	none	6.29.04	0.88	3.27	12	Plots 1,4,12	1	46	Plots 4,12 missing TKN; Plot 1 high TKN
Golay 2 nd Derivative, avg 10	Log TKN	7.19.04	0.87	0.14	14	Plot 5	1	9	Plot 5 high reflectance
Untransformed	Excluding TKN >15	7.19.04	0.87	4.04	11	Plots 1,5,6,13	3	74	Plots 1,6,13 high TKN; Plot 5 high reflect.
Golay 1 st Derivative	none	6.29.04	0.81	4.38	12	Plots 1,4,12	5	28	Plots 4,12 missing TKN; Plot 1 high TKN
Untransformed (350-1075nm)	none	7.19.04	0.79	4.78	14	Plot 5	5	124	Plot 5 high reflectance
Golay 2 nd Derivative, avg 10	none	7.19.04	0.78	4.71	14	Plot 5	1	64	Plot 5 high reflectance
Kubelka-Munk Transform	none	7.19.04	0.78	5.17	14	Plot 5	4	159	Plot 5 high reflectance
Golay 1 st Derivative	none	7.19.04	0.76	5.06	14	Plot 5	6	212	Plot 5 high reflectance
Transform 1/R	none	7.19.04	0.68	5.78	15	none	4	130	none
Absorbance Transformation	none	7.19.04	0.66	5.66	14	Plot 5	3	190	Plot 5 high reflectance
Transform 1/R	Arcsine sqrt (TKN)	7.19.04	0.65	0.09	14	Plot 5	3	122	Plot 5 high reflectance
Log R	none	7.19.04	0.63	5.81	14	Plot 5	3	181	Plot 5 high reflectance
Log R	Sqrt TKN	7.19.04	0.63	0.84	14	Plot 5	3	189	Plot 5 high reflectance
MSC Transformation	none	7.19.04	0.63	5.89	14	Plot 5	3	194	Plot 5 high reflectance

Spectra Transformations	TKN Transformations	Date	r	RMSEP	n	Name of plots removed	PCs	Number of sig. spectral bands	Comments
Truncated spectra (400-950nm)	none	7.19.04	0.62	6.10	14	Plot 5	3	99	Plot 5 high reflectance
Truncated spectra (400-950nm)	Log TKN	7.19.04	0.62	0.24	14	Plot 5	3	184	Plot 5 high reflectance
Truncated spectra (400-950nm)	Arcsine sqrt (TKN)	7.19.04	0.61	0.09	14	Plot 5	5	158	Plot 5 high reflectance
Truncated spectra (400-950nm)	4th root TKN	7.19.04	0.61	0.25	14	Plot 5	3	117	Plot 5 high reflectance
Truncated spectra (400-950nm)	Sqrt TKN	7.19.04	0.56	0.90	14	Plot 5	3	156	Plot 5 high reflectance
Normalized spectra (R/R410)	none	7.19.04	0.50	6.80	14	Plot 5	3	172	Plot 5 high reflectance
Truncated spectra, random test	none	8.24.04	0.49	17.10	5	none	1	none	none
Truncated spectra, manual test	none	8.24.04	0.48	32.60	5	none	1	none	none
Untransformed (350-1075nm)	none	6.29.04	0.32	7.32	11	Plots 1,4,8,12	3	27	Plots 4,12 missing TKN; Plot 1 high TKN; Plot 8 low reflect.
PLS2 Untransformed	TKN, TP	7.19.04	0.18	8.07	14	Plot 5	1	none	Plot 5 high reflectance
Golay 2 nd Derivative, avg 10	Log TKN	8.24.04	0.16	0.16	14	Plot 1	1	none	Plot 1 high TKN conc
Untransformed (350-1075nm)	none	6.16.04	0.07	7.07	14	Plot 1	1	145	Plot 1 high TKN conc
Norris 1 st Derivative	Log TKN	8.24.04	-0.01	0.31	15	none	1	none	none
Normalized spectra (R/R410)	none	8.24.04	-0.04	28.32	14	Plot 6	1	22	Plot 6 high reflectance
Golay 1 st Derivative	none	8.24.04	-0.06	29.79	15	none	1	none	none
Norris 1 st Derivative	none	8.24.04	-0.08	29.72	15	none	1	none	none
Untransformed (350-1075nm)	none	8.24.04	-0.09	30.49	14	Plot 6	1	none	Plot 6 high reflectance
Truncated spectra (400-950nm)	none	8.24.04	-0.10	30.51	14	Plot 6	1	none	Plot 6 high reflectance
Untransformed (350-1075nm)	none	9.21.04	-0.14	25.92	15	none	1	none	none
Transform 1/R	none	8.24.04	-0.17	26.64	15	none	1	none	none

Table 3.4.14. PLS-regression transformations tested on TKN concentrations collected from the *Phragmites*-dominant site.

[illegible][illegible]

Table 3.4.15. PLS-regression for total nitrogen at the *Phragmites*-absent (PA) site. r = regression coefficient, RMSEP = root mean square error of prediction, PCs = PLS-components

Spectra Transformations	TKN Transformations	Date	r	RMSEP	n	Name of plots removed	PCs	# bands used	Comments
Golay 2 nd Derivative, avg 10	none	8.24.04	0.98	0.83	13	Plots 12,14	4	6	Plots 12,14 low TKN conc.
Norris 1 st Derivative	Log TKN	8.24.04	0.96	0.04	13	Plots 12,14	7	21	Plots 12,14 low TKN conc.
Golay 2 nd Derivative	none	7.19.04	0.91	1.45	14	Plot 2	1	31	Plot 2 high TKN conc.
Norris 1 st Derivative	none	8.24.04	0.90	1.62	13	Plots 12,14	2	3	Plots 12,14 low TKN conc.
Golay 1 st Derivative	none	9.21.04	0.87	2.88	13	Plots 10,13	5	20	Plot 10 high reflect; Plot 13 high TKN
Golay 2 nd Derivative	Log TKN	8.24.04	0.79	0.08	13	Plots 12,14	1	45	Plots 12,14 low TKN conc.
Truncated spectra, manual test set	none	8.24.04	0.62	3.28	5	none	1	none	none
Norris 1 st Derivative, avg 5	none	8.24.04	0.60	3.12	13	Plots 12,14	9	60	Plots 12,14 low TKN conc.
Golay 2 nd Derivative	none	9.21.04	0.58	5.04	14	Plot 12	1	9	Plot 12 low reflectance
Untransformed (350-1075nm)	none	8.24.04	0.43	4.13	14	Plot 14	2	36	Plot 14 low TKN conc.
Norris 1 st Derivative	Log TKN	9.21.04	0.43	0.21	13	Plots 10,13	1	5	Plot 10 high reflect; Plot 13 high TKN
Truncated spectra (400-950nm)	none	8.24.04	0.42	4.07	14	Plot 14	1	9	Plot 14 low TKN conc.
Transform 1/R	none	8.24.04	0.42	3.54	13	Plots 12,14	1	1	Plots 12,14 low TKN conc.
Golay 1 st Derivative	none	8.24.04	0.42	3.62	13	Plots 12,14	2	85	Plots 12,14 low TKN conc.
Golay 1 st Derivative, avg 5	none	8.24.04	0.42	3.62	13	Plots 12,14	2	85	Plots 12,14 low TKN conc.
Absorbance Transformation	none	8.24.04	0.42	3.55	13	Plots 12,14	1	1	Plots 12,14 low TKN conc.
Truncated spectra, random test set	none	8.24.04	0.41	3.37	5	none	1	none	none
Transform 1/R	Arcsine sqrt (TKN)	8.24.04	0.39	0.05	13	Plots 12,14	1	2	Plots 12,14 low TKN conc.
Normalized spectra (R/R410)	none	8.24.04	0.37	4.73	13	Plots 1,6	1	123	Plot 1 high reflect; Plot 6 low reflect

Spectra Transformations	TKN Transformations	Date	r	RMSEP	n	Name of plots removed	PCs	# bands used	Comments
Norris 1 st Derivative, avg 10	none	8.24.04	0.37	3.61	13	Plots 12,14	1	4	Plots 12,14 low TKN conc.
Untransformed (350-1075nm)	none	6.29.04	0.35	2.62	14	Plot 2	1	5	Plot 2 high TKN conc.
Log R	none	6.29.04	0.34	2.58	14	Plot 12	2	107	Plot 12 low TKN conc.
Log R	Square root TKN	8.24.04	0.27	0.67	14	Plot 14	1	41	Plot 14 low TKN conc.
Untransformed (350-1075nm)	none	6.16.04	0.22	2.92	13	Plots 2,5	3	13	Plots 2,5 missing TKN
Truncated spectra (400-950nm)	Arcsine sqrt (TKN)	8.24.04	0.20	0.07	14	Plot 14	1	5	Plot 14 low TKN conc.
Truncated spectra (400-950nm)	Square root TKN	8.24.04	0.20	0.67	14	Plot 14	1	5	Plot 14 low TKN conc.
Truncated spectra (400-950nm)	4th root TKN	8.24.04	0.17	0.19	14	Plot 14	1	6	Plot 14 low TKN conc.
Golay 1 st Derivative, avg 10	none	8.24.04	0.15	4.10	13	Plots 12,14	1	115	Plots 12,14 low TKN conc.
Truncated spectra (400-950nm)	Log TKN	8.24.04	0.14	0.19	14	Plot 14	1	5	Plot 14 low TKN conc.
Kubelka-Munk Transformation	none	8.24.04	0.14	4.56	14	Plot 14	1	none	Plot 14 low TKN conc.
Untransformed (350-1075nm)	none	7.19.04	0.12	7.16	14	Plot 6	1	none	Plot 6 high reflectance
Golay 2 nd Derivative	Log TKN	9.21.04	0.12	0.25	14	Plot 12	1	2	Plot 12 low reflectance
MSC Transformation	none	8.24.04	0.03	5.26	13	Plots 12,14	1	none	Plots 12,14 low TKN conc.
Log R	Square root TKN	6.29.04	0.02	0.56	15	none	1	127	none
Transform 1/R	none	9.21.04	-0.26	6.14	14	Plot 13	1	none	Plot 13 high TKN conc.
Untransformed (350-1075nm)	none	9.21.04	-0.53	7.28	15	none	1	none	none
Truncated spectra (400-950nm)	none	9.21.05	-0.65	7.06	15	none	1	none	none

Table 3.4.16. PLS-regressions transformations performed on TKN concentrations collected from the *Phragmites*-absent site.

	Untransformed (350-1075 nm)	Truncated spectra (400-950 nm)	Truncated, Arcsine sqrt (TKN)	Truncated, 4th root TKN	Truncated Sqrt (TKN)	Truncated Log ₁₀ TKN	Truncated Manual test set	Truncated Random test set	Normalized spectra	Transform 1/R	Transform 1/R, Arcsine sqrt (TKN)	Log R	Log R, Sqrt (TKN)	PLS2
6/16/2004	X													
6/29/2004	X											X	X	
7/19/2004	X													
8/24/2004	X	X	X	X	X	X	X	X	X	X	X		X	X
9/21/2004	X	X								X				

	Norris 1st Derivative	Norris 1st Derivative, avg 5	Norris 1st Derivative, avg 10	Norris 1st Derivative, Log TKN	Golay 1st Derivative	Golay 1st Derivative, avg 5	Golay 1st Derivative, avg 10	Golay 2nd Derivative	Golay 2nd Deriv, Log (TKN)	Discriminant Analysis	MSC Transform	Absorbance Transform	Kubelka- Munk Transform	Avg 5 wavelengths	Avg 10 wavelengths
6/16/2004															
6/29/2004															
7/19/2004								X							
8/24/2004	X	X	X	X	X	X	X	X	X	X	X	X	X	X	X
9/21/2004				X	X			X	X						

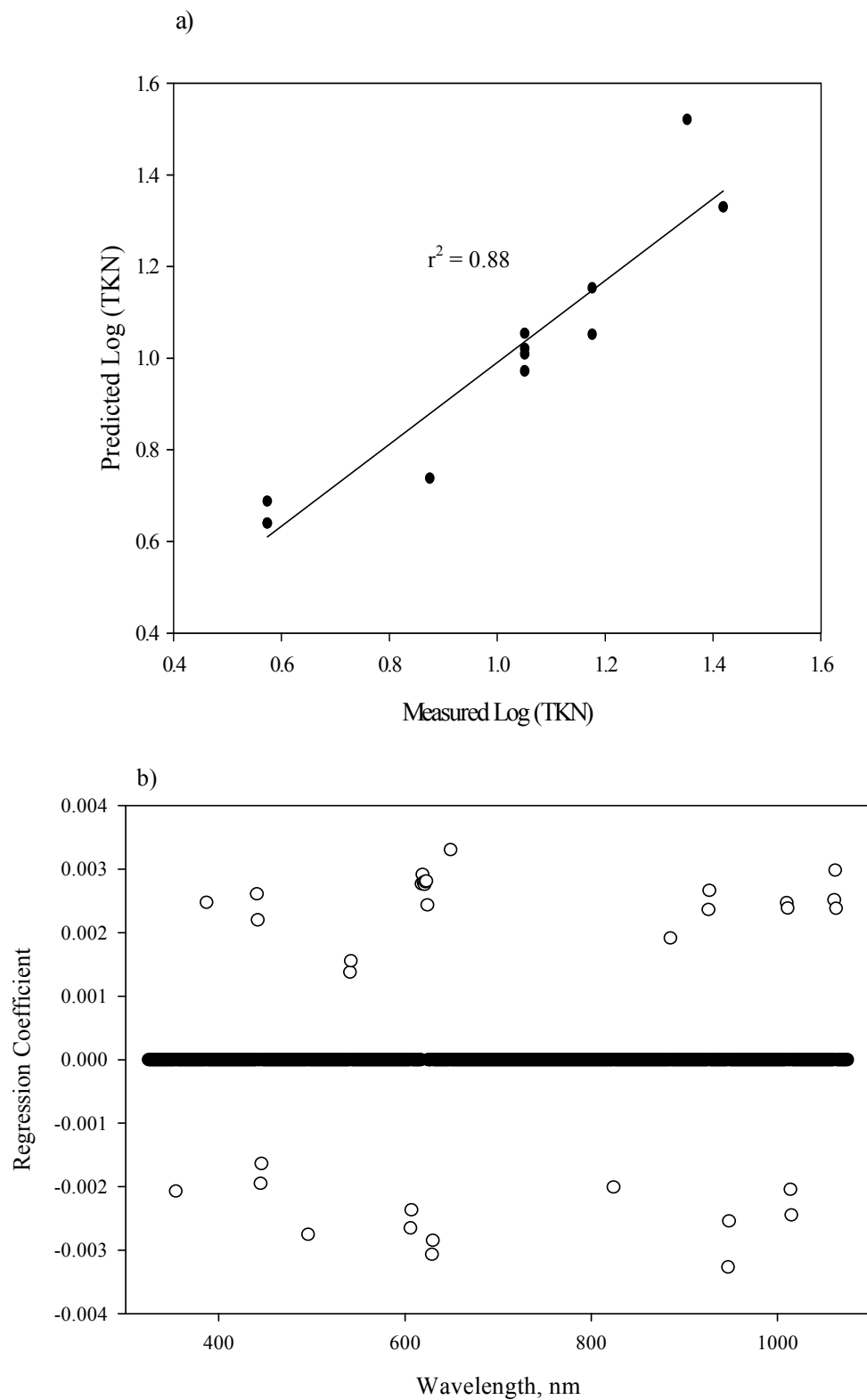


Figure 3.4.16. (a) Predicted vs measured log of total nitrogen PLS-regression at the *Phragmites*-dominant site which used 33 spectral bands of the 1st derivative of the 6/29/04 reflectance to form three PLS-components with $r = 0.94$ and RMSEP of 0.09. (b) Loading plot showing significant spectral bands used in the regression as open circles.

At the *Phragmites*-absent site, the best PLS model used 115 spectral bands of 2nd derivative transformed reflectance that were combined into four PLS-components with RMSEP of 0.83 and $R^2 = 0.96$ (Figure 3.4.17).

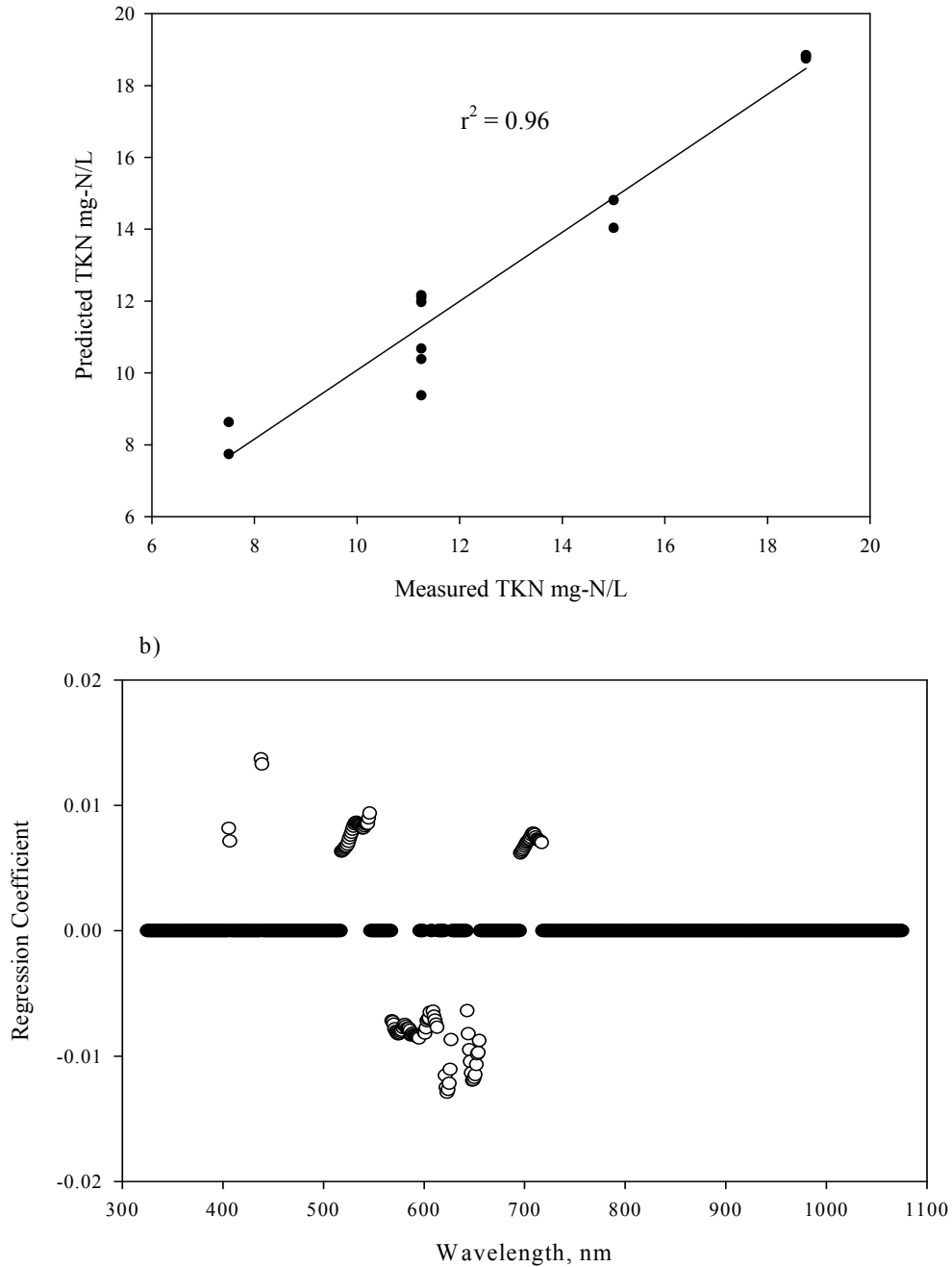


Figure 3.4.17. (a) Predicted vs measured total nitrogen PLS-regression at the *Phragmites*-absent site which used 115 spectral bands of the 2nd derivative of the 8/24/04 reflectance to form four PLS-components with $r = 0.98$ and RMSEP of 0.83. (b) Loading plot showing significant spectral bands used in the regression as open circles.

Spectral bands used in the PLS models are summarized according to regression transformations for the *Phragmites*-dominant and *Phragmites*-absent sites (Figures 3.4.18 and 3.4.19, respectively). At the *Phragmites*-dominant site several models used similar spectral bands in the blue (420 – 510 nm), green (520 – 600 nm), and red-edge (700 – 710 nm), as Figure 3.4.18b further illustrates by highlighting spectral bands used in ten or more regressions. At the *Phragmites*-absent site, spectral bands in the green and red-edge were used in ten or more regressions (Figure 3.4.19). A list of the illustrated bands, significant to ten or more regressions, can be found in the Appendix.

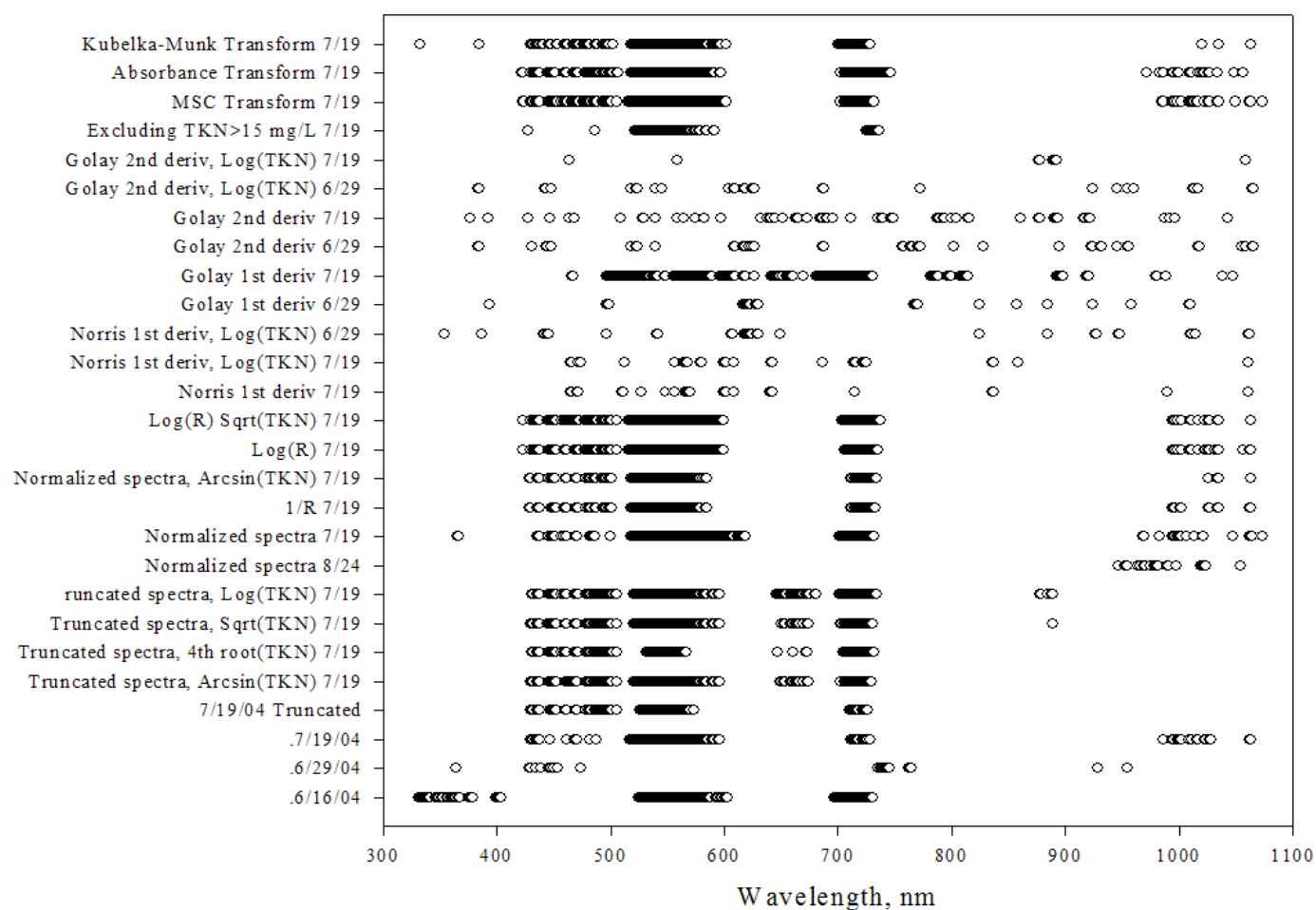


Figure 3.4.18a. Significant spectral bands for total nitrogen according to PLS-regressions at the *Phragmites*-dominant site.

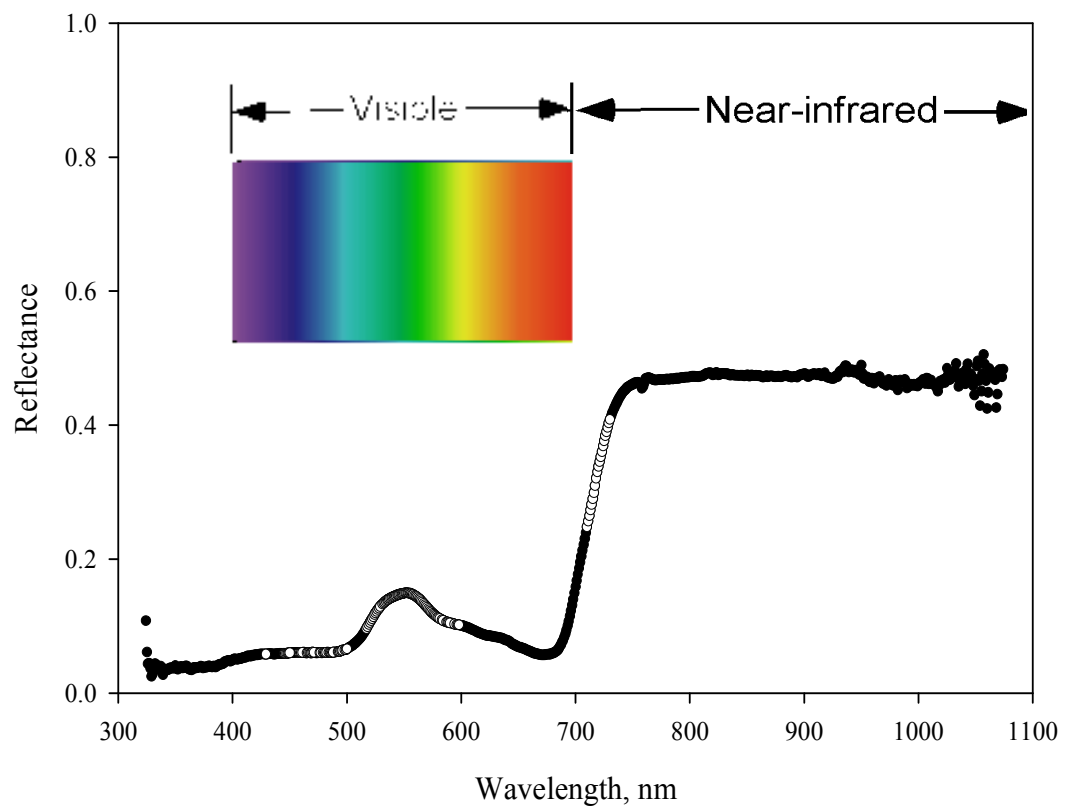


Figure 3.4.18b. Spectral bands significant for ten or more regressions for total nitrogen at the *Phragmites*-dominant site are indicated by an open circle.

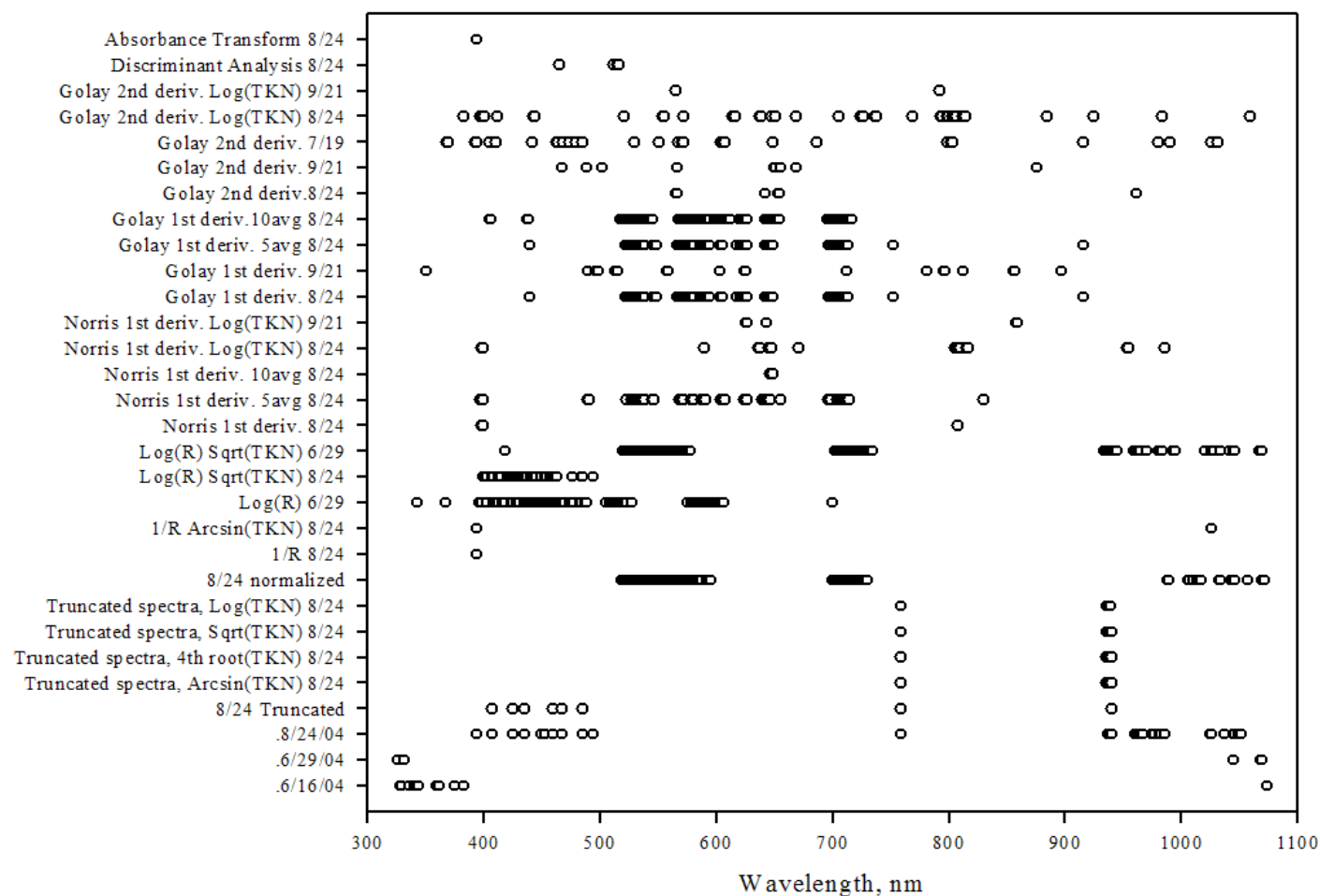


Figure 3.4.19a. Significant spectral bands for total nitrogen according to PLS-regressions at the *Phragmites*-absent site.

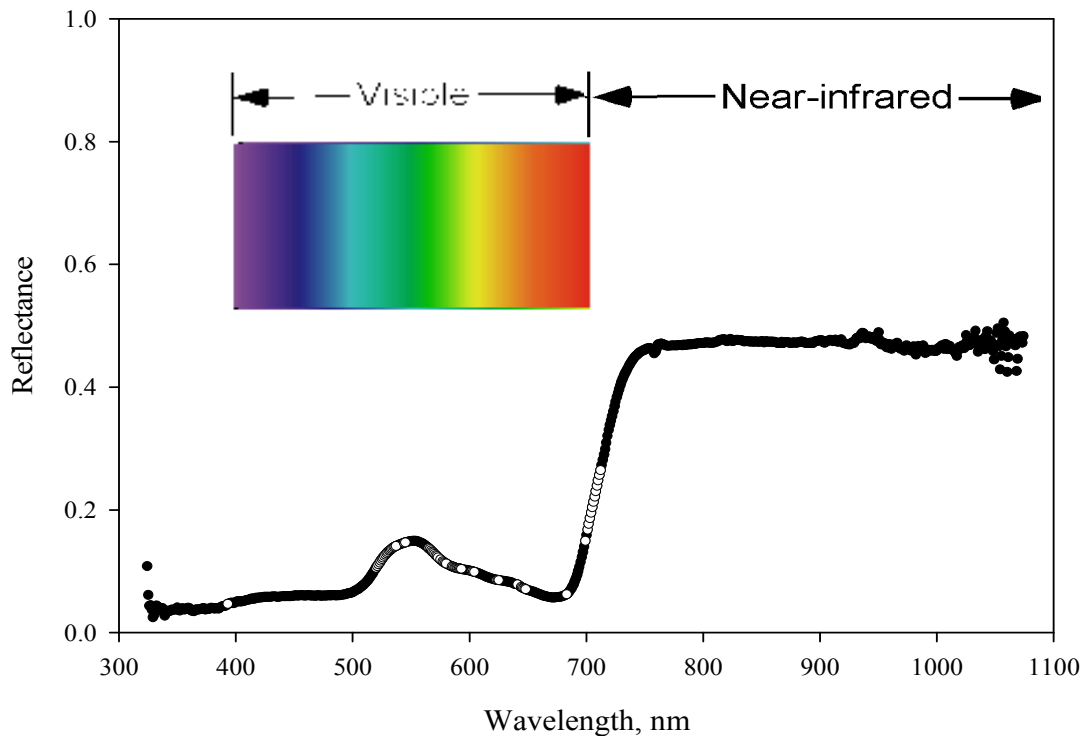


Figure 3.4.19b. Spectral bands significant for ten or more regressions for total nitrogen at the *Phragmites*-absent site are indicated by an open circle.

PLS Models of Total Phosphorus

PLS models at the *Phragmites*-dominant site were very successful at predicting total phosphorus concentrations, particularly during August and September of both years using the 1st and 2nd derivative of reflectance and log of total phosphorus (Table 3.4.17). The best PLS model at the *Phragmites*-dominant site used the log of total phosphorus (9/21/04 data) and seven spectral bands of first derivative transformed reflectance that were combined into one PLS-component with an RMSEP of 0.08 and $R^2 = 0.92$ (Figure 3.4.20). The second highest regression correlation used nine spectral bands of 1st derivative spectra combined into two PLS-components and untransformed total phosphorus (9/21/04 data), yielding an RMSEP of 0.02 and R^2 of 0.90 (Figure 3.4.21).

Table 3.4.17. PLS-regression for total phosphorus at the *Phragmites*-dominant (PD) site. r = regression coefficient, RMSEP = root mean square error of prediction, PCs = PLS-components

Spectra Transformations	TP Transformations	Date	r	RMSEP	n	Name of plots removed	PCs	# bands used	Comments
Norris 1 st Derivative	Log TP	9.21.04	0.96	0.08	13	Plots 2,3	1	7	Plot 2 high reflect; Plot 3 low TP conc.
Golay 1 st Derivative	none	9.21.04	0.95	0.02	14	Plot 2	2	9	Plot 2 high reflectance
Norris 1 st Derivative	none	9.21.04	0.90	0.03	14	Plot 2	3	99	Plot 2 high reflectance
Golay 2 nd Derivative	Log TP	8.24.04	0.83	0.27	13	Plots 2,3	6	7	Plots 2,3 low TP conc
Untransformed d (350-1075nm)	none	6.06.05	0.82	0.16	14	Plot 2	3	48	Plot 2 low TP conc.
Untransformed d (350-1075nm)	none	9.21.04	0.75	0.04	13	Plots 2,7	2	67	Plots 2,7 high reflect
Golay 2 nd Derivative	none	9.21.04	0.70	0.04	13	Plots 2,3	1	13	Plot 2 high reflect; Plot 3 low TP conc.
Untransformed d (350-1075nm)	none	8.24.04	0.67	0.06	13	Plots 2,9 Plots 3,5,7	3	91	Plot 9 high reflect; Plot 2 low TP conc
Golay 2 nd Derivative	Log TP	7.19.04	0.65	0.36	12	3,5,7	1	5	Plots 3,5,7 low TP conc.
Log R	Sqrt TP	9.21.04	0.60	0.10	14	Plot 2	2	24	Plot 2 high reflectance
Normalized spectra (R/R410)	none	8.24.04	0.59	0.08	14	Plot 2	3	36	Plot 2 low TP conc.
Transform 1/R	none	9.21.04	0.56	0.05	14	Plot 2	3	586	Plot 2 high reflectance
Golay 1 st Derivative	none	8.24.04	0.55	0.08	15	none	1	81	none
Norris 1 st Derivative	none	8.24.04	0.54	0.08	14	Plot 2	1	82	Plot 2 low TP conc.
Truncated spectra (400-950nm)	none	9.21.04	0.52	0.06	13	Plots 2,7	7	263	Plots 2,7 high reflect
Golay 2 nd Derivative	none	8.24.04	0.50	0.07	14	Plot 6	1	10	Plot 6 high reflectance
Kubelka-Munk Transformation	none	8.24.04	0.49	0.08	15	none	1	17	none
Untransformed d (350-1075nm)	none	6.16.04	0.47	1.87	14	Plot 15	3	91	Plot 15 high reflect.
Untransformed d (350-1075nm)	Arcsine sqrt (TP)	8.24.04	0.47	0.01	14	Plot 2	1	414	Plot 2 low TP conc.

Spectra Transformations	TP Transformations	Date	r	RMSEP	n	Name of plots removed	PCs	# bands used	Comments
Untransformed (350-1075nm)	Sqrt TP	8.24.04	0.47	0.13	14	Plot 2	1	415	Plot 2 low TP conc.
Norris 1 st Derivative	Log TP	8.24.04	0.44	0.40	13	Plots 2,3	1	90	Plots 2,3 low TP conc
Golay 2 nd Derivative	Log TP	9.21.04	0.43	0.28	14	Plot 3	1	4	Plot 3 low TP conc.
Absorbance Transformation	none	8.24.04	0.41	0.08	14	Plot 2	1	330	Plot 2 low TP conc.
Transform 1/R	Arcsine sqrt (TP)	8.24.04	0.40	0.02	14	Plot 2	3	20	Plot 2 low TP conc.
Untransformed (350-1075nm)	Arcsine sqrt (TP)	7.19.04	0.38	0.02	14	Plot 10	1	113	Plot 10 low reflectance
Untransformed (350-1075nm)	4th root TP	8.24.04	0.35	0.17	14	Plot 2	1	420	Plot 2 low TP conc.
Log R	none	8.24.04	0.35	0.09	14	Plot 2	1	334	Plot 2 low TP conc.
Untransformed (350-1075nm)	Log TP	8.24.04	0.31	0.42	13	Plots 2,3	1	416	Plots 2,3 low TP conc Remaining samples used in calibration
Truncated spectra, manual test	none	8.24.04	0.31	0.06	5	none	1	none	none
Log R	Sqrt TP	8.24.04	0.31	0.15	14	Plot 2	2	399	Plot 2 low TP conc.
Truncated spectra (400-950nm)	none	7.19.04	0.28	0.18	14	Plot 10	1	79	Plot 10 low reflectance
Transform 1/R	none	8.24.04	0.27	0.09	14	Plot 2	1	12	Plot 2 low TP conc.
Untransformed (350-1075nm)	none	7.19.04	0.26	0.18	14	Plot 10	1	63	Plot 10 low reflectance
MSC Transformation	none	8.24.04	0.17	0.12	15	none	1	none	none Remaining samples used in calibration
Truncated spectra, random test	none	8.24.04	0.14	0.11	4	Plot 2	1	none	none
Untransformed (350-1075nm)	none	6.29.04	-0.11	0.56	13	Plots 4,12	1	none	Plots 4,12 missing

Table 3.4.18. PLS-regressions transformations tested on total phosphorus concentrations collected at the *Phragmites*-dominant site.

[illegible][illegible]

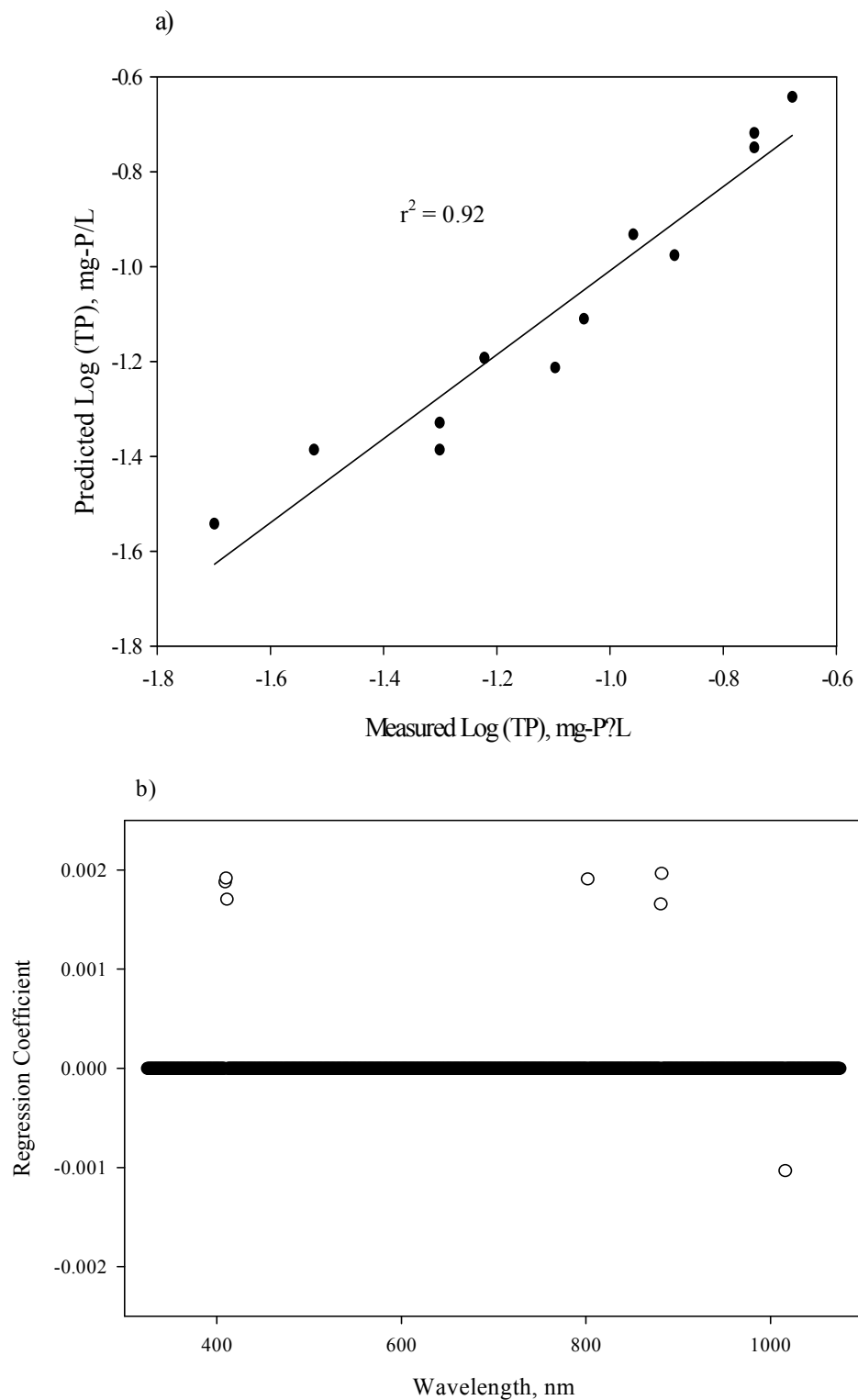


Figure 3.4.20. (a) Predicted vs measured log of total phosphorus PLS-regression at the *Phragmites*-dominant site which used seven spectral bands of the 1st derivative of the 9/21/04 reflectance to form one PLS-component with $r = 0.96$ and RMSEP of 0.08. (b) Loading plot showing significant spectral bands used in the regression as open circles.

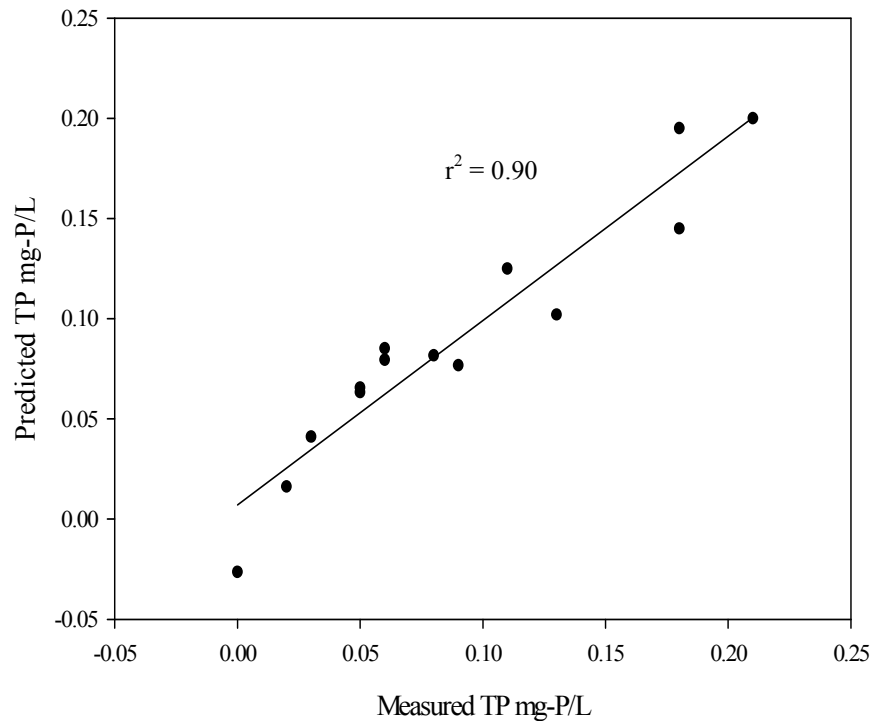


Figure 3.4.21. Predicted vs measured total phosphorus PLS-regression at the *Phragmites*-dominant site which used nine spectral bands of the 1st derivative of the 9/21/04 reflectance to form two PLS-components with $r = 0.95$ and RMSEP of 0.02.

At the *Phragmites*-absent site, PLS models were capable of quantifying total phosphorus concentrations for untransformed spectra during July and August (Table 3.4.19). The best PLS model used 73 spectral bands from the 7/19/04 sample date that formed three PLS-components with RMSEP of 0.06 and $R^2 = 0.79$ (Figure 3.2.22).

Table 3.4.19. PLS-regression for total phosphorus at the *Phragmites*-absent (PA) site. r = regression coefficient, RMSEP = root mean square error of prediction, PCs = PLS-components

Spectra Transformations	TP Transformations	Date	r	RMSEP	n	Name of plots removed	PCs	# bands used	Comments
Untransformed (350-1075nm)	none	7.19.04	0.89	0.06	14	Plot 2	3	73	Plot 2 high TP conc.
Truncated spectra (400-950nm)	none	7.19.04	0.86	0.07	14	Plot 2	4	89	Plot 2 high TP conc.
Untransformed (350-1075nm)	none	9.21.04	0.85	0.05	13	Plots 7,12	3	10	Plot 7 high TP conc; Plot 12 high reflect.
Transform 1/R	none	9.21.04	0.84	0.05	13	Plots 7,12	8	28	Plot 7 high TP conc; Plot 12 high reflect.
Kubelka-Munk Transformation	none	8.24.04	0.83	0.04	14	Plot 7	3	88	Plot 7 high TP conc
Normalized spectra (R/R410)	none	8.24.04	0.77	0.06	15	none	4	73	none
Absorbance Transformation	none	8.24.04	0.75	0.05	14	Plot 7	3	76	Plot 7 high TP conc
Log R	Sqrt TP	8.24.04	0.74	0.07	14	Plot 7	3	26	Plot 7 high TP conc
Untransformed (350-1075nm)	Arcsine sqrt (TP)	7.19.04	0.72	0.00	14	Plot 2	3	192	Plot 2 high TP conc.
Norris 1 st Derivative	Log TP	9.21.04	0.71	0.24	15	none	1	32	none
Truncated spectra (400-950nm)	none	9.21.04	0.68	0.06	13	Plots 7,12	3	53	Plot 7 high TP conc; Plot 12 high reflect.
Log R	Sqrt TP	9.21.04	0.68	0.09	13	Plots 7,12	2	32	Plot 7 high TP conc; Plot 12 high reflect.
Transform 1/R	Arcsine sqrt (TP)	8.24.04	0.66	0.01	15	none	3	53	none
Golay 2 nd Derivative	Log TP	9.21.04	0.65	0.26	15	none	1	32	none
MSC Transformation	none	8.24.04	0.64	0.07	15	none	1	228	none
Truncated spectra, random test	none	8.24.04	0.61	0.05	5	none	1	none	Remaining samples used for calibration
Norris 1 st Derivative	none	9.21.04	0.60	0.07	13	Plots 7,12	1	15	Plot 7 high TP conc; Plot 12 high reflect.
Golay 1 st Derivative	none	9.21.04	0.58	0.07	13	Plots 7,12	2	3	Plot 7 high TP conc; Plot 12 high reflect.
Golay 1 st Derivative	none	8.24.04	0.55	0.06	14	Plot 7	1	222	Plot 7 high TP conc

Spectra Transformations	TP Transformations	Date	r	RMSEP	n	Name of plots removed	PCs	# bands used	Comments
Golay 2 nd Derivative	none	9.21.04	0.55	0.10	15	none	1	15	none
Norris 1 st Derivative	none	8.24.04	0.53	0.06	14	Plot 7	1	194	Plot 7 high TP conc
Log R	none	8.24.04	0.51	0.06	14	Plot 7	1	511	Plot 7 high TP conc
Untransformed d (350-1075nm)	none	8.24.04	0.50	0.08	15	none	2	4	none
Transform 1/R	none	8.24.04	0.50	0.08	15	none	3	458	none
Untransformed d (350-1075nm)	Arcsine sqrt (TP)	8.24.04	0.49	0.00	15	none	2	61	none
Untransformed d (350-1075nm)	Sqrt TP	8.24.04	0.49	0.10	15	none	2	60	none
Untransformed d (350-1075nm)	Log TP	8.24.04	0.49	0.25	15	none	4	25	none
Golay 2 nd Derivative	none	8.24.04	0.49	0.08	15	none	1	53	none
Golay 2 nd Derivative	Log TP	8.24.04	0.49	0.24	15	none	1	61	none
Untransformed d (350-1075nm)	4th root TP	8.24.04	0.48	0.08	15	none	2	50	none
Golay 2 nd Derivative	Log TP	7.19.04	0.47	0.28	15	none	1	12	none
Untransformed d (350-1075nm)	none	6.29.04	0.41	0.09	14	Plot 2	6	57	Plot 2 missing TP
Norris 1 st Derivative	Log TP	8.24.04	0.40	0.23	14	Plot 7	1	179	Plot 7 high TP conc
Untransformed d (350-1075nm)	none	6.06.05	0.12	0.35	13	Plots 3,10	1	none	Plot 3 high reflect; Plot 10 high TP conc
Truncated spectra, manual test	none	8.24.04	0.11	0.11	5	none	4	none	Remaining samples used for calibration
Untransformed d (350-1075nm)	none	6.16.04	0.03	0.91	13	Plots 5,9	1	none	Plot 5 missing TP, Plot 9 high TP conc.

Table 3.4.20. PLS-regressions transformations tested on total phosphorus concentrations collected at the *Phragmites*-absent site.

[illegible][illegible]

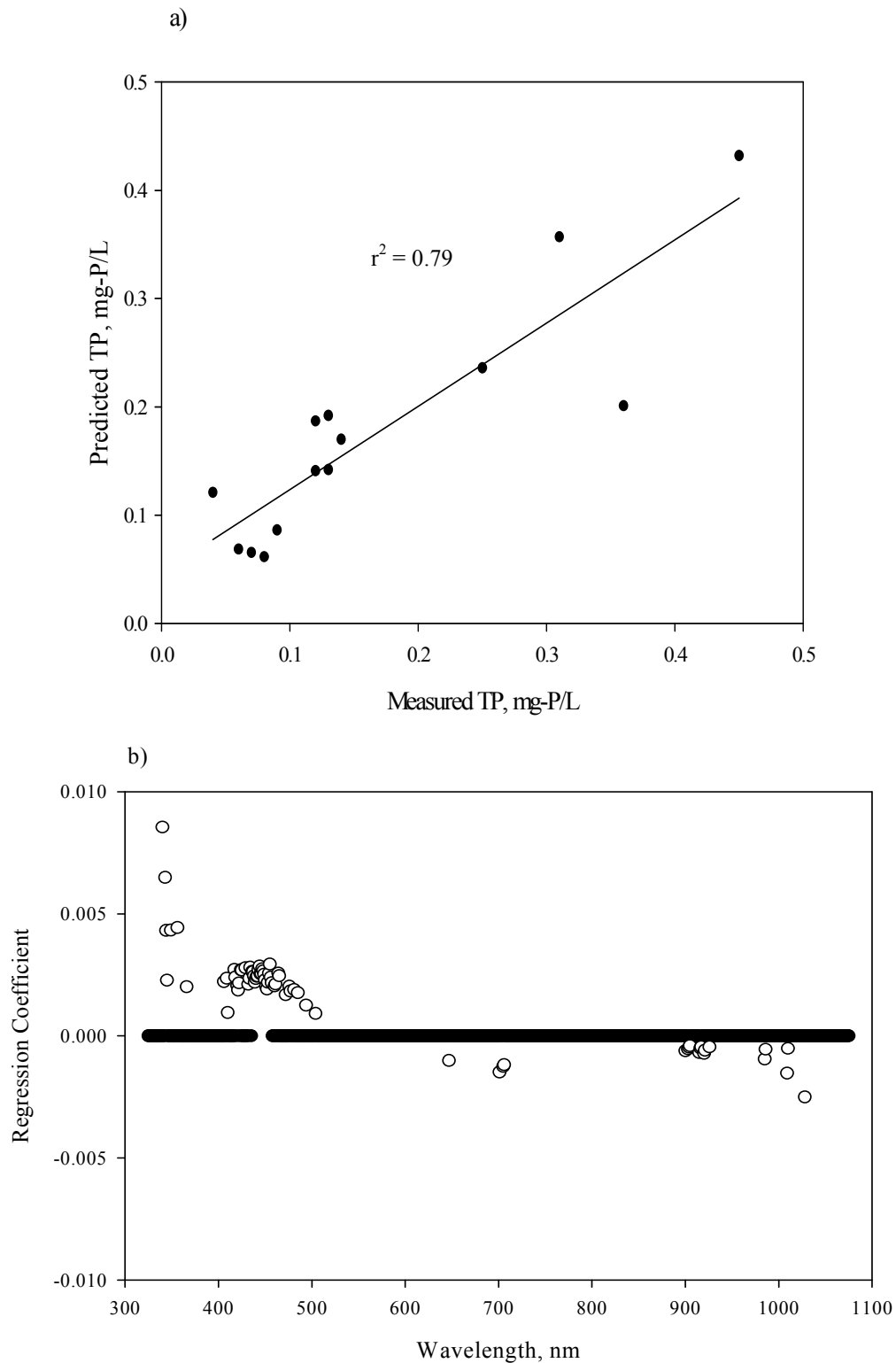


Figure 3.4.22. (a) Predicted vs measured total phosphorus PLS-regression at the *Phragmites*-absent site which used 73 untransformed spectral bands from 7/19/04 to form three PLS-components with $r = 0.89$ and RMSEP of 0.06. (b) Loading plot shows significant spectral bands used in the regression as open circles.

A summary of spectral bands used in each PLS model predicting phosphorus concentrations at the *Phragmites*-dominant site shows that regressions using a transformation of total phosphorus (log, square root, fourth root) used more spectral bands than untransformed total phosphorus data (Figure 3.4.23a). Spectral bands used in ten or more regressions were in the green and near-infrared wavebands (Figure 3.4.23b). Spectral bands used at the *Phragmites*-absent site are primarily concentrated in the visible green, with a few in the near-infrared (Figure 3.4.24b). A list of the illustrated bands, significant to ten or more regressions, can be found in the Appendix.

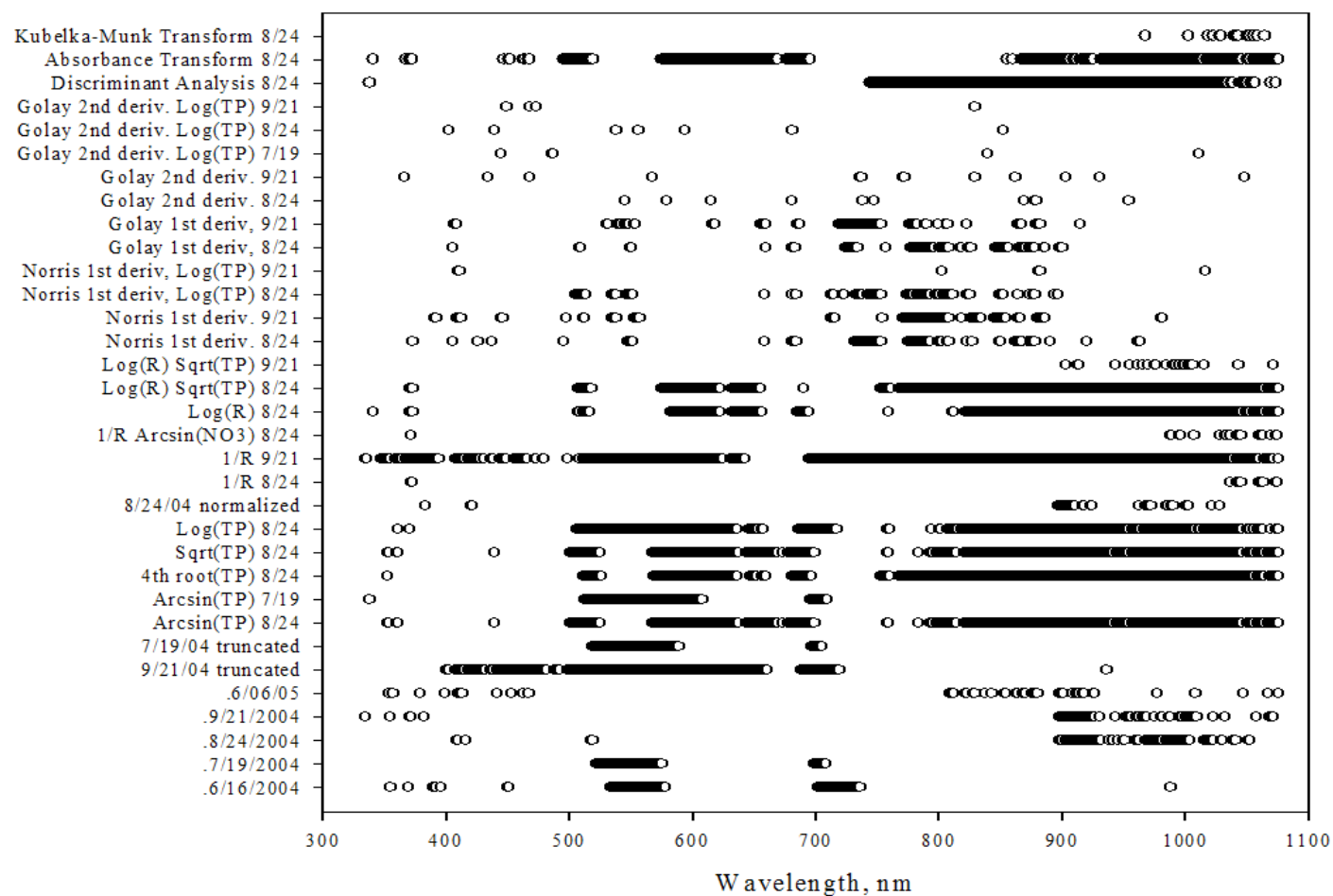


Figure 3.4.23a. Significant spectral bands for total phosphorus according to PLS-regressions at the *Phragmites*-dominant site.

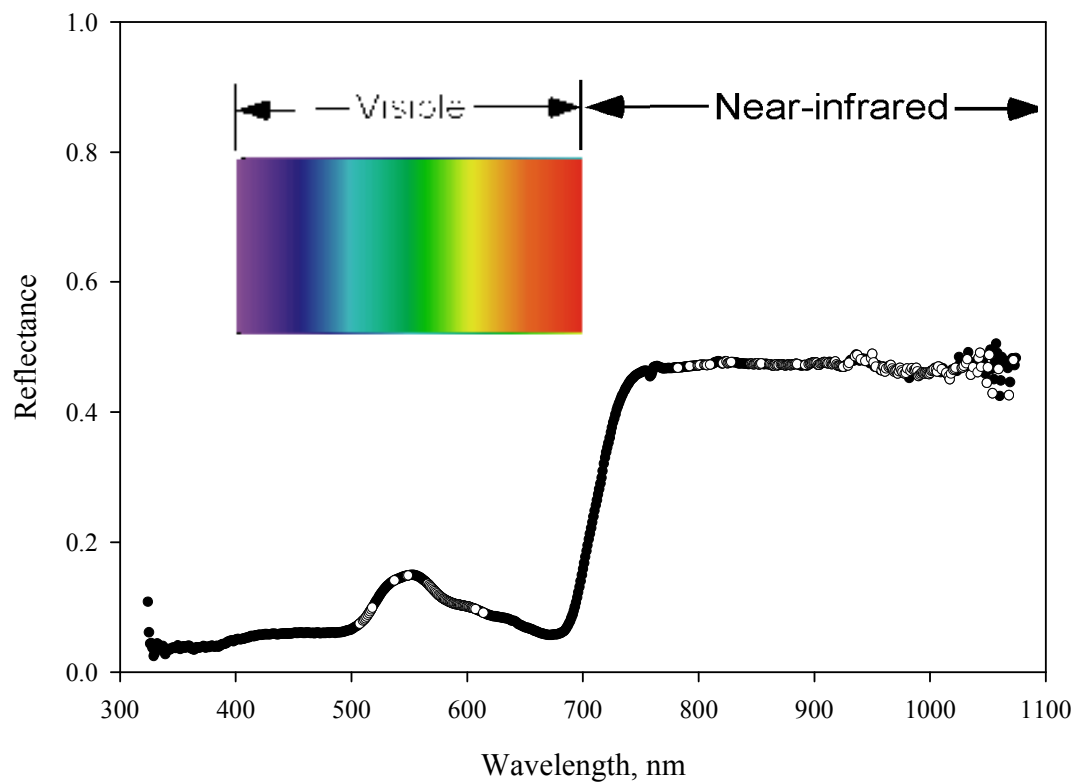


Figure 3.4.23b. Spectral bands significant for ten or more regressions for total phosphorus at the *Phragmites*-dominant site are indicated by an open circle.

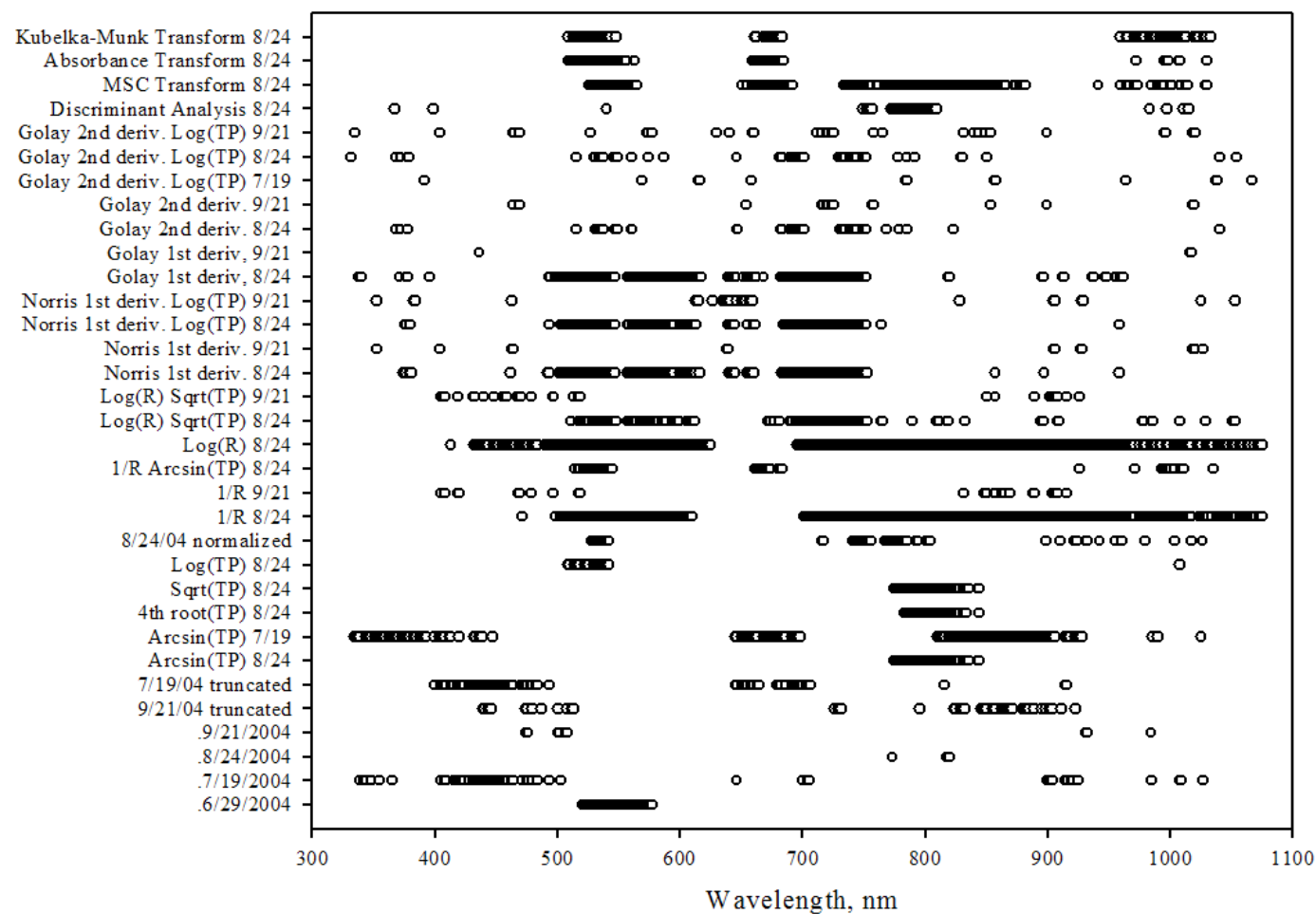


Figure 3.4.24a. Significant spectral bands for total phosphorus according to PLS-regressions at the *Phragmites*-absent site.

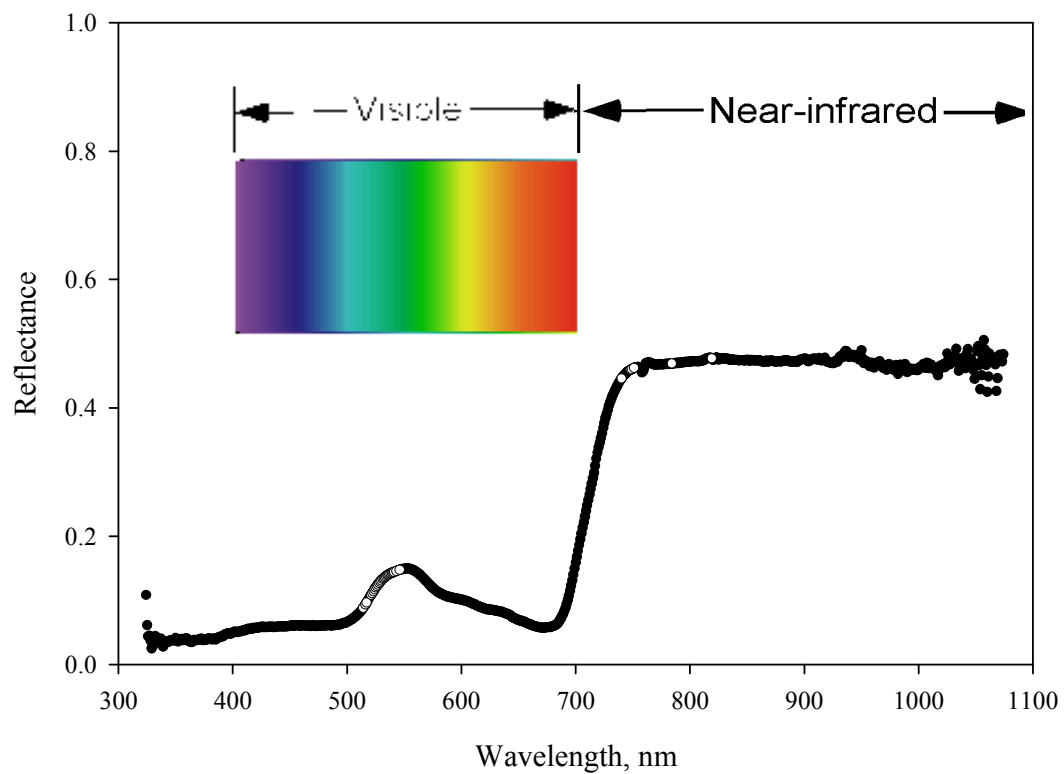


Figure 3.4.24b. Spectral bands significant for ten or more regressions for total phosphorus at the *Phragmites*-absent site are indicated by an open circle.

3.4.2 Prediction of canopy nutrients

Since it would be useful to detect vegetation nutrient concentrations using remote sensing techniques, we explored the ability of PLS-regression to quantify canopy nitrogen, canopy phosphorus and biomass within our study sites.

PLS was able to quantify canopy nitrogen, canopy phosphorus and biomass for all thirty marsh plots (Table 3.4.21). Canopy nitrogen (g/m^2 and %) and biomass were best predicted with the first derivative of the reflectance ($R^2 = 0.77$, 0.80 , and 0.83 , respectively), while canopy phosphorus was best predicted using the second derivative of the reflectance ($R^2 = 0.76$ and $R^2 = 0.71$) (Table 3.4.21).

Table 3.4.21. PLS-regressions for leaf nitrogen, leaf phosphorus, and plot biomass for all thirty plots on 8/02/05. R^2 = regression correlation coefficient; RMSEP = root mean square error of prediction; PCs = Partial Least Squares components; # bands used = number of spectral bands

Species	Cover range	R^2	RMSEP	PCs	Transformation	# bands used
Canopy N	4 - 43 (g/m^2)	0.67	4.6	2	untransformed	19
	5 - 43 (g/m^2)	0.77	4.4	2	1 st derivative	11
	6 - 43 (g/m^2)	0.67	5.4	3	2 nd derivative	8
	1 - 2.3 (%)	0.64	0.2	4	untransformed	45
	1.2 - 2.7 (%)	0.80	0.1	3	1 st derivative	35
	1.3 - 2.7 (%)	0.70	0.2	1	2 nd derivative	14
Canopy P	0.7 - 2.7 (g/m^2)	0.30	0.6	1	untransformed	446
	0.7 - 2.8 (g/m^2)	0.44	0.5	1	1 st derivative	298
	0.7 - 2.9 (g/m^2)	0.76	0.3	2	2 nd derivative	19
	0.2 - 0.4 (%)	0.00	0.1	1	untransformed	-
	0.2 - 0.4 (%)	0.04	0.0	1	1 st derivative	27
	0.2 - 0.4 (%)	0.71	0.0	3	2 nd derivative	10
Biomass	190 - 2300 g	0.79	294.0	3	untransformed	122
	191 - 2300 g	0.83	258.4	2	1 st derivative	17
	192 - 2300 g	0.61	390.1	1	2 nd derivative	15

Total canopy nitrogen of the plot was compared to canopy nitrogen relative to the total biomass of the plot (Table 3.4.22). The PLS regressions yielded similar R^2 's and the two models both used spectral bands 735 – 739 nm (Figure 3.4.25).

Table 3.4.22. PLS-regressions for canopy nitrogen of the plot (g/m^2) and in reference to total biomass (%) for all thirty plots on 8/02/05. R^2 = regression correlation coefficient; RMSEP = root mean square error of prediction; PCs = Partial Least Squares components; # bands used = number of spectral bands used in the PLS-regression.

Response	Data Range	R^2	RMSEP	PCs	Transformation	# bands used
Leaf N (g/m^2)	4 - 43	0.67	4.6	2	350 - 1075 nm	19
Leaf N (%)	1 - 2.3	0.64	0.2	4	350 - 1075 nm	45

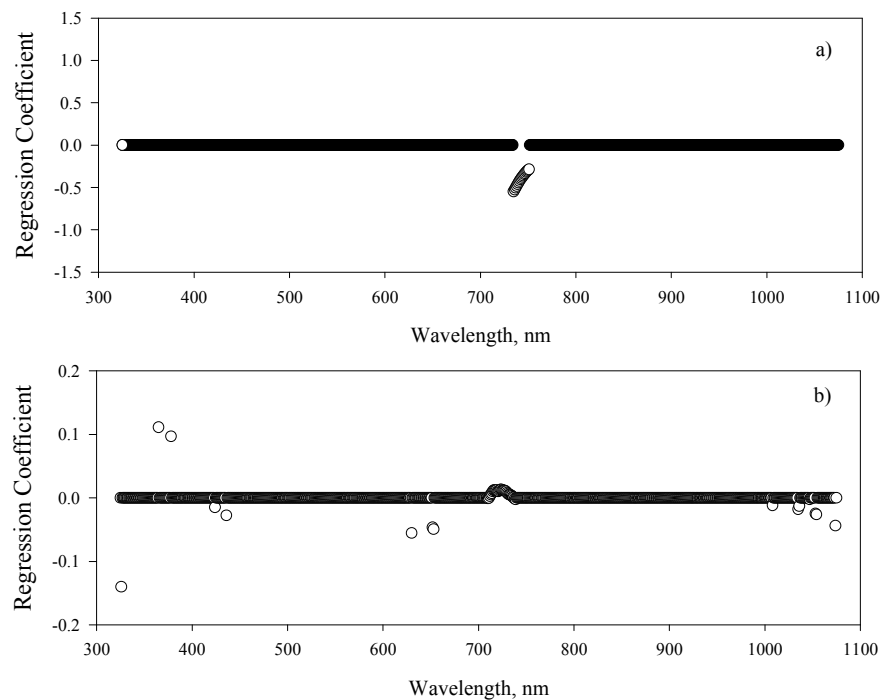


Figure 3.4.25. PLS regression coefficients for (a) canopy nitrogen of the plot (g/m^2) and (b) canopy nitrogen according to total biomass (%) using untransformed reflectance data.

No spectral band used in any PLS-regression for canopy nitrogen (transformations 350 – 1075 nm, 1st derivative R, 2nd derivative R) was shared between regressions (Figure 3.4.26a, b, and c). Phosphorus PLS-regressions, however, used several similar spectral bands, including single bands in the visible and near-infrared and a

cluster of spectral bands at the red-edge, in all three regressions (Figure 3.4.26d, e, and f). Biomass PLS-regressions shared spectral bands at 600 nm for all three regressions (Figure 3.4.26g, h, and i).

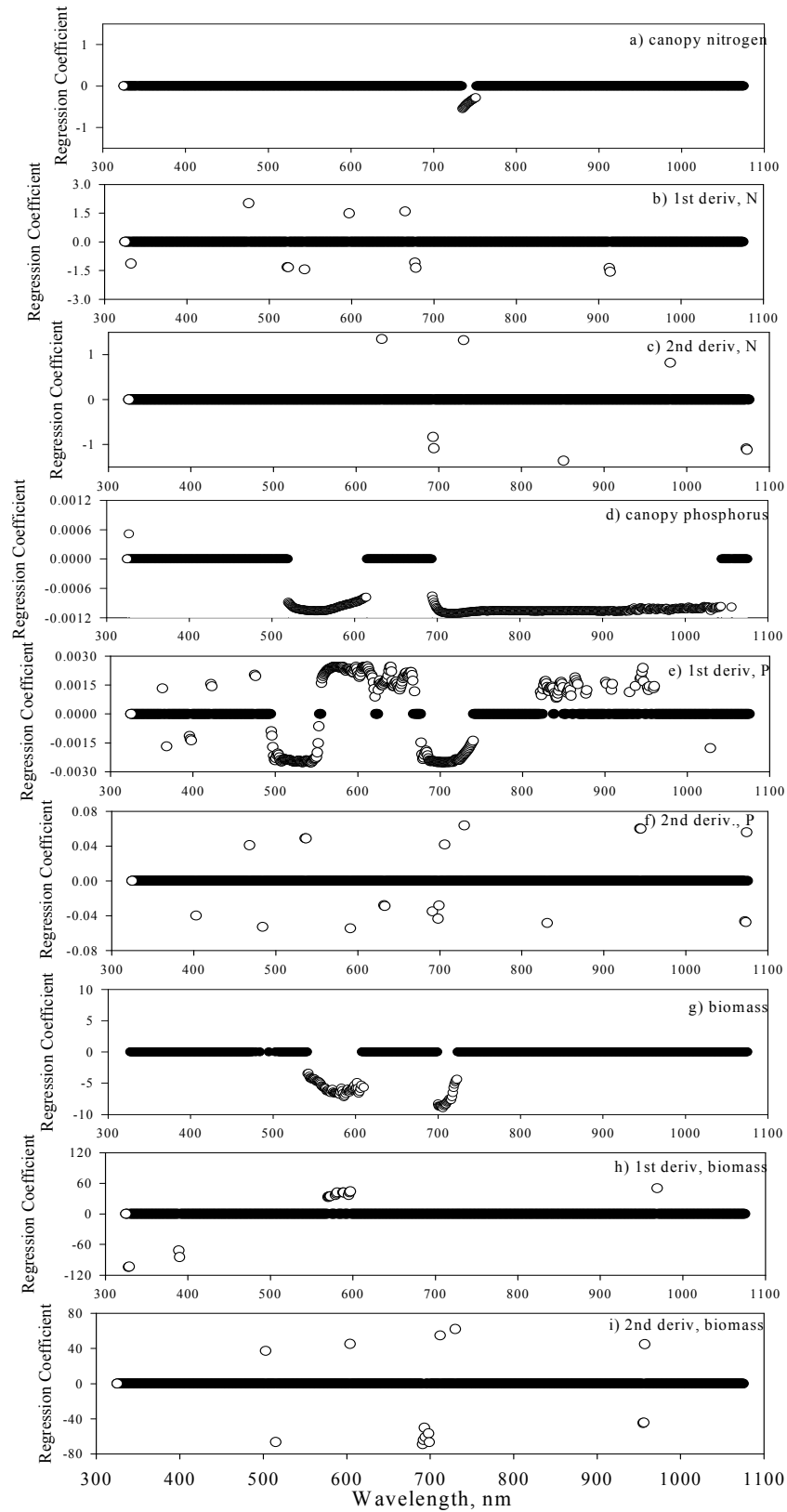


Figure 3.4.26. PLS regression coefficients for (a) canopy nitrogen, (b) 1st derivative R, canopy N, (c) 2nd derivative R, canopy N, (d) canopy phosphorus, (e) 1st derivative R, canopy P, (f) 2nd derivative R, canopy P, (g) biomass, (h) 1st derivative R, biomass, (i) 2nd derivative R, biomass.

3.4.3 Prediction of vegetation composition and surface cover

We explored the ability of PLS-regression to quantify the percent cover of six common plant species that were present at our study sites because assessment of marsh vegetation composition with remote sensing could improve the frequency and reduce the cost of wetland assessment.

PLS was able to adequately quantify (i.e., $R^2 > 0.70$) species cover of five of the six species as well as cover of dead material and exposed soil (Table 3.4.23). The amount of exposed soil at the *Phragmites*-dominant site had the overall best PLS model, using 351 untransformed spectral bands from the August 2004 sample date to form six PLS-components with an R^2 of 0.94 and RMSEP of 3.6%. *P. australis*, *A. calamus*, *P. virginica* and dead material cover also had high coefficients of determination, which indicates that hyperspectral reflectance may be capable of identifying the mix of dominant species, the cover of dead vegetation and cover of soil in marshes. *Typha* species at the *Phragmites*-absent site and dead material at the *Phragmites*-dominant site had weaker predictive PLS models ($R^2=0.67$ each and RMSEP= 0.4% and 15.3%, respectively; Table 3.4.23). Other PLS models tested, but found to be less predictive than those in Table 3.4.23 can be found in the Appendix.

Unfortunately, the PLS models best at predicting species at one marsh site did not transfer well to the other site (Table 3.4.24). For example, the best PLS model of exposed soil at the *Phragmites*-dominant site with an R^2 of 0.94 (untransformed August 2004 data) yielded an R^2 of 0.01 at the *Phragmites*-absent site.

Table 3.4.23. The best PLS-regression(s) for each species cover at individual marsh sites. R^2 = regression correlation coefficient; RMSEP = root mean square error of prediction; PCs = Partial Least Squares components; # bands used = number of spectral bands used in the PLS-regression.

Species	Site	Cover range	Date	R^2	RMSEP	PCs	Transformation	# bands used
<i>P. australis</i>	PD	5 - 90	8.02.05	0.85	12.0	3	1 st derivative	142
<i>A. calamus</i>	PD	0 - 65	6.16.04	0.85	6.8	8	1/R	128
	PD	0 - 65	6.16.04	0.85	6.8	8	1/R, arcsin (cover) ^{1/2}	128
<i>P. arifolium</i>	PD	0 - 60	9.21.04	0.74	8.9	3	350 - 1075nm	27
	PA	30 - 100	8.24.04	0.79	7.7	3	R/R410	169
<i>P. virginica</i>	PD	0 - 40	5.25.04	0.83	7.6	3	400 - 950nm	27
	PA	0 - 18	9.21.04	0.86	0.5	4	Log R, (cover) ^{1/2}	243
<i>Typha sp.</i>	PA	0 - 1.5	8.24.04	0.67	0.4	4	Log R	13
<i>I. capensis</i>	PD	0 - 70	7.19.04	0.81	10.7	4	1 st deriv (Norris)	45
	PD	0 - 70	7.19.04	0.81	10.9	2	1 st deriv. (Golay)	60
	PD	0 - 65	8.24.04	0.81	0.9	9	Log R, (cover) ^{1/2}	44
	PA	0 - 90	7.19.04	0.81	13.0	3	1/R	26
	PA	0 - 90	7.19.04	0.79	15.0	8	Log R	59
Dead	PD	0 - 90	9.21.04	0.67	15.3	6	350-1075nm	34
	PA	0 - 20	5.25.04	0.85	2.0	3	350-1075nm	165
Exposed	PD	0 - 40	8.24.04	0.94	3.6	6	350-1075nm	351
	PA	0 - 18	7.19.04	0.83	0.5	2	2 nd deriv.	88

Table 3.4.24. The best PLS models of each species cover applied to the opposite marsh site. R^2 = regression correlation coefficient; RMSEP = root mean square error of prediction; PCs = Partial Least Squares components; # bands used = number of spectral bands used in the PLS-regression. Regressions were not performed for *P. australis* and *A. calamus* at the PD site and *Typha* species at the PA site because the species was not present at that site.

Species	Site	Cover range	Date	R^2	RMSEP	PCs	Transformation	# bands used
<i>P. australis</i>	N/A	-	-	-	-	-	-	-
<i>A. calamus</i>	N/A	-	-	-	-	-	-	-
	N/A	-	-	-	-	-	-	-
<i>P. arifolium</i>	PA	0 - 18	9.21.04	0.28	5.0	3	350 - 1075 nm	60
	PD	3 - 100	8.24.04	0.59	17.4	3	R/R410	4
<i>P. virginica</i>	PA	0 - 8	8.24.04	0.64	1.2	3	400 - 950 nm	56
	PD	0 - 65	6.03.04	0.30	0.7	9	Log R, (cover) ^{1/2}	353
<i>Typha sp.</i>	N/A	-	-	-	-	-	-	-
<i>I. capensis</i>	PA	0 - 90	7.19.04	0.55	20.2	1	1 st deriv (Norris)	20
	PA	0 - 90	7.19.04	0.58	19.8	3	1 st deriv (Golay)	10
	PA	0 - 85	8.24.04	0.71	1.7	5	Log R, (cover) ^{1/2}	42
	PD	0 - 70	7.19.04	0.19	22.2	3	1/R	21
	PD	0 - 70	7.19.04	0.59	15.8	3	Log R	14
Dead	PA	18 - 100	9.21.04	0.59	12.0	2	350 - 1075 nm	168
	PD	0 - 40	5.25.04	0.53	7.4	2	350 - 1075 nm	93
Exposed	PA	0 - 18	8.24.04	0.01	1.0	1	350 - 1075 nm	-
	PD	0 - 40	8.24.04	0.50	11.3	1	2 nd derivative	20

The majority of the best models for each species occurred in the latter half of the season (late July to late September) and when that species cover was at a maximum. *P. australis* cover was decreasing in August when its best model was established, but *A. calamus* was at its maximum cover in mid-June when its best model was established (Figure 3.4.27). Best *P. arifolium* PLS models were established in late September at the *Phragmites*-dominant site when *P. arifolium* cover had decreased (Figure 3.4.27) and in August at the *Phragmites*-absent site when *P. arifolium* cover was at a maximum (Figure 3.4.28). Similarly, *P. virginica*'s best models were

established in late May at the *Phragmites*-dominant site when *P. virginica* was at its highest cover of the season (Figure 3.4.27) and in late September at the *Phragmites*-absent site when *P. virginica* was at its lowest cover of the season (Figure 3.4.28). Only *I. capensis* had consistent models for both sites since the best PLS model was established at both sites when *I. capensis* cover was very high (Figures 3.4.27 and 3.4.28).

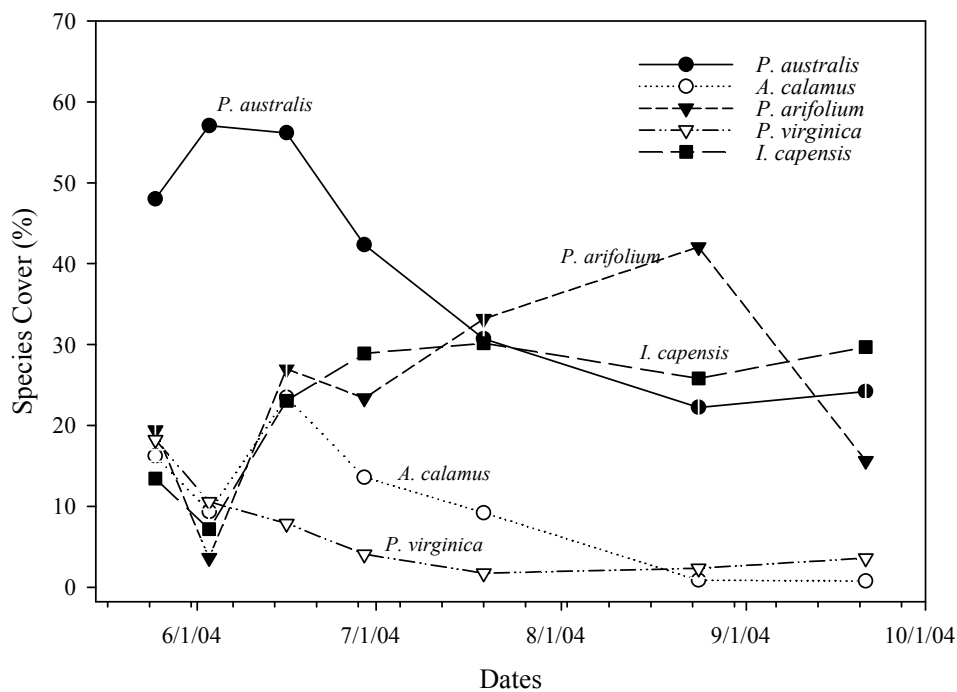


Figure 3.4.27. Mean species cover for the five most common species present at the *Phragmites*-dominant site during the 2004 growing season.

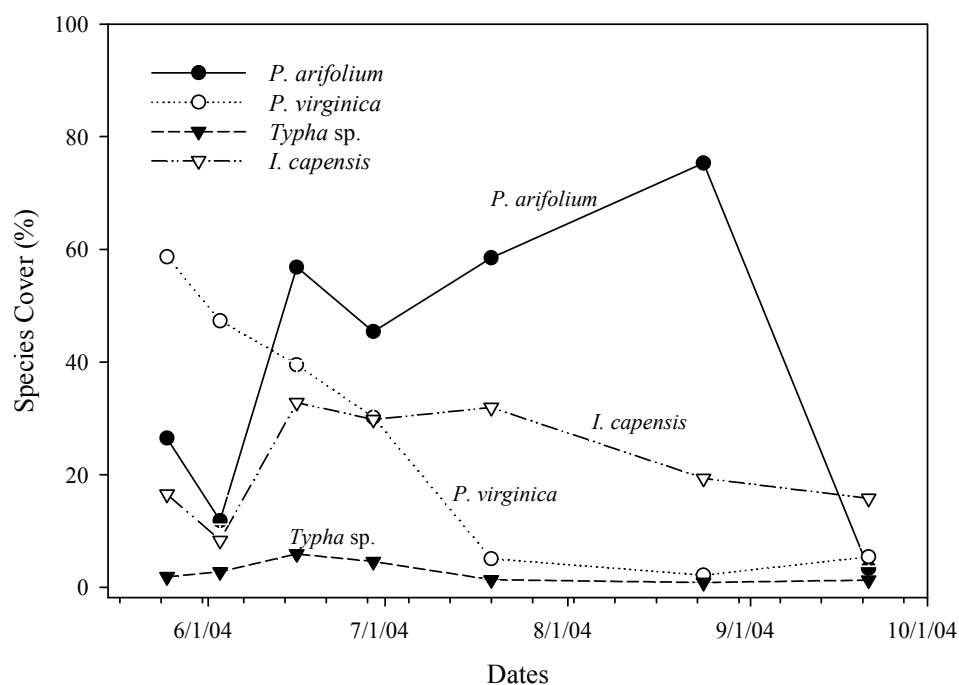


Figure 3.4.28. Mean species cover for the four most common species present at the *Phragmites*-absent site during the 2004 growing season.

Several transformations were used to create the best PLS models for the cover of each species. In addition to untransformed reflectance data, 1st and 2nd derivatives, inverse, normalized, and log of the reflectance were used in one or more PLS model (Table 3.4.23). The two cover transformations used in the best PLS models for *A. calamus*, *P. virginica* and *I. capensis* were the square root of the cover and the arcsine of the square root of cover.

Spectral bands used in PLS models for various transformations were compared using plots of regression coefficients. *P. australis* regression models used bands in the blue and red-edge for untransformed reflectance data and the first derivative of the reflectance (Figure 3.4.29a and b). Models using the first derivative of the reflectance

and the first derivative with the log of *P. australis* cover both used green spectral bands, despite the differences in the sample dates between the models (Figure 3.4.29a and c).

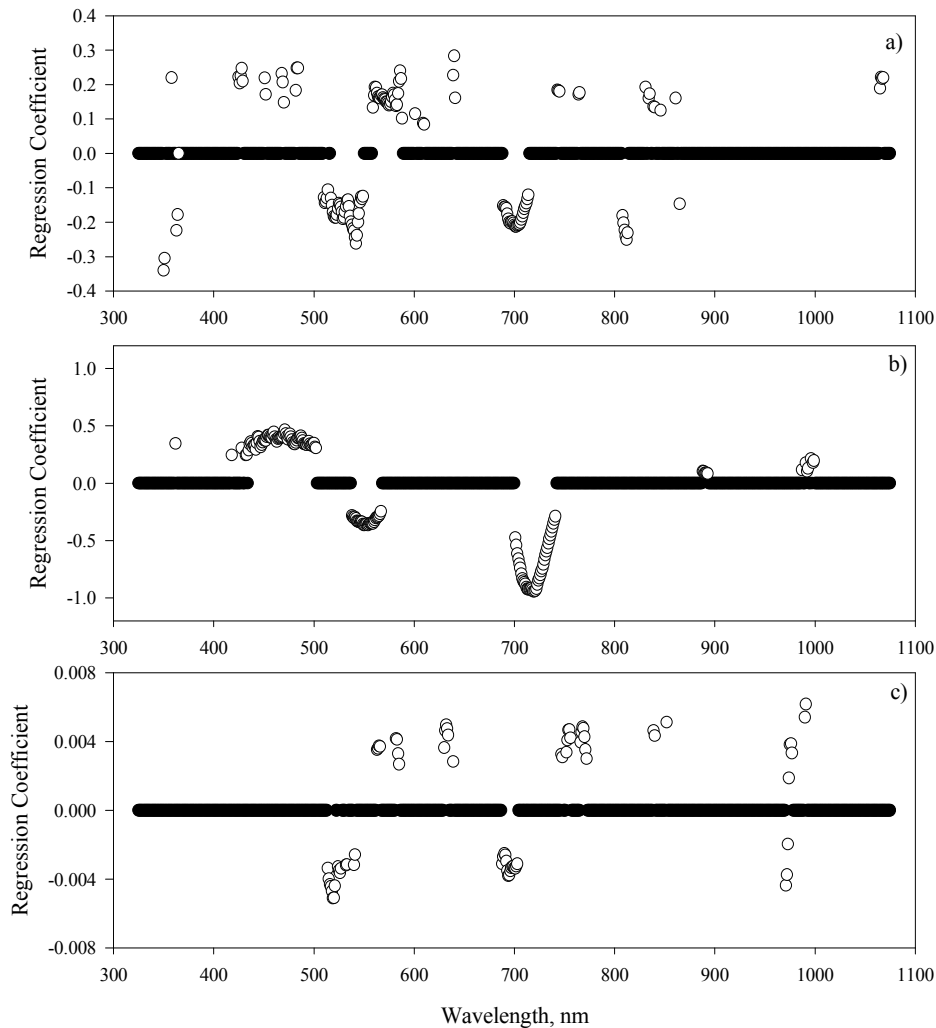


Figure 3.4.29. PLS regression coefficients for (a) 1st derivative R, *P. australis* 8/02/05 (b) untransformed *P. australis* cover 8/02/05 and (c) 1st derivative R, Log (*P. australis* cover) 8/24/04.

Regression coefficients for *A. calamus* showed similarities between spectral bands used in PLS models for untransformed data from mid-June, inverse reflectance data for the same sample date, and inverse data with the arcsine of the square root of *A. calamus* (Figure 3.4.30). The models involving the inverse reflectance shared many spectral bands, including bands near 450 nm, 530 nm, 570 nm, 710 nm, and 880 nm

(Figure 3.4.30a and c). All three PLS models shown used spectral bands at 950 nm and 1000 nm (Figure 3.4.30).

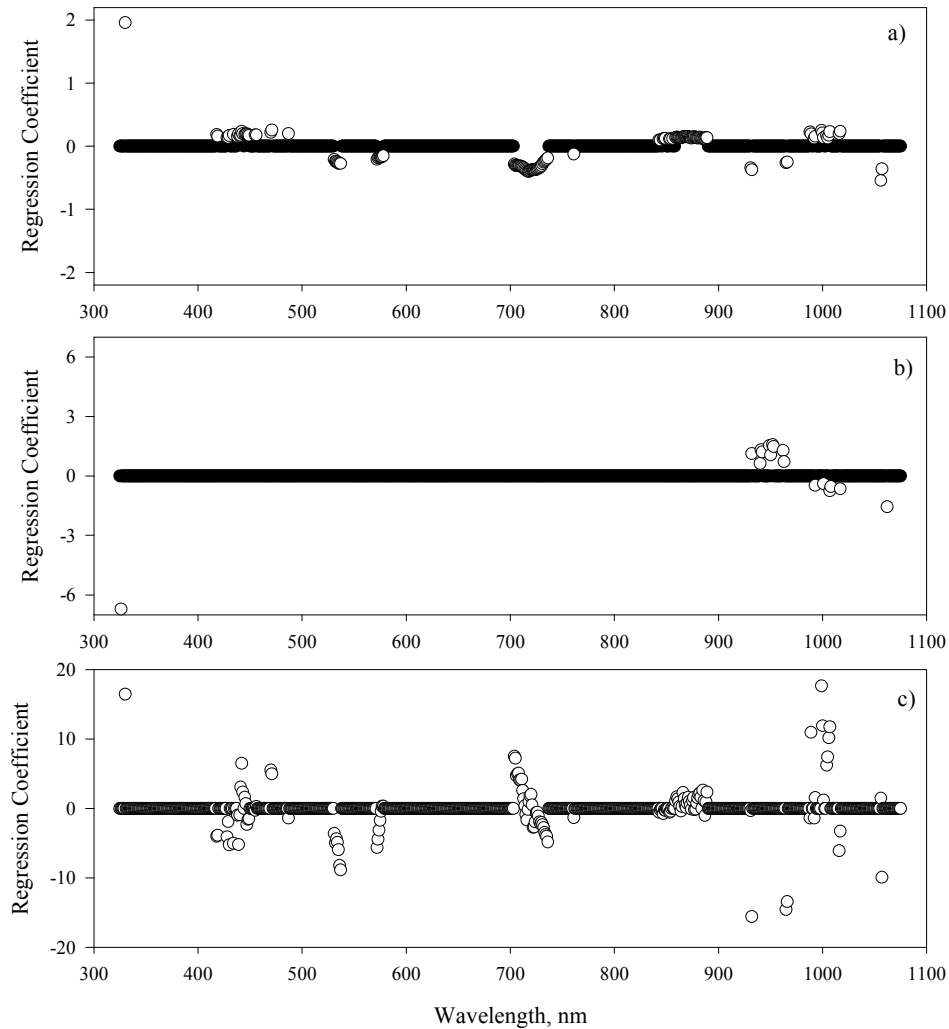


Figure 3.4.30. PLS regression coefficients for (a) 1/R, *A. calamus* 6/16/04 (b) untransformed *A. calamus* cover 6/16/04 and (c) 1/R, Arcsine Sqrt(*A. calamus* cover) 6/16/04.

P. arifolium regression models using untransformed data from the *Phragmites*-dominant site (8/24/04) and normalized data from the *Phragmites*-absent site (8/24/04) both used spectral bands in the green (Figure 3.4.31b and c), while models of untransformed data from the *Phragmites*-dominant site (9/21/04) and the two sites together (8/24/04) both used spectral bands along the red-edge (Figure 3.4.31a and e).

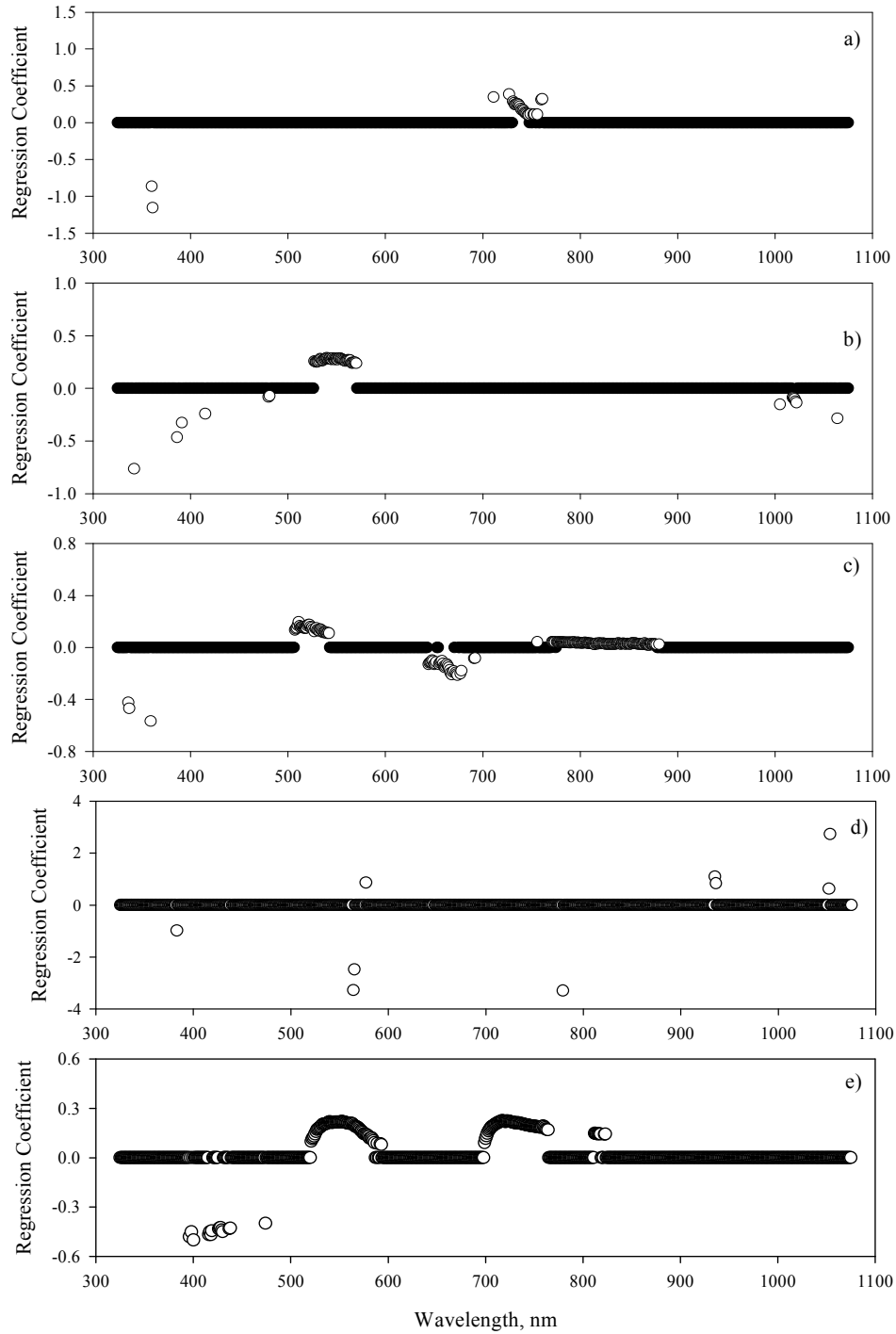


Figure 3.4.31. PLS regression coefficients for (a) *P. arifolium* cover, *Phragmites*-dominant site, 9/21/04 (b) *P. arifolium* cover, *Phragmites*-dominant site, 8/24/04, (c) Normalized reflectance, *P. arifolium* at the *Phragmites*-absent site, 8/24/04, (d) 2nd golay of the reflectance, *P. arifolium* at the *Phragmites*-absent site, 8/24/04, (e) untransformed *P. arifolium* data for both sites, 8/24/04.

PLS models at the *Phragmites*-absent site for *P. virginica* in late September used the same spectral bands between 600 – 700 nm and 710 – 810 nm (Figure 3.4.32b and c).

The regression model of truncated data from the *Phragmites*-dominant site shared spectral bands at 630 nm with the *Phragmites*-absent site models (Figure 3.4.32a) and a model of the two sites shared bands in the red-edge with the three other regressions (Figure 3.4.32d).

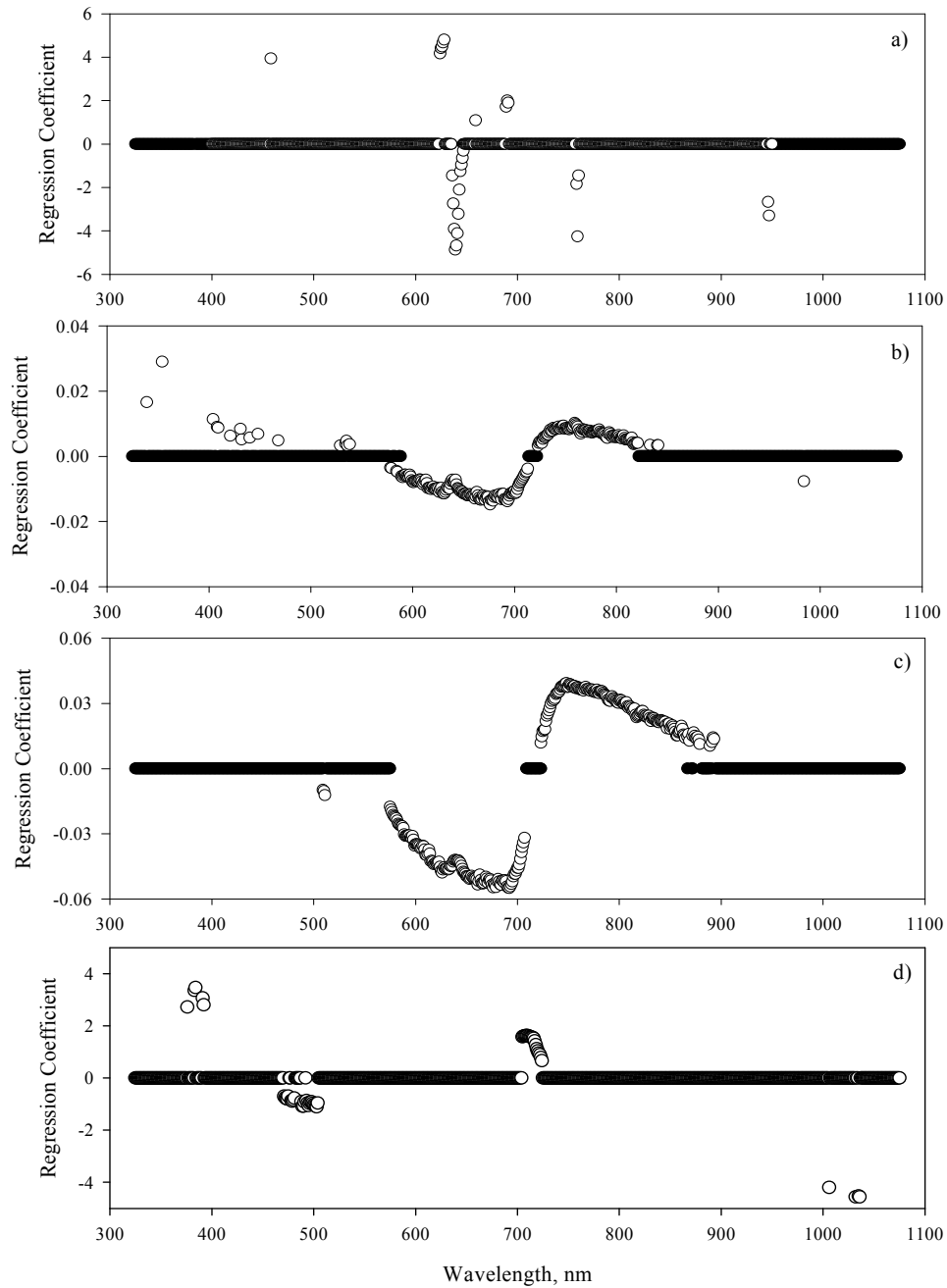


Figure 3.4.32 PLS regression coefficients for (a) *P. virginica* cover, truncated reflectance from the *Phragmites*-dominant site (5/25/04) (b) Log R, Sqrt (*P. virginica*) 9/21/04, *Phragmites*-absent site, (c) *P. virginica* 9/21/04, *Phragmites*-absent site, (d) combined sites for *P. virginica*, 5/25/04.

PLS models for *Typha* species had few spectral bands in common (Figure 3.4.33).

For two of the best regression models for *Typha* cover, only one band, 580 nm, was used in both (Figure 3.4.33).

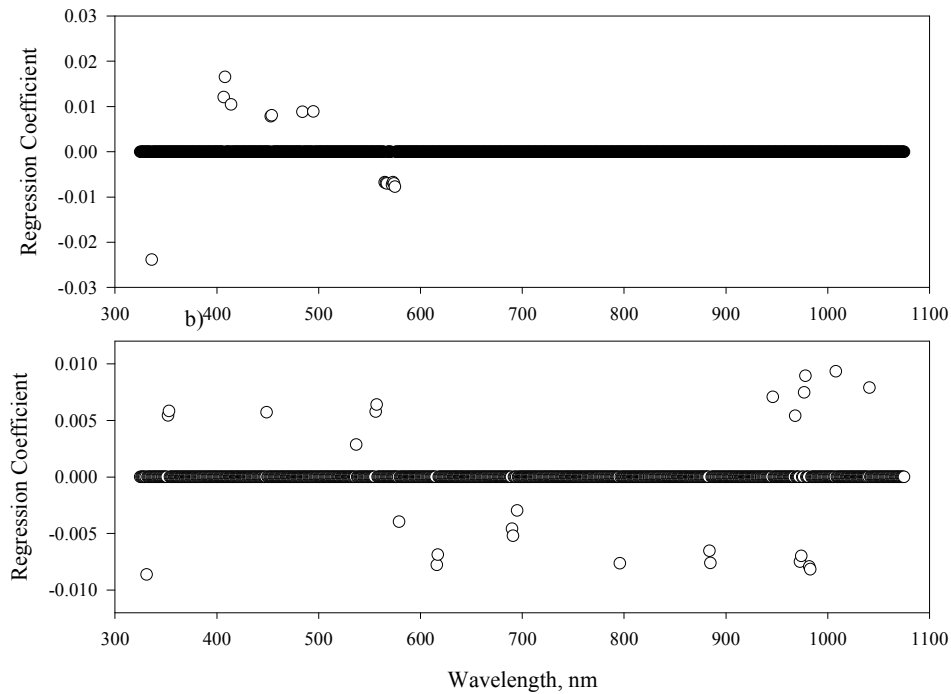


Figure 3.4.33 PLS regression coefficients for (a) Log R, *Typha* species, 8/24/04 (b) 2nd derivative R, *Typha* sp. 8/24/04

Regression models of *I. capensis* shared spectral bands near 400 nm and 500 nm, as well as 1000 nm (Figure 3.4.34). In general, more spectral bands were similar between *I. capensis* regression models of the same site.

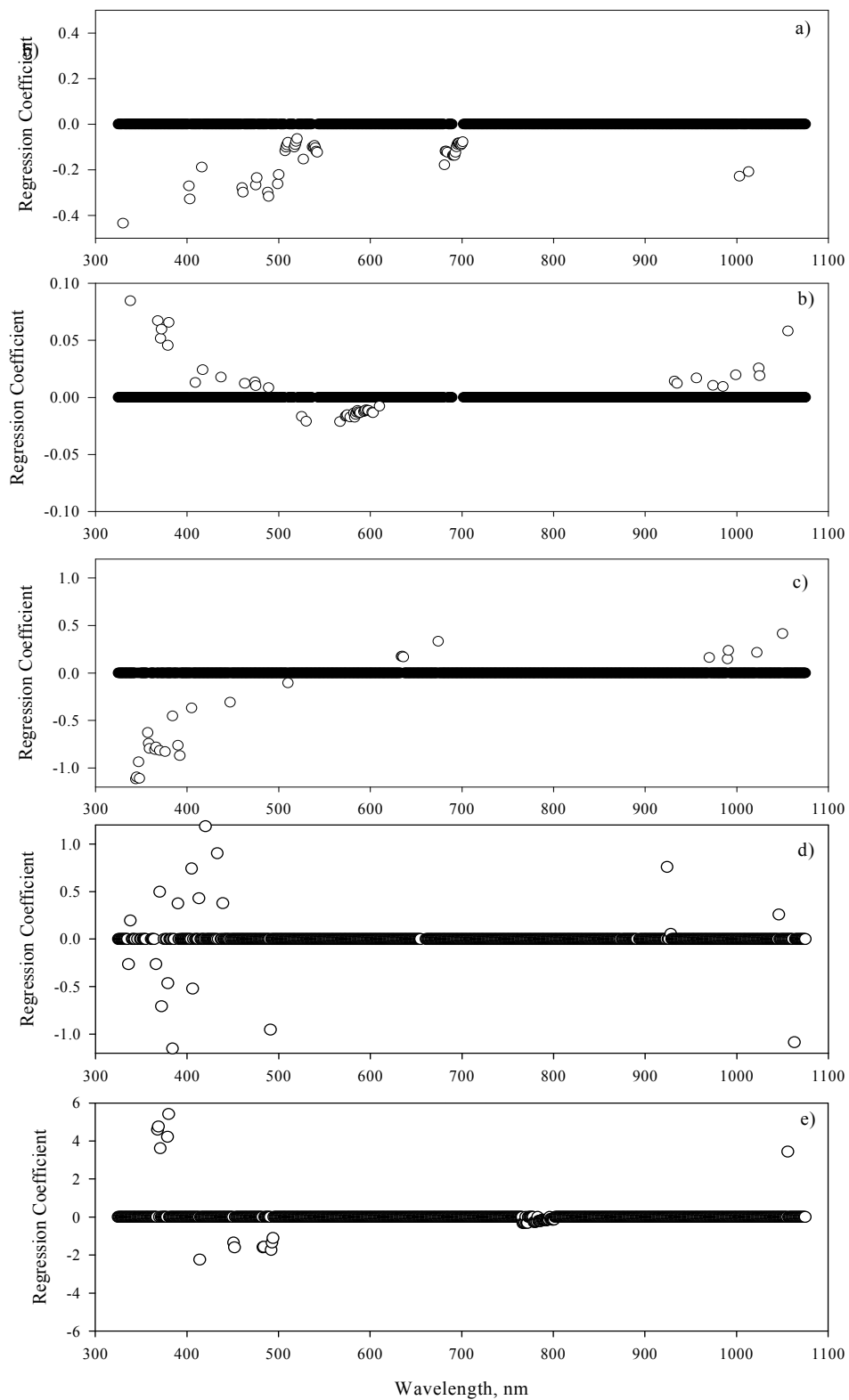


Figure 3.4.34. PLS regression coefficients for (a) 1st derivative R, *I. capensis*, *Phragmites*-dominant site, 7/19/04, (b) Log R, Sqrt (*I. capensis*), *Phragmites*-dominant site 8/24/04 (c) 1/R, *Phragmites*-absent site, 7/19/04, (d) Log R, *Phragmites*-absent site 7/19/04 (e) untransformed *I. capensis* for both sites, 8/24/04.

PLS regression models for dead material shared a spectral band at 325 nm, around 650 nm, and at 770 nm (Figure 3.4.35) for models that used the *Phragmites*-dominant site, *Phragmites*-absent site, and combined sites for different sample dates.

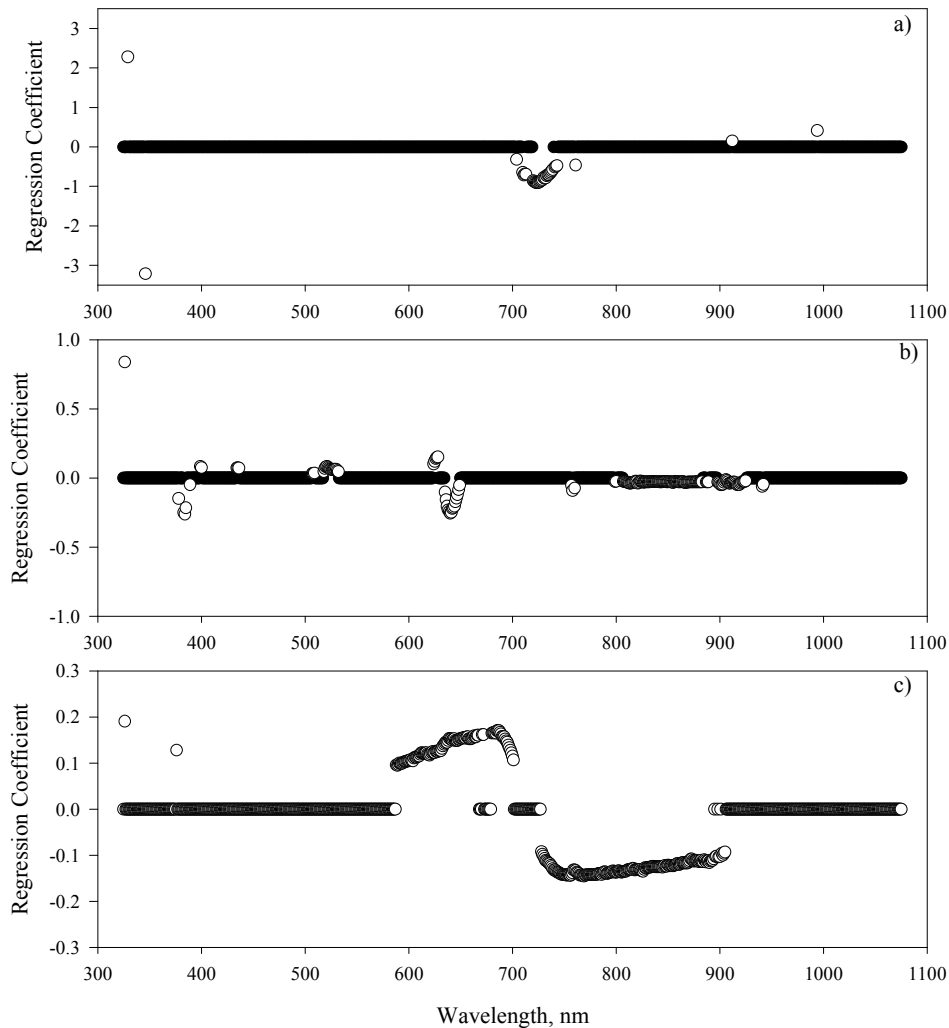


Figure 3.4.35. PLS regression coefficients for (a) dead material at the *Phragmites*-dominant site on 9/21/04, (b) dead material at the *Phragmites*-absent site on 5/25/04, and (c) dead material at combined sites on 9/21/04.

Exposed soil regression models for untransformed reflectance at the *Phragmites*-dominant and combined sites used spectral bands at 500 nm and the red-edge (Figure 3.4.36a and c). Models using the 2nd derivative of reflectance at the *Phragmites*-

absent site and reflectance at the *Phragmites*-dominant site shared bands near 590 nm, 710 nm, and 805 nm (Figure 3.4.36a and b).

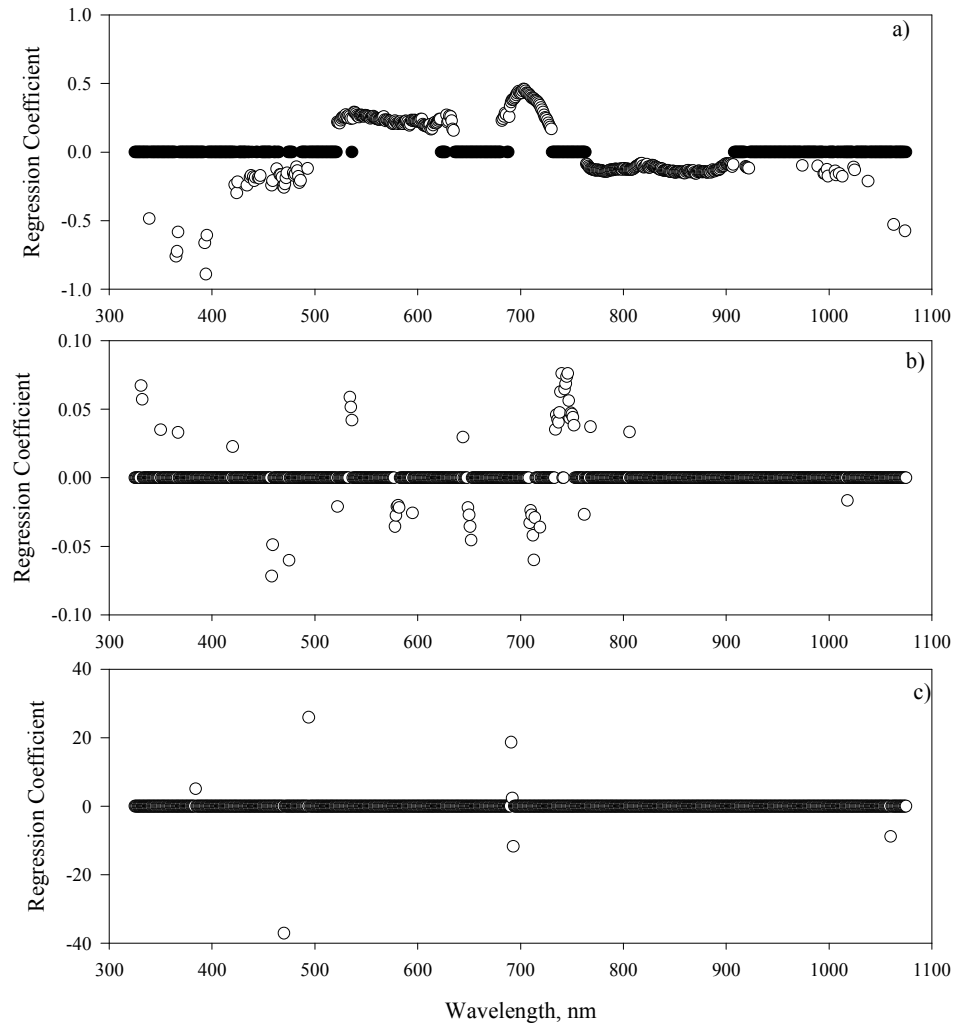


Figure 3.4.36. PLS regression coefficients for (a) exposed soil at the *Phragmites*-dominant site 8/24/04, (b) 2nd derivative of reflectance at the *Phragmites*-absent site, 7/19/04, and (c) combined sites on 8/24/04

It would also be useful to remotely sense marsh characteristics such as leaf area index, species richness and diversity, so we explored the ability of PLS-regression to quantify the characteristics within our study sites using hyperspectral reflectance.

PLS was able to quantify LAI sufficiently at both sites but at different dates during the 2004 growing season. The best LAI model at the *Phragmites*-absent site during August had five PLS-components with an R^2 of 0.90 and RMSEP of 1.5, and at the *Phragmites*-dominant site 107 spectral bands combined into ten PLS-components with an R^2 of 0.81 and RMSEP of 0.4 during June (Table 3.4.25). Species richness and Shannon-Wiener diversity index, however, were not well predicted with PLS models. The best model for species richness at the *Phragmites*-absent marsh site used nine spectral bands to form one PLS-component with an R^2 of 0.31 and RMSEP of 0.8 (Table 3.4.25).

Similar to species cover models, the best vegetation characteristic models did not predict the characteristic well at the opposite marsh site (Table 3.4.26). For example, the PLS model most predictive of LAI at the *Phragmites*-absent site was a poor predictor of LAI at the *Phragmites*-dominant site (Table 3.4.26), although both sites had comparable LAI statistics.

Table 3.4.25. The best PLS-regression(s) for each vegetation characteristic at individual marsh sites. LAI at the PA site used no spectral bands in its PLS-regression. R^2 = regression correlation coefficient; RMSEP = root mean square error of prediction; PCs = Partial Least Squares components; # bands used = number of spectral bands used in the PLS-regression.

Species	Site	Range	Date	R^2	RMSEP	PCs	Transformation	# bands used
LAI	PD	4 - 8	6.16.04	0.81	0.4	10	350 - 1075 nm	107
	PA	3 - 7.5	8.24.04	0.90	1.5	5	350 - 1075 nm	-
Sp. Richness	PD	4 - 10	7.19.04	0.18	1.3	2	350 - 1075 nm	420
	PA	5 - 9	6.29.04	0.31	0.8	1	350 - 1075 nm	9
Diversity	PD	0.5 - 2	6.03.04	0.46	0.2	3	350 - 1075 nm	261
	PA	0.1 - 1.5	9.21.04	0.71	0.3	8	350 - 1075 nm	207

Table 3.4.26. The best PLS models of each vegetation characteristic applied to the opposite marsh site. R^2 = regression correlation coefficient; RMSEP = root mean square error of prediction; PCs = Partial Least Squares components; # bands used = number of spectral bands used in the PLS-regression.

Species	Site	Range	Date	R^2	RMSEP	PCs	Transformation	# bands used
LAI	PA	3.5 - 7	6.16.04	0.01	1.0	1	350 - 1075 nm	-
	PD	3 - 7.5	8.24.04	0.27	1.1	6	350 - 1075 nm	-
Sp. richness	PA	4 - 11	7.19.04	0.02	1.9	1	350 - 1075 nm	-
	PD	5 - 10	6.29.04	0.06	1.0	6	350 - 1075 nm	3
Diversity	PA	0.5 - 2	6.03.04	0.12	0.4	3	350 - 1075 nm	-
	PD	1.2 - 1.9	9.21.04	0.04	0.2	1	350 - 1075 nm	-

Chapter 4: Discussion

4.1 Nitrogen fertilization effect on sub-surface marsh N and P levels

Applying nitrogen as urea to tidal freshwater marshes increases sub-surface marsh nitrogen levels but not phosphorus concentrations. As expected, the highest fertilized treatment yielded the highest concentration of ammonia, nitrate, and total nitrogen for the majority of sample dates, while ambient conditions yielded the lowest concentrations (Figures 3.1.1, 3.1.3, and 3.1.5, respectively). Sub-surface phosphorus concentrations were not affected by nitrogen treatments for either site in the 2004-5 growing seasons.

Contrary to my findings, Harvey et al. (1996) found that mean total nitrogen and total nitrate concentrations in sub-surface water were similar between a high and low treatment of nitrogen fertilizer applied as swine lagoon effluent to Bermuda grass pastures. Leaf nitrogen analyzed in the same experiment, however, found higher leaf nitrogen concentrations in the field with the higher nitrogen application, indicating that the vegetation in the highly fertilized field used the excess nitrogen from the soil and sub-surface water. I found similar results that the addition of nitrogen as fertilizer increased the canopy nitrogen and phosphorus (Figure 3.2.36 – 39).

The fact that sub-surface water nutrients were affected by fertilization in my research implies that nitrification and plant uptake rates could not match the fertilization rate at the *Phragmites*-dominant site. In plots receiving low nitrogen fertilization amounts,

the ammonification of urea, nitrification of ammonia, and plant uptake of nitrate were equally fast, therefore little ammonia and nitrate remained in the sub-surface water. In highly fertilized plots, though, nitrification and plant uptake were presumably less than the application rate, resulting in excess ammonia and nitrate in the sub-surface water.

At the *Phragmites*-absent site, plots receiving both low and high nitrogen fertilization amounts had similar ammonia and nitrate water concentrations, implying that ammonification, nitrification and plant uptake had equal rates and that nitrogen was a limiting factor at the site.

Plots receiving nitrogen as urea in dialysis tubes had a slow-release of nitrogen over the growing season, which was reflected by the constant sub-surface ammonia levels for treatments N200/1D and N200/2D (Figure 3.1.1). Several studies on nitrogen fertilizer released slowly over time have shown an enhancement of crop growth and seed yield (Quiroga-Garza et al. 2001; Kaushal et al. 2005) and a reduction of ammonia volatilization, leaching, and denitrification losses, thereby reducing the nitrogen load on the environment (Rathier and Frink 1989; Quiroga-Garza et al. 2001; Prasad 2005). In contrast, one greenhouse study by Hawkins et al. (2005) found no differences in seedling height, biomass, or nutrient concentration between slow-released and regularly applied nitrogen fertilizer on western hemlock.

4.2 Nitrogen fertilization effect on vegetation composition and canopy nutrients

Nitrogen fertilization affected vegetation composition and canopy nutrient concentrations at both study sites. High nitrogen additions produced a low percent cover in *P. australis*, *P. virginica*, and *Typha* species, while moderate nitrogen additions produced a high percent cover (Figures 3.2.4, 3.2.12, and 3.2.15). Meanwhile, percent cover was high for high nitrogen additions for *A. calamus*, *P. arifolium*, and *I. capensis*, and low for moderate urea additions (Figures 3.2.6, 3.2.8, 3.2.9, 3.2.17, and 3.2.18). Canopy nitrogen and phosphorus concentrations were both high for large additions of nitrogen (Figures 3.2.36 – 39).

The effect of nitrogen on species cover in my study had the ability to change the composition of plant communities. Similar findings of nutrient enrichment to wetlands altering community composition have been reported by Cronk and Fennessy (2001). The Environmental Protection Agency has even proposed that vegetation species composition, percent cover, and spectral greenness be used as indicators of health or ecological integrity of wetlands (Cronk and Fennessy, 2001). Also, some have found nitrogen to decrease the diversity index and increase the dominance of a few species (Cronk and Fennessy, 2001), but my results showed no adverse effects on diversity index or species richness due to nitrogen fertilization (Figures 3.2.23 – 24 and 3.2.29 – 30).

In order to recognize a change in species community composition at a wetland, you must first be familiar with its original composition. In my research, the original

vegetation community compositions between study sites differed significantly. Although close in proximity to one another, the *Phragmites*-dominant site had an abundance of *Phragmites australis* (Figure 3.2.1), while the *Phragmites*-absent site had no *P. australis*, but a lot of *Polygonum arifolium* (Figure 3.2.2). Surprisingly, the *Phragmites*-dominant site had more species and a higher species diversity index than the *Phragmites*-absent site (Figures 3.2.22 and 3.2.28), despite the monoculture tendency of the invasive species, *P. australis*. The vegetation community composition also fluctuated greatly throughout the growing season. At the beginning of the season, *Peltandra virginica* had a high percent cover in both marsh sites, but by mid-summer had given way to *P. arifolium*, *P. australis*, and *I. capensis* (Figure 3.4.27 – 8). By the end of the summer, all species were senescing.

Other research on nitrogen effects on vegetation supported my results that excess nitrogen caused an increase to marsh vegetation biomass (Figures 3.2.31 – 32) (Gibson et al., 1994; Kiehl et al., 1997).

4.3 Effects of fertilizer and vegetation on canopy reflectance

Canopy reflectance of the tidal freshwater marsh was affected by vegetation composition and, to an extent, nitrogen fertilization. Certain individual untransformed spectral bands were affected by the addition of nitrogen (Figure 3.3.18), but more bands were affected by nitrogen when the second derivative of the reflectance curve was used (Figure 3.3.19).

Nitrogen had no effect on the three simple ratios, R_{493}/R_{678} , R_{415}/R_{710} , and R_{564}/R_{768} , and two reflectance indices, PRI and NDVI (Figures 3.3.4 – 13), which was contrary to several other studies. NDVI was successfully correlated to nitrogen treatment in cotton (Bronson et al., 2005), and the indices PRI and RE were used to detect changes in total ammonia in a brackish marsh (Tilley et al., 2003). In a greenhouse experiment on four individual marsh plants, however, indices PRI and NDVI distinguished treatment differences in only two species, *A. calamus* and *P. virginica* (Tilley et al., unpublished). It is possible that the diversity of species in the tidal freshwater marsh prevented a nitrogen effect on reflectance ratios or indices.

Canopy reflectance of the two marsh sites had visually different curves, most likely due to the differences in vegetation at each site (Figure 3.3.14). Each species produced a unique reflectance curve due to morphological differences in the plant. Physical differences between species are easy to detect, for instance *P. australis* has smooth leaves and stem versus the shiny, slick leaves of *P. virginica* and the soft, hairy leaves of *P. arifolium*.

Previous research has also been able to distinguish between vegetation types using reflectance. Several studies have found reflectance in the visible and red-edge capable of identifying weeds from crops (Smith and Blackshaw 2003; Chang et al., 2004; Henry et al., 2004). Individual reflectance signatures were also used successfully to discriminate between salt marsh vegetation communities (Schmidt and Skidmore 2003; Silvestri et al., 2003). Clearly, based on the results of this study and

previous research, vegetation in the wetland affected the reflectance curve of each plot. The differences in species at each site produced significant reflectance distinctions between marsh sites.

4.4 Models predictive of nutrient level, vegetation cover, and canopy nutrients

My analyses indicated that partial least squares (PLS) regression can be used to predict sub-surface water nutrient concentrations and vegetation composition in tidal freshwater marshes.

Partial least squares regression models successfully predicted sub-surface water nutrient concentrations at both tidal freshwater marsh sites. Ammonia concentrations were best estimated with untransformed canopy reflectance from August and September (Tables 3.4.1, 3.4.3, and 3.4.5), which was consistent with the ANOVA analysis, where data from the August and September dates were most affected by nitrogen (Figures 3.1.7 – 8). Sub-surface nitrate concentrations were best estimated in August by PLS regressions (Tables 3.4.7, 3.4.9, and 3.4.11), and total phosphorus concentrations were best predicted in August and September (Tables 3.4.17 and 3.4.19). Total nitrogen concentrations were best predicted in July, when N400 suddenly decreased in concentration (Figure 3.1.5).

In my research, I tested several reflectance transformations in the PLS-regression models. Overall, the transformations that worked consistently well for all water quality data regressions were the first and second derivatives of the reflectance curve with the untransformed water quality data or the logarithm of the water quality

concentration. Other researchers have found the first and second derivative useful for predicting nitrogen in vegetation (Townsend et al., 2003; Petisco et al., 2005).

My results also demonstrated that predictive models of vegetation cover could be developed using PLS regression. The percent cover of *P. australis* was well predicted from canopy reflectance in August ($r^2 = 0.85$), while *A. calamus* showed the best results in June when its percent cover was highest ($r^2 = 0.85$) (Table 3.4.23). *P. arifolium* was well predicted at both the *Phragmites*-absent and *Phragmites*-dominant sites during August when it was the dominant species in the marsh ($r^2 = 0.79$) (Table 3.4.23).

For *P. virginica*, predictive models were best in June at the *Phragmites*-dominant site, when *P. virginica* was at a maximum and in August and September at the *Phragmites*-absent site, when *P. virginica* was at a minimum (Figure 3.2.12 and Table 3.4.23). Although *Typha* species had a cover of 8% or less throughout the growing season, a predictive model was developed using PLS-regressions (Table 3.4.23). The best predictive models of *I. capensis* were in July, which was also the date of peak percent cover of *I. capensis* (Figure 3.2.16). I also found PLS-regression models able to predict the amount of exposed soil and the percent cover of dead material in the marsh, as well as LAI ($r^2 = 0.81$ and 0.90) for both marsh sites (Table 3.4.23 and 3.4.25).

My research agrees with earlier studies and concludes that PLS-regression models are able to predict plant species composition using canopy reflectance data. In previous research, Almeida and De Souza Filho (2004) were able to discriminate between vegetation types in riparian forests, burn grasslands, crops and savannahs using principal component analysis of hyperspectral data. Similarly, Schmidtlein and Sassini (2004) modeled the distribution of plant species in grasslands using high-resolution hyperspectral airborne imagery and PLS-regression. Their model agreed with ground-based observations ($r^2 = 0.71$), but they concluded that distinguishing between plant communities with remote sensing techniques was difficult and needed further development.

Other vegetation components measured in my study did not prove to be as predictable with reflectance data as species cover. I was unable to estimate species richness and species diversity index from the marsh canopy reflectance using PLS-regression. However, in a study by Maestre (2004), species richness and diversity were predicted from reflectance using PLS-regression.

Canopy nitrogen, phosphorus, and biomass were also predicted from canopy reflectance using PLS regressions. The first derivative of the reflectance was the best for predicting canopy nitrogen and biomass, whereas the second derivative of the reflectance was best for canopy phosphorus (Table 3.4.21). Other researchers have agreed with my results. Petisco et al. (2005) predicted the leaf nitrogen, phosphorus, and calcium concentrations in several woody plant species using PLS-regressions,

obtaining an $r^2 = 0.99$ for the best nitrogen prediction model. Bronson et al. (2005) and Fridgen and Varco (2004) both developed predictive models of leaf nitrogen in cotton when it was in peak bloom.

4.5 Spectral bands significant to nutrient availability

Spectral bands offering information on canopy nutrients and nutrient availability were identified using PLS regression and ANOVA. Canopy nitrogen and phosphorus both used spectral bands in the red-edge, while canopy phosphorus also had several significant bands in the visible green.

For sub-surface ammonia concentrations, spectral bands in the visible green and along the red-edge were consistently used in PLS-regressions at both the *Phragmites*-dominant and the *Phragmites*-absent sites. Applied ammonia increases the chlorophyll content of plants, which affects both the visible green and the red-edge. Few studies have investigated chlorophyll's relationship to green reflectance, but several have linked chlorophyll to the red-edge, including work by Fridgen and Varco (2004) and Tarpley et al. (2000) on cotton leaf nitrogen where the red-edge was shifted to longer wavelengths as nitrogen supply increased. Other studies found the red-edge increased significantly with less nitrogen fertilization (Zhao et al., 2003; Zhao et al., 2005).

Nitrate PLS-regressions showed significant spectral bands in the red-edge, like ammonia, and also in the near-infrared. Bands in the near-infrared have been correlated to vegetation biomass and nitrogen uptake (Li et al., 2001). Other research

has shown near-infrared spectral bands able to predict wetland vegetation characteristics (Thenkabail et al. 2000; Becker et al. 2005).

Results from total nitrogen regressions had significant spectral bands in the visible green and along the red-edge. Changes in the visible green spectral bands have been linked to nitrogen deficits in plant leaves (Buscaglia and Varco 2002; Zhao et al., 2003; Zhao et al., 2005). Also, green spectral bands have been identified as optimal bands for characterization of agricultural crops (Thenkabail et al., 2000).

Total phosphorus PLS-regressions showed significant spectral bands concentrated primarily in the near-infrared. Vegetation biomass is closely related to near-infrared reflectance and increases with ample phosphorus (Thenkabail et al., 2000).

4.6 Conclusions

The following conclusions were made from the work contained in this thesis:

1. Nitrogen additions to the tidal freshwater marsh plots increased sub-surface nitrogen levels, biomass in the *Phragmites*-absent site, and canopy nitrogen and phosphorus, but did not affect sub-surface phosphorus levels, or biomass of the *Phragmites*-dominant marsh.
2. Applying nitrogen with slow-release dialysis tubes created constant levels of sub-surface nitrogen across the growing season.
3. The percent cover of *P. australis*, *P. virginica*, and *Typha* species was highest for the middle nitrogen application rate, whereas it was highest for *A. calamus*, *P. arifolium*, and *I. capensis* at the highest nitrogen fertilization rate.

4. Canopy reflectance differed due to vegetation composition.
5. Spectral bands in the red-edge (700 – 730 nm) were useful in vegetation and sub-surface water nutrient predictive models.
6. Models developed using Partial Least Squares regression of hyperspectral canopy reflectance were predictive of sub-surface water nutrient concentrations, vegetation composition, exposed soil, dead material, and canopy nutrients in tidal freshwater marshes.

4.7 Implications

The results of this study suggested that the addition of nitrogen to a tidal freshwater marsh increased the concentration of nitrogen in the sub-surface water, increased the amount of nitrogen and phosphorus stored in the vegetation canopy, increased above ground biomass at the marsh that contained no *Phragmites*, and altered the vegetation composition. All of these variables influence the canopy reflectance signature, which indicates that hyperspectral radiometry can be used to detect their changes. PLS modeling of hyperspectral canopy reflectance was found to be useful for indirectly detecting the affects of additional nitrogen. In effect the PLS models could estimate canopy nitrogen, above ground biomass, and the cover of dominant species.

Reflectance differences caused by nitrogen fertilization, biomass, and vegetation composition, radiometry could be a useful tool for assessing wetlands. That is, hyperspectral radiometry could estimate marsh sub-surface water nitrogen, identify dominant marsh species, assess the percent cover of exposed soil and dead material, and estimate canopy nutrient concentrations.

My results also implied that the species *P. australis*, *P. virginica*, and *Typha* species were not nitrogen – limited, because their percent cover did not continue to increase with the addition of nitrogen. Conversely, *A. calamus*, *P. arifolium*, and *I. capensis* did increase in percent cover with high additions of nitrogen, implying these species were nitrogen – limited in the marsh.

APPENDIX A

List of Abbreviations

ANOVA	Analysis of variance
LAI	Leaf area index
N100	100 g – N
N200/1D	200 g – N, 1 dialysis tube
N200/2D	200 g – N, 2 dialysis tubes
N400	400 g
NDVI	$(R_{\text{nir}} - R_{\text{red}}) / (R_{\text{nir}} + R_{\text{red}})$
NH ₃	Ammonia
NIR	Near-infrared
NO ₃	Nitrate
PA site	<i>Phragmites</i> -absent site
PCs	PLS components
PD site	<i>Phragmites</i> -dominant site
PLS	Partial least squares
PRI	$(R_{531} - R_{570}) / (R_{531} + R_{570})$
R	Correlation coefficient
R ²	Coefficient of determination
RE	Red edge
RMSEP	Root mean square error of prediction
TKN	Total nitrogen
TP	Total phosphorus
VNIR	Visible and near-infrared

APPENDIX B Spectral Bands Used in ANOVA and PLS-regressions

B1. List of significant spectral bands used in PLS regression models for sub-surface water nutrients.

NH ₃						NH ₃	NO ₃							
Both sites	NH ₃ PD site					PA site	Both sites	NO ₃ PD site			NO ₃ PA site			
511	513	560	704	793	910	492	530	446	533	562	512	697	725	765
512	514	561	705	794	914	493	538	447	534	563	530	698	729	766
513	527	562	706	803	915	508	539	448	536	564	531	699	730	767
514	528	569	707	807	916	509	549	449	537	565	537	700	731	832
515	529	570	708	808	917	511	550	450	538	566	573	701	732	894
533	530	573	709	809	918	532	551	496	539	567	574	702	733	895
534	531	574	710	813	919	547	552	497	540	568	575	703	734	896
812	532	575	711	814	923	590	553	498	541	569	576	704	735	
821	533	578	712	815	924	592	558	499	542	570	577	705	736	
824	534	582	713	816	925	601	559	500	543	571	578	706	737	
976	535	583	714	822	926	935	560	501	544	572	579	707	738	
	536	584	715	862	927		561	510	545	573	580	708	739	
	537	585	716	863	928		562	511	546	574	587	709	740	
	538	586	717	864	967		563	515	547	576	588	710	741	
	539	599	718	871	1035		564	516	548	577	589	711	742	
	543	606	720	872			565	517	549	578	597	712	743	
	544	611	729	874			567	521	550	580	598	713	744	
	545	677	732	875			573	522	551	602	606	714	745	
	547	682	759	876			574	523	552	615	607	715	746	
	551	695	760	898			575	524	553	616	608	716	747	
	552	696	761	899			576	525	554	617	609	717	748	
	553	697	762	900			577	526	555	618	610	718	749	
	554	698	787	901			579	527	556	619	611	719	750	
	555	699	788	903			580	528	557	620	612	720	751	
	556	700	789	906			581	529	558	659	689	721	752	
	557	701	790	907			582	530	559	864	694	722	753	
	558	702	791	908			584	531	560		695	723	763	
	559	703	792	909			617	532	561		696	724	764	

TKN PD site					TKN PA site			TP PA site	
430	489	538	566	712	394	573	684	515	750
446	493	539	567	713	521	574	700	517	752
447	494	540	568	714	522	576	702	518	785
448	495	541	569	715	523	578	703	522	820
449	496	542	570	716	524	579	704	523	
450	497	543	571	717	525	580	705	524	
451	499	544	572	718	526	581	706	525	
459	500	545	573	719	527	586	707	526	
460	501	546	574	720	528	587	708	527	
461	518	547	575	721	529	588	709	528	
462	519	548	576	722	530	589	710	529	
466	520	549	577	723	531	590	711	530	
467	521	550	578	724	532	591	712	531	
468	522	551	579	725	533	592	713	532	
469	523	552	580	726	534	593		533	
470	524	553	581	727	535	594		534	
471	525	554	582	728	536	603		535	
472	526	555	584	729	537	604		536	
477	527	556	585	730	538	605		537	
478	528	557	588	731	545	624		538	
480	529	558	589		546	625		539	
481	530	559	590		566	626		540	
482	532	560	591		567	642		541	
483	533	561	595		568	645		542	
485	534	562	597		569	646		544	
486	535	563	598		570	647		547	
487	536	564	599		571	648		741	
488	537	565	711		572	649		749	

TP PD site							
508	582	783	865	902	941	985	1022
511	583	793	866	903	945	987	1023
512	584	800	867	904	950	988	1028
513	585	801	868	905	951	989	1029
514	586	802	869	906	952	990	1030
515	587	806	870	907	954	991	1032
516	588	807	872	908	959	992	1033
517	589	808	873	909	960	993	1036
518	590	811	874	910	961	994	1038
519	591	822	875	911	962	995	1042
538	592	825	876	912	963	996	1043
549	593	826	877	913	965	997	1044
550	594	827	878	915	966	998	1045
567	595	828	879	916	967	999	1050
568	596	829	880	917	968	1000	1051
569	597	846	881	918	969	1001	1052
570	598	847	882	919	970	1002	1055
571	599	848	883	920	971	1003	1060
572	600	849	884	921	972	1004	1069
573	601	850	885	922	973	1006	1073
574	602	851	886	923	974	1007	
575	603	852	893	924	975	1008	
576	604	853	896	925	976	1011	
577	605	854	897	926	977	1015	
578	606	855	898	930	979	1017	
579	607	862	899	931	980	1018	
580	608	863	900	936	981	1019	
581	615	864	901	938	984	1021	

<i>P. australis</i> PD site				<i>A. calamus</i> PD site				<i>P. arifolium</i> PA site								
483	546	574	728	429	706	849	881	432	539	569	607	682	751	808	840	875
484	547	575	729	430	707	852	882	507	540	570	608	683	752	809	841	876
500	548	576	730	431	712	853	883	508	541	571	609	684	753	810	842	877
518	549	577	731	432	718	854	885	509	542	572	610	685	758	811	843	878
520	550	700	732	438	719	856	886	512	543	573	622	686	775	812	844	881
521	551	701	733	439	720	857	887	513	544	574	644	687	776	813	845	887
522	552	702	734	455	721	859	888	514	545	575	645	689	777	814	846	891
523	553	704	1002	471	722	860	889	515	546	576	646	691	778	815	847	958
524	554	705		532	723	861	992	517	547	577	647	692	779	816	848	962
526	555	706		533	724	862	993	518	548	578	650	694	781	817	849	
527	556	707		534	725	863	999	519	549	579	651	709	784	818	850	
528	557	708		535	726	864	1000	522	550	584	655	710	785	819	851	
529	558	709		536	727	865	1001	523	551	585	656	716	786	820	852	
531	559	710		537	728	866	1004	524	552	586	657	717	787	821	853	
532	560	711		554	729	867	1007	525	553	587	658	724	788	822	854	
533	561	712		555	730	868	1016	526	556	588	659	725	794	825	855	
534	562	713		556	731	869	1017	527	557	589	660	726	795	826	856	
535	563	714		557	732	870	1056	528	558	590	661	727	796	827	857	
536	564	718		558	733	871	1062	529	559	591	665	728	797	828	858	
537	565	719		559	734	872		530	560	592	666	729	798	829	859	
538	566	720		560	761	873		531	561	593	667	730	800	830	860	
539	567	721		561	762	874		532	562	594	668	731	801	832	863	
540	568	722		562	842	875		533	563	595	669	732	802	833	864	
541	569	723		563	843	876		534	564	599	672	733	803	834	865	
542	570	724		564	844	877		535	565	602	673	734	804	835	866	
543	571	725		574	845	878		536	566	603	674	744	805	836	867	
544	572	726		575	847	879		537	567	604	678	748	806	838	868	
545	573	727		578	848	880		538	568	605	679	749	807	839	874	

B2. List of significant spectral bands determined through PLS regression analysis for vegetation.

<i>P. arifolium</i> PD site											<i>P. virginica</i> PD site	
386	543	571	604	714	742	772	800	828	856	990	882	925
466	544	572	605	715	743	773	801	829	857	991	883	926
517	545	573	610	716	744	774	802	830	858	993	890	927
518	546	574	611	717	745	775	803	831	859	994	891	928
519	547	575	612	718	746	776	804	832	860	1003	892	929
520	548	576	613	719	747	777	805	833	861	1005	893	930
521	549	577	614	720	748	778	806	834	862	1006	894	931
522	550	578	686	721	749	779	807	835	863	1018	895	964
523	551	579	691	722	750	780	808	836	864	1019	896	968
524	552	580	692	723	751	781	809	837	865	1020	897	969
525	553	581	693	724	752	782	810	838	866	1021	898	970
526	554	582	694	725	753	783	811	839	867	1022	900	971
527	555	583	695	726	754	784	812	840	873	1023	905	972
528	556	584	696	727	755	785	813	841	874	1028	906	973
529	557	585	697	728	756	786	814	842	888		907	974
530	558	586	698	729	757	787	815	843	889		908	975
531	559	588	699	730	758	788	816	844	899		909	987
532	560	589	703	731	759	789	817	845	900		910	988
533	561	590	704	732	760	790	818	846	912		911	1021
534	562	591	705	733	761	791	819	847	913		912	1022
535	563	592	706	734	762	792	820	848	915		913	1028
536	564	593	707	735	763	793	821	849	916		914	1035
537	565	596	708	736	764	794	822	850	917		916	1051
538	566	599	709	737	767	795	823	851	919		918	1054
539	567	600	710	738	768	796	824	852	920		921	1067
540	568	601	711	739	769	797	825	853	921		922	
541	569	602	712	740	770	798	826	854	922		923	
542	570	603	713	741	771	799	827	855	959		924	

<i>P. virginica</i> PA site															
514	545	573	603	659	694	722	750	778	806	834	862	890	918	947	998
518	546	574	604	660	695	723	751	779	807	835	863	891	919	948	1000
519	547	575	605	661	696	724	752	780	808	836	864	892	920	949	1001
520	548	576	606	662	697	725	753	781	809	837	865	893	921	950	1013
521	549	577	611	663	698	726	754	782	810	838	866	894	922	951	1022
522	550	578	612	664	699	727	755	783	811	839	867	895	923	952	1039
523	551	579	613	665	700	728	756	784	812	840	868	896	924	953	
524	552	580	614	666	701	729	757	785	813	841	869	897	925	954	
525	553	581	615	667	702	730	758	786	814	842	870	898	926	955	
526	554	582	616	668	703	731	759	787	815	843	871	899	927	956	
527	555	583	617	669	704	732	760	788	816	844	872	900	928	957	
528	556	584	618	670	705	733	761	789	817	845	873	901	929	958	
529	557	585	619	671	706	734	762	790	818	846	874	902	930	961	
530	558	586	640	672	707	735	763	791	819	847	875	903	931	965	
531	559	587	641	673	708	736	764	792	820	848	876	904	932	966	
532	560	588	642	674	709	737	765	793	821	849	877	905	933	967	
533	561	589	643	675	710	738	766	794	822	850	878	906	934	968	
534	562	590	644	676	711	739	767	795	823	851	879	907	935	969	
535	563	591	645	677	712	740	768	796	824	852	880	908	936	970	
536	564	592	646	680	713	741	769	797	825	853	881	909	937	971	
537	565	593	650	681	714	742	770	798	826	854	882	910	938	978	
538	566	594	651	683	715	743	771	799	827	855	883	911	939	979	
539	567	595	652	687	716	744	772	800	828	856	884	912	941	980	
540	568	598	653	688	717	745	773	801	829	857	885	913	942	984	
541	569	599	654	689	718	746	774	802	830	858	886	914	943	987	
542	570	600	655	691	719	747	775	803	831	859	887	915	944	988	
543	571	601	656	692	720	748	776	804	832	860	888	916	945	989	
544	572	602	657	693	721	749	777	805	833	861	889	917	946	997	

					<i>I. capensis</i>				
<i>Typha</i> species PA site					PD site	<i>I. capensis</i> PA site		LAI PD site	
400	582	610	717	796	337	339	656	354	612
401	583	611	718	813	406	344	657	355	613
408	584	612	719	814	520	347	658	365	614
414	585	613	720	816	523	348	659	366	615
424	586	620	721	817	528	356	660	509	616
430	587	621	722	818	530	357	661	510	617
453	588	622	723	819	537	358	674	512	618
454	589	695	724	820	539	359		513	619
463	590	696	725	823	540	360		518	620
464	591	697	726	829	541	365		519	621
484	592	698	727	830	542	366		588	622
495	593	699	728	834	554	368		589	638
496	594	700	729		555	370		592	640
566	595	701	730		596	371		593	641
567	596	702	731		606	374		594	651
569	597	703	732		607	376		595	652
570	598	704	733			384		596	
571	599	705	734			390		597	
572	600	706	735			392		598	
573	601	707	736			405		599	
574	602	708	737			447		600	
575	603	710	738			448		601	
576	604	711	739			449		602	
577	605	712	740			460		603	
578	606	713	748			619		604	
579	607	714	749			653		605	
580	608	715	776			654		606	
581	609	716	777			655		607	

LAI PA site													
358	520	549	582	612	677	705	733	761	789	817	845	873	901
359	521	555	583	613	678	706	734	762	790	818	846	874	902
362	522	556	584	614	679	707	735	763	791	819	847	875	904
371	523	557	585	622	680	708	736	764	792	820	848	876	905
374	525	558	586	639	681	709	737	765	793	821	849	877	908
387	526	559	587	640	682	710	738	766	794	822	850	878	909
393	527	560	588	641	683	711	739	767	795	823	851	879	913
394	528	561	591	642	684	712	740	768	796	824	852	880	914
408	529	562	592	646	685	713	741	769	797	825	853	881	915
434	530	563	593	647	686	714	742	770	798	826	854	882	916
438	531	564	594	652	687	715	743	771	799	827	855	883	923
502	532	565	595	653	688	716	744	772	800	828	856	884	934
503	533	566	596	654	689	717	745	773	801	829	857	885	935
505	534	567	597	656	690	718	746	774	802	830	858	886	936
506	535	568	598	657	691	719	747	775	803	831	859	887	937
507	536	569	599	661	692	720	748	776	804	832	860	888	938
508	537	570	600	662	693	721	749	777	805	833	861	889	939
509	538	571	601	664	694	722	750	778	806	834	862	890	941
510	539	572	602	665	695	723	751	779	807	835	863	891	942
511	540	573	603	666	696	724	752	780	808	836	864	892	943
512	541	574	604	667	697	725	753	781	809	837	865	893	957
513	542	575	605	670	698	726	754	782	810	838	866	894	958
514	543	576	606	671	699	727	755	783	811	839	867	895	1041
515	544	577	607	672	700	728	756	784	812	840	868	896	
516	545	578	608	673	701	729	757	785	813	841	869	897	
517	546	579	609	674	702	730	758	786	814	842	870	898	
518	547	580	610	675	703	731	759	787	815	843	871	899	
519	548	581	611	676	704	732	760	788	816	844	872	900	

Species												
Richness	Percent Dead Material						Diversity Index			Bare Area		
706	638	755	784	812	840	868	648	749	830	416	449	486
707	639	756	785	813	841	869	658	750	831	417	450	490
708	715	757	786	814	842	870	661	751	841	419	451	491
1023	730	758	787	815	843	871	662	752	944	420	452	493
	731	760	788	816	844	872	722	753	952	421	453	494
	732	761	789	817	845	873	723	754	953	422	454	806
	733	762	790	818	846	874	725	755	955	424	455	807
	734	763	791	819	847	875	727	756	960	425	456	808
	735	764	792	820	848	876	729	757	974	427	457	882
	736	765	793	821	849	877	730	758	985	428	458	889
	737	766	794	822	850	878	731	761	986	430	459	890
	738	767	795	823	851	879	732	766	987	431	463	891
	739	768	796	824	852	880	733	767	988	432	466	
	740	769	797	825	853	882	734	768	990	433	467	
	741	770	798	826	854	883	735	769	995	434	468	
	742	771	799	827	855	885	736	775	996	435	469	
	743	772	800	828	856	887	737	778	998	436	470	
	744	773	801	829	857	888	738	779	1002	437	471	
	745	774	802	830	858	889	739	782	1013	438	472	
	746	775	803	831	859	891	740	784	1019	439	473	
	747	776	804	832	860	904	741	785		440	475	
	748	777	805	833	861	912	742	786		441	476	
	749	778	806	834	862	915	743	791		442	479	
	750	779	807	835	863	916	744	794		443	480	
	751	780	808	836	864	922	745	801		444	481	
	752	781	809	837	865	941	746	806		446	483	
	753	782	810	838	866	942	747	809		447	484	
	754	783	811	839	867		748	813		448	485	

B3. List of significant spectral bands identified by an ANOVA model as significantly affected by nitrogen for the second derivative of reflectance (Golay)

6/16/04 <i>Phragmites</i> -dominant site									
415	506	538	569	611	672	703	743	785	895
442	507	539	572	621	673	704	744	786	896
448	508	540	573	622	677	705	745	790	897
453	509	541	574	623	678	706	746	791	903
454	510	542	575	624	679	707	747	795	914
455	511	543	576	625	680	708	748	796	919
456	512	547	577	626	681	709	749	797	920
457	513	548	578	627	682	710	750	802	921
458	514	549	579	640	683	711	751	803	928
467	515	550	580	641	684	712	752	810	929
468	516	551	581	642	685	713	756	811	934
478	517	552	582	643	686	714	757	816	941
479	518	553	583	644	687	718	758	817	946
485	519	554	584	648	688	719	762	818	975
489	520	555	590	649	689	720	763	822	976
490	525	556	591	655	690	721	764	823	
491	526	557	592	660	691	722	765	824	
492	527	558	593	661	692	723	768	832	
493	528	559	594	662	693	733	769	840	
494	529	560	597	663	694	734	770	868	
495	530	561	603	664	695	735	771	869	
499	531	562	604	665	696	736	772	870	
500	532	563	605	666	697	737	773	880	
501	533	564	606	667	698	738	774	886	
502	534	565	607	668	699	739	775	887	
503	535	566	608	669	700	740	776	888	
504	536	567	609	670	701	741	777	889	
505	537	568	610	671	702	742	784	890	

6/16/04 <i>Phragmites</i> -absent site									
406	506	536	564	603	640	673	701	739	869
420	507	537	565	604	641	674	702	740	873
421	508	538	566	605	642	675	703	741	874
422	509	539	567	606	643	676	704	742	891
427	510	540	568	607	647	677	705	743	892
428	511	541	569	608	648	678	706	744	906
445	512	542	570	609	649	679	707	745	923
455	513	543	572	610	650	680	708	746	924
456	514	544	573	613	651	681	709	747	925
466	515	545	574	618	652	682	710	748	926
467	516	546	575	619	653	683	711	749	927
479	517	547	576	620	656	684	712	750	931
480	518	548	577	621	657	685	713	751	932
481	519	549	578	622	658	686	714	752	933
485	520	550	579	623	659	687	725	757	934
486	521	551	580	624	660	688	726	758	936
490	524	552	581	625	661	689	727	759	937
491	525	553	582	627	662	690	728	760	938
492	526	554	583	628	663	691	729	771	973
493	527	555	584	629	664	692	730	772	974
494	528	556	585	630	665	693	731	773	975
495	529	557	592	631	666	694	732	774	996
496	530	558	593	632	667	695	733	787	
501	531	559	594	633	668	696	734	792	
502	532	560	595	636	669	697	735	793	
503	533	561	596	637	670	698	736	812	
504	534	562	601	638	671	699	737	813	
505	535	563	602	639	672	700	738	828	

6/29/04 <i>Phragmites</i> -dominant site								6/29/04 <i>Phragmites</i> -absent site										
471	534	569	642	693	721	752	815	996	412	513	546	576	621	668	700	734	767	955
472	535	574	649	694	722	753	816		417	514	547	577	622	673	701	735	768	
495	536	575	650	695	723	755	817		433	515	548	578	623	674	702	736	769	
496	537	576	667	696	724	756	825		435	516	549	579	624	675	703	737	770	
497	538	577	668	697	725	757	826		436	517	550	580	625	676	704	738	771	
498	539	578	669	698	726	758	827		459	518	551	581	626	677	705	739	772	
499	540	579	671	699	727	759	830		464	519	552	582	627	678	706	740	773	
505	541	580	672	700	731	761	831		491	520	553	583	635	679	707	741	774	
506	547	581	673	701	732	762	832		492	525	554	584	636	680	708	742	780	
507	550	582	674	702	733	763	862		493	526	555	585	637	681	709	743	781	
508	551	584	675	703	734	764	863		494	527	556	588	638	682	710	744	787	
509	552	585	676	704	735	767	889		495	528	557	590	639	683	711	745	793	
510	553	586	677	705	736	768	890		496	529	558	591	640	684	712	746	798	
511	554	591	678	706	737	769	894		497	530	559	592	641	685	713	747	804	
512	555	592	679	707	738	770	895		499	531	560	593	642	686	714	748	811	
513	556	593	680	708	739	771	896		500	532	561	594	643	687	715	749	824	
516	557	594	681	709	740	772	901		501	533	562	600	647	688	716	750	825	
517	558	608	682	710	741	773	903		502	534	563	601	648	689	717	751	826	
518	559	610	683	711	742	774	904		503	535	564	602	649	690	721	752	827	
519	560	622	684	712	743	790	905		504	536	565	603	650	691	722	753	828	
522	561	627	685	713	744	791	920		505	537	566	604	651	692	726	754	830	
527	562	628	686	714	745	807	936		506	538	567	605	652	693	727	755	831	
528	563	632	687	715	746	808	966		507	539	568	606	661	694	728	756	834	
529	564	637	688	716	747	809	972		508	540	569	607	662	695	729	757	835	
530	565	638	689	717	748	810	977		509	541	572	610	663	696	730	761	836	
531	566	639	690	718	749	811	986		510	542	573	611	665	697	731	762	918	
532	567	640	691	719	750	812	987		511	543	574	619	666	698	732	763	919	
533	568	641	692	720	751	814	990		512	545	575	620	667	699	733	766	941	

7/19/04 <i>Phragmites</i> -dominant site								7/19/04 <i>Phragmites</i> -absent site							
421	540	579	679	709	745	773	922	413	530	560	594	680	713	751	963
458	541	580	680	710	746	774	923	414	531	561	595	681	714	756	964
477	548	581	681	711	747	780	931	417	532	562	600	682	725	757	
489	549	582	682	712	748	781	932	418	533	563	601	683	726	758	
497	550	583	683	713	749	805	938	422	534	564	604	684	727	762	
500	551	585	686	714	750	806	972	452	535	565	620	685	728	763	
501	552	592	687	715	751	807	974	497	536	566	621	686	729	764	
502	553	593	688	716	752	808		502	537	567	622	687	730	768	
503	554	594	689	717	753	809		503	538	568	623	688	731	769	
504	555	595	690	718	754	810		504	539	569	624	689	732	770	
505	556	600	691	719	755	811		505	540	572	637	690	733	771	
506	557	601	692	720	756	815		506	541	573	638	691	734	772	
509	558	610	693	724	757	816		507	542	574	639	692	735	773	
510	559	620	694	725	758	817		508	543	575	640	693	736	857	
513	560	622	695	731	759	820		509	546	576	641	694	737	858	
514	561	623	696	732	760	827		510	547	577	642	695	738	861	
515	562	624	697	733	761	828		511	548	578	650	696	739	862	
516	563	625	698	734	762	829		512	549	579	651	697	740	872	
518	564	626	699	735	763	830		513	550	580	652	698	741	879	
519	565	636	700	736	764	831		514	551	581	667	699	742	896	
520	566	641	701	737	765	846		515	552	582	670	700	743	902	
524	567	642	702	738	766	860		516	553	583	671	701	744	903	
525	568	643	703	739	767	889		520	554	584	672	702	745	916	
534	569	650	704	740	768	890		525	555	585	674	703	746	917	
535	573	654	705	741	769	895		526	556	590	675	708	747	918	
537	576	672	706	742	770	896		527	557	591	676	709	748	935	
538	577	677	707	743	771	897		528	558	592	678	711	749	936	
539	578	678	708	744	772	920		529	559	593	679	712	750	941	

8/24/04 <i>Phragmites</i> -dominant site					8/24/04 <i>Phragmites</i> -absent site								
492	553	671	704	755	487	519	550	582	625	672	700	748	
494	554	674	705	756	492	520	551	583	636	673	701	749	
504	555	675	706	762	493	524	552	584	637	674	702	750	
505	556	676	707	767	494	525	553	585	638	675	713	751	
509	557	680	708	768	495	526	554	587	639	676	722	752	
510	558	681	709	769	496	527	555	588	640	677	723	756	
512	559	682	710	772	497	528	556	590	641	678	726	761	
513	560	683	718	812	498	529	557	591	642	679	727	762	
521	561	684	733	813	499	530	558	592	645	680	728	767	
527	563	685	734	835	500	531	559	593	647	681	729	768	
528	564	686	735	841	501	532	560	594	648	682	730	769	
529	565	687	736	847	502	533	561	600	649	683	731	807	
530	566	688	737	851	503	534	562	601	650	684	732	808	
531	567	689	738	861	504	535	563	602	651	685	733	809	
532	568	690	739	864	505	536	564	603	652	686	734	815	
533	576	691	740	870	506	537	565	604	655	687	735	821	
534	577	692	741	896	507	538	566	605	656	688	736	822	
535	578	693	742	901	508	539	567	606	657	689	737	823	
536	579	694	743	917	509	540	568	607	658	690	738	831	
537	580	695	744	940	510	541	569	608	663	691	739	832	
541	611	696	745	955	511	542	574	617	664	692	740	891	
542	619	697	746		512	543	575	618	665	693	741	899	
546	620	698	747		513	544	576	619	666	694	742	924	
547	622	699	748		514	545	577	620	667	695	743	956	
549	623	700	749		515	546	578	621	668	696	744	961	
550	624	701	750		516	547	579	622	669	697	745	965	
551	625	702	751		517	548	580	623	670	698	746		
552	655	703	752		518	549	581	624	671	699	747		

9/21/04 <i>Phragmites</i> -dominant site					9/21/04 <i>Phragmites</i> -absent site		6/06/05 PD site	6/06/05 PA site		8/02/05 PD site		8/02/05 PA site
410	567	687	745	955	440	803	457	387	1068	390	822	352
414	568	688	746	956	531	809	458	389	1069	470	823	353
433	569	689	747	957	548	815	478	390	1071	471	824	354
442	570	690	748	958	567	816	523	420		492	827	452
500	573	691	749	959	572	863	529	421		493	847	524
501	574	692	750	960	577	885	530	493		502	867	629
502	575	693	751	992	582	886	539	505		503	875	648
503	576	694	768	993	583	983	572	506		504	880	670
504	580	695	769		584	1000	574	545		528	929	671
511	581	696	839		623		576	546		529	930	692
512	582	697	840		624		593	587		530	934	704
513	592	698	858		682		594	860		531	936	728
530	597	699	897		683		601	861		547	988	739
533	607	700	940		684		602	862		581	996	766
534	608	701	941		685		629	901		640	1038	767
535	667	728	942		686		787	926		644	1046	790
536	675	729	943		687		793	936		645	1048	791
548	676	730	944		688		794	940		654		822
549	677	734	945		689		838	941		656		823
550	678	735	946		690		846	966		697		827
551	679	736	947		711			967		698		865
557	680	738	948		727			985		726		866
558	681	739	949		728			986		727		896
559	682	740	950		729			1033		728		902
560	683	741	951		735			1034		736		907
561	684	742	952		736			1035		763		966
565	685	743	953		737			1064		764		
566	686	744	954		797			1067		795		

<i>Phragmites</i> -dominant site summary						<i>Phragmites</i> -absent site summary							
500	540	576	682	710	755	492	527	556	590	648	688	732	773
501	541	577	683	711	756	493	528	557	591	649	689	733	
502	547	578	684	712	757	494	529	558	592	650	690	734	
503	548	579	685	713	758	495	530	559	593	651	691	735	
504	549	580	686	714	762	496	531	560	594	652	692	736	
505	550	581	687	718	763	497	532	561	600	663	693	737	
506	551	582	688	719	764	501	533	562	601	665	694	738	
509	552	592	689	720	767	502	534	563	602	666	695	739	
510	553	593	690	733	768	503	535	564	603	667	696	740	
511	554	594	691	734	769	504	536	565	604	668	697	741	
512	555	608	692	735	770	505	537	566	605	670	698	742	
513	556	610	693	736	771	506	538	567	606	671	699	743	
516	557	622	694	737	772	507	539	568	607	672	700	744	
518	558	623	695	738	773	508	540	569	619	673	701	745	
519	559	624	696	739	774	509	541	572	620	674	702	746	
527	560	625	697	740	810	510	542	573	621	675	703	747	
528	561	641	698	741	811	511	543	574	622	676	708	748	
529	562	642	699	742	816	512	545	575	623	677	709	749	
530	563	667	700	743	817	513	546	576	624	678	711	750	
531	564	671	701	744	889	514	547	577	625	679	712	751	
532	565	672	702	745	890	515	548	578	636	680	713	752	
533	566	675	703	746	895	516	549	579	637	681	714	756	
534	567	676	704	747	896	517	550	580	638	682	726	757	
535	568	677	705	748	897	518	551	581	639	683	727	762	
536	569	678	706	749	920	519	552	582	640	684	728	768	
537	573	679	707	750		520	553	583	641	685	729	769	
538	574	680	708	751		525	554	584	642	686	730	771	
539	575	681	709	752		526	555	585	647	687	731	772	

Table C1. PLS-regressions for *P. australis* percent cover at the *Phragmites*-dominant (PD) site. r = regression coefficient, RMSEP = root mean square error of prediction, PCs = PLS-components

Spectra Transformations	<i>P. australis</i> Transformations	Date	r	RMSEP	n	Name of plots removed	PCs	# bands used	Comments
Norris 1 st Derivative	none	8.02.05	0.92	12.03	15	none	3	142	none
Untransformed d (350-1075nm)	none	8.02.05	0.87	15.81	15	none	3	157	none
Golay 2 nd Derivative, avg 10	none	8.02.05	0.86	16.12	15	none	2	13	none
Norris 1 st Derivative	Log PHAU	8.24.04	0.83	0.28	14	Plot 6	3	70	Plot 6: high reflectance
Truncated spectra (400-950nm)	none	8.24.04	0.81	13.82	14	Plot 6	5	20	Plot 6: high reflectance
Untransformed d (350-1075nm)	none	6.06.05	0.79	16.09	15	none	3	213	none
Untransformed d (350-1075nm)	Square root PHAU Log (base 10)	8.24.04	0.79	1.55	15	none	5	24	none
Untransformed d (350-1075nm)	PHAU	8.24.04	0.79	0.32	15	none	4	36	none
Norris 1 st Derivative	none	8.24.04	0.79	14.39	14	Plot 6	2	52	Plot 6: high reflectance
Untransformed d (350-1075nm)	none	5.25.04	0.78	10.47	14	Plot 6	6	40	Plot 10: high <i>Phragmites</i> concentration
Untransformed d (350-1075nm)	4th root PHAU	8.24.04	0.78	0.38	15	none	4	37	none
Golay 2 nd Derivative, avg 10	Log PHAU	8.24.04	0.77	0.33	15	none	1	53	none
MSC Transformation	none	8.24.04	0.75	15.69	15	none	3	21	none
Log R	Square root PHAU	7.19.04	0.73	1.44	13	Plots 5, 10	5	387	Plot 5: high reflectance; Plot 10: low reflectance
Log R	Square root PHAU	8.24.04	0.72	1.79	15	none	5	231	none
Golay 1 st Derivative	none	8.24.04	0.71	16.75	15	Plot 6	1	84	Plot 6: high reflectance
Golay 2 nd Derivative, avg 10	none	8.24.04	0.71	16.20	15	none	1	27	none
Absorbance Transformation	none	8.24.04	0.71	16.59	15	none	3	12	none
Untransformed d (350-1075nm)	none	6.16.04	0.69	14.87	15	none	3	42	none
Untransformed d (350-1075nm)	Arcsine sqrt (PHAU)	8.24.04	0.63	0.22	14	Plot 6	4	136	Plot 6: high reflectance
Untransformed d (350-1075nm)	none	8.24.04	0.60	19.67	14	Plot 6	4	110	Plot 6: high reflectance
Untransformed d (350-1075nm)	none	6.03.04	0.57	21.25	14	Plot 3	3	115	Plot 3: high reflectance

Spectra Transformations	<i>P. australis</i> Transformations	Date	r	RMSEP	n	Name of plots re moved	PCs	# bands used	Comments
Log R	none	8.24.04	0.56	19.25	15	none	3	125	none
Golay 1 st Derivative	none	7.19.04	0.54	19.27	13	Plots 5,10	1	33	Plot 5: high reflectance; Plot 10: low reflectance
Transform 1/R	Arcsine sqrt (PHAU)	8.24.04	0.53	0.25	15	none	3	156	none
Kubelka-Munk Transformation	none	8.24.04	0.53	19.97	15	none	3	162	none
Golay 2 nd Derivative, avg 10	Log PHAU	7.19.04	0.52	0.31	15	none	1	32	none
Transform 1/R	none	8.24.04	0.52	19.97	15	none	3	126	none
Untransformed (350-1075nm)	none	7.19.04	0.49	20.00	13	Plots 5,10	1	113	Plot 5: high reflectance; Plot 10: low reflectance
Truncated spectra (400-950nm)	none	7.19.04	0.49	20.14	13	Plots 5,10	1	129	Plot 5: high reflectance; Plot 10: low reflectance
Transform 1/R	none	7.19.05	0.49	20.71	13	Plots 5,10	7	none	Plot 5: high reflectance; Plot 10: low reflectance
Untransformed (350-1075nm)	none	9.21.04	0.48	20.16	13	Plots 2,11	3	123	Plot 2: high reflectance; Plot 11: high <i>Phragmites</i> conc.
Manual test set	none	8.24.04	0.42	22.07	5	Plot 6	2	none	Plot 6: high reflectance; Remainder used in calib.
Golay 2 nd Derivative, avg 10	none	7.19.04	0.41	22.48	15	none	2	8	none
Norris 1 st Derivative	none	7.19.04	0.35	21.29	15	none	2	11	none
Normalized spectra (R/R410)	none	8.24.04	0.32	22.37	15	none	1	23	none
Random test set	none	8.24.04	0.01	24.18	5	none	1	none	Remainder used for calibration
Untransformed (350-1075nm)	none	6.29.04	-0.24	25.42	15	none	1	none	none

Table C2. PLS-regression transformations tested on *P. australis* percent cover at the *Phragmites*-dominant site.

	Untransformed (350-1075 nm)	Truncated spectra (400-950 nm)	Arcsine sqrt (PHAU)	4th root PHAU	Sqrt (PHAU)	Log ₁₀ PHAU	Manual test set	Random test set	Normalized spectra	Transform 1/R	Transform 1/R, Arcsine sqrt (PHAU)	Log R	Log R, Sqrt (PHAU)
5/25/2004	X												
6/3/2004	X												
6/16/2004	X												
6/29/2004	X												
7/19/2004	X	X								X			X
8/24/2004	X	X	X	X	X	X	X	X	X	X	X	X	X
9/21/2004	X												
6/6/2005	X												
8/2/2005	X												

	Norris 1st Derivative	Norris 1st Deriv, Log (PHAU)	Golay 1st Derivative	Golay 2nd Derivative	Golay 2nd Deriv, Log (PHAU)	MSC Transform	Absorbance Transform	Kubelka-Munk Transform
5/25/2004								
6/3/2004								
6/16/2004								
6/29/2004								
7/19/2004	X		X	X	X			
8/24/2004	X	X	X	X	X	X	X	X
9/21/2004								
6/6/2005								
8/2/2005	X			X				

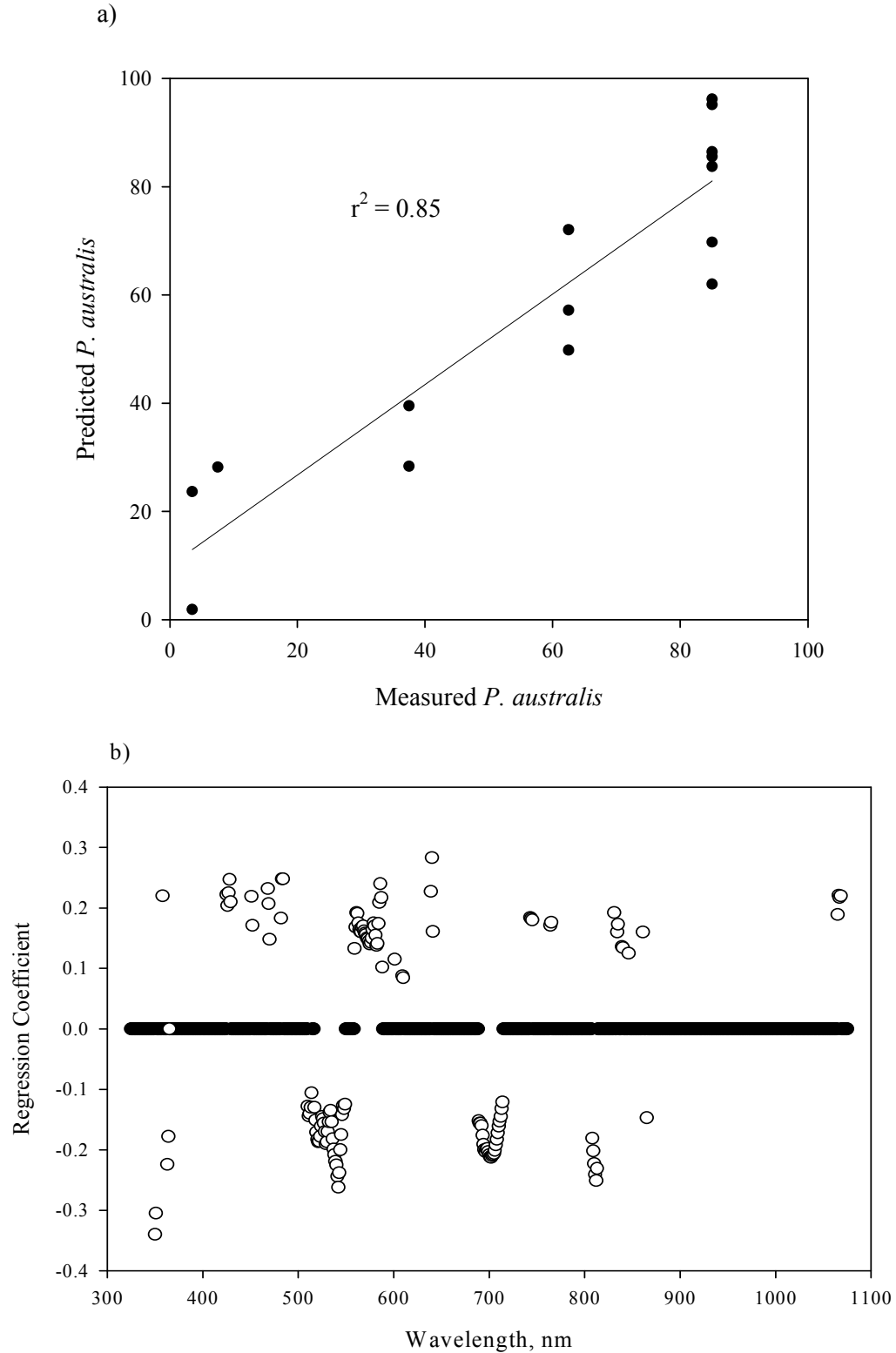


Figure C1. (a) Predicted vs measured *P. australis* PLS-regression at the *Phragmites*-dominant site, 8/02/05 data, which used 142 spectral bands of first derivative reflectance that were combined into three PLS-components with $r = 0.92$ and RMSEP = 12%. (b) Loading plot of regression coefficients for the PLS-regression where significant spectral bands used in the regression are depicted by open circles.

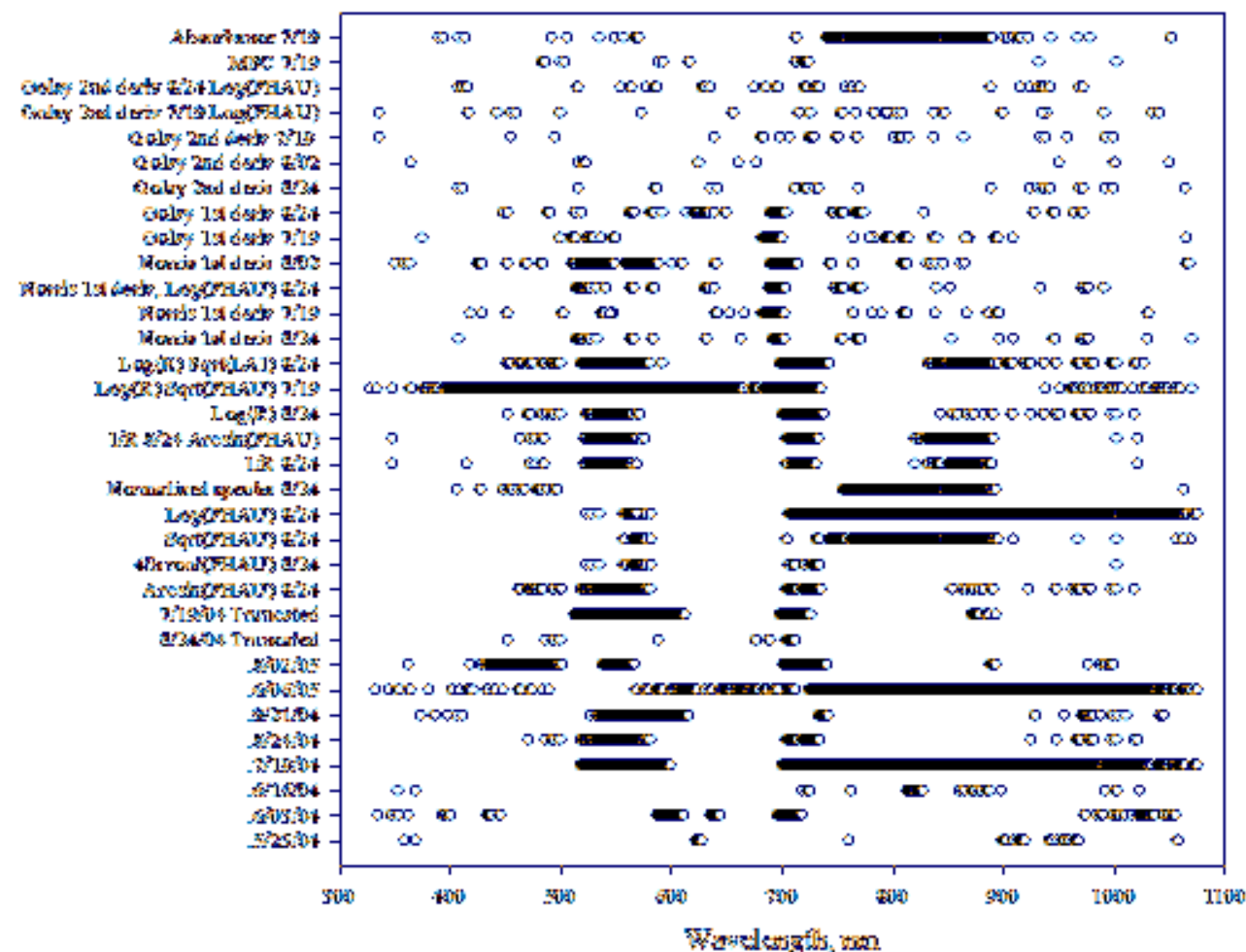


Figure C2. Significant spectral bands for *P. australis* according to PLS-regressions at the *Phragmites*-dominant site.

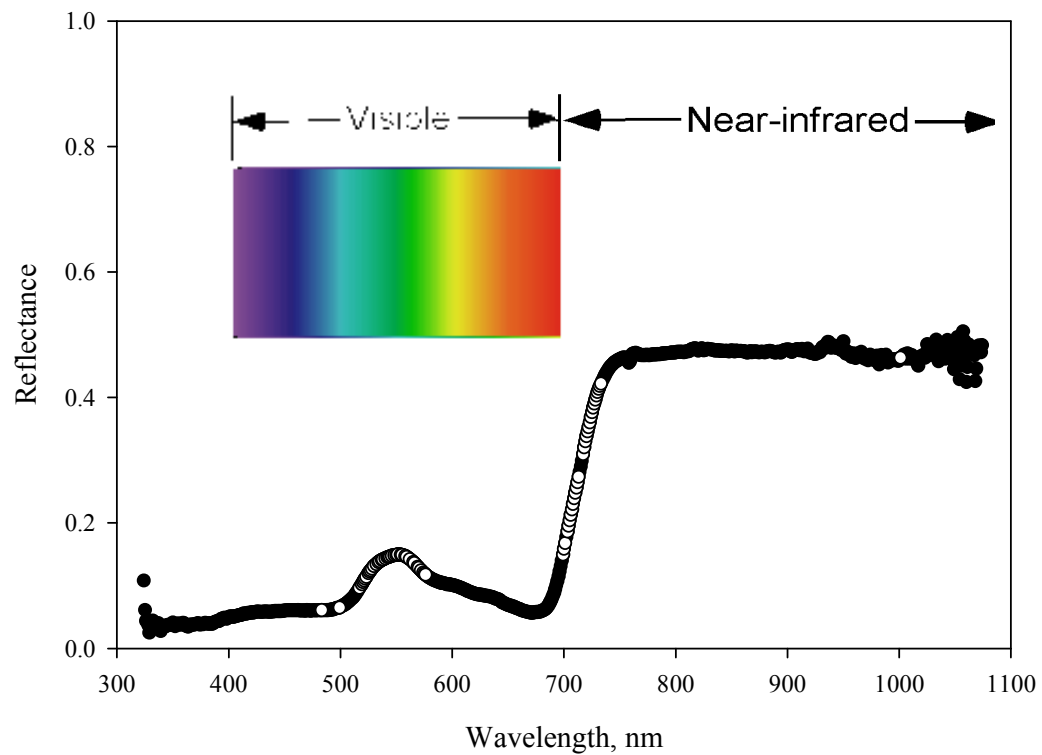


Figure C3. Spectral bands significant for ten or more regressions for *P. australis* at the *Phragmites*-dominant site are indicated by an open circle.

Table C3. PLS-regressions for *A. calamus* cover (%) at the *Phragmites*-dominant (PD) site. *r* = regression coefficient, RMSEP = root mean square error of prediction, PCs = PLS-components

Spectra Transformations	<i>A. calamus</i> Transformations	Date	<i>r</i>	RMSEP	n	Name of plots re moved	PCs	# bands used	Comments
Transform 1/R	none	6.16.04	0.92	6.78	15	none	8	128	none
Transform 1/R	Arcsine sqrt (ACCA)	6.16.04	0.92	6.78	15	none	8	128	none
Kubelka-Munk Transformation	none	6.16.04	0.81	9.95	15	none	4	121	none
Norris 1 st Derivative	none	6.16.04	0.80	10.33	15	none	1	11	none
Golay 2 nd Derivative, avg 10	Log ACCA	6.16.04	0.79	0.33	15	none	1	62	none
Untransformed d (350-1075nm)	none	6.16.04	0.77	10.76	15	none	5	17	none
Untransformed d (350-1075nm)	4th root ACCA Arcsine sqrt (ACCA)	6.16.04	0.75	0.08	13	Plots 3,5	6	24	Plots 3,5: no <i>A. calamus</i> in plot
Untransformed d (350-1075nm)	none	6.16.04	0.74	0.17	15	none	4	35	none
MSC Transformation	none	6.16.04	0.73	11.71	15	none	4	11	none
Log R	none	6.16.04	0.72	11.87	15	none	3	177	none
Absorbance Transformation	none	6.16.04	0.72	11.83	15	none	3	175	none
Untransformed d (350-1075nm)	Square root ACCA	6.16.04	0.71	1.54	15	none	4	34	none
Log R	Square root ACCA	6.16.04	0.71	1.61	15	none	3	115	none
Untransformed d (350-1075nm)	none	8.24.04	0.68	0.87	14	Plot 6	3	82	Plot 6: high reflectance
Golay 1 st Derivative	none	6.16.04	0.67	12.63	15	none	1	57	none
Untransformed d (350-1075nm)	none	7.19.04	0.67	9.15	14	Plot 5	2	38	Plot 5: high reflectance
Norris 1 st Derivative	none	6.29.04	0.63	12.90	14	Plot 4	2	79	Plot 4: high reflectance
Golay 2 nd Derivative, avg 10	none	6.29.04	0.63	13.06	14	Plot 4	1	17	Plot 4: high reflectance
Untransformed d (350-1075nm)	none	5.25.04	0.62	9.19	12	Plots 1-3	2	115	Plots 1-3: missing reflectance
Untransformed d (350-1075nm)	Log (base 10) ACCA	6.16.04	0.58	0.44	15	none	4	16	none

Spectra Transformations	<i>A. calamus</i> Transformations	Date	r	RMSEP	n	Name of plots re moved	PCs	# bands used	Comments
Golay 2 nd Derivative, avg 10	none	6.16.04	0.58	14.85	15	none	1	36	none
Truncated spectra (400-950nm)	none	6.16.04	0.55	15.90	14	Plot 9	3	155	Plot 9: high reflectance
Golay 1 st Derivative	none	6.29.04	0.53	14.13	14	Plot 4	1	10	Plot 4: high reflectance
Untransformed d (350-1075nm)	none	6.06.05	0.50	13.67	15	none	2	316	none
Untransformed d (350-1075nm)	none	6.29.04	0.50	14.38	14	Plot 4	3	10	Plot 4: high reflectance
Transform 1/R	none	6.29.04	0.15	17.11	14	Plot 4	1	none	Plot 4: high reflectance
Untransformed d (350-1075nm)	none	8.02.05	0.15	2.02	14	Plot 11	1	none	Plot 11: low reflectance
Truncated spectra (400-950nm)	none	6.29.04	0.14	17.28	14	Plot 4	2	none	Plot 4: high reflectance
Untransformed d (350-1075nm)	none	6.03.04	0.10	6.36	12	Plots 1-3	1	none	Plots 1-3: high reflectance
Log R	Square root ACCA	6.29.04	0.07	2.09	14	Plot 4	1	none	Plot 4: high reflectance
Untransformed d (350-1075nm)	none	9.21.04	0.20	0.76	15	none	1	none	none

Table C4. PLS-regression transformations tested on spectrum and *A. calamus* percent cover at the *Phragmites*-dominant site.

	Untransformed (350-1075 nm)	Truncated spectra (400-950 nm)	Arcsine sqrt (ACCA)	4th root ACCA	Sqrt (ACCA)	Log ₁₀ ACCA	Transform 1/R	Transform 1/R, Arcsine sqrt (ACCA)	Log R	Log R, Sqrt (ACCA)
5/25/2004	X									
6/3/2004	X									
6/16/2004	X	X	X	X	X	X	X	X	X	X
6/29/2004	X	X					X			X
7/19/2004	X									
8/24/2004	X									
9/21/2004	X									
6/6/2005	X									
8/2/2005	X									

	Norris 1st Derivative	Golay 1st Derivative	Golay 2nd Derivative	Golay 2nd Deriv, Log (ACCA)	MSC Transform	Absorbance Transform	Kubelka-Munk Transform
5/25/2004							
6/3/2004							
6/16/2004	X	X	X	X	X	X	X
6/29/2004	X	X	X				
7/19/2004							
8/24/2004							
9/21/2004							
6/6/2005							
8/2/2005							

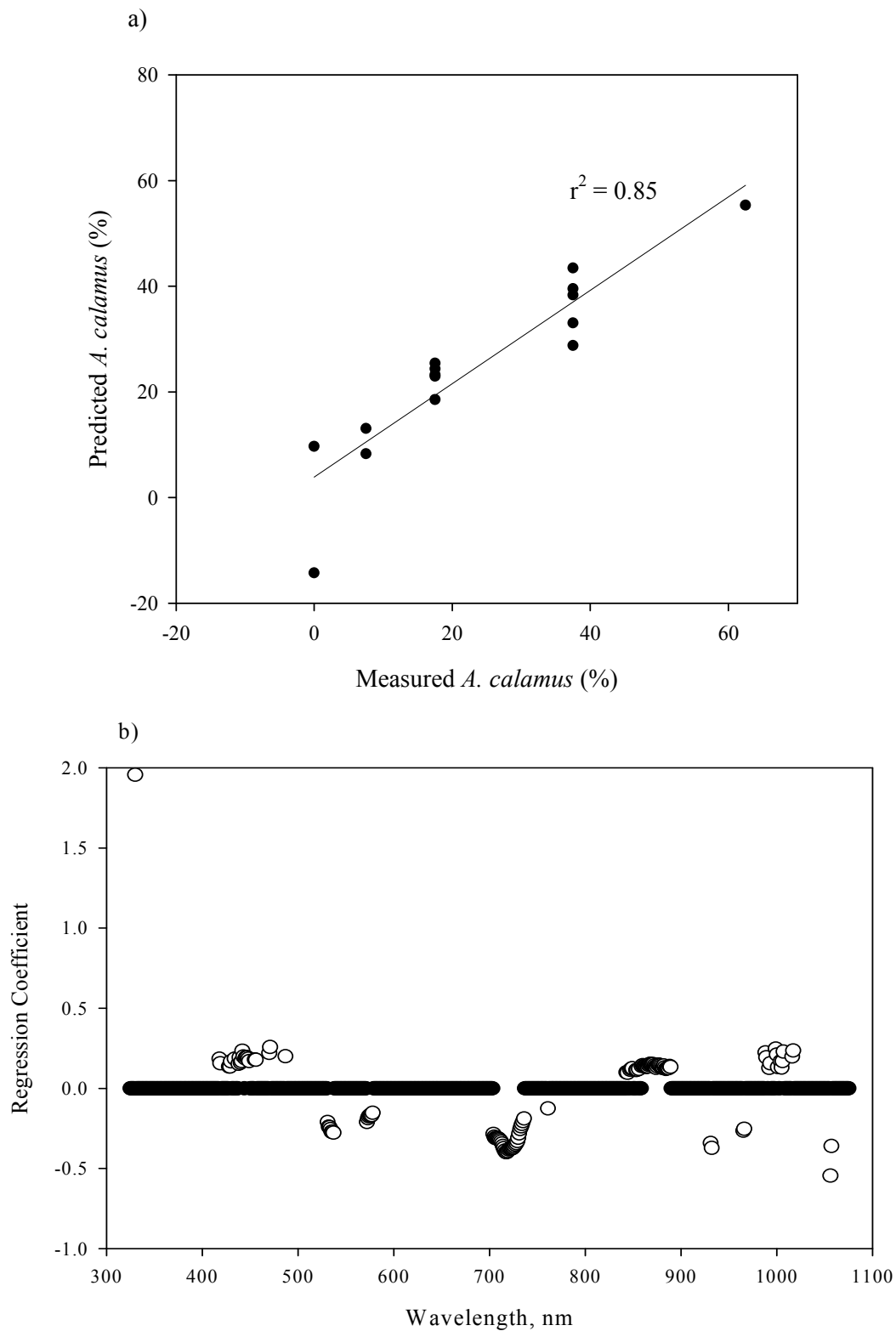


Figure C4. (a) Predicted vs measured *A. calamus* cover (%) PLS-regression of the inverse reflectance for the *Phragmites*-dominant site, 6/16/04 data, which used 128 spectral bands that were combined into eight PLS-components with $r = 0.92$ and RMSEP of 6.8%. (b) Loading plot of regression coefficients, where spectral bands used in the regression are depicted by open circles.

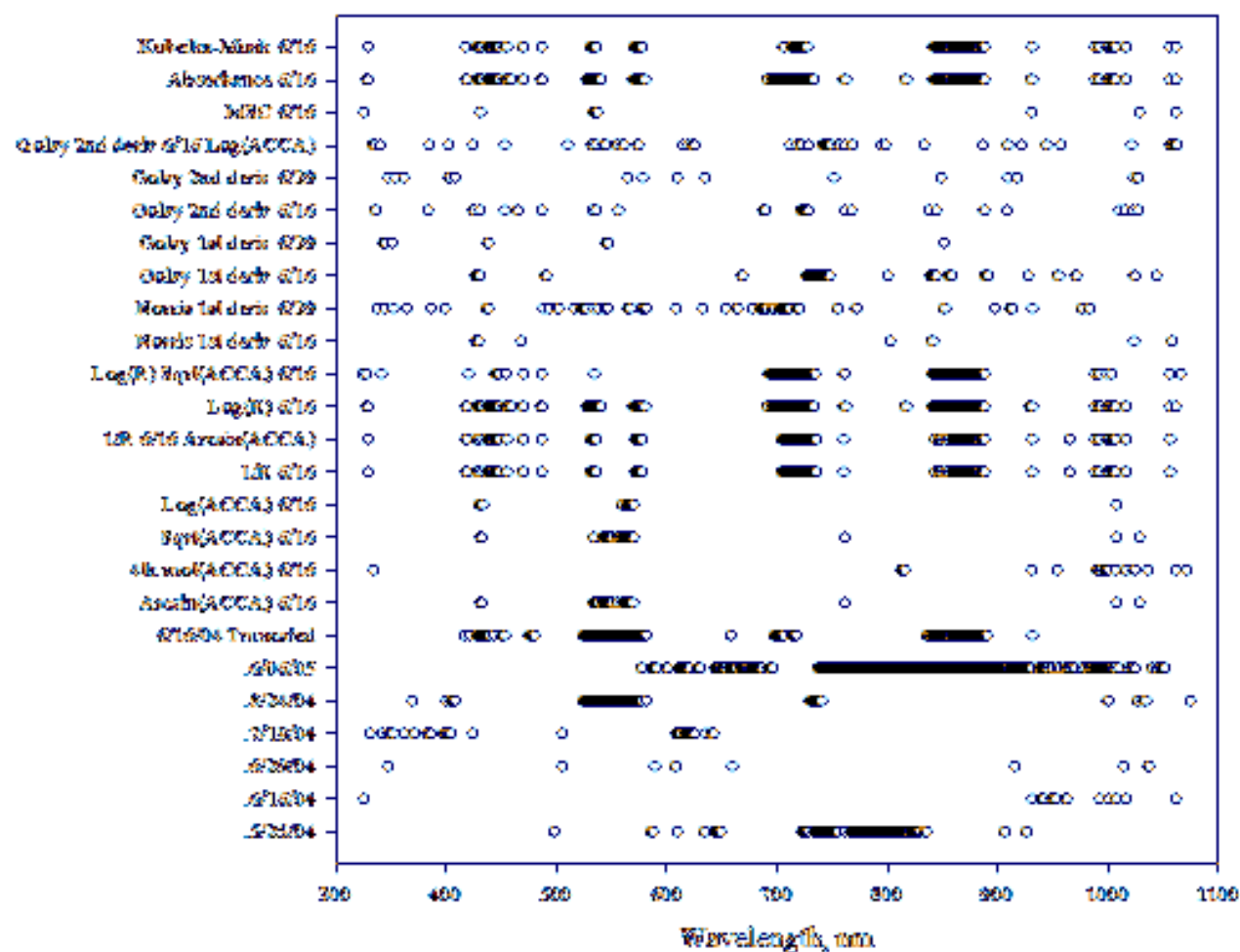


Figure C5. Significant spectral bands for *A. calamus* according to PLS-regressions at the *Phragmites*-dominant site.

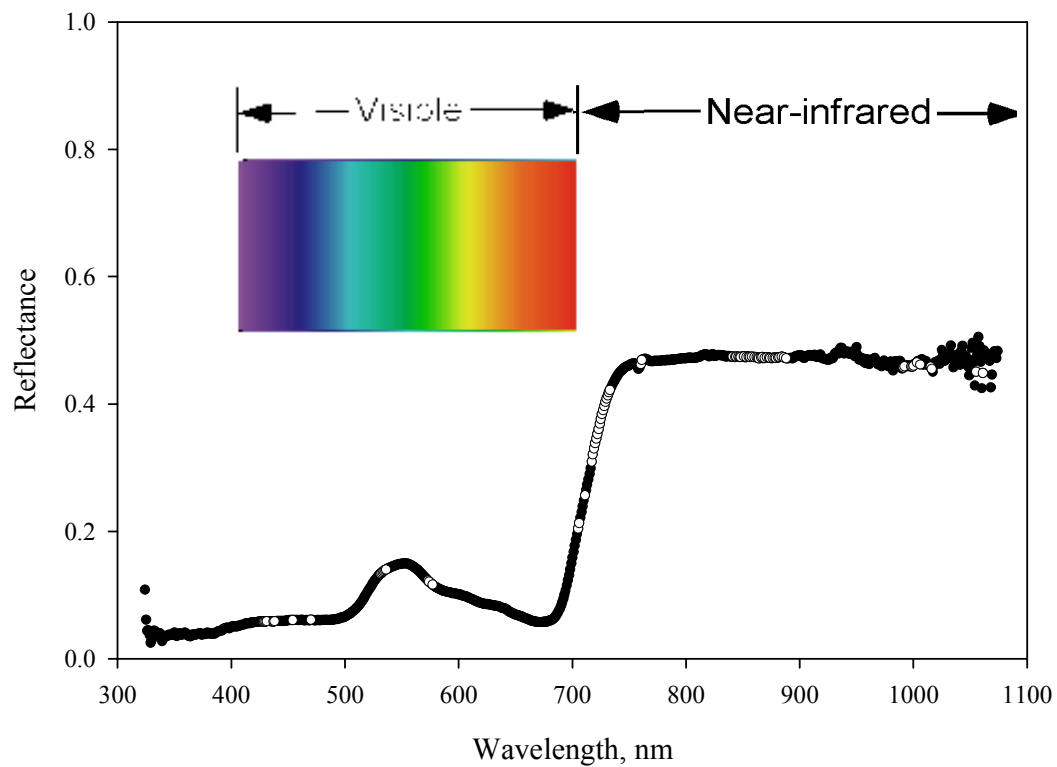


Figure C6. Spectral bands significant for seven or more regressions for *A. calamus* cover at the *Phragmites*-dominant site are indicated by an open circle.

Table C5. PLS-regressions for *P. arifolium* cover (%) at the *Phragmites*-dominant (PD) site. *r* = regression coefficient, RMSEP = root mean square error of prediction, PCs = PLS-components

Spectra Transformations	<i>P. arifolium</i> Transformations	Date	<i>r</i>	RMSEP	n	Name of plots removed	PCs	# bands used	Comments
Untransformed (350-1075nm)	none	9.21.04	0.86	8.87	15	none	3	27	none
Golay 2 nd Derivative, avg 10	none	8.24.04	0.83	15.24	15	none	1	76	none
Norris 1 st Derivative	none	9.21.04	0.83	9.37	15	none	4	49	none
Truncated spectra (400-950nm)	none	9.21.04	0.81	9.97	15	none	7	36	none
Untransformed (350-1075nm)	none	8.24.04	0.80	16.40	15	none	3	59	none
Untransformed (350-1075nm)	Arcsine sqrt (POAR)	8.24.04	0.78	0.20	15	none	3	100	none
Log R	none	8.24.04	0.78	16.79	15	none	3	151	none
Transform 1/R	Arcsine sqrt (POAR)	9.21.04	0.78	0.14	15	none	3	56	none
Normalized spectra (R/R410)	none	8.24.04	0.77	17.36	15	none	3	4	none
Untransformed (350-1075nm)	4th root POAR	8.24.04	0.73	0.39	14	Plot 6	4	35	Plot 6: high reflectance
Untransformed (350-1075nm)	Square root POAR	8.24.04	0.73	1.60	15	none	2	13	none
Log R	Square root POAR	8.24.04	0.73	1.59	15	none	3	128	none
Golay 2 nd Derivative, avg 10	none	9.21.04	0.71	12.03	15	none	1	21	none
Golay 2 nd Derivative, avg 10	Log POAR	8.24.04	0.69	0.29	15	none	1	67	none
Untransformed (350-1075nm)	none	5.25.04	0.67	11.33	12	Plots 1,2,3	5	522	Plots 1,2,3: missing reflectance data
Absorbance Transformation	none	8.24.04	0.67	20.30	15	none	2	125	none
Kubelka-Munk	none	8.24.04	0.66	22.12	15	none	4	298	none
Transformation	none	9.21.04	0.66	12.79	15	none	3	27	none
Transform 1/R	none	9.21.04	0.66	12.64	15	none	1	34	none
Golay 1 st Derivative	none	9.21.04	0.66	12.64	15	none	1	34	none

Spectra Transformations	<i>P. arifolium</i> Transformations	Date	r	RMSEP	n	Name of plots re moved	PCs	# bands used	Comments
Transform 1/R	none	8.24.04	0.64	21.00	15	none	3	88	none
Norris 1 st Derivative	none	8.24.04	0.64	21.73	15	none	1	233	none
Untransformed (350-1075nm)	none	6.03.04	0.63	1.92	14	Plot 3	4	175	Plot 3: high reflectance
Golay 1 st Derivative	none	8.24.04	0.62	22.45	15	none	1	233	none
Untransformed (350-1075nm)	none	7.19.04	0.58	18.85	14	Plot 3	2	231	Plot 3: high reflectance
Untransformed (350-1075nm)	none	8.02.05	0.55	6.17	13	Plots 11, 13	3	23	Plots 11, 13: high <i>P. arifolium</i> concentrations
Truncated spectra (400-950nm)	none	8.24.04	0.55	23.94	15	none	1	282	none
Log R	Square root POAR Log (base 10)	9.21.04	0.55	1.69	15	none	3	8	none
Untransformed (350-1075nm)	POAR	8.24.04	0.54	0.35	14	Plot 6	2	257	Plot 6: high reflectance
Untransformed (350-1075nm)	none	6.29.04	0.52	14.48	14	Plot 3	1	322	Plot 3: high <i>P. arifolium</i> concentration
MSC Transformation	none	8.24.04	0.39	23.80	14	Plot 4 Plots	1	20	Plot 4: low <i>P. arifolium</i> concentration
Untransformed (350-1075nm)	none	6.06.05	0.29	1.19	13	8,11	1	334	Plots 3,11: high <i>P. arifolium</i> concentrations
Untransformed (350-1075nm)	none	6.16.04	0.23	15.27	14	Plot 3	2	566	Plot 3: high <i>P. arifolium</i> concentration

Table C6. PLS-regressions for *P. arifolium* cover (%) at the *Phragmites*-absent (PA) site. r = regression coefficient, RMSEP = root mean square error of prediction, PCs = PLS-components

Spectra Transformations	<i>P. arifolium</i> Transformations	Date	r	RMSEP	n	Name of plots removed	PCs	# bands used	Comments
Normalized spectra (R/R410)	none	8.24.04	0.89	7.66	13	Plots 1,7	3	169	Plot 1: high reflect.; Plot 7: low <i>P. arifolium</i> conc.
Golay 2 nd Derivative, avg 10	none	8.24.04	0.87	8.55	14	Plot 7	2	11	Plot 7: low <i>P. arifolium</i> concentration
Truncated spectra (400-950nm)	none	8.24.04	0.77	10.99	13	Plots 1,7	2	16	Plot 1: high reflect.; Plot 7: low <i>P. arifolium</i> conc.
Golay 2 nd Derivative, avg 10	none	9.21.04	0.77	4.08	14	Plot 11	1	86	Plot 11: no <i>P. arifolium</i>
Log R	none	8.24.04	0.75	11.39	13	Plots 1,7	4	54	Plot 1: high reflect.; Plot 7: low <i>P. arifolium</i> conc.
Golay 1 st Derivative	none	9.21.04	0.74	4.60	13	Plots 11,13	1	85	Plots 11: no <i>P. arifolium</i> ; Plot 13: low reflectance
Untransformed (350-1075nm)	Arcsine sqrt (POAR)	8.24.04	0.73	0.15	13	Plots 1,7	3	230	Plot 1: high reflect.; Plot 7: low <i>P. arifolium</i> conc.
Log R	Square root POAR	8.24.04	0.73	0.72	13	Plots 1,7	4	39	Plot 1: high reflect.; Plot 7: low <i>P. arifolium</i> conc.
Golay 2 nd Derivative, avg 10	Log POAR	8.24.04	0.73	0.07	14	Plot 7	1	46	Plot 7: low <i>P. arifolium</i> concentration
Kubelka-Munk Transformation	none	8.24.04	0.73	11.95	13	Plots 1,7	3	314	Plot 1: high reflect.; Plot 7: low <i>P. arifolium</i> conc.
Absorbance Transformation	none	8.24.04	0.72	11.95	13	Plots 1,7	3	47	Plot 1: high reflect.; Plot 7: low <i>P. arifolium</i> conc.
Norris 1 st Derivative	none	9.21.04	0.71	6.24	15	none	1	25	Plot 1: high reflect.; Plot 7: low <i>P. arifolium</i> conc.
Transform 1/R	none	8.24.04	0.70	12.22	13	Plots 1,7	3	374	Plot 1: high reflect.; Plot 7: low <i>P. arifolium</i> conc.
Norris 1 st Derivative	none	8.24.04	0.67	12.87	13	Plots 1,7	1	282	Plot 1: high reflect.; Plot 7: low <i>P. arifolium</i> conc.
Untransformed (350-1075nm)	none	8.24.04	0.66	13.19	13	Plots 1,7	6	7	Plot 1: high reflect.; Plot 7: low <i>P. arifolium</i> conc.
Golay 1 st Derivative	none	8.24.04	0.66	12.93	13	Plots 1,7	1	244	Plot 1: high reflect.; Plot 7: low <i>P. arifolium</i> conc.
Truncated spectra (400-950nm)	none	9.21.04	0.66	5.58	14	Plot 11	4	11	Plot 11: no <i>P. arifolium</i>
Untransformed (350-1075nm)	none	8.02.05	0.65	23.87	14	Plot 8	5	353	Plot 8: high reflectance
Untransformed (350-1075nm)	Square root POAR	8.24.04	0.65	0.82	13	Plots 1,7	6	8	Plot 1: high reflect.; Plot 7: low <i>P. arifolium</i> conc.

Table C7. PLS-regression transformations tested on *P. arifolium*.cover (%). Site is identified as PD (*Phragmites*-dominant) or PA (*Phragmites*-absent)

	Untransformed (350-1075 nm)	Truncated spectra (400-950 nm)	Arcsine sqrt (POAR)	4th root POAR	Sqrt (POAR)	Log ₁₀ POAR	Normalized spectra	Transform 1/R	Transform 1/R, Arcsine sqrt (POAR)	Log R	Log R, Sqrt (POAR)
5/25/2004	PD site and PA site										
6/3/2004	PD, PA										
6/16/2004	PD, PA										
6/29/2004	PD, PA										
7/19/2004	PD, PA										
8/24/2004	PD, PA	PD, PA	PD, PA	PD, PA	PD, PA	PD, PA	PD, PA	PD, PA		PD, PA	PD, PA
9/21/2004	PD, PA	PD, PA						PD, PA	PD, PA		PD, PA
6/6/2005	PD, PA										
8/2/2005	PD, PA										

	Norris 1st Derivative	Golay 1st Derivative	Golay 2nd Derivative	Golay 2nd Deriv, Log (POAR)	MSC Transform	Absorbance Transform	Kubelka-Munk Transform
5/25/2004							
6/3/2004							
6/16/2004							
6/29/2004							
7/19/2004							
8/24/2004	PD, PA	PD, PA	PD, PA	PD, PA	PD, PA	PD, PA	PD, PA
9/21/2004	PD, PA	PD, PA	PD, PA				
6/6/2005							
8/2/2005							

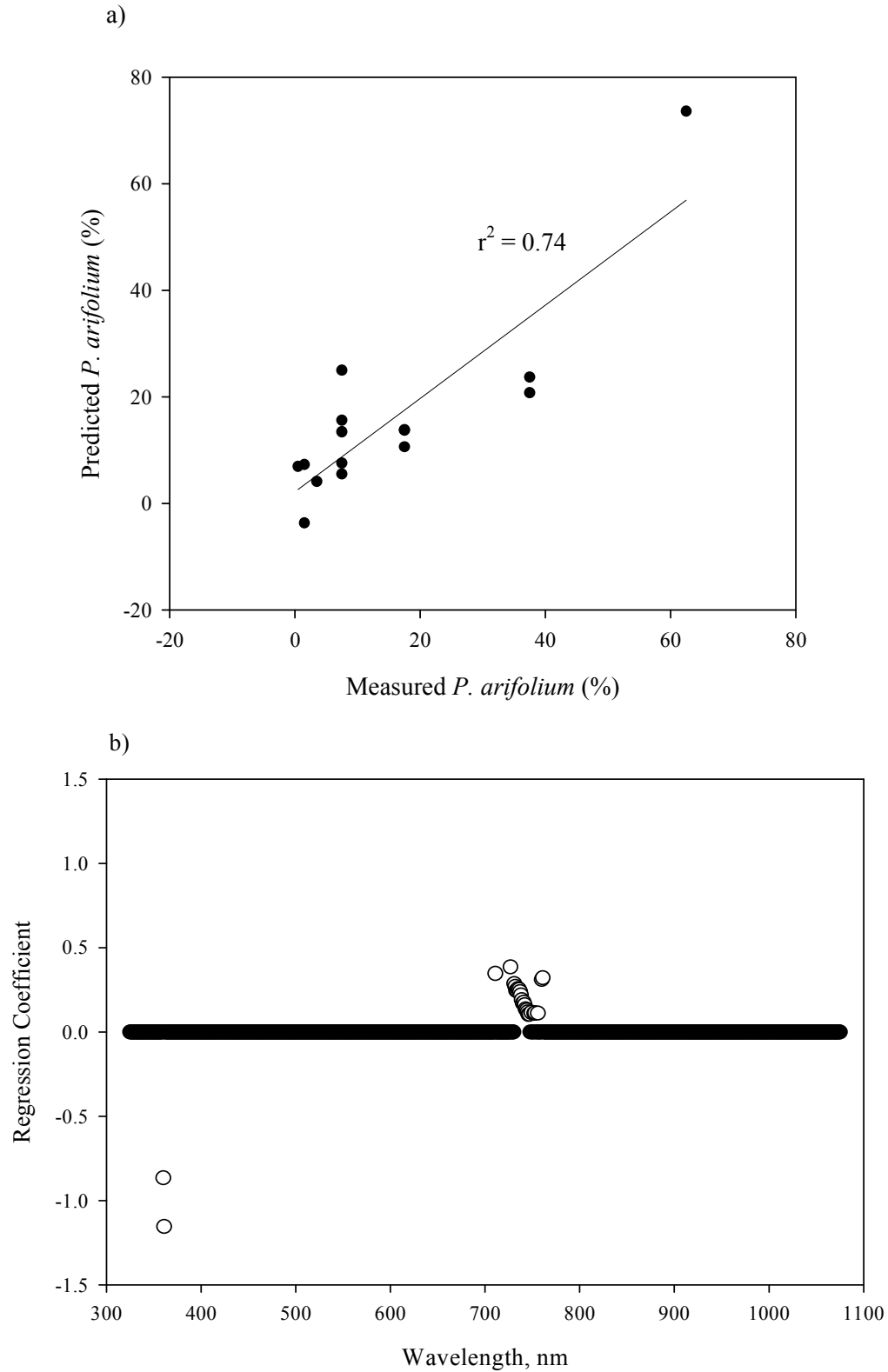


Figure C7 (a) Predicted vs measured *P. arifolium* cover at the *Phragmites*-dominant site, 9/21/04, using 27 untransformed spectral bands to form three PLS-components with an RMSEP of 8.9% and $r = 0.86$. (b) Loading plot of regression coefficients for the PLS-regression where spectral bands used in the regression are depicted by open circles.

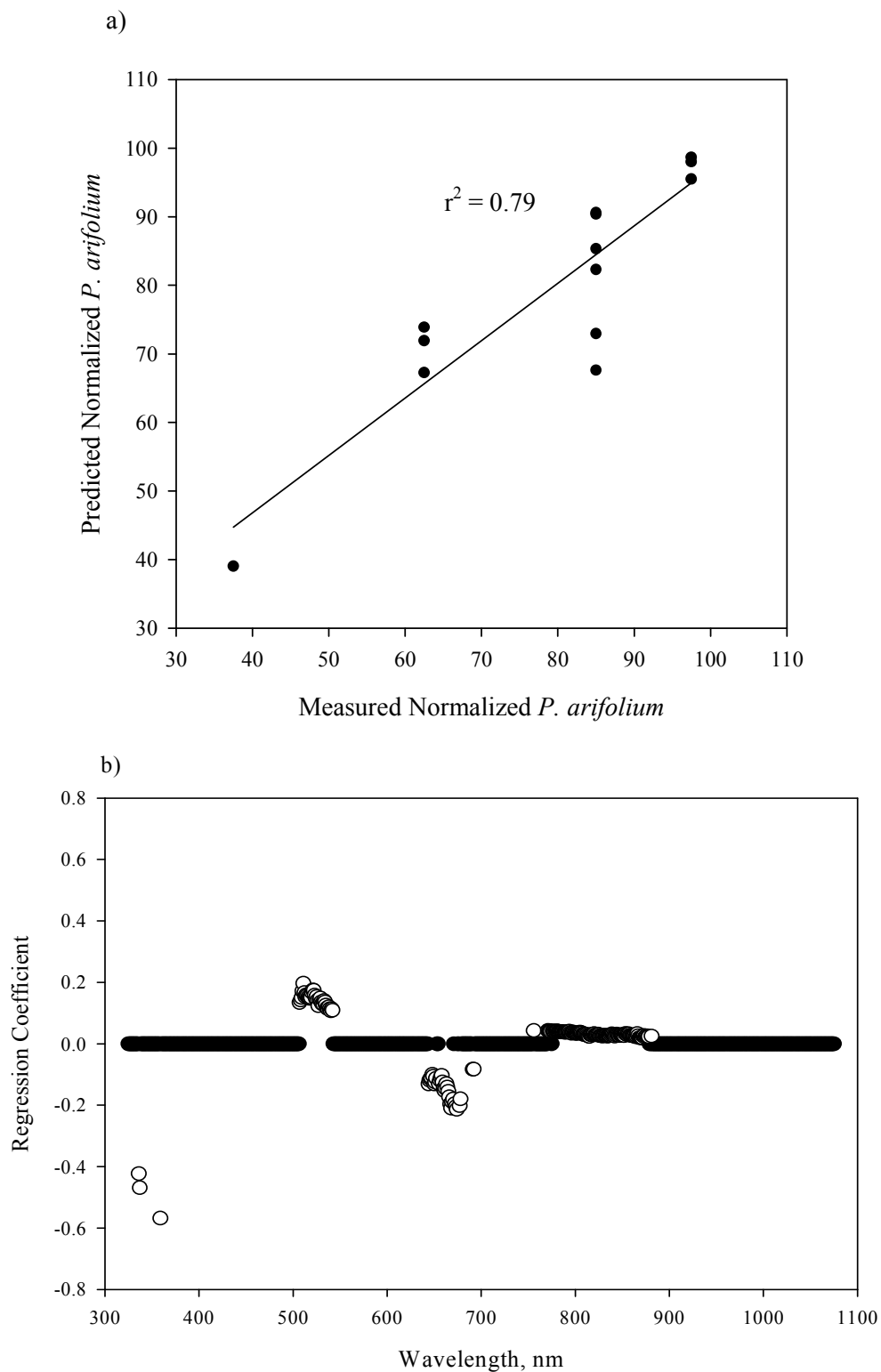


Figure C8 (a) Predicted vs measured *P. arifolium* cover using 169 spectral bands of normalized spectra at the *Phragmites*-absent site on 8/24/04 to create three PLS-components with RMSEP of 7.7% and $r = 0.89$. (b) Loading plot of regression coefficients for the PLS-regression where spectral bands used in the regression are depicted by open circles.

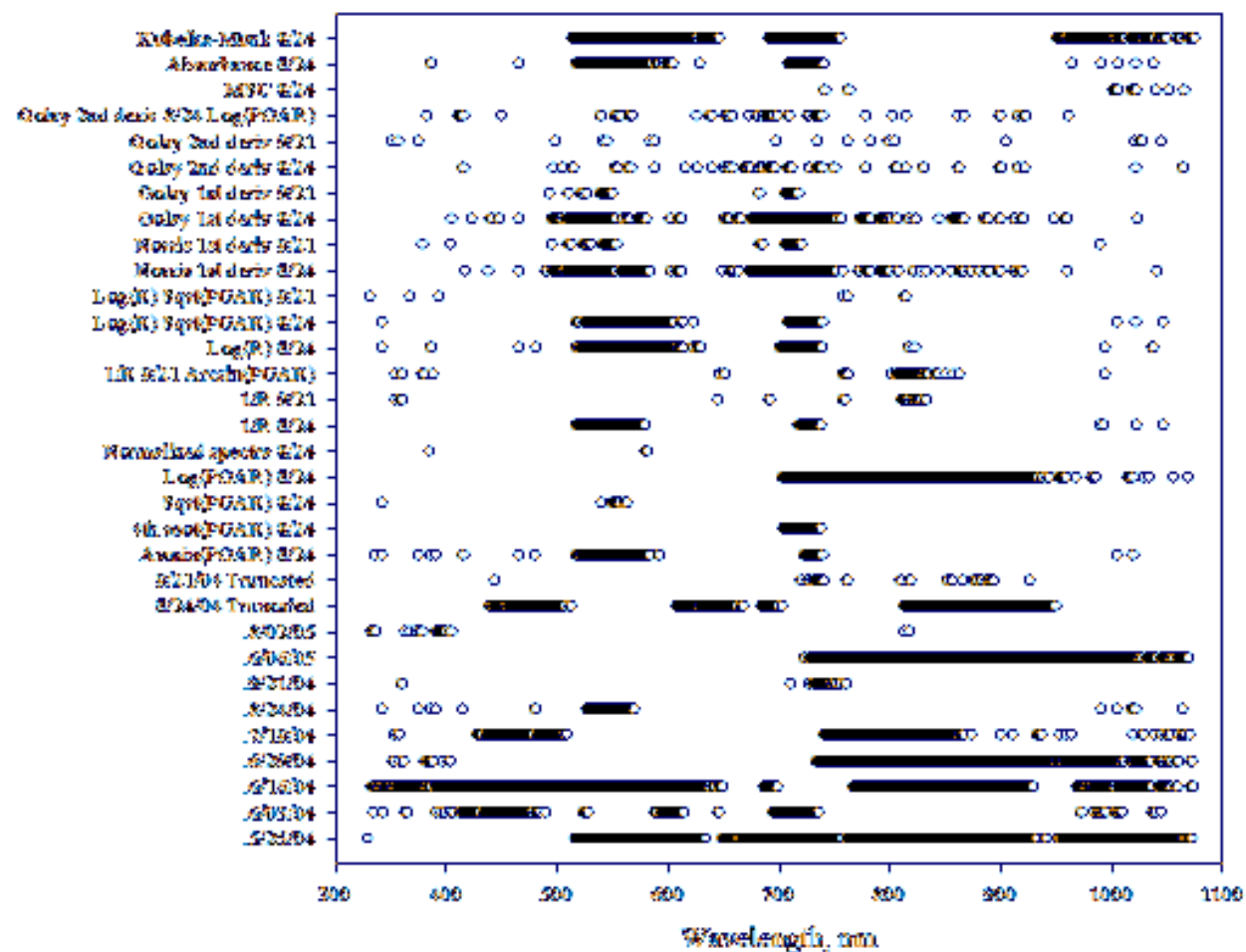


Figure C9. Significant spectral bands for *P. arifolium* according to PLS-regressions at the *Phragmites*-dominant site.

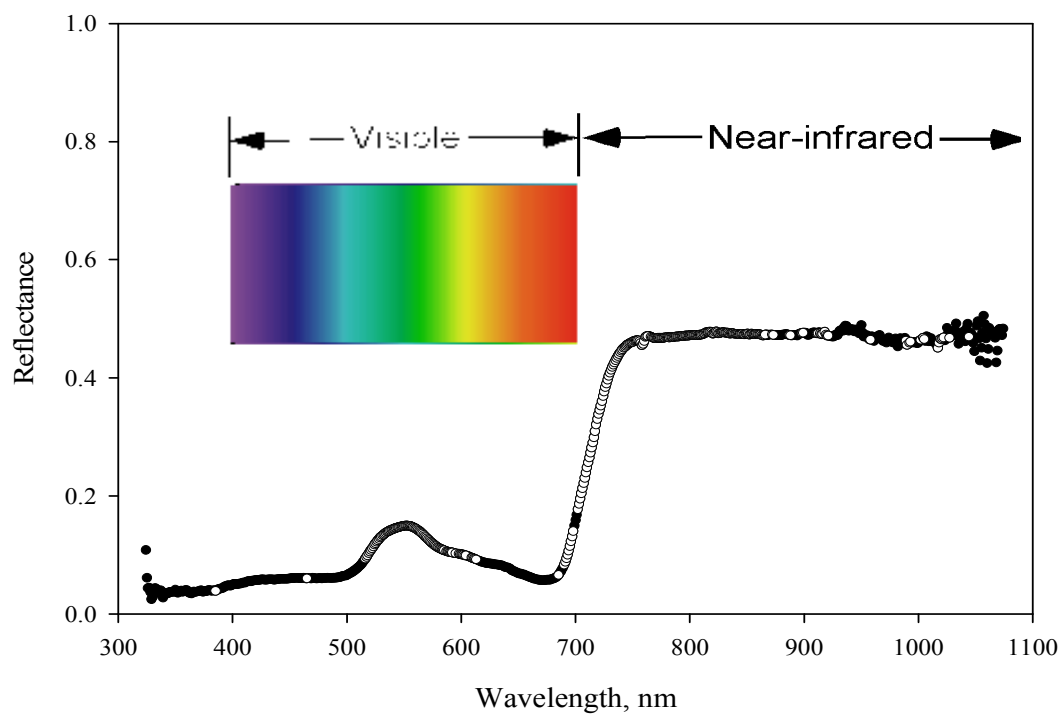


Figure C10. Spectral bands significant for seven or more regressions for *P. arifolium* at the *Phragmites*-dominant site are indicated by an open circle.

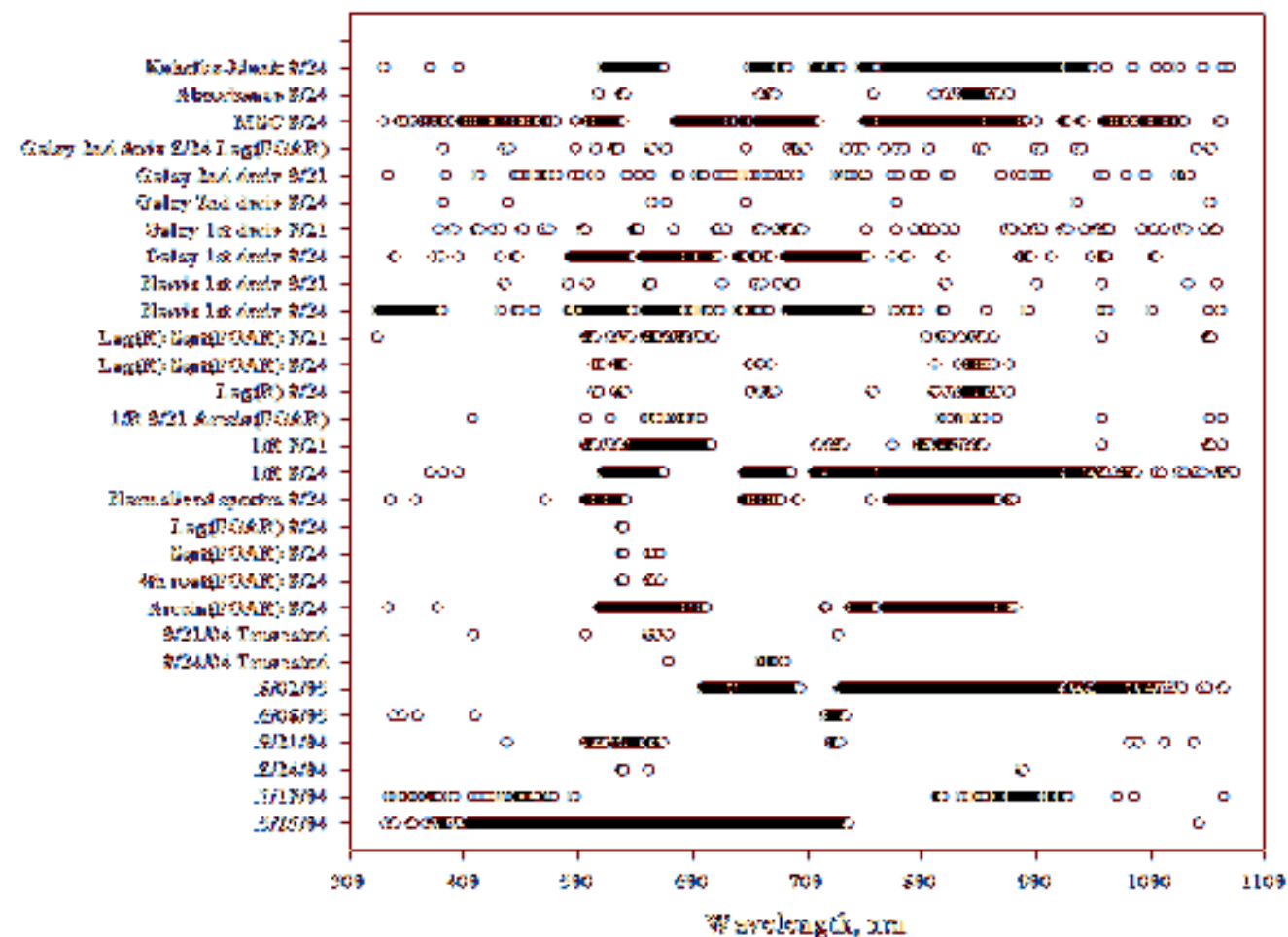


Figure C11. Significant spectral bands for *P. arifolium* according to PLS-regressions at the *Phragmites*-absent site.

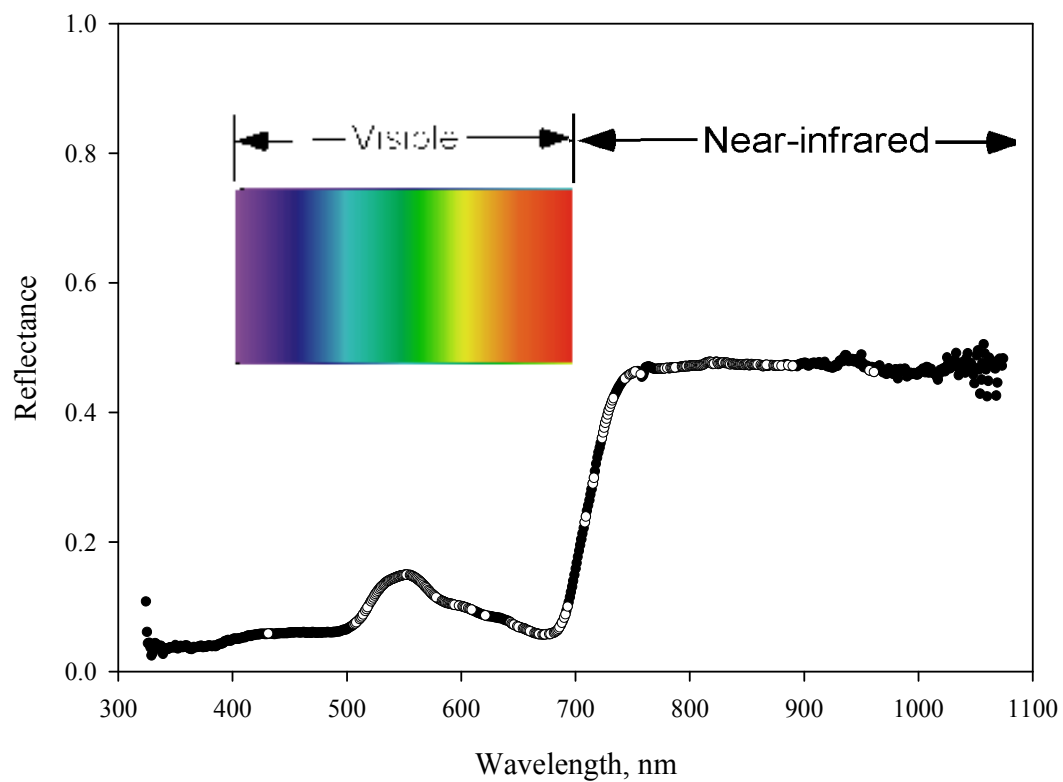


Figure C12. Spectral bands significant for seven or more regressions for *P. arifolium* at the *Phragmites*-absent site are indicated by an open circle.

Table C8. PLS-regressions for *P. virginica* cover (%) at the *Phragmites*-dominant (PD) site. r = regression coefficient, RMSEP = root mean square error of prediction, PCs = PLS-components

Spectra Transformations	<i>Peltandra virginica</i> Transformations	Date	r	RMSEP	n	Name of plots removed	PCs	# bands used	Comments
Truncated spectra (400-950nm)	none	5.25.04	0.91	7.57	11	Plots 1-3, 12	3	27	Plots 1-3: missing refl.; Plot 12: low refl
Truncated spectra (400-950nm)	none	6.03.04	0.87	8.61	14	Plot 3	8	24	Plot 3: high reflectance
Untransformed (350-1075nm)	none	5.25.04	0.80	11.05	10	Plots 1-3, 9,12	2	102	Plots 1-3: missing refl.; Plot 9: hi refl; Plot 12: low refl
Golay 1 st Derivative	none	5.25.04	0.79	11.06	12	Plots 1-3	1	69	Plots 1-3: missing reflectance
Untransformed (350-1075nm)	Square root PEVI	6.03.04	0.78	1.39	14	Plot 3	3	65	Plot 3: high reflectance
Untransformed (350-1075nm)	none	6.03.04	0.75	11.57	14	Plot 3	3	33	Plot 3: high reflectance
Untransformed (350-1075nm)	Arcsine sqrt (PEVI)	6.03.04	0.60	0.21	14	Plot 3	6	34	Plot 3: high reflectance
Log R	Square root PEVI	6.03.04	0.55	0.73	14	Plot 3	9	353	Plot 3: high reflectance
Norris 1 st Derivative	none	6.03.04	0.52	16.37	15	none	1	93	none
Transform 1/R	none	5.25.04	0.50	17.34	11	Plots 1-3, 12	3	39	Plots 1-3: missing refl; Plot 12: low refl
Transform 1/R	none	6.03.04	0.49	17.35	14	Plot 3	2	55	Plot 3: high reflectance
Untransformed (350-1075nm)	none	6.16.04	0.48	10.03	15	none	3	56	none
Kubelka-Munk Transformation	none	6.03.04	0.46	16.88	14	Plot 3	3	none	Plot 3: high reflectance
Log R	none	6.03.04	0.45	16.57	15	none	3	17	none
Absorbance Transformation	none	6.03.04	0.41	16.24	14	Plot 3	3	60	Plot 3: high reflectance
Untransformed (350-1075nm)	4th root PEVI	6.03.04	0.37	0.71	15	none	1	41	none
Transform 1/R	Arcsine sqrt (PEVI)	6.03.04	0.37	0.25	14	Plot 3	2	323	Plot 3: high reflectance

Spectra Transformations	<i>Peltandra virginica</i> Transformations	Date	r	RMSEP	n	Name of plots removed	PCs	# bands used	Comments
Norris 1 st Derivative	none	5.25.04	0.35	18.12	12	Plots 1-3	1	47	Plots 1-3: missing reflectance
Untransformed (350-1075nm)	none	6.06.05	0.32	12.67	13	Plots 7, 9	1	357	Plot 7: low reflectance; Plot 9: high reflectance
Golay 2 nd Derivative, avg 10	none	5.25.04	0.23	18.38	12	Plots 1-3	1	89	Plots 1-3: missing reflectance
Untransformed (350-1075nm)	none	6.29.04	0.17	6.53	14	Plot 8	2	6	Plot 8: no <i>P. virginica</i> concentration
Golay 1 st Derivative	none	6.03.04	0.13	17.33	15	none	1	124	none
Golay 2 nd Derivative, avg 10	none	6.03.04	0.13	17.33	15	none	1	124	none
MSC Transformation	none	6.03.04	0.13	17.33	15	none	1	124	none
Normalized spectra (R/R410)	none	7.19.04	0.01	2.96	15	none	1	none	none
Untransformed (350-1075nm)	none	9.21.04	-0.11	6.45	15	none	1	none	none
Untransformed (350-1075nm)	none	8.02.05	-0.31	11.15	15	none	1	none	none
Log R	Square root PEVI	6.16.04	-0.38	1.24	15	none	1	none	none
Untransformed (350-1075nm)	none	7.19.04	-0.42	2.93	15	none	1	none	none
Untransformed (350-1075nm)	none	8.24.04	-0.50	5.70	15	none	1	none	none
Untransformed (350-1075nm)	Log (base 10) PEVI	6.03.04	-0.72	0.89	13	Plots 3,4	1	none	Plots 3,4: no <i>P. virginica</i> concentration

Table C9. PLS-regressions for *P. virginica* cover (%) at the *Phragmites*-absent (PA) site. *r* = regression coefficient, RMSEP = root mean square error of prediction, PCs = PLS-components

Spectra Transformations	<i>Peltandra virginica</i> Transformations	Date	<i>r</i>	RMSEP	<i>n</i>	Name of plots removed	PCs	# bands used	Comments
Log R	Square root PEVI	9.21.04	0.93	0.51	15	none	4	243	none
Transform 1/R	none	9.21.04	0.90	2.94	15	none	5	294	none
Norris 1 st Derivative	none	9.21.04	0.86	3.28	15	none	1	139	none
Untransformed d (350-1075nm)	none	9.21.04	0.84	3.65	15	none	3	294	none
Golay 1 st Derivative	none	9.21.04	0.83	3.54	15	none	1	223	none
Truncated spectra (400-950nm)	none	9.21.04	0.82	3.90	15	none	2	220	none
Untransformed d (350-1075nm)	Arcsine sqrt (PEVI)	8.24.04	0.81	0.04	15	none	2	70	none
Untransformed d (350-1075nm)	Square root PEVI	8.24.04	0.81	0.43	15	none	2	70	none
Norris 1 st Derivative	none	8.24.04	0.81	1.17	15	none	2	104	none
Truncated spectra (400-950nm)	none	8.24.04	0.80	1.15	15	none	3	56	none
Normalized spectra (R/R410)	none	8.24.04	0.80	1.18	15	none	3	64	none
Untransformed d (350-1075nm)	none	8.02.05	0.79	4.00	15	none	2	564	none
Golay 2 nd Derivative, avg 10	none	9.21.04	0.75	4.28	14	Plot 14	1	17	Plot 14: low reflectance
Transform 1/R	none	8.24.04	0.74	1.35	15	none	3	164	none
Untransformed d (350-1075nm)	none	8.24.04	0.72	1.36	15	none	2	21	none
Untransformed d (350-1075nm)	4th root PEVI	8.24.04	0.70	0.29	15	none	2	43	none
Log R	Square root PEVI	8.24.04	0.70	0.51	15	none	1	378	none
Untransformed d (350-1075nm)	none	7.19.04	0.69	3.24	15	none	2	165	none
Golay 1 st Derivative	none	8.24.04	0.68	1.44	15	none	1	247	none

Table C10. PLS-regression transformations performed on spectra and *P. virginica*. cover. Site is identified as PD (*Phragmites*-dominant) or PA (*Phragmites*-absent).

	Untransformed (350-1075 nm)	Truncated spectra (400-950 nm)	Arcsine sqrt (PEVI)	4th root PEVI	Sqrt (PEVI)	Log ₁₀ PEVI	Normalized spectra	Transform 1/R	Transform 1/R, Arcsine sqrt (PEVI)	Log R	Log R, Sqrt (PEVI)
5/25/2004	PD site and PA site	PD						PD			
6/3/2004	PD, PA	PD	PD	PD	PD	PD		PD	PD	PD	PD
6/16/2004	PD, PA										PD
6/29/2004	PD, PA										
7/19/2004	PD, PA						PD				
8/24/2004	PD, PA	PA	PA	PA	PA	PA	PA	PA	PA	PA	PA
9/21/2004	PD, PA	PA						PA			PA
6/6/2005	PD, PA										
8/2/2005	PD, PA										

	Norris 1st Derivative	Golay 1st Derivative	Golay 2nd Derivative	MSC Transform	Absorbance Transform	Kubelka-Munk Transform
5/25/2004	PD	PD	PD			
6/3/2004	PD	PD	PD	PD	PD	PD
6/16/2004						
6/29/2004						
7/19/2004						
8/24/2004	PA	PA	PA	PA	PA	PA
9/21/2004	PA	PA	PA			
6/6/2005						
8/2/2005						

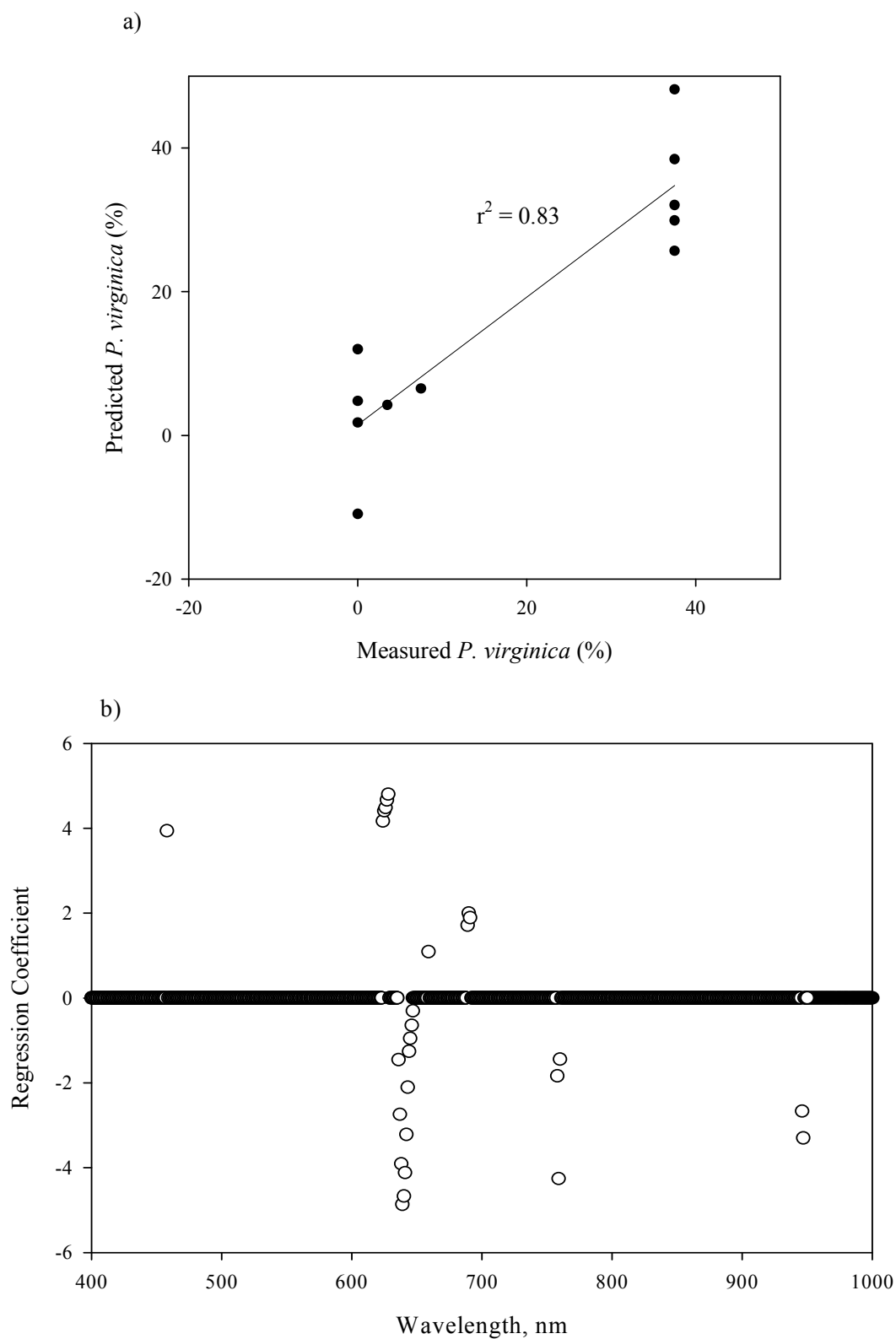


Figure C13 (a) Predicted vs measured *P. virginica* cover PLS-regression using 27 spectral bands of the truncated spectra at the *Phragmites*-dominant site, 5/25/04 data, that were combined into three PLS-components with an RMSEP of 7.6% and $r = 0.91$. **(b)** Loading plot of regression coefficients where spectral bands used in the regression are depicted by open circles.

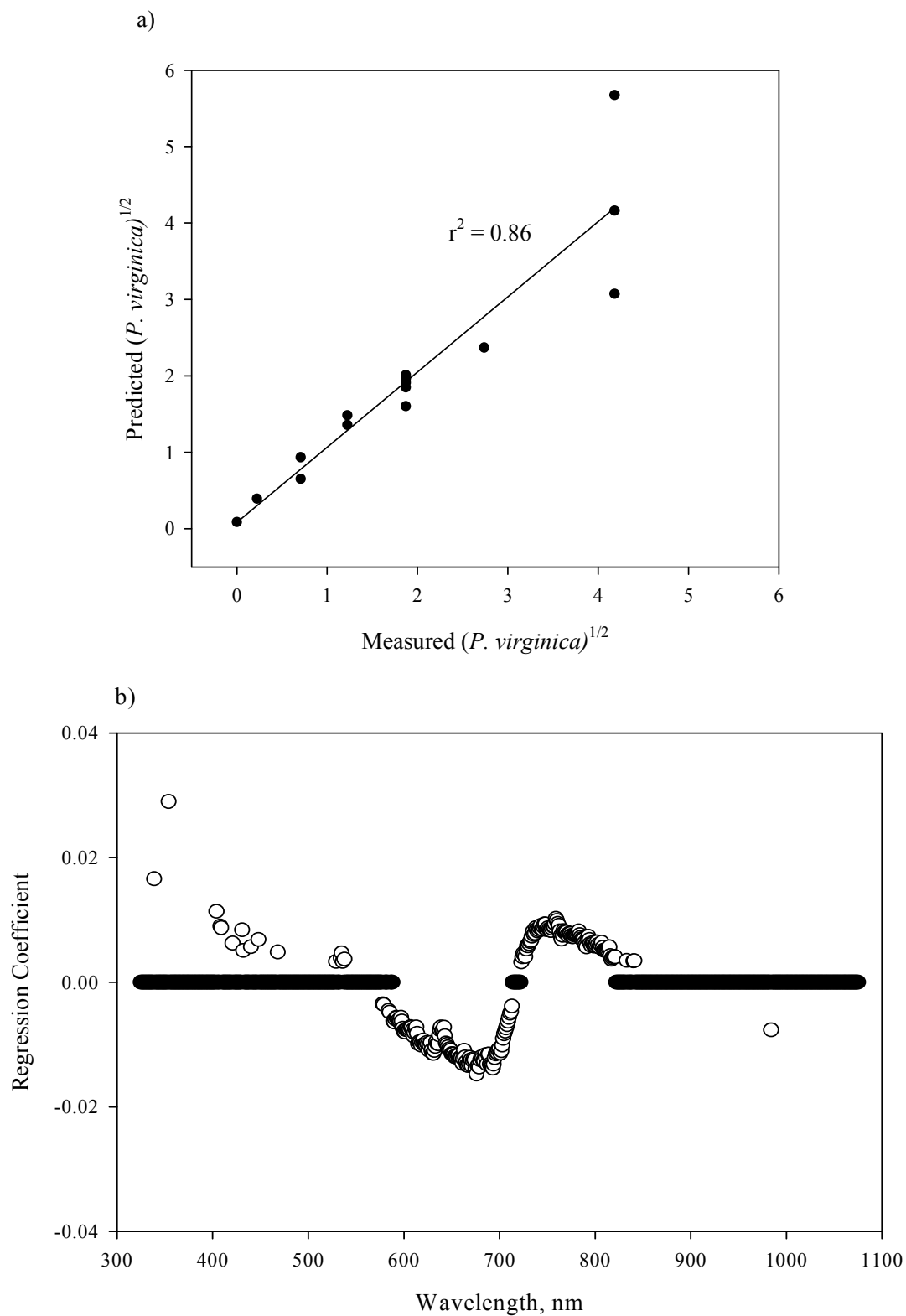


Figure C14 (a) Predicted vs measured PLS-regression using the square root of *P. virginica* and 243 spectral bands of the log (base 10) of the spectra at the *Phragmites*-absent site, 9/21/04, that were combined into four PLS-components with an RMSEP of 0.51% and $r = 0.93$. (b) Loading plot of regression coefficients. Spectral bands used in the regression are depicted by open circles.

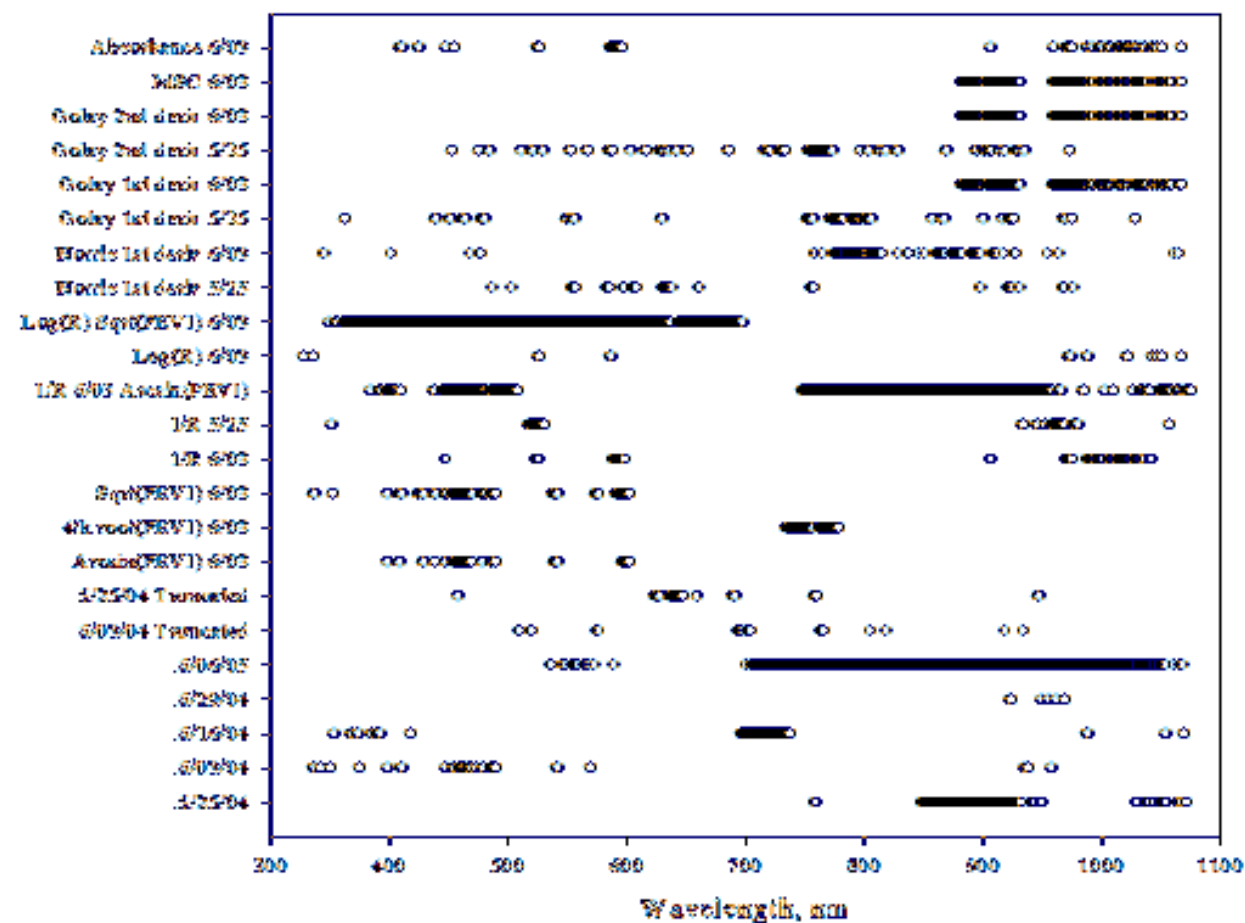


Figure C15. Significant spectral bands for *P. virginica* according to PLS-regressions at the *Phragmites*-dominant site.

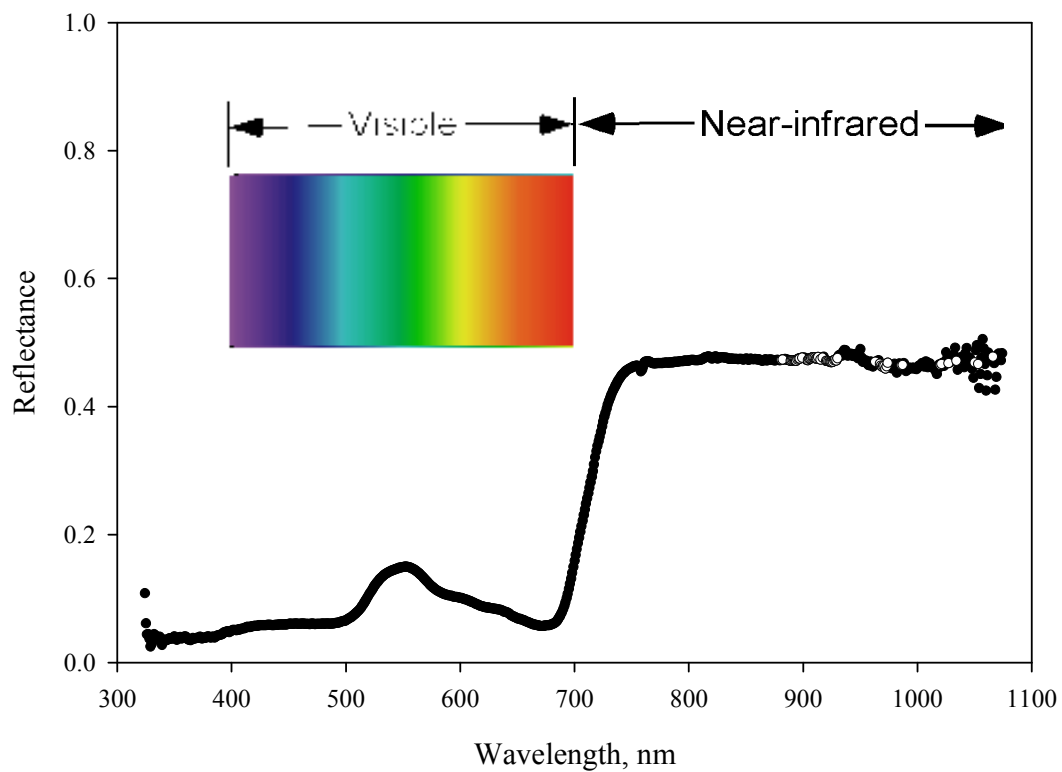


Figure C16. Spectral bands significant for seven or more regressions for *P. virginica* at the *Phragmites*-dominant site are indicated by an open circle.

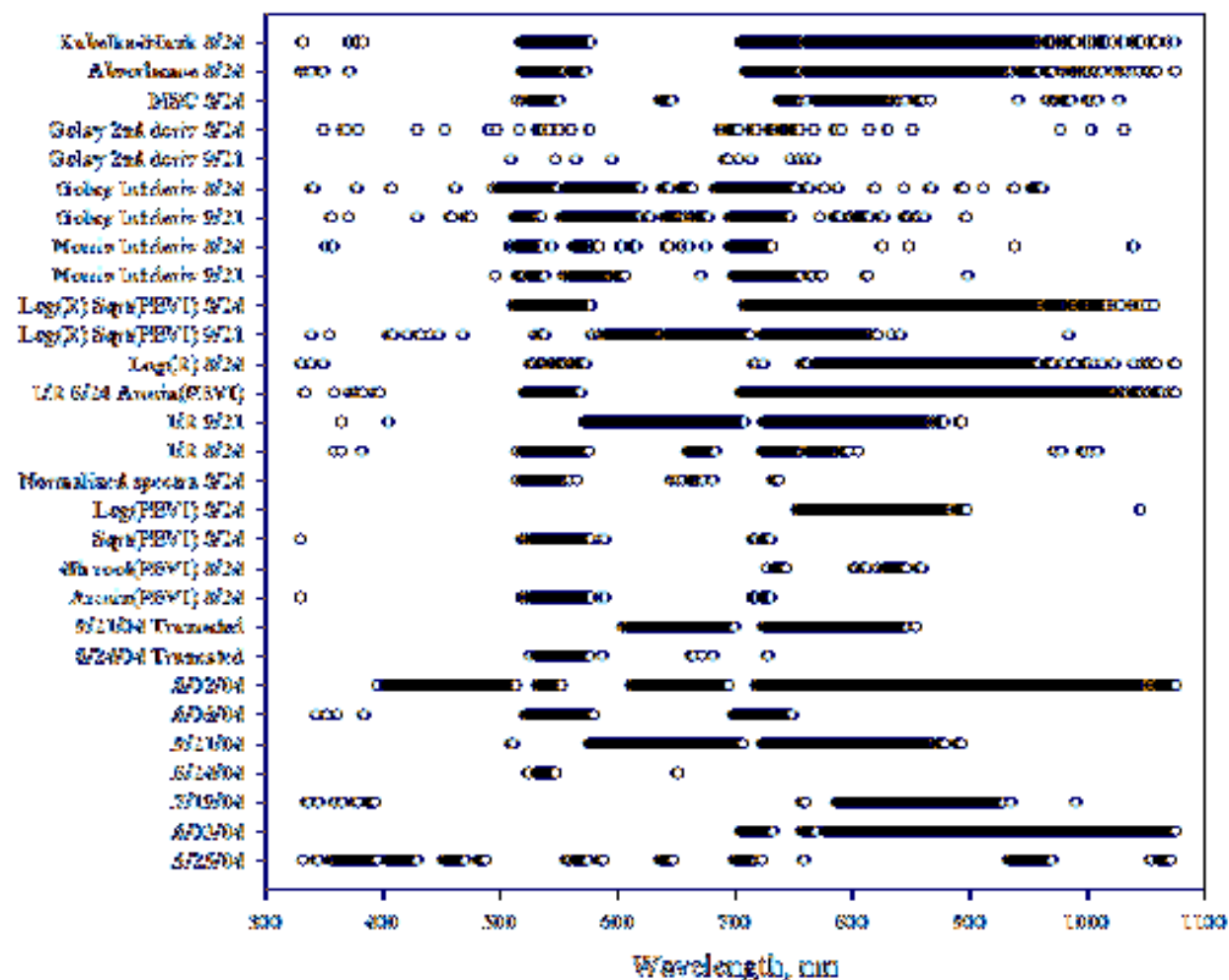


Figure C17. Significant spectral bands for *P. virginica* according to PLS-regressions at the *Phragmites*-absent site.

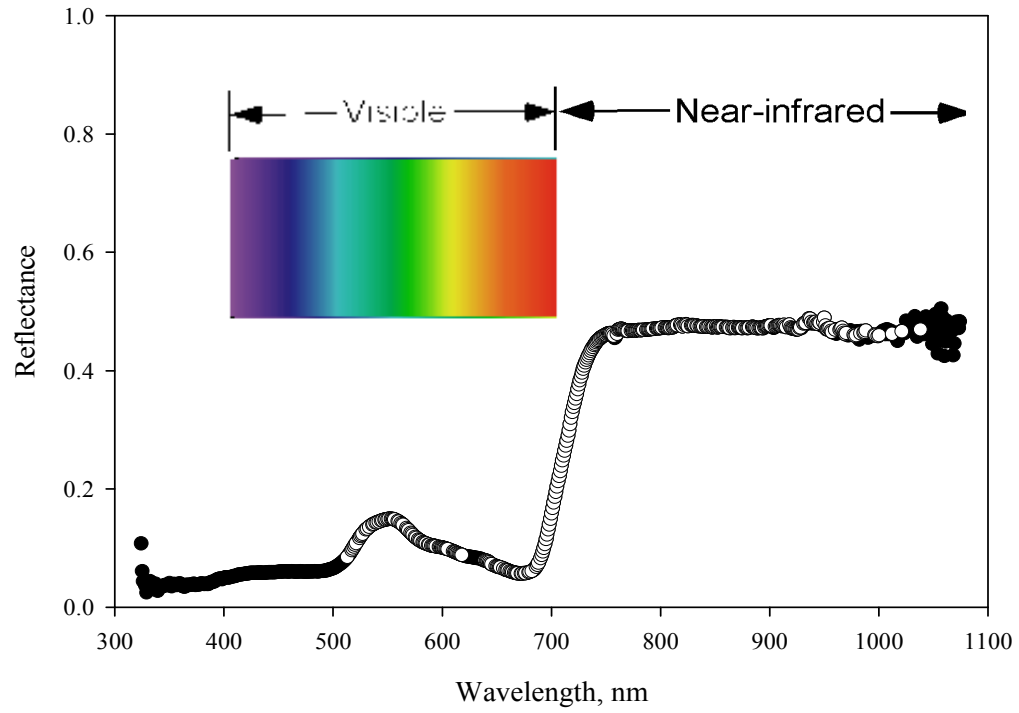


Figure C18. Spectral bands significant for seven or more regressions for *P. virginica* at the *Phragmites*-absent site are indicated by an open circle.

Table C11. PLS-regressions for *Typha* species percent cover at the *Phragmites*-absent (PA) site. r = regression coefficient, RMSEP = root mean square error of prediction, PCs = PLS-components

Spectra Transformations	<i>Typha</i> species Transformations	Date	r	RMSEP	n	Name of plots removed	PCs	# bands used	Comments
Log R	none	8.24.04	0.82	0.40	15	none	4	13	none
Untransformed (350-1075nm)	none	8.24.04	0.81	0.41	15	none	5	91	none
Golay 2 nd Derivative, avg 10	none	8.24.04	0.81	0.39	15	none	1	26	none
Norris 1 st Derivative	none	8.24.04	0.79	0.43	13	Plots 1, 2	2	47	Plots 1 and 2: high reflectance
Normalized spectra (R/R410)	none	8.24.04	0.78	0.43	14	Plot 1	3	118	Plot 1: high reflectance
Untransformed (350-1075nm)	none	6.16.04	0.76	3.39	14	Plot 10	2	42	Plot 10: low reflectance
Untransformed (350-1075nm)	Arcsine sqrt (TYSP)	8.24.04	0.76	0.03	15	none	2	20	none
Untransformed (350-1075nm)	Log (base 10) TYSP	8.24.04	0.76	0.32	15	none	2	8	none
Untransformed (350-1075nm)	Square root TYSP	8.24.04	0.75	0.35	15	none	2	19	none
Golay 2 nd Derivative, avg 10	Log TYSP	8.24.04	0.74	0.33	15	none	1	18	none
Kubelka-Munk Transformation	none	8.24.04	0.73	0.46	15	none	2	37	none
Absorbance Transformation	none	8.24.04	0.72	0.48	14	Plot 1	3	245	Plot 1: high reflectance
Untransformed (350-1075nm)	none	7.19.04	0.71	0.60	15	none	4	50	none
Transform 1/R	Arcsine sqrt (TYSP)	8.24.04	0.71	0.04	14	Plot 1	2	126	Plot 1: high reflectance
Truncated spectra (400-950nm)	none	8.24.04	0.70	0.48	14	Plot 1	2	148	Plot 1: high reflectance
Transform 1/R	none	8.24.04	0.69	0.49	14	Plot 1	2	226	Plot 1: high reflectance
Transform 1/R	none	7.19.04	0.68	0.60	15	none	3	20	none

Spectra Transformations	<i>Typha</i> species Transformations	Date	r	RMSEP	n	Name of plots removed	PCs	# bands used	Comments
Log R	Square root TYSP	8.24.04	0.68	0.39	15	none	4	56	none
Untransformed (350-1075nm)	none	9.21.04	0.68	1.48	15	none	7	214	none
Norris 1 st Derivative	none	7.19.04	0.67	0.58	15	none	1	9	none
Truncated spectra (400-950nm)	none	7.19.04	0.65	0.60	15	none	3	66	none
Untransformed (350-1075nm)	4th root TYSP	8.24.04	0.65	0.34	14	Plot 1	3	330	Plot 1: high reflectance
Log R	Square root TYSP	7.19.04	0.63	0.37	15	none	8	2	none
Untransformed (350-1075nm)	none	8.02.05	0.58	5.58	14	Plot 1	9	244	Plot 1: low reflectance
Untransformed (350-1075nm)	none	6.29.04	0.47	1.94	14	Plot 6	1	498	Plot 6: low reflectance
Untransformed (350-1075nm)	none	5.25.04	0.45	0.97	13	Plots 2, 5	2	110	Plot 2: high <i>Typha</i> conc.; Plot 5: missing reflect.
MSC Transformation	none	8.24.04	0.44	0.62	14	Plot 1	1	134	Plot 1: high reflectance
Golay 1 st Derivative	none	8.24.04	0.42	0.64	13	Plots 1,2	1	174	Plots 1 and 2: high reflectance
Golay 2 nd Derivative, avg 10	none	7.19.04	0.39	0.73	14	Plot 11	1	1	Plot 11: noisy reflectance derivative
Golay 1 st Derivative	none	7.19.04	0.30	0.74	14	Plot 11	1	none	Plot 11: noisy reflectance derivative Plot 1: high reflectance; Plot 9: missing reflectance
Untransformed (350-1075nm)	none	6.03.04	0.17	2.16	13	Plots 1,9	1	none	reflectance
Untransformed (350-1075nm)	none	6.06.05	0.05	1.61	14	Plot 6	1	none	Plot 6: high <i>Typha</i> concentration

Table C12. PLS-regression transformations tested on spectra and *Typha* species percent cover at the *Phragmites*-absent site.

	Untransformed (350-1075 nm)	Truncated spectra (400-950 nm)	Arcsine sqrt (TYSP)	4th root TYSP	Sqrt (TYSP)	Log ₁₀ TYSP	Normalized spectra	Transform 1/R	Transform 1/R, Arcsine sqrt (TYSP)	Log R	Log R, Sqrt (TYSP)
5/25/2004	X										
6/3/2004	X										
6/16/2004	X										
6/29/2004	X										
7/19/2004	X	X						X			X
8/24/2004	X	X	X	X	X	X	X	X	X	X	X
9/21/2004	X										
6/6/2005	X										
8/2/2005	X										

	Norris 1st Derivative	Golay 1st Derivative	Golay 2nd Derivative	Golay 2nd Derivative, Log (TYSP)	MSC Transform	Absorbance Transform	Kubelka-Munk Transform
5/25/2004							
6/3/2004							
6/16/2004							
6/29/2004							
7/19/2004	X	X	X				
8/24/2004	X	X	X	X	X	X	X
9/21/2004							
6/6/2005							
8/2/2005							

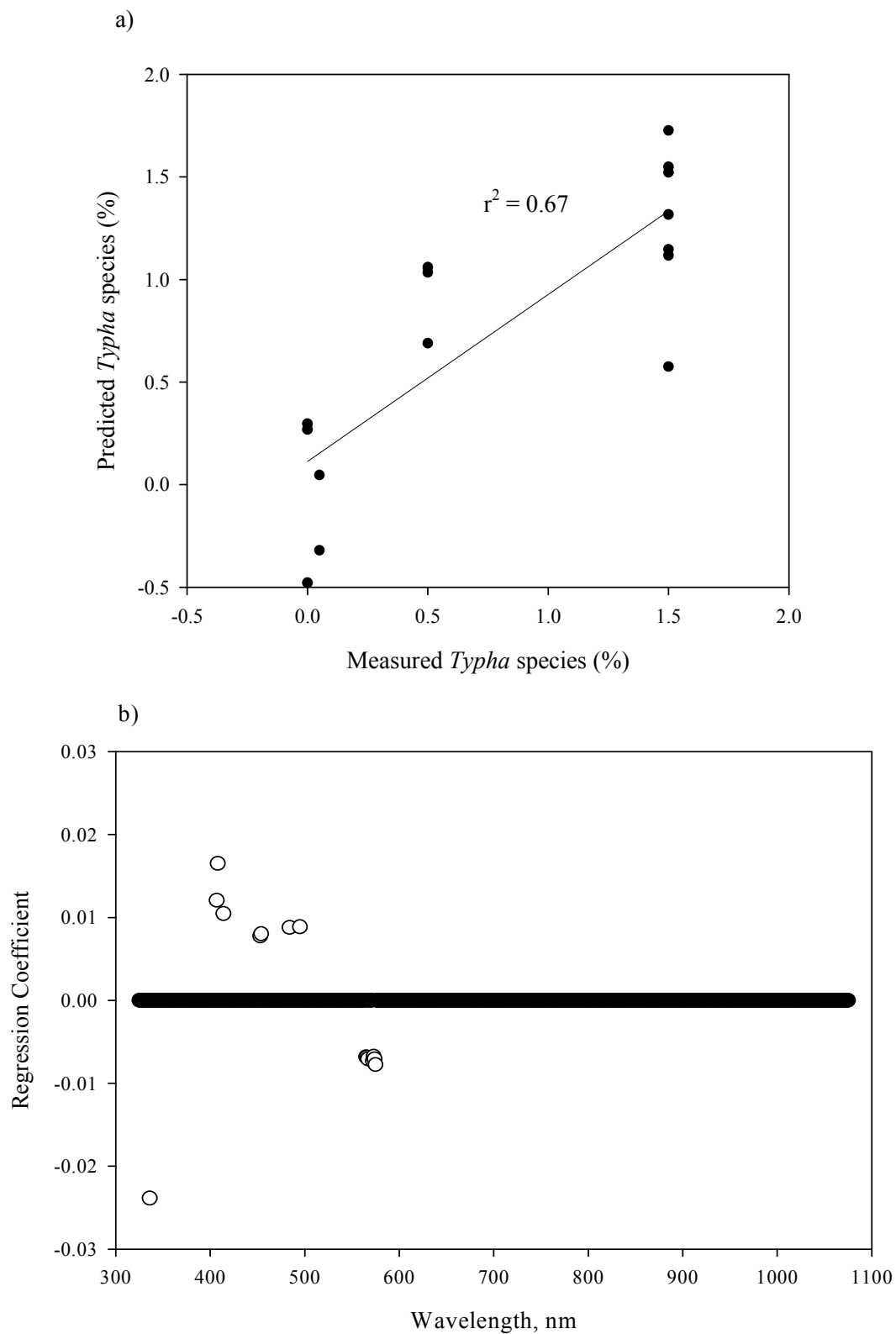


Figure C19. (a) Predicted vs measured *Typha* species cover PLS-regression using 13 spectral bands of the log of the reflectance at the *Phragmites*-absent site on 8/24/04 to form four PLS-components with an RMSEP of 0.4% and $r = 0.82$. (b) Loading plot of regression coefficients. Spectral bands used in the regression are depicted by open circles.

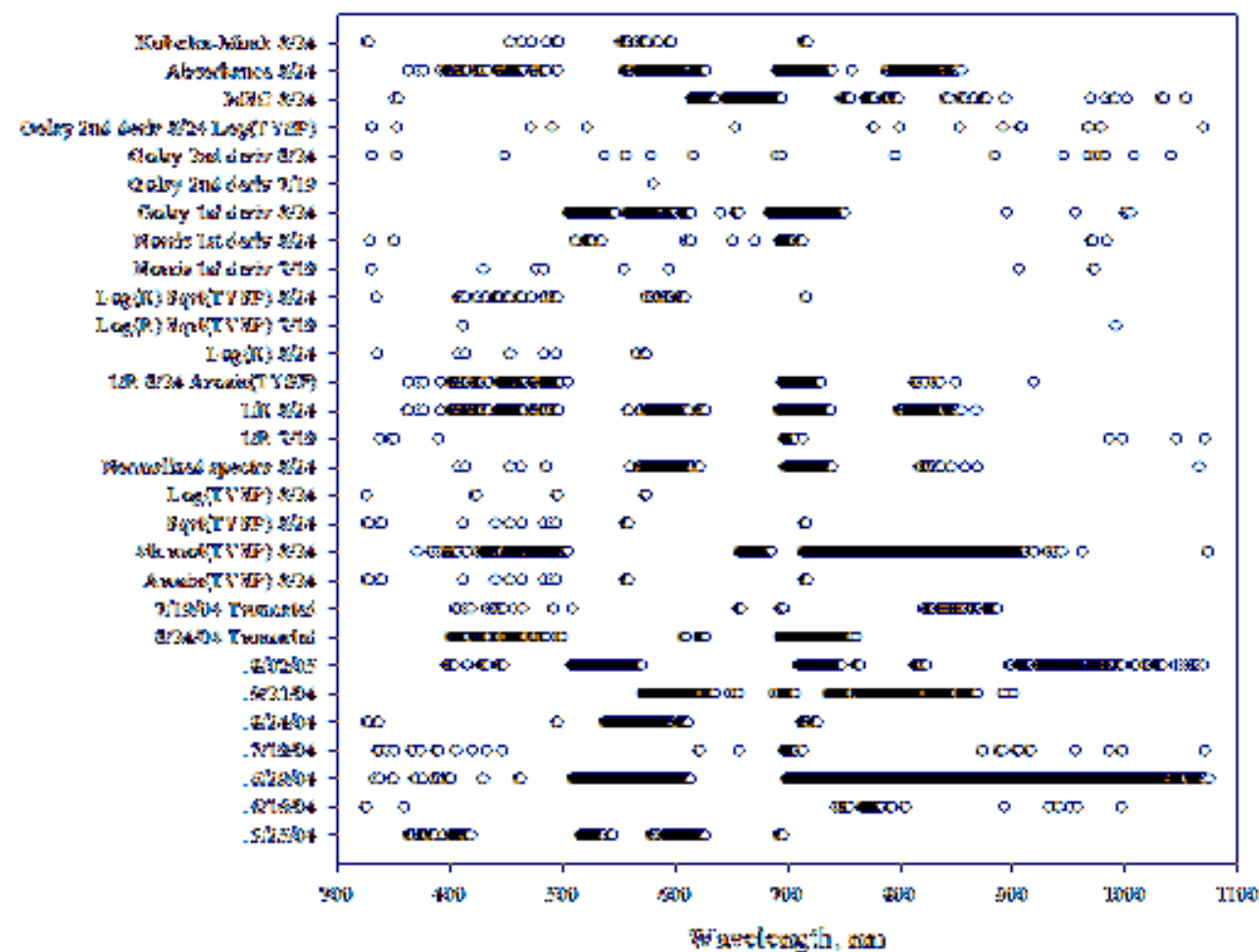


Figure C20. Significant spectral bands for *Typha* species according to PLS-regressions at the *Phragmites*-absent site.

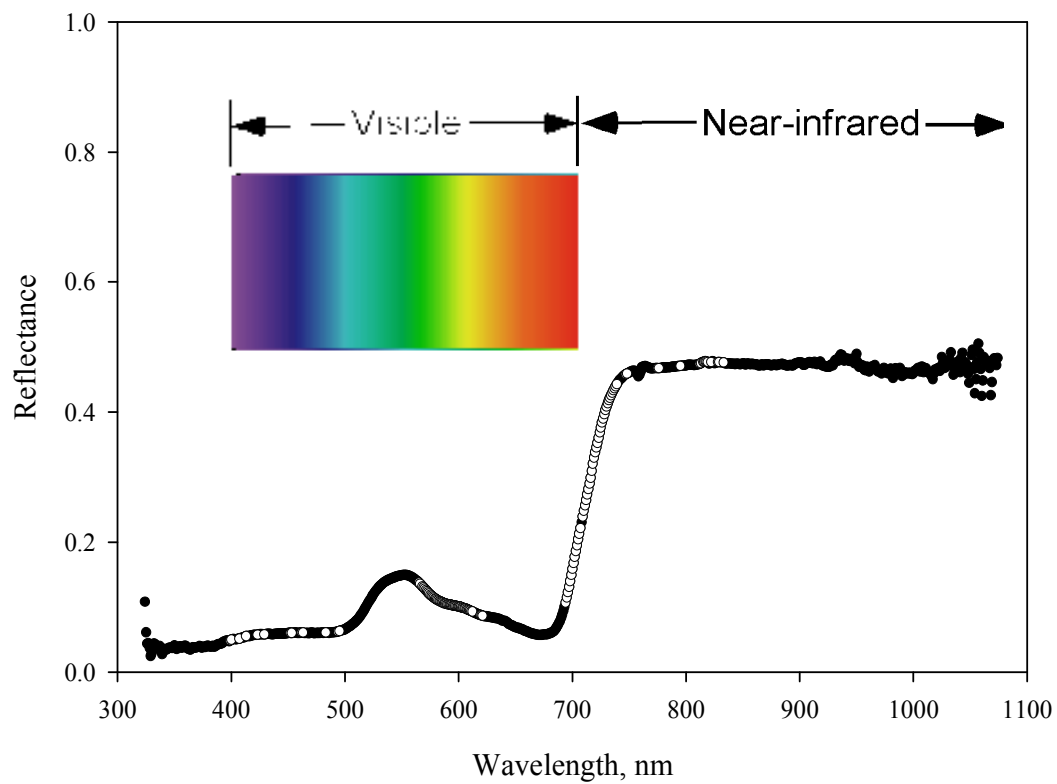


Figure C21. Spectral bands significant for seven or more regressions for *Typha* species at the *Phragmites*-absent site are indicated by an open circle.

Table C13. PLS-regressions for *I. capensis* percent cover at the *Phragmites*-dominant (PD) site. *r* = regression coefficient, RMSEP = root mean square error of prediction, PCs = PLS-components

Spectra Transformations	<i>I. capensis</i> Transformations	Date	<i>r</i>	RMSEP	n	Name of plots removed	PCs	# bands used	Comments
Norris 1 st Derivative	none	7.19.04	0.90	10.74	13	Plot 1, 14	4	45	Plot 1: high reflect.; Plot 14: low <i>I. capensis</i> conc.
Golay 1 st Derivative	none	7.19.04	0.90	10.85	13	Plots 1,14	2	60	Plot 1: high reflect.; Plot 14: low <i>I. capensis</i> conc.
Log R	Square root IMCA	8.24.04	0.90	0.87	14	Plot 4	9	44	Plot 4: low reflectance
Untransformed d (350-1075nm)	Arcsine sqrt (IMCA)	7.19.04	0.83	0.18	14	Plot 1	2	9	Plot 1: high reflectance
Untransformed d (350-1075nm)	Square root IMCA	7.19.04	0.83	1.49	14	Plot 1	2	11	Plot 1: high reflectance
Untransformed d (350-1075nm)	4th root IMCA	7.19.04	0.82	0.39	14	Plot 1	3	14	Plot 1: high reflectance
Golay 2 nd Derivative, avg 10	Log IMCA	7.19.04	0.79	0.34	13	Plots 3,14	1	60	Plot 3: high reflect. ; Plot 14: low <i>I. capensis</i> conc.
Log R	none	7.19.04	0.77	15.82	14	Plot 1	3	14	Plot 1: high reflectance
Untransformed d (350-1075nm)	none	7.19.04	0.75	17.55	14	Plot 1	2	6	Plot 1: high reflectance
Untransformed d (350-1075nm)	Arcsine sqrt (IMCA)	8.24.04	0.73	0.18	14	Plot 6	3	61	Plot 6: high reflectance
Untransformed d (350-1075nm)	Log (base 10) IMCA	7.19.04	0.72	0.38	13	Plot 1, 14	3	10	Plot 1: high reflect.; Plot 14: low <i>I. capensis</i> conc.
Log R	Square root IMCA	7.19.04	0.72	1.79	14	Plot 1	2	16	Plot 1: high reflectance
Untransformed d (350-1075nm)	none	6.06.05	0.69	21.45	14	Plot 7	2	50	Plot 7: low reflectance
Untransformed d (350-1075nm)	none	8.24.04	0.68	15.53	14	Plot 6	3	148	Plot 6: high reflectance
Golay 1 st Derivative	none	8.24.04	0.67	15.13	14	Plot 6	1	15	Plot 6: high reflectance
MSC Transformation	none	7.19.04	0.66	18.06	14	Plot 14	6	none	Plot 14: low <i>I. capensis</i> concentration
Norris 1 st Derivative	none	8.24.04	0.66	15.23	14	Plot 6	1	9	Plot 6: high reflectance

Spectra Transformations	<i>I. capensis</i> Transformations	Date	r	RMSEP	n	Name of plots removed	PCs	# bands used	Comments
Golay 2 nd Derivative, avg 10	none	8.24.04	0.61	16.29	13	Plots 4,6	1	4	Plot 4: low reflectance; Plot 6: high reflectance
Untransformed (350-1075nm)	none	6.16.04	0.54	14.92	15	none	2	448	none
Golay 2 nd Derivative, avg 10	none	7.19.04	0.54	22.08	14	Plot 3	1	16	Plot 3: high amount of noise in reflect. derivative
Untransformed (350-1075nm)	none	6.29.04	0.52	13.69	15	none	3	50	none
Transform 1/R	Arcsine sqrt (IMCA)	7.19.04	0.50	0.25	14	Plot 14	5	4	Plot 14: low <i>I. capensis</i> concentration
Untransformed (350-1075nm)	none	5.25.04	0.49	12.24	12	Plots 1,2,3	2	50	Plots 1,2,3: missing reflectance
Truncated spectra (400-950nm)	none	7.19.04	0.48	20.36	14	Plot 14	1	269	Plot 14: low <i>I. capensis</i> concentration
Normalized spectra (R/R410)	none	7.19.04	0.47	23.34	13	Plot 1, 14	3	38	Plot 1: high reflect.; Plot 14: low <i>I. capensis</i> conc.
Kubelka-Munk Transformation	none	7.19.04	0.47	21.34	14	Plot 14	3	13	Plot 14: low <i>I. capensis</i> concentration
Transform 1/R	none	7.19.04	0.44	22.24	14	Plot 14	3	21	Plot 14: low <i>I. capensis</i> concentration
Untransformed (350-1075nm)	none	8.02.05	0.37	28.25	15	none	1	none	none
Absorbance Transformation	none	7.19.04	0.30	22.17	14	Plot 14	1	73	Plot 14: low <i>I. capensis</i> concentration
Truncated spectra (400-950nm)	none	8.24.04	0.27	14.55	13	Plots 10,12	1	124	Plots 10,12: high <i>I. capensis</i> concentration
Untransformed (350-1075nm)	none	6.03.04	0.19	10.17	13	Plots 3,13	1	none	Plot 3: high reflectance; Plot 13: low reflectance
Untransformed (350-1075nm)	none	9.21.04	-0.31	27.30	15	none	1	none	none

Table C14. PLS-regressions for *I. capensis* percent cover at the *Phragmites*-absent (PA) site. r = regression coefficient, RMSEP = root mean square error of prediction, PCs = PLS-components

Spectra Transformations	<i>I. capensis</i> Transformations	Date	r	RMSEP	n	Name of plots removed	PCs	# bands used	Comments
Transform 1/R	none	7.19.04	0.90	13.09	14	Plot 15	3	26	Plot 15: <i>I. capensis</i> missing
Log R	none	7.19.04	0.89	15.04	14	Plot 15	8	59	Plot 15: <i>I. capensis</i> missing
Untransformed (350-1075nm)	none	6.16.04	0.87	14.63	13	Plots 11, 14	7	50	Plot 11: high reflectance; Plot 14: low reflectance
Untransformed (350-1075nm)	none	7.19.04	0.86	15.85	14	Plot 15	6	34	Plot 15: <i>I. capensis</i> missing
Untransformed (350-1075nm)	none	6.03.04	0.85	6.92	12	Plots 1, 9, 15	8	99	Plot 1: high refl; Plot 9: no refl; Plot 15: low refl.
Log R	Square root IMCA	7.19.04	0.84	1.70	14	Plot 15	5	42	Plot 15: <i>I. capensis</i> missing
Absorbance Transformation	none	7.19.04	0.84	16.65	14	Plot 15	3	53	Plot 15: <i>I. capensis</i> missing
Transform 1/R	Arcsine sqrt (IMCA)	7.19.04	0.82	0.21	14	Plot 15	4	34	Plot 15: <i>I. capensis</i> missing
MSC Transformation	none	7.19.04	0.81	19.64	14	Plot 15	2	13	Plot 15: <i>I. capensis</i> missing
Untransformed (350-1075nm) Kubelka-Munk Transformation	Arcsine sqrt (IMCA)	7.19.04	0.80	0.25	14	Plot 15	2	10	Plot 15: <i>I. capensis</i> missing
Untransformed (350-1075nm)	none	7.19.04	0.79	18.67	14	Plot 15	3	78	Plot 15: <i>I. capensis</i> missing
Untransformed (350-1075nm)	Square root IMCA	7.19.04	0.77	2.13	14	Plot 15	2	6	Plot 15: <i>I. capensis</i> missing
Normalized spectra (R/R410)	none	7.19.04	0.77	19.64	14	Plot 15	2	72	Plot 15: <i>I. capensis</i> missing
Golay 1 st Derivative	none	7.19.04	0.76	19.78	14	Plot 15	3	10	Plot 15: <i>I. capensis</i> missing
Norris 1 st Derivative	none	7.19.04	0.74	20.21	14	Plot 15	1	20	Plot 15: <i>I. capensis</i> missing
Untransformed (350-1075nm)	4th root IMCA	7.19.04	0.72	0.59	14	Plot 15	2	4	Plot 15: <i>I. capensis</i> missing
Untransformed (350-1075nm)	none	8.24.04	0.71	19.40	13	Plots 1,15	2	56	Plot 1: high reflectance; Plot 15: low reflectance

Spectra Transformations	<i>I. capensis</i> Transformations	Date	r	RMSEP	n	Name of plots removed	PCs	# bands used	Comments
Golay 1 st Derivative	none	8.24.04	0.69	18.90	15	none	1	75	none
Log R	Square root IMCA	8.24.04	0.68	2.33	13	Plots 1,15	2	408	Plot 1: high reflectance; Plot 15: low reflectance
Untransformed (350-1075nm)	none	6.29.04	0.67	23.33	14	Plot 6	2	43	Plot 6: low reflectance
Norris 1 st Derivative	none	8.24.04	0.67	19.75	15	none	2	51	none
Untransformed (350-1075nm)	none	8.02.05	0.66	23.33	15	none	2	63	none
Untransformed (350-1075nm)	Log (base 10) IMCA	7.19.04	0.64	0.64	14	Plot 15	2	4	Plot 15: <i>I. capensis</i> missing
Golay 2 nd Derivative, avg 10	none	8.24.04	0.61	21.30	14	Plot 1	1	18	Plot 1: high reflectance
Untransformed (350-1075nm)	none	6.06.05	0.56	19.78	14	Plot 3	1	385	Plot 3: high reflectance
Truncated spectra (400-950nm)	none	7.19.04	0.55	29.52	14	Plot 15	3	11	Plot 15: <i>I. capensis</i> missing
Truncated spectra (400-950nm)	none	8.24.04	0.55	23.27	13	Plots 1,15	2	298	Plot 1: high reflectance; Plot 15: low reflectance
Transform 1/R	none	8.24.04	0.51	24.75	13	Plots 1,15	2	none	Plot 1: high reflectance; Plot 15: low reflectance
Golay 2 nd Derivative, avg 10	none	7.19.04	0.46	28.19	13	Plots 8, 15	1	18	Plot 8: noisy derivative; Plot 15: <i>I. capensis</i> missing
Golay 2 nd Derivative, avg 10	Log IMCA	7.19.04	0.25	0.68	13	Plots 8, 15	1	5	Plot 8: noisy derivative; Plot 15: <i>I. capensis</i> missing
Untransformed (350-1075nm)	none	9.21.04	0.20	26.50	14	Plot 12	1	64	Plot 12: high reflectance
Untransformed (350-1075nm)	none	5.25.04	-0.10	31.49	15	none	1	none	none

Table C15. PLS-regression transformations tested on spectra and *I. capensis* percent cover. Site is identified as PD (*Phragmites*-dominant) or PA (*Phragmites*-absent).

	Untransformed (350-1075 nm)	Truncated spectra (400-950 nm)	Arcsine sqrt (IMCA)	4th root IMCA	Sqrt (IMCA)	Log ₁₀ IMCA	Normalized spectra	Transform 1/R	Transform 1/R, Arcsine sqrt (IMCA)	Log R	Log R, Sqrt (IMCA)
5/25/2004	PD site and PA site										
6/3/2004	PD, PA										
6/16/2004	PD, PA										
6/29/2004	PD, PA										
7/19/2004	PD, PA	PD, PA	PD, PA	PD, PA	PD, PA	PD, PA	PD, PA	PD, PA	PD, PA	PD, PA	PD, PA
8/24/2004	PD, PA	PD, PA	PD					PA			PD, PA
9/21/2004	PD, PA										
6/6/2005	PD, PA										
8/2/2005	PD, PA										

	Norris 1st Derivative	Golay 1st Derivative	Golay 2nd Derivative	Golay 2nd Derivative, Log (IMCA)	MSC Transform	Absorbance Transform	Kubelka-Munk Transform
5/25/2004							
6/3/2004							
6/16/2004							
6/29/2004							
7/19/2004	PD, PA	PD, PA	PD, PA	PD, PA	PD, PA	PD, PA	PD, PA
8/24/2004	PD, PA	PD, PA	PD, PA				
9/21/2004							
6/6/2005							
8/2/2005							

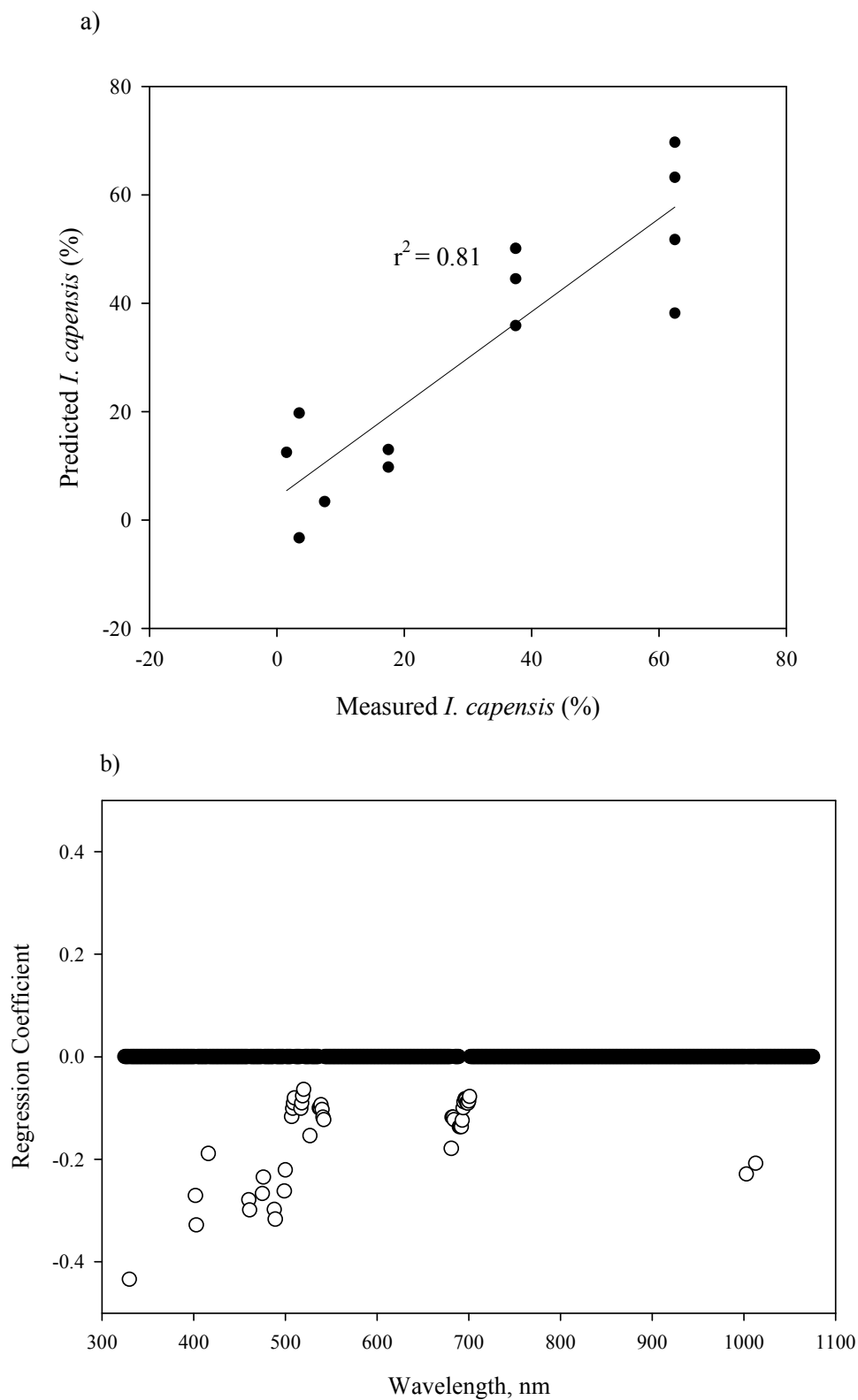


Figure C22 (a) Predicted vs measured *I. capensis* cover using 45 spectral bands of first derivative transformed reflectance at the *Phragmites*-dominant site on 7/19/04 to combine into four PLS-components with an RMSEP of 10.8% and $r = 0.90$. (b) Loading plot of regression coefficients where spectral bands used in the regression are depicted by open circles.

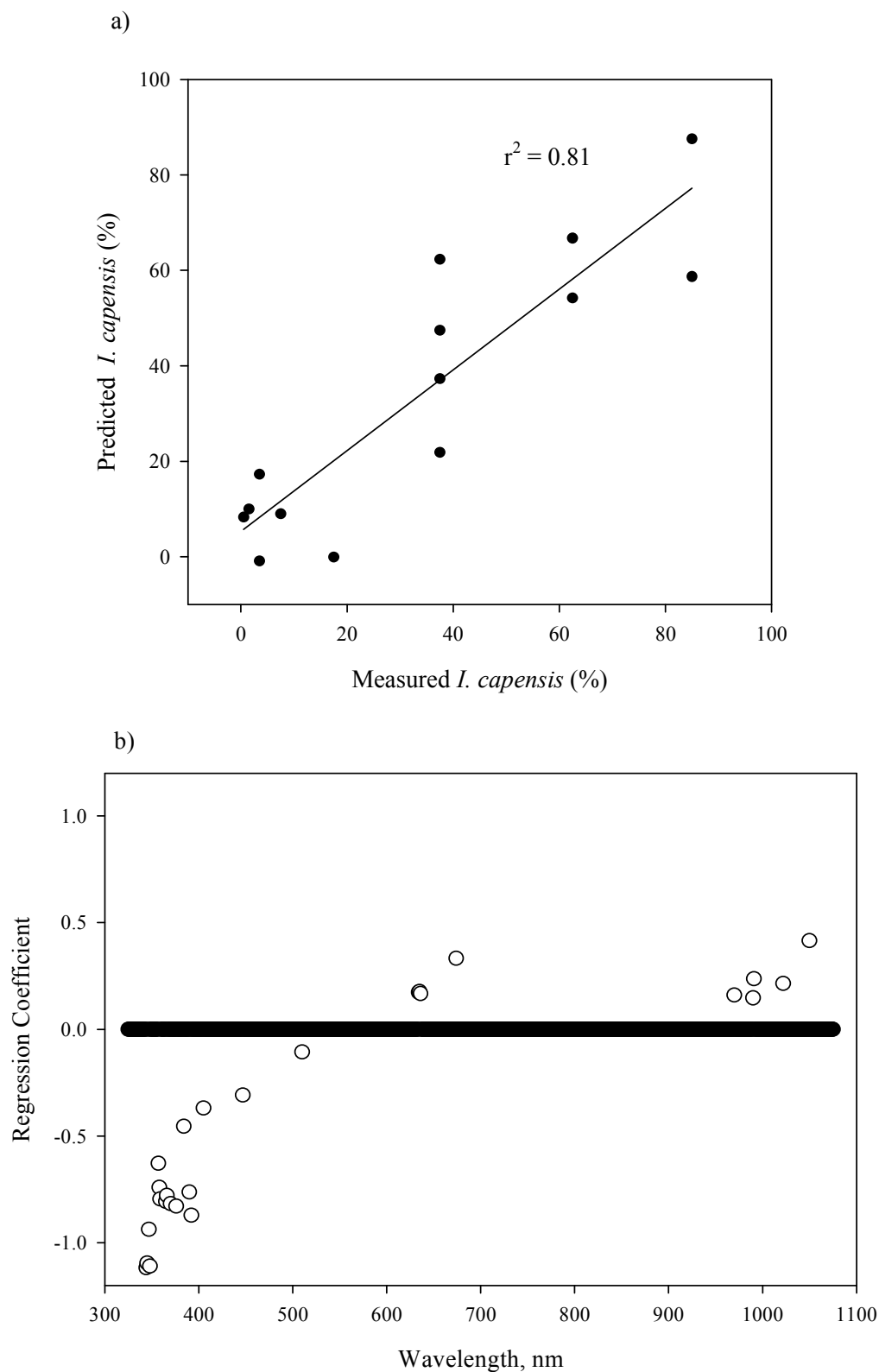


Figure C23. (a) Predicted vs measured *I. capensis* percent cover PLS-regression using 26 spectral bands of inverse reflectance at the *Phragmites*-absent site on 7/19/04 to combine into three PLS-components with an RMSEP of 13% and $r = 0.90$. (b) Loading plot of regression coefficients where spectral bands used in the regression are depicted by open circles.

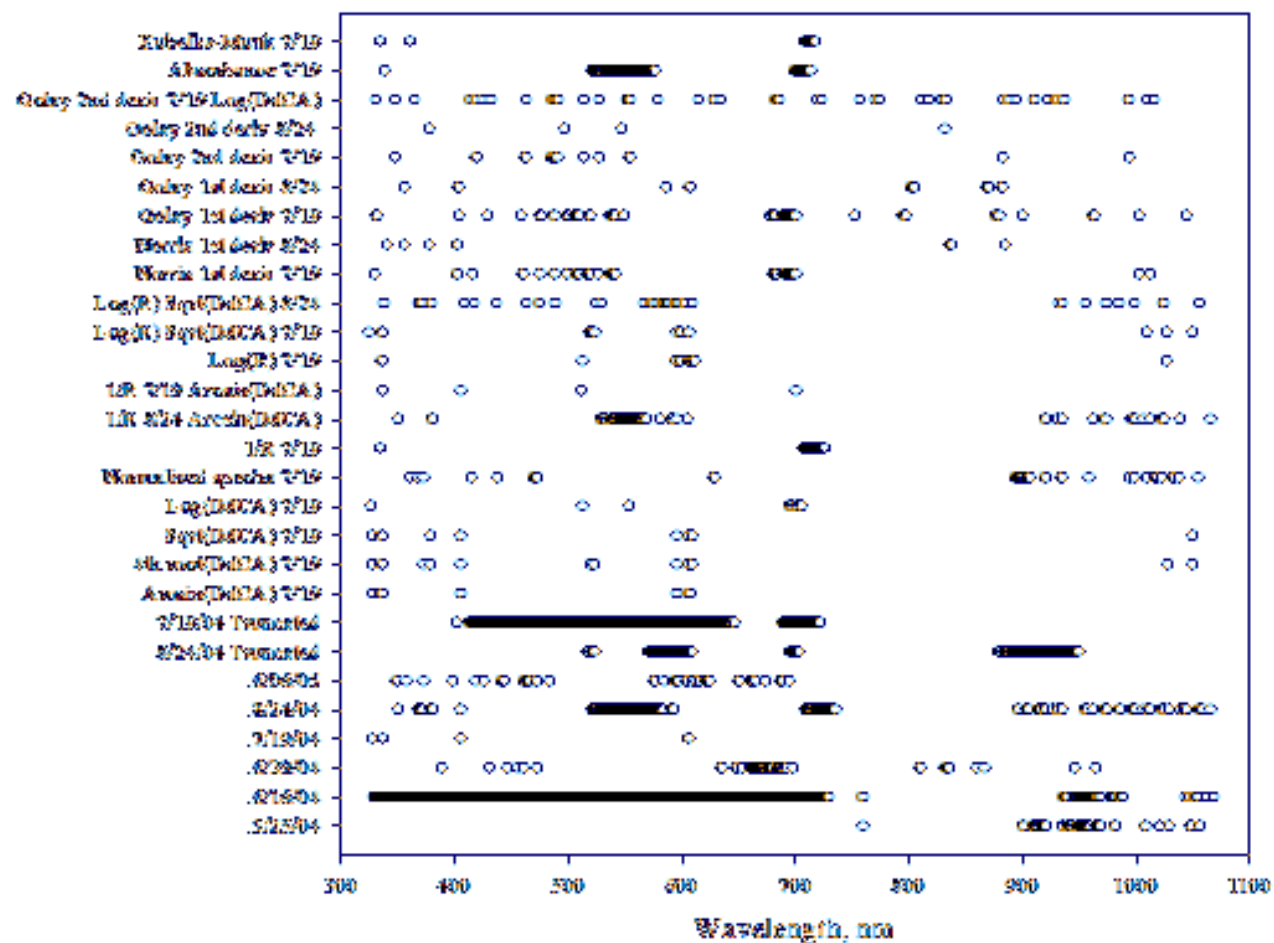


Figure C24. Significant spectral bands for *I. capensis* according to PLS-regressions at the *Phragmites*-dominant site.

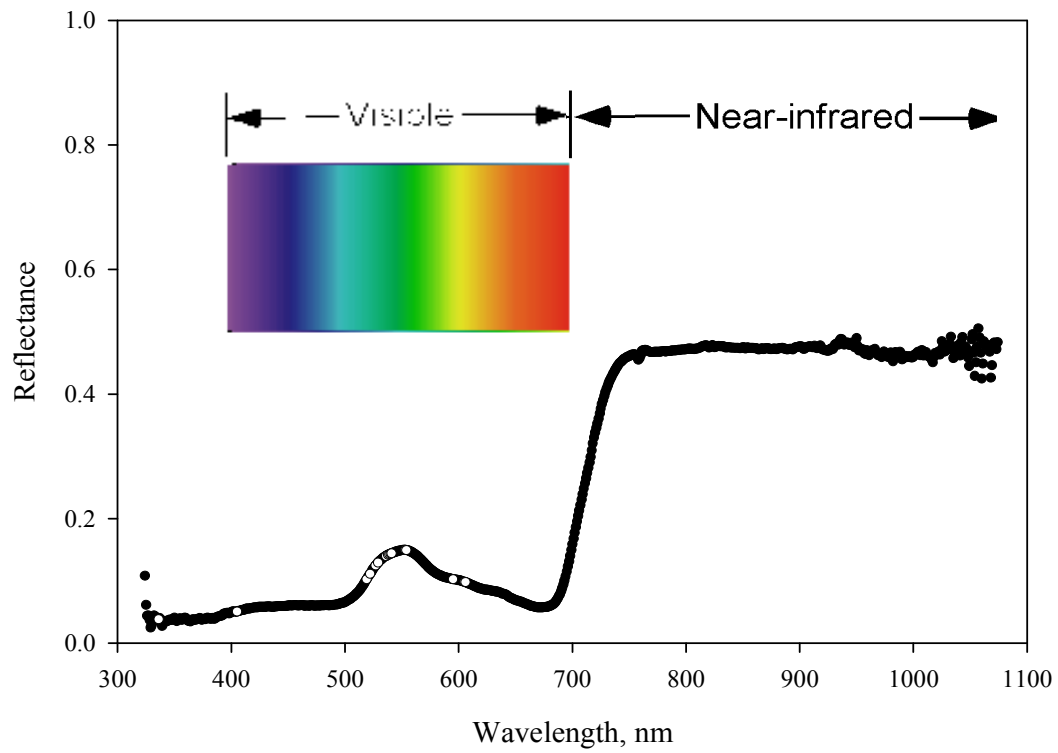


Figure C25. Spectral bands significant for seven or more regressions for *I. capensis* at the *Phragmites*-dominant site are indicated by an open circle.

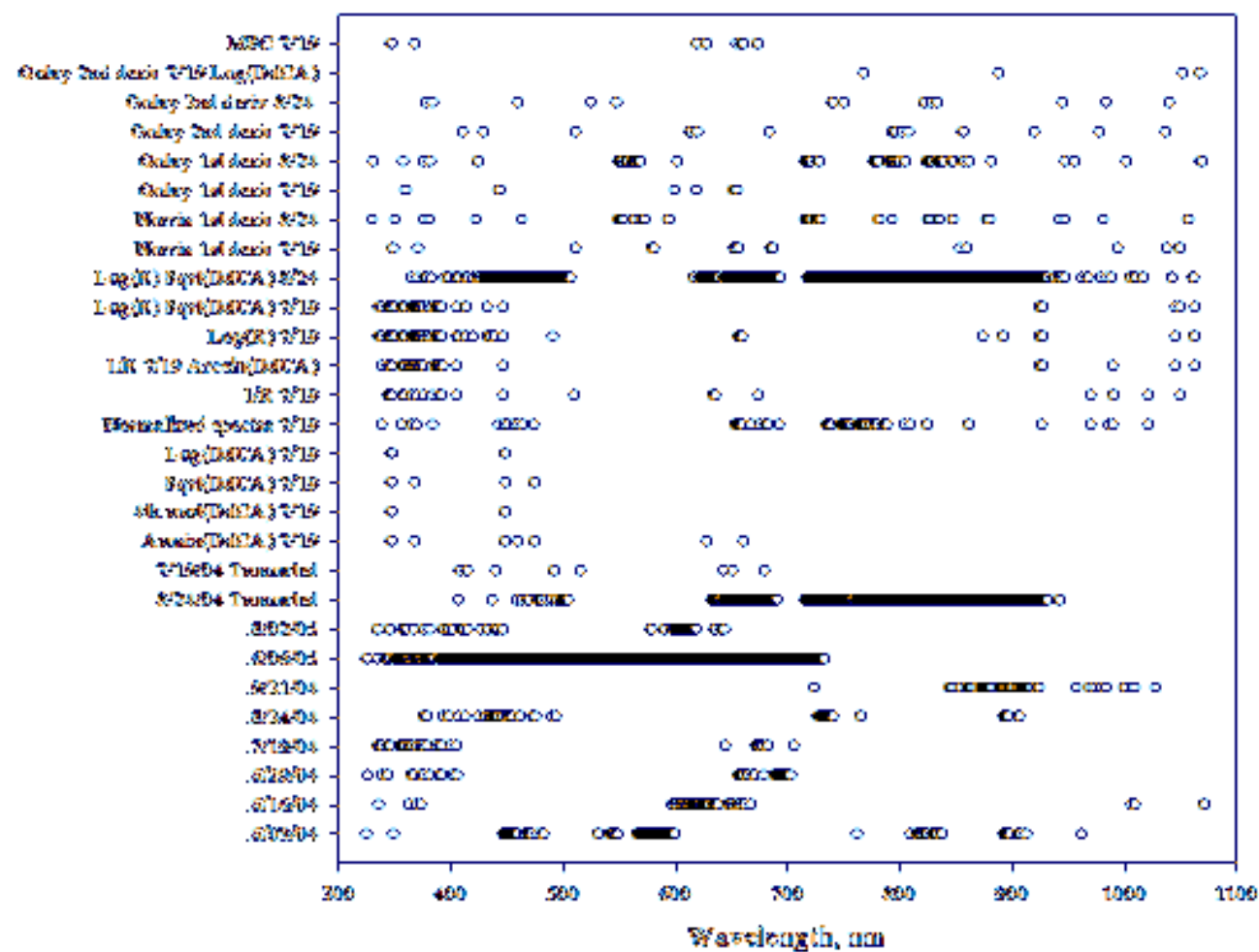


Figure C26. Significant spectral bands for *I. capensis* according to PLS-regressions at the *Phragmites*-absent site.

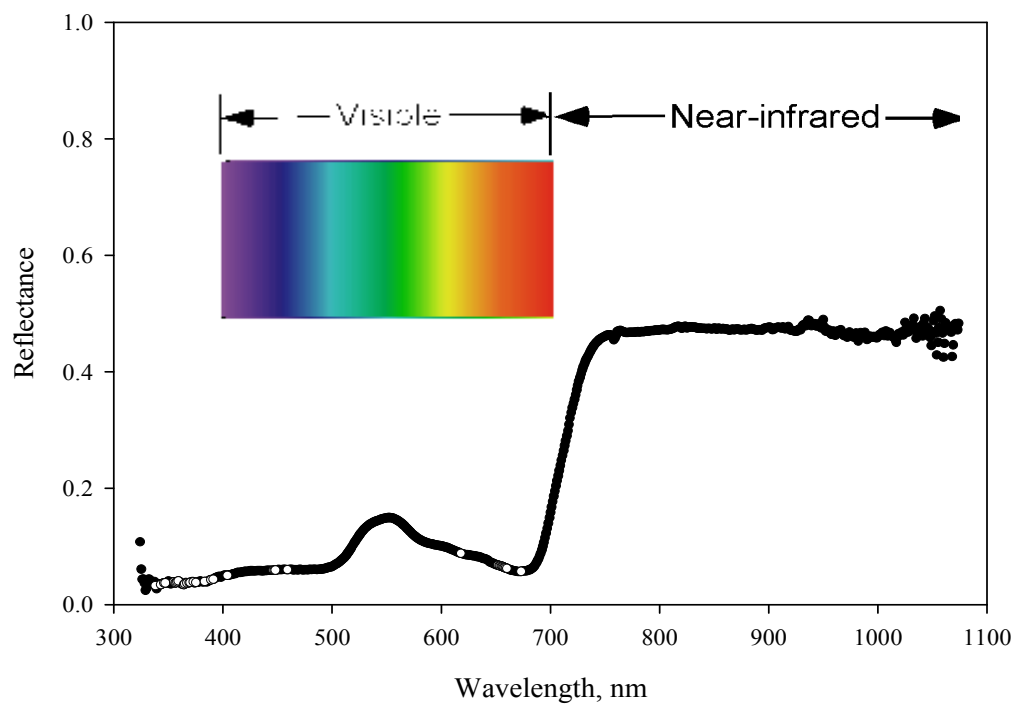


Figure C27. Spectral bands significant for seven or more regressions for *I. capensis* at the *Phragmites*-absent site are indicated by an open circle.

Table C16. PLS-regressions for LAI at the *Phragmites*-dominant (PD) site. r = regression coefficient, RMSEP = root mean square error of prediction, PCs = PLS-components

Spectra Transformations	LAI Transformations	Date	r	RMSEP	n	Name of plots removed	PCs	# bands used	Comments
Untransformed (350-1075nm)	none	6.16.04	0.90	0.46	15	none	10	107	none
Untransformed (350-1075nm)	none	7.19.04	0.89	0.42	14	Plot 8	10	31	Plot 8: high LAI
Untransformed (350-1075nm)	Arcsine sqrt (LAI)	7.19.04	0.89	0.01	14	Plot 8	10	30	Plot 8: high LAI
Untransformed (350-1075nm)	Square root LAI	7.19.04	0.89	0.09	14	Plot 8	10	30	Plot 8: high LAI
Truncated spectra (400-950nm)	none	7.19.04	0.87	0.45	14	Plot 8	5	38	Plot 8: high LAI
Transform 1/R	Arcsine sqrt (LAI)	7.19.04	0.84	0.01	14	Plot 8	3	97	Plot 8: high LAI
MSC Transformation	none	7.19.04	0.84	0.50	14	Plot 8	4	34	Plot 8: high LAI
Untransformed (350-1075nm)	4th root LAI	7.19.04	0.83	0.04	14	Plot 8	10	27	Plot 8: high LAI
Transform 1/R	none	7.19.05	0.82	0.51	14	Plot 8	3	93	Plot 8: high LAI
Golay 2 nd Derivative, avg 10	Log LAI	9.21.04	0.80	0.05	15	none	1	17	none
Log R	Square root LAI	7.19.04	0.76	0.13	14	Plot 8	3	93	Plot 8: high LAI
Untransformed (350-1075nm)	none	8.24.04	0.76	0.76	14	Plot 6	3	80	Plot 6: high reflectance
Untransformed (350-1075nm)	none	6.06.05	0.74	0.89	14	Plot 11	2	559	Plot 11: missing LAI data
Log R	none	7.19.04	0.74	0.62	14	Plot 8	3	91	Plot 8: high LAI
Golay 1 st Derivative	none	7.19.04	0.73	0.61	14	Plot 7	4	57	Plot 7: low LAI
Norris 1 st Derivative	none	7.19.04	0.72	0.62	14	Plot 7	2	51	Plot 7: low LAI
Norris 1 st Derivative	Log LAI	7.19.04	0.72	0.05	14	Plot 7	2	37	Plot 7: low LAI
Truncated spectra (400-950nm)	none	8.24.04	0.69	0.93	14	Plot 6	5	30	Plot 6: high reflectance
Golay 2 nd Derivative, avg 10	none	8.24.04	0.69	0.84	15	none	1	13	none
Absorbance Transformation	none	7.19.04	0.68	0.68	13	Plots 8, 10	4	9	Plot 8: high LAI; Plot 10: high absorbance
Untransformed (350-1075nm)	Log (base 10) LAI	7.19.04	0.67	0.07	14	Plot 8	4	21	Plot 8: high LAI
Norris 1 st Derivative	Log LAI	8.02.05	0.66	0.08	14	Plot 10	1	33	Plot 10: low LAI
Golay 2 nd Derivative, avg 10	Log LAI	7.19.04	0.65	0.05	14	Plot 7	1	16	Plot 7: low LAI

Spectra Transformations	LAI Transformations	Date	r	RMSEP	n	Name of plots removed	PCs	# bands used	Comments
Kubelka-Munk Transformation	none	7.19.04	0.65	0.81	15	none	2	11	none
Golay 2 nd Derivative, avg 10	Log LAI	8.24.04	0.65	0.07	15	none	1	15	none
Golay 2 nd Derivative, avg 10	none	7.19.04	0.63	0.68	14	Plot 7	1	17	Plot 7: low LAI
Normalized spectra (R/R410)	none	7.19.04	0.60	0.70	14	Plot 7	3	28	Plot 7: low LAI
Log R	Square root LAI	8.24.04	0.60	0.20	14	Plot 6	8	11	Plot 6: high reflectance
Transform 1/R	none	8.24.04	0.56	1.03	14	Plot 6	9	14	Plot 6: high reflectance
Untransformed (350-1075nm)	none	8.02.05	0.53	1.20	14	Plot 5	5	6	Plot 5: high reflectance
Norris 1 st Derivative	Log LAI	8.24.04	0.53	0.08	14	Plot 6	1	74	Plot 6: high reflectance
Untrans. spectra, manual test set	none	8.24.04	0.52	1.12	5	none	6	none	Remaining plots used in the calibration set
Golay 1 st Derivative	none	8.24.04	0.48	1.02	14	Plot 6	1	88	Plot 6: high reflectance Remaining used in the cal. set; Plot 6: high refl
Untrans. spectra, random test set	none	8.24.04	0.38	0.79	5	Plot 6	2	none	
Untransformed (350-1075nm)	none	9.21.04	0.12	0.61	14	Plot 10	1	24	Plot 10: low reflectance
Untransformed (350-1075nm)	none	6.29.04	0.08	1.02	14	Plot 8	1	none	Plot 8: low reflectance
PLS2 Untransformed (325-1075nm)	LAI, Species, Diver.	7.19.04	0.21	0.99	14	Plot 7	1	none	Plot 7: low LAI
Untransformed (350-1075nm)	none	5.25.04	0.48	0.93	15	none	1	none	none
Untransformed (350-1075nm)	none	6.03.04	0.69	0.80	15	none	1	none	none

Table C17. PLS-regressions for LAI at the *Phragmites*-absent (PA) site. r = regression coefficient, RMSEP = root mean square error of prediction, PCs = PLS-components

Spectra Transformations	LAI Transformations	Date	r	RMSEP	n	Name of plots removed	PCs	# bands used	Comments
Untrans. spectra, manual test set	none	8.24.04	0.95	1.54	5	none	5	none	Remainder used in calibration
Untrans. spectra, random test set	none	8.24.04	0.87	0.98	5	none	2	none	Remainder used in calibration
Golay 2 nd Derivative, avg 10	Log LAI	8.24.04	0.83	0.06	15	none	2	46	none
Norris 1 st Derivative	none	8.02.05	0.81	0.84	14	Plot 3	2	154	Plot 3: high reflectance
Normalized spectra (R/R410)	none	7.19.04	0.80	0.70	15	none	4	409	none
Untransformed (350-1075nm)	none	8.24.04	0.79	0.76	14	Plot 1	2	445	Plot 1: high reflectance
Untransformed (350-1075nm)	Arcsine sqrt (LAI)	7.19.04	0.78	0.02	15	none	5	144	none
Untransformed (350-1075nm)	4th root LAI	7.19.04	0.78	0.06	15	none	5	143	none
Untransformed (350-1075nm)	Square root LAI	7.19.04	0.78	0.18	15	none	5	144	none
Log R	none	7.19.04	0.78	0.74	15	none	4	174	none
Golay 2 nd Derivative, avg 10	Log LAI	7.19.04	0.76	0.07	15	none	1	37	none
Transform 1/R	none	8.24.04	0.76	0.80	14	Plot 1	2	418	Plot 1: high reflectance
Log R	Square root LAI	8.24.04	0.76	0.18	15	none	3	29	none
Golay 2 nd Derivative, avg 10	none	7.19.04	0.75	0.78	15	none	1	31	none
Truncated spectra (400-950nm)	none	8.24.04	0.75	0.82	14	Plot 1	2	333	Plot 1: high reflectance
Golay 2 nd Derivative, avg 10	Log LAI	9.21.04	0.75	0.10	14	Plot 5	1	31	Plot 5: high LAI
Untransformed (350-1075nm)	none	7.19.04	0.73	0.76	13	Plots 6, 15	2	173	Plots 6, 15: high reflectance
MSC Transformation	none	7.19.04	0.72	0.81	15	none	2	165	none
Absorbance Transformation	none	7.19.04	0.72	0.84	15	none	3	179	none
Untransformed (350-1075nm)	Log (base 10) LAI	7.19.04	0.71	0.07	15	none	2	176	none
Transform 1/R	Arcsine sqrt (LAI)	7.19.04	0.71	0.02	15	none	2	154	none
Transform 1/R	none	7.19.05	0.71	0.82	15	none	2	161	none
Untransformed (350-1075nm)	none	8.02.05	0.71	0.70	15	none	2	555	none
Golay 2 nd Derivative, avg 10	none	8.24.04	0.71	0.87	15	none	2	89	none
Log R	Square root LAI	7.19.04	0.70	0.19	15	none	4	168	none

Spectra Transformations	LAI Transformations	Date	r	RMSEP	n	Name of plots removed	PCs	# bands used	Comments
Norris 1 st Derivative	none	7.19.04	0.68	0.86	15	none	2	57	none
Norris 1 st Derivative	Log LAI	7.19.04	0.68	0.08	15	none	2	62	none
Norris 1 st Derivative	Log LAI	8.24.04	0.68	0.08	14	Plot 1	1	215	Plot 1: high reflectance
Golay 1 st Derivative	none	8.24.04	0.67	0.92	14	Plot 1	1	237	Plot 1: high reflectance
Golay 1 st Derivative	none	7.19.04	0.65	0.89	15	none	2	73	none
Truncated spectra (400-950nm)	none	7.19.04	0.64	0.64	14	Plot 6	7	421	Plot 6: high reflectance
Untransformed (350-1075nm)	none	5.25.04	0.60	0.88	14	Plot 5	4	39	Plot 5: missing reflectance
Kubelka-Munk Transformation	none	7.19.04	0.55	0.98	15	none	2	230	none
PLS2 Untransformed (325-1075nm)	LAI, species, diver.	7.19.04	0.55	1.04	15	none	3	196	none
Untransformed (350-1075nm)	none	6.29.04	0.47	0.84	14	Plot 5	2	321	Plot 5: high LAI
Untransformed (350-1075nm)	none	9.21.04	0.31	0.57	14	Plot 5	1	96	Plot 5: high LAI
Untransformed (350-1075nm)	none	6.06.05	0.24	1.12	13	Plots 1,3	1	160	Plots 1,3: high reflectance
Untransformed (350-1075nm)	none	6.16.04	0.06	1.01	15	none	1	none	none
Untransformed (350-1075nm)	none	6.03.04	0.01	0.94	11	Plots 8,9,10,14	1	none	Plots 8,10,14: no LAI data; Plot 9: no reflect.

Table C18. PLS-regressions transformations tested on spectra and LAI. Site is identified as PD (*Phragmites*-dominant) or PA (*Phragmites*-absent).

	Untransformed (350-1075 nm)	Truncated spectra (400-950 nm)	Arcsine sqrt (LAI)	4th root LAI	Sqrt (LAI)	Log ₁₀ LAI	Manual test set	Random test set	Normalized spectra	Transform 1/R	Transform 1/R, Arcsine sqrt (LAI)	Log R	Log R, Sqrt (LAI)
5/25/2004	PD site and PA site												
6/3/2004	PD, PA												
6/16/2004	PD, PA												
6/29/2004	PD, PA												
7/19/2004	PD, PA	PD, PA	PD, PA	PD, PA	PD, PA	PD, PA			PD, PA	PD, PA	PD, PA	PD, PA	PD, PA
8/24/2004	PD, PA	PD, PA					PD, PA	PD, PA		PD, PA			PD, PA
9/21/2004	PD, PA												
6/6/2005	PD, PA												
8/2/2005	PD, PA												

	Norris 1st Derivative	Norris 1st Deriv, Log (LAI)	Golay 1st Derivative	Golay 2nd Derivative	Golay 2nd Derivative, Log (LAI)	MSC Transform	Absorbance Transform	Kubelka-Munk Transform
5/25/2004								
6/3/2004								
6/16/2004								
6/29/2004								
7/19/2004	PD, PA	PD, PA	PD, PA	PD, PA	PD, PA	PD, PA	PD, PA	PD, PA
8/24/2004		PD, PA	PD, PA	PD, PA	PD, PA			
9/21/2004					PD, PA			
6/6/2005								
8/2/2005	PA	PD						

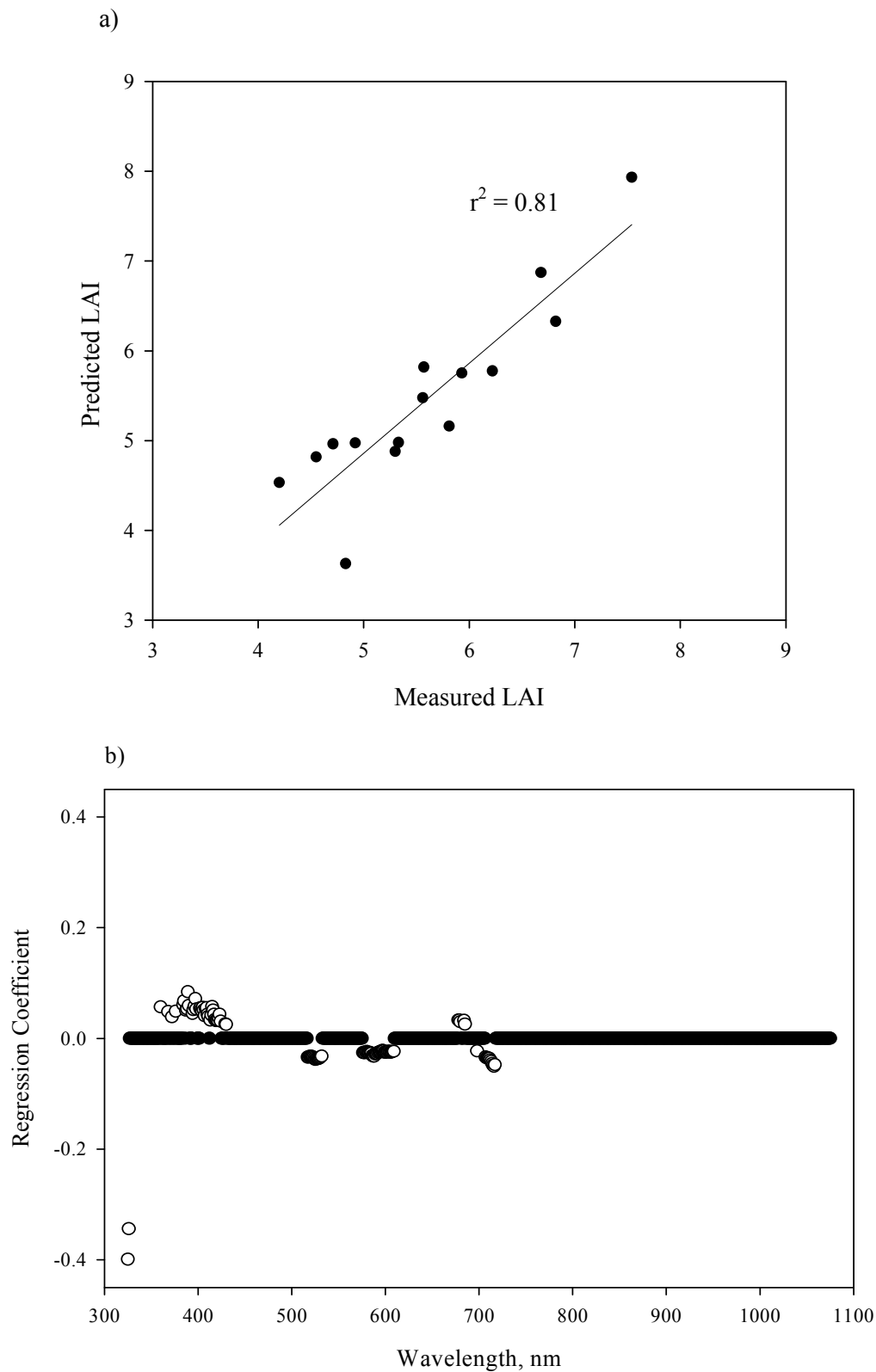


Figure C28. (a) Predicted vs measured LAI PLS-regression at the *Phragmites*-dominant site on 6/16/04 using 107 untransformed spectral bands that were combined into ten PLS-components with an RMSEP of 0.46% and $r = 0.90$. (b) Loading plot of regression coefficients for the PLS-regression where spectral bands used in the regression are depicted by open circles.

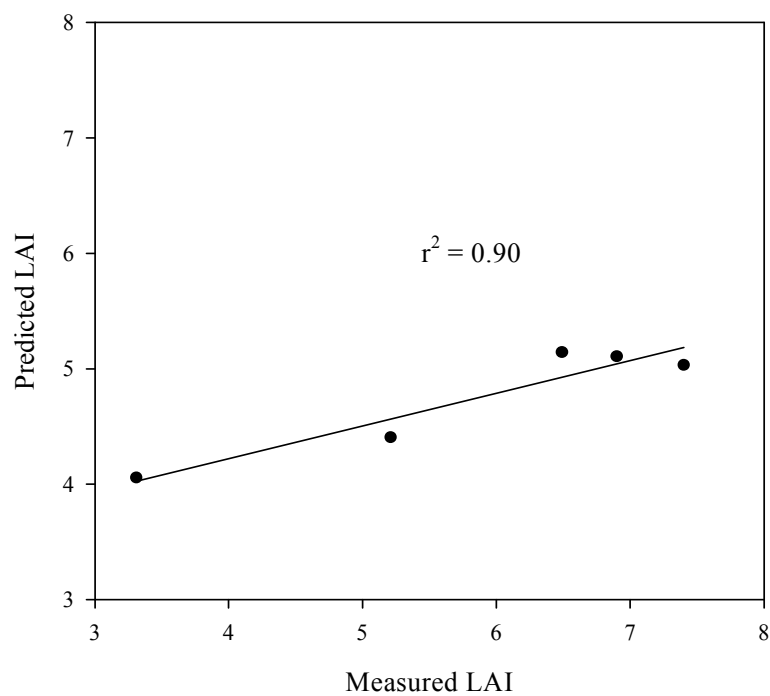


Figure C29. Predicted vs measured LAI PLS-regression at the *Phragmites*-absent site on 8/24/04 using test set validation with five PLS-components and an RMSEP of 1.5% and $r = 0.95$.

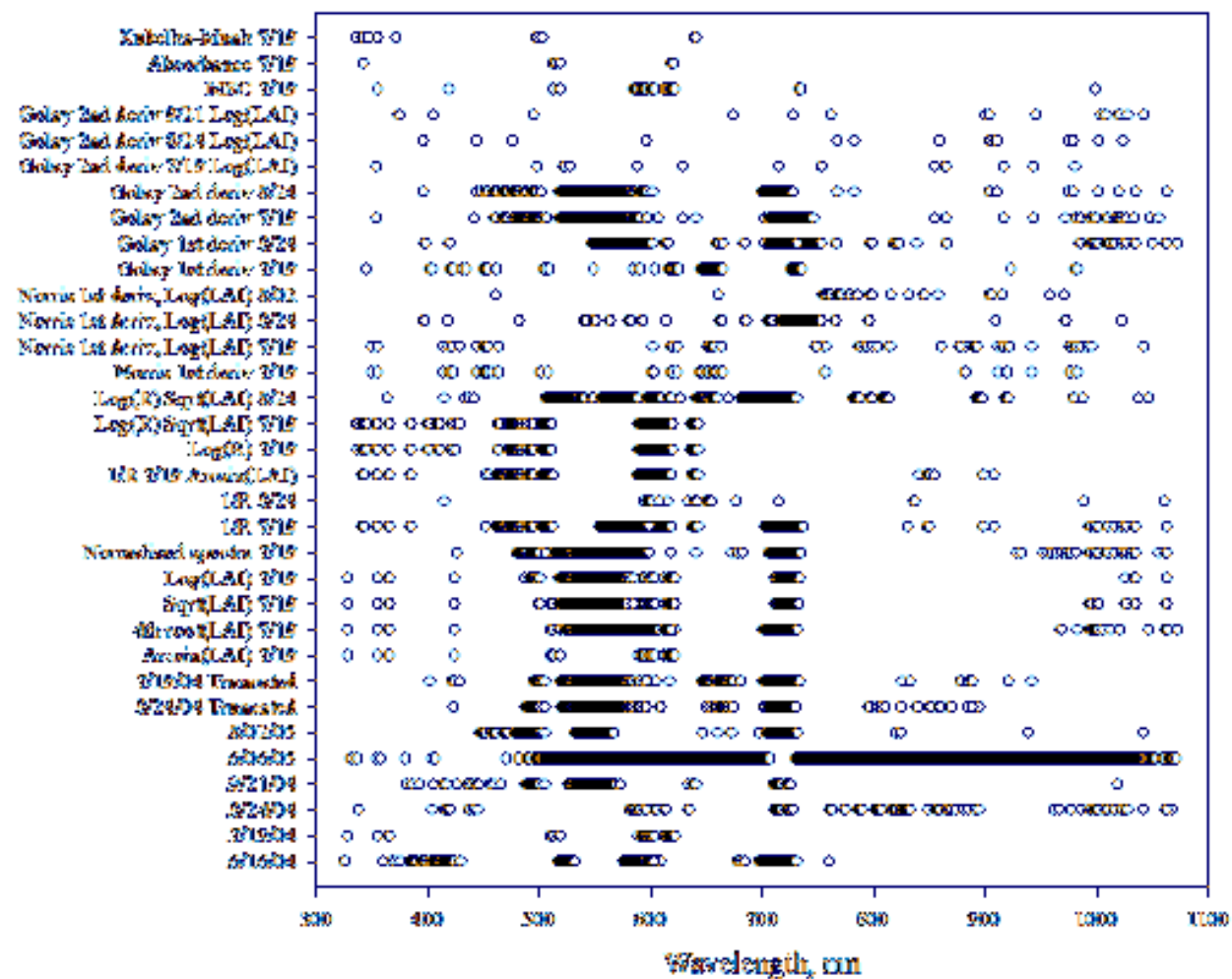


Figure C30. Significant spectral bands for LAI according to PLS-regressions at the *Phragmites*-dominant site.

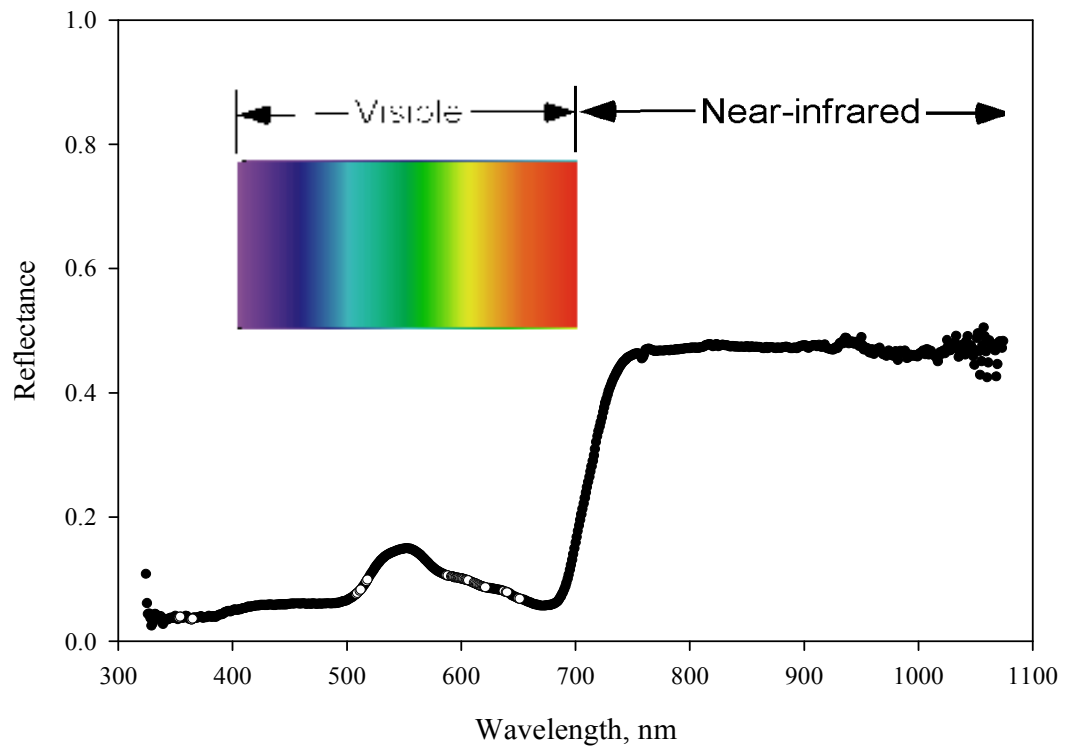


Figure C31. Spectral bands significant for seven or more regressions for LAI at the *Phragmites*-dominant site are indicated by an open circle.

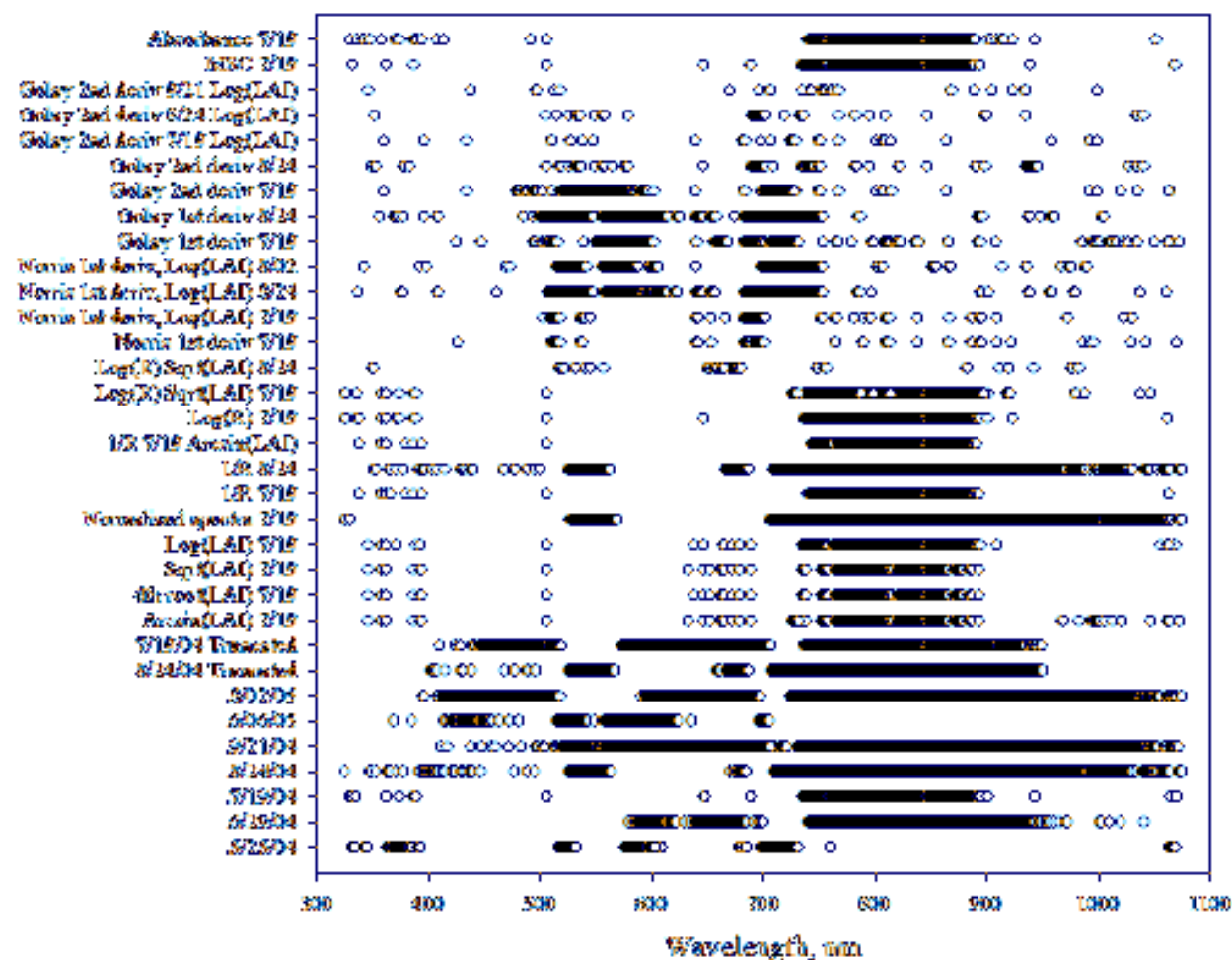


Figure C32. Significant spectral bands for LAI according to PLS-regressions at the *Phragmites*-absent site.

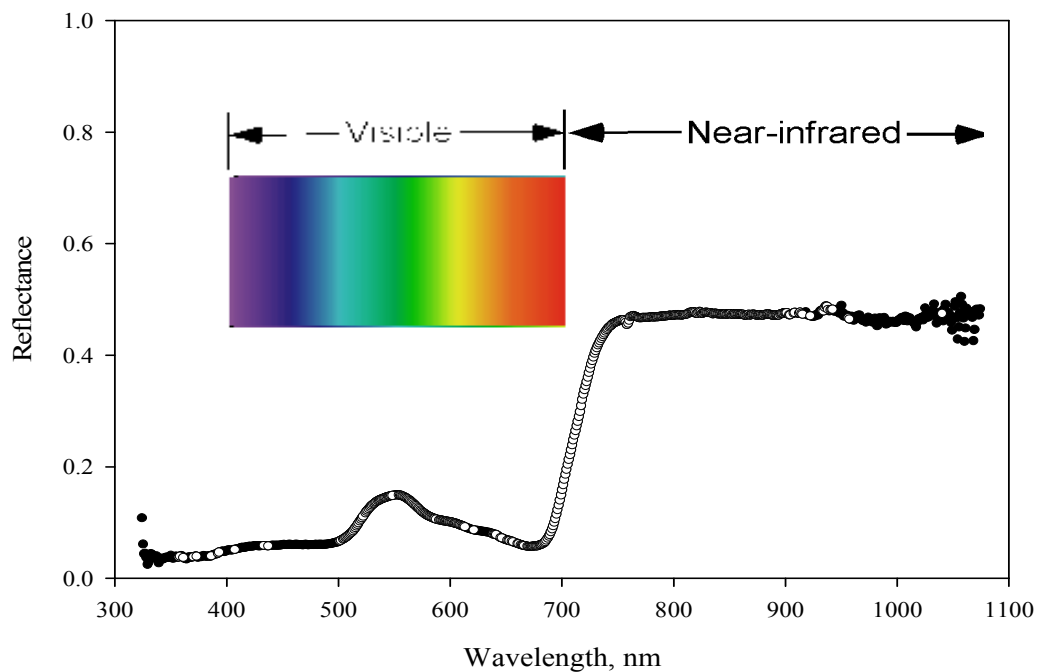


Figure C33. Spectral bands significant for seven or more regressions for LAI at the *Phragmites*-absent site are indicated by an open circle.

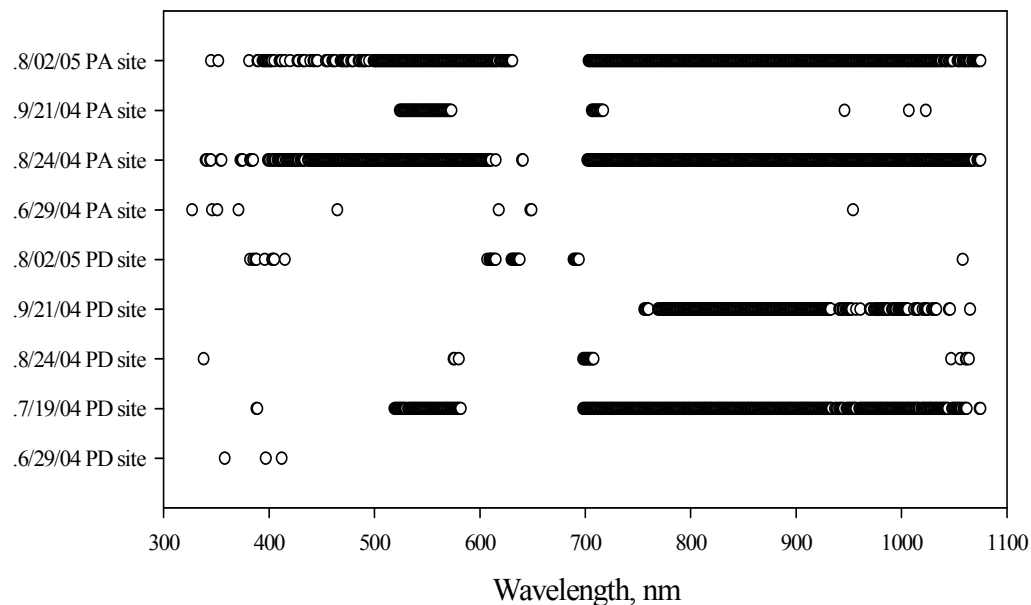


Figure C34. Significant spectral bands for species richness according to PLS-regressions at the *Phragmites*-dominant (PD) site and the *Phragmites*-absent (PA) site.

Table C19. PLS-regressions for species richness on data from both the *Phragmites*-dominant (PD) and *Phragmites*-absent (PA) sites.

Spectra Transformations	Marsh Site	Date	r	RMSEP	n	Name of plots removed	PCs	# bands used	Comments
Untransformed (350-1075nm)	<i>Phragmites</i> -absent	6.29.04	0.56	0.78	14	Plot 10	1	9	Plot 10: many species
Untransformed (350-1075nm)	<i>Phragmites</i> -absent	8.02.05	0.53	1.08	15	none	5	555	none
Untransformed (350-1075nm)	<i>Phragmites</i> -dominant	7.19.04	0.43	1.30	14	Plot 10	2	420	Plot 10: low reflectance
Untransformed (350-1075nm)	<i>Phragmites</i> -dominant	5.25.04	0.42	1.81	11	Plots 1-3, 12	2	none	Plots 1-3: missing refl; Plot 12: low refl
Untransformed (350-1075nm)	<i>Phragmites</i> -absent	8.24.04	0.41	0.95	15	none	1	595	none
Untransformed (350-1075nm)	<i>Phragmites</i> -absent	9.21.04	0.41	0.86	15	none	1	65	none
Untransformed (350-1075nm)	<i>Phragmites</i> -dominant	8.02.05	0.39	1.28	14	Plot 12	1	33	Plot 12: high reflectance
Untransformed (350-1075nm)	<i>Phragmites</i> -dominant	9.21.04	0.32	1.14	14	Plot 5	2	232	Plot 5: low reflectance
Untransformed (350-1075nm)	<i>Phragmites</i> -dominant	8.24.04	0.26	1.28	14	Plot 5	1	20	Plot 5: low reflectance
Untransformed (350-1075nm)	<i>Phragmites</i> -dominant	6.29.04	0.24	1.04	14	Plot 11	6	3	Plot 11: few species present
Untransformed (350-1075nm)	<i>Phragmites</i> -absent	5.25.04	0.15	1.14	14	Plot 10	1	none	Plot 10: low reflectance
Untransformed (350-1075nm)	<i>Phragmites</i> -absent	7.19.04	0.12	1.91	15	none	1	none	none
Untransformed (350-1075nm)	<i>Phragmites</i> -absent	6.16.04	-0.01	1.23	15	none	1	none	none
Untransformed (350-1075nm)	<i>Phragmites</i> -absent	6.06.05	-0.03	1.55	14	Plot 3	1	none	Plot 3: high reflectance Plot 9: no reflect.; Plot 10: no species data
Untransformed (350-1075nm)	<i>Phragmites</i> -absent	6.03.04	-0.06	1.38	13	Plots 9,10	1	none	data
Untransformed (350-1075nm)	<i>Phragmites</i> -dominant	6.03.04	-0.22	1.87	15	none	1	none	none
Untransformed (350-1075nm)	<i>Phragmites</i> -dominant	6.16.04	-0.54	2.19	15	none	1	none	none
Untransformed (350-1075nm)	<i>Phragmites</i> -dominant	6.06.05	-0.68	1.99	15	none	1	none	none

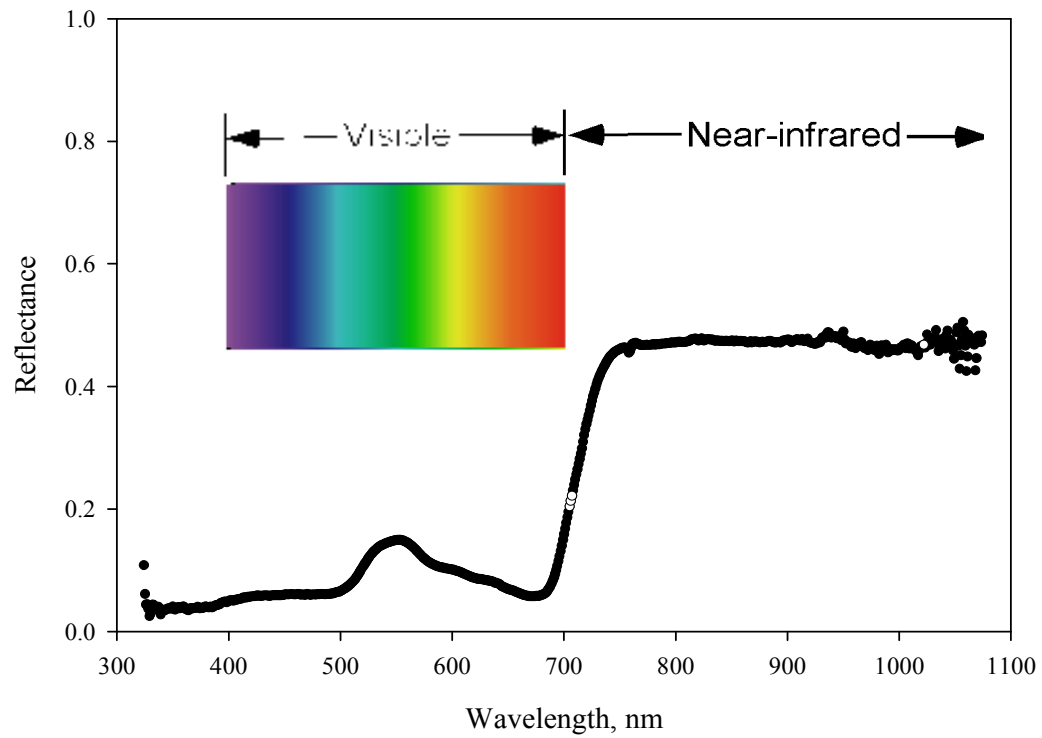


Figure C35. Spectral bands significant for five or more regressions for species richness at the *Phragmites*-dominant (PD) site and the *Phragmites*-absent (PA) site are indicated by an open circle.

Table C20. PLS-regressions for diversity index on data from both the *Phragmites*-dominant (PD) and *Phragmites*-absent (PA) sites.

Spectra Transformations	Marsh Site	Date	r	RMSEP	n	Name of plots removed	PCs	# bands used	Comments
Untransformed (350-1075nm)	<i>Phragmites</i> -absent	9.21.04	0.84	0.25	15	none	8	207	none
Untransformed (350-1075nm)	<i>Phragmites</i> -absent	8.24.04	0.83	0.22	15	none	5	385	none
Golay 2 nd Derivative, avg 10	<i>Phragmites</i> -absent	8.24.04	0.81	0.23	15	none	2	104	none
Untransformed (350-1075nm)	<i>Phragmites</i> -absent	8.02.05	0.80	0.21	15	none	2	609	none
Untransformed (350-1075nm)	<i>Phragmites</i> -absent	5.25.04	0.70	0.21	15	none	5	65	none
Untransformed (350-1075nm)	<i>Phragmites</i> -dominant	6.03.04	0.68	0.22	15	none	3	261	none
Untransformed (350-1075nm)	<i>Phragmites</i> -dominant	6.06.05	0.65	0.10	13	Plots 2,10	3	17	Plot 2: high reflectance; Plot 10: low refl
Untransformed (350-1075nm)	<i>Phragmites</i> -dominant	7.19.04	0.65	0.14	15	none	2	10	none
Untransformed (350-1075nm)	<i>Phragmites</i> -absent	6.29.04	0.64	0.21	14	Plot 6	3	35	Plot 6: low reflectance
Golay 2 nd Derivative, avg 10	<i>Phragmites</i> -absent	7.19.04	0.62	0.27	14	Plot 13	1	74	Plot 13: high reflectance
Untransformed (350-1075nm)	<i>Phragmites</i> -absent	7.19.04	0.59	0.28	14	Plot 13	2	494	Plot 13: high reflectance
Untransformed (350-1075nm)	<i>Phragmites</i> -dominant	8.24.04	0.54	0.22	15	none	1	411	none
Golay 2 nd Derivative, avg 10	<i>Phragmites</i> -absent	9.21.04	0.53	0.40	14	Plot 11	1	49	Plot 11: high reflectance
Golay 2 nd Derivative, avg 10	<i>Phragmites</i> -dominant	8.24.04	0.49	0.23	15	none	1	58	none
Untransformed (350-1075nm)	<i>Phragmites</i> -dominant	5.25.04	0.46	0.14	11	Plot 1-3, 6	2	146	Plots 1-3: missing reflectance; Plot 6: low refl
Untransformed (350-1075nm)	<i>Phragmites</i> -dominant	8.02.05	0.44	0.24	14	Plot 5	3	48	Plot 5: high reflectance
Untransformed (350-1075nm)	<i>Phragmites</i> -absent	6.06.05	0.39	0.26	14	Plot 3	2	32	Plot 3: high reflectance
Untransformed (350-1075nm)	<i>Phragmites</i> -absent	6.03.04	0.35	0.35	13	Plots 9,10	3	none	Plot 9: missing refl.; Plot 10: missing veg data
Untransformed (350-1075nm)	<i>Phragmites</i> -dominant	6.29.04	0.15	0.25	15	none	1	75	none
Golay 2 nd Derivative, avg 10	<i>Phragmites</i> -dominant	7.19.04	0.07	0.20	14	Plot 1	1	8	Plot 1: high reflectance
Untransformed (350-1075nm)	<i>Phragmites</i> -absent	6.16.04	0.03	0.18	13	Plots 5,14	1	none	Plot 5: high reflectance; Plot 14: low refl
Untransformed (350-1075nm)	<i>Phragmites</i> -dominant	6.16.04	0.01	0.13	14	Plot 11	1	24	Plot 11: low reflectance
Untransformed (350-1075nm)	<i>Phragmites</i> -dominant	9.21.04	-0.19	0.21	15	none	1	none	none

Table C21. Transformations performed on data for the diversity index PLS-regressions. Site is identified as PD (*Phragmites*-dominant) or PA (*Phragmites*-absent).

	Untransformed (350-1075 nm)	Golay 2nd Derivative
5/25/2004	PD site and PA site	
6/3/2004	PD, PA	
6/16/2004	PD, PA	
6/29/2004	PD, PA	
7/19/2004	PD, PA	PD, PA
8/24/2004	PD, PA	PD, PA
9/21/2004	PD, PA	PA
6/6/2005	PD, PA	
8/2/2005	PD, PA	

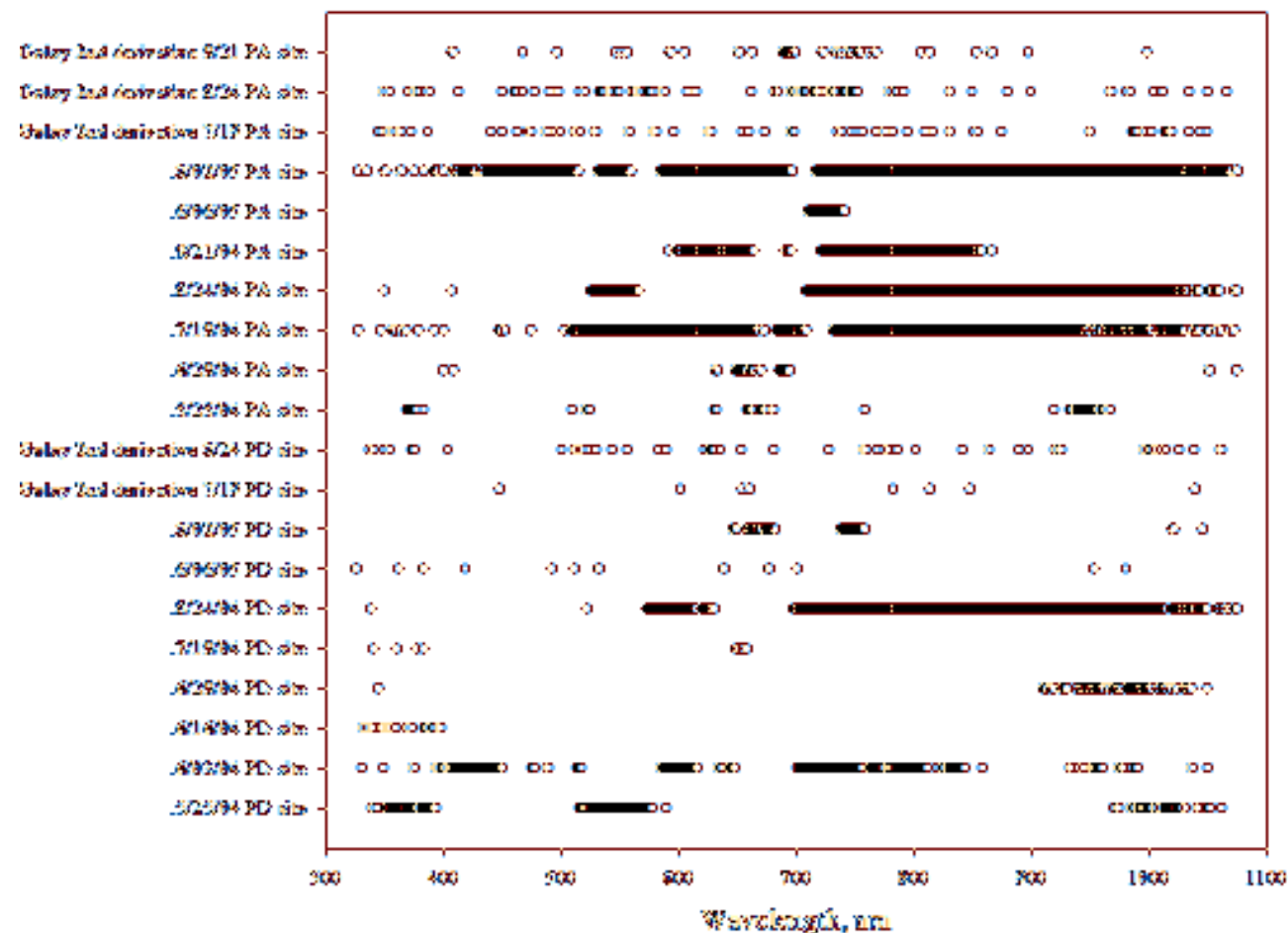


Figure C36. Significant spectral bands for species diversity index according to PLS-regressions for both the *Phragmites*-dominant (PD) and the *Phragmites*-absent (PA) sites.

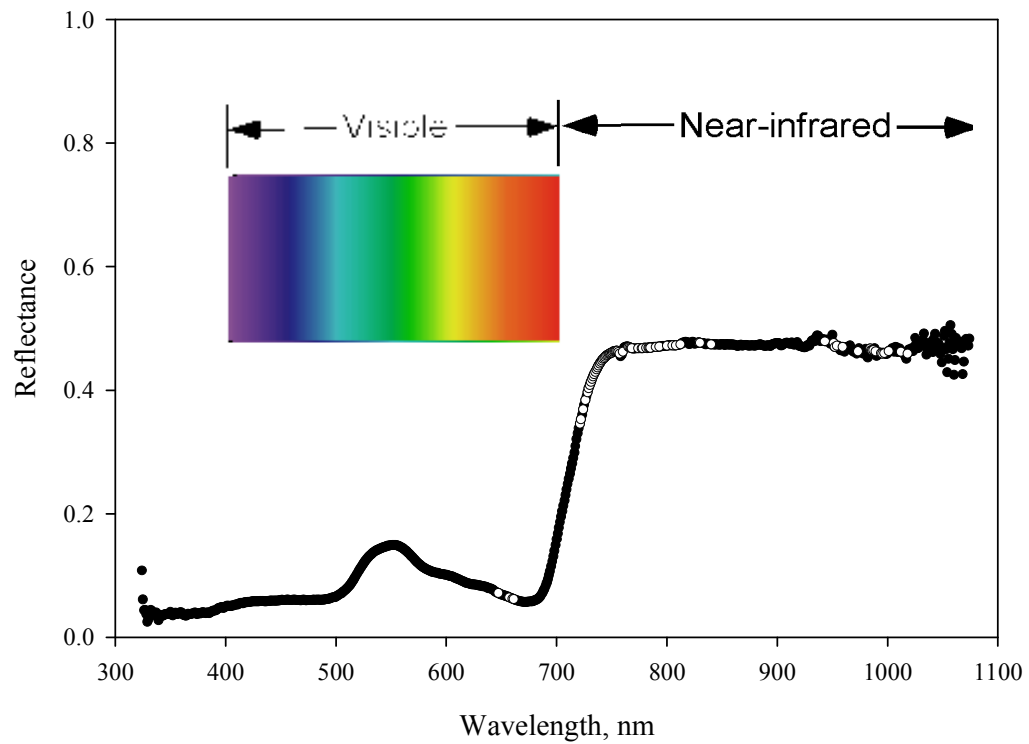


Figure C37. Spectral bands significant for seven or more regressions for diversity index at the *Phragmites*-dominant (PD) site and the *Phragmites*-absent (PA) site are indicated by an open circle.

Table C22. PLS-regressions for percent cover of dead material on data from both the *Phragmites*-dominant (PD) and *Phragmites*-absent (PA) sites.

Spectra Transformations	Marsh Site	Date	r	RMSEP	n	Name of plots removed	PCs	# bands used	Comments
Untransformed (350-1075nm)	<i>Phragmites</i> -absent	5.25.04	0.92	2.00	14	Plot 6	3	165	Plot 6: high dead material conc.
Untransformed (350-1075nm)	<i>Phragmites</i> -dominant	9.21.04	0.82	15.25	14	Plot 12	6	34	Plot 12: low reflectance
Golay 2 nd Derivative, avg 10	<i>Phragmites</i> -dominant	8.24.04	0.77	9.35	15	none	1	26	none
Untransformed (350-1075nm)	<i>Phragmites</i> -absent	9.21.04	0.77	12.04	14	Plot 7	2	168	Plot 7: high reflectance
Untransformed (350-1075nm)	<i>Phragmites</i> -dominant	5.25.04	0.73	7.35	12	Plot 1-3	2	93	Plots 1-3: missing reflectance
Golay 2 nd Derivative, avg 10	<i>Phragmites</i> -absent	7.19.04	0.68	0.17	15	none	1	47	none
Untransformed (350-1075nm)	<i>Phragmites</i> -dominant	6.03.04	0.65	0.78	13	Plot 3, 7	2	20	Plot 3: high refl; Plot 7: high dead conc.
Golay 2 nd Derivative, avg 10	<i>Phragmites</i> -dominant	9.21.04	0.64	21.28	14	Plot 12	1	37	Plot 12: low reflectance
Untransformed (350-1075nm)	<i>Phragmites</i> -absent	7.19.04	0.61	0.19	15	none	2	531	none
Untransformed (350-1075nm)	<i>Phragmites</i> -absent	8.02.05	0.58	0.45	15	none	8	124	none
Untransformed (350-1075nm)	<i>Phragmites</i> -absent	8.24.04	0.52	0.82	15	none	2	404	none
Golay 2 nd Derivative, avg 10	<i>Phragmites</i> -absent	8.24.04	0.52	0.82	15	none	1	17	none
Untransformed (350-1075nm)	<i>Phragmites</i> -dominant	8.24.04	0.42	13.53	15	none	2	315	none
Untransformed (350-1075nm)	<i>Phragmites</i> -absent	6.16.04	0.33	1.31	13	Plots 5,14	2	49	Plot 5: high refl; Plot 14: low refl
Untransformed (350-1075nm)	<i>Phragmites</i> -absent	6.03.04	0.17	1.17	13	Plots 9,10	1	9	Plot 9: missing refl; Plot 10: no veg data
Untransformed (350-1075nm)	<i>Phragmites</i> -dominant	7.19.04	-0.01	2.87	14	Plot 5	1	none	Plot 5: high reflectance
Untransformed (350-1075nm)	<i>Phragmites</i> -dominant	8.02.05	-0.10	2.76	14	Plot 5	1	none	Plot 5: high reflectance
Untransformed (350-1075nm)	<i>Phragmites</i> -dominant	6.16.04	-0.43	12.73	15	none	1	none	none
Untransformed (350-1075nm)	<i>Phragmites</i> -absent	6.29.04	-0.54	1.08	15	none	1	none	none
Untransformed (350-1075nm)	<i>Phragmites</i> -dominant	6.29.04	-0.69	2.75	15	none	1	none	none

Table C23. Transformations performed on data for percent dead material PLS-regressions. Site is identified as PD (*Phragmites*-dominant) or PA (*Phragmites*-absent).

	Untransformed (350-1075 nm)	Golay 2nd Derivative
5/25/2004	PD site and PA site	
6/3/2004	PD, PA	
6/16/2004	PD, PA	
6/29/2004	PD, PA	
7/19/2004	PD, PA	PA
8/24/2004	PD, PA	PD, PA
9/21/2004	PD, PA	PD
6/6/2005	PD, PA	
8/2/2005	PD, PA	

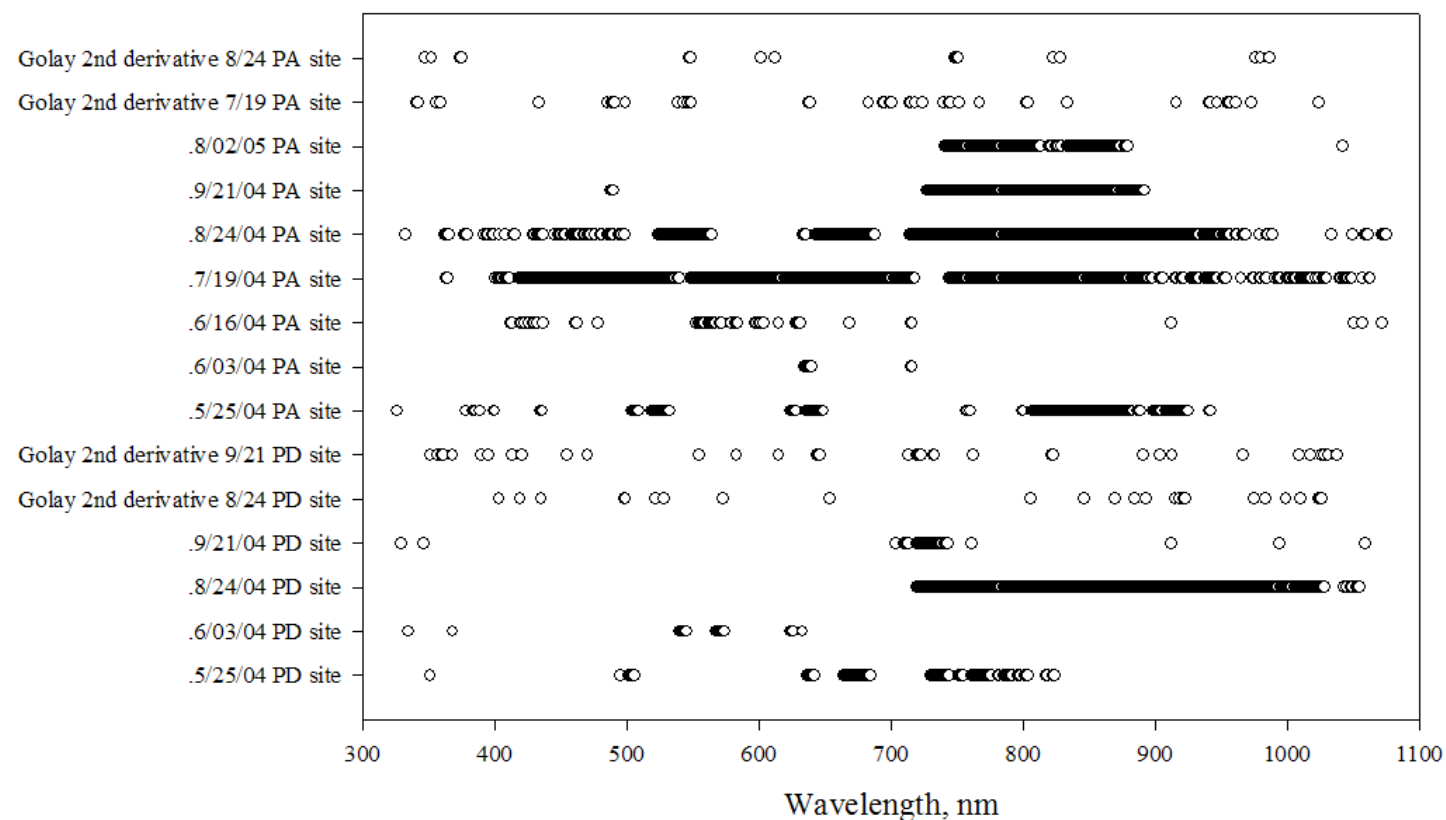


Figure C38. Significant spectral bands for percent dead material according to PLS-regressions for both the *Phragmites*-dominant (PD) and the *Phragmites*-absent (PA) sites.

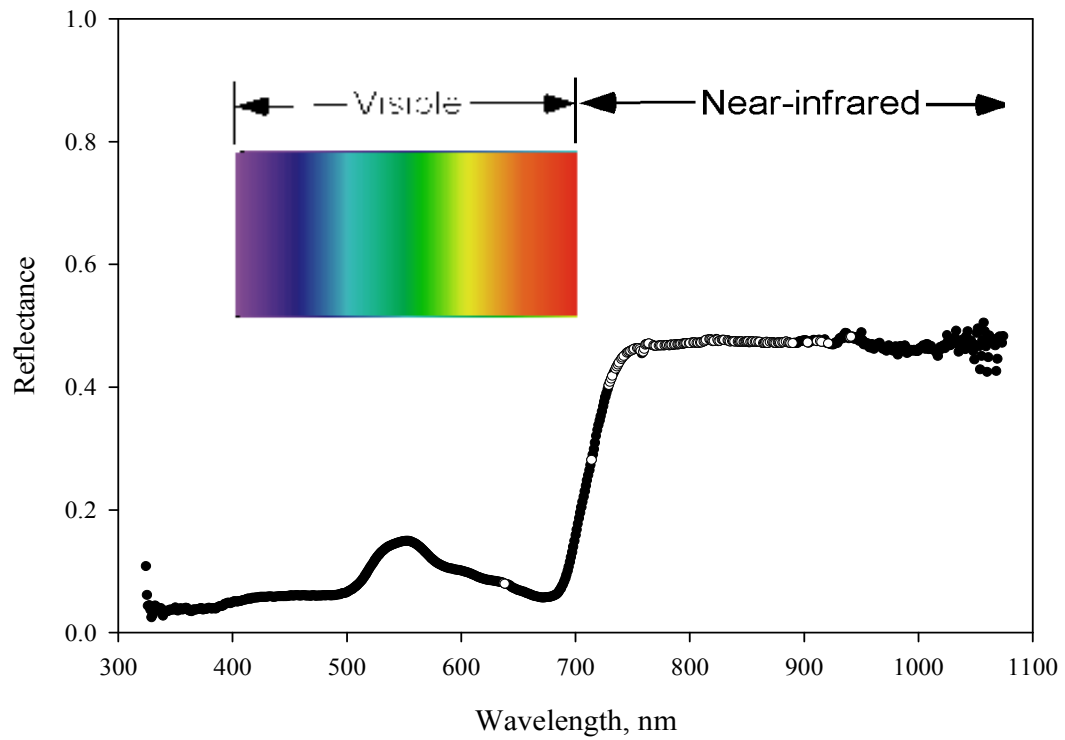


Figure C39. Spectral bands significant for five or more regressions for percent dead material at the *Phragmites*-dominant (PD) site and the *Phragmites*-absent (PA) site are indicated by an open circle.

Table C24. PLS-regressions for percent exposed soil on data from both the *Phragmites*-dominant (PD) and *Phragmites*-absent (PA) sites.

Spectra Transformations	Marsh Site	Date	r	RMSEP	n	Name of plots removed	PCs	# bands used	Comments
Untransformed (350-1075nm)	<i>Phragmites</i> -dominant	8.24.04	0.97	3.62	15	none	6	351	none
Golay 2 nd Derivative, avg 10	<i>Phragmites</i> -absent	7.19.04	0.91	0.53	15	none	2	88	none
Untransformed (350-1075nm)	<i>Phragmites</i> -absent	6.29.04	0.82	1.28	15	none	3	118	none
Untransformed (350-1075nm)	<i>Phragmites</i> -absent	7.19.04	0.76	0.83	15	none	2	150	none
Golay 2 nd Derivative, avg 10	<i>Phragmites</i> -absent	6.29.04	0.75	1.49	15	none	1	none	none
Golay 2 nd Derivative, avg 10	<i>Phragmites</i> -dominant	8.24.04	0.71	11.25	14	Plot 14	1	20	Plot 14: noisy derivative of reflectance
Untransformed (350-1075nm)	<i>Phragmites</i> -absent	8.02.05	0.65	0.77	14	Plot 4	4	78	Plot 4: low reflectance
Untransformed (350-1075nm)	<i>Phragmites</i> -absent	5.25.04	0.63	1.56	15	none	6	none	none
Untransformed (350-1075nm)	<i>Phragmites</i> -absent	6.03.04	0.61	0.43	13	Plots 9,10	4	8	Plot 9: missing refl; Plot 10: no veg data
Untransformed (350-1075nm)	<i>Phragmites</i> -absent	6.16.04	0.56	1.44	14	Plot 2	3	431	Plot 2: high reflectance
Untransformed (350-1075nm)	<i>Phragmites</i> -absent	9.21.04	0.56	10.34	15	none	1	138	none
Untransformed (350-1075nm)	<i>Phragmites</i> -dominant	5.25.04	0.41	2.51	11	Plots 1-3,6	1	171	Plots 1-3: missing refl; Plot 6: low refl
Untransformed (350-1075nm)	<i>Phragmites</i> -dominant	6.16.04	0.36	1.93	15	none	2	57	none
Untransformed (350-1075nm)	<i>Phragmites</i> -dominant	6.29.04	0.33	1.08	14	Plot 12	1	2	Plot 13: high reflectance
Untransformed (350-1075nm)	<i>Phragmites</i> -dominant	7.19.04	0.27	4.62	15	none	1	18	none
Untransformed (350-1075nm)	<i>Phragmites</i> -dominant	9.21.04	0.15	15.29	14	Plot 12	2	141	Plot 12: low reflectance
Untransformed (350-1075nm)	<i>Phragmites</i> -absent	8.24.04	0.06	0.98	14	Plot 6	1	none	Plot 6: low reflectance
Untransformed (350-1075nm)	<i>Phragmites</i> -dominant	6.03.04	-0.39	2.34	14	Plot 3	1	none	Plot 3: high reflectance
Golay 2 nd Derivative, avg 10	<i>Phragmites</i> -dominant	9.21.04	-0.50	16.89	15	none	1	none	none
Untransformed (350-1075nm)	<i>Phragmites</i> -dominant	8.02.05	-0.55	1.34	15	none	1	none	none

Table C25 Transformations performed on data for percent exposed soil PLS-regressions. Site is identified as PD (*Phragmites*-dominant) or PA (*Phragmites*-absent).

	Untransformed (350-1075 nm)	Golay 2nd Derivative
5/25/2004	PD site and PA site	
6/3/2004	PD, PA	
6/16/2004	PD, PA	
6/29/2004	PD, PA	PA
7/19/2004	PD, PA	PA
8/24/2004	PD, PA	PD
9/21/2004	PD, PA	PD
6/6/2005	PD, PA	
8/2/2005	PD, PA	

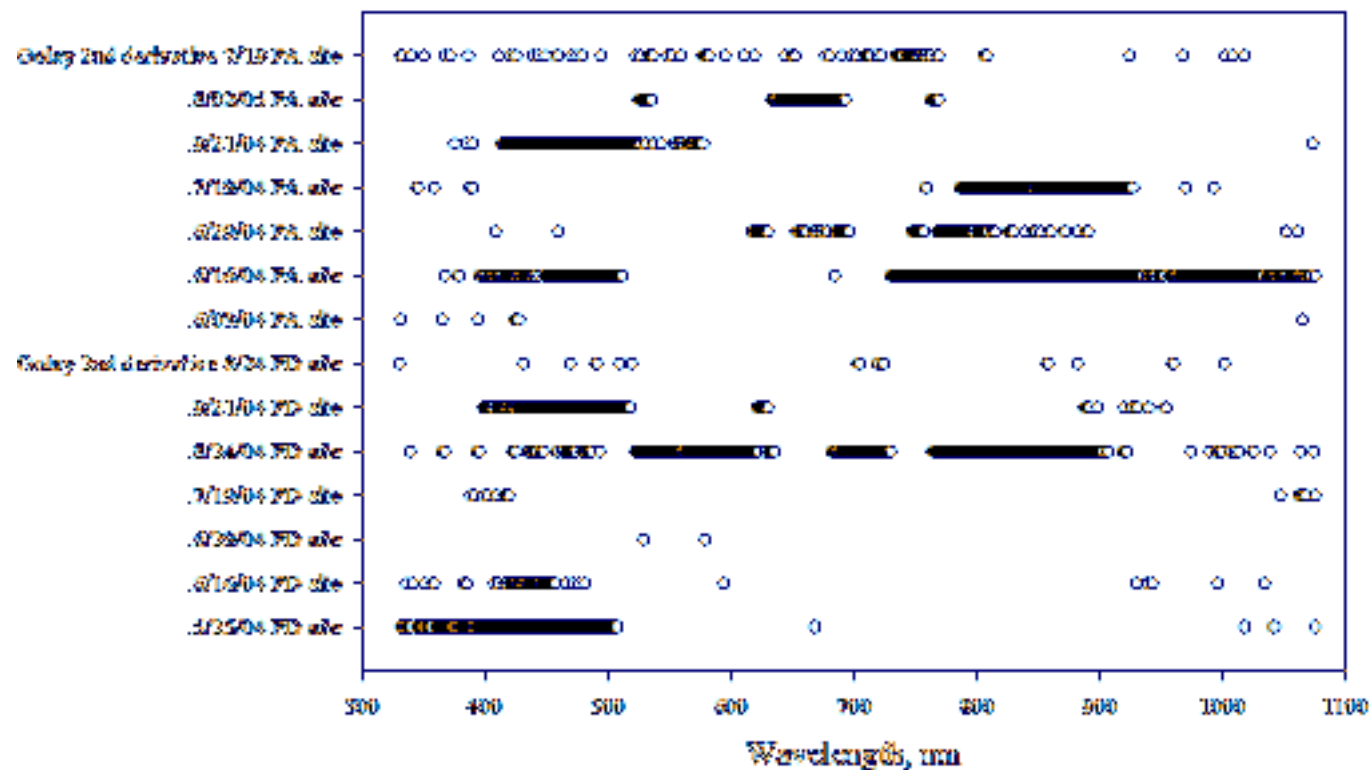


Figure C40. Significant spectral bands for percent bare area according to PLS-regressions for both the *Phragmites*-dominant (PD) and the *Phragmites*-absent (PA) sites.

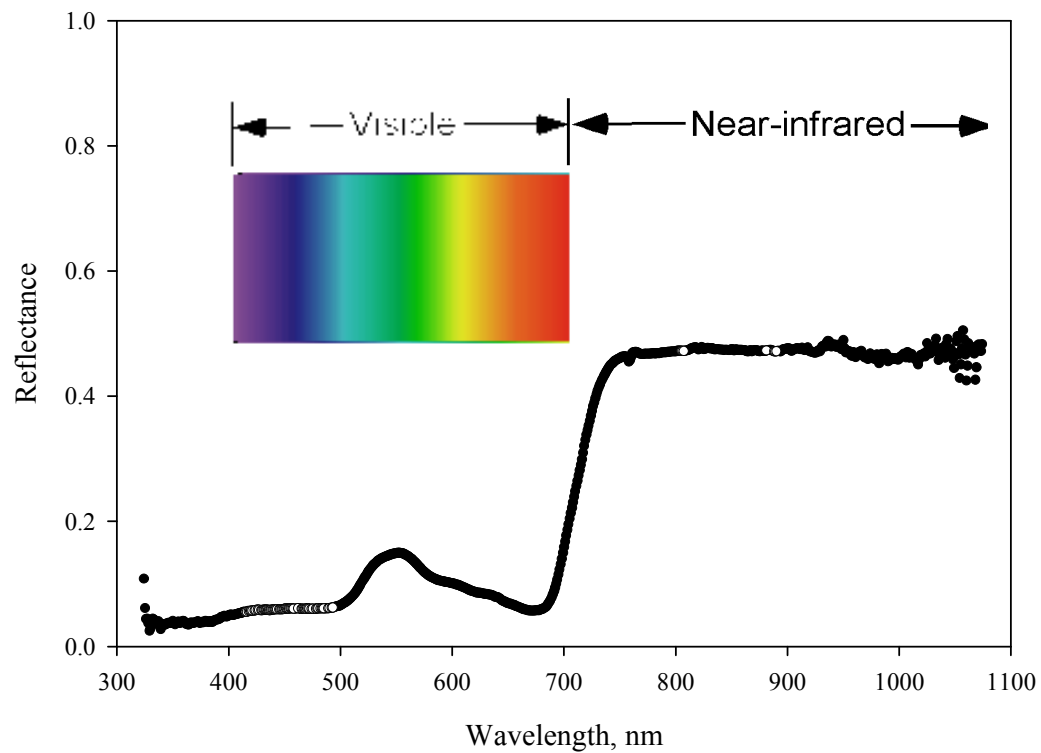


Figure C41. Spectral bands significant for five or more regressions for percent bare area at the *Phragmites*-dominant (PD) site and the *Phragmites*-absent (PA) site are indicated by an open circle.

APPENDIX D Raw vegetation data across the 2004-05 seasons

LAI and species cover according to the Peet classification system are recorded for each plot on each sample date, as well as notes about each plot and time of day plot was observed.

Table D1. Explanation of species abbreviations

Species Code	Species Name
TYSP	<i>Typha</i> species
PEVI	<i>Peltandra virginica</i>
HIMO	<i>Hibiscus moscheutos</i>
POAR	<i>Polygonum arifolium</i>
IMCA	<i>Impatiens capensis</i>
BILA	<i>Bidens laevis</i>
SISU	<i>Sium suave</i>
CIAR	<i>Cinna arundinacea</i>
LEOR	<i>Leersia oryzoides</i>
ZIAQ	<i>Zizania aquatica</i>
AMCA	<i>Amaranthus cannabinus</i>
BTS5B	<i>Bidens</i> species
SALA	<i>Sagittaria latifolia</i>
LIAR	<i>Limnophila aromatica</i>
ELOB	<i>Eleocharis obtusa</i>
	<i>Schoenoplectus</i>
SCTA	<i>tabernaemontani</i>
NULU	<i>Nuphar lutea</i>
ACCA	<i>Acorus calamus</i>
SCFL	<i>Schoenoplectus fluviatilis</i>
MISC	<i>Mikania scandens</i>
PIPU	<i>Pilea pumila</i>
PHAU	<i>Phragmites australis</i>
CASE	<i>Calystegia sepium</i>
APAM	<i>Apios americana</i>
BOCY	<i>Boehmeria cylindrica</i>
EUPSP	<i>Eupatorium</i> species
CIMA	<i>Cicuta maculata</i>
FRPE	<i>Fraxinus pennsylvanica</i>
MEAR	<i>Mentha arvensis</i>
Cyperacene	<i>Cyperacene</i> species
LEVI	<i>Lepidium virginicum</i>
CUGR	<i>Cuscuta gronovii</i>
DEAD	Dead material
WATER	Water present
BARE	Exposed soil
PERL	Exposed perlite
POSA	<i>Polygonum sagittatum</i>
ASSP	<i>Asclepias speciosa</i>
POAP	<i>Polypodium appalachianum</i>
SPEU	<i>Sparganium eurycarpum</i>
Aster Sp	<i>Aster</i> species
Sparganium	<i>Sparganium</i> species

Table D2. Raw vegetation data from each plot at the *Phragmites*-dominant site on 5/25/04.

plot #	8d221	9d202	10d203	11d222	12d103	13d223	14d113	15d003
LAI	6.57	4.41	4.61	4.79	3.79	4.85	5.37	4.04
SEL	0.03	0.12	0.04	0.02	0.16	0.14	0.18	0.24
Notes:	11:25, sun	sun	sun	13:03, sun* ahead tilley	13:10, sun* ahead tilley	13:42, sun* ahead tilley	13:19, sun* ahead tilley	13:34, sun, 3
TYSP		2	2		3	2	3	3
PEVI	8	7	8	7	8	7	8	9
HIMO	5							
POAR	7	6	7	7	6	6	7	6
IMCA	5		2	6	2	6	1	0
BILA		7	2	4	3	2	3	2
SISU	1	3	5			5	1	
CIAR						2	1	
LEOR	7	2						
ZIAQ		2						
AMCA			2	2	3		4	2
BTS5B	2							
SALA	2							2
LIAR			5					
ELOB			5					
SCTA			1	5	2			
NULU							6	
ACCA						1		
SCFL								
MISC								
PIPU								
PHAU								
STPA?								
CASE								
MEAR								
Cyperacene								
LEVI								
CUGR								
DEAD	2	3	1	2	3	5	2	2
WATER	1	4	4	1	1	0	2	2
BARE	2	2	2	2	4	2	2	3
PERL								
Species								
Richness	8	7	10	6	7	8	9	7
NH3 (mg/L)	NA	NA	NA	NA	NA	NA	NA	NA
RP (mg/L)	NA	NA	NA	NA	NA	NA	NA	NA

Table D2 continued.

plot #	7m102	6m222	5m111	4m001	3m101	2m201	1m221
LAI	4.6	7.73	6.3	6.43	5.58	5.97	5.8
SEL	0.45	0.05	0.1	0.02	0.17	0.02	0.05
		16.48 haze, whorled leaves		17.24 haze	17.40 haze	17.55 sun	18.10 sun
Notes:	16.31 haze					5	2
TYSP						7	7
PEVI	7		7				4
HIMO							6
POAR	2	7	7	6	7		5
IMCA		6	3	5		7	
BILA	1		2				
SISU							
CIAR							
LEOR							
ZIAQ							
AMCA			3		2		
BTS5B							
SALA							
LIAR							
ELOB							
SCTA							
NULU							
ACCA	6	6		4		6	7
SCFL	3	2		2			
MISC			6	2			
PIPU	2			2	2		
PHAU	7	6	8	8	7	7	6
STPA?	2						
CASE				6	7		
APAM		2	4				
BOCY	5	5	2		5		
EUPSP		5					
CIMA			6				
FRPE			2				
MEAR					6	6	
Cyperacene							
LEVI			33/34				
CUGR					1		
DEAD	3	2	6	7	6	2	3
WATER	0	0	0	0	0	0	1
BARE	5		2	3	3	3	3
PERL		2					
Species							
Richness	9	8	11	8	8	6	7
NH3 (mg/L)	NA	NA	NA	NA	NA	NA	NA
RP (mg/L)	NA	NA	NA	NA	NA	NA	NA

Table D3. Raw vegetation data from each plot at the *Phragmites*-absent site on 5/25/04.

plot #	1d001	2d101	3d002	4d111	5d112	6d201	7d102
LAI	6.55	6.24	6.82	5.87	5.02	5.59	4.22
SEL	0.13	0.29	0.83	0.06	0.98	0.03	0.36
Notes:	partly cloudy	photo of a.b.		moved sm. post	sun	sun	sun
TYSP	3	5	4	4	4	3	3
PEVI	8	9	8	9	8	7	7
HIMO	4				7		3
POAR	8	7	5	7	6	5	5
IMCA	4	4	8	6	6	7	8
BILA	3	4	2	3	3	5	5
SISU			2			2	2
CIAR			3	2			
LEOR				3	2	4	
ZIAQ							3
AMCA		2					2
BTS5B							
SALA					2		
LIAR							
ELOB							
SCTA							
NULU							
ACCA	1						
SCFL							
MISC							
PIPU							
PHAU							
STPA?							
CASE							
APAM							
BOCY							
EUPSP							
CIMA							
FRPE							
MEAR							
Cyperacene							
LEVI							
CUGR							
DEAD	2	2	2	4	6	7	5
WATER	4	3	2	2	2	3	1
BARE	0	0	0	0	5	0	4
PERL							
Species Richness	7	6	7	7	8	7	9
NH3 (mg/L)	NA	NA	NA	NA	NA	NA	NA
RP (mg/L)	NA	NA	NA	NA	NA	NA	NA

Table D3 continued.

plot #	8d221	9d202	10d20 3	11d22 2	12d103	13d22 3	14d11 3	15d00 3
LAI	6.57	4.41	4.61	4.79	3.79	4.85	5.37	4.04
SEL	0.03	0.12	0.04	0.02	0.16	0.14	0.18	0.24
Notes:	11:25, sun	sun	sun	13:03, sun* ahead tilley	13:10, sun* ahead tilley	13:42, sun* ahead tilley	13:19, sun* ahead tilley	13:34, sun, 3
TYSP		2	2		3	2	3	3
PEVI	8	7	8	7	8	7	8	9
HIMO	5							
POAR	7	6	7	7	6	6	7	6
IMCA	5		2	6	2	6	1	0
BILA		7	2	4	3	2	3	2
SISU	1	3	5			5	1	
CIAR						2	1	
LEOR	7	2						
ZIAQ		2						
AMCA			2	2	3		4	2
BTS5B	2							
SALA	2							2
LIAR			5					
ELOB			5					
SCTA			1	5	2			
NULU							6	
ACCA						1		
SCFL								
MISC								
PIPU								
PHAU								
STPA?								
CASE								
APAM								
BOCY								
EUPSP								
CIMA								
FRPE								
MEAR								
Cyperacene								
LEVI								
CUGR								
DEAD	2	3	1	2	3	5	2	2
WATER	1	4	4	1	1	0	2	2
BARE	2	2	2	2	4	2	2	3
PERL								
Species								
Richness	8	7	10	6	7	8	9	7
NH3 (mg/L)	NA	NA	NA	NA	NA	NA	NA	NA
RP (mg/L)	NA	NA	NA	NA	NA	NA	NA	NA

Table D4. Raw vegetation data from each plot at the *Phragmites*-dominant site on 6/03/04.

plot #	15M003	14M112	13m202	12m223	11m002	10m203	9m103
LAI	3.96	4.02	5.7	4.67	4.35	4.99	4.45
SEL	0.23	0.45	0.36	0.69	0.2	0.22	0.26
Notes:	11:00, sun	11:18, sun	11:35 sun	11:44 sun	11:53 sun & wind	12:03 full sun and wind	12:12 sun
TYSP			4				
PEVI	3	8	4	3	3	2	5
HIMO			4				
POAR	4	3	5	4	4	5	3
IMCA	4	3	4	3	7	5	5
BILA				1			
SISU							
CIAR							
LEOR							
ZIAQ							
AMCA		1		1			
SALA							
LIAR							
ELOB							
SCTA							
NULU							
ACCA	5	6	6	5	5	5	4
SCFL	4	1					
MISC	5	2	2	3		0	
PIPU				1			1
PHAU	8	9	7	9	9	8	9
CASE						4	
APAM							
BOCY							
EUPSP							
CIMA							
FRPE							
MEAR							
Cyperacene							
LEVI							
CUGR							
DEAD	3	3	2	4	4	3	3
WATER	0	0	3	0	0	0	3
BARE	3	2	3	3	4	4	3
PERL		2	3	3	5	4	4
Species Richness	7	8	8	9	5	7	6
NH3 (mg/L)	0.3	5.2	NA	7.8	2.3	1.7	2.4
RP (mg/L)	0.13	0.12	NA	0.02	0.01	0.02	0.08

Table D4 continued.

plot #	8m113	7m102	6m222	5M111	4m001	3m101	2m201	1m221
LAI	5.73	3.41	4.69	3.23	4.6	4.85	4.75	5.62
SEL	0.38	0.26	0.12	1.11	0.51	0.02	0.12	0.42
Notes:	12:27:00 sun PM	12:32 sun	12.42 SUN	12.56 SUN	13.05 Some clouds, sun	13.14 sun	13.19 Cloudy	13.30 Sun
TYSP							5	3
PEVI	2	6	4	4			7	6
HIMO	3							3
POAR	2	3	5	3	2	5	4	4
IMCA	5		5	1	4	3	6	5
BILA		0		0				
SISU								
CIAR								
LEOR								
ZIAQ								
AMCA				0		1		
SALA								
LIAR								
ELOB								
SCTA								
NULU								
ACCA	2	6	4	4	3		5	7
SCFL		0	3		1			
MISC				0	0			
PIPU		0			1	1		
PHAU	9	7	6	8	7	7	7	7
CASE				4	6	7		
APAM	5		0	1				
BOCY		1	2	1		1		
EUPSP			4					
CIMA				1				
FRPE				0				
MEAR						0	1	
Cyperacene								
LEVI								
CUGR						0		
DEAD	2	5	2	2	3	3	3	2
WATER	0	0	0	0	0	0	0	1
BARE	2	5	1	4	1	1	1	4
PERL	1	3	0	1	2	3	1	1
Species								
Richness	7	8	9	13	8	9	7	7
NH3 (mg/L)	1.8	1.7	3.1	3.3	2	3.7	NA	6.7
RP (mg/L)	0.01	0.12	0.91	NA	0.01	0.35	NA	0.05

Table D5. Raw vegetation data from each plot at the *Phragmites*-absent site on 6/03/04.

plot #	1d001	2d101	3d002	4d111	5d112	6d201	7d102
LAI	3.62	3.71	3.41	4.86	5.19	4.07	4.14
SEL	0.06	1.19	0.03	0.56	0.48	0.68	1.01
				14.52 Some clouds, Sun for LAI			14.45 Sun, partly cloudy
Notes:	14.22 Sun	14.29 Sun	14.37 Sun		14.59 Sun	15.19 Sun	
TYSP	4	5	4	4	4	4	4
PEVI	8	7	8	8	8	6	7
HIMO	4		3		6		0
POAR	5	8	4	3	5	3	5
IMCA	4	2	6	5	3	6	7
BILA	1	1	2	0		3	2
SISU				1			0
CIAR			2	4			
LEOR				0		4	
ZIAQ							0
AMCA		1					
SALA							
LIAR							
ELOB							
SCTA							
NULU							
ACCA	0				1		
SCFL							
MISC							
PIPU							
PHAU							
CASE							
APAM							
BOCY							
EUPSP							
CIMA							
FRPE							
MEAR							
Cyperacene							
LEVI							
CUGR							
DEAD	1	2	3	4	3	4	3
WATER	1	1	1	3	1	1	2
BARE	1	2	1	1	2	2	2
PERL	2	2	3	4	1	2	3
Species Richness	7	6	7	8	6	6	8
NH3 (mg/L)	NA	NA	0.3	0.1	0.8	NA	NA
RP (mg/L)	NA	NA	0.11	0.13	0.05	NA	NA

Table D5 continued.

plot #	8d221	9d202	10d203	11d222	12d103	13d223	14d113	15d003
LAI	5.63	5.37		3.28	3.72	3.18	2.27/2.99	2.4
SEL	1.75	0.02		0.47	0.5	0.35	0.63/0.89	0.08
				15.34 Cloudy with sun	15.40 Partly cloudy	16.01 Sun	15.48 Sun	15.55 Partly cloudy
Notes:	15.08 Sun	15.28 Sun						
TYSP		3		2	2	4	4	4
PEVI	6	9		6	8	7	8	9
HIMO	3			4				
POAR	3	3		6	6	5	7	4
IMCA	3	4		6	0	6		
BILA	1	1		4	3	3	2	2
SISU		0				1		
CIAR						3	1	
LEOR	5	3						
ZIAQ								
AMCA				0	0			
SALA								
LIAR								
ELOB								
SCTA				5	2			
NULU							5	
ACCA								
SCFL								
MISC								
PIPU								
PHAU								
CASE								
APAM								
BOCY								
EUPSP								
CIMA								
FRPE								
MEAR								
Cyperacene								
LEVI								
CUGR								
DEAD	2	2		1	2	2	2	2
WATER	1	3		2	3	2	2	4
BARE	3	1		3	3	2	2	2
PERL	3	1		3	3	3	2	2
Species								
Richness	6	7		8	7	7	6	4
NH3								
(mg/L)	0.5	0.4		NA	NA	NA	0	0.1
RP								
(mg/L)	0.02	0.08		NA	NA	NA	0.13	0.03

Table D6. Raw vegetation data from each plot at the *Phragmites*-dominant site on 6/16/04.

plot #	15M003	14M112	13m202	12m223	11m002	10m203	9m103
LAI	5.56	4.2	5.93	4.92	4.55	6.68	5.33
SEL	0.06	0.02	0.26	0.37	0.16	0.11	0.04
Notes:	9.10, Cl, LAI away from water	9.43, cl., LAI - inland	10.03, cl. LAI - inland	10.19, cl. LAI - inland	10.34, cl. LAI - inland	10.45, cl. LAI - inland	10.58, cl. LAI - inland
TYSP	2						
PEVI	2	7	5		3	4	6
HIMO			6	1			
POAR	7	6	7	8	6	6	5
IMCA	5	5	6	7	8	7	6
BILA				2			
SISU							
CIAR							
LEOR							
ZIAQ							
AMCA		1				1	
BTS5B							
SALA							
LIAR							
ELOB							
SCTA							
NULU							
ACCA	7	7	7	6	6	7	6
SCFL	5	4					
MISC	4	4		4		4	
PIPU		1		2		1	4
PHAU	8	8	8	8	9	8	8
STPA?	3						
CASE						4	
APAM							
LEVI							
BISPC				1			
POSA							
ASSP							
STPA2							
CUGR		2					1
DEAD	5	6	6	7	6	6	7
WATER	0	0	0	0	0	0	0
BARE	2	3	2	3	3	2	4
PERL	2	3	3	2	3	1	3
Richness	9	10	6	9	5	9	7
NH3 (mg/L)	0.38	2.66	25.3	14.9	0.8	1.8	1.04
Total							
Nitrate	1.4	2	1.6	3.2	1.4	2.7	1.5
Total N	15	11.25	26.25	18.75	11.25	11.25	11.25
TP (mg/L)	0.06	2.5	0.31	0.22	0.77	0.22	0.7

Table D6 continued.

plot #	8m113	7m102	6m222	5M111	4m001	3m101	2m201	1m221
LAI	7.54	4.71	5.57	4.83	5.3	6.82	5.81	6.22
SEL	0.39	0.38	0.04	0.37	0	0.06	0.8	0.11
Notes:	11.10, cl, LAI - inland	11.24, cl. LAI - water	11.34, cl. LAI - water	11.48, cl, LAI - water	12.01, p.cl	12.12, p.sunny	12.26, p. sunny	12.37, p. sunny
TYSP							6	
PEVI		5	6				6	5
HIMO	5							6
POAR	5	5	7	6	6	9	6	6
IMCA	6		7	4	7	5	7	6
BILA				2		2		
SISU								
CIAR								
LEOR								
ZIAQ								
AMCA								
ELOB								
SCTA								
NULU								
ACCA	5	6	7	4	5		6	8
SCFL		4				4		
MISC			4					
PIPU				1	3			
PHAU	9	7	6	8	8	8	7	6
STPA?	9							
CASE				6	6	6		
APAM	4			5				
BOCY		5	4	3		5		
EUPSP			5					
CIMA				5				
MEAR						5	5	
BISPC				4				
POSA			3					
ASSP						3		
STPA2		4						
CUGR					2	4		
DEAD	7	5	3	6	6	6	6	5
WATER	0	0	0	0	0	0	0	0
BARE	1	5	4	4	4	2	4	4
PERL	1	3	0	4	3	2	0	2
Richness	7	7	9	11	7	10	7	6
NH3 (mg/L)	3.06	1.06	16.3	2.44	1.12	1.9	6.6	90.8
Nitrate (mg/L)	1.7	1.2	3.2	1.8	2	3.2	2	1.1
Total N	11.25	7.5	26.25	3.75	15	15	3.75	97.5
TP (mg/L)	0.68	0.05	5	0.24	2.7	0.13	6.4	0.28

Table D7. Raw vegetation data from each plot at the *Phragmites*-absent site on 6/16/04.

plot #	1d001	2d101	3d002	4d111	5d112	6d201	7d102
LAI	3.75	5.83	4.81	5.81	6.43	5.01	6.32
SEL	0.1	0.57	0.65	0.16	0.14	0.19	0.2
Notes:	13.27, cl, lai - - dstream	13.35, p. cloudy	13.45, p. sunny	13.55, p. sunny	15.18, p.sunny	15.11, p.sunny	14.04, cl, lai - dstr.
TYSP	3	6	5	4	5	6	5
PEVI	7	7	7	7	7	7	7
HIMO	5				6		4
POAR	8	9	6	8	9	5	7
IMCA	6	5	7	7	6	9	9
BILA		5	3	4	1	1	4
SISU						4	
CIAR		2	4	3			
LEOR				5	5	6	
ZIAQ							4
AMCA	3	1					
BTS5B							
SALA					6		
LIAR							
ELOB							
SCTA							
NULU							
ACCA							
SCFL							
MISC							
PIPU							
PHAU							
LEVI							
BISPC							
POSA							
ASSP							
STPA2							
CUGR				3			
DEAD	4	4	2	3	4	2	4
WATER	0	0	2	0	0	0	0
BARE	4	2	2	4	3	4	4
PERL	4	4	3	4	2	4	4
Richness	6	7	6	8	8	7	7
NH3 (mg/L)	0.42	31.6	0.54	1		1.6	3.3
Nitrate (mg/L)	1.5		1.4	0.8		0	1.4
Total N	11.25	37.5	11.25	7.5		11.25	11.25
TP (mg/L)	0.2	2.6	0.15	0.24		0.29	0.62

Table D7 continued

plot #	8d221	9d202	10d203	11d222	12d103	13d223	14d113	15d003
LAI	5.52	6.48	4.97	6.62	4.71	5.93	6.57	3.51
SEL	0.32	0.27	0.66	0.04	0.19	0.3	0.23	0.08
		14.13, p. sun, lai - upstrea m		14.20, p. sun. lai - upstr.	14.28, p.sun, lai- upstr.	14.49, cl. Lai - upstr.	14.34, cl. Lai - upstr.	14.41, cl, lai - upstrea m
Notes:	15.05, p.cl.lai - dstr.		14.56, p.cl.					
TYSP	1	4	2	2	4	5	4	5
PEVI	6	7	7	7	8	7	7	8
HIMO	6							
POAR	9	8	7	8	8	8	9	7
IMCA	7	6	4	8	4	8	6	
BILA		6	4	4	5	2	2	
SISU	2	3	5	3		5		
CIAR			6			5		
LEOR	7		5	1				1
ZIAQ		4						
AMCA							2	4
BTS5B	3							
SALA								
LIAR								
ELOB			6					
SCTA			2	6	2			
NULU							6	
ACCA						2		
SCFL								
MISC								
PIPU								
PHAU								
LEVI								
BISPC								
POSA								
ASSP								
STPA2								
CUGR								
DEAD	3	3	2	0	3	4	3	4
Water	0	3	0	0	0	0	0	3
BARE	4	3	4	2	4	4	4	5
PERL	4	4	2	3	4	5	4	0
Richne ss	8	7	10	8	6	8	7	5
NH ₃ (mg- N/L)	0.92	4.34	1.62	37	0.82	3.4	0.64	0.42
Nitrate (mg/L)	0.9	0.9	1.5	1.3	2.3	3.9	1.7	2.1
Total N	11.25	11.25	15	15	18.75	11.25	11.25	11.25
TP (mg- P/L)	0.67	4.5	1.2	0.47	0.48	0.18	1.8	2.7

Table D8. Raw vegetation data from each plot at the Phragmites-dominant site on 6/29/04.

plot #	15M003	14M112	13m202	12m223	11m002	10m203	9m103
LAI	4.42	2.98	6.54	4.48	4.8	4.86	5.01
SEL	0.33	0.04	0.7	0.31	0.07	0.06	0.05
Notes:	3:25, full sun	3:27, full sun	3:29, full sun	3:32, full sun	3:33, full sun	3:35, full sun	3:39, full sun
TYSP			5				
PEVI	1	6		5	1	2	5
HIMO			6				
POAR	6	5	8	6	4	7	4
IMCA	7	6	6	7	7	7	7
BILA				1			
SISU							
CIAR							
LEOR							
ZIAQ							
AMCA		3					4
BTS5B							
SALA							
LIAR							
ELOB							
SCTA							
NULU							
ACCA	5	4	6	6	5	4	6
SCFL	4	4					
MISC	4						
PIPU				4		3	3
PHAU	7	9	8	7	8	8	8
STPA?							
CASE						5	
APAM							
BOCY							
EUPSP							
CIMA							
FRPE							
MEAR							
STPA2							
unknown1							
CUGR							2
DEAD	4	5	4	4	4	3	5
WATER	0	0	0	0	0	0	0
BARE	1	3	1	2	3	2	3
PERL	1	2	0	2	2	2	2
Richness	7	7	6	7	5	7	8
NH3 (mg/L)	0.4	1.06	29.6		0.56	0.92	0.66
Nitrate	1.6		0.7		1.1	2.1	1.6
Total N	11.25	3.75	26.25		15	3.75	11.25
TP (mg/L)	0.06	1.7	0.16		0.03	0.01	0.02

Table D8 continued.

plot #	8m113	7m102	6m222	5M111	4m001	3m101	2m201	1m221
LAI	6.86	3.38	4.72	5.18	4.36	5.29	5.25	3.31
SEL	0.08	0.48	0	0.11	0	0.35	0.07	0.11
Notes:	3:37, full sun	3:41, full sun	3:44, full sun	3:46, full sun	3:47, full sun	3:49, cloud	3:51, cloud 5	3:52, cloud 4
TYSP								
PEVI		6	1	5	3			3
HIMO	1		4					5
POAR	4	6	7	6	7	8	6	5
IMCA	5	5	6	4	7	7	8	7
BILA			3					
SISU								
CIAR								
LEOR								
ZIAQ								
AMCA								
BTS5B								
SALA								
LIAR								
ELOB								
SCTA								
NULU								
ACCA	5	7	5	5	4		4	8
SCFL		6	6				4	
MISC								
PIPU		2		3	3			
PHAU	8	7	6	6	7	6	6	6
STPA?	8							
CASE				6	5	5		
APAM	4			4				
BOCY		5	5	2		3		
EUPSP								
CIMA				5				
FRPE								
MEAR						5	4	
STPA2		3						
unknown1								
CUGR	3				3	2		
DEAD	4	3	3	4	5	3	4	2
WATER	0	0	0	0	0	0	0	0
BARE	1	4	3	2	3	2	3	4
PERL	1	2	1	1	0	0	0	0
Richness	8	9	9	10	8	7	7	7
NH3								
(mg/L)	1.24	1	20.5	2.18		1.12	1.28	79.5
Nitrate	0.9	1.2	4.4	2.9	2.2		1.5	0.6
Total N	15	3.75	22.5	11.25		11.25	7.5	97.5
TP (mg/L)	0.07	0.02	0.62	0		0.02	0.04	0.1

Table D9. Raw vegetation data from each plot at the *Phragmites*-absent site on 6/29/04.

plot #	1d001	2d101	3d002	4d111	5d112	6d201	7d102
LAI	4.37	3.71	2.32	4.43	5.1	2.97	4.97
SEL	0	0.42	0	0	0.14	0	0.17
Notes:	1:05pm	1:15pm, sun	1:20pm, sun	1:31pm, full sun	1:40pm. Full sun	1:59pm, full sun	2:25pm, sun
TYSP	5	5	5	4	4	5	4
PEVI	6	7	8	8	5	6	5
HIMO	6				7		1
POAR	8	9	6	8	8	4	5
IMCA	5	5	8	8	4	9	9
BILA	3	4		1		1	3
SISU						4	
CIAR		1	5	3			
LEOR				4	5	4	
ZIAQ					1		4
AMCA	5	3					
BTS5B							
SALA					5		
LIAR							
ELOB							
SCTA							
NULU							
ACCA							
SCFL							
MISC							
PIPU							
PHAU							
LEVI							
BISPC							
POSA							
ASSP							
STPA2							
unknown1							
CUGR				4			
DEAD	2	4	1	1	2	1	3
WATER	0	0	0	0	0	0	0
BARE	3	4	3	2	1	2	3
PERL	1	3	0	0	1	2	0
Richness	7	7	5	8	8	7	7
NH3 (mg/L)	0.5	44.4	0.62	1.16	1.12	1.1	3.12
Total Nitrate	0.9		2.2	0	0.2	1.8	0.8
Total N	11.25	15	3.75	7.5	11.25	11.25	11.25
TP (mg/L)	0.09		0.17	0.21	0.15	0.27	0.42

Table D9 continued.

plot #	8d221	9d202	10d203	11d222	12d103	13d223	14d113	15d003
LAI	3.55	4.41	1.94	4.99	3.94	4.25	4.78	3.11
SEL	0.65	0.18	0.42	0.16	1.14	0.08	0.05	0.18
Notes:	1:50pm, full sun	2:05pm, small cloud	3:05, full sun	2:10pm, sun	2:30pm, sun	2:56pm, full sun	2:40pm, sun	2:50pm, full sun
TYSP		5	4	4	4	4	4	4
PEVI	5	6	6	6	7	6	8	8
HIMO	5							
POAR	7	8	6	8	8	7	8	7
IMCA	4	6	4	8	3	7	5	
BILA		5	2		4	2	2	
SISU	5	5	5	4		6		
CIAR			6			4		
LEOR	6		4					
ZIAQ		6		3		2		4
AMCA				2	2		2	4
BTS5B	2							
SALA				2				6
LIAR								
ELOB								
SCTA				4	3			
NULU							7	
ACCA			5					
SCFL								
MISC								
PIPU								
PHAU								
LEVI								
BISPC								
POSA								
ASSP								
STPA2								
unknown1					2			
CUGR								
DEAD	3	3	2	1	1	1	3	2
WATER	0	0	0	0	2	0	0	4
BARE	5	4	5	3	2	3	3	3
PERL	3	0	3	2	0	3	3	1
Richness	7	7	9	9	8	8	7	6
NH3 (mg/L)	0.66	2.1	0.88	5.2	0.68	1.4	0.9	0.34
Total								
Nitrate	1.2	0.9	2.3	0.9	1.8	1.6	1.7	1.1
Total N	7.5	11.25	11.25	7.5	3.75	11.25	11.25	11.25
TP (mg/L)	0.15	0.31	0.22	0.2	0.34	0.15	0.21	0.19

Table D10. Raw vegetation from each plot at the Phragmites-dominant site on 7/19/04.

plot #	15M003	14M112	13m202	12m223	11m002	10m203	9m103
LAI	6.16	4.79	6.19	6.2	6.45	5.64	5.8
SEL	0.1	0.05	0.07	0.19	0.21	0.22	0.27
Notes:	10:50, cloudy	11:20, p. sunny	11, sunny	11:30, p. sunny	11:50, p. sunny	11:40, p. sunny	11:55, p.sunny
TYSP	2		2				
PEVI	1	5	2	2		1	4
HIMO							
POAR	8	6	8	7	6	5	4
IMCA	8	3	7	8	8	8	7
BILA							
SISU							
CIAR							
LEOR							
ZIAQ							
AMCA		3					3
BIS5B							
SALA							
LIAR							
ELOB							
SCTA							
NULU							
ACCA	2	4	4	5	6	5	5
SCFL	4	4					
MISC	2	1	3	1		4	
PIPU							
PHAU	7	9	6	7	7	6	7
STPA?							
CASE							
APAM							
BOCY	2			4		2	1
EUPSP							
MEAR							
POAP							
unknown6							2
CUGR		4					
DEAD	5	5	1	4	4	4	3
WATER	0	0	0	0	0	0	0
BARE	1	4	3	2	1	3	3
PERL	0	0	0	0	1	2	0
Species							
Richness	9	9	7	7	4	7	8
NH3 (mg/L)	0.96	1.28	22.2	5.5	0.88	1.3	0.6
Total Nitrate	1.5	1.7	1.2	8.2	0.9	2.3	1.6
Total N	6	6	21	7.5	4.5	6	4.5
TP (mg/L)	0.05	0.32	0.29	0.43	0.06	0.03	0.03

Table D10 continued

plot #	8m113	7m102	6m222	5M111	4m001	3m101	2m201	1m221
LAI	7.87	3.38	6.03	6.02	4.89	5.59	5.53	3.96
SEL	0.2	0.09	0.09	0.87	0.27	0.44	0.23	0.17
Notes:	12:05, sunny	12:14, sunny	12:23, p. sunny	12:32, sunny	12:51, p. sunny	12:42, p. sunny	1:03, sun	1:12, p. sunny
TYSP		3					3	5
PEVI		5	3	3	3		3	2
HIMO		3		3				4
POAR	3	6	8	8	7	8	5	7
IMCA	6	4	5	3	6	4	7	7
BILA						5		
SISU								
CIAR								
LEOR								
ZIAQ								
AMCA								
BIS5B				4				
SALA								
LIAR								
ELOB								
SCTA								
NULU								
ACCA	3	7	3	3	5		4	7
SCFL		1	4			2	7	
MISC								
PIPU								
PHAU	8	6	4	7	7	6	5	5
STPA?	9							
CASE				4	6	5		
APAM	5			5				
BOCY			5	3	2			
EUPSP								
MEAR						3		
STPA2		4						
POAP			2					
unknown6								
CUGR	4					3		
DEAD	5	3	2	4	3	3	2	2
WATER	0	0	0	0	0	0	0	0
BARE	2	5	1	5	2	3	4	6
PERL	0	0	0	0	0	0	0	0
Species								
Richness	7	9	8	10	7	8	7	7
NH3 (mg/L)	2.4	0.62	30	1.86	1.54	1.08	0.78	75
Total Nitrate	1.5	1.2	8.5	5	4	1.9	1.7	0.6
Total N	6	4.5	25.5	6	7.5	4.5	3	22.5
TP (mg/L)	0.35	0	0.41	0	0.51	0.01	0.05	0.19

Table D11. Raw vegetation data from each plot at the Phragmites-absent site on 7/19/04.

plot #	1d001	2d101	3d002	4d111	5d112	6d201	7d102	8d221
LAI	3.49	6.95	3.9	5.07	6.71	3.31	5.52	4.05
SEL	0.67	0.21	0	0.07	0.15	0.44	0.02	0.24
	14:13, p. sunny	14:13, p. sunny	14:24, p. sunny	15:21, sun	15:15, p. sunny	15:28, sunny	14:29, p. sunny	15:09, sunny
Notes:								
TYSP	3	3	4	3	1	3	3	
PEVI	5	4	6	5	3	5	2	2
HIMO	6				7		4	5
POAR	8	9	6	7	10	5	6	8
IMCA	4	6	8	7	5	9	9	3
BILA		2				2		
SISU						4		
CIAR				2	2			
LEOR				2		3		3
ZIAQ					2	2	2	
AMCA	4	2				3		
BIS5B								
SALA					4			2
LIAR								
ELOB								
SCTA								
NULU								
ACCA						1		2
SCFL								
MISC								
PIPU								
PHAU								
STPA?								
CASE								
APAM								
BOCY								
EUPSP								
CIMA								
POAP								
unknown1								
unknown6								
CUGR				5				
DEAD	0	1	2	2	2	2	2	2
WATER	0	0	2	1	0	0	2	0
BARE	4	2	4	3	0	3	1	2
PERL	0	0	0	0	0	0	0	0
Species								
Richness	6	6	4	7	8	10	6	7
NH3 (mg/L)	0.54	27.4	0.52	1.66	0.44	1.2	0.9	0.82
Total Nitrate	1.5		2.2	1	1.4	0.4	1.6	1.1
Total N	11.25	30	11.25	11.25	0	11.25	15	11.25
TP (mg/L)	0.04	0.35	0.45	0.25	0.06	0.31	0.36	0.08

Table D11 continued.

plot #	9d202	10d203	11d222	12d103	13d223	14d113	15d003
LAI	4.71	3.69	4.18	6.18	4.95	5.97	3.69
SEL	0.06	0.41	0.05	0.27	0.64	0.58	0.82
				14:39, p sunny			14:49, p. sunny
Notes:	15:34, sunny	15:05, sunny	15:39, sunny		14:55, sun	14:47, sunny	
TYSP	3	3	2	3	3	3	3
PEVI	4	5	5	2	5	2	4
HIMO							
POAR	8	7	8	9	8	9	9
IMCA	7	7	8	2	7	4	
BILA	3	2		2			
SISU	4	4			7		
CIAR		3			3		
LEOR							
ZIAQ	4		3				1
AMCA			3	2	7		3
BIS5B							
SALA							5
LIAR							
ELOB		2					
SCTA			3				
NULU						4	
ACCA		2			2		
SCFL							
MISC							
PIPU							
PHAU		2			2		
STPA?							
CASE							
APAM							
BOCY							
MEAR							
POAP							
unknown1							
unknown6							
CUGR		3					
DEAD	1	2	1	1	1	1	2
WATER	1	0	1	0	1	0	3
BARE	3	4	2	2	0	0	2
PERL	0	0	0	0	0	0	0
Species							
Richness	7	11	7	6	9	5	6
NH3 (mg/L)	0.94	1.16	2.8	0.82	1.3	0.5	0.54
Total Nitrate	2.1	1.7	1.6	1.3	1.2	1.6	1.1
Total N	11.25	11.25	11.25	15	11.25	7.5	7.5
TP (mg/L)	0.12	0.13	0.13	0.09	0.14	0.07	0.12

Table D12. Raw vegetation data from each plot at the *Phragmites*-dominant site on 8/24/04.

plot #	15M003	14M112	13m202	12m223	11m002	10m203	9m103
LAI	6.79	4.86	6.62	7.32	5.05	4.87	4.04
SEL	0.09	0.1	0.03	0.28	0.02	0.36	0.29
Notes:	11:06, mostly cloudy	11:31, mostly cloudy	11:20	11:49	11:41	11:54, mostly cloudy	12:02, mostly sunny
TYSP	3						
PEVI				5	2	2	6
HIMO							
POAR	10	7	8	7	5	5	7
IMCA	4	5	7	8	6	8	7
BILA							
SISU							
CIAR							
LEOR							
ZIAQ							
AMCA		2					4
BIS5B							
SALA							
LIAR							
ELOB							
SCTA							
NULU							
ACCA		2	2		2	3	4
SCFL		2				3	
MISC							
PIPU				3		2	3
PHAU	4	8	5	4	8	6	8
STPA?							
CASE						3	
APAM							
BOCY							
EUPSP							
CIMA							
FRPE							
MEAR							
POAP							
unknown1							
unknown6							
CUGR		4		3			
DEAD	3	7	6	5	6	7	7
WATER	10	9	4	2	7	1	1
BARE	1	4	3	3	5	4	4
PERL	0	0	0	0	0	0	0
Species							
Richness	4	7	4	6	5	8	7
NH3 (mg/L)	0.28	0.79	7.12	1.87	0.31	2.96	0.52
Total Nitrate	1.6	1.4	1.8	2.6	1.1	2.2	1.9
Total N	11.25	15	48.75	15	11.25	15	15
TP (mg/L)	0.04	0.03	0.12	0.01	0.04	0.04	0.29

Table D12 continued.

plot #	8m113	7m102	6m222	5M111	4m001	3m101	2m201	1m221
LAI	5.8	6.14	4.09	4.08	3.98	4.55	4.77	3.34
SEL	0.34	0.52	0.28	0	0.12	0.24	0.11	0.27
Notes:	12:08	12:18	12:31	12:37, sunny	12:42	12:48	12:53	12:58
TYSP		3					3	3
PEVI		2	2	4	2		2	4
HIMO								3
POAR	6	7	9	7	4	7	8	8
IMCA	6	7	7	4		5	7	6
BILA								
SISU								
CIAR								
LEOR								
ZIAQ								
AMCA								
BIS5B								
SALA								
LIAR								
ELOB								
SCTA								
NULU								
ACCA	2	4	1	2			3	2
SCFL			3	3			4	
MISC								
PIPU			1	3	4	3		
PHAU	7	6	4	7	5	4	4	4
STPA?	6							
CASE					6	4		
APAM	4			6				
BOCY			3	3		5		
EUPSP		3						
CIMA								
FRPE								
MEAR								
unknown6								
CUGR	3				1	3		
DEAD	7	5	3	6	7	7	6	4
WATER	1	2	1	0	0	0	0	0
BARE	4	4	1	7	6	7	7	7
PERL	0	0	0	0	0	0	0	0
Species Richness	7	8	8	9	6	7	7	7
NH3 (mg/L)	1.16	0.44	16.48	5.4	1.08	1.53	1.75	20.48
Total Nitrate	1.4	1.3	1.8	3.3	4.3	5.2	1.2	0.1
Total N	11.25	15	18.75	15	11.25	15	11.25	105
TP (mg/L)	0.17	0.02	0.27	0.03	0.02	0	0	0.09

Table D13. Raw vegetation data from each plot at the *Phragmites*-absent site on 8/24/04.

plot #	1d001	2d101	3d002	4d111	5d112	6d201	7d102
LAI	4.34	6.49	5.21	4.86	7.4	2.8	4.36
SEL	0.32	0.25	0.1	0.55	0.1	0.24	0.02
Notes:	13:45	13:49	13:59	15:08	15:14	15:00	14:08, sunny
TYSP	3	2	3	1		3	3
PEVI	2		2	4	3	5	4
HIMO	3	4	3				4
POAR	9	10	9	8	10	7	6
IMCA	3	2	7	6	3	7	9
BILA							
SISU						2	
CIAR				2			
LEOR							
ZIAQ					1		2
AMCA	1						
BIS5B							
SALA							
LIAR							
ELOB							
SCTA							
NULU							
ACCA							
SCFL							
MISC							
PIPU							
PHAU							
STPA?							
CASE							
APAM							
BOCY							
EUPSP							
CIMA							
POAP							
unknown1							
unknown6							
CUGR				5			
DEAD	1	1	3	2	1	3	3
WATER	1	2	2	3	3	1	2
BARE	0	0	2	2	0	6	3
PERL	0	0	0	0	0	0	0
Species							
Richness	6	4	5	6	4	5	6
NH3 (mg/L)	0.22	1.54	0.35	1.34	0.35	2.3	0.1
Total Nitrate	1.2	0.8	1.4	0.8	1.3	0.1	0.7
Total N	15	18.75	11.25	11.25	11.25	11.25	18.75
TP (mg/L)	0.06	0.1	0.14	0.26	0.09	0.24	0.34

Table D13 continued

plot #	8d221	9d202	10d203	11d222	12d103	13d223	14d113	15d003
LAI	6.9	4.42	3.31	4.35	5.12	4.86	5.36	4.73
SEL	0.22	0.06	0.57	0.26	0.04	0.3	0.06	0.13
Notes:	15:21	14:16	14:51	14:23	14:30	14:46	14:33	14:39
TYSP	0	2	3	3	1	2		3
PEVI	3	2	4	4	3	4	1	3
HIMO	3							
POAR	9	9	8	9	9	8	10	9
IMCA	1	5		7	3	8	2	
BILA		1						
SISU	3		4			4		
CIAR			3					
LEOR								
ZIAQ		3						
AMCA				2				2
BIS5B								
SALA								5
LIAR								
ELOB			2					
SCTA				3				
NULU								
ACCA								
SCFL								
MISC								
PIPU								
PHAU								
STPA?								
CASE								
APAM								
BOCY								
EUPSP								
POAP								
unknown1								
unknown6								
CUGR			2					
DEAD	1	3	2	4	1	2	0	2
WATER	1	3	0	0	1	1	0	1
BARE	2	2	1	3	4	2	0	2
PERL	0	0	0	0	0	0	0	0
Species Richness	6	6	7	6	4	5	3	5
NH3 (mg/L)	2.29	0.4	1.11	5.42	0.43	8.04	1.11	0.17
Total Nitrate	1	0.9	1.1	0.7	1.1	1.3	1.3	1.1
Total N	7.5	7.5	11.25	15	3.75	18.75	3.75	11.25
TP (mg/L)	0.1	0.07	0.24	0.13	0.09	0.11	0.07	0.03

Table D14. Raw vegetation data from each plot at the *Phragmites*-dominant site on 9/21/04.

plot #	15M003	14M112	13m202	12m223	11m002	10m203	9m103
LAI	3.72	2.72	3.95	3.15	3.19	2.7	2.53
SEL	0.06	0.12	0.14	0.43	0.2	0.3	0
Notes:	sunny, 11:24	sunny, 11:04	sunny, 11:18	11:38, sunny	sun, 11:33	11:44, sun	11:50, sun
TYSP	2						
PEVI	2	4	2	4	2		4
HIMO							
POAR	5	5	2	4	3	5	5
IMCA	6		8	8	4	8	6
BILA							2
SISU							
CIAR							
LEOR							
ZIAQ							
AMCA		1					
BIS5B							
SALA							
LIAR							
ELOB							
SCTA							
NULU							
ACCA		3	3	2	3	3	2
SCFL							
MISC						4	
PIPU							3
PHAU	6	8	5	7	9	7	8
STPA?							
CASE							
APAM							
BOCY		3					
FRPE							
MEAR							
SPEU							
Aster Sp							2
unknown6							
CUGR				3			
DEAD	9	9	7	5	8	7	8
WATER	9	10	9	4	9	2	2
BARE	6	7	4	6	6	7	6
PERL	0	0	0	0	0	0	0
Species							
Richness	5	6	5	6	5	5	8
NH3 (mg/L)	0.21	1.33	2.59	0.55	2.88	6.4	0.43
Total Nitrate	1.7	1.3	1.8	1.7	0.8	2.2	2.5
Total N	11.25	11.25	67.5	15	7.5	18.75	11.25
TP (mg/L)	0.05	0.18	0.21	0.08	0.06	0.11	0.05

Table D14 continued

plot #	8m113	7m102	6m222	5M111	4m001	3m101	2m201	1m221
LAI	3.67	3.8	3.56	3.93	3.19	2.63	4.38	2.4
SEL	0.47	0	0.19	0	0	0	0.03	0.05
Notes:	12:05, sun	12:13, sun	12:20, cloud	12:26, cloud	12:32, thin cloud	12:36, thin cloud/ partly sunny	12:40, thin cloud	12:45, thin cloud, partly sunny
TYSP	3						2	3
PEVI		6	3	4	2	1	3	6
HIMO								
POAR	6	7	8	6	3	6	7	5
IMCA	4	7	7		8	4	7	7
BILA								
SISU								
CIAR								
LEOR								
ZIAQ								
AMCA								
BIS5B								
SALA								
LIAR								
ELOB								
SCTA								
NULU								
ACCA	2	3		2			2	3
SCFL		1	1	3			3	
MISC					7			
PIPU				3	4			
PHAU	7	5	3	4	3	2	2	2
STPA?	7							
CASE								
APAM	4			5				
BOCY		4	4	3				
EUPSP		3						
MEAR						5		
SPEU								
Aster Sp								
unknown6								
CUGR	3				1			
DEAD	8	6	5	7	6	8	5	8
WATER	1	1	1	0	0	0	1	1
BARE	7	6	4	7	3	7	6	7
PERL	0	0	0	2	0	0	0	0
Species								
Richness	8	8	6	8	7	5	7	6
NH3 (mg/L)	2.63	0.33	6.2	0.96	1.14	1.86	4.58	1.05
Total Nitrate	1.7	1.4	0.9	1.5	3.2	5.2	1.8	0.2
Total N	15	15	22.5	11.25	7.5	11.25	7.5	93.75
TP (mg/L)	0.18	0.06	0.09	0.02	0.03	0	0.03	0.13

Table D15. Raw vegetation data from each plot at the Phragmites-absent site on 9/21/04.

plot #	1d001	2d101	3d002	4d111	5d112	6d201	7d102
LAI	1.47	2.28	2.61	0.98	5.06	2.98	2.39
SEL	0	0.2	0.67	0	0.28	0	0.17
Notes:	14:14, sunny	14:18	14:10, sunny	15:06, sun	15:10, sun	15:02, sun	14:22, sun
TYSP	2	1	2	2		4	2
PEVI	3	2	1	6		6	3
HIMO			2				
POAR	2	3	3	4	2	2	3
IMCA	5	1	8		1	7	8
BILA							
SISU							
CIAR				3		2	
LEOR							
ZIAQ							
AMCA							
BIS5B							
SALA					3		
LIAR							
ELOB							
SCTA							
NULU							
ACCA							
SCFL							
MISC							
PIPU							
PHAU							
LEVI							
BISPC							
POSA				2			
ASSP							
STPA2							
Aster Sp							
unknown6							
CUGR							
DEAD	8	9	8	8	10	7	6
WATER	1	1	2	4	1	4	3
BARE	6	1	5	4	1	6	7
PERL	0	0	0	0	0	0	0
Species							
Richness	4	4	5	5	3	5	4
NH3 (mg/L)	0.42	4.36	0.29	1.16	0.24	5.04	10.32
Total Nitrate	0.5	1.1	0.5	0.2	1.5	0.3	1.2
Total N	11.25	15	11.25	11.25	11.25	3.75	22.5
TP (mg/L)	0.14	0.26	0.13	0.17	0.13	0.03	0.45

Table D15 continued.

plot #	8d221	9d202	10d203	11d222	12d103	13d223	14d113	15d003
LAI	2.04	2.43	2.54	1.33	1	2.09	2.05	2.09
SEL	0.19	0.37	0.25	0	0	0.46	0.16	0.07
Notes:	14:58, sun	14:27, sun	14:55, sun	14:34, sun	14:37, sun	14:50, sun	14:40, sun	14:45, sun
TYSP			5	4	3	2	2	2
PEVI	4	4	6	4	4	5	2	4
HIMO								
POAR	3	2	2		6	4	1	6
IMCA	3		3			8	3	
BILA								
SISU								
CIAR		1						
LEOR								
ZIAQ								
AMCA						3		
BIS5B								
SALA	2							2
LIAR								
ELOB			3					
SCTA				1				1
NULU								
ACCA								
SCFL								
MISC								
PIPU								
PHAU								
LEVI								
BISPC								
POSA								
ASSP								
STPA2								
Aster Sp								
CUGR								
DEAD	8	9	7	9	8	8	10	9
WATER	1	2	5	3	2	2	1	3
BARE	3	5	5	6	7	3	2	3
PERL	0	0	0	0	0	0	0	0
Species Richness	4	3	5	3	3	6	4	5
NH3 (mg/L)	1.41	0.67	1.16	8.6	0.29	0.58	0.91	0.14
Total Nitrate	1.2	1	1.8	1.4	1.2	1.4	0.9	1
Total N	11.25	15	18.75	18.75	11.25	26.25	15	3.75
TP (mg/L)	0.03	0.06	0.32	0.05	0.06	0.06	0.1	0.08

Table D16. Raw vegetation data from each plot at the *Phragmites*-dominant site on 6/06/05.

plot #	15M003	14M112	13m202	12m223	11m002	10m203	9m103
LAI	2.35	3.49	3.36	4.96	3.75	5.15	7.92
SEL	0	0.41	0.83	0.33	0.04	0.35	0.13
Notes:	12:58	13:14	13:26	13:32	13:38	13:47	13:52
TYSP	clear	clear	clear	clear	clear	clear	clear
PEVI	4	6	5	7		3	7
HIMO			2				
POAR					5	3	3
IMCA	4		4	8	7	9	7
BILA							
SISU							
CIAR							
LEOR							
ZIAQ							
AMCA						1	
BIS5B							
SALA							
LIAR							
ELOB							
SCTA							
NULU							
ACCA	7	7	6	5	7	4	4
SCFL	4						
MISC							
PIPU							
PHAU	4	6	9	9	9	7	9
STPA?							
CASE						4	
APAM							
BOCY							
EUPSP							
CIMA							
FRPE							
MEAR							
Aster Sp							
CUGR							
DEAD	5	4	1	3	6	3	3
WATER	0	0	0	0	0	0	0
BARE	7	2	6	0	0	0	0
PERL	0	0	0	0	0	0	0
Species							
Richness	5	3	5	4	4	7	5
NH3 (mg/L)	1.14	4.88	4.3	0.65	0.79	6.08	0.57
Total Nitrate	3.2		2.4	7	3.9	6.7	3.1
Total N							
TP (mg/L)	0.12	0.58	0.58	0.18	0.14	0.36	0.09
max ht (cm)	180	160	210	220	240	230	250
avg ht (cm)	110	120	200	190	200	190	200

Table D16 continued.

plot #	8m113	7m102	6m222	5M111	4m001	3m101	2m201	1m221
LAI	4.84	3.82	6.34	4.14	4.78	5.09	4.74	5.55
SEL	0.52	0.05	0.11	0.28	0.41	0.23	0.13	0.38
Notes:	14:33	14:40	14:46	14:50	14:56	15:01	15:08	15:15
TYSP	clear	clear	clear	clear	clear	clear	clear	clear
PEVI	1							2
HIMO		7	6	7	3		6	6
POAR	6		3	4	3	2	4	3
IMCA	8	1	8	8	8	9	7	5
BILA	4	2						
SISU								
CIAR								
LEOR								
ZIAQ								
AMCA						2		
BIS5B								
SALA								
LIAR								
ELOB								
SCTA								
NULU								
ACCA		7	5	1	4		3	5
SCFL		3				3	5	
MISC								
PIPU								
PHAU	9	8	8	7	8	8	8	9
STPA?						4		
CASE		2	3	3	3	4		
APAM	1			3	2			
BOCY				3	2			
EUPSP								
CIMA								
FRPE								
MEAR								
Aster Sp								
CUGR						2		
DEAD	3	2	2	4	4	5	3	2
WATER	0	0	0	0	0	0	0	0
BARE	0	2	0	0	0	0	0	0
PERL	0	0	0	0	0	0	0	0
Species								
Richness	6	7	6	8	8	8	6	6
NH3 (mg/L)	0.71	0.87	1.56	1.14	1.06	3.3	1.3	16.88
Total Nitrate	2.4	3.4	8.8	1.7	4.5	5.8	2.5	1.3
Total N								
TP (mg/L)	0.21	0.35	0.88	0.05	0.08	0.34	0.04	0.96
max ht (cm)	270	240	210	210	240	200	240	240
avg ht (cm)	200	160	160	140	160	140	170	170

Table D17. Raw vegetation data from each plot at the Phragmites-absent site on 6/06/05.

plot #	1d001	2d101	3d002	4d111	5d112	6d201	7d102
LAI	3.71	4.32	6.3	5.73	3.55	4.77	4.24
SEL	0.68	0.64	0.11	0.52	0.21	0.03	0.26
Notes:	10:30 clear	10:34 clear	10:41 clear	12:00 clear	12:05 clear	11:54 clear	10:52 clear
TYSP		4	2	2	1	6	4
PEVI	10	9	9	7	8	8	8
HIMO	2						
POAR	3	3	5	2		6	7
IMCA	5	6	6	6	3	3	7
BILA			2				
SISU							4
CIAR			2	1		2	
LEOR							2
ZIAQ							2
AMCA		2					
BIS5B							
SALA							
LIAR							
ELOB							
SCTA							
NULU							
ACCA	2				2	1	
SCFL							
MISC							
PIPU							
PHAU							
LEVI							
BISPC							
POSA							
ASSP							
STPA2							
SPEU							
Aster Sp							
unknown6							
Sparganium							
CUGR							
DEAD	0	0	2	0	4	0	2
WATER	0	0	0	0	0	1	0
BARE	0	0	0	3	6	1	1
PERL	0	0	0	0	0	0	0
Species Richness	5	5	6	5	4	6	7
NH3 (mg/L)	0.76	1.35	0.64	9.8	1.28	4.98	21.28
Total Nitrate	3.5	2.8	1.1	2.2	1.6	1.7	0
Total N							
TP (mg/L)	0.22	1.16	0.26	0.37	0.75	0.21	0.56
max ht (cm)	110	160	150	130	120	170	160
avg ht (cm)	90	120	90	90	95	120	100

Table D17 continued.

plot #	8d221	9d202	10d203	11d222	12d103	13d223	14d113	15d003
LAI	7.24	7.23	5.67	5.36	4.73	6.23	4.58	4.27
SEL	0.19	0.35	0.11	0.06	0.6	0.02	0.08	0.21
Notes:	11:49 clear	11:01 clear	11:42 clear	11:08 clear	11:15 clear	11:34 clear	11:20 clear	11:27 clear
TYSP		1	4	3	2	4	3	1
PEVI	8	8	8	8	7	9	10	9
HIMO								
POAR	5	7	4	3	4	4	4	4
IMCA	8	6	4	8	5	8	2	2
BILA								
SISU		3	4		4	3		
CIAR	3		5					2
LEOR		1		1				
ZIAQ		2		2				
AMCA		2						
BIS5B								
SALA								
LIAR								
ELOB			3					
SCTA			2	3	1			
NULU							4	
ACCA			2					
SCFL								
MISC								
PIPU								
PHAU								
POSA								
ASSP								
SPEU								
Aster Sp								
CUGR								
DEAD	2	0	1	0	1	0	0	0
WATER	0	1	0	0	0	1	0	1
BARE	0	0	0	0	3	0	0	4
PERL	0	0	0	0	0	0	0	0
Species								
Richness	4	8	9	7	6	6	5	5
NH3								
(mg/L)	5.48	0.88	4.28	0.18	0.48	7.84	1.5	2.59
Total								
Nitrate	1.8	0.1	2.7	1		1.5	8.6	
Total N								
TP								
(mg/L)	0.65	0.28	1.2	0.12	0.09	0.44	0.73	1.04
max ht								
(cm)	110	100	190	180	115	180	125	100
avg ht								
(cm)	100	80	100	95	90	110	95	95

Table D18. Raw vegetation data from each plot at the *Phragmites*-dominant site on 8/02/05.

plot #	15M003	14M112	13m202	12m223	11m002	10m203	9m103
LAI	2.14	3.66	3.61	5.48	5.33	5.18	3.52
SEL	0.04	0.05	0.06	0.17	0.05	0.41	0.1
Notes:	10:02 v. sunny	10:18 v sunny	10:26 v sunny	10:44 v sunny	10:37	11:02 v sunny	10:52 v sunny
TYSP	3						
PEVI	4	6	5	3		3	4
HIMO			2				
POAR	5	6	7		7	3	
IMCA	1		6	9	7	6	6
BILA							
SISU							
CIAR							
LEOR							
ZIAQ							
AMCA							3
BIS5B							
SALA							
LIAR							
ELOB							
SCTA							
NULU							
ACCA	5	4	4	2	3	3	3
SCFL	6	5					
MISC		2				2	
PIPU							
PHAU	4	8	8	9	9	9	9
STPA?							
CASE	3						
APAM							
BOCY							
MEAR							
POSA							
ASSP							
STPA2							
CUGR			2		2	1	
DEAD	1	2	2	3	4	4	5
WATER	0	1	0	0	0	0	0
BARE	4	1	3	1	0	1	3
PERL							
Species Richness	8	6	7	4	5	7	5
NH3 (mg/L)	0.41	1.04	0.73	16.56	0.67		
Total Nitrate	1.6	1.5	1.6	9.8	0.7		0
max ht (cm)	200	240	290	325	300	325	315
avg ht (cm)	150	190	150	200	180	250	210

Table D18 continued.

plot #	8m113	7m102	6m222	5M111	4m001	3m101	2m201	1m221
LAI	4.43	4.14	3.98	5.55	3.46	4.75	4.1	4.11
SEL	0.02	0.25	0.33	0.05	0.02	0.04	0.05	0.08
	11:16	11:27	11:35	11:43	11:40	11:58	12:17	12:11
	v	v	vs	v	v	v	v	v
Notes:	sunny	sunny	unny	sunny	sunny	sunny	sunny	sunny
TYSP							2	3
PEVI	1	4	4	5			7	3
HIMO		1						2
POAR	3	5	6	2		4	3	6
IMCA	6	8	9	8	8	8	6	8
BILA								
SISU								
CIAR								
LEOR								
ZIAQ								
AMCA						3		
BIS5B								
SALA								
LIAR								
ELOB								
SCTA								
NULU								
ACCA	3	4	3	3	3		4	4
SCFL		2	3	3		3	3	
MISC		2						
PIPU								
PHAU	9	9	4	9	7	5	8	7
STPA?	4							
CASE					2	8		
APAM	2			7	2			
BOCY			4	3	2	5		
MEAR						4		
POSA		2						
ASSP								
STPA2								
CUGR	2		2	1	2	2		
DEAD	4	3	2	3	5	1	2	2
WATER	0	0	0	0	0	0	0	0
BARE	1	2	1	1	4	2	2	3
PERL								
Species								
Richness	8	9	8	9	7	9	7	7
NH3 (mg/L)	36.8	0.99		14.8	0.62		2.63	18.8
Total Nitrate	4	2.1		6.4	1.5		2	
max ht (cm)	300	300	190	290	310	250	310	290
avg ht (cm)	200	190	150	200	200	140	175	150

Table D19. Raw vegetation data from each plot at the Phragmites-absent site on 8/02/05.

plot #	1d001	2d101	3d002	4d111	5d112	6d201	7d102
LAI	1.34	3.67	4.28	1.5	3.14	4.96	3.92
SEL	0.27	0.32	0.37	0.39	0.17	0.07	0.06
	13:29	13:37	13:42	14:42	14:46	14:36	13:50
	v	v	v	v	v	v	v
Notes:	sunny	sunny	sunny	sunny	sunny	sunny	sunny
TYSP		5	2	3		6	1
PEVI	6	6	2	6	5	2	3
HIMO	4				7		
POAR	6	6	8	6	8	10	9
IMCA	7	8	7	6		1	6
BILA							
SISU	3				3		
CIAR			1				
LEOR				1			
ZIAQ					4	2	
AMCA	2						
BIS5B							
SALA							
LIAR							
ELOB							
SCTA			1				
NULU							
ACCA	1						
SCFL							
MISC							
PIPU							
PHAU			1				
STPA?							
CASE							
APAM							
BOCY							
Sparganium							
CUGR			1	5	2		2
DEAD	2	3	2	3	1	1	3
WATER	0	1	0	2	0	0	0
BARE	3	4	1	6	2	0	2
PERL							
Species							
Richness	7	4	8	6	6	5	5
NH3 (mg/L)	0.52	4.78	0.72	4.74	2.94	5.04	19.52
Total Nitrate	1	1.1	1.1	0.8	0.1	0.8	0.1
max ht (cm)	130	210	170	110	210	210	140
avg ht (cm)	100	130	120	70	110	150	110

Table D19 continued.

plot #	8d221	9d202	10d203	11d222	12d103	13d223	14d113	15d003
LAI	4.17	4.53	3.36	3.96	3.4	3.91	3.97	4.24
SEL	0.08	0.11	0.14	0.23	0.04	0.06	0.07	0.1
	14:51 v sunny	13:51 v sunny	14:32 v sunny	14:26 v sunny	14:03 v sunny	14:21	14:11 v sunny	14:16 v sunny
Notes:								
TYSP		1	6	4	1	3	2	1
PEVI	5	4	5	6	3	4	4	5
HIMO	4							
POAR	7	9	9	8	9	9	9	9
IMCA	9	4	6	2	9	8	6	
BILA	5							
SISU				3				
CIAR								
LEOR								
ZIAQ	4	3			1			1
AMCA					2			
BIS5B								
SALA	2							7
LIAR								
ELOB								
SCTA		2		3	1			
NULU							5	
ACCA						2		
SCFL								
MISC								
PIPU								
PHAU								
STPA?								
CASE								
APAM								
BOCY								
Sparganium								
CUGR	2	2		7		1		2
DEAD	1	2	2	2	1	2	2	2
WATER	0	0	0	1	3	1	2	5
BARE	1	1	1	3	2	0	3	0
PERL								
Species Richness	8	7	4	7	7	6	5	6
NH3 (mg/L)	34.24	1.95	2.94	1.31		0.3	0.85	0.37
Total								
Nitrate	0.5	0.4	0.8	1.6		0.3	1.1	1.1
max ht (cm)	170	180	200	210	140	190	190	120
avg ht (cm)	130	100	130	150	110	130	110	95

Table D20. Diversity data from each plot at the *Phragmites*-dominant site. Diversity index was calculated with the percent cover of each species and the total percent cover of all species.

	15m003	14m112	13m202	12m223	11m002	10m203	9m103	8m113	7m102	6m222	5m111	4m001	3m101	2m201	1m221
5/25/2004	1.73	1.40	1.76	1.42	1.46	1.48	1.63	1.52	1.58	1.71	1.84	1.56	1.74	1.72	1.68
6/3/2004	1.25	1.11	1.67	0.84	1.14	1.22	0.91	1.04	1.55	1.77	0.86	1.05	1.10	1.55	1.57
6/16/2004	1.63	1.78	1.78	1.64	1.43	1.71	1.72	1.58	1.88	1.94	1.78	1.70	1.65	2.03	1.75
6/29/2004	1.54	1.40	1.60	1.67	1.15	1.42	1.58	1.34	1.95	1.88	2.11	1.67	1.44	1.54	1.53
7/19/2004	1.35	1.36	1.24	1.42	1.33	1.30	1.41	1.37	1.80	1.12	1.58	1.61	1.37	1.51	1.72
8/24/2004	0.92	1.57	1.31	1.33	1.55	1.43	1.75	1.76	1.64	0.92	1.82	1.51	1.67	1.54	1.39
9/21/2004	1.46	1.51	1.30	1.48	1.39	1.59	1.52	1.74	1.83	1.20	1.62	1.27	1.27	1.43	1.52
6/6/2005	1.41	1.20	1.10	1.21	1.36	0.99	1.18	1.07	1.20	1.24	1.38	1.09	1.11	1.34	0.97
8/2/2005	1.78	1.23	1.35	0.80	1.16	0.81	0.97	0.89	1.13	0.99	1.33	1.13	1.33	1.25	1.28

Table D21. Diversity data from each plot at the *Phragmites*-absent site

	15m003	14m112	13m202	12m223	11m002	10m203	9m103	8m113	7m102	6m222	5m111	4m001	3m101	2m201	1m221
5/25/2004	1.73	1.40	1.76	1.42	1.46	1.48	1.63	1.52	1.58	1.71	1.84	1.56	1.74	1.72	1.68
6/3/2004	1.25	1.11	1.67	0.84	1.14	1.22	0.91	1.04	1.55	1.77	0.86	1.05	1.10	1.55	1.57
6/16/2004	1.63	1.78	1.78	1.64	1.43	1.71	1.72	1.58	1.88	1.94	1.78	1.70	1.65	2.03	1.75
6/29/2004	1.54	1.40	1.60	1.67	1.15	1.42	1.58	1.34	1.95	1.88	2.11	1.67	1.44	1.54	1.53
7/19/2004	1.35	1.36	1.24	1.42	1.33	1.30	1.41	1.37	1.80	1.12	1.58	1.61	1.37	1.51	1.72
8/24/2004	0.92	1.57	1.31	1.33	1.55	1.43	1.75	1.76	1.64	0.92	1.82	1.51	1.67	1.54	1.39
9/21/2004	1.46	1.51	1.30	1.48	1.39	1.59	1.52	1.74	1.83	1.20	1.62	1.27	1.27	1.43	1.52
6/6/2005	1.41	1.20	1.10	1.21	1.36	0.99	1.18	1.07	1.20	1.24	1.38	1.09	1.11	1.34	0.97
8/2/2005	1.78	1.23	1.35	0.80	1.16	0.81	0.97	0.89	1.13	0.99	1.33	1.13	1.33	1.25	1.28

Table D22. Leaf nutrient data for the six species most present at each plot at the *Phragmites*-dominant site. The first number in each description code designates the plot number of the sample. The first letter indicates which site the sample was taken from: M = *Phragmites*-dominant site; D = *Phragmites*-absent site. The last four letters are the species code of the sample. Table D1 explains each species code.

Description	Lab#	N (%)	P (%)	K (%)	Ca (%)	Mg (%)	S (%)	B (ppm)	Fe (ppm)	Mn (ppm)	Cu (ppm)	Zn (ppm)	Al (ppm)
1MACCA	1	1.83	0.360	2.64	0.52	0.515	0.336	17.3	388.2	845.1	6.3	25.7	118.5
1MHIMO	2	2.61	0.285	1.71	0.98	0.679	0.235	25.0	300.0	470.1	4.2	29.3	43.4
1MIMCA	3	2.96	0.282	3.79	1.26	0.595	0.188	33.9	752.2	452.5	3.1	53.6	220.4
1MPEVI	4	3.52	0.715	4.47	1.59	0.386	0.341	46.1	1584.2	1009.0	15.4	77.3	505.3
1MPHAU	5	1.29	0.114	0.66	0.10	0.066	0.119	7.3	118.9	113.0	11.9	18.9	69.0
1MPOAR	6	2.59	0.327	2.14	0.67	0.631	0.206	33.6	1827.3	1995.0	15.6	59.1	565.6
1MTYSP	7	1.76	0.358	2.44	0.63	0.555	0.351	26.5	860.2	931.1	11.0	36.8	326.2
2MACCA	8	1.89	0.365	2.72	0.63	0.554	0.347	28.4	485.9	1145.0	16.2	33.9	240.3
2MPEVI	9	3.68	0.769	6.09	1.60	0.319	0.330	46.8	1008.8	1529.3	8.8	84.9	495.6
2MPHAU	10	1.74	0.145	0.58	0.19	0.113	0.162	5.4	178.7	285.4	13.2	45.7	69.7
2MSCFL	11	1.49	0.275	1.34	0.19	0.210	0.182	12.3	355.9	1401.2	39.6	46.9	147.7
2MTUSP	12	1.38	0.213	1.21	0.58	0.488	0.209	18.2	339.3	1715.7	10.7	23.9	193.6
3MBOCY	13	1.84	0.241	1.79	1.79	0.496	0.311	37.2	74.9	184.2	8.9	40.3	74.4
3MCASE	14	1.85	0.306	1.75	0.83	0.681	0.210	35.6	70.5	260.0	8.8	27.1	50.8
3MIMCA	15	2.07	0.361	3.35	1.83	0.706	0.319	22.4	100.8	193.0	7.5	100.0	50.1
3MMEAR	16	1.72	0.243	2.06	0.71	0.428	0.238	22.8	72.0	227.3	12.8	37.8	18.3
3MPHAU	17	1.58	0.124	0.70	0.16	0.086	0.139	5.1	89.5	303.6	12.3	21.8	18.4
4MACCA	18	2.58	0.289	1.57	0.69	0.597	0.257	28.8	123.1	635.2	4.2	21.8	77.2
4MCASE	19	2.00	0.267	2.02	0.79	0.582	0.188	36.5	66.7	261.7	6.4	18.0	23.8
4MCUGR	20	1.43	0.235	1.81	0.47	0.224	0.160	23.8	505.9	139.7	42.9	396.3	61.5
4MIMCA	21	2.68	0.385	3.76	1.40	0.759	0.266	26.9	128.2	179.4	6.4	80.6	51.0
4MPHAU	22	1.04	0.082	0.54	0.13	0.065	0.097	3.6	63.6	277.8	5.3	12.4	24.6
5MAPAM	23	2.53	0.247	1.70	1.40	0.384	0.192	20.7	78.5	248.7	11.8	41.5	23.6
5MCASE	24	2.61	0.218	2.57	1.05	0.557	0.195	36.2	67.7	192.4	8.3	32.4	17.6
5MIMCA	25	2.55	0.245	3.68	1.36	0.570	0.179	21.0	100.8	136.2	5.1	91.4	35.3
5MPHAU	26	2.18	0.188	1.02	0.21	0.111	0.202	5.3	83.0	296.4	12.4	22.0	27.7
5MSCFL	27	1.30	0.219	1.88	0.19	0.149	0.165	11.2	92.3	928.7	39.1	37.7	30.6
6MACCA	28	1.95	0.319	2.74	0.70	0.550	0.298	18.4	410.5	691.5	14.7	36.5	224.5
6MIMCA	29	2.05	0.244	3.37	1.10	0.625	0.178	18.7	570.4	240.5	7.2	75.4	264.0
6MPEVI	30	3.62	0.679	5.22	1.50	0.413	0.323	66.2	1827.5	1363.8	5.3	93.1	711.5
6MPHAU	31	1.53	0.148	0.96	0.13	0.092	0.148	5.8	150.2	228.7	16.2	19.7	50.3
6MSCFL	32	1.42	0.260	1.34	0.16	0.188	0.157	5.8	179.0	1309.5	25.2	36.7	66.7
7MACCA	33	1.73	0.275	3.27	0.78	0.529	0.322	21.1	216.8	789.4	7.1	27.0	66.7
7MIMCA	34	3.24	0.283	3.86	1.18	0.446	0.214	20.7	1109.4	321.0	11.9	81.8	328.6
7MPEVI	35	3.66	0.512	4.60	1.79	0.326	0.352	52.4	581.0	1980.6	6.8	78.9	228.9
7MPHAU	36	1.10	0.110	0.61	0.11	0.058	0.122	3.8	88.6	175.5	9.8	17.4	35.6

Table D22 continued.

Description	Lab#	N (%)	P (%)	K (%)	Ca (%)	Mg (%)	S (%)	B (ppm)	Fe (ppm)	Mn (ppm)	Cu (ppm)	Zn (ppm)	Al (ppm)
8MAPAM	37	0.00	0.274	1.52	0.97	0.443	0.209	23.8	210.6	395.0	9.3	32.8	53.8
8MIMCA	38	3.49	0.246	3.35	0.98	0.525	0.175	22.9	121.1	202.4	4.7	55.9	52.5
8MPHAU	39	1.04	0.058	0.35	0.08	0.041	0.087	5.8	49.2	83.2	7.3	11.8	75.3
8MPOAR	40	2.56	0.287	2.30	0.66	0.810	0.220	43.6	1013.2	1509.5	7.3	109.4	538.7
8MTYSP	41	2.74	0.378	2.78	0.68	0.566	0.269	18.4	177.6	631.4	6.5	33.0	71.2
9MACCA	42	2.14	0.371	2.66	0.67	0.589	0.333	22.5	213.7	802.1	8.7	32.5	109.1
9MAMCA	43	1.97	0.232	2.94	0.55	0.340	0.189	36.1	164.5	400.3	10.7	53.1	95.2
9MIMCA	44	2.97	0.265	3.55	1.19	0.662	0.207	25.0	1217.8	339.6	9.9	65.9	655.0
9MPHAU	45	1.12	0.083	0.42	0.11	0.065	0.112	2.9	116.0	159.1	10.2	16.5	33.4
10MACCA	46	2.24	0.396	2.86	0.83	0.617	0.338	24.9	260.5	676.6	15.3	38.5	152.4
10MIMCA	47	2.88	0.269	4.45	1.45	0.751	0.190	22.4	155.3	152.6	6.9	82.1	89.4
10MMISC	48	3.16	0.178	3.30	1.27	0.611	0.245	34.3	108.0	167.6	8.1	32.5	36.9
10MPHAU	49	1.50	0.102	0.58	0.13	0.091	0.134	9.6	76.0	247.4	9.9	15.6	20.3
10MPOAR	50	3.33	0.298	2.55	0.74	0.793	0.221	57.5	115.0	1292.9	7.3	110.6	52.4
11MACCA	51	2.20	0.368	2.83	0.73	0.578	0.339	22.9	154.5	956.2	7.0	26.3	56.4
11MIMCA	52	2.16	0.251	4.26	1.14	0.530	0.164	20.7	176.9	222.8	4.9	49.4	90.3
11MPEVI	53	3.27	0.606	6.15	1.40	0.319	0.263	64.4	160.9	777.8	22.6	57.7	92.6
11MPHAU	54	0.99	0.092	0.68	0.12	0.058	0.105	2.9	67.4	156.9	12.4	17.3	10.9
11MPOAR	55	2.20	0.338	3.49	0.58	0.744	0.184	26.8	211.6	1412.9	4.6	50.2	42.1
12MACCA	56	2.34	0.284	2.72	0.72	0.557	0.293	26.0	114.7	576.4	5.6	28.0	64.9
12MIMCA	57	2.76	0.279	3.78	1.29	0.717	0.221	24.7	100.1	152.1	6.4	76.1	51.7
12MPEVI	58	3.42	0.385	3.83	1.03	0.246	0.246	42.2	127.9	838.3	2.4	66.9	42.7
12MPHAU	59	1.46	0.108	0.71	0.15	0.079	0.138	3.8	70.7	252.2	12.9	18.7	1.7
13MACCA	60	1.97	0.310	2.37	0.74	0.572	0.280	19.0	272.6	1185.2	9.4	24.6	136.8
13MHIMO	61	1.92	0.188	1.34	1.24	0.670	0.170	28.8	135.9	609.6	2.9	34.1	52.9
13MIMCA	62	1.92	0.150	3.03	1.09	0.503	0.142	24.8	96.8	234.4	2.6	39.6	49.3
13MPEVI	63	3.57	0.390	3.48	1.26	0.307	0.306	42.2	415.9	780.8	4.2	48.7	242.7
13MPHAU	64	1.58	0.117	0.65	0.15	0.106	0.137	4.6	118.5	238.0	19.3	19.2	19.6
13MPOAR	65	2.42	0.295	2.02	0.75	0.780	0.209	25.0	283.5	2340.2	4.0	58.2	116.4
14MACCA	66	1.97	0.293	2.83	0.65	0.496	0.326	21.7	225.7	616.3	7.3	20.6	147.6
14MPEVI	67	2.60	0.499	4.70	1.46	0.286	0.287	43.7	718.5	976.9	38.2	54.6	449.0
14MPHAU	68	1.32	0.096	0.67	0.13	0.094	0.144	3.6	88.3	122.5	23.1	19.9	30.2
14MPOAR	69	3.16	0.316	2.20	0.78	0.772	0.254	21.1	656.4	1881.7	23.6	73.7	315.5
14MSCFL	70	1.61	0.283	1.62	0.19	0.168	0.185	6.4	121.4	588.1	34.1	31.9	35.5
15MACCA	71	2.02	0.310	2.52	0.73	0.498	0.278	19.2	258.1	1146.3	10.0	27.2	152.5
15MCASE	72	2.84	0.225	2.17	1.46	0.411	0.386	26.9	234.4	535.5	3.9	37.6	118.1
15MPHAU	73	1.09	0.103	0.74	0.15	0.101	0.119	3.8	131.2	209.5	18.9	18.7	50.5
15MSCFL	74	1.33	0.265	1.40	0.18	0.142	0.146	7.7	113.4	889.5	45.6	36.8	37.1
15MTYSP	75	1.93	0.152	0.42	0.88	0.388	0.218	35.3	948.4	1199.2	10.6	29.0	780.0

Table D23. Leaf nutrient data for the six species most present at each plot at the *Phragmites*-absent site

Description	Lab #	N (%)	P (%)	K (%)	Ca (%)	Mg (%)	S (%)	B (ppm)	Fe (ppm)	Mn (ppm)	Cu (ppm)	Zn (ppm)	Al (ppm)
1Dacca	1	2.84	0.277	2.15	0.59	0.493	0.606	21.7	977.1	597.8	3.8	37.5	472.3
1DHIMO	2	0.98	0.225	1.45	0.45	0.471	0.142	17.3	754.1	284.2	6.4	33.3	485.0
1DIMCA	3	1.33	0.171	3.97	1.02	0.504	0.138	22.6	841.6	249.5	5.6	49.3	460.1
1DPEVI	4	2.15	0.510	5.45	1.38	0.279	0.193	40.3	2117.5	974.8	6.8	50.8	1149.9
1DPOAR	5	1.43	0.253	2.49	0.76	0.749	0.226	24.8	2807.7	1056.6	8.1	62.0	1861.3
2DCUGR	6	2.08	0.350	3.25	0.35	0.262	0.198	16.4	314.7	371.7	3.9	42.1	146.4
2DIMCA	7	1.82	0.219	3.60	1.02	0.390	0.154	19.8	192.1	162.1	3.2	51.6	121.4
2DPEVI	8	2.62	0.493	5.20	1.30	0.329	0.253	39.6	1025.5	1073.6	7.2	62.4	546.7
2DPOAR	9	1.89	0.263	2.98	0.68	0.768	0.204	24.8	398.9	1187.5	3.9	57.5	210.3
2DTYSP	10	0.90	0.095	0.62	0.35	0.307	0.163	9.3	170.4	809.6	1.0	12.5	74.1
3DCIAR	11	1.03	0.121	1.52	0.16	0.116	0.117	6.3	313.5	134.3	3.8	24.5	77.8
3DIMCA	12	1.54	0.238	3.16	1.09	0.433	0.166	22.5	160.1	183.7	3.0	46.0	105.5
3DPEVI	13	2.32	0.512	4.93	1.27	0.325	0.221	89.5	620.9	805.9	6.6	56.8	616.8
3DPOAR	14	1.06	0.269	2.94	0.60	0.659	0.146	25.0	296.4	1151.1	2.1	42.0	114.5
3DTYSP	15	0.83	0.123	1.07	0.41	0.331	0.155	10.3	157.0	717.1	1.3	14.0	49.7
4DCUGR	16	1.56	0.286	2.38	0.24	0.120	0.148	14.3	113.6	71.4	2.2	21.3	52.2
4DIMCA	17	1.45	0.229	3.44	1.03	0.423	0.188	25.0	423.6	244.5	3.8	43.7	171.5
4DPEVI	18	3.51	0.544	5.49	1.66	0.379	0.375	50.7	1584.2	1066.2	6.2	66.3	697.1
4DPOAR	19	1.34	0.263	2.22	0.59	0.588	0.174	23.8	831.0	1159.9	2.5	41.9	354.5
4DTYSP	20	1.25	0.155	1.16	0.40	0.375	0.154	10.4	429.3	464.2	4.4	19.4	221.6
5Dacca	21	1.53	0.315	2.86	0.63	0.431	0.451	16.7	674.7	971.6	11.2	33.1	326.1
5DHIMO	22	2.64	0.360	2.27	1.13	0.614	0.253	43.0	266.7	475.0	81.1	41.8	85.2
5DPEVI	23	2.73	0.574	5.45	1.05	0.309	0.278	38.4	521.0	532.9	4.9	48.9	333.1
5DPOAR	24	1.35	0.259	2.77	0.66	0.735	0.174	25.0	231.9	1592.5	3.4	74.3	131.9
5DZIAQ	25	1.49	0.294	2.07	0.33	0.168	0.174	10.2	170.1	396.8	514.5	39.2	100.6
6DIMCA	26	1.96	0.277	3.19	1.03	0.475	0.227	22.1	273.3	454.0	8.7	47.3	133.1
6DPEVI	27	3.72	0.538	3.94	1.65	0.438	0.402	60.0	527.9	1504.9	6.4	62.2	338.9
6DPOAR	28	1.35	0.224	2.45	0.68	0.702	0.179	22.9	301.1	1436.2	2.5	52.3	164.5
6DTYSP	29	0.81	0.075	0.54	0.50	0.409	0.189	10.7	139.5	430.6	1.7	16.4	65.7
7DHIMO	30	1.52	0.331	4.09	0.67	0.246	0.186	35.3	428.7	332.0	5.5	41.4	208.0
7DIMCA	31	1.24	0.242	3.65	1.11	0.549	0.200	27.6	368.2	323.5	4.3	48.2	174.5
7DPEVI	32	3.07	0.436	4.13	0.97	0.322	0.276	40.0	916.8	843.4	2.1	51.6	487.3
7DPOAR	33	1.12	0.185	2.59	0.61	0.619	0.141	20.3	564.2	977.8	3.3	40.1	230.6
7DTYSP	34	1.25	0.159	1.42	0.47	0.372	0.204	17.3	961.0	669.9	6.4	24.6	462.1

Table D23 continued

Description	Lab #	N (%)	P (%)	K (%)	Ca (%)	Mg (%)	S (%)	B (ppm)	Fe (ppm)	Mn (ppm)	Cu (ppm)	Zn (ppm)	Al (ppm)
8DBILA	35	1.36	0.258	2.74	1.89	0.348	0.376	31.9	118.6	518.5	7.3	43.6	47.9
8DHIMO	36	1.66	0.255	1.46	0.77	0.522	0.158	21.5	123.5	278.1	4.2	32.8	60.9
8DIMCA	37	1.76	0.238	4.03	1.12	0.462	0.210	23.0	240.4	155.9	4.4	55.4	131.2
8DPEVI	38	4.00	0.840	6.54	1.33	0.425	0.412	51.4	330.5	789.7	10.3	74.6	166.6
8DPOAR	39	2.01	0.331	2.65	0.73	0.776	0.238	25.0	728.1	1164.7	5.0	81.2	468.4
9DIMCA	40	1.35	0.192	3.23	1.17	0.686	0.183	34.2	635.3	511.4	9.0	66.5	278.5
9DPEVI	41	3.55	0.485	4.79	1.18	0.406	0.420	38.4	2840.9	1125.8	7.6	90.4	1578.7
9DPOAR	42	1.68	0.264	3.18	0.79	0.806	0.246	25.5	1283.4	1368.2	4.4	57.9	656.8
9DSCTA	43	1.93	0.248	2.72	0.90	0.590	0.418	28.6	252.1	1109.5	5.3	56.4	94.6
9DTYSP	44	1.13	0.194	1.89	0.25	0.195	0.182	8.6	485.8	276.8	23.2	30.9	254.9
10DIMCA	45	1.09	0.183	2.63	0.84	0.367	0.155	13.2	267.5	233.1	5.4	38.0	92.9
10DPEVI	46	2.82	0.624	5.42	1.09	0.355	0.330	37.4	1133.5	628.7	3.3	56.5	432.4
10DPOAR	47	1.64	0.275	2.41	0.76	0.654	0.191	22.2	791.8	1537.6	3.0	116.1	313.9
10DSPEU	48	1.26	0.214	2.36	0.47	0.449	0.591	15.4	828.1	521.6	3.0	22.6	303.8
10DTYSP	49	1.07	0.125	0.78	0.50	0.335	0.164	31.9	339.8	504.8	2.6	17.7	324.9
11DCUGR	50	2.49	0.327	3.09	0.31	0.315	0.208	25.0	158.4	576.3	1.7	34.5	111.3
11DPEVI	51	3.10	0.410	4.47	1.44	0.333	0.332	50.4	855.1	1706.9	4.8	54.4	416.3
11DPOAR	52	1.54	0.193	2.62	0.66	0.830	0.188	23.8	212.9	1598.7	1.3	43.9	77.8
11DSCTA	53	1.22	0.220	1.85	0.44	0.287	0.427	9.6	180.8	560.0	28.9	33.9	73.6
11DSISU	54	1.92	0.285	1.85	0.86	0.301	0.275	43.8	91.2	219.5	3.0	47.1	27.7
11DTYSP	55	0.60	0.128	1.18	0.49	0.386	0.197	11.1	105.9	532.8	6.9	17.7	55.7
12DIMCA	56	1.84	0.167	3.75	1.26	0.486	0.177	33.9	554.2	273.8	4.6	57.7	412.3
12DPEVI	57	3.42	0.608	6.16	1.62	0.389	0.364	61.4	3385.5	1176.6	7.8	83.4	2202.3
12DPOAR	58	1.71	0.245	2.89	0.65	0.734	0.202	23.0	1692.0	1137.7	30.8	60.2	1233.7
12DTYSP	59	1.41	0.215	2.25	0.57	0.355	0.166	19.1	1124.5	969.8	3.8	25.8	689.6
12DZIAQ	60	1.89	0.194	2.11	0.23	0.098	0.168	7.3	322.5	148.6	11.4	20.7	164.8
13DIMCA	61	1.67	0.189	3.52	1.17	0.455	0.232	65.2	179.3	205.7	4.3	52.4	197.2
13DPEVI	62	3.59	0.515	5.13	1.67	0.381	0.394	66.5	651.5	1286.3	3.8	66.7	413.7
13DPOAR	63	1.35	0.190	2.37	0.65	0.742	0.195	26.8	267.5	1222.8	2.2	55.5	122.6
13DSPEU	64	1.36	0.127	1.44	0.49	0.534	0.284	52.5	295.4	632.8	1.7	19.2	363.7
13DTYSP	65	0.87	0.087	0.62	0.34	0.325	0.151	13.9	191.0	442.9	1.7	11.9	109.6
14DIMCA	66	1.71	0.187	3.85	1.49	0.533	0.172	39.8	395.7	371.1	78.0	56.1	203.7
14DNULU	67	1.24	0.225	2.43	0.54	0.128	0.146	28.4	328.8	326.0	2.6	16.0	159.3
14DPEVI	68	3.51	0.621	5.66	1.78	0.352	0.340	75.9	1705.8	857.4	8.4	71.3	1079.6
14DPOAR	69	1.85	0.296	3.23	0.77	0.619	0.183	22.8	766.9	1848.5	5.6	70.1	367.4
14DTYSP	70	0.91	0.117	0.86	0.41	0.329	0.106	8.4	272.4	789.1	1.2	13.4	69.9
15DPEVI	71	3.40	0.606	6.08	1.56	0.405	0.375	67.1	5967.3	1152.0	10.7	166.9	2761.2
15DPOAR	72	1.92	0.306	3.21	0.78	0.746	0.219	26.2	1815.3	1795.2	7.7	69.4	1012.7
15DSALA	73	1.75	0.385	4.17	0.63	0.428	0.181	28.8	2094.6	737.1	6.9	44.9	1386.0
15DTYSP	74	1.25	0.178	2.40	0.42	0.231	0.121	11.5	1096.2	485.3	16.6	25.9	725.5
15DZIAQ	75	1.76	0.245	3.77	0.25	0.154	0.166	7.7	786.9	280.8	9.0	29.0	447.2

Table D24. Biomass data (g) for each species at each 1m² plot at the *Phragmites*-dominant site. X = species absent.

Plot Number	1M	2M	3M	4M	5M	6M	7M	8M	9M	10M	11M	12M	13M	14M	15M
ACCA	189.9	40.3	X	15	8	85.2	132.8	X	49.4	44.9	51	42.5	136.9	142.8	159.7
AMCA	X	X	9	X	X	X	X	X	64.4	X	X	X	X	X	X
APAM	X	X	4.4	2	168	X	X	30	X	X	X	X	X	X	X
BILA	X	X	X	X	X	X	X	X	X	X	X	X	X	X	X
BOCY	X	X	24.9	3.1	X	14.1	X	X	X	X	X	X	X	X	X
CASE	X	X	174.8	17.1	87.9	18.6	X	X	X	X	X	X	X	X	3.9
CIAR	X	X	X	X	X	X	X	X	X	X	X	X	X	X	X
CUGR	X	X	6.3	3.9	X	X	X	X	X	0.8	X	X	3.9	X	X
ELOB	X	X	X	X	X	X	X	X	X	X	X	X	X	X	X
HIMO	46.7	X	X	X	X	X	X	X	X	X	X	X	23.4	X	X
IMCA	26.2	17.3	117.3	43.2	46.4	124.6	6.8	4.3	18.3	85.5	55.3	154.5	38.9	X	2.7
LEOR	X	X	X	X	X	X	X	X	X	X	X	X	X	X	X
MEAR	X	X	24.4	X	X	X	X	X	X	X	X	X	X	X	X
MISC	X	X	X	X	X	X	0.1	X	X	9.7	X	X	X	0.8	X
NULU	X	X	X	X	X	X	X	X	X	X	X	X	X	X	X
PEVI	33.9	60.4	4.6	X	12.7	21.8	19.8	X	0.1	2.8	3.9	12	22.9	142	3
PHAU	1149.9	1070.3	107.4	1672.2	1610.3	885.6	1100.4	1616.3	2140.5	1310.7	1629.9	1786.6	970.8	930.5	211.8
POAR	22.3	7.8	9.2	X	X	13.4	X	3.1	X	6.9	77.4	X	46.7	9.6	X
SALA	X	X	X	X	X	X	X	X	X	X	X	X	X	X	X
SCFL	X	85	20.7	X	30.1	21.1	X	X	X	X	X	X	X	56.5	157.3
SCTA	X	X	X	X	X	X	X	X	X	X	X	X	X	X	X
SISU	X	X	X	X	X	X	X	X	X	X	X	X	X	X	X
SPEU	X	X	X	X	X	X	X	X	X	X	X	X	X	X	X
TYSP	46.9	40.1	X	X	X	X	X	2.7	X	X	X	X	X	X	14.1
ZIAQ	X	X	X	X	X	X	X	X	X	X	X	X	X	X	X
Total Biomass	1515.8	1321.2	503	1756.5	1963.4	1184.4	1259.9	1656.4	2272.7	1461.3	1817.5	1995.6	1243.5	1282.2	552.5

Table D25. Biomass data (g) for each species at each 1m² plot at the *Phragmites*-absent site. X = species absent.

Plot number	1D	2D	3D	4D	5D	6D	7D	8D	9D	10D	11D	12D	13D	14D	15D
ACCA	4.9	X	X	X	35.4	X	X	X	X	X	X	X	3.7	X	X
AMCA	X	X	X	X	X	X	X	X	X	X	X	0.1	X	X	X
APAM	X	X	X	X	X	X	X	X	X	X	X	X	X	X	X
BILA	X	X	X	X	X	X	X	84.7	X	X	X	X	X	X	X
BOCY	X	X	X	X	X	X	X	X	X	X	X	X	X	X	X
CASE	X	X	X	X	X	X	X	X	X	X	X	X	X	X	X
CIAR	X	X	6.4	X	X	X	X	X	X	4.3	X	X	X	X	X
CUGR	X	4.2	X	3.1	X	X	X	0.01	X	0.1	58.5	X	1.3	X	0.01
ELOB	X	X	X	X	X	X	X	X	X	15.8	X	X	X	X	X
HIMO	21.2	X	X	X	10.9	X	7.5	62.1	X	X	X	X	X	X	X
IMCA	49.2	118.3	54.8	40.7	X	2.9	19.3	226.4	22.3	27.8	13.7	72.5	90.3	27.2	X
LEOR	X	X	X	1.5	X	X	X	X	X	0.1	X	X	X	X	X
MEAR	X	X	X	X	X	X	X	X	X	X	X	X	X	X	X
MISC	X	X	X	X	X	X	X	X	X	X	X	X	X	X	X
NULU	X	X	X	X	X	X	X	X	X	X	X	X	X	38.7	X
PEVI	148.7	87.7	28.2	75.5	51.4	17.7	28.5	29.8	64.8	58.1	40.8	90.5	101.2	63	53.3
PHAU	X	X	1.3	X	X	X	X	X	X	X	X	X	X	X	X
POAR	80.8	98.6	165.5	70.6	372.8	370.2	247.5	88.8	254.7	412.4	206.7	127.9	313.8	106.6	115.2
SALA	X	X	X	X	X	X	X	6.5	X	X	X	X	X	X	19.7
SCFL	X	X	X	X	X	X	X	X	X	X	X	X	X	X	X
SCTA	X	X	X	X	X	X	X	X	7.2	X	111.8	X	X	X	X
SISU	X	X	X	X	X	X	X	X	X	0.2	19.5	X	X	X	X
SPEU	X	X	X	X	X	X	X	X	X	44.9	X	X	55	X	X
TYSP	X	128.2	69.9	46.8	X	234.7	31	X	22.9	225.2	166.8	2.2	131.4	21.8	5
ZIAQ	X	X	X	X	12.1	0.3	X	2.8	3.9	X	X	4.4	X	X	1.6
Total Biomass	304.8	437	326.1	238.2	482.6	625.8	333.8	501.11	375.8	788.9	617.8	297.6	696.7	257.3	194.81

Table D26. Elevation (cm) of marsh plots above base of data-logging well (see A. Baldwin, unpublished data) located on tidal creek equidistant from each marsh site.

Plot	cm	ft
1D001	15.5	0.51
2D101	21.9	0.72
3D002	18.3	0.6
4D111	20.4	0.67
5D112	8.2	0.27
6D201	18.3	0.6
7D102	18.0	0.59
8D221	18.9	0.62
9D202	14.9	0.49
10D203	18.6	0.61
11D222	14.6	0.48
12D103	12.8	0.42
13D223	17.4	0.57
14D113	15.8	0.52
15D003	8.5	0.28
1M221	18.3	0.6
2M201	18.9	0.62
3M101	32.9	1.08
4M001	33.2	1.09
5M111	29.0	0.95
6M222	29.3	0.96
7M102	26.2	0.86
8M113	35.4	1.16
9M103	30.8	1.01
10M203	29.0	0.95
11M002	21.6	0.71
12M223	23.2	0.76
13M202	18.9	0.62
14M112	2.4	0.08
15M003	16.5	0.54

Literature Cited

- Almeida, T.I.R., C.R. de Souza Filho, 2004. Principal component analysis applied to feature-oriented band ratios of hyperspectral data: a tool for vegetation studies. *International Journal of Remote Sensing* 20: 5005-5023.
- Anderson, J.E., J.E. Perry, 1996. Characterization of wetland plant stress using leaf spectral reflectance: Implications for wetland remote sensing. *Wetlands* 16(4):477-487.
- Becker, B.L., D.P. Lusch, J. Qi, 2005. Identifying optimal spectral bands from in situ measurements of Great Lakes coastal wetlands using second-derivative analysis. *Remote Sensing of the Environment* 97: 238-248.
- Bedford, B.C., M.R. Walbridge, A. Aldous, 1999. Patterns in nutrient availability and plant diversity of temperate North American wetlands. *Ecology* 80(7):2151.
- Blackburn, G.A., 2004. Wavelet decomposition of hyperspectral reflectance data for quantifying photosynthetic pigment concentrations in vegetation. Preceedings at the Geo-Imagery Bridging Continents Conference, Istanbul, Turkey.
- Blicher-Mathiesen, G., C.C. Hoffman, 1999. Denitrification as a sink for dissolved nitrous oxide in a freshwater riparian fen. *Journal of Environmental Quality* 28(1):257.
- Bowden, W.B., 1986. Nitrification, nitrate reduction, and nitrogen immobilization in a tidal freshwater marsh sediment. *Ecology* 67(1): 88-99.
- Bronson, K.F., J.D. Booker, J.W. Keeling, R.K. Boman, T.A. Wheeler, R.J. Lascano, R.L. Nichols, 2005. Cotton canopy reflectance at landscape scale as affected by nitrogen fertilization. *Agronomy Journal*, 97: 654-660.
- Carter, G.A., R.L. Miller, 1994. Early detection of plant stress by digital imaging within narrow stress-sensitive wavebands. *Remote Sensing of Environment* 50(3):295-302.
- Casa, R., H.G. Jones, 2003. Retrieval of crop canopy properties: a comparison between model inversion from hyperspectral data and image classification. *International Journal of Remote Sensing* 25(6):1119-1130.
- Chang, J., S.A. Clay, D.E. Clay, K. Dalsted, 2004. Detecting weed-free and weed-infested areas of a soybean field using near-infrared spectral data. *Weed Science* 52:642-648.
- Cronk, J.K., M.S. Fennessy, 2001. *Wetland Plants: Biology and Ecology*. Lewis Publishers, New York, New York.

- Denver, J.M., S.W. Ator, L.M. Debrewer, M.J. Ferrari, J.R. Barbaro, T.C. Hancock, M.J. Brayton, M.R. Nardi, 2001. Water Quality in the Delmarva Peninsula, Delaware, Maryland, and Virginia, 1999-2001: Reston, Va., U.S. Geological Survey Circular 1228, 36p.
- Diker, K., W.C. Bausch, 2003. Radiometric field measurements of Maize for estimating soil and plant nitrogen. *Biosystems Engineering* 86(4):411-420.
- Drexler, J.Z., B.L. Bedford, 2002. Pathways of nutrient loading and impacts on plant diversity in a New York peatland. *Wetlands* 22(2):263-281.
- Esbensen, K.H., 2002. *Multivariate Data Analysis In Practice: An Introduction to Multivariate Data Analysis and Experimental Design*. 5th Edition. Camo Technologies, Woodbridge, NJ.
- Feller, I.C., D.F. Whigham, J.P. O'Neill, and K.L. McKee, 1999. Effects of nutrient enrichment on within-stand cycling in a mangrove forest. *Ecology* 80: 2193-2205.
- Filella, Il, L. Serrano, J. Serra, J. Peñuelas, 1995. Evaluating wheat nitrogen status with canopy reflectance indices and discriminant analysis. *Crop Science* 35(5):1400.
- Forina, M., S. Lanteri, M.C. Cerrato Oliveros, C. Pizarro Millan, 2004. Selection of useful predictors in multivariate calibration. *Anal. Bioanal Chem* 380: 397-418.
- Fridgen, J.L., J.J. Varco, 2004. Dependency of cotton leaf nitrogen, chlorophyll, and reflectance on nitrogen and potassium availability. *American Society of Agronomy* 96:63-69.
- Garthwaite, P.H., 1994. An interpretation of partial least squares. *Journal of the American Statistical Association* 89(425):122-127.
- Geladi, P., E. Dabakk, 2000. *Computational Methods and Chemometrics in Near-IR Spectroscopy*. *Encyclopedia of Spectroscopy and Spectrometry*. Academic Press, New York, New York.
- Gibson, K.D., J.B. Zedler, R. Langis, 1994. Limited response of cordgrass (*Spartina fabiosa*) to soil amendments in a constructed marsh. *Ecological Applications* 4(4): 757-767.
- Glenn, N.F., J.T. Mundt, K.T. Weber, T.S. Prather, L.W. Lass, J. Pettingill, 2005. Hyperspectral data processing for repeat detection of small infestations of leafy spurge. *Remote Sensing of the Environment* 95: 399-412.

- Gomez, R.B., 1999. Key issues of hyperspectral sensing technology applications. American Institute of Aeronautics and Astronautics 99-4563, 11p.
- Grossman, Y.L., S.L. Ustin, S. Jacquemoud, E.W. Sanderson, G. Schmuck, J. Verdebout, 1996. Critique of stepwise multiple linear regression for the extraction of leaf biochemistry information from leaf reflectance data. Remote Sensing of the Environment 56: 182-193.
- Haboudane, D., J.R. Miller, E. Pattey, P.J. Zarco-Tejada, I.B. Strachan, 2004. Hyperspectral vegetation indices and novel algorithms for predicting green LAI of crop canopies: Modeling and validation in the context of precision agriculture. Remote Sensing of Environment 90(3):337-352.
- Hansen, P.M., J.K. Schjoerring, 2003. Reflectance measurement of canopy biomass and nitrogen status in wheat crops using normalized difference vegetation indices and partial least squares regression. Remote Sensing of Environment 86(4):542-553.
- Harvey, R.W., J.P. Mueller, J.A. Barker, M.H. Poore, J.P. Zublena, 1996. Forage characteristics, steer performance, and water quality from bermuda grass pastures fertilized with two levels of nitrogen from swine lagoon effluent. Journal of Animal Science 74(2): 457-464.
- Hawkins, B.J., D. Burgess, A.K. Mitchell, 2005. Growth and nutrient dynamics of western hemlock with conventional or exponential greenhouse fertilization and planting in different fertility conditions. Canadian Journal of Forest Research 35(4): 1002-1016.
- Henry, W.B., D.R. Shaw, L.M. Bruce, 2004. Spectral reflectance curves to distinguish soybean from common cocklebur (*Xanthium strumarium*) and sicklepod (*Cassia obtusifolia*) grown with varying soil moisture. Weed Science 52:788-796.
- Hochberg, E.J., M.J. Atkinson, S. Andréfouët, 2003. Spectral reflectance of coral reef bottom-types worldwide and implications for coral reef remote sensing. Remote Sensing of Environment 85(2):159-173.
- Hogan, D.M., T.E. Jordan, M. Walbridge, 2004. Phosphorus retention and soil organic carbon in restored and natural freshwater wetlands. Wetland 24(3):573-585.
- Hurcom, S.J., A.R. Harrison, M. Taberner, 1996. Assessment of biophysical vegetation properties through spectral decomposition techniques. Remote Sensing of the Environment 56: 203-214.
- Kahn, J., W.M. Kemp, 1985. Economic losses associated with the degradation of an

- ecosystem: The case of submerged aquatic vegetation in Chesapeake Bay. *Journal of Environmental Economics and Management* 12:246-263.
- Kaushal, T., M. Ond, S. Ito, A. Yamazaki, H. Fujikake, N. Ohtake, K. Sueyoshi, Y. Takahashi, T. Ohyama, 2005. N-15 analysis of the promotive effect of deep placement of slow-release nitrogen fertilizers on growth and seed yield of soybeans. *Soil Science and Plant Nutrition* 51(6): 885-892.
- Kiehl, K., P. Esselink, J.P. Bakker, 1997. Nutrient limitation and plant species composition in temperate salt marshes. *Oecologia (Berlin)* 11(3): 325-330.
- Kodani, E., Y. Awaya, K. Tanaka, N. Matsumura, 2002. Seasonal patterns of canopy structure, biochemistry and spectral reflectance in a broad-leaved deciduous *Fagus crenata* canopy. *Forest Ecology and Management* 167(1-3):233-249.
- Koger, C.H., D.R. Shaw, K.N. Reddy, L.M. Bruce, 2004. Detection of pitted morningglory (*Ipomoea lacunosa*) by hyperspectral remote sensing. I. Effects of tillage and cover crop residue. *Weed Science* 52:222-229.
- Kooistra, L., R.S.E.W. Leuven, R. Wehrens, P.H. Nienhuis, L.M.C. Buydens, 2003. A comparison of methods to relate grass reflectance to soil metal contamination. *International Journal of Remote Sensing*, 20(20): 4995-5010.
- Koponen, S., J. Pulliainen, K. Kallio, M. Hallikainen, 2002. Lake water quality classification with airborne hyperspectral spectrometer and simulated MERIS data. *Remote Sensing of Environment* 79:51-59.
- Krieger, K.A., 2003. Effectiveness of a coastal wetland in reducing pollution of a Laurentian Great Lake: hydrology, sediment, and nutrients. *Wetlands* 23(4):778-791.
- Landgrebe, D.A. 2003. *Signal Theory Methods in Multispectral Remote Sensing*. Wiley Interscience: A John Wiley & Sons Publication. Hoboken, New Jersey.
- Landsat, USA. Remote Sensing – Center for Remote Imaging, Sensing and Processing. 28 January 2005.
<<http://www.crisp.nus.edu.sg/~research/tutorial/landsat.htm>>
- Larcher, W, 2001. *Physiological Plant Ecology: Ecophysiology and stress physiology of functional groups*, Fourth edition. Springer, New York.
- Leardi, R., 2000. Application of genetic algorithm-PLS for feature selection in spectral data sets. *Journal of Chemometrics*, 14: 643-655.
- Li, H., R.J. Laascano, E.M. Barnes, J. Booker, L.T. Wilson, K.F. Bronson, E. Segarra,

2001. Multispectral reflectance of cotton related to plant growth, soil water and texture, and site elevation. *Agronomy Journal* 93:1327-1336.
- Lovelock, C.E., S.A. Robinson, 2002. Surface reflectance properties of Antarctic moss and their relationship to plant species, pigment composition and photosynthetic function. *Plant, Cell and Environment* 25:1239-1250.
- Ma, B.L., L.M. Dwyer, C. Costa, E.R. Cober, M.J. Morrison, 2001. Early Prediction of soybean yield from canopy reflectance measurements. *Agronomy Journal* 93:1227-1234.
- Maestre, F.T., 2004. On the importance of patch attributes, environmental factors and past human impacts as determinants of perennial plant species richness and diversity in Mediterranean semi-arid steppes. *Diversity and Distributions* 10(1): 20-28.
- Maheu-Giroux, M., S. de Blois, 2005. Mapping the invasive species *Phragmites australis* in linear wetland corridors. *Aquatic Botany* 83: 310-320.
- McNulty, S.G., J. Boggs, J.D. Aber, L. Rustad, A. Magill, 2005. Red Spruce ecosystem level changes following fourteen years of chronic nitrogen fertilization. *Forest Ecology and Management* 219(2-3): 279-291.
- Mitsch, W.J. and J.G. Gosselink. 2000. *Wetlands*, Third edition. John Wiley and Sons, New York.
- Ott, R.L. and M. Longnecker. 2001. *An Introduction to Statistical Methods and Data Analysis*. Fifth edition. Duxbury: Thomson Learning. Pacific Grove, CA.
- Pattey, E., I.B. Strachan, J.B. Boisvert, R.L. Desjardins, N.B. McLaughlin, 2001. Detecting effects of nitrogen rate and weather on corn growth using micrometeorological and hyperspectral reflectance measurements. *Agricultural and Forest Meteorology*, 108(2): 85-99.
- Pauli, D., M. Peintinge, B. Schmid, 2002. Nutrient enrichment in calcareous fens: effects on plant species and community structure. *Basic and Applied Ecology* 3(3):255-266.
- Peet, R.K., T.R. Wentworth, P.S. White, 1998. A flexible, multipurpose method for recording vegetation composition and structure. *Castanea* 63:262-274.
- Petisco, C., B. Garcia-Criado, B.R. Vazquez de Aldana, I. Zabalgoeazcoa, S. Mediavilla, A. Garcia-Ciudad, 2005. Use of near-infrared reflectance spectroscopy in predicting nitrogen, phosphorus and calcium contents in heterogeneous woody plant species. *Anal Bioanal Chem* 382: 458-465.

- Phillips, R.L., O. Beerli, E.S. DeKeyser., 2005. Remote wetland assessment for Missouri Coteau Prairie glacial basins. *Wetlands* 25(2): 335-349.
- Phillips, S.W., M.J. Focazio, L.J. Bachman, 1999. Discharge, nitrate load, and residence time of ground water in the Chesapeake Bay watershed. U.S. Geological Survey, FS-150-99, 6p.
- Poe, A.C., M.F. Piehler, S.P. Thompson, H.W. Paerl, 2003. Denitrification in a constructed wetland receiving agricultural runoff. *Wetlands* 23(4):817-826.
- Prasad, R. 2005. Research on nitrification inhibitors and slow-release nitrogen fertilizers in India: A review. *Proceedings of the Indian National Science Academy Part B: Biological Sciences* 75(Part3): 149-157.
- Quiroga-Garza, H., G.A. Picchioni, M.D. Remmenga, 2001. Bermudagrass fertilized with slow-release nitrogen sources. I. Nitrogen uptake and potential leaching losses. *Journal of Environmental Quality* 20(2): 440-448.
- Rathier, T.M., C.R. Frink, 1989. Nitrate in runoff water from container grown Juniper and Alberta spruce under different irrigation and nitrogen fertilization regimes. *Journal of Environmental Horticulture* 7(1): 32-35.
- Rautiainen, M., 2005. Retrieval of leaf area index for a coniferous forest by inverting a forest reflectance model. *Remote Sensing of the Environment* 99: 295-303.
- Read, J.J., L. Tarpley, J.M. McKinion, K.R. Reddy, 2002. Narrow-waveband reflectance ratios for remote estimation of nitrogen status in cotton. *Journal of Environmental Quality* 31:1442-1452.
- Rosso, P.H., J.C. Pushnik, M. Lay, S.L. Ustin, 2005. Reflectance properties and physiological responses of *Salicornia virginica* to heavy metal and petroleum contamination. *Environmental Pollution* 137: 241-252.
- Salem, F., M. Kafatos, T. El-Ghazawi, R. Gomez, R. Yang, 2005. Hyperspectral image assessment of oil-contaminated wetland. *International Journal of Remote Sensing*, 26(4): 811-821.
- Schmidt, K.S., A.K. Skidmore, 2003. Spectral discrimination of vegetation types in a coastal wetland. *Remote Sensing of Environment* 85: 92-108.
- Schmidtlein, S., J. Sassan, 2004. Mapping of continuous floristic gradients in grasslands using hyperspectral imagery. *Remote Sensing of Environment* 92:126-138.

- Schuerger, A.C., G.A. Capelle, J.A. Di Benedetto, C. Mao, C.N. Thai, M.D. Evans, J.T. Richards, T.A. Blank, E.C. Stryjewski, 2003. Comparison of two hyperspectral imaging and two laser-induced fluorescence instruments for the detection of zinc stress and chlorophyll concentration in bahia grass (*Paspalum notatum* Flugge). *Remote Sensing of the Environment* 84: 572-588.
- Shippert, P., 2004. Why use hyperspectral imagery? *Photogrammetric Engineering and Remote Sensing* 377, 379-380.
- Siebielec, G., G.W. McCarty, T.I. Stuczynski, J.B. Reeves III, 2004. Near- and mid-infrared diffuse reflectance spectroscopy for measuring soil metal content. *Journal of Environmental Quality*, 33: 2056-2069.
- Silliman, B.R., M. Bertness, 2004. Shoreline development drives invasion of *Phragmites australis* and the loss of plant diversity on New England salt marshes. *Conservation Biology* 18(5):1424.
- Silvestri, S., M. Marani, A. Marani, 2003. Hyperspectral remote sensing of salt marsh vegetation, morphology and soil topography. *Physics and Chemistry of the Earth* 28:15-25.
- Sims, D.A., J.A. Gamon, 2002. Relationships between leaf pigment content and spectral reflectance across a wide range of species, leaf structures and developmental stages. *Remote Sensing of Environment*, 81: 337-354.
- Smith, A.M., R.E. Blackshaw, 2003. Weed-crop discrimination using remote sensing: a detached leaf experiment. *Weed Technology* 17: 811-820.
- Smith, M.L., S.V. Ollinger, M.E. Martin, J.D. Aber, R.A. Hallett, C.L. Goodale, 2002. Direct estimation of aboveground forest productivity through hyperspectral remote sensing of canopy nitrogen. *Ecological Applications* 12(5): 1286-1302.
- Smith, M.L., M.E. Martin, L. Plourde, S.V. Ollinger, 2003. Analysis of hyperspectral data for estimation of temperate forest canopy nitrogen concentration: comparison between an airborne (AVIRIS) and a spaceborne (Hyperion) sensor. *IEEE Transactions on Geoscience and Remote Sensing*, 41(6): 1332-1337.
- Strachan, I.B., E. Pattey, J.B. Boisvert, 2002. Impact of nitrogen and environmental conditions on corn as detected by hyperspectral reflectance. *Remote Sensing of Environment* 80(2):213-224.

- Tarpley, L., K.R. Reddy, G.F. Sassenrath-Cole, 2000. Reflectance indices with precision and accuracy in predicting cotton leaf nitrogen concentration. *Crop Science* 40:1814-1819.
- Thenkabail, P.S., R.B. Smith, E. De Pauw, 2000. Hyperspectral vegetation indices and their relationships with agricultural crop characteristics. *Remote Sensing of the Environment* 71: 158-182.
- Thomson, A.G., A. Huiskes, R. Cox, R.A. Wadsworth, L.A. Boorman, 2004. Short-term vegetation succession and erosion identified by airborne remote sensing of Westerschelde salt marshes, The Netherlands. *Int. Journal of Remote Sensing* 20: 4151-4176.
- Thoren, A.K., C. Legrand, K.S. Tonderski, 2004. Temporal export of nitrogen from a constructed wetland: influence of hydrology and senescing submerged plants. *Ecological Engineering* 23: 233-249.
- Tilley, D.R., M. Ahmed, J.H. Son, H. Badrinarayanan, 2003. Hyperspectral reflectance of emergent macrophytes as an indicator of water column ammonia in an oligohaline, subtropical marsh. *Ecological Engineering* 21:153-163.
- Tilley, D.R., A. Baldwin, E. Poynter, 2004. A Progress Report to Maryland Sea Grant College on the project: Hyperspectral Reflectance of Freshwater Tidal Emergent Macrophytes as a Remote Sensing Tool for Assessing Wetland Nitrogen Status (R/CT-03). Maryland Sea Grant College, University of Maryland, College Park.
- Tilley, D.R., A. Baldwin, E.P. Jenkins, (in review). Hyperspectral reflectance response of four freshwater emergent macrophytes to nitrogen fertilization.
- Tiner, R.W., 2004. Remotely-sensed indicators for monitoring the general condition of “natural habitat” in watersheds: an application for Delaware’s Nanticoke River watershed. *Ecological Indicators* 4: 227-243.
- Townsend, P.A., J.R. Folster, R.A. Chastain, Jr., W.S. Currie, 2003. Application of imaging spectroscopy to mapping canopy nitrogen in the forests of the central Appalachian Mountains using Hyperion and AVIRIS. *IEEE Transactions on Geoscience and Remote Sensing* 41(6):1347-1354.
- Truscott, A.M., S.C.F. Palmer, G.M. McGowan, J.N. Cape, S. Smart, 2005.

- Vegetation composition of roadside verges in Scotland: the effects of nitrogen deposition, disturbance, and management. *Environmental Pollution* 136(1): 109-118.
- Turkington, R., E. John, S. Watson, P. Seccombe-Hett, 2002. The effects of fertilization and herbivory on the herbaceous vegetation of the boreal forest in Northwest Canada: a ten-year study. *Journal of Ecology* 90(2): 325-337.
- Underwood, E., S. Ustin, D. DiPietro, 2003. Mapping nonnative plants using hyperspectral imagery. *Remote Sensing of Environment*, 86: 150-161.
- USEPA, 2002. National Water Quality Inventory 2000 Report. U.S. Environmental Protection Agency, Office of Water, EPA-841-R-02-001. Washington, D.C.
- Wilson, M.D., S.L. Ustin, D.M. Rocke, 2004. Classification of contamination in salt marsh plants using hyperspectral reflectance. *IEEE Transactions on Geoscience and Remote Sensing* 42(5):1088-1095.
- Xue, L., W. Cao, W. Luo, T. Dai, Y. Zhu, 2004. Monitoring leaf nitrogen status in rice with canopy spectral reflectance. *Agronomy Journal* 96:135-142.
- Yang, C.M., R.K. Chen, 2004. Modeling rice growth with hyperspectral reflectance data. *Crop Science*, 44: 1283-1290.
- Yao, H., L. Tian, 2003. A genetic-algorithm-based selective principal component analysis (GA-SPCA) method for high-dimensional data feature extraction. *IEEE Transactions on Geoscience and Remote Sensing* 41(6):1469-1478.
- Zha, Y., J. Gao, S. Ni, Y. Liu, J. Jiang, Y. Wei, 2003. A spectral reflectance-based approach to quantification of grassland cover from Landsat TM imagery. *Remote Sensing of Environment* 87(2-3):371-375.
- Zhang, M., S.L. Ustin, E. Rejmankova, E.W. Sanderson, 1997. Monitoring pacific coast salt marshes using remote sensing. *Ecological Applications* 7(3):1039-1053.
- Zhao, D., K.R. Reddy, V.G. Kakani, J.J. Read, G.A. Carter, 2003. Corn (*Zea mays* L.) growth, leaf pigment concentration, photosynthesis and leaf hyperspectral reflectance properties as affected by nitrogen supply. *Plant and Soil* 257: 205-217.
- Zhao, D., K.R. Reddy, V.G. Kakani, J.J. Read, S. Koti, 2005. Selection of optimum reflectance ratios for estimating leaf nitrogen and chlorophyll concentrations of field-grown cotton. *Agronomy Journal*, 97: 89-98.